National Technical University of Athens

School of Civil Engineering

Bearing Capacity and Strengthening of a Multi-Storey Reinforced Concrete Hotel

ALEXANDROS BELIVANIS

Supervisor: Professor Vlassis Koumousis

A dissertation submitted in partial fulfilment of the requirements for the Degree of Master of Science in Analysis and Design of Earthquake Resistant Structures

Athens, July 2016

My originality declaration

"This dissertation entitled Bearing Capacity and Strengthening of a Multi-Storey Reinforced Concrete Hotel for the fulfilment of the degree of M.Sc. in Analysis and Design of Earthquake Resistant Structures, has been made by myself based on references listed in appendices. All sources of information have been acknowledged by references including those from the internet."

Acknowledgment

I would like to acknowledge my supervisor, Professor Vlassis Koumousis for his supervision during all the period I worked on this dissertation and because he gave me the opportunity to learn about this interesting subject.

Abstract

This project's aim is not only to study the bearing capacity of a multi-storey reinforced concrete hotel, but also to study its strengthening. The hotel constructed in 1967 in Greece in seismic zone 2 area (Z2, $a_{GR}/g=0.24$) under the provision of the national codes of Members of Reinforced Concrete (1954) and of the Design Code for Earthquake Resistant structures (1959). It is a 5-storey reinforced concrete building with underground floor, ground floor (two levels), mezzanine floor, approachable and non approachable roof. Its overall high is 27.53m, including the non approachable roof, while the typical high of floors is 3.2m. SAP2000 is used for the analyses of the building. Modal response spectrum analysis, nonlinear static (pushover) analyses and nonlinear dynamic time-history analyses are performed. Three pairs of acceleration time histories are used. They are the earthquakes events of Corinth (1981, magnitude: 6.6), Kalamata (1986, magnitude 6.2) and L'Aquila-Italy (2009 magnitude: 6.3). The acceleration time-histories are obtained by the PEER Ground Motion Data Base-Beta version. The acceleration time-histories are scaled. The assessment of the bearing capacity shows that the structure requires rehabilitation. The rehabilitation aim is to reach the life safety performance level. Nonlinear static (pushover) analyses and nonlinear dynamic time-history analyses are performed to the retrofitted structure, showing that the target-performance level is succeeded, when seismic action corresponding to seismic return period of 475 years, or the scaled L'Aquila, Corinth, Kalamata acceleration time-histories are imposed to the structure.

Table of Contents

CHAPTER 1 1
Introduction 1
1.1 Motivation 1
1.2 Research Objective 1
1.3 Research Approach 2
1.4 Report Outline 2
Chapter 2 5
Assessment of the Bearing Capacity of Structures-Background Concepts 5
2.1 Required Information for the Assessment of the Structure 5
2.1.1 General Information and History of the Building 5
2.1.2 Required Input Data 6
2.1.3 Materials 6
2.1.4 Knowledge Level 7
2.1.5 Confidence Factors 7
2.2 Seismic Action for the Assessment of the Structure 8
2.2.1 Seismic Action 8
2.2.2 Combination of the Effects of the Components of the Seismic Action 11
2.3 Methods of Analysis 11
2.3.1 Modal Response Spectrum Analysis 12
2.3.2 Nonlinear Static (Pushover) Analysis 14
2.3.3 Nonlinear Time-History Dynamic Analysis 17
2.4 Performance Based Design 18
2.4.1 Rehabilitation Objectives 20
2.4.2 Structural Performance Levels 21
2.4.3 Capacity Curve 22
2.4.4 Primary and Secondary Elements and Components 22
2.4.5 Component Behaviour F-δ Curve 23
2.4.6 Performance Levels of the Elements 26
2.4.7 Performance Levels of the Structure 29
2.4.8 Target Displacement Check 30
2.4.9 Performance Point Estimation 32
2.4.10 ATC-40 Methodology 36
CHAPTER 3 45
Retrofit Strategies and Systems 45
3.1 Introduction 45
3.2 Technical Strategies 46
3.2.1 Local Modification of Components 47
3.2.2 Removal or Lessening of Existing Irregularities 48
3.2.3 Global Structural Strengthening and Stiffening 48
3.2.4 Reducing Earthquake Demands (mass reduction, seismic isolation, energy dissipation systems) 49

3.3 Management Strategies 50
3.4 Retrofit System Selection 51
3.5 Traditional Methods for the Retrofitting of Buildings 52
3.5.1 Addition of shear walls 52
3.5.2 Addition of braces in Frames 54
3.5.3 Extension of Existing Columns with additional Shear Walls 54
3.5.4 Columns Retrofitting-The Application of Jackets to Columns 55
CHAPTER 4 59
Modelling of the structure using SAP 2000 59
4.1 SAP2000 Overview 59
4.2 History and Description of the Structure 61
4.3 Modelling of the Structure in SAP2000 72
4.3.1 Material Properties 73
4.3.2 Frame Sections 78
4.3.3 Stiffness- Property Modifiers 82
4.3.4 Loading 84
4.3.5 Diaphragms 98
Chapter 5 101
Modal Response Spectrum Analysis of the Existing Structure 101
5.1 Modal Analysis 101
5.2 Response Spectrum Analysis 105
5.3 Modal Response Spectrum Analysis Results 108
Chapter 6 115
Nonlinear Static (Pushover) Analysis of the Existing Structure 115
6.1 Limitations on Use of the Nonlinear Static Analysis-Higher Mode Participation Check 115
6.2 Secant Stiffness 117
6.3 Plastic Hinges 120
6.4 Nonlinear Static (Pushover) Analysis 125
6.5 Results of Nonlinear Static (Pushover) Analysis 128
6.6 Discussions on the Pushover Analysis Results 145
Chapter 7 147
Nonlinear Time-History Dynamic Analyses of the Existing Structure 147
7.1 Nonlinear Characteristics of the structure elements 147
7.2 Earthquake Ground Motion Time-Histories 147
7.3 Time-History Function Definition in SAP 2000 154
7.4 Load Case Definition in SAP 2000 155
7.5 Results of Nonlinear Time-History Analyses 157
7.6 Discussions on Nonlinear Time History Analyses Results 168
7.7 Conclusions on the Assessment of the Bearing Capacity of the Structure 170
Chapter 8 173

Strengthening of the Structure 173
8.1 Modal Analysis Results 177
8.2 Wall System Check 178
Chapter 9 179
Nonlinear Static (Pushover) Analysis Results of the Retrofitted Structure ... 179
9.1 Discussions on Pushover Analyses Results 195
Chapter 10 197
Nonlinear Time-History Dynamic Analyses Results of the Retrofitted Structure 197
10.1 Discussions on Nonlinear Time-History Analyses Results of the Retrofitted Structure 207
10.2 Conclusions on the Assessment of the Bearing Capacity of the Retrofitted Structure 208
Chapter 11 209
Shear Resistance Checks 209
11.1 Check of Shear Resistance of Shear Walls 209
11.2 Check of Shear Resistance of Existing Members 211
Chapter 12 215
Retrofitted and Non-retrofitted Building Comparison 215
12.1 Modal Analyses Comparison 216
12.2 Pushover Analyses 218
12.2.1 Comparison of the Capacity Curves of the Non-Retrofitted and the Retrofitted Building 218
12.2.2 Hinges Limit States Results 222
12.2.3 Maximum Absolute Displacements Comparison 223
12.2.4 Inter-Storey Drift Ratios Comparison 225
12.3 Nonlinear Time-History Dynamic Analyses 227
12.3.1 Hinges Limit States 227
12.3.2 Comparison of the Maximum Absolute Displacements of the Non-Retrofitted and the Retrofitted Building due to the Earthquake events: L'Aquila, Corinth, Kalamata 228
12.3.3 Comparison of the Inter-storey Drift Ratios of the of the Non-Retrofitted and the Retrofitted Building due to the Earthquake events: L'Aquila, Corinth, Kalamata 229
12.3.4 Comparison of the Maximum Forces along the Column C20 of the Retrofitted and the Non-Retrofitted Building (L'Aquila Earthquake Event) 231
Chapter 13 237
Summary and Conclusions 237
13.1 Summary 237
13.2 Conclusions 238
References 241
Appendices 245

List of Tables:

Table 2.1 Values of the Parameters describing the recommended Type 1 Elastic Response Spectra (EN 1998-1:2004, Greek National Annex)..... 9
Table 2.2 Rehabilitation Objectives (FEMA 356, 2000) (EN 1998-3, 2005).... 21
Table 2.3 Minimum values of reduction factors (Psycharis, 2015)..... 41
Table 4.1 Stiffness of Cracked Sections (KANEPE, 2013)..... 83
Table 4.2 Actions on Structures 84
Table 4.3 Load to the Beams-Ground Floor (hotel) z=4m 87
Table 4.5 Load to the Beams-Ground Floor-Shops (z=5.06m)..... 90
Table 4.6 Load to the Beams – Floor A (z= 9.03m)..... 91
Table 4.7 Load to the beams – Floors B,C,D,E (z= 12.23m, 15.43m, 18.63m, 21.83m respectively)..... 93
Table 4.8 Slab load to the Beams –Approachable Roof (z=25.03m)..... 94
Table 4.9 Slab load to the beams –non approachable roof (z=27.53m) 96
Table 5.1 Modal Analysis Results: Modal Participating Mass Ratios of the first 5 and the last five modes of the structure 102
Table 5.2 Maximum Column Forces per Floor Level for Load Combinations: G+0.3Q+Ex+0.3Ey, G+0.3Q+Ex-0.3Ey, G+0.3Q-Ex+0.3Ey, G+0.3Q+Ex-0.3Ey, G+0.3Q+SRSS (Ex,Ey)..... 109
Table 5.3 Maximum Column Forces per Floor Level for Load Combinations: G+0.3Q+0.3Ex+Ey, G+0.3Q+0.3Ex-Ey, G+0.3Q-0.3Ex+Ey, G+0.3Q-0.3Ex-Ey, G+0.3Q+SRSS (Ex,Ey) 110
Table 5.4 Maximum displacements U1,U2,U3 per floor level due to earthquake along the X axis G+0.3Q+Ex+0.3Ey, G+0.3Q-Ex+0.3Ey, G+0.3Q Ex-0.3Ey, G+0.3Q -Ex-0.3Ey and G+0.3Q+SRSS (Ex, Ey)..... 112
Table 5.5 Maximum displacements U1,U2,U3 per Floor Level due to Earthquake along the Y axis G+0.3Q+0.3Ex+Ey, G+0.3Q-0.3Ex+Ey, G+0.3Q+0.3Ex-Ey, G+0.3Q -0.3Ex-Ey, and G+0.3Q+SRSS (Ex, Ey)..... 113
Table 6.1 Higher mode participation check for earthquake imposed along the X axis. 116
Table 6.2 Higher mode participation check for earthquake imposed along the Y axis 116
Table 6.3 Secant Stiffness of Beams..... 120
Table 6.4 Secant Stiffness of Columns..... 120
Table 6.5 Modal Participating Mass Ratios of the first 5 Modes..... 125
Table 6.6 Hinges Limit State Results at Performance Point (Step 91-92).... 129
Table 6.7 Hinges Limit State Results 131
Table 6.8 Hinges Limit State Results at Performance Point (Step 82)..... 133
Table 6.9 Hinges Limit States at Performance Point (Step 84)..... 135

Table 6.10 Hinges Limit State Results at Performance Point (Step 89)..... 137
Table 6.11 Hinges Limit State Results..... 139
Table 6.12 Hinges Limit State Results at Performance Point (Step 66)..... 140
Table 6.13 Hinges Limit State Results at Performance Point (Step 84)..... 142
Table 8.1 Modal Participating mass ratios of the retrofitted structure using the secant stiffness..... 177
Table 8.2 Modal Participating mass ratios of the retrofitted structure using the stiffness proposed by the table 4.1 of KANEPE..... 178
Table 8.3 Wall System Check..... 178
Table 9.1 Higher Mode Participation Check for Earthquake Imposed along the X Axis..... 179
Table 9.2 Higher Mode Participation Check for Earthquake Imposed along the y Axis..... 180
Table 9.3 Hinges Limit State Results at Performance Point (Step 59)..... 191
Table 9.4 Hinges Limit State Results at Performance Point (Step 57)..... 192
Table 9.5 Hinges Limit State Results at Performance Point (Step 173)..... 188
Table 9.6 Hinges Limit State Results at Performance Point (Step 176)..... 189
Table 9.7 Hinges Limit State Results at Performance Point (Step 12)..... 185
Table 9.8 Hinges Limit State Results at Performance Point (Step 13)..... 186
Table 9.9 Hinges Limit State Results at Performance Point (Step 79)..... 182
Table 9.10 Hinges Limit State Results at Performance Point (Step 84)..... 183
Table 11.1 Check of Shear Resistance of Sheart Wall 7 210
Table 11.2 Results of Checks of Shear Resistance of Shear Walls..... 211
Table 11.3 Shear check of the column C10 (no jacket is applied)..... 213
Table 12.1 Modal Participating Mass Ratios of the Non-Retrofitted Structure using the Stiffness proposed in Table 4.1 of KANEPE..... 216
Table 12.2 Modal Participating Mass Ratios of the Retrofitted Structure using the Stiffness proposed in Table 4.1 of KANEPE 216
..... 216
Table 12.3 Modal Participating Mass Ratios of the Non-Retrofitted Structure using the Secant Stiffness..... 216
Table 12.4 Modal Participating Mass Ratios of the Retrofitted Structure using the Secant Stiffness 216

List of Figures:

Figure 2.1 Shape of the Elastic Response Spectrum (EN 1998-1:2004) 8
Figure 2.2 Capacity Curves (ATC-40, 1996) 16
Figure 2.3 Example of Lateral Loads Distribution (Psycharis, 2015) 17
Figure 2.4 Capacity Curve with Global Strength Degradation Modelled (ATC-40, 1996) 19
Figure 2.5 Definition of Rotation Angle θ (Psycharis, 2015) 24
Figure 2.6 Backbone Curve-Deformation Controlled Actions (Psycharis, 2015) 24
Figure 2.7 Backbone Curve-Force Controlled Actions (Psycharis, 2015) 25
Figure 2.8 Idealized F-δ curve of structural elements (Psycharis, 2015) 25
Figure 2.9 Definition of the performance levels on the capacity curve of the structure (Psycharis, 2015) 30
Figure 2.10 Definition of the Target Displacement of the Equivalent Single-Degree of Freedom System (Psycharis, 2015) 31
Figure 2.11 Example Modal Participation Factors and Modal Mass Coefficients (ATC-40, 1996) 34
Figure 2.12 Response Spectra in Traditional and ADRS formats (ATC-40, 1996) 35
Figure 2.13 Capacity Spectrum superimposed over Response Spectra in Traditional and ADRS formats (ATC-40, 1996) 36
Figure 2.14 Calculation of the first trial performance point (Psycharis, 2015) 37
Figure 2.15 Construction of Bilinear Representation of Capacity Spectrum (Psycharis, 2015) 38
Figure 2.16 Calculation of hysteretic damping according to Chopra cited in Psycharis (2015) 39
Figure 2.17 Construction of elastic response spectrum for $\zeta=\zeta_{eff}$ and calculation of new performance point 42
Figure 3.1 Addition of Shear Wall (KANEPE, 2013) 53
Figure 3.2 Effectiveness of Structural Walls and Bracings (Sugano (1989) cited in Fardis et al (2003)) 53
Figure 3.3 Steel Bracings in Frames (Fardis et al.2003) 54
Figure 3.4 Addition of shear walls in the sides of existing columns (Fardis et al.2003) 55
Figure 3.5 Reinforcement of the concrete jacket (Spyrakos, 2004) 56
Figure 3.6 Confinement using spiral reinforcement (Fardis et al.2003) 58
Figure 3.7 Confinement using steel sheets (Fardis et al.2003) 58
Figure 3.7 Complete FRP wrapping (Belarbi et al.2013) 58
Figure 4.1Typical Floor Plan 62
Figure 4.2 Building Model in SAP2000 63
Figure 4.3 Section A-A' 64

Figure 4.4 Ground Floor-Hotel (4m) 65
Figure 4.5 Ground Floor-Shops (5.06m)..... 66
Figure 4.6 Mezzanine Floor (6.52m) 67
Figure 4.7 Floor A (9.03m) 68
Figure 4.7 Floor B (12.23m)..... 69
Figure 4.8 Floor C (15.43m)..... 70
Figure 4.9 Floors D and E (18.63m and 21.83m respectively) 71
Figure 4.10 Model of the Building in SAP2000 (Extrude View) 72
Figure 4.11 Elevation View of the Building 73
Figure 4.12 Definition of Material's Properties 74
Figure 4.13 Definition of Nonlinear Concrete Properties and Stress-Strain Curve 75
Figure 4.14 Definition of Nonlinear Steel Properties and Stress-Strain Curve 76
Figure 4.15 Definition of Weight per Unit Volume of the Underground Shear Walls..... 78
Figure 4.16 Selection of "Concrete Column" and "Reinforcement to be Checked" options 79
Figure 4.17 Beam Longitudinal Reinforcement at the Bottom of the Section in the Mid-spans and at the Upper Side at the Edge-spans 80
Figure 4.18 a) B20x50 4Φ14 (mid-span) b) B20x50 4Φ14 (edge-span)..... 81
Figure 4.19 a) Column (C11A) b) Strip Foundation (in the perimeter of the foundation)..... 81
Figure 4.20 Stiffness Modification Factors 84
Figure 4.21 Slab Division into Areas for Loading Transfer to the Beams..... 85
Figure 4.22 Distribution of Slab Load to the Beams - Ground Floor and Mezzanine Floor (z= 4m and 6.52m respectively)..... 86
Table 4.4 Load to the beams-mezzanine floor (z=6.52m) 88
Figure 4.23 Distribution of Slab Load to the Beams-Ground Floor-Shops (z=5.06m)..... 89
Figure 4.24 Distribution of Slab Load to the Beams – floor A (z= 9.03m)..... 91
Figure 4.25 Distribution of Slab Load to the Beams – Floors B,C,D,E, Approachable Roof (z= 12.23m, 15.43m, 18.63m, 21.83m, 25.03m respectively)..... 92
Figure 4.26 Distribution of Slab Load to the Beams –Non Approachable Roof (z=27.53m)..... 96
Figure 4.27 Load Patterns Definition..... 97
Figure 4.28 Loads Assignment to the Beams..... 98
Figure 4.29 Use of Diaphragm Constraint to Model a Rigid Floor Slab (CSi, 1995)..... 99
Figure 4.30 Diaphragm Constraints Definition 100
Figure 5.1 Mass Sources Definition..... 102

Figure 5.2 Deformed Shape of Mode 1: T1= 1.627sec. Translational along X axis 103
Figure 5.3 Deformed Shape of Mode 2: T2= 1.405sec. Translational along Y axis 104
Figure 5.4 Deformed Shape of Mode 3: T3= 1.142sec. Rotational about Z axis 105
Figure 5.5 Response Spectrum Function Definition 106
Figure 5.6 Vertical Loads-Case Definition 107
Figure 5.7 Definition of Load Case of Seismic Action Imposed to the Building along the X axis. 107
Figure 5.7 Definition of The combination of the Vertical Loads+Ex+0.3Ey . 108
Figure 5.8 Column Frames Facing the Maximum Values of Magnitudes..... 111
Figure 5.9 Joint that maximum displacement (-0.0891m) along the U2 axis is observed at the approachable roof level (25.03m) 114
Figure 5.10 Joints that maximum displacement (-0.0758m) along the U1 axis is observed at the approachable roof level (25.03m) 114
Figure 6.1 Moment-Curvature diagram of column C11 at the A floor level.. 118
Figure 6.2 Auto Hinge Assignment Data for Concrete Columns..... 121
Figure 6.3 Auto Hinge Assignment Data for Concrete Beams 121
Figure 6.4 Hinge Backbone Curve according to FEMA 356 (2000)..... 122
Figure 6.5 Modelling Parameters and Numerical Acceptance Criteria for Nonlinear Procedures-Reinforced Concrete Beams (FEMA 356, 2000)..... 123
Figure 6.6 Modelling Parameters and Numerical Acceptance Criteria for Nonlinear Procedures-Reinforced Concrete Columns (FEMA 356, 2000)..... 124
Figure 6.7 Definition of the Load Case of a Nonlinear Static Analysis. Uniform Distribution of Lateral Loads along the +Y axis. 126
Figure 6.8 Load Application Control for Nonlinear Static Analysis..... 127
Figure 6.9 The results are saved in multiple states. 127
Figure 6.10 a) Pushover Curve (Uniform Distribution of Lateral Loads along –X Axis) b) ATC-40 Capacity Spectrum-ADRS (Uniform Distribution of Lateral Loads along –X Axis)..... 128
Figure 6.11 Deformed Shape of the Structure at Performance Point- Step 91-92 (Uniform Distribution of Lateral Loads along –X Axis) 129
Figure 6.12 a) Pushover Curve (Uniform Distribution of Lateral Loads along +X Axis) b) ATC-40 Capacity Spectrum-ADRS (Uniform Distribution of Lateral Loads along +X Axis) 130
Figure 6.13 Deformed Shape of the Structure at Maximum Step of the Analysis (Uniform Distribution of Lateral Loads along +X Axis)..... 131
Figure 6.14 a) Pushover Curve (Uniform Distribution of Lateral Loads along +Y Axis) b) ATC-40 Capacity Spectrum-ADRS (Uniform Distribution of Lateral Loads along +Y Axis) 132

Figure 6.15 Deformed Shape of the Structure at Performance Point-Step 82 (Uniform Distribution of Lateral Loads along +Y Axis) 133
Figure 6.16 a) Pushover Curve (Uniform Distribution of Lateral Loads along –Y Axis) b) ATC-40 Capacity Spectrum-ADRS (Uniform Distribution of Lateral Loads along -Y Axis)..... 134
Figure 6.17 Deformed Shape of the Structure at Performance Point-Step 84 (Uniform Distribution of Lateral Loads along -Y Axis)..... 135
Figure 6.18 a) Pushover Curve (Modal Distribution of Lateral Loads along +X Axis) b) ATC-40 Capacity Spectrum-ADRS (Modal Distribution of Lateral Loads along +X Axis)..... 136
Figure 6.19 Deformed Shape of the Structure at Performance Point-Step 89 (Modal Distribution of Lateral Loads along +X Axis) 137
Figure 6.20 a) Pushover Curve (Modal Distribution of Lateral Loads along -X Axis) b) ATC-40 Capacity Spectrum-ADRS (Modal Distribution of Lateral Loads along -X Axis) 138
Figure 6.21 Deformed Shape of the Structure at Maximum Step of the Analysis (Modal Distribution of Lateral Loads along -X Axis)..... 138
Figure 6.22 a) Pushover Curve (Modal Distribution of Lateral Loads along +Y Axis) b) ATC-40 Capacity Spectrum-ADRS (Modal Distribution of Lateral Loads along +Y Axis)..... 139
Figure 6.23 Deformed Shape of the Structure at Performance Point-Step 66 (Modal Distribution of Lateral Loads along +Y Axis) 140
Figure 6.24 a) Pushover Curve (Modal Distribution of Lateral Loads along -Y Axis) b) ATC-40 Capacity Spectrum-ADRS (Modal Distribution of Lateral Loads along -Y Axis) 141
Figure 6.25 Deformed Shape of the Structure at Performance Point-Step 84 (Modal Distribution of Lateral Loads along -Y Axis)..... 141
Figure 6.26 Hinge Results-Backbone Curve..... 142
Figure 6.27 Maximum Displacement per Height along X axis for Uniform and Modal Distribution of Lateral Loads 143
Figure 6.28 Maximum Displacement per Height along Y axis for Uniform and Modal Distribution of Lateral Loads 143
Figure 6.29 Inter-story Drift Ratios along X Axis for Uniform and Modal Distribution of Lateral Loads 144
Figure 6.30 Inter-story Drift Ratios along Y Axis for Uniform and Modal Distribution of Lateral Loads 144
Figure 7.1 Non Scaled Acceleration Time History of Corinth Earthquake (longitudinal axis) 148
Figure 7.2 Scaled Acceleration Time History of Corinth Earthquake (longitudinal axis) 149
Figure 7.3 Scaled and Non-scaled Acceleration Response Spectrum of Corinth Earthquake (longitudinal axis)..... 149

Figure 7.4 Non Scaled Acceleration Time History of Corinth Earthquake (transverse axis) 149
Figure 7.5 Scaled Acceleration Time History of Corinth Earthquake (transverse axis) 150
Figure 7.6 Scaled and Non-scaled Acceleration Response Spectrum of Corinth Earthquake (transverse axis) 150
Figure 7.7 Non Scaled Acceleration Time History of Kalamata Earthquake (longitudinal axis) 150
Figure 7.8 Scaled Acceleration Time History of Kalamata Earthquake (longitudinal axis) 151
Figure 7.9 Scaled and Non-scaled Acceleration Response Spectrum of Kalamata Earthquake (longitudinal axis) 151
Figure 7.10 Non Scaled Acceleration Time History of Kalamata Earthquake (transverse axis) 151
Figure 7.11 Scaled Acceleration Time History of Kalamata Earthquake (transverse axis) 152
Figure 7.12 Scaled and Non-scaled Acceleration Response Spectrum of Kalamata Earthquake (transverse axis) 152
Figure 7.13 Non Scaled Acceleration Time History of L'Aquila Earthquake (longitudinal axis) 152
Figure 7.14 Scaled Acceleration Time History of L'Aquila Earthquake (longitudinal axis) 153
Figure 7.15 Scaled and Non-scaled Acceleration Response Spectrum of L'Aquila Earthquake (longitudinal axis) 153
Figure 7.16 Non Scaled Acceleration Time History of L'Aquila Earthquake (transverse axis) 153
Figure 7.17 Scaled Acceleration Time History of L'Aquila Earthquake (transverse axis) 154
Figure 7.18 Scaled and Non-scaled Acceleration Response Spectrum of L'Aquila Earthquake (transverse axis) 154
Figure 7.19 Time History Function Definition 155
Figure 7.20 Load Case Definition: L'Aquila. Load Combination: G+0.3Q+0.3Ex+Ey 156
Figure 7.21 Mass and Stiffness Proportional Damping Coefficients 157
Figure 7.22 Earthquake Event: L'Aquila. Most Unfavourable Load Combination: G+0.3Q+Ex+0.3Ey 158
Figure 7.23 Displacement Time-History of the Center of Mass (joint 130) of the Approachable Roof due to L'Aquila Earthquake Event 159
Figure 7.24 Hysteretic Loop of base shear force along X- Displacement along X of joint 130–(center of mass of the approachable roof) - L'Aquila 159
Figure 7.25 Earthquake Event: Corinth. Most Unfavourable Load Combination: G+0.3Q-Ex-0.3Ey 160

Figure 7.26 Displacement Time-History of the Center of Mass (joint 130) of the Approachable Roof due to Corinth Earthquake Event 161
Figure 7.27 Hysteretic Loop of base shear force along X- Displacement along X of joint 130–(center of mass of the approachable roof)- Corinth 161
Figure 7.28 Earthquake Event: Kalamata. Most Unfavourable Load Combination: G+0.3Q-Ex-0.3Ey 162
Figure 7.29 Displacement Time-History of the Center of Mass (joint 130) of the Approachable Roof due to Kalamata Earthquake Event 163
Figure 7.30 Hysteretic Loop of base shear force along X- Displacement along X of joint 130–(center of mass of the approachable roof)- Kalamata 163
Figure 7.31 Maximum Absolute Displacement per Floor Level for Earthquakes imposed along the X axis 164
Figure 7.32 Maximum Absolute Displacement per Floor Level for Earthquakes imposed along the Y axis 164
Figure 7.33 Inter-story Drift Ratios along X axis 165
Figure 7.34 Inter-story Drift Ratios along Y axis 165
Figure 7.35 Time-History of Bending Moments of Column C20 along axis X (M3-3) 166
Figure 7.36 Time-History of Shear Forces of Column C20 along axis X (V2-2) 166
Figure 7.37 Time-History of Bending Moments of Column C20 along axis Y (M2-2) 167
Figure 7.38 Time-History of Shear Forces of Column C20 along axis Y (V3-3) 167
Figure 7.39 Deformed shape and hinges results of the Columns C19,C20,C21 due to the L'Aquila earthquake event (Load Combination: G+0.3Q+Ex+0.3Ey) 170
Figure 8.1 Structural Interventions- Addition of Shear walls and jackets 174
Figure 8.2 Section of Shear Wall 5 (section designer) 175
Figure 8.3 Jacket of Column C5 at the floor level E. Jacket Width:10cm, Reinforcing Steel: 16Φ16+ 4Φ20 Bar Cover: 4cm 176
Figure 9.1 a) Pushover Curve (Uniform Distribution of Lateral Loads along +X Axis) b) ATC-40 Capacity Spectrum-ADRS (Uniform Distribution of Lateral Loads along +X Axis) 190
Figure 9.2 Deformed Shape of the Structure at Performance Point-Step 59 (Uniform Distribution of Lateral Loads along +X Axis) 190
Figure 9.3 a) Pushover Curve (Uniform Distribution of Lateral Loads along -X Axis) b) ATC-40 Capacity Spectrum-ADRS (Uniform Distribution of Lateral Loads along -X Axis) 191
Figure 9.4 Deformed Shape of the Structure at Performance Point-Step 57 (Uniform Distribution of Lateral Loads along -X Axis) 192

Figure 9.5 a) Pushover Curve (Uniform Distribution of Lateral Loads along +Y Axis) b) ATC-40 Capacity Spectrum-ADRS (Uniform Distribution of Lateral Loads along +Y Axis) 187
Figure 9.6 Deformed Shape of the Structure at Performance Point-Step 173 (Uniform Distribution of Lateral Loads along +Y Axis) 187
Figure 9.7 a) Pushover Curve (Uniform Distribution of Lateral Loads along -Y Axis) b) ATC-40 Capacity Spectrum-ADRS (Uniform Distribution of Lateral Loads along -Y Axis)..... 188
Figure 9.8 Deformed Shape of the Structure at Performance Point-Step 176 (Uniform Distribution of Lateral Loads along -Y Axis)..... 189
Figure 9.9 a) Pushover Curve (Modal Distribution of Lateral Loads along +X Axis) b) ATC-40 Capacity Spectrum-ADRS (Modal Distribution of Lateral Loads along +X Axis) 184
Figure 9.10 Deformed Shape of the Structure at Performance Point-Step 12 (Modal Distribution of Lateral Loads along +X Axis) 184
Figure 9.11 a) Pushover Curve (Modal Distribution of Lateral Loads along -X Axis) b) ATC-40 Capacity Spectrum-ADRS (Modal Distribution of Lateral Loads along -X Axis) 185
Figure 9.12 Deformed Shape of the Structure at Performance Point-Step 13 (Modal Distribution of Lateral Loads along -X Axis)..... 186
Figure 9.13 a) Pushover Curve (Modal Distribution of Lateral Loads along +Y Axis) b) ATC-40 Capacity Spectrum-ADRS (Modal Distribution of Lateral Loads along +Y Axis) 181
Figure 9.14 Deformed Shape of the Structure at Performance Point-Step 79 (Modal Distribution of Lateral Loads along +Y Axis) 181
Figure 9.15 a) Pushover Curve (Modal Distribution of Lateral Loads along -Y Axis) b) ATC-40 Capacity Spectrum-ADRS (Modal Distribution of Lateral Loads along -Y Axis) 182
Figure 9.16 Deformed Shape of the Structure at Performance Point-Step 84 (Modal Distribution of Lateral Loads along -Y Axis)..... 183
Figure 9.17 Maximum Displacement per Height along X axis for Uniform and Modal Distribution of Lateral Loads 193
Figure 9.18 Maximum Displacement per Height along Y axis for Uniform and Modal Distribution of Lateral Loads 193
Figure 9.19 Inter-story Drift Ratios along X Axis for Uniform and Modal Distribution of Lateral Loads 194
Figure 9.20 Inter-story Drift Ratios along Y Axis for Uniform and Modal Distribution of Lateral Loads 194
Figure 10.1 Earthquake Event: L'Aquila, Load Combination: G+0.3Q+Ex+0.3Ey 197
Figure 10.2 Displacement Time-History of the Center of Mass (joint 130) of the Approachable Roof due to L'Aquila Earthquake Event 198

Figure 10.3 Hysteretic Loop of base shear force along X- Displacement along X of joint 130–(center of mass of the approachable roof)- L'Aquila..... 198
Figure 10.4 Earthquake Event: Corinth, Load Combination: G+0.3Q-Ex-0.3Ey 199
Figure 10.5 Displacement Time-History of the Center of Mass (joint 130) of the Approachable Roof due to Corinth Earthquake Event..... 199
Figure 10.6 Hysteretic Loop of base shear force along X- Displacement along X of joint 130–(center of mass of the approachable roof)- Corinth 200
Figure 10.7 Earthquake Event: Kalamata, Load Combination: G+0.3Q-Ex-0.3Ey 201
Figure 10.8 Displacement Time-History of the Center of Mass (joint 130) of the Approachable Roof due to Kalamata Earthquake Event..... 201
Figure 10.9 Hysteretic Loop of base shear force along X- Displacement along X of joint 130–(center of mass of the approachable roof)- Kalamata 202
Figure 10.10 Maximum Absolute Displacement per Floor Level for Earthquakes imposed along the X axis..... 203
Figure 10.11 Maximum Absolute Displacement per Floor Level for Earthquakes imposed along the Y axis..... 203
Figure 10.12 Inter-story Drift Ratios along X axis 204
Figure 10.13 Inter-story Drift Ratios along Y axis 204
Figure 10.14 Time-History of Bending Moments of Column C20 along axis X (M3-3)..... 205
Figure 10.15 Time-History of Shear Forces of Column C20 along axis X (V2-2) 205
Figure 10.16 Time-History of Bending Moments of Column C20 along axis Y (M2-2)..... 206
Figure 10.17 Time-History of Shear Forces of Column C20 along axis Y (V3-3) 206
Figure 12.1 Pushover Analysis-Uniform Distribution of Lateral Loads along +X Axis..... 218
Figure 12.2 Pushover Analysis-Uniform Distribution of Lateral Loads along -X Axis..... 218
Figure 12.3 Pushover Analysis-Uniform Distribution of Lateral Loads along +Y Axis..... 219
Figure 12.4 Pushover Analysis-Uniform Distribution of Lateral Loads along -Y Axis..... 219
Figure 12.5 Pushover Analysis-Modal Distribution of Lateral Loads along +X Axis..... 220
Figure 12.6 Pushover Analysis-Modal Distribution of Lateral Loads along -X Axis..... 220
Figure 12.7 Pushover Analysis-Modal Distribution of Lateral Loads along +Y Axis..... 221

Figure 12.8 Pushover Analysis-Modal Distribution of Lateral Loads along -Y Axis 221
Figure 12.9 Maximum Absolute Displacements along X axis for Uniform and Modal Distribution of Lateral Loads for the Non-Retrofitted and the Retrofitted Building 224
Figure 12.10 Maximum Absolute Displacements along Y axis for Uniform and Modal Distribution of Lateral Loads for the Non-Retrofitted and the Retrofitted Building 224
Figure 12.11 Inter-Storey Drift Ratios along X axis for Uniform and Modal Distribution of Lateral Loads for the Non-Retrofitted and the Retrofitted Building 226
Figure 12.12 Inter-Storey Drift Ratios along Y axis for Uniform and Modal Distribution of Lateral Loads for the Non-Retrofitted and the Retrofitted Building 226
Figure 12.13 Maximum Absolute Displacements along X axis of the Non-Retrofitted and the Retrofitted Building due to the Earthquake events: L'Aquila, Corinth, Kalamata 228
Figure 12.14 Maximum Absolute Displacements along Y axis of the Non-Retrofitted and the Retrofitted Building due to the Earthquake events: L'Aquila, Corinth, Kalamata 229
Figure 12.15 Inter-Storey Drift Ratios along X axis for the Non-Retrofitted and the Retrofitted Building due to the Earthquake events: L'Aquila, Corinth, Kalamata 230
Figure 12.16 Inter-Storey Drift Ratios along Y axis for the Non-Retrofitted and the Retrofitted Building due to the Earthquake events: L'Aquila, Corinth, Kalamata 230
Figure 12.17 Envelope of the Bending Moments of Column C20 along Axis X (M3-3) per Floor Level of the Non-Retrofitted (blue) and the Retrofitted (red) Building 232
Figure 12.18 Envelope of the Shear Forces of Column C20 along Axis X (V2-2) per Floor Level of the Non-Retrofitted (blue) and the Retrofitted (red) Building 233
Figure 12.19 Envelope of the Bending Moments of Column C20 along Axis Y (M2-2) per Floor Level of the Non-Retrofitted (blue) and the Retrofitted (red) Building 234
Figure 12.20 Envelope of the Shear Forces of Column C20 along Axis Y (V3-3) per Floor Level of the Non-Retrofitted (blue) and the Retrofitted (red) Building 235

Abbreviations

ADRS Acceleration-Displacement Response Spectra

ATC-40 Applied Technology Council

CF Confidence Factor

CQC Complete Quadratic Combination

FRP Fibre Reinforced Polymer

KL Knowledge Level

SRSS Square Root of the Sum of the Squares

CHAPTER 1

Introduction

1.1 Motivation

The majority of buildings constructed in Greece until the mid 80's are reinforced concrete buildings. A significant portion of those buildings have faced light or severe damages due to the earthquakes occurred during their lifetime (Spyrakos, 2004). The Design Code for Earthquake Resistant structures was introduced in Greece in 1959. However the buildings that were designed under its provisions, especially the multi-storey, do not have adequate resistance to earthquakes. Their members do not have adequate, ductility, most buildings do not have a lateral force resisting system in both directions and in many cases architectonic factors define the positions of the beams and columns, so the structural system do have many indirect supports (beam to beam) and do not have frames. Those structural systems may be adequate to transfer the vertical loads; however their resistance to seismic loads is inadequate. As a result, the buildings designed under the provision of the Design Code for Earthquake Resistant structures of 1959 or earlier, are extremely vulnerable to earthquakes and they may be dangerous for human or economic losses (Fardis et al. 2003).

Thus the study of the assessment of the bearing capacity of buildings and their strengthening is a very interesting subject and will be in high demand in the next few years in Greece.

1.2 Research Objective

The objective of this research is to study the methods of assessment of the bearing capacity of structures, the nonlinear static and the non linear dynamic analyses using performance based design. In addition its objective is to study the methods of seismic retrofitting and to apply the appropriate methods in order to rehabilitate the structure under examination.

1.3 Research Approach

In this paper the bearing capacity of a multi-storey reinforced concrete hotel is examined. Information about the assessment of the bearing capacity, the seismic actions, the methods of analyses, the performance based design and the retrofit strategies and systems is provided. After background information is given, the modelling of the structure in SAP2000 software is described and all the values that are used as inputs are set and explained. Furthermore, three types of analyses are performed. They are the modal response spectrum analyses, the nonlinear static (pushover) analysis and the non linear dynamic time-history analysis. The results of the analyses are discussed and the building is rehabilitated. The nonlinear static and the nonlinear dynamic analyses are performed for the retrofitted building.

1.4 Report Outline

The first chapter is an introduction to this study by explaining the motivation, the objectives and the research approach.

In the second chapter background information about the assessment of the bearing capacity of structures, the methods of analyses and the performance based design is provided.

In the third chapter information for the retrofit strategies and systems are included.

Chapter four consists of the modelling procedure in SAP2000. The history and description of the structure are explained and the material properties, the frame sections, the stiffness of the structure, the loads and the diaphragms are defined.

In the fifth chapter the modal response spectrum analysis is explained and its results are discussed.

In the sixth chapter the non linear static (pushover) analysis of the existing structure is explained and its results are provided and discussed.

Chapter seven consists of information about the non linear time-history analysis of the existing structure. In addition the acceleration time-histories are provided and the results are discussed.

In the chapter eight the interventions on the structure are explained.

In the ninth chapter the non linear static analysis of the retrofitted structure is explained and its results are discussed.

In the tenth chapter the non linear dynamic time-history analysis of the retrofitted structure is explained and its results are discussed.

Chapter eleven consists of the shear resistance checks.

In the chapter twelve the results of the analyses of the non retrofitted and retrofitted structure are compared and discussed.

In the chapter thirteen the summary and the concluding remarks are included.

Chapter 2

Assessment of the Bearing Capacity of Structures-Background Concepts

2.1 Required Information for the Assessment of the Structure

The assessment of existing structures follows the procedure:

- Collection of data and history of the structure
- Analyses
- Verification of limit states (KANEPE, 2013)

The goal of the assessment is to estimate the bearing capacity of the structure, and to testify whether the requirements provided by the standards are met (KANEPE, 2013).

A damaged structure should be assessed by a different procedure than non-damaged structures. The assessment of a non-damaged structure determines the rehabilitation need, in relation to the target performance. In case the structure is already damaged, the first step is the assessment of the structure at its current condition, which leads to the decision to repair it or not. The second step is the assessment of the repaired structure, which helps to decide whether the rehabilitation is necessary. (KANEPE, 2013)

2.1.1 General Information and History of the Building

In assessing the earthquake resistance of existing structures, the input data shall be collected from a variety of sources which include:

- Available documentation of the building
- Relevant generic data sources (e.g. contemporary codes and standards)
- Field investigations
- In-situ and/or laboratory measurements and tests (EN 1998-3, 2005).

2.1.2 Required Input Data

The required information is:

- The structural system and its compliance with the regularity criteria in EN 1998-1:2004, 4.2.3 should be identified. The information should be collected either from the original design drawings, or from on site investigation. Information on possible structural changes since construction should also be collected.
- The type of the building foundations should be identified.
- The ground condition as categorized in EN 1998-1:2004, 3.1 should be identified.
- Information about the mechanical properties and the condition of constituent materials, such as the overall dimensions and cross-sectional properties of the building elements should be collected.
- Information about identifiable material defects and inadequate detailing.
- Information on the seismic criteria used for the initial design. The value of the force reduction factor (q-factor) should also be known, if applicable.
- The present use of the building (with identification of its importance class, as described in EN 1998-1:2004, 4.2.5) should be described.
- Re-assessment of the imposed actions taking into account the use of the building.
- Information about any present or previous damage, if any, including earlier repair measures. (EN 1998-3, 2005)

2.1.3 Materials

Data for the current condition of the concrete and the reinforcement steel should be gathered. The necessary mechanical properties for the concrete are its compression strength (fc) and the modulus of elasticity (E), while for the reinforcement steel, they are the yield strength f_y, its tensile strength (f_t) and its stain at maximum load (ε_u) (KANEPE, 2013).

2.1.4 Knowledge Level

The engineer is able to decide the appropriate type of analysis and the appropriate confidence factor values, once the knowledge level is known.

KL1: Limited knowledge

KL2: Normal knowledge

KL3: Full knowledge

The factors that determine the appropriate knowledge level are:

- Geometry: the geometry of the structural system, and of non- structural elements (e.g. masonry infill panels) that may affect the structural response.
- Details: the amount and detailing of the reinforcement in reinforced concrete and the connection of floor diaphragms to lateral resisting structure.
- Materials: the mechanical properties of the constituent materials.

2.1.5 Confidence Factors

The mean values of the material properties that are obtained from in-situ tests and from additional sources of information and are used in the calculation of the capacity, when capacity is to be compared with the demand for safety verification, shall be divided by the confidence factor, CF, for the appropriate knowledge level.

The mean values of the properties of the materials that are obtained from in-situ tests and from additional sources of information shall be multiplied by the confidence factor, CF, for the appropriate knowledge level, when the determination of the properties to be used in the calculation of the force capacity (strength) of ductile components, delivering action effects to brittle components/ mechanisms, is requested (EN 1998-3, 2005).

The proposed values are: CF_{KL1}=1.35, CF_{KL2}=1.20, CF_{KL3}=1.00

2.2 Seismic Action for the Assessment of the Structure

The aim of the assessment of the structure is to check whether an existing undamaged or damaged building satisfies the required limit state appropriate to the seismic action under consideration (EN 1998-3, 2005).

2.2.1 Seismic Action

The earthquake motion at a given point on the surface is represented by an elastic ground acceleration response spectrum, which is called an "elastic response spectrum".

Two orthogonal components which are assumed as being independent describe the horizontal seismic action. The two components are described by the same response spectrum (EN 1998-1, 2004).

In addition, time-history representation of the earthquake motion may be used (EN 1998-1, 2004).

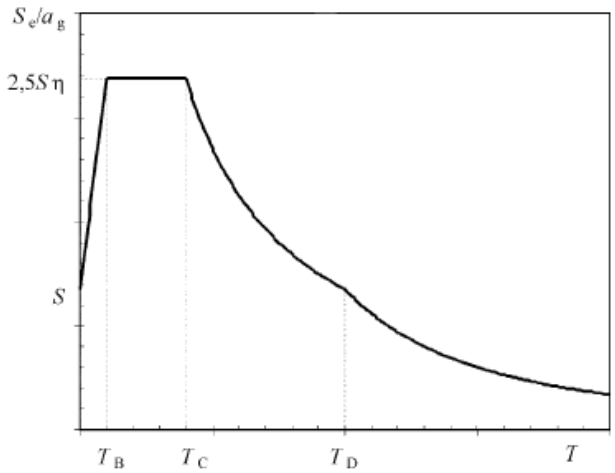

Figure 2.1 Shape of the Elastic Response Spectrum (EN 1998-1:2004)

The values of periods T_B, T_C, T_D and of the soil factor S, which describe the shape of the elastic response spectrum depend upon the ground type.

Table 2.1 Values of the Parameters describing the recommended Type 1 Elastic Response Spectra (EN 1998-1:2004, Greek National Annex)

Ground Type	S	T_B (s)	T_C (s)	T_D (s)
A	1	0.15	0.4	2.5
B	1.2	0.15	0.5	2.5
C	1.15	0.2	0.6	2.5
D	1.35	0.2	0.8	2.5
E	1.4	0.15	0.5	2.5

2.2.1.1 Design Spectrum for Elastic Analysis

The design of structures to resist seismic forces, lower than those that correspond to a linear elastic response is permitted, due to the capacity of structures to resist seismic actions in the non-linear range.

The reduction is achieved through the introduction of the behaviour factor q. As a result, explicit inelastic structural analysis in design is avoided. The ability of the structure to dissipate energy, though the ductile behaviour of its elements, and/or other mechanisms, is taken into account by performing an elastic analysis based on a reduced (by the behaviour factor q) response spectrum, with respect to the elastic one. Thus it is called a "design spectrum".

The design spectrum $S_d(T)$, for the horizontal components of the seismic actions, is defined as follows:

$$0 \le T \le T_B : S_d(T) = a_g \cdot S \cdot \left[\frac{2}{3} + \frac{T}{T_B} \cdot \left(\frac{2,5}{q} - \frac{2}{3} \right) \right]$$

$$T_B \le T \le T_C : S_d(T) = a_g \cdot S \cdot \frac{2,5}{q}$$

$$T_C \le T \le T_D : S_d(T) \begin{cases} = a_g \cdot S \cdot \frac{2,5}{q} \cdot \left[\frac{T_C}{T} \right] \\ \ge \beta \cdot a_g \end{cases} \qquad \text{(1-4) (EN 1998-1, 2004)}$$

$$T_D \le T : S_d(T) \begin{cases} = a_g \cdot S \cdot \frac{2,5}{q} \cdot \left[\frac{T_C \cdot T_D}{T^2} \right] \\ \ge \beta \cdot a_g \end{cases}$$

Where $S_d(T)$ is the design spectrum;

T is the vibration period of a linear single-degree of freedom system;

a_g is the design ground acceleration on type A ($a_g = \gamma_I \cdot a_{gR}$);

T_B is the lower limit of the period of the constant spectral acceleration branch;

T_C is the upper limit of the period of the constant spectral acceleration branch;

T_D is the value defining the beginning of the constant displacement response range of the spectrum;

S is the soil factor;

η is the damping correction factor with a reference values of η=1 for 5% viscous damping; $\eta = \sqrt{10/(5+\xi)} \geq 0,55$ where ξ is the viscous damping ratio of the structure, expressed as a percentage. (EN 1998-1, 2004)

q is the behaviour factor;

β is the lower bound factor for the horizontal design spectrum; β=0.2 (EN 1998-1:2004, Greek National Annex).

2.2.1.2 Time-History Representation

The motion due to an earthquake event can also be presented in terms of ground acceleration time-histories and related quantities (velocity and displacement) (CSi, 1995).

The samples should be carefully chosen to correspond to the seismogenetic features of the sources and the soil conditions of the site. The accelerograms may be recorded or generated through a physical simulation of source and travel path mechanisms. More information about the time-history analysis is given in section 2.3.3 (EN 1998-1, 2004).

2.2.2 Combination of the Effects of the Components of the Seismic Action

The horizontal components of the seismic action are taken as acting simultaneously. The square root of the sum of the squared values of the action effect due to each horizontal component can be used for the estimation of the maximum value of each action effect on the structure due to the two horizontal components of the seismic action.

Alternatively the effects of the horizontal components of the seismic action may be computed using the following combinations:

- E_{Edx} '+' 0.30 E_{Edy} (5)
- 0.30 E_{Edx} '+' E_{Edy} (6) (EN 1998-1, 2004)

where '+' implies "to be combined with" and

E_{Edx} are the action effects due to the application of the seismic action along the chosen horizontal axis of the structure.

E_{Edy} are the action effects due to the application of the same seismic action along the orthogonal horizontal axis y of the structure (EN 1998-1, 2004).

2.3 Methods of Analysis

The effects of the seismic action, which are combined with the effects of the other permanent and variable loads in accordance with the seismic load combination, may be evaluated using one of the following methods:

- Lateral force analysis (linear)
- Modal response spectrum analysis (linear)
- Nonlinear static (pushover) analysis
- Nonlinear time-history dynamic analysis
- q-factor approach

Linear static procedure (lateral force analysis) is appropriate when higher modes effects are not significant, which is generally true for short, regular buildings.

Dynamic procedures are required for tall buildings, or buildings with torsional irregularities, or non-orthogonal systems. (FEMA 356, 2000)

The modal response spectrum analysis, the nonlinear static (pushover) analysis and the nonlinear time-history dynamic analysis are explained below.

2.3.1 Modal Response Spectrum Analysis

According to the modal response spectrum analysis the response of all modes of vibration which contribute significantly to the global response of the structure, should be taken into account. This claim is satisfied if either of the following can be demonstrated:

- the sum of the effective modal masses for the modes taken into account amounts at least 90% of the total mass of the structure;
- all modes with effective modal mass greater than 5% of the total mass are taken into account (EN 1998-1, 2004).

The above conditions should be met for each relevant direction, in case a spatial model is used (EN 1998-1, 2004). The sum of the effective modal masses (for all modes and a given direction) is equal to the mass of the structure (CSi, 1995).

According to EN 1998-1, 2004 the response in two vibration modes i and j (including translational and torsional modes) may be taken as independent of each other, if the following criterion is met:

$T_j \leq 0.9\ T_i$ where T_j and T_i are periods (with $T_j \leq T_i$)

In case the above condition is met, so all relevant mode responses are considered independent of each other, the maximum value E_e of a seismic action effect can be estimated by the use of the square root of the sum of the squares method (SRSS):

$$E_e = \sqrt{\Sigma E_{Ei}^2} \qquad (7) \text{ (EN 1998-1, 2004)}$$

where:

E_E is the seismic action effect under consideration (force, displacement, etc.);

E_{Ei} is the value of the seismic action effect due to the vibration mode i.

In case the modal responses are not independent of each other, more accurate methods such as the "Complete Quadratic Combination" (CQC), should be used for the combination of the modal maxima (EN 1998-1, 2004).

Modal Analysis is used for the determination of the vibration modes of the structure. The modes are useful to understand the behaviour of the structure. In addition, they can be used as the basis for modal superposition in response spectrum analysis. The Eigenvector Analysis is the type of modal analysis that determines the undamped free-vibration mode shapes and frequencies of the structure. An excellent insight into the behaviour of the structure is provided by these natural modes (CSi, 1995).

Eigenvector analysis involves the solution of the generalized eigenvalue problem:

$$[K - \Omega^2 M]\, \Phi = 0 \qquad (8) \quad \text{(CSi, 1995)}$$

Where K is the stiffness matrix, M is the diagonal mass matrix, Ω^2 is the diagonal matrix of the eigenvalues and Φ is the matrix of the corresponding eigenvectors (mode shapes).

A natural vibration mode is determined by each eigenvalue-eigenvector pair. The eigenvalue is the square of the circular frequency ω for that mode.

A mass degree of freedom is any active degree of freedom that possesses translational mass or rotational mass moment of inertia (CSi, 1995).

The Response Spectrum Analysis is a statistical type of analysis. Its aim is to determine the likely response of the structure to seismic loading.

According to CSi (1995) the dynamic equilibrium equations that are associated with the response of the structure to ground motion are given by:

$$K\,u(t) + C\,\dot{u}(t) + M\,\ddot{u}\,(t) = m_x\,\ddot{u}_{gx}\,(t) + m_y\,\ddot{u}_{gy}\,(t) + m_z\,\ddot{u}_{gz}(t) \qquad (9)$$

Where K is the stiffness matrix, C is the proportional damping matrix and M is the diagonal mass matrix. u, $\dot{u}$, $\ddot{u}$ are the relative displacements, velocities and accelerations with respect to the ground respectively, m_x , m_y m_z are the unit acceleration loads and $\ddot{u}_{gx}$, $\ddot{u}_{gy}$, $\ddot{u}_{gz}$ are the components of uniform ground acceleration.

Through the response spectrum analysis the likely maximum response to these equations is calculated. The information about the time that this extreme value occurs during the seismic loading is not available. To this it is necessary that the earthquake ground acceleration in each direction is given as a digitalized response-spectrum curve of pseudo-spectral acceleration response versus period of the structure.

The response quantities that are estimated include displacements, forces and stresses. A single, positive result is produced for each response quantity, even though accelerations may be specified in three directions. A statistical measure of the likely maximum magnitude for a specific response quantity is represented by each computed result. The actual response can be expected to vary within a range from this positive result to its negative (CSi, 1995).

Response spectrum analysis is performed using mode superposition method. A modal load case that computes the modes should be defined, and then that modal case should be referred in the definition of the response spectrum (Wilson and Button, (1982) cited in CSi (1995)).

2.3.2 Nonlinear Static (Pushover) Analysis

The main objective of the nonlinear static analysis is the estimation of inelastic deformation that is caused to the elements of the structure, under the imposed seismic action. A mathematical model of the structure, which incorporates the nonlinear load-deformation characteristics of its individual components and elements, should be subjected to monotonically increasing lateral loads, representing inertia forces in an earthquake, until a target displacement is

succeeded. The calculated displacements and internal forces should meet the acceptance criteria of the target performance level (FEMA 356, 2000).

The maximum displacement that is likely to be experienced during the design earthquake is represented by the target displacement. The calculated internal forces are reasonable approximations of the real ones expected during the design earthquake, due to the direct account for effects of material inelastic response by the mathematical model.

The node where the structure displacement is calculated, due to the imposed lateral loads, is called the "control node". It should be located at the centre of mass of the roof of the building. If a penthouse exists, the level of the control node should be at the level of the floor of the penthouse (FEMA 356, 2000).

The relation between the lateral displacement of the control node and the base shear force should be established for control node displacements ranging from zero to 150% of the target displacement, unless the building is earlier collapsed (KANEPE, 2013).

The gravity loads should be included in the mathematical model and combined with the lateral loads. The lateral loads should be imposed not only in positive, but also in negative direction. For the design, the maximum seismic effects shall be used.

The load-deformation response of each component along its length should be represented by a discretized analysis model, so as the identification of locations of inelastic actions is able.

All the lateral-force-resisting elements, either primary or secondary, should be included in the model.

It is important that the force-displacement behaviour of all components is included in the model, using full backbone curves that include strength degradation and residual strength, if any (FEMA 356, 2000).

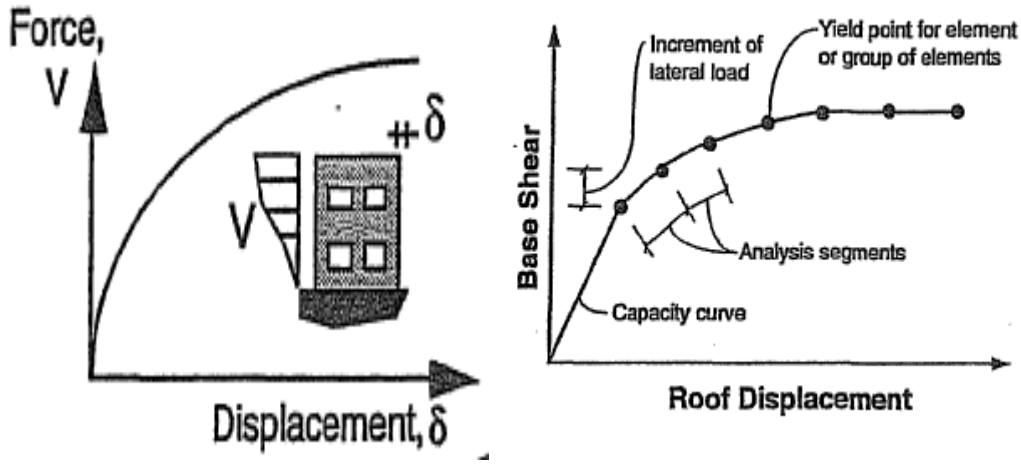

Figure 2.2 Capacity Curves (ATC-40, 1996)

2.3.2.1 Limitations on Use of the Nonlinear Static Analysis

The non linear static analysis is permitted for structures that higher mode effects are not significant.

To determine if higher modes are significant, a modal response spectrum analysis shall be performed for the structure using sufficient modes to capture 90% of the mass participation. In addition another response spectrum analysis should be performed, considering only the first mode participation. Higher mode effects shall be considered significant if the shear in any story resulting from the modal response spectrum analysis considering modes required to obtain 90% of mass participation exceeds 130% of the corresponding story shear considering only the first mode response.

If higher mode effects are significant, the non linear static procedure shall be permitted if a linear dynamic procedure (e.g. modal response spectrum analysis) is also performed to supplement the nonlinear static analysis (KANEPE, 2013).

2.3.2.2 Lateral Load Distribution

Lateral loads shall be applied in the plane of each floor diaphragm, in proportion to the distribution of inertia forces. The distribution of lateral inertia forces determines relative magnitudes of shears, moments, and deformations within the structure. During an earthquake, the distribution of these forces is going to

vary continuously, as portions of the structure yield and stiffness characteristics change. The distribution extremes depend on the intensity of the earthquake motion and the degree of the nonlinear response of the structure. Thus, using more than one lateral load pattern is recommended, in order to take into account the range of design actions that may occur during actual dynamic response (FEMA 356, 2000).

At least two vertical distributions of lateral load should be applied:

- A uniform distribution: The lateral loads at each level are proportional to the total mass of each level
- A modal pattern: The vertical distribution is proportional to the shape of fundamental mode in the direction under consideration (KANEPE, 2013).

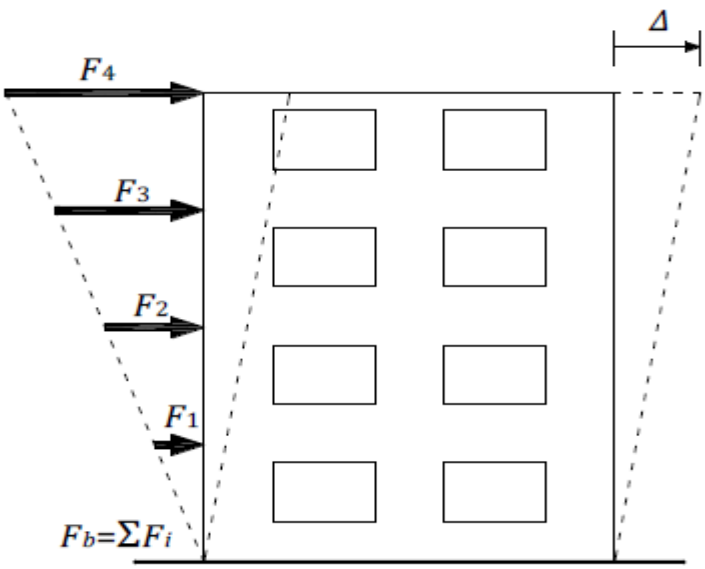

Figure 2.3 Example of Lateral Loads Distribution (Psycharis, 2015)

2.3.3 Nonlinear Time-History Dynamic Analysis

Nonlinear time-history dynamic analysis may be used for the calculation of the response of the building in discrete time steps, using discretized recorded or synthetic time histories as base motion (FEMA 356, 2000).

The parameters of response should be calculated for each one time-history analysis performed. If three or more analyses are performed, the maximum

response of the parameter of interest should be used. If seven or more consistent pairs of horizontal time-histories are used, it is permitted to use the average of all responses of the parameter of interest (FEMA 356, 2000).

The nonlinear time-history analysis (dynamic) is similar to the nonlinear static analysis as it concerns the modelling approaches and the acceptance criteria. The main difference is that the design displacements are not established using a target displacement. Instead they are directly calculated through dynamic analysis using ground motion time histories (FEMA 356, 2000).

For the analysis of a spatial model, simultaneously imposed consistent pairs of earthquake ground motion records, along each of the horizontal axes of the building shall be permitted (FEMA 356, 2000).

Their values should be scaled to the value of $a_g.S$ for the zone under consideration.

In addition, the accelerograms should comply with the following rules:

- At least 3 accelerograms should be used;
- The mean of the zero period spectral response acceleration values (calculated from the individual time histories) should not be smaller than the value of $a_g.S$ for the site in question.
- In the range of periods between $0.2T_1$ and $2T_1$, where T_1 is the fundamental period of the structure in the direction where the accelerogram will be applied; no value of the mean 5% damping elastic spectrum, calculated from all time histories, should be less than 90% of the corresponding value of the 5% damping elastic response spectrum (EN 1998-1, 2004).

2.4 Performance Based Design

The nonlinear static (pushover) analysis is focused on the generation of the capacity curve (or the pushover curve), which represents the lateral displacement as a function of the force applied to the structure. This process is

independent of the method used to calculate the demand and provides valuable insight for the engineer.

It can be combined with the "performance based design". Using the performance point or target displacement, the global response of the structure and the deformations of the individual components are compared to limits in light of the specific performance goal for the building (ATC-40, 1996).

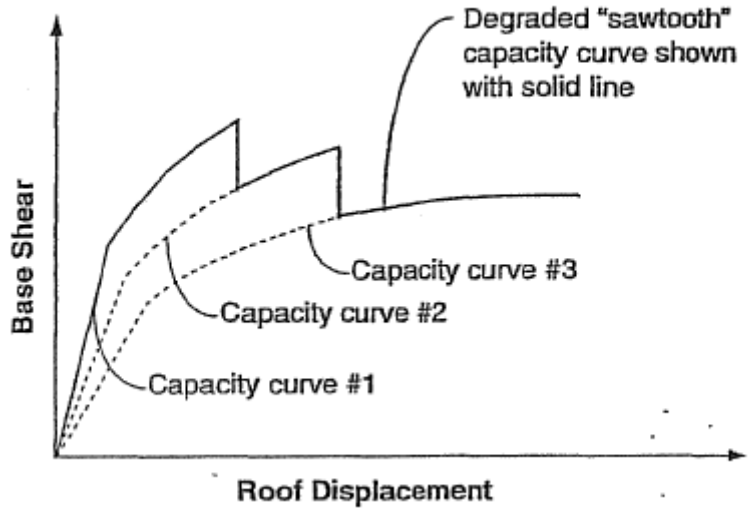

Figure 2.4 Capacity Curve with Global Strength Degradation Modelled (ATC-40, 1996)

The "performance based design" is based on the definition of an acceptable level of damage (performance), considering the possibility to occur the "design earthquake". The method is focused on the real behaviour of the structure in relation with the level of the earthquake demand and the corresponding expected damage level. As a result, the optimum combination of safety and economy is ensured. In other words, a performance level describes a limiting damage condition which may be considered satisfactory for a given building and a given ground motion. (ATC-40, 1996)

On the one hand, the classic design methodology applied for the design of the modern earthquake resistant structures takes into account the behaviour of the structure before the yield point (elastic response) and does not take into

account the behaviour of the structure when it is damaged. The minimum safety level is achieved through the behaviour factor that is used. However in many cases this way of design may not guarantee the maximum safety level, especially for non regular buildings.

On the other hand, the performance based design is primarily applied for the bearing capacity assessment and the retrofitting of existing buildings. It is used by international codes such as the EN 1998-3, KANEPE, FEMA 356, ATC-40.

The behaviour of the structure from the appearance of the first damages to the collapse should be known. Thus the performance based design is applied in combination with non-linear analyses methods such as the non-linear static analysis (pushover), or the non-linear time history analysis (Psycharis, 2015).

2.4.1 Rehabilitation Objectives

A seismic rehabilitation objective shall be selected for the building, consisting of one or more rehabilitation goals. Each goal should consist of a Target Building Performance Level and an Earthquake Hazard Level (FEMA 356, 2000).

Prior to embarking on a rehabilitation program, an evaluation should be performed to determine whether the building in its existing condition, has the desired seismic performance capability (FEMA 356, 2000).

It is mentioned that the design of usual new buildings, according to the current codes corresponds to the B2 target of performance level (EAK 2000 cited in Psycharis (2015)).

Table 2.2 Rehabilitation Objectives (FEMA 356, 2000) (EN 1998-3, 2005)

		Performance Level		
		Damage Limitation (DL) or Immediate Occupancy (IO)	Life Safety (LS)	Near Collapse (NC) or Collapse Prevention (CP)
Earthquake Hazard Level (Earthquake having probability of exceedance in 50 years)	20 % (Mean Return Period 225 years)	A1	B1	G1
	10% (Mean Return Period 475 years)	A2	B2	G2
	2 % (Mean Return Period 2475 years)	A3	B3	G3

2.4.2 Structural Performance Levels

<u>Limit State of Near Collapse (NC)</u>

The structure is heavily damaged. Vertical elements are still capable to sustain vertical loads, however the residual lateral strength and stiffness is low. Most non-structural components have collapsed and large permanent drifts are present. It is likely that the structure will not survive another earthquake, even of moderate intensity (EN 1998-3, 2005). There is significant danger for people to be injured from broken elements inside or outside of the structure. Probably its repair is not feasible.

Limit State of Significant Damage (SD) or Life Safety (LS)

The damages to the structure are significant. There is some residual lateral strength and stiffness, and vertical elements are capable of sustaining vertical loads. Non-structural components are damaged. Partitions and infills are not failed out of plane. Moderate permanent drifts are present. It is likely that the structure is uneconomic to be repaired and can sustain after-shocks of moderate intensity (EN 1998-3, 2005). Most of the damages can be repaired. Non-significant injuries may occur.

Limit State of Damage Limitation (DL) or Immediate Occupancy (IO)

The building is lightly damaged. The structural elements do not face significant yielding and retain their strength and stiffness properties. Non-structural elements, such as infills and partitions, may show distributed cracking. However the damage is economically repaired. Permanent drifts are negligible and the structure does not need any repair measures (EN 1998-3, 2005).The building is functional during or immediately after the earthquake. There is no danger of injuries (Psycharis, 2015).

2.4.3 Capacity Curve

The relation between the base shear force and the displacement of the control node is called "capacity curve" (EN 1998-1, 2004).The limit states of the performance are defined on the capacity curve. The non-linear displacement of the centre of mass of the roof is calculated for several values and specific distribution of the lateral load (pushover analysis), considering the reduced stiffness of the elements that have exceeded their yield point (Psycharis, 2015).

2.4.4 Primary and Secondary Elements and Components

All the elements and components that affect the distribution of forces in a structure, or the lateral stiffness, shall be classified as primary or secondary, even if they are not part of the intended lateral-force resisting system (FEMA 356, 2000).

Primary elements and components

Primary elements and components are considered the ones that provide the capacity to the structure to resist collapse under seismic loading induced by ground motion in any direction (FEMA 356, 2000).

Nearly all the elements of a typical building, including many nonstructural components make a contribution to the building's overall stiffness, mass, and damping, and consequently to its response to earthquake ground motion. However not all of those elements are critical to the ability of the structure to resist collapse when subjected to strong ground shaking (FEMA 356, 2000).

Secondary elements and components

The elements and components that do not contribute significantly in resisting earthquake effects because of low lateral stiffness, strength or deformation capacity are classified as secondary (FEMA 356, 2000).

For a given performance level, acceptance criteria for primary elements is typically more restrictive than those for secondary.

By the use of secondary elements classification, certain elements are allowed to experience greater damage and larger displacements than would otherwise be permitted for primary elements (FEMA 356, 2000).

2.4.5 Component Behaviour F-δ Curve

The inelastic behaviour of each element of the structure should be taken into account. On the F-δ diagrams the limits of the performance levels are determined. The "F" may represent forces or moments while the "δ" may represent deformation, curvature or rotation. Flexural coexist with shear deformation at the reinforced concrete frames and the rotation of the edge sections are influenced by anchorage. Thus the best choice for F-δ is the bending moment M and the rotation angle θ. θ is the rotation angle of the chord that connects the base and the top of a theoretical cantilever of length equal to shear length Lv. $\theta=\delta_v/L_v$ where $L_v=M/V$ (M= bending moment at the base,

V=shear force), δ_v is the displacement at the top of the theoretical cantilever (Psycharis, 2015).

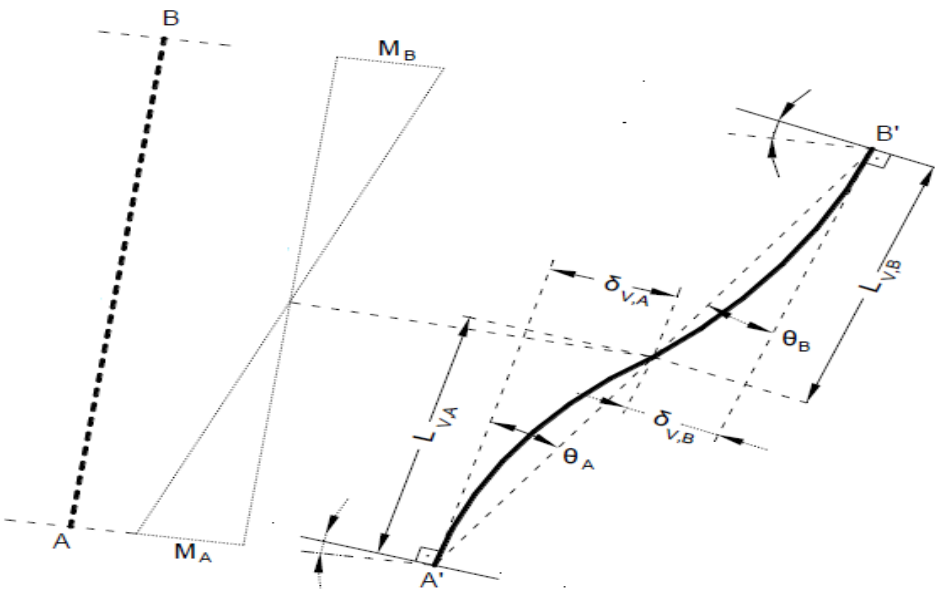

Figure 2.5 Definition of Rotation Angle θ (Psycharis, 2015)

For deformation-controlled actions, a "backbone curve" should represent an upper bound to the forces and a drop in resistance when degradation becomes apparent in the cyclic data. The backbone curve is approximated by a multi-linear "idealized" load deformation relation as shown in figure 2.6 (ATC-40, 1996).

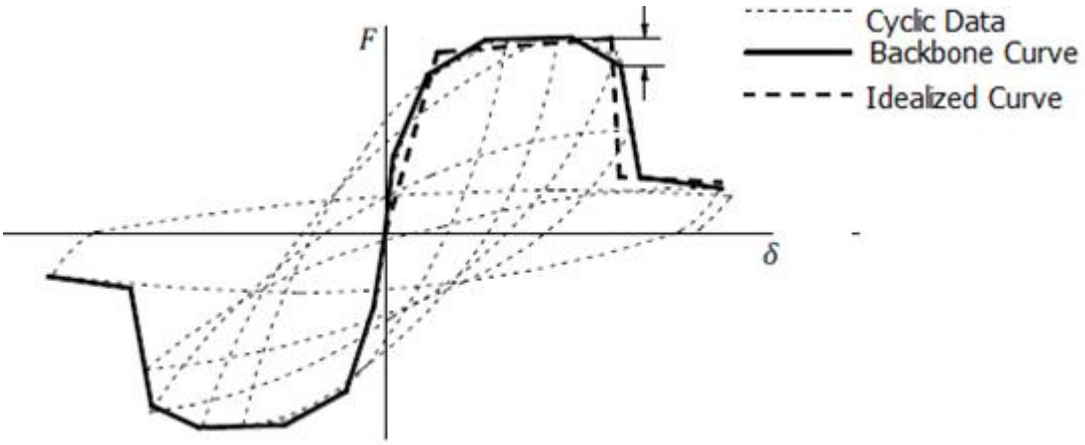

Figure 2.6 Backbone Curve-Deformation Controlled Actions (Psycharis, 2015)

For force-controlled actions, the backbone curve represents a lower bound to the forces, followed by a drop in resistance to match cyclic data. Displacement ductility should not be shown in the "idealized" deformation relation, as shown in the figure 2.7 (ATC-40, 1996).

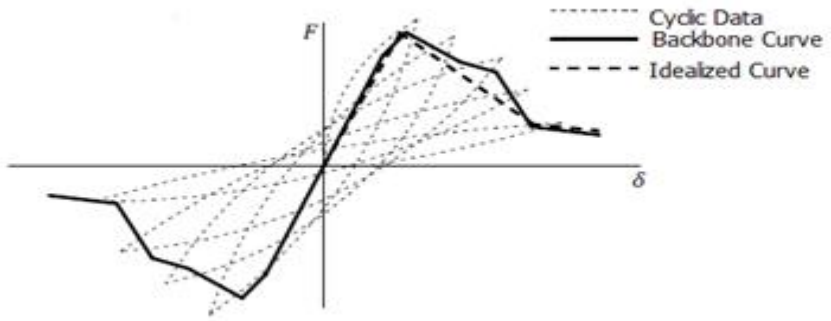

Figure 2.7 Backbone Curve-Force Controlled Actions (Psycharis, 2015)

Strengths and deformation capacities are defined for earthquake loadings that involve about three fully reserved cycles to the specified deformation level, in addition to similar cycles to lesser deformation levels (ATC-40, 1996).

The idealized "F-δ" curve is generally taken into account as shown in the figure 2.8.

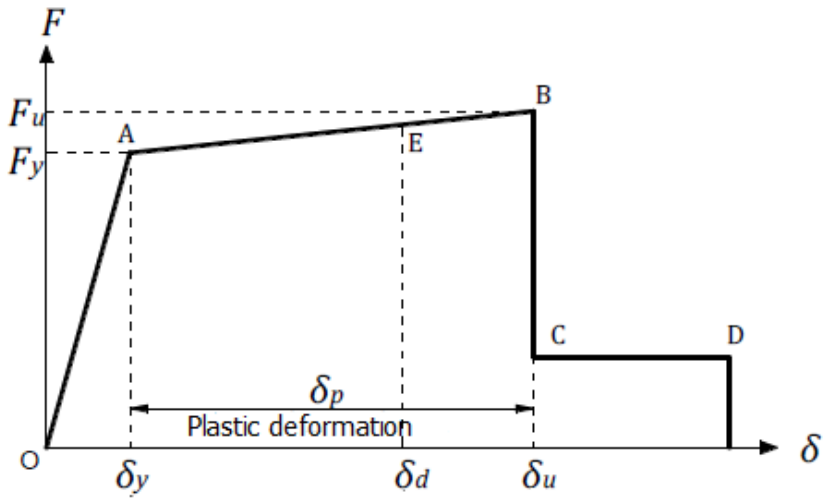

Figure 2.8 Idealized F-δ curve of structural elements (Psycharis, 2015)

where:

OA:

Linear response is considered between the points O (unloaded component) and an effective yield point A. The slope of the OA represents the elastic stiffness. It is mentioned that if the deformation is given as rotation angle, the value of $\delta_y = \theta_y$ should be calculated taking into account the participation of shear deformation and the anchorage slip of bars as explained in EC8-3 and KANEPE.

AB:

The AB part represents the nonlinear response at reduced stiffness from A to B. It is the plastic deformation of the component. At point B significant strength degradation begins and resistance to reserved cyclic lateral forces is no longer guaranteed beyond this deformation. The slope from A to B is typically small, representing phenomena such as stain hardening. However, the AB is often considered totally horizontal, so the yield strength F_y is equal to the ultimate strength F_u. The plastic deformation capacity is the ultimate minus the yield deformation: $\delta_p = \delta_u - \delta_y$.

CD:

The residual resistance of the component is represented by the CD part. Its estimation is difficult and it is usually assumed to be equal to 20% of the nominal strength. The purpose of this segment is to allow modelling of components that have lost most of their lateral force resistance, but they are still capable of sustaining gravity loads.

2.4.6 Performance Levels of the Elements

The limit states of the performance levels are defined on the capacity curve of each element according to the corresponding deformations δ_d. For example, in the figure 2.8 the point E represents the performance level "life safety". The limit states of the performance levels are depended on the frame type (e.g. column, beam e.t.c). In addition the classification to deformation-controlled or

force-controlled and primary or secondary is taken into account (Psycharis, 2015).

For ductile components subject to deformation controlled actions, performance is measured by the relation of deformation demand to deformation capacity. For those components forces and stresses are of lesser importance (ATC-40, 1996).

For components subject to force-controlled actions, where brittle behaviour is expected, the main measure of performance is the force or stress level (ATC-40, 1996).

According to EN 1998-3 (2005) the deformation capacity of beams, columns and walls are defined in terms of the chord rotation θ. Thus the limit states of the performance levels of the elements are defined on the backbone curve of each element.

<u>Limit State of Near Collapse (NC)</u>

The value of the chord rotation capacity (elastic plus inelastic part) at ultimate θ_u of concrete members under cyclic loading may be calculated from the following expression:

$$\theta_{um} = \frac{1}{\gamma el}\left(\theta_y + \left(\varphi_u - \varphi_y\right) L_{pl}\left(1 - \frac{0.5 \cdot L_{pl}}{L_v}\right)\right) \qquad (10) \text{ (EN 1998-3, 2005)}$$

Where:

Θy is the chord rotation at yield.

Φu is the ultimate curvature at the end section.

Φy is the yield curvature at the end section.

The value of the length L_{pl} of the plastic hinge depends on how the enhancement of strength and deformation capacity of concrete due to the confinement is taken into account in the calculation of the ultimate curvature of the end section φ_u (EN 1998-3, 2005).

Limit State of Significant Damage (SD)

The chord rotation capacity corresponding to significant damage Θ_{SD} may be assumed to be ¾ of the ultimate chord rotation θ_u (EN 1998-3, 2005).

Limit State of Damage Limitation (DL)

The capacity for this limit state used in the verifications is the yielding bending moment under the design value of the axial load.

In case the verification is carried out in terms of deformations the corresponding capacity is given by the chord rotation at yielding θy, evaluated as:

For beams and columns:

$$\theta_y = \varphi_y \cdot \frac{Lv + a_v \cdot z}{3} + 0.0013 \cdot \left(1 + 1.5\frac{h}{Lv}\right) + 0.13 \cdot \varphi_y \frac{d_b \cdot f_y}{\sqrt{f_c}} \qquad (11) \text{ (EN 1998-3, 2005)}$$

And for walls of rectangular, T- barbelled section:

$$\theta_y = \varphi_y \cdot \frac{L_v + a_v \cdot z}{3} + 0.002 \cdot \left(1 - 0.125 \cdot \frac{L_v}{h}\right) + 0.13 \cdot \varphi_y \cdot \frac{d_b \cdot f_y}{\sqrt{f_c}} \qquad (12) \text{ (EN 1998-3, 2005)}$$

Where:

Φ_y is the yield curvature of the end section

$a_v z$ is the tension shift of the bending moment diagram with

z length of internal level arm, taken equal to d-d' in beams, columns or walls with barbelled or T-section, or to 0.8h in walls with rectangular section, and

a_v=1 if shear cracking is expected to precede flexural yielding at the end section (i.e. when the yield moment at the end section, M_y, exceeds the product of L_v times the shear resistance of the member considered without shear reinforcement, $V_{R,C}$, taken in accordance with EN 1992-1-1:2004, 6.2.2 (1)); otherwise, (i.e. if $M_y < L_v V_{R,C}$) a_v=0,

f_y and f_c are the steel yield stress and the concrete strength, respectively, both in MPa

d and d’ are the depths to the tension and compression reinforcement respectively, and

d_{bl} is the (mean) diameter of the tension reinforcement.

The first term in above expressions, accounts for the flexural contribution. The second term represents the contribution of shear deformation and the third anchorage slip of bars. (EN 1998-3, 2005)

2.4.7 Performance Levels of the Structure

The procedure described above for each element, is followed by the determination of the limit states of the performance levels on the capacity curve of the structure. This step is not a clear procedure and requires engineering judgement. The reason is that a performance level for the whole structure is not always corresponding to the point that the first element of the structure reaches the corresponding performance level. A number of the structure elements may have reached a performance level, however the structure may still be below that level. Consequently, the engineer should assess the importance of damages of the elements to the structure behaviour. The classification of the elements into primary and secondary plays significant role. For example the limit states of the performance levels on the capacity curve, could be set for the first primary element that reaches each performance level (Psycharis, 2015).

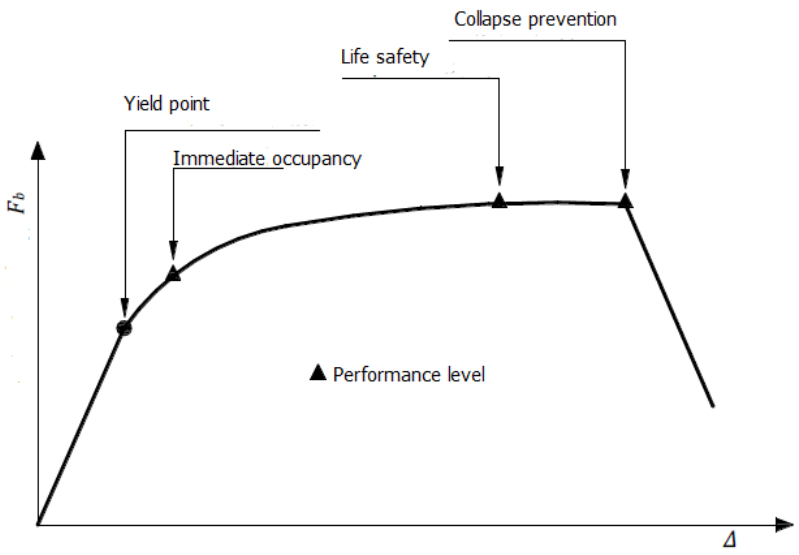

Figure 2.9 Definition of the performance levels on the capacity curve of the structure (Psycharis, 2015)

2.4.8 Target Displacement Check

A displacement along the capacity curve that is consistent with the seismic demand should be calculated in order to determine compliance with a given performance level. The capacity spectrum method is suitable for this purpose. It is based on finding a point on the capacity spectrum, which also lies on the appropriate demand response spectrum, reduced for non linear effects. The condition, for which the seismic demand, imposed on the structure by the specified ground motion, is equal to the seismic capacity of the structure, is represented by the "performance point" (ATC-40, 1996).

The performance point may be estimated accurately by nonlinear time history analysis. However, specialized software is required, the analysis is time consuming and it is highly dependent on the time history used. Thus many nonlinear time-history analyses, using accelerograms of various characteristics are required in order to obtain reliable results.

In addition, methods such as the coefficient method or the nonlinear static (pushover) analysis may be used for the estimation of the target displacement. The nonlinear static analysis shall be applied in combination with other methods

such as the N2 method, the modal pushover, the adaptive pushover or the ATC-40, which is explained below.

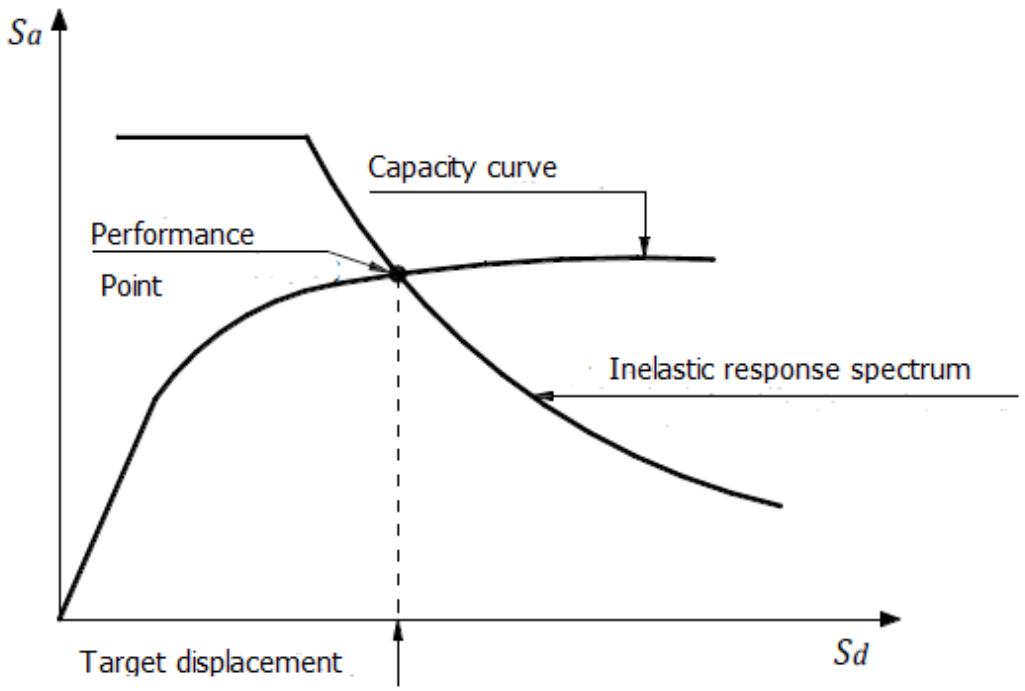

Figure 2.10 Definition of the Target Displacement of the Equivalent Single-Degree of Freedom System (Psycharis, 2015)

Once the expected displacement of the structure (of the control node) is calculated, the relevant performance point is marked on the capacity curve, which is compared with the desirable performance level for the considered ground motion. Subsequently, it is checked if the target performance level is exceeded or not.

The same procedure shall be followed for each element, at its own "F-δ" curve. If the target performance level for some elements is exceeded, their rehabilitation is necessary and the whole procedure should be repeated.

As mentioned earlier, unless nonlinear dynamic time-history analysis is performed, the accuracy of the results obtained by alternative methods (the "static" methods) is not adequate. The reason is that they are based on the response of an equivalent single degree of freedom system and that the

estimation of the response at each floor level of the structure is based on a determined vertical distribution of lateral loads (Psycharis, 2015).

2.4.9 Performance Point Estimation

2.4.91 Equivalent single degree of freedom system

The equivalent single degree of freedom system is dependent on the distribution of the lateral loads, which are used for the generation of the capacity curve.

In general the following expression is used for the distribution of lateral loads:

$$Fi = V \cdot \frac{m_i \varphi_i}{\sum_j m_j \varphi_j} \qquad (13) \quad \text{(Psycharis, 2015)}$$

Where: $V = \sum F_i$ is the base shear force.

This method is usually applied for planar motion of the structure to the seismic force direction, so the φ_i factor represents the distribution of the displacements at the floor levels. Commonly, they are considered equal to the first mode value, however any other distribution, representative of the expected displacement of the structure, may be used. The values of the φ_i are normalized, so that the value at the top is equal to one: $\varphi_{top}=1$.

As long as the previous formula is used for the distribution of lateral loads and $\varphi_{top}=1$, the correspondence between the multi-degree and the single-degree of freedom systems (for forces, displacements, energy etc) is given by:

$$Q = \Gamma \cdot Q^* \qquad (14) \quad \text{(Psycharis, 2015)}$$

where

Q^*= the magnitude at the single degree of freedom system (e.g. force F^*, displacement d^*)

Q= corresponding magnitude at the multi degree of freedom system (e.g. base shear force V, top displacement Δ)

Γ= participation factor, which is given (for planar motion of the structure) by the expression:

$$\Gamma = \frac{\sum m_i \varphi_i}{\sum m_i \varphi_i^2}$$ (15) (Psycharis, 2015)

The numerator of the above expression is equal to the mass of the equivalent single-degree of system:

$$m^* = \sum m_i \varphi_i$$ (16) (Psycharis, 2015)

Both the forces and the displacements are converted from a single-degree of freedom to a multi-degree of freedom system and vice versa, following the same rule, so the stiffness of the two systems is common. However the natural period of the equivalent single-degree of freedom system is not equal to the fundamental period of the multi-degree of freedom system (Psycharis, 2015).

2.4.9.2 Conversion of the capacity curve to the capacity spectrum

Prerequisite to use the capacity spectrum method is the conversion of the capacity curve, which is in terms of base shear force and roof displacement, to what is called a capacity spectrum, which is a representation of the capacity curve in Acceleration-Displacement Response Spectra (ADRS) format (i.e. S_a versus S_d). The equations that are required for the transformation are (ATC-40, 1996):

$$S_a = \frac{V}{a \cdot m_{tot}}$$ (17,18) (Psycharis, 2015)

$$S_d = \frac{\Delta}{\Gamma}$$ or $$S_d = \frac{\Delta}{\Gamma \cdot \varphi_{top}}$$ if $\varphi_{top} \neq 1$

Where:

V is the base shear force of the multi-degree of freedom system

m_{tot}= total mass of the multi-degree of freedom system

α= modal mass coefficient for the first natural mode (ATC-40, 1996)

Δ= displacement of the top

$$a = \frac{\left[\sum m_i \varphi_i\right]^2}{m_{tot} \cdot \sum m_i \varphi_i^2} = \frac{\Gamma \cdot \sum m_i \varphi_i}{m_{tot}} = \Gamma \cdot \frac{m^*}{m_{tot}}$$ (19) (Psycharis, 2015)

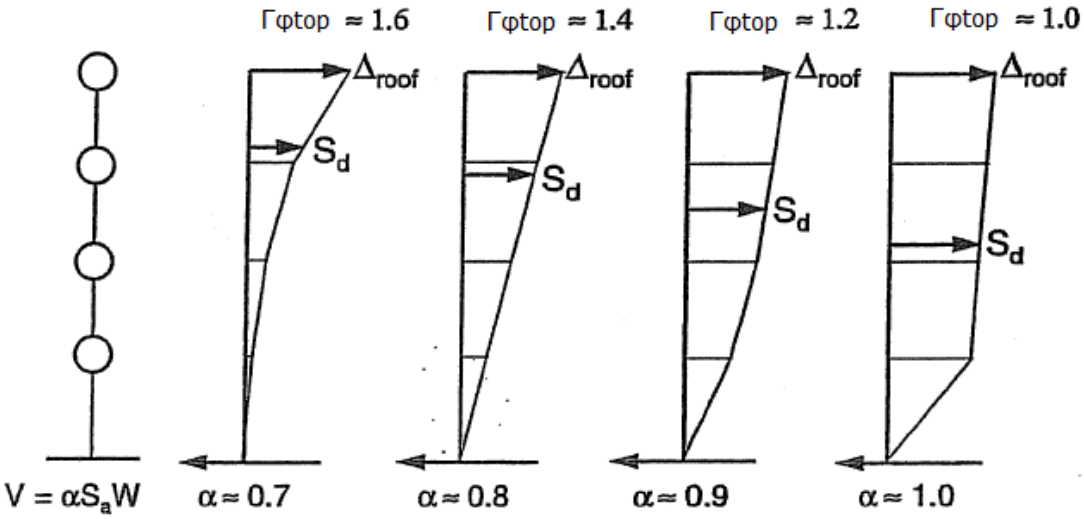

Figure 2.11 Example Modal Participation Factors and Modal Mass Coefficients (ATC-40, 1996)

As shown in the figure 2.11, the modal mass coefficient and the participation factor, vary according to the relative inter-story displacement over the building height (ATC-40, 1996).

The general process for converting the capacity curve to the capacity spectrum, that is, converting the capacity curve into the ADRS format, is to first calculate the modal participation factor Γ and the modal mass coefficient α using the equations above. Then for each point on the capacity curve, V, δtop, the associated point S_a, S_d on the capacity spectrum is calculated using the equations (17,18) (ATC-40, 1996).

The traditional S_a versus T representation of response spectra is familiar to the majority of engineers. However the S_a versus S_d (ADRS) representation is less familiar to them. Lines radiating from the origin have constant period in the

ADRS format. The period T, for any point of the ADRS spectrum, can be calculated by the relationship:

$$T = 2\pi \cdot \sqrt{\frac{S_d}{S_a}} \qquad (20) \text{ (Psycharis, 2015)}$$

Similarly, for any point on the traditional spectrum, the spectral displacement S_d can be computed using the formula:

$$S_d = \frac{S_a \cdot T^2}{4\pi^2} \quad . \qquad (21) \text{ (Psycharis, 2015)}$$

These two relationships are the same formula arranged in different ways.

Figure 2.13 shows the same capacity spectrum superimposed on each of the response spectra plots shown in figure 2.12. Following along the capacity spectrum, the period is constant at T1, up until point A. When point B is reached, the period is T2. This is important since it indicates that as the structure undergoes inelastic displacement, the period lengthens. The lengthening period is clear on the ADRS plot (remembering that lines of constant period radiate from origin), even if it is more apparent on the traditional spectrum plot (ATC-40, 1996).

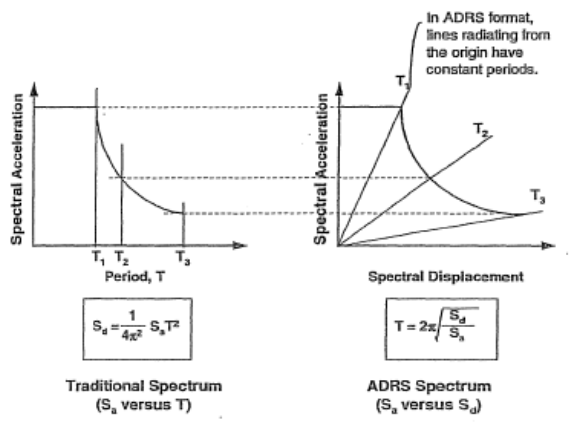

Figure 2.12 Response Spectra in Traditional and ADRS formats (ATC-40, 1996)

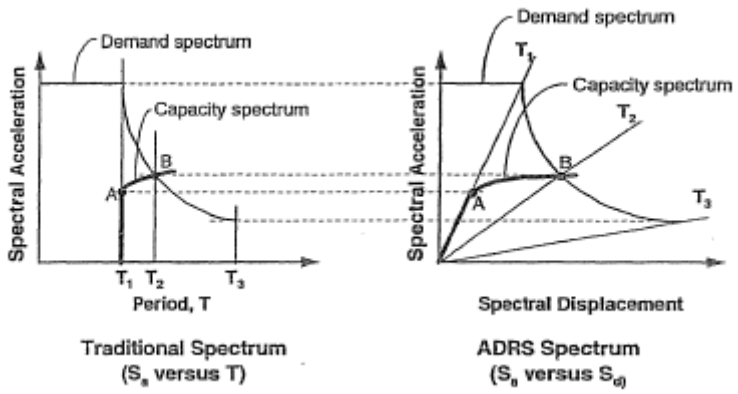

Figure 2.13 Capacity Spectrum superimposed over Response Spectra in Traditional and ADRS formats (ATC-40, 1996)

2.4.10 ATC-40 Methodology

Three procedures of the methodology are proposed, which results are similar. (Psycharis, 2015). In the following the procedure A is described, which is the most direct application of the concepts and relationships mentioned above. This procedure is iterative. It is more an analytical method than a graphical method (ATC-40, 1996). Its steps are:

1) <u>Elastic Response Spectrum Conversion</u>

The 5% damped (elastic) response spectrum, appropriate for the site, should be developed and transformed into Acceleration Displacement Response Spectra (ADRS) (Psycharis, 2015) using the following equations:

$$S_a = \frac{4 \cdot \pi^2}{T^2} \cdot S_d \qquad (22)$$

$$S_d = \frac{T^2}{4 \cdot \pi^2} \cdot S_a \qquad (23)$$

$$T = 2\pi \sqrt{\frac{S_d}{S_a}} \qquad (24)$$ (Psycharis, 2015)

2) <u>Generation of the capacity curve of the structure and conversion to capacity spectrum</u>

The capacity curve of the structure should be found and transformed into a capacity spectrum (ADRS format) of the equivalent single-degree of freedom system as mentioned above. The capacity spectrum and the 5% damped response spectrum should be plotted on the same chart.

3) <u>Selection of a trial performance point</u>

The trial performance point is estimated by the engineer to develop a reduced demand response spectrum. A line is drawn up from the origin, at the stiffness that corresponds to cracked sections (effective stiffness). The intersection of the line and the elastic spectrum (5% damped) determines the displacement d_1 of the equivalent single-degree of freedom system. For displacement d_1 is estimated the trial performance point on the capacity spectrum as shown in the figure, and the corresponding acceleration a_1 (Psycharis, 2015).

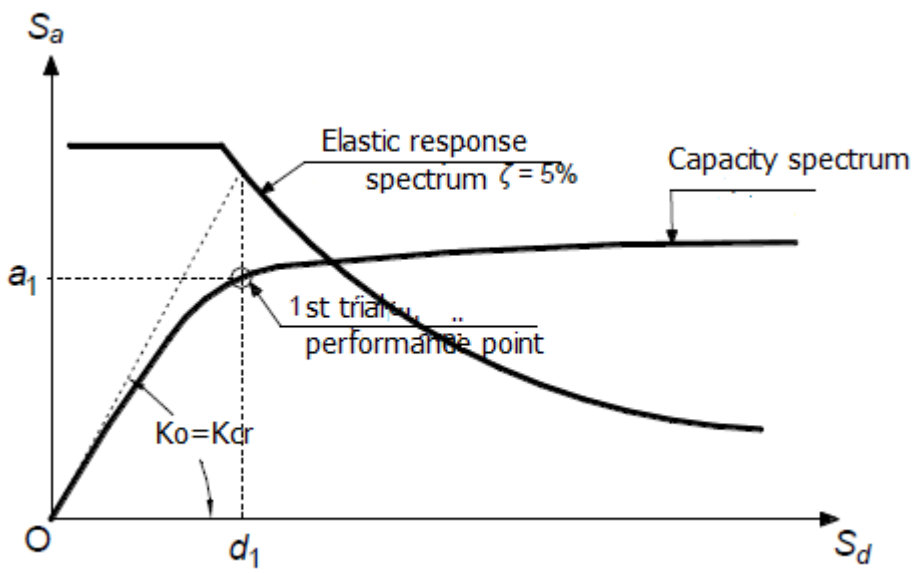

Figure 2.14 Calculation of the first trial performance point (Psycharis, 2015)

4) Construction of Bilinear Representation of Capacity Spectrum

The definition of the first performance point is followed by a bilinear representation of the capacity spectrum. It is necessary in order to estimate the effective damping and appropriate reduction of the spectral demand. If the capacity spectrum is found to intersect the reduced response spectrum at the estimated point, then this is the performance point (ATC-40, 1996).

To construct the bilinear representation, a line back from the trial performance point should be drawn. The slope of the line should be such, that when it intersects the first line, drawn up before from the origin at the stiffness that corresponds to cracked sections, the area designated A_1 in the figure should be approximately equal to the area designated A_2. The intent of setting the areas A_1 and A_2 equals is to have equal area under the capacity spectrum and its bilinear representation, that is, to have equal energy associated with each curve (ATC-40, 1996). The intersection of the first and second line determines the yield point, according to the bilinear curve, and its coordinates on the plot are the yield displacement δ_y and the yield acceleration a_y (Psycharis, 2015).

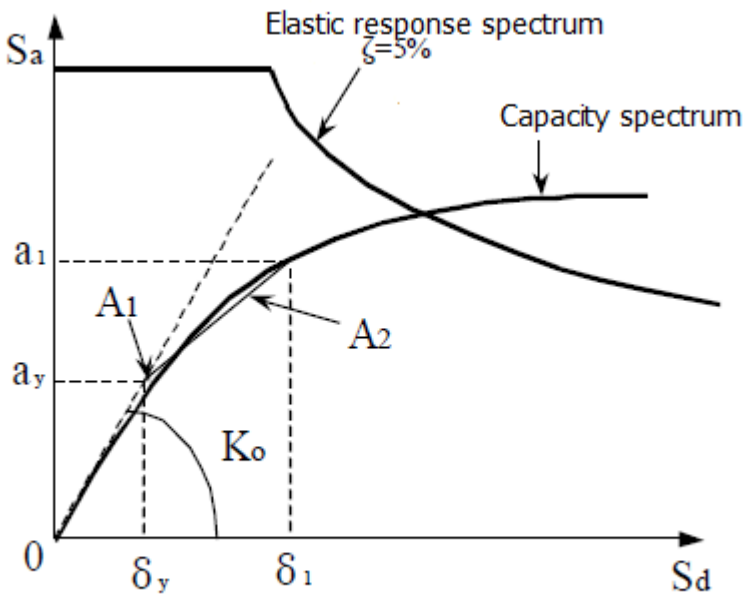

Figure 2.15 Construction of Bilinear Representation of Capacity Spectrum (Psycharis, 2015)

5) <u>Estimation of effective damping and reduction of 5% damped response spectrum</u>

The damping occurring when a structure is driven into the inelastic range by an earthquake ground motion is a combination of viscous damping (that is inherent in the structure) and the hysteretic damping (ATC-40, 1996).

$$\zeta_{eff} = \zeta_{el} + \zeta_{hyst} \qquad (25) \quad \text{(Psycharis, 2015)}$$

Where

ζ_{el} =viscous damping inherent in the structure (5% for reinforced concrete structures)

ζ_{hyst} = hysteretic damping due to inelastic behaviour of the structure (Psycharis, 2015)

Hysteretic damping is related to the area inside the loops formed when the earthquake force (base shear) is plotted against the structure displacement (ATC-40, 1996).

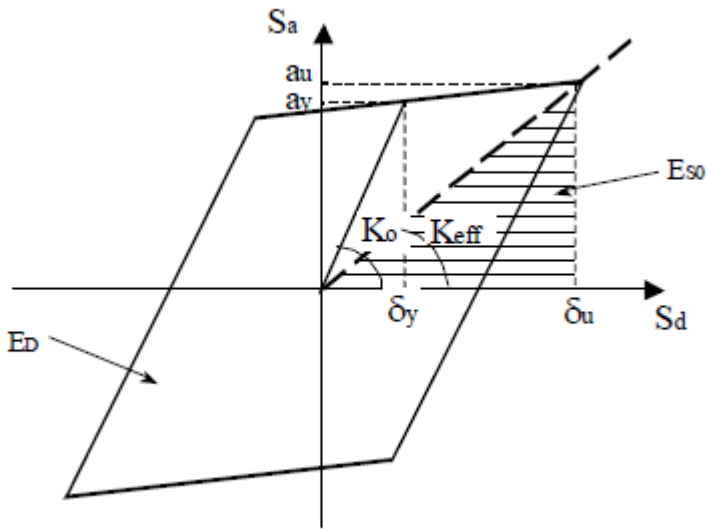

Figure 2.16 Calculation of hysteretic damping according to Chopra cited in Psycharis (2015)

The hysteretic damping can be calculated as (Chopra 1995):

$$\zeta_{hyst} = \frac{1}{4\pi} \cdot \frac{E_D}{E_{S0}} \Rightarrow \zeta_{hyst} = \frac{0.637 \cdot \left(a_y \cdot \delta_u - \delta_y \cdot a_u\right)}{a_u \cdot \delta_u} \qquad (26) \quad \text{(Psycharis, 2015)}$$

where

E_D= energy dissipated by damping

E_{S0}=maximum strain energy

As shown in the figure 2.16, E_D is the area enclosed by a single hysteresis loop. In other words it is the energy dissipated by the structure in a single cycle motion.

E_{S0} is the area of the hatched triangle. It is the maximum strain energy associated to that cycle of motion (ATC-40, 1996).

The hysteretic damping can be used to estimate the effective damping of the structure.

The idealized hysteresis loop shown in the figure overestimates the effective damping, unless the building is ductile (concrete buildings are not typically ductile structures), subjected to ground shaking of short duration (not enough cycles to degrade elements significantly) and with effective damping less than 30%. The overestimation of realistic levels of dumping occurs because the actual hysteresis loops are imperfect. They are reduced in area, or pinched.

Thus, according to ATC-40 a damping modification factor, k, is used. It is a measure of how well is the actual building hysteresis represented by the idealized hysteresis loop shown in the figure, either initially, or after degradation.

The structural behaviour of the building determines the κ-factor. However the structural behaviour of the building is dependent on the duration of the ground shaking and on the quality of the seismic resisting system. Values for the κ-factor and the types of structural behaviour are given in the tables.

Finally the effective damping is:

$$\zeta_{eff}(\%) = 5 + \frac{63.7 \cdot \kappa \cdot \left(a_y \cdot \delta_1 - \delta_y \cdot a_1\right)}{a_1 \cdot \delta_1}$$

(27) (Psycharis, 2015)

The effective damping can be used for the calculation of the spectral reduction factors, which are used for the decrease of the elastic (5% damped) response spectrum to a reduced response spectrum with damping greater than 5% of critical damping (ATC-40, 1996).

The equations of the reduction factors are given by:

$$SR_A = \frac{1}{B_S} = \frac{3.21 - 0.68 \cdot \ln \zeta_{eff}}{2.12} \geq SR_{A.\min}$$

$$SR_V = \frac{1}{B_L} = \frac{2.31 - 0.41 \cdot \ln \zeta_{eff}}{1.65} \geq SR_{V.\min}$$

(28,29) (Psycharis, 2015)

Table 2.3 Minimum values of reduction factors (Psycharis, 2015)

Structural Behaviour Type	$SR_{A.min}$	$SR_{L.min}$
A	0.33	0.50
B	0.44	0.56
C	0.56	0.67

Then the reduced demand spectrum is produced, by multiplication of the reduction factors with the elastic spectrum (5% damping). The SR_A and SR_L are multiplied with the parts that correspond to the constant acceleration and velocity, respectively.

The intersection point between the reduced response spectrum for $\zeta=\zeta_{eff}$ and the capacity spectrum is the new trial performance point. The projection of this point to the axes S_a and S_d, defines the new acceleration a_2 and the new displacement δ_2, respectively (Psycharis, 2015).

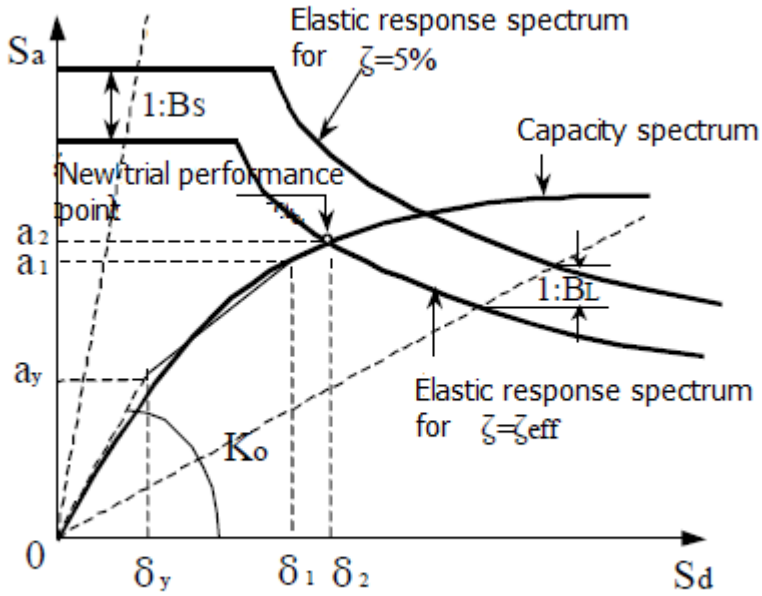

Figure 2.17 Construction of elastic response spectrum for $\zeta=\zeta_{eff}$ and calculation of new performance point

6) <u>Intersection of Capacity Spectrum and Demand Spectrum</u>

It is an iterative procedure. Adequate tolerance must be succeeded. If the demand spectrum intersects the capacity spectrum within acceptable tolerance, then the trial performance point is the performance point and its displacement represents the maximum structural displacement of the equivalent single-degree of freedom system, expected for the demand earthquake (ATC-40, 1996).

The acceptable tolerance criterion is:

$$0.95 \cdot \delta_1 < \delta_2 < 1.05 \cdot \delta_1$$

If the acceptable tolerance is not succeeded, then a new a_i, δ_i point is selected and the process is repeated from the step 4.

7) <u>Target displacement of the structure</u>

The displacement of the top of the structure, which corresponds to the displacement δ of the equivalent single degree of freedom system, is calculated by the equation:

$$S_d = \frac{\Delta}{\Gamma} \quad \text{or} \quad S_d = \frac{\Delta}{\Gamma \cdot \varphi_{top}} \quad \text{if} \quad \varphi_{top} \neq 1$$ (30) (Psycharis, 2015)

Solving for Δ and taking into account that S_d=δ=the target displacement

CHAPTER 3

Retrofit Strategies and Systems

3.1 Introduction

Once the seismic evaluation of the structure has been conducted and the presence of unacceptable seismic deficiencies has been detected, the retrofit strategy should be decided. For most buildings, acceptable design solutions may result by a number of alternative strategies and systems. The most favourable solutions among a number of feasible and applicable alternatives should be decided by the engineer together with the owner (ATC-40, 1996).

"A retrofit strategy is a basic approach adopted to improve the probable seismic performance of the building or otherwise reduce the existing risk to an acceptable level" (ATC-40, 1996).To obtain seismic risk reduction, both technical and management strategies may be employed. Approaches such as increasing building strength, correcting critical deficiencies, altering stiffness and reducing demand, are included in technical strategies. Approaches such as the change of occupancy, incremental improving and phased construction are included in the management strategies (ATC-40, 1996).

"A Retrofit system is the specific method used to achieve the selected strategy" (ATC-40, 1996). If the basic strategy, for example, is to increase building strength, the addition of new shear walls, thickening of existing shear walls, or addition of braced frames, may be used to accomplish this strategy. The selection of a specific system in order to evaluate the applicability of a given strategy is not necessary. However it is necessary to select a specific system in order to complete a design (ATC-40, 1996).

Systems and strategies are sometimes being confused by the engineers. Strategies are related to the modification or control of the basic parameters that affect the earthquake performance of a building. The building stiffness, strength, deformation capacity, ability to dissipate energy, the strength of

ground motion, the occupancy and the contents exposure within the building are included. Strategies can also include combinations of those approaches. Retrofit systems are the specific methods, used to implement the strategies. For example the addition of shear walls or braced frames to increase stiffness and strength, or the use of confinement jackets to enhance deformability (ATC-40, 1996).

3.2 Technical Strategies

The basic demand and response parameters of the building for the design earthquake are modified by technical strategies (ATC-40, 1996).

Lateral displacements experienced by the building as it responds to earthquake ground motion, lead to deformations of each individual element. The element deformations remain elastic, at low levels of response, and no damage is occurring. However, at higher levels of response, elements deformations exceed their linear elastic capacities and the building experience damages. A building must have a complete lateral force resisting system, capable of limiting earthquake-induced lateral displacements to levels that the damage sustained by the elements of the building will be within acceptable levels for the indented performance objective, in order to provide reliable seismic performance. The mass, stiffness, damping, the deformation capacity of the elements, the strength and character of the ground motion, are the basic factors that affect the lateral force resisting system of the building.

The technical strategies provide for improved seismic performance by directly operating on these basic response factors, either individually or in concert. The traditional approaches to seismic retrofitting-the addition of braced frames and shear walls-operate in building stiffness and strength. Energy dissipation systems operate on the structure damping capability. Base isolation operates on the character and strength of ground motion transmitted to the structure (ATC-40, 1996).

Furthermore, although not specifically required by any of the strategies, it is extremely beneficial for the retrofitted lateral-force resisting system to have an

appropriate level of redundancy. As a result, any localized failure of a few elements of the system will not lead to local collapse or instability. The redundancy should be considered when developing retrofitting designs. (FEMA 356, 2000)

3.2.1 Local Modification of Components

Some elements may not have adequate strength, toughness or deformation capacity to satisfy the retrofit objective, although the building may have substantial strength and stiffness. In such a case, local modification of the elements that are inadequate shall be performed. The basic configuration of the lateral-force resisting system should be retained. Local modifications could be the improvement of component connectivity, deformation capacity and component strength (FEMA 356, 2000).

In addition, local strengthening may be applied to the under-strength elements or connections, without affecting the overall structure. Measures such as cover plating steel beams or columns, plywood sheathing to an existing timber diagram could be included. Such measures increase the strength of the element or component and allow it to resist more earthquake-induced force before the onset of damage.

Local measures that intend to improve the deformation capacity or ductility of the element make it able to resist large deformation levels. For example, the placement of a confinement jacket around a reinforced concrete column for the improvement of its ability to deform without spalling or degrading reinforcement slices could be used. In addition the reduction of the cross section to increase the flexibility and response displacement capacity could be used (FEMA 356, 2000). The increase of deformation capacity is more efficient when the number of elements that require modification is low. Otherwise, it may be extremely costly and cause significant problems to the occupants of the building, during the construction period (Spyrakos, 2004).

3.2.2 Removal or Lessening of Existing Irregularities

It can be detected by reviewing the results of the nonlinear analysis, by examining the distribution of structural displacements and inelastic deformation demands. If they are non uniform with disproportionally high values within one storey relative to the adjacent story, or at one side of the building relative to the other, then an irregularity exists.

Irregularities are common. However they are not always caused by the presence of a discontinuity in the structure, as for example the termination of a perimeter shear wall above the first story. Often, the demands predicted by the analysis may be reduced to acceptable levels by simple removal of the irregularity.

The addition of braced frames, or shear walls are effective corrective measures for removal or reduction of irregularities, such as soft or weak storeys. Moment frames, braced frames, or shear walls could be used to balance the distribution of mass and stiffness within a storey if torsional irregularities exist. Another corrective measure against irregularities may be the partial demolition. Portions of the structure, such as setback towers, or side wings, that may create the irregularity, could be removed. However the last measure has significant impact on the appearance of the structure (FEMA 356, 2000).

3.2.3 Global Structural Strengthening and Stiffening

It can be a great retrofitting strategy, if the deficiencies shown by the analysis are related to excessive lateral deflection of the building, and critical primary elements have inadequate ductility to resist the resulting deformations. By structural stiffening, the deformation demand is reduced (Spyrakos, 2004).

Effective measures for adding stiffness are the construction of new braced frames or shear walls within an existing structure (FEMA 356, 2000).

If there is an unacceptable performance deficiency in structural strength, global strengthening can be an effective rehabilitation strategy. This can be identified when the onset of global inelastic behaviour occurs at levels of ground shaking

that are substantially less than the selected level of ground shaking, or inelastic deformation demands are present throughout the structure. The threshold of ground motion at which the onset of damage occurs is possible to be raised by providing supplemental strength to such a lateral-force resisting system. Effective elements for this purpose are the shear walls and the braced frames. However they may be significantly stiffer than the structure to which they are added, which requires their design to provide nearly all of the structure's lateral resistance. On the other hand, moment-resisting frames are more flexible, consequently they may be more compatible with existing elements in some structures. However, such flexible elements may not become effective in the building response until existing brittle elements have already been damaged (FEMA 356, 2000).

If the strength increase is succeed without the increase of stiffness, for example by the use of FRP, then the retrofitted structure can sustain higher seismic actions, before damaging.

The global structural stiffening and strengthening are strategies usually applied simultaneously, since the majority of systems which increase the strength of the structure, such as the addition of shear walls, increase its stiffness, as well (Spyrakos, 2004).

3.2.4 Reducing Earthquake Demands (mass reduction, seismic isolation, energy dissipation systems)

3.2.4.1 Mass Reduction

The amount of force and deformation induced in a structure by ground motion is controlled by mass and stiffness. The reduction of mass may be an effective strategy of retrofitting, if deficiencies attributable to excessive building mass, global structural flexibility or global structural weakness are shown by the results of a seismic evaluation. The force and deformation demand produced by earthquakes can be reduced by mass reduction, so it can be used instead of structural strengthening and stiffening. Mass can be reduced in many ways, such as the demolition of upper stories, replacement of heavy cladding and

interior partitions, or removal of heavy storage and equipment loads (FEMA 356, 2000).

3.2.4.2 Seismic isolation

According to the seismic isolation strategy, compliance bearings are inserted between the superstructure and its foundations. In this way the structure above the bearings is translated nearly as a rigid body, since most of the deformation induced in the isolated system by the ground motion occurs within the compliant bearings, which are especially designed to resist these concentrated displacements. Moreover, most bearings have excellent energy dissipation characteristics (damping). The result is that the demand on the existing elements of the structure is greatly reduced. Thus seismic isolation is an appropriate strategy to achieve enhanced retrofitting objectives, like the protection of historic fabric, valuable contents, and equipment, or for buildings that contain important operations and functions. This strategy is more effective for relatively stiff buildings with low profiles and larger mass. It is less effective for light flexible structures (FEMA 356, 2000).

3.2.4.3 Supplemental Energy Dissipation

It is effective when excessive deformations due to global structural flexibility are occurred in a building. Technologies such as fluid viscous dampers (hydraulic cylinders), yielding plates, or friction pads allow the energy imparted to the structure by the ground motion to be dissipated in a controlled manner. The energy is dissipated by those devices, when they undergo significant deformation (or stroke), which requires that the structure experience substantial lateral displacements. Thus, those systems are most effective in structures that are relatively flexible and have some inelastic deformation capacity. They are most commonly installed in structures as components of braced frames (FEMA 356, 2000).

3.3 Management Strategies

Management strategies are mainly controlled by the owner of the building, rather than the engineer. They are categorized in those strategies that affect

the acceptability of the probable performance of the building, and in those that regulate the way in which a technical strategy is implemented. The occupancy change, the demolition, the temporary retrofit, the phased retrofit, the retrofit while occupied, the retrofit while vacant, the exterior retrofit and the interior retrofit are included.

The management strategies are very important and affect the way a seismic risk reduction project is executed. They should be considered by the engineer in collaboration with the owner, since the last one probably do not have the relevant knowledge and may be unaware of the available alternative strategies (ATC-40, 1996).

3.4 Retrofit System Selection

The selection of the optimum retrofit system should be based on the established performance objectives which are desired for the building, and the existing deficiencies relative to those performance objectives. Once those have been determined, the evaluation of each of the strategy is necessary, to determine whether they are technically and practically capable of mitigating the deficiencies (ATC-40, 1996).

Summarizing the information provided above, the retrofit system selection is dependent on the desired performance objective, as follows:

Once the objective is the increase of stiffness and strength of the structure, the most effective method of retrofitting is the addition of shear walls. It is followed by the addition of braced frames, the extension of the existing columns with additional shear walls and the use of FRPs.

Once the objective is the improvement of the ductility, then the proposed method is the addition of confinement jackets to the columns that are inadequate, or the use of FRP's.

Once the objective is the improvement of the strength, stiffness and ductility of the structure simultaneously, then all of the methods of seismic retrofit can be

used, taking into account the desired level of improvement for each of the above (Spyrakos, 2004).

Usually the optimum solution, technically and in terms of cost, is a combination of the proposed retrofit systems (Spyrakos, 2004).

3.5 Traditional Methods for the Retrofitting of Buildings

As mentioned above, the basic approaches for seismic retrofitting of buildings are either the intervention to the structure as a whole, so as the stress at its weak elements will be reduced, or the retrofit of the weak elements of the structure. Usually the first is selected when the elements that are not adequate are too many (Fardis et al. 2003).

The most common methods of global retrofitting of a structure, which are explained in the following, are:

- The addition of shear walls
- The addition of braces in frames
- Extension of existing columns with additional shear walls

While the most common method of local retrofitting is:

- The application of jackets to columns

No matter which one of the above methods is selected, the new components must be connected to the existing structure. Thus special checks are necessary, to guarantee that the connection between the existing and the new materials can transfer the forces adequately (Fardis et al.2003).

3.5.1 Addition of shear walls

It is considered the most efficient method of increasing strength and stiffness of the structure. The number of additional shear walls and their position in the structure are the most crucial factors.

The techniques used for the addition of shear walls are:

- In-situ constructed shear walls
- Pre-cast walls (panels)
- Masonry of solid clay bricks or concrete masonry units

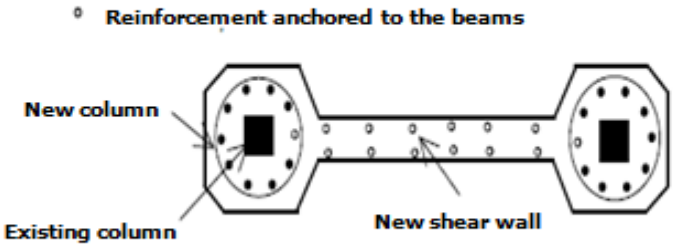

Figure 3.1 Addition of Shear Wall (KANEPE, 2013)

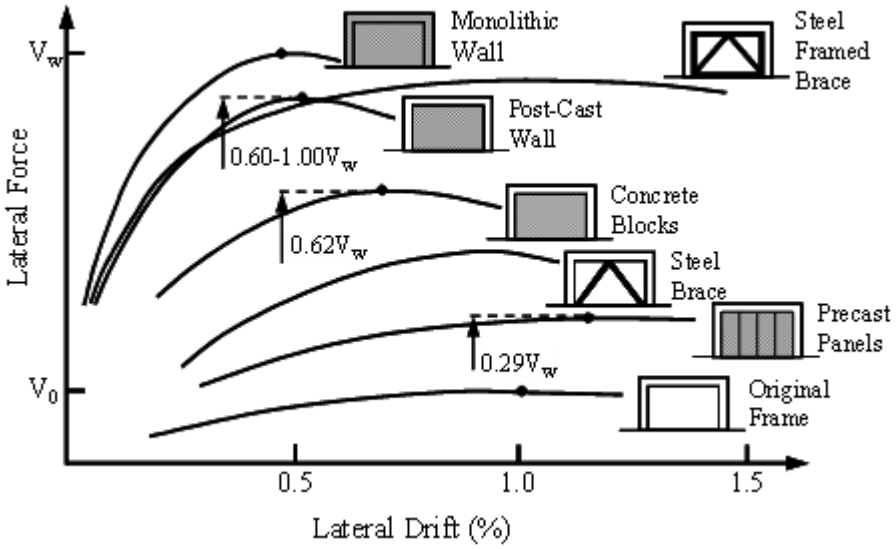

Figure 3.2 Effectiveness of Structural Walls and Bracings (Sugano (1989) cited in Fardis et al (2003))

3.5.2 Addition of Braces in Frames

This method can make a significant contribution not only to the increase of the strength and stiffness of the existing structure, but also to its ductility. Usually these systems are made of steel (Fardis et al.2003). The diagonals work in axial stress and therefore call for minimum member sizes in providing stiffness and strength against horizontal shear (Viswanath et al.2010).

It is used in a similar way as in steel structures. Its application to industrial buildings or in soft-storeys in the ground floor of buildings is easy. Its self-weigh is low and it can be constructed quickly (Fardis et al.2003).

In addition, this system offers the ability to accommodate openings. If it is realized with external steel systems (external bracing), the minimum disruption of the full operationality of the building is obtained. There are two types of bracing systems, concentric bracing system and eccentric bracing system.

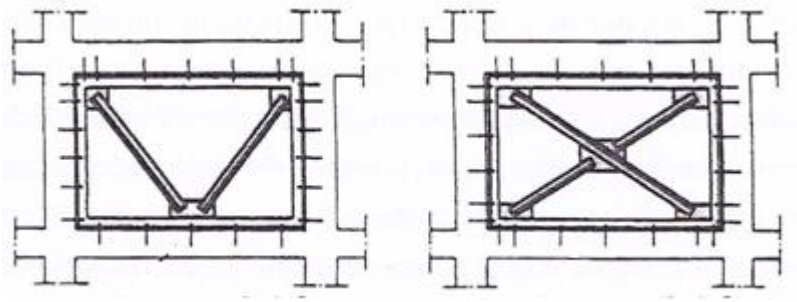

Figure 3.3 Steel Bracings in Frames (Fardis et al.2003)

3.5.3 Extension of Existing Columns with additional Shear Walls

It is an efficient way to increase the ductility of the structure. Furthermore it offers moderate increase of strength and stiffness. It is applied to carefully selected locations of the structure, usually combined with retrofitting of those columns which have inadequate strength and/or ductility.

The shear wall is added towards the direction that the resistance of the structure is inadequate. The addition of shear walls in two directions is common in corner columns.

The shear walls are usually constructed by cast-concrete or they are pre-cast. Unloading of the structure before their construction is recommended, so the shear walls would be able to take part of the vertical loading.

This method is widely applied in Greece, because no specialized personnel are required. Moreover, the uncertainties as it concerns the analysis are much lesser that those of the other methods described above (Fardis et al.2003).

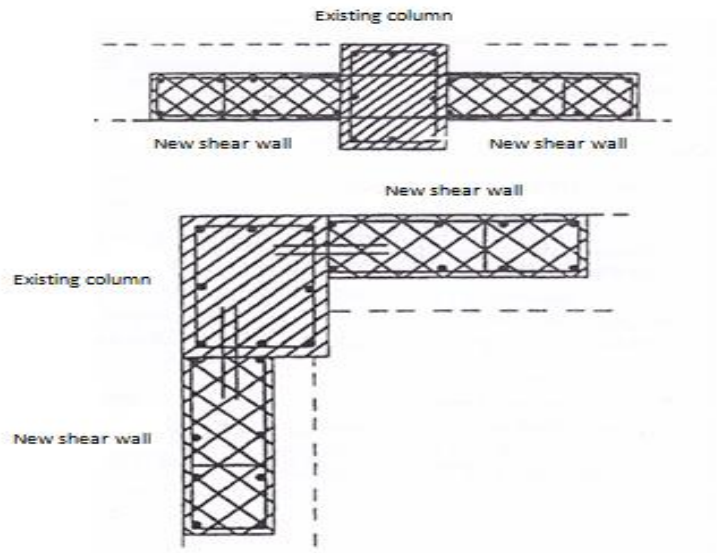

Figure 3.4 Addition of shear walls in the sides of existing columns (Fardis et al.2003)

3.5.4 Columns Retrofitting-The Application of Jackets to Columns

It is the most common method of local retrofitting. The column retrofit is required when the elements have to take loads that exceed their strength. There are two main categories of methods for column retrofitting. The first is the retrofit of columns by increase of their sections and is applied by the application of jackets to the columns. The second one is the retrofit by providing confinement (Spyrakos, 2004).

3.5.4.1 Concrete Jacketing

Concrete jacketing technique is applied by the enlargement of the section of the existing concrete, by adding new concrete, longitudinal and transverse reinforcement.

Figure 3.5 Reinforcement of the concrete jacket (Spyrakos, 2004)

The concrete jackets are applied to columns (or to walls) for the following purposes:

- Increasing of the bearing capacity
- Increasing the flexural and/or shear strength
- Increasing the deformation capacity
- Improving the strength of deficient lap-slices

The thickness of the jacket should be enough for the placement of longitudinal and transverse reinforcement, with an adequate cover (EN 1998-3, 2005).

3.5.4.2 Retrofitting of Columns with Confinement

Retrofitting of columns with confinement is capable under the following circumstances:

- When increase of the ductility of the column is required
- When increase of the shear strength of the column is required
- When a maximum increase of 30% of the compression strength of the concrete is sufficient
- When the bond failure of the vertical reinforcement of the column at the area of overlap, is probable.

The confinement of reinforced concrete columns may be achieved by several techniques:

- Steel angle collars: they usually are steel sheets of thickness 1-2mm or FRP sheets.
- Prestressed steel angle collars
- Spiral reinforcement made of steel sheet or FRP.
- Steel jacket made of steel sheets or FRP

The use of FRPs is widely used nowadays (Fardis et al.2003). Their properties, such as the high-strength-to-weight and the stiffness-to-weight ratios, the resistance to electrochemical corrosion and their easily handling make FRP material superior in comparison with other conventional materials in strengthening applications (Belarbi et al.2013).

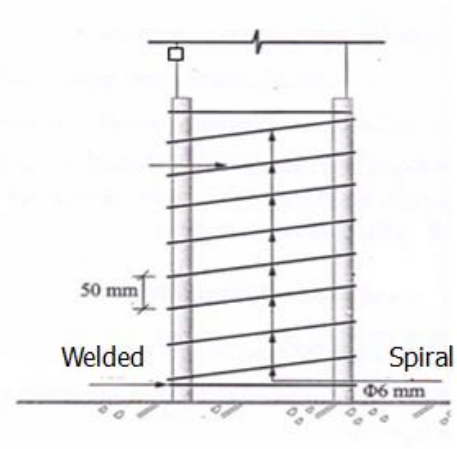

Figure 3.6 Confinement using spiral reinforcement (Fardis et al.2003)

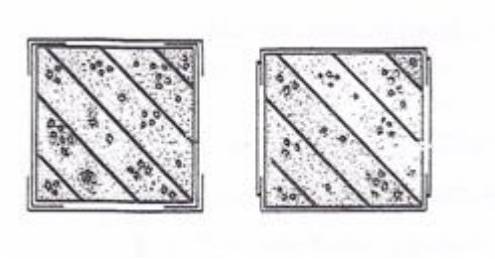

Figure 3.7 Confinement using steel sheets (Fardis et al.2003)

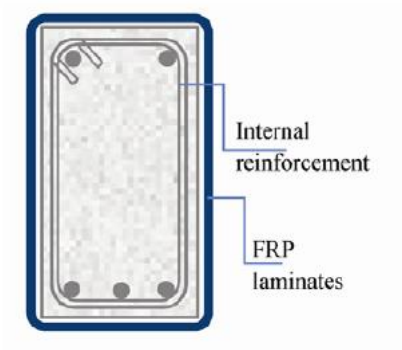

Figure 3.7 Complete FRP wrapping (Belarbi et al.2013)

No matter which technique is used, confinement has a significant impact to concrete behaviour. The ductility and the compressive strength of the confined element are extremely increased.

CHAPTER 4

Modelling of the structure using SAP 2000

4.1 SAP2000 Overview

SAP2000 is general-purpose civil engineering software. It is ideal for the analysis and design of any type of structural system. 2D, or 3D systems of complex or simple geometry may be modelled, analyzed and designed. The object-based modelling environment streamlines and simplifies the engineering process. Its features include integrated modelling templates, code-based loading assignments, design-optimization procedures, advanced analysis options, and customizable output reports (CSi Knowledge Base, 2013).

Modelling

There is a broad range of modelling options. Model domain may be component, system, or global-level in scope, while encompassing sub-grade components and soil-structure interaction.

The members may be linear or curved, cables and post-tensioned tendons, link elements to model springs, dampers, isolators and the associated nonlinear and hysteretic behaviour. Moreover, modelling options are the frame elements, shells or multi-parametric shells, solid elements with isoparametric formulation, and nonlinear response. Section designer is available for the design of custom cross sections. The member properties are automatically calculated by the section designer once the user specifies the geometry of the section and the material composition. In addition, bi-axial interaction and moment-curvature diagrams are generated by the section designer.

Once the object-based model is created, it is automatically converted into a finite-element model by meshing the material domain with an efficient network of quadrilateral sub-elements.

It is an exceptional tool for modelling structural systems of any complexity and any project type (CSi Knowledge Base, 2013).

Loading

Forces such as seismic, wind, vehicle, wave, and thermal may be automatically generated and assigned according to a suite of code-based guidelines. An unlimited number of load cases and combinations may be defined and enveloped by the user (CSi Knowledge Base, 2013).

Analysis

SAP2000 is capable of any analysis type, ranging from simple static, linear-elastic, to more complex dynamic and nonlinear-inelastic. Eigen analysis and Ritz analysis are also included in the options.

Material nonlinearity can be used to capture inelastic and limit-state behaviour. Plastic hinging may be specified in flexural members according to code-based standards or empirical data (CSi Knowledge Base, 2013).

Available for earthquake simulation are both static and dynamic methods. Modal, uniform, or user-defined lateral load patterns may be considered in nonlinear static pushover analysis. The plastic-hinging behaviour of slender elements, shear walls and steel plates may be determined. The formulation of demand capacity spectrum and the performance point calculations may be performed (CSi Knowledge Base, 2013).

Dynamic methods include:

- Response Spectrum (for likely maximum seismic response given pseudo-statical acceleration vs structural period curve)
- Power-spectral-density and steady state (for fatigue behaviour with optional damping and complex-impedance properties)

- Time history analysis, which may follow modal or direct integration methods.

Design and Output

Design is fully integrated with the analysis process. The results are enveloped, before the steel members are sized or the reinforced-concrete sections are designed. American, Canadian, and a variety of international standards (including EN 1998-2) are available (CSi Knowledge Base, 2013).

Output and display options are intuitive and practical. A few of the graphics available upon the conclusion of analysis are: finalized member design, deformed geometry per load combination or mode shape, moment, shear, and axial-force diagrams, section-cut response displays and animation of time-dependent displacements. Reports for the presentation of images and data are automatically generated. (CSi Knowledge Base, 2013).

4.2 History and Description of the Structure

The reinforced concrete hotel was constructed in 1967 in Greece. The building was designed and constructed under the provision of the national codes of Members of Reinforced Concrete (1954) and of the Design Code for Earthquake Resistant structures (1959). The code of 1959 did not provide safety against earthquakes in comparison with the modern codes. Furthermore, the seismic actions according to the code of 1959 were significantly reduced in comparison with the ones supposed by the Eurocodes. The detailıng of members and other particular rules were not included in the code for concrete members of 1954. In other words, the code was adequate for structures subjected only to vertical loads. As a result the majority of the buildings that were built before 1984 (when the basis of the modern codes was introduced) do not have a structural system to resist lateral loads in their both main horizontal axes. They are unsafe and vulnerable to earthquake motion. Inelastic behaviour, ductility and capacity design were completely unknown.

The hotel is in seismic zone 2 (Z2, $a_{GR}/g=0.24$). It is a 5-storey reinforced concrete building with underground floor, ground floor (two levels), mezzanine

floor, approachable and non approachable roof. The total number of levels is 11. Its overall high is 27.53m, including the non approachable roof, while the typical high of floors is 3.2m (except the underground, ground and mezzanine floor). The reception of the hotel is at the North of the ground floor, while at the south of the ground floor there are shops. The floor plan for all the stories is common.

The floor plan of the building is polygonal, with dimensions 21.00m, 14.85m, 12.7m, 10.76m as shown in the typical floor plan (figure 4.1).

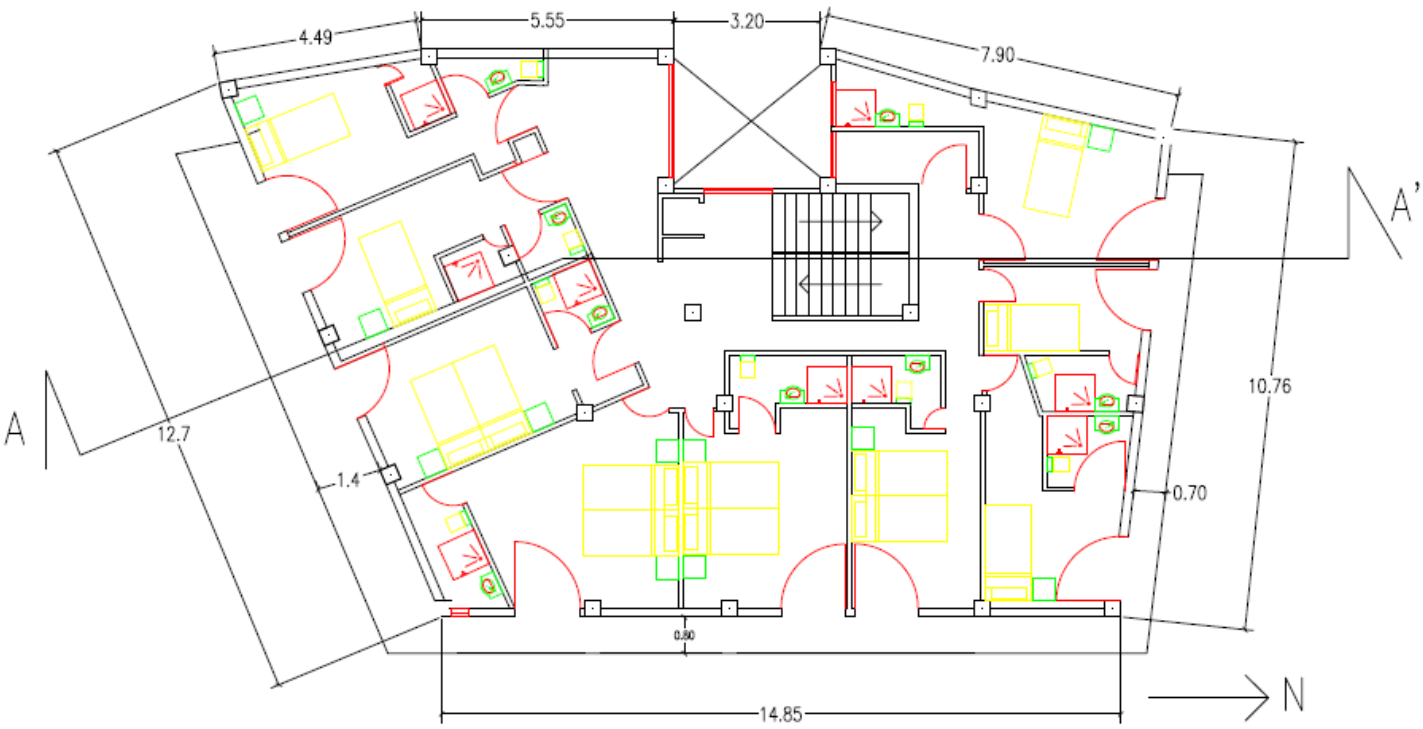

Figure 4.1Typical Floor Plan

The structural system consists of columns, beams and slabs. Hence it is a frame system (in both X and Y axes), which according to EN 1998-1 (2004) is a structural system in which both the vertical and lateral loads are mainly resisted by spatial frames, whose total shear resistance at the building base exceeds 65% of the total shear resistance of the whole structure. In the perimeter of the underground floor, there are reinforced concrete shear walls. The underground floor is considered to be unshakable.

The slenderness $\lambda=L_{max}/L_{min}$ of the building in plan is $\lambda=21.00/11.7134=1.79<4$. However the plan configuration is not compact, since the area between the outline of the floor and a convex polygonal line enveloping the floor exceeds 5% of the floor area for some of the set-backs (EN 1998-1, 2004). Hence the criteria for regularity in plan are not satisfied and a spatial model is required for the analysis of the building.

The building is regular in elevation, since setbacks do not exist at any floor level, the frames run from their foundations to the top of the building without interruptions and both the lateral stiffness and the mass of the building remain constant from the base to the top.

The building floor slabs including the approachable roof act as horizontal diagrams, collecting and transmitting the inertia forces to the vertical structural system and ensure that those systems act together in resisting the horizontal seismic action.

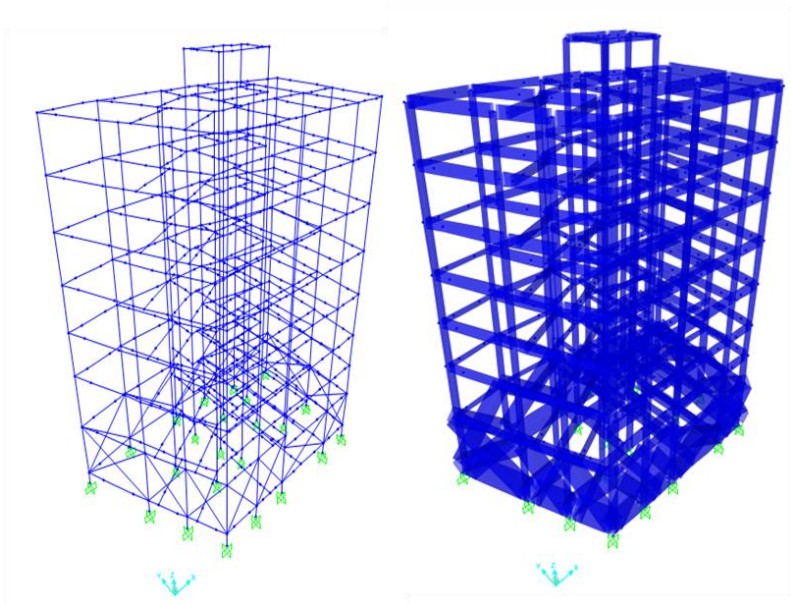

Figure 4.2 Building Model in SAP2000

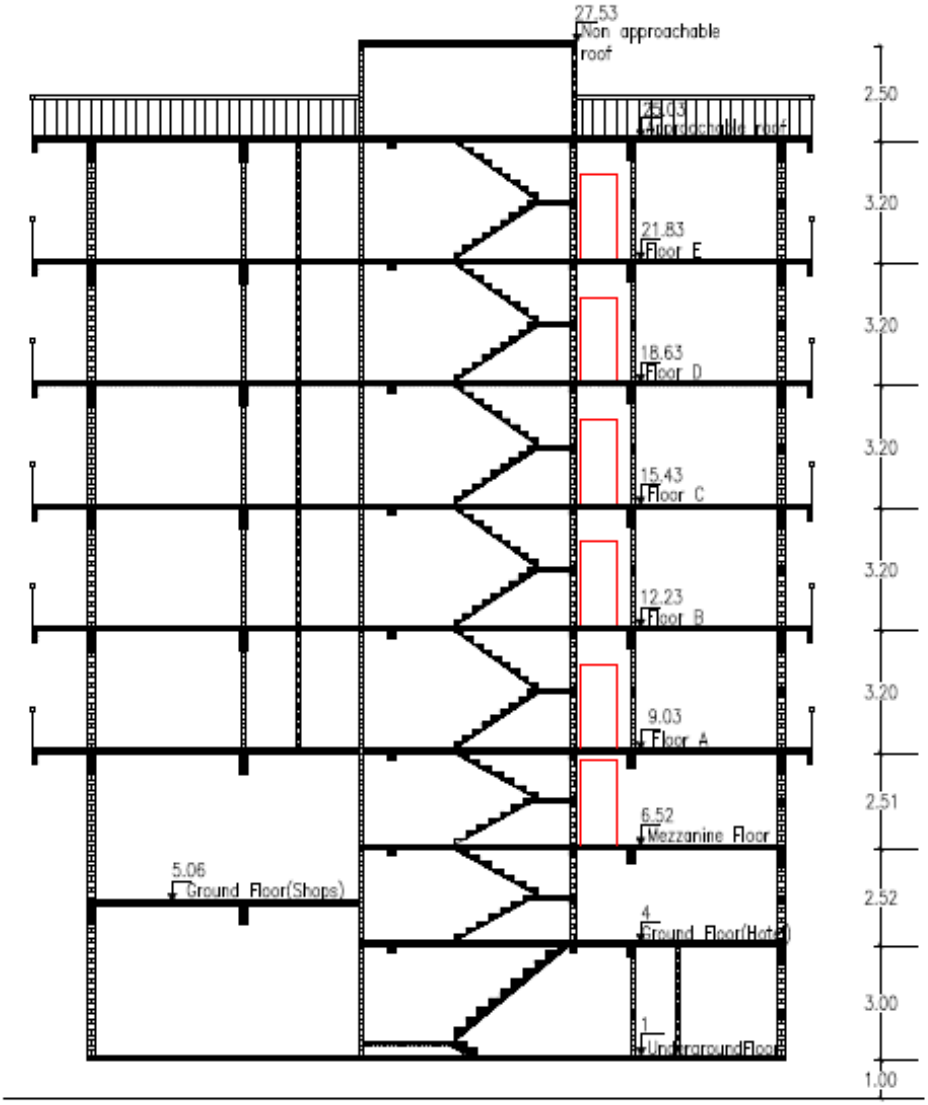

Figure 4.3 Section A-A'

As shown in the A-A' section, the level z=0m is considered at the foundation level in order to be compatible with SAP2000 model, and not at the ground level.

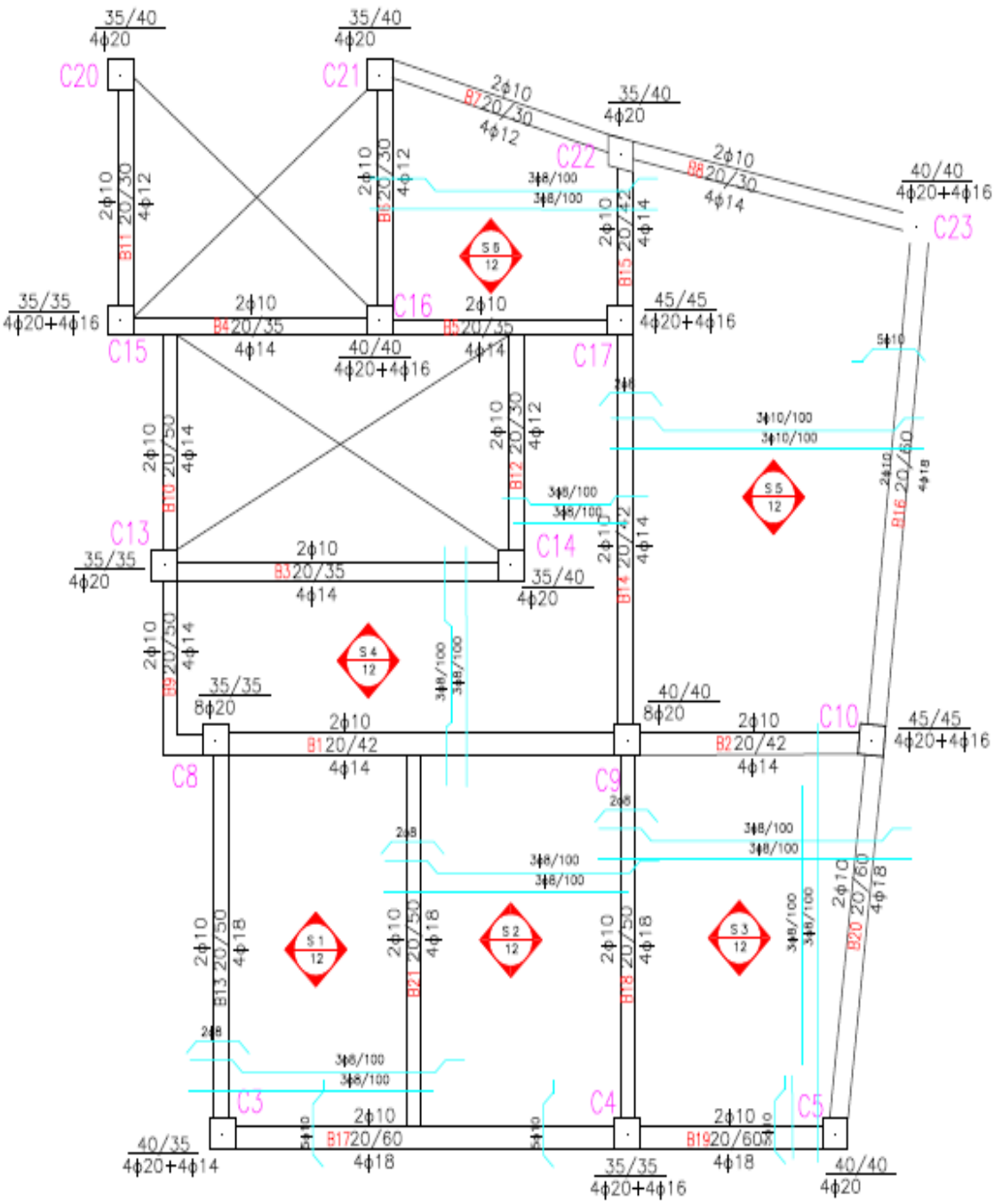

Figure 4.4 Ground Floor-Hotel (4m)

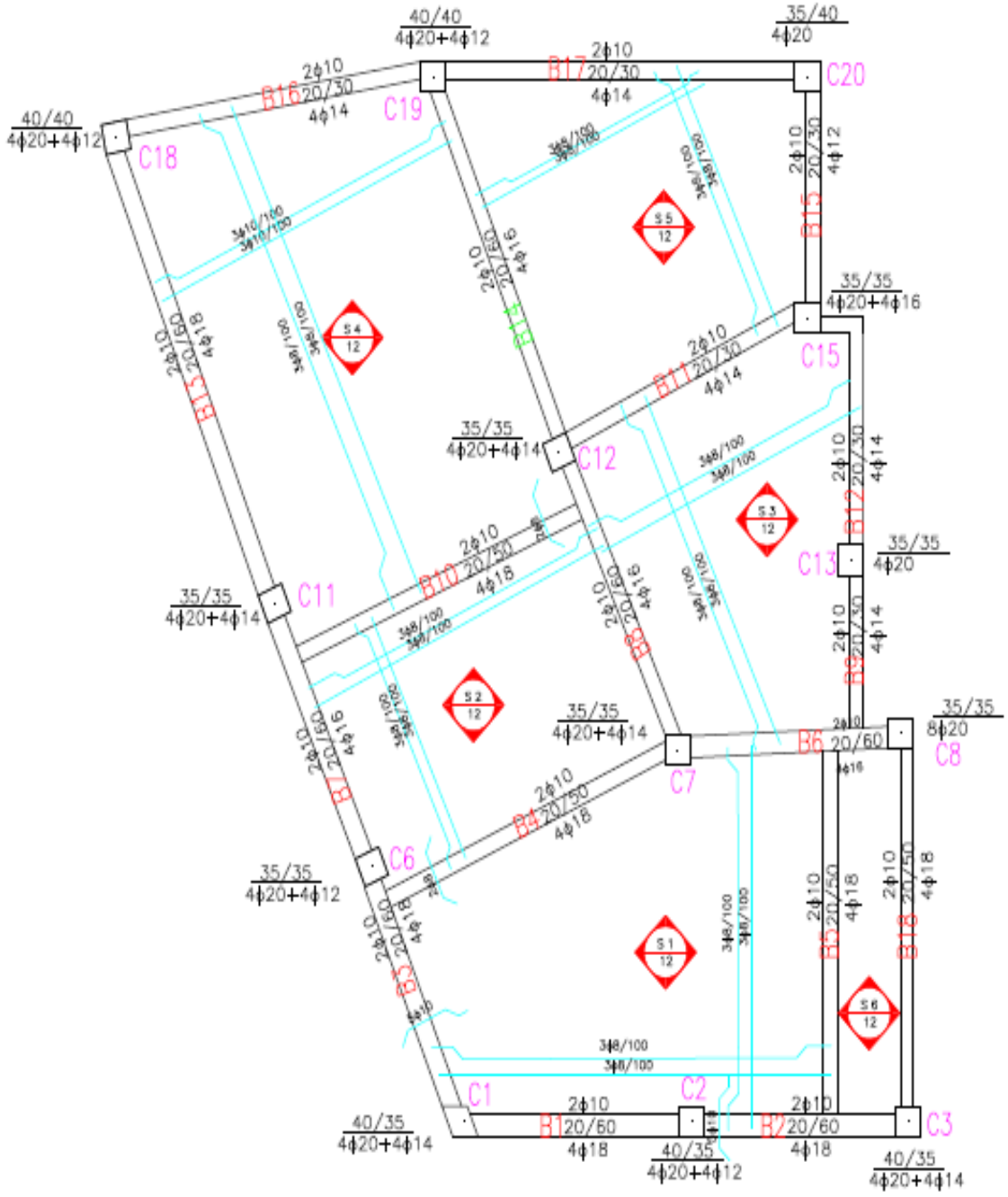

Figure 4.5 Ground Floor-Shops (5.06m)

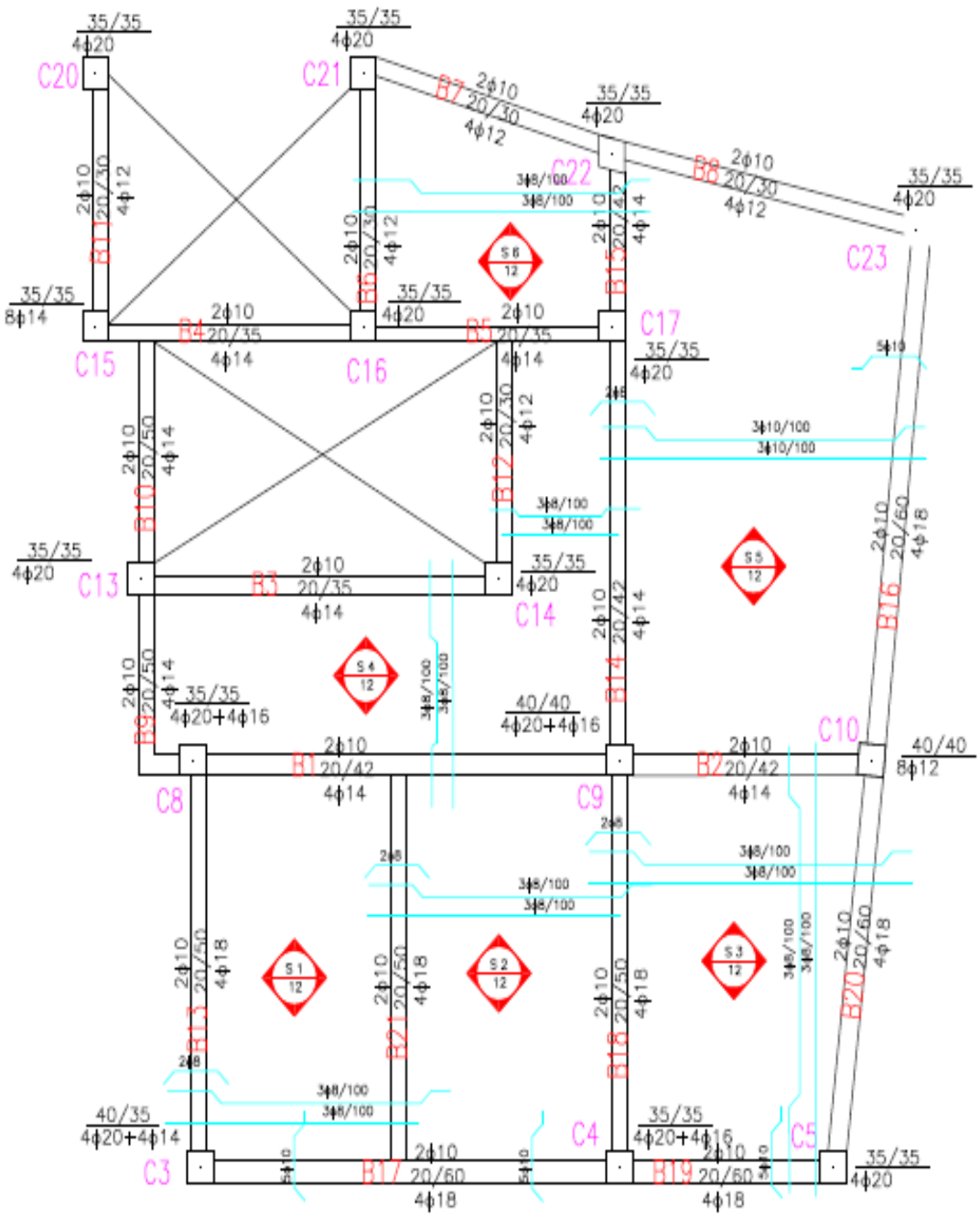

Figure 4.6 Mezzanine Floor (6.52m)

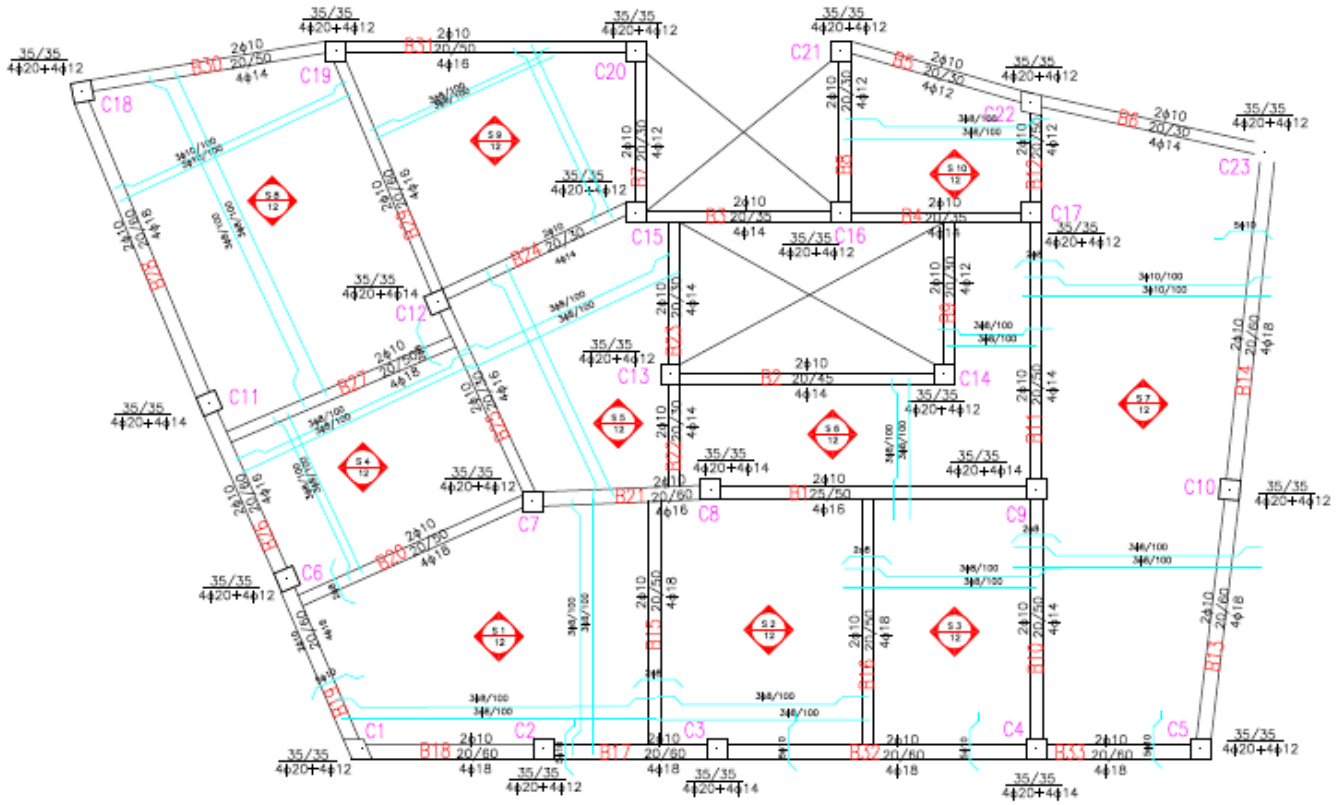

Figure 4.7 Floor A (9.03m)

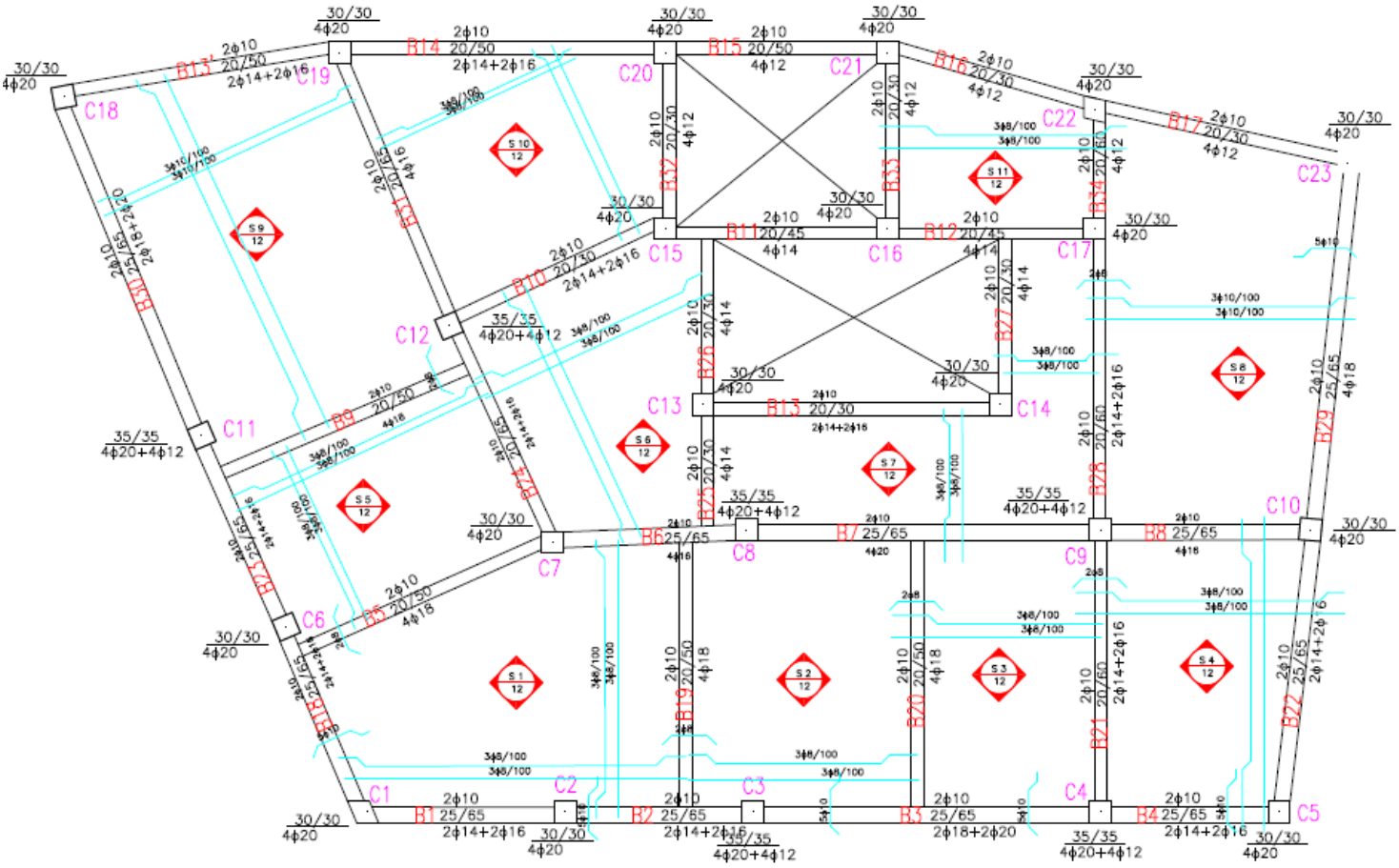

Figure 4.7 Floor B (12.23m)

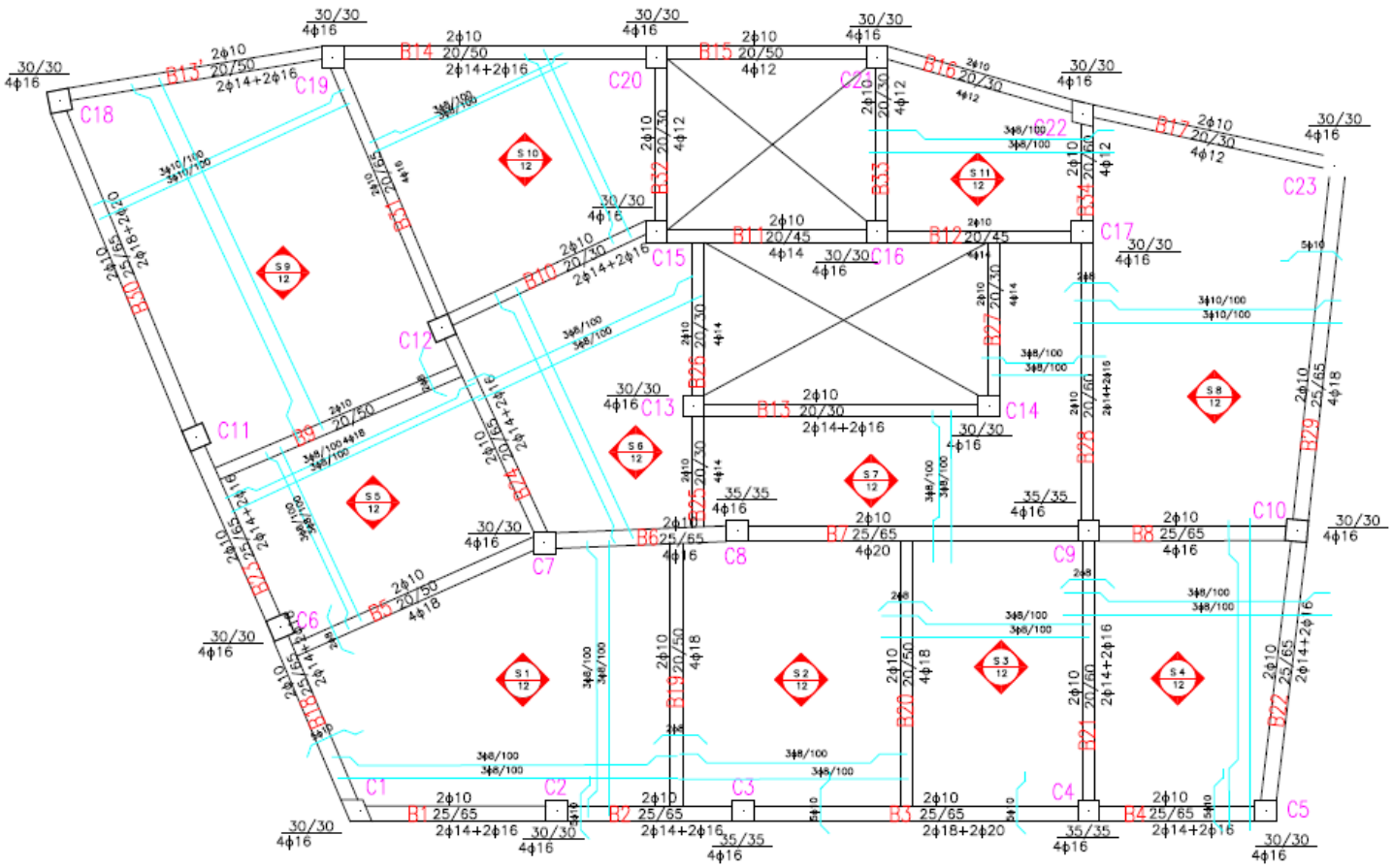

Figure 4.8 Floor C (15.43m)

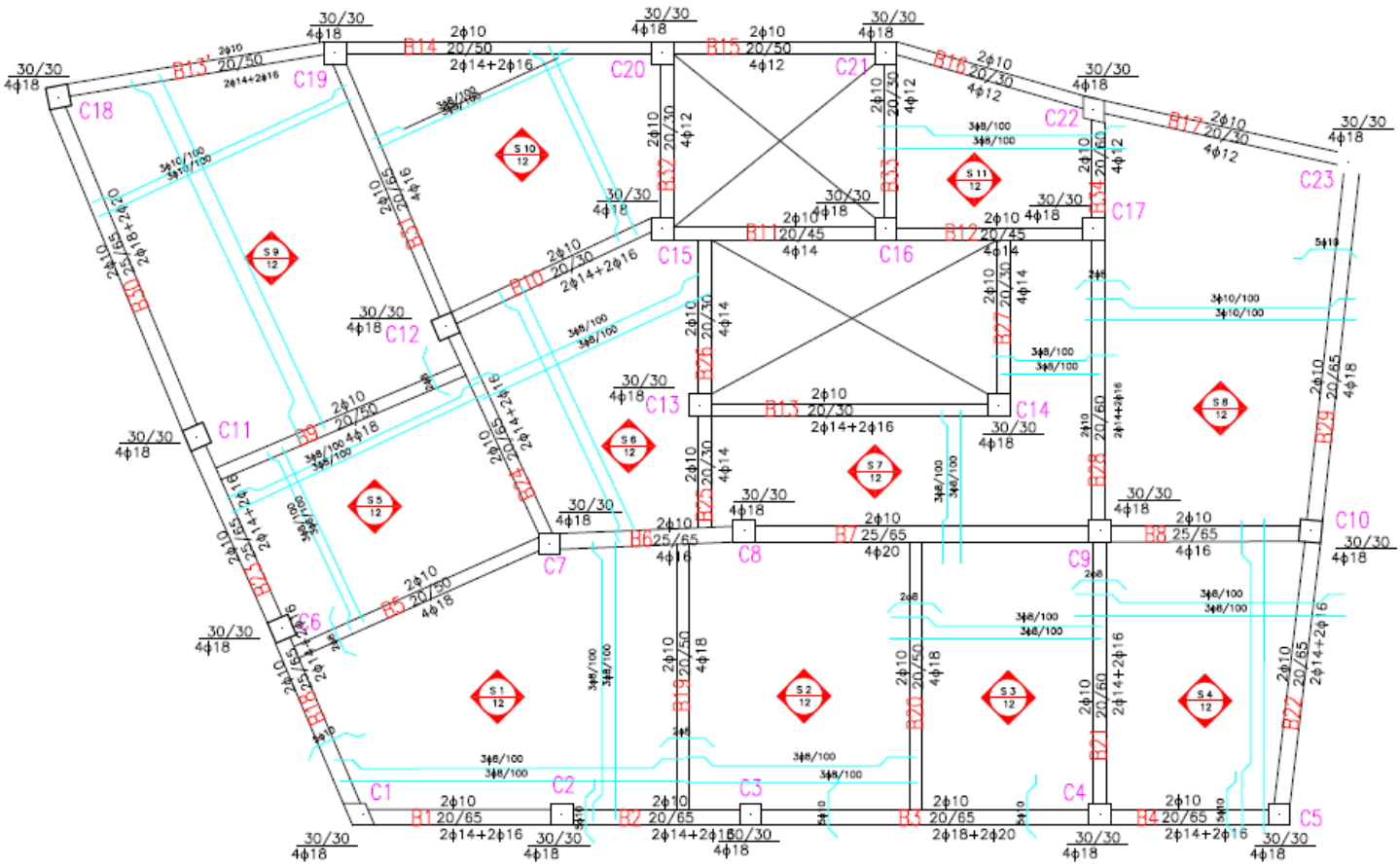

Figure 4.9 Floors D and E (18.63m and 21.83m respectively)

4.3 Modelling of the Structure in SAP2000

The model is spatial. It consists of vertical and horizontal frame elements of orthogonal sections, representing the columns and the beams, respectively. It is mentioned that the beams are modelled as orthogonal sections, not as flanges. The slabs and the infill walls are not modelled, however not only their permanent and imposed loads, but also the diaphragmatic behaviour of the slabs, are taken into account. The shear walls in the perimeter of the underground level are modelled as extremely stiffed bracings. Soil-structure interaction is neglected. The foundation is considered fixed into the ground.

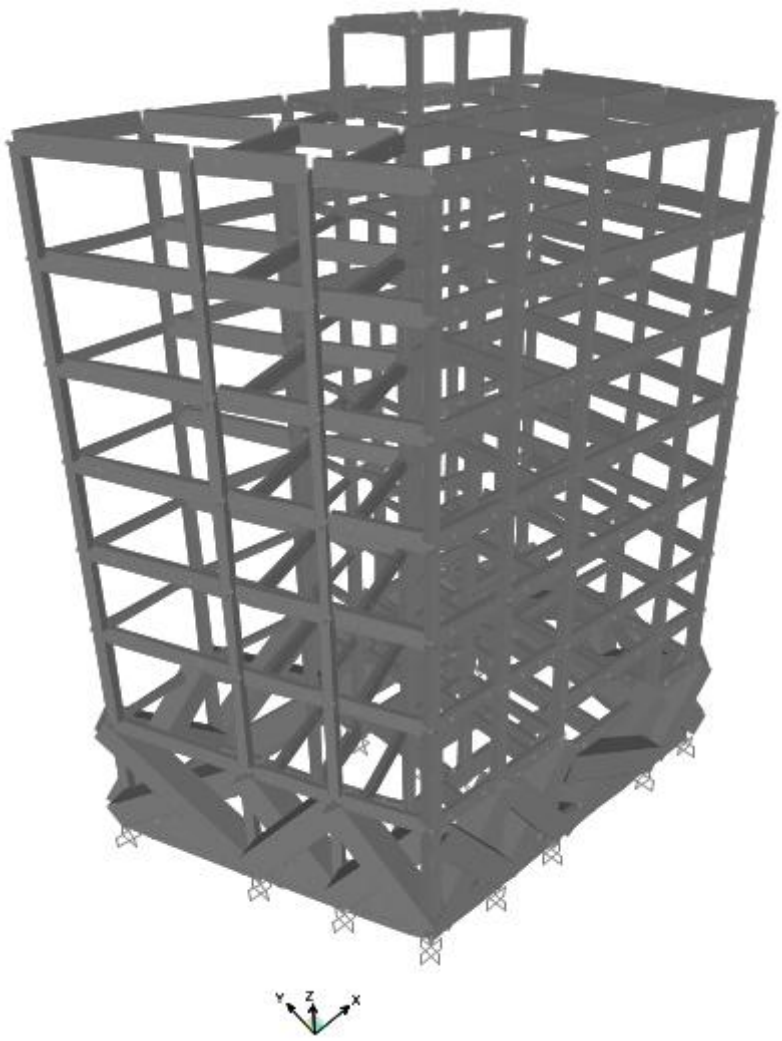

Figure 4.10 Model of the Building in SAP2000 (Extrude View)

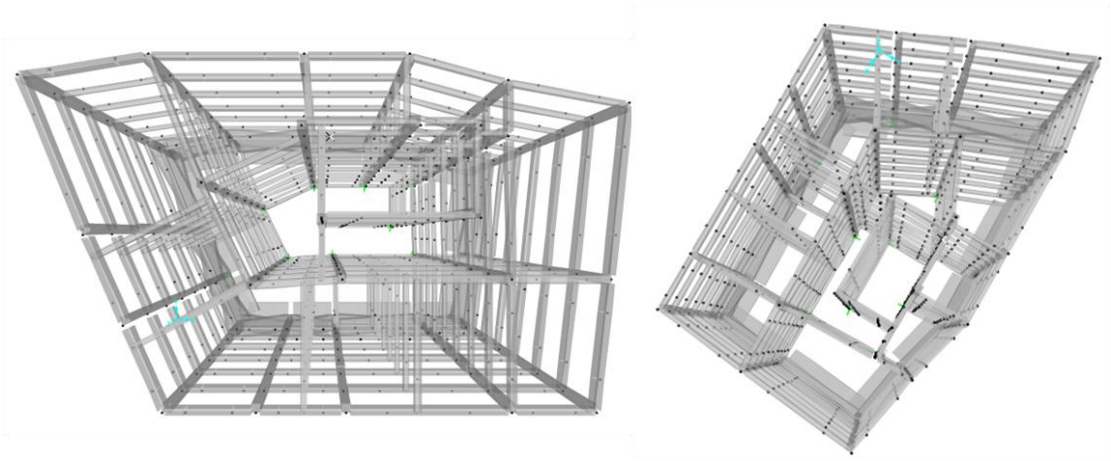

Figure 4.11 Elevation View of the Building

4.3.1 Material Properties

The required information about the geometry of the structure and its elements is taken from the existing construction drawings. They were collected by the local town planning authorities having the owner's consent. However information about the reinforcement details is not available.

Assumptions are made about the mechanical properties of the materials, according to common practices of the time of the construction. In addition, it is assumed that full knowledge is succeeded; hence the confidence factor is taken equal to the unit (CF=1).

Concrete B160 is used. It corresponds to strength class C12/15 according to EN1992-1 (2004). Its most important strength and deformation characteristics are:

Characteristic compressive cylinder strength of concrete at 28 days: f_{ck}=12 MPa

Characteristic compressive cube strength of concrete at 28 days: $f_{ck,cube}$=15 MPa

Mean value of concrete cylinder compressive strength: f_{cm}=20 MPa (f_{cm}= f_{ck}+8)

Mean value of axial tensile strength of concrete: f_{ctm}=1.6 MPa

Young's modulus: E_{cm}=27 GPa

Stain at maximum unconfined compressive strength, f'_c: ε_{c1}=1,8 ‰

Ultimate unconfined stain capacity: ε_{cu1}=3,5 ‰

The steel class of reinforcing bars is assumed STAHL 1, with minimum yield point 2200kg/cm^2 and minimum tensile stress 3400-5000 kg/cm^2, according to the reinforced concrete code of 1954. The young modulus of the steel is assumed equal to E_s=200 GPA. STAHL 1 corresponds to S220. (Reinforcing Steel New Regulation, 2008)

The material properties are defined following the steps shown below:

Define ⇒ Materials ⇒ Add New Material

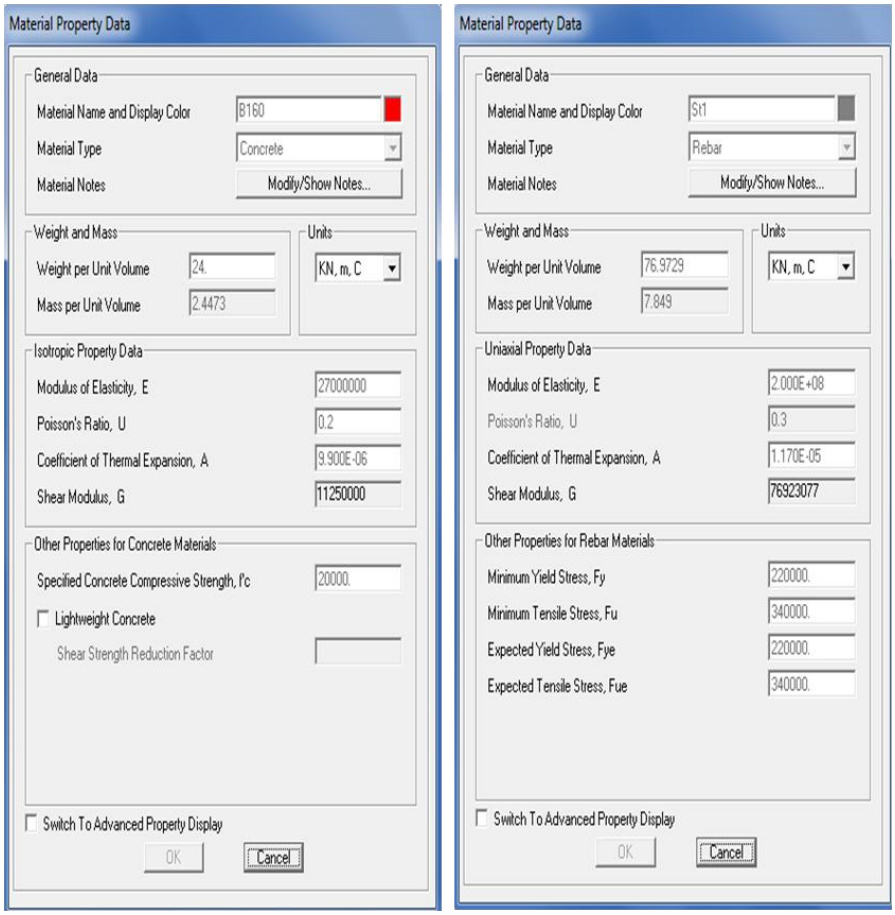

Figure 4.12 Definition of Material's Properties

The weight per unit volume of the concrete is defined 24kN/m^3 since the sections are considered lightly reinforced.

The Nonlinear Material Data, which is necessary for the inelastic analyses, is also defined for both materials, as shown in the figures 4.13 and 4.14.

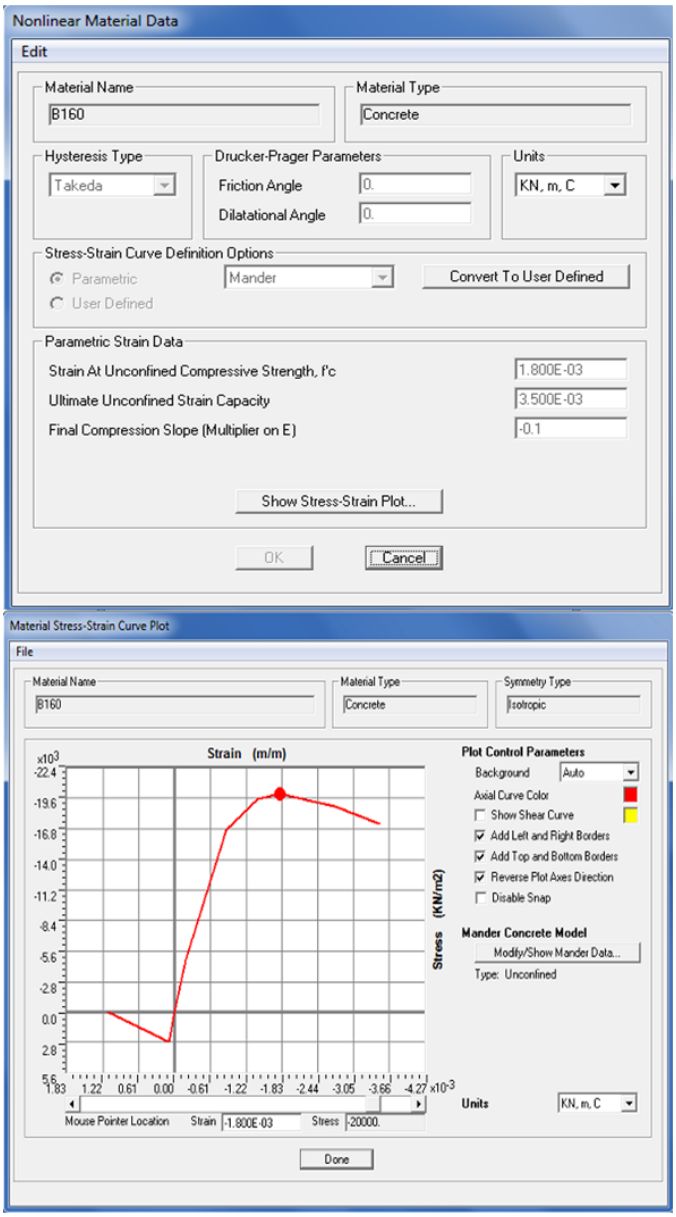

Figure 4.13 Definition of Nonlinear Concrete Properties and Stress-Strain Curve

Nonlinear material behaviour may be taken into account through a directional material model, in which uncoupled stress-strain behaviour is modelled for one or more stress-strain components (CSi, 1995).

For each material an axial stress-strain curve that represents the direct (tension-compression) stress-strain behaviour of the material along any material axis may be specified.

Concrete is an isotropic material. Thus the stress-strain curve represents the behaviour along each of the three axes σ11-ε11, σ22-ε22, σ33-ε33. The nonlinear stress-strain is the same in each direction (CSi, 1995).

Steel is a uniaxial material, thus the stress-strain curve represents the relationship between σ11 and ε11.

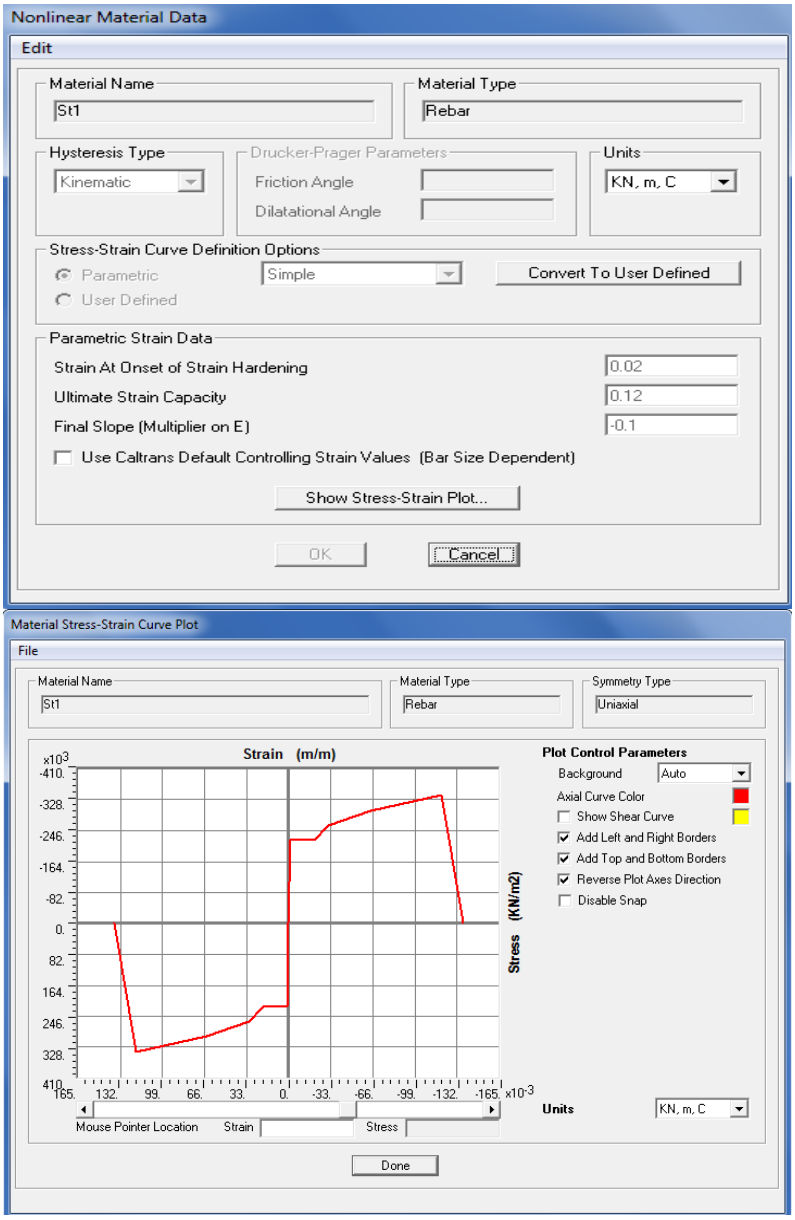

Figure 4.14 Definition of Nonlinear Steel Properties and Stress-Strain Curve

The hysteresis type defines the nonlinear stress-strain behaviour of the material when the load is reversed.

Kinematic hysteresis type is the default hysteresis model for all metal materials in the program, because it is based upon kinematic hardening behaviour that is commonly observed in metals. A significant amount of energy is dissipated by this model, thus it is appropriate for ductile materials (CSi, 1995).

Takeda model uses a degrading hysteretic loop. It is suitable for concrete or other brittle materials. Less energy is dissipated than the Kinematic model (CSi, 1995).

It is mentioned that the weight per unit volume of the concrete of the underground shear walls is not equal to the weight per unit volume of the concrete material shown in figure 4.12. The shear walls are modelled as bracings of $1m^2$ sections, and the weight per unit volume is adjusted in order to result in the real self-weight of the shear walls, which dimensions are:

Width: 0.2m

Height: 3m (for the shear walls underneath the hotel)

Height: 4.06m (for the shear walls underneath shops)

Their self-weight is:

Shear wall underneath hotel: $W = 24 \cdot 0.2 \cdot 3 = 14.4 kN/m$

Shear wall underneath shops: $W = 24 \cdot 0.2 \cdot 4.06 = 19.488 kN/m$

The weight per unit volume is adjusted so as the self-weight of the two bracings modelled in each frame is equal to the self-weight of the real existing shear walls.

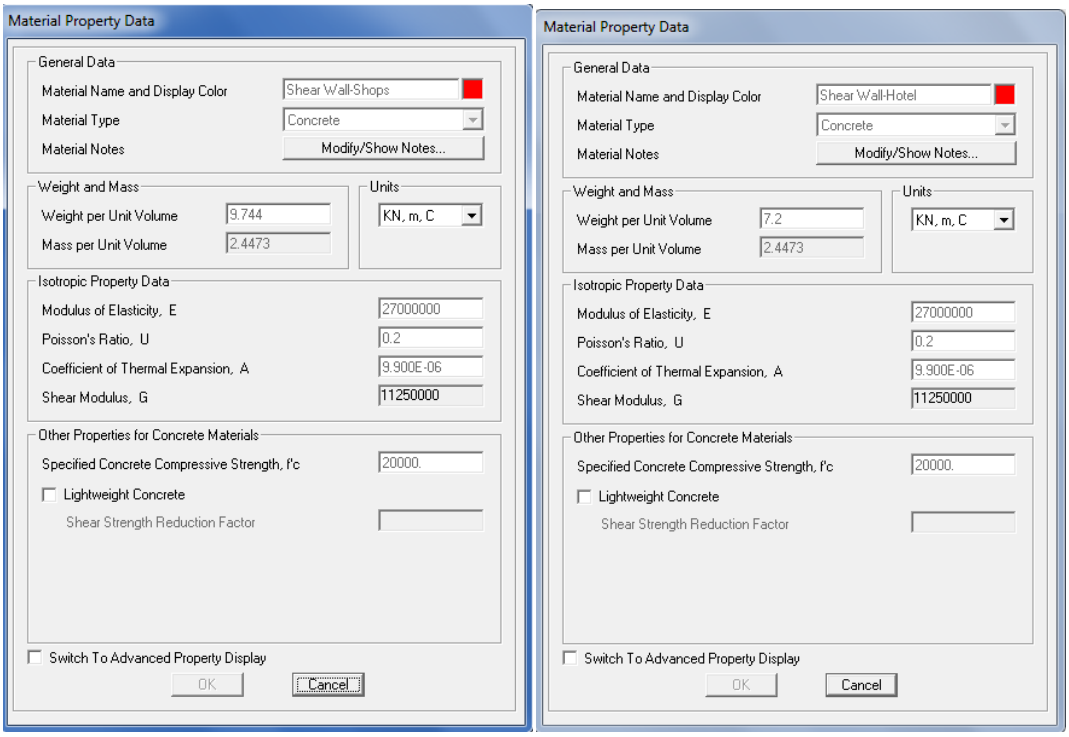

Figure 4.15 Definition of Weight per Unit Volume of the Underground Shear Walls

4.3.2 Frame Sections

All the elements of the structure (except slabs) are designed using the section designer, where sections of arbitrary geometry and combination of materials may be designed. The geometric properties (areas, moments of inertia etc) are computed automatically. Furthermore, the reinforcing bars may be defined by the user (CSi, 1995).

The sections are modelled following the commands:

Define ⇒ Section Properties ⇒ Frame Properties ⇒ Add New Property ⇒ Other ⇒ Section Designer

The "concrete column" (even though the element may not be a column) and "reinforcement to be checked" options must be selected as indicated in the figure 4.16. This option is used to specify whether the concrete member is to have its specified reinforcing checked, or new longitudinal reinforcing designed, when it is run through the concrete frame design postprocessor (CSi, 1995).

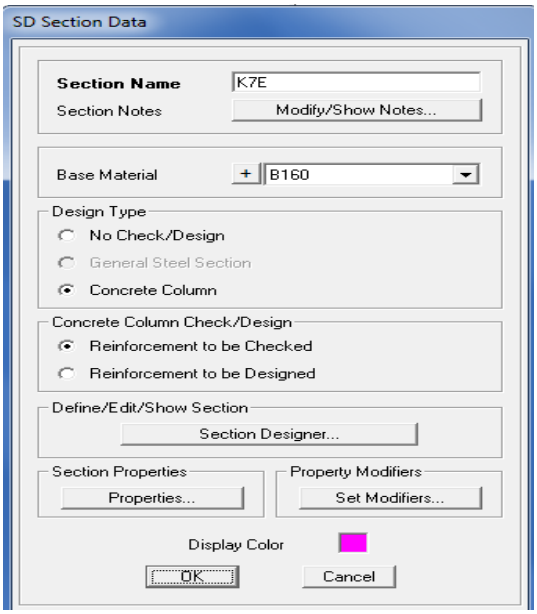

Figure 4.16 Selection of "Concrete Column" and "Reinforcement to be Checked" options

The steel and concrete characteristics that defined in 4.3.1 are selected. It is assumed that the concrete cover is 0.02m.

In addition, all the frame sections are considered unconfined. The significance of the shear reinforcement was underestimated by the codes of 1954 and 1959. Thus, it is assumed that the long spacing between the stirrups do not provide confinement to the sections.

As known, the bending moments act at the bottom, in the mid-span of a beam and at the upper side of the section in the edge-spans. Thus the longitudinal reinforcing bars were placed at the bottom of the section in the mid-spans and at the upper side at the edge-spans of the beams.

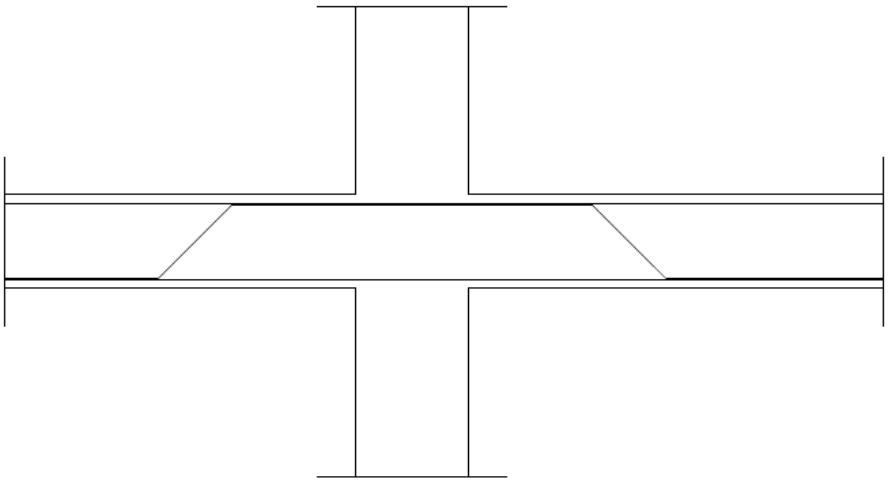

Figure 4.17 Beam Longitudinal Reinforcement at the Bottom of the Section in the Mid-spans and at the Upper Side at the Edge-spans

Each beam is divided into 3 parts, one mid-span-longitudinal reinforcing bars at the bottom and two edge-spans-longitudinal reinforcing bars at the top of the section. It is assumed that each edge-span length is 25% and the mid-span length is 50% of the total length of the beam. The beam parts are connected through joints.

This is the best way to design the beams using the section designer. The section designer is useful because it is able to calculate the yield bending moment (M_y) and curvature (Φ_y) of the section (which is required for the calculation of secant stiffness-explained in 6.2) automatically.

Besides the main longitudinal reinforcement of the beams, 2Φ10 is considered at the top for both the mid-span and the edge-span.

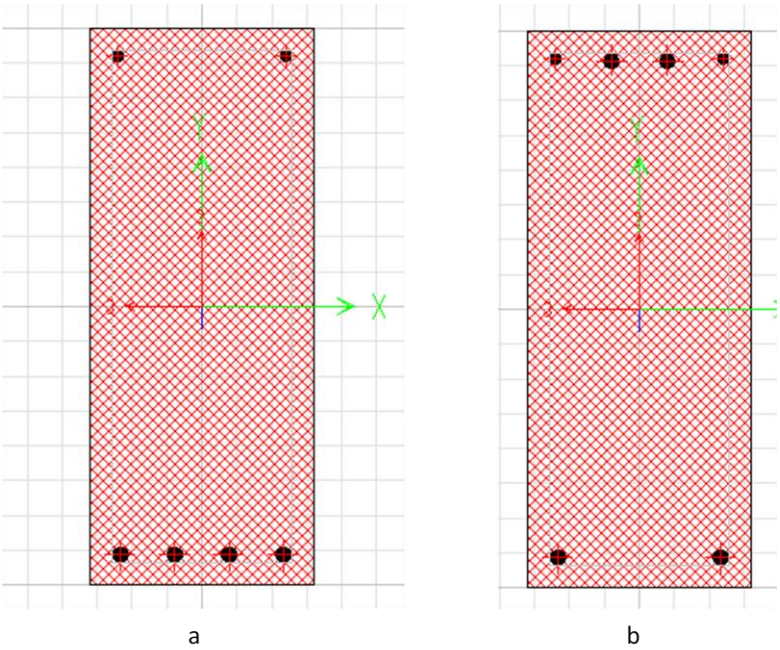

Figure 4.18 a) B20x50 4Φ14 (mid-span) b) B20x50 4Φ14 (edge-span)

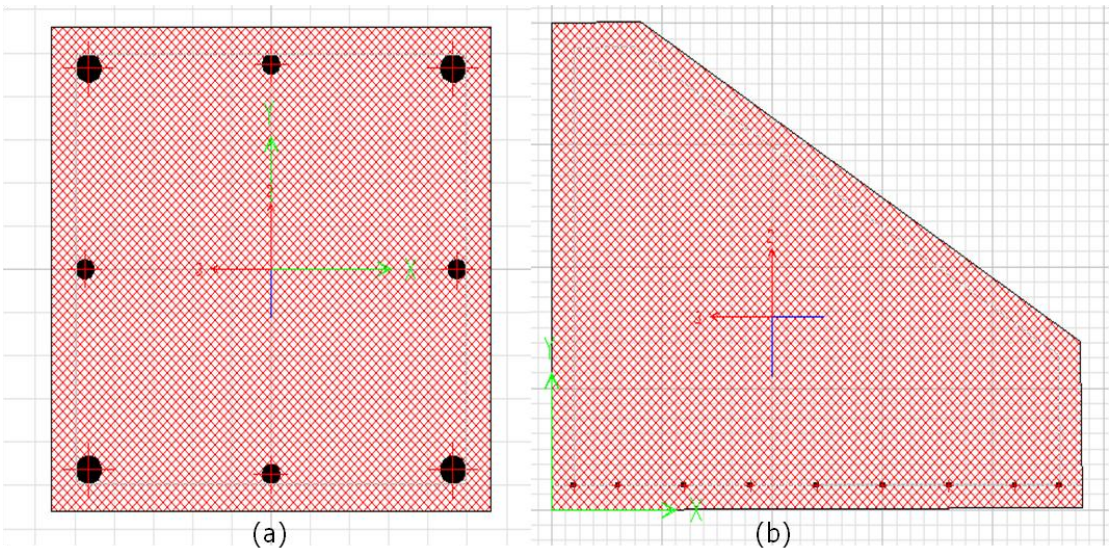

Figure 4.19 a) Column (C11A) b) Strip Foundation (in the perimeter of the foundation)

The columns in the foundation level of the building are connected to each other through connecting beams.

Strip foundation is modelled in the perimeter of the building at the foundation level. The underground shear walls are based on the strip foundation.

Once the definition of the frame sections is completed, the elements are designed using a spatial grid, which intersections are exactly at the positions of the joints of the building. It is mentioned that if the beams do not frame into the centre of a column or there are other eccentricities that should be taken into account, the "insertion point" command is used.

Frame elements are modelled as line elements connected at points (joints). However, all the structural members do have finite cross-sectional dimensions. As a result when two elements, for example a column and a beam are connected at a joint, there is some overlap of their cross sections. This overlapping is taken into account in SAP2000 by using the command "end length offsets". The dimensions of the members may be large and the length of overlap may be significant fraction of the total length of an element (CSi, 1995).

The end offsets are automatically calculated from the connectivity. It is considered that the reinforced concrete elements are connected monolithically, thus the "rigid zone factor" is taken equal to the unit. This indicates that the end offsets are fully rigid.

4.3.3 Stiffness- Property Modifiers

The stiffness of the elements has to be modified due to the cracking of the concrete sections. Unless a more accurate analysis of the cracked elements is performed and if linear analyses are applied and the behaviour factor q corresponds to the whole of the structure, the stiffness can be estimated as a percentage of the stiffness of the uncracked sections.

The values that are shown in the table can be used when no more accurate information is available.

Table 4.1 Stiffness of Cracked Sections (KANEPE, 2013)

Structural Element	**Stiffness**
Internal Column	$0.8*(E_cI_g)$
Outer Column	$0.6*(E_cI_g)$
Shear Wall-non cracked	$0.7*(E_cI_g)$
Shear Wall, cracked	$0.5*(E_cI_g)$
Beam	$0.4*(E_cI_g)$

Where: E_cI_g is the stiffness of the uncracked section (elastic).

The values shown in the table 4.1 are used for the linear response spectrum analysis. The secant stiffness of the sections, which is explained in section 6.2 is used for the non linear analyses.

The stiffness may be modified by the option "Property Modifiers" in Sap 2000. Modification factors may be defined as frame section properties and assigned directly to frame objects, or they may be assigned to the frames by selecting them.

For example the commands:

Assign ⇒ Frame ⇒ Property Modifiers may be selected.

The factors that must be modified are the moment of inertia about 3 for the beams and the moment of inertia about 3 and about 2 for the columns, since the columns receive biaxial bending moment about those two local axes.

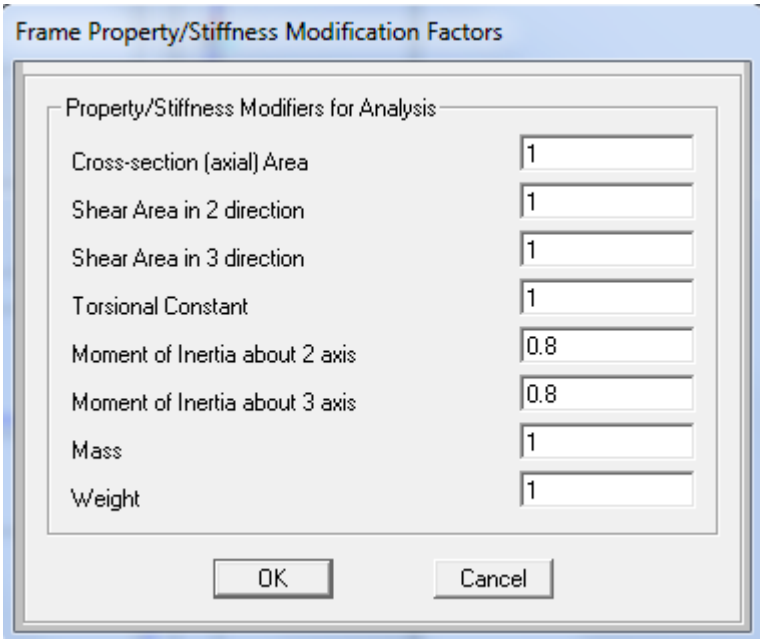

Figure 4.20 Stiffness Modification Factors

4.3.4 Loading

The codes "Rules for Actions on Structures FEK 171A/1946" and the "EN 1991-1-1:2002" (Eurocode 1 Actions on Structures) provide the load values listed in table 4.2.

Table 4.2 Actions on Structures

Actions on the structure	
Self-weight (Permanent Loads)	
Concrete self weight	24 KN/m^3
Floors	1.5 KN/m^2
Roof	1.3 KN/m^2
Strecher Bond	2.1 KN/m^2
Header Bond	3.6 KN/m^2
Imposed Loads (Live Loads)	
Floors	2 KN/m^2
Stairs	3.5 KN/m^2
Balconies	5 KN/m^2
Shops	5 KN/m^2
Approachable Roof	2 KN/m^2
Non Approachable Roof	1 KN/m^2

As mentioned in 4.3 the slabs are not included in the model. Thus the slab load is distributed to the beams according to EKOS (2000) (Greek Code of Reinforced Concrete 2000). The slab is divided into areas through yield lines as shown in the figure 4.21. Each beam is considered receiving the load transmitted through its corresponding slab area. The division of the slab into areas is dependent on the corner supports of the slab. If in the two sides of a corner, the support is common (for example fixed supports) the division angle is 45˚. If one of the sides is completely fixed and the other one is free edge, the division angle towards the fix support is 60˚. For partially fixed supports the angle ranges between 45˚ and 60˚.

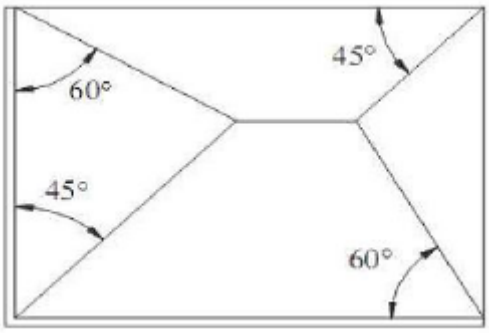

Figure 4.21 Slab Division into Areas for Loading Transfer to the Beams

In the figures 4.22-4.26, the division areas of the slabs are shown. In the tables 4.3-4.9, the total permanent load (due to the slabs and the walls) and the total imposed load (due to the slabs) transmitted to the beams is presented. Detailed calculations are cited in the appendix B.

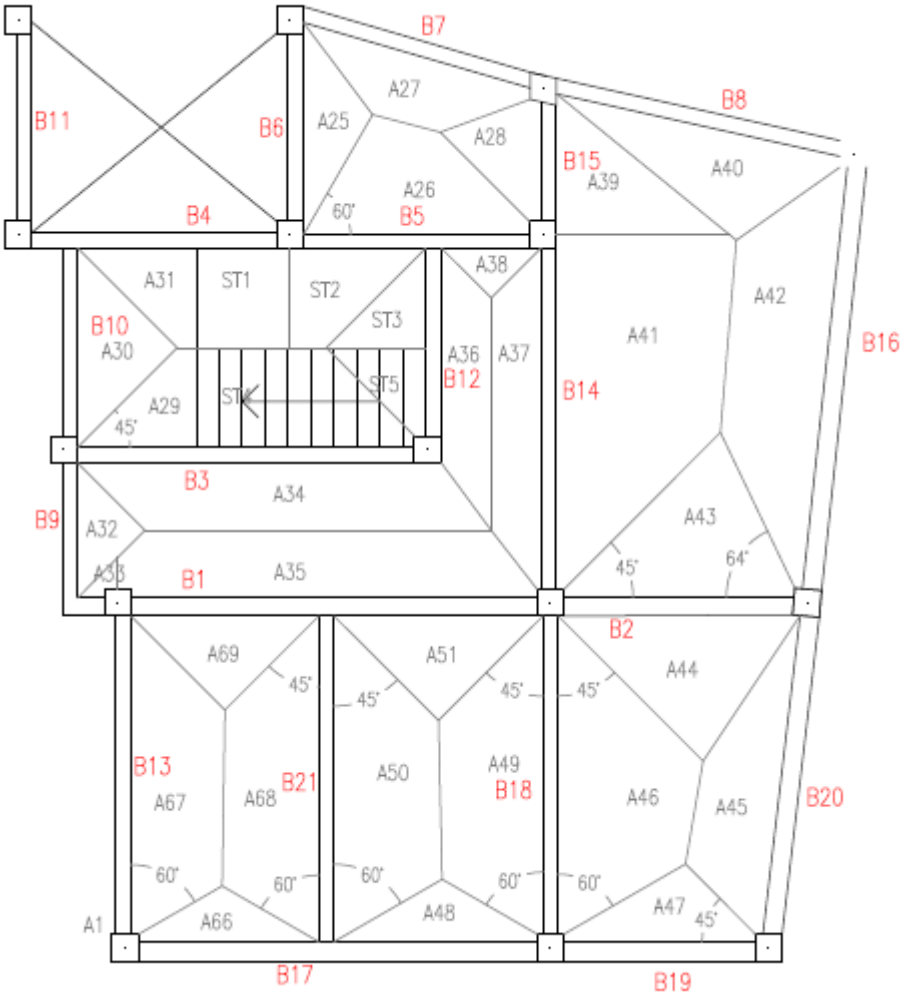

Figure 4.22 Distribution of Slab Load to the Beams - Ground Floor and Mezzanine Floor (z= 4m and 6.52m respectively)

Table 4.3 Load to the Beams-Ground Floor (hotel) z=4m

Beams	Total Permanent Load (KN/m)	Total Imposed Load (KN/m)
B1	6.446	2.943
B2	13.739	4.260
B3	16.074	4.809
B4	11.590	2.470
B5	14.879	3.969
B6	10.227	1.020
B7	10.637	1.208
B8	11.078	1.409
B9	6.179	0.884
B10	7.263	1.380
B11	4.662	0.000
B12	14.374	3.937
B13	8.390	1.894
B14	10.384	4.742
B15	9.386	4.286
B16	11.174	1.946
B17	8.639	0.788
B18	13.920	4.419
B19	9.347	1.112
B20	10.068	1.441
B21	8.708	3.976

Table 4.4 Load to the beams-mezzanine floor (z=6.52m)

Beams	Total Permanent Load (KN/m)	Total Imposed Load (KN/m)
B1	8.456	2.943
B2	11.389	4.260
B3	10.422	4.809
B4	5.938	2.470
B5	9.277	3.969
B6	4.445	1.020
B7	4.855	1.208
B8	5.296	1.409
B9	4.147	0.884
B10	5.031	1.380
B11	2.010	0.000
B12	8.392	3.937
B13	6.058	1.894
B14	12.294	4.742
B15	11.296	4.286
B16	6.272	1.946
B17	3.737	0.788
B18	11.588	4.419
B19	4.345	1.112
B20	5.166	1.441
B21	10.618	3.976

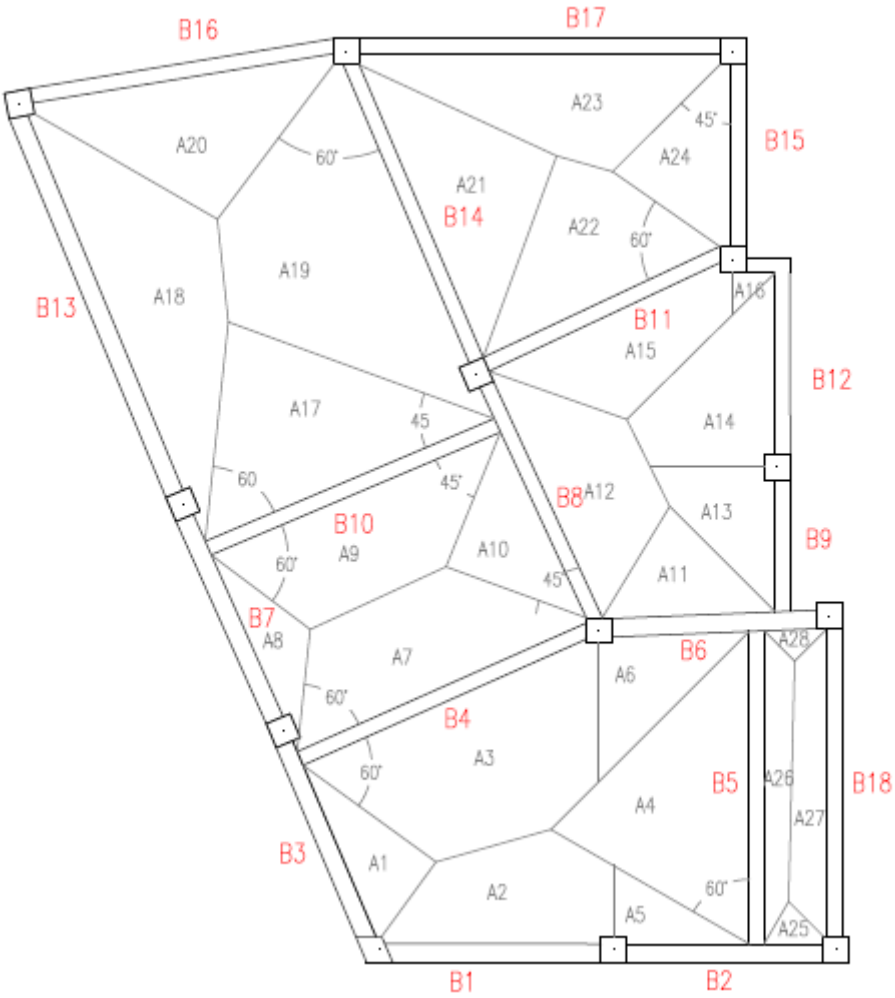

Figure 4.23 Distribution of Slab Load to the Beams-Ground Floor-Shops (z=5.06m)

Table 4.5 Load to the Beams-Ground Floor-Shops (z=5.06m)

Beams	Total Permanent Load (KN/m)	Total Imposed Load (KN/m)
B1	17.685	6.339
B2	14.082	2.226
B3	14.378	2.564
B4	14.337	8.047
B5	7.274	8.304
B6	10.467	3.870
B7	13.831	1.940
B8	6.895	7.871
B9	12.176	5.102
B10	17.328	11.702
B11	16.449	9.980
B12	13.321	6.408
B13	17.028	5.589
B14	12.935	14.766
B15	11.515	4.347
B16	17.730	5.157
B17	17.186	4.536
B18	9.176	2.157

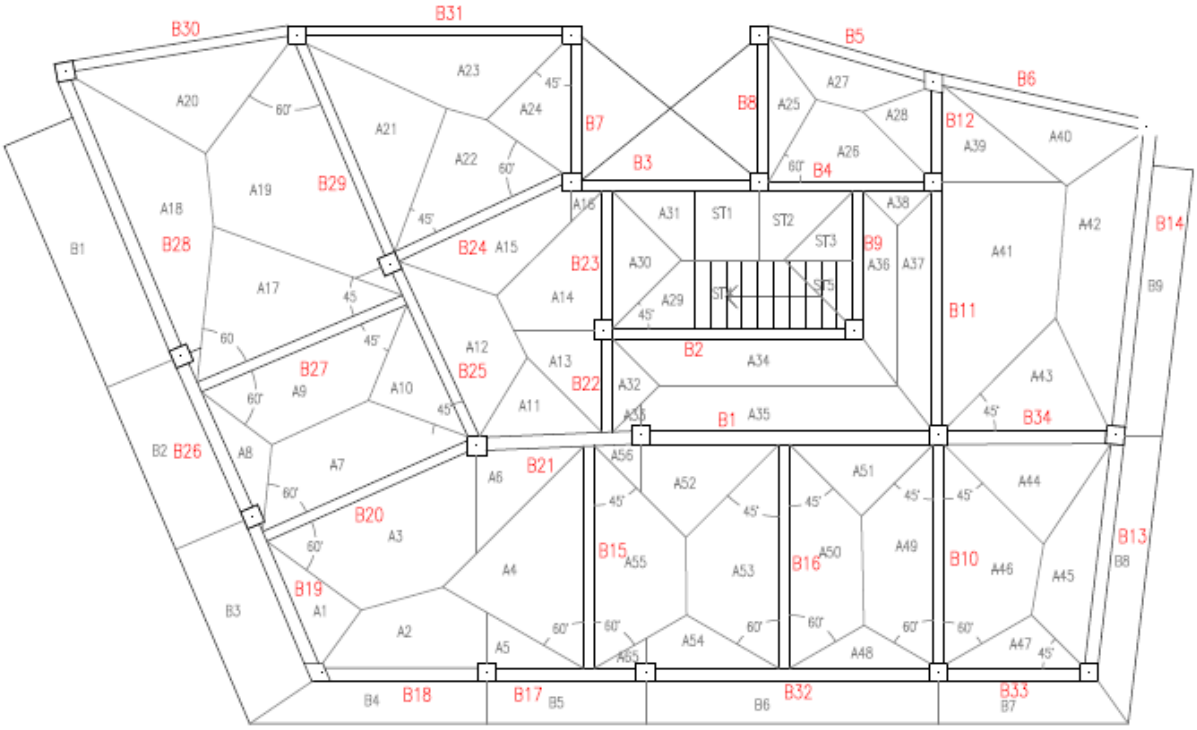

Figure 4.24 Distribution of Slab Load to the Beams – floor A (z= 9.03m)

Table 4.6 Load to the Beams – Floor A (z= 9.03m)

Beams	Total Permanent Load (KN/m)	Total Imposed Load (KN/m)
B1	9.160	3.385
B2	8.262	4.809
B3	3.778	2.470
B4	7.067	3.969
B5	13.085	1.208
B6	13.526	1.409
B7	9.898	1.739
B8	8.325	1.020
B9	6.382	3.937
B10	15.138	4.419
B11	19.667	4.742
B12	14.846	4.286
B13	15.986	5.608
B14	18.454	5.334
B15	16.659	5.018
B16	15.368	4.428
B17	15.097	5.419
B18	19.629	8.125

B19	18.835	9.484
B20	17.552	5.426
B21	6.478	2.958
B22	6.381	2.914
B23	11.326	3.943
B24	10.595	3.992
B25	6.895	3.149
B26	17.676	8.515
B27	15.921	4.681
B28	21.848	8.458
B29	16.974	5.907
B30	17.123	2.063
B31	13.694	1.814
B32	15.127	5.277
B33	16.241	6.404
B34	14.743	4.287

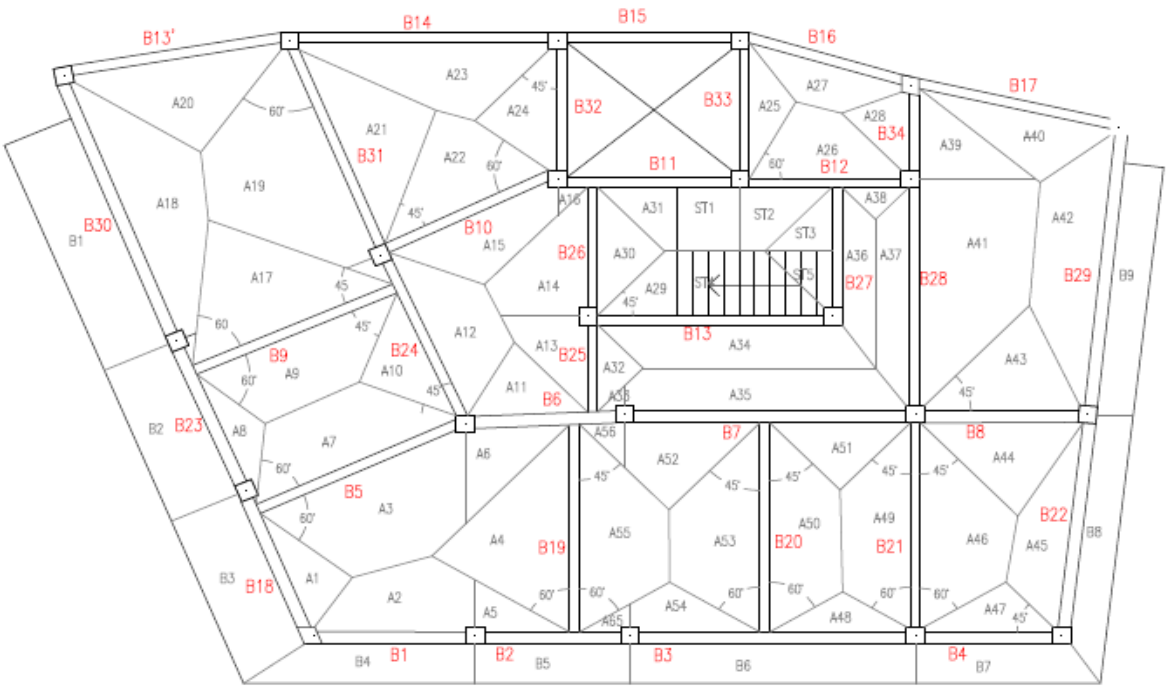

Figure 4.25 Distribution of Slab Load to the Beams – Floors B,C,D,E, Approachable Roof (z= 12.23m, 15.43m, 18.63m, 21.83m, 25.03m respectively)

Table 4.7 Load to the beams – Floors B,C,D,E (z= 12.23m, 15.43m, 18.63m, 21.83m respectively)

Beams	Total Permanent Load (KN/m)	Total Imposed Load (KN/m)
B1	19.629	8.125
B2	15.097	5.419
B3	15.127	5.277
B4	16.241	6.404
B5	17.342	5.426
B6	6.478	2.958
B7	9.160	3.385
B8	14.743	4.287
B9	15.921	4.681
B10	10.595	3.992
B11	13.678	1.739
B12	17.507	3.969
B13	18.702	4.809
B13'	17.123	2.063
B14	13.694	1.814
B15	0.000	0.000
B16	12.005	1.208
B17	13.526	1.409
B18	18.835	9.484
B19	16.659	5.018
B20	9.698	4.428
B21	15.138	4.419
B22	15.986	5.608
B23	17.676	8.515
B24	6.895	3.149
B25	6.381	2.914
B26	11.326	3.943
B27	16.822	3.937

B28	19.877	4.742
B29	18.454	5.334
B30	21.848	8.458
B31	16.974	5.907
B32	9.898	1.739
B33	8.325	1.020
B34	14.846	4.286

Table 4.8 Slab load to the Beams –Approachable Roof (z=25.03m)

Beams	Total Permanent Load (KN/m)	Total Imposed Load (KN/m)
B1	9.972	8.125
B2	5.647	5.419
B3	5.675	5.277
B4	6.738	6.404
B5	11.340	5.426
B6	6.182	2.958
B7	7.074	3.385
B8	8.959	4.287
B9	9.783	4.681
B10	8.343	3.992
B11	13.505	1.739
B12	17.185	3.969
B13	18.325	4.809
B13'	4.311	2.063
B14	3.792	1.814
B15	0.000	0.000
B16	2.524	1.208
B17	2.946	1.409
B18	9.214	9.484
B19	10.487	5.018

B20	9.255	4.428
B21	9.236	4.419
B22	6.495	5.608
B23	8.108	8.515
B24	6.581	3.149
B25	6.090	2.914
B26	18.681	3.943
B27	16.531	3.937
B28	9.910	4.742
B29	6.900	5.334
B30	9.874	8.458
B31	12.345	5.907
B32	3.634	1.739
B33	2.133	1.020
B34	8.957	4.286

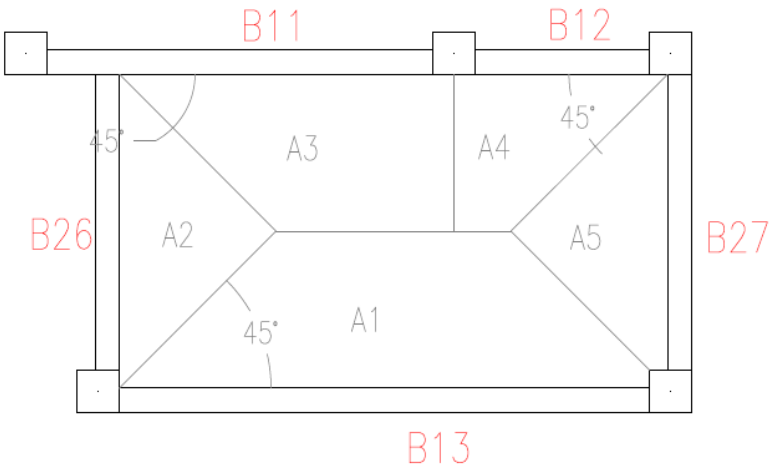

Figure 4.26 Distribution of Slab Load to the Beams –Non Approachable Roof (z=27.53m)

Table 4.9 Slab load to the beams –non approachable roof (z=27.53m)

Beams	Total Permanent Load (KN/m)	Total Imposed Load (KN/m)
B11	3.605	0.863
B12	2.564	0.495
B13	5.913	0.957
B26	4.953	0.690
B27	5.609	0.686

Prior the application of the loads to the model, the load patterns should be defined. The load patterns are:

Dead load: it is the self weight of the elements-calculated automatically by the SAP2000.

Dead load (slabs-permanent load): it is the permanent load of the slabs (including the infill walls) as calculated above. Since its calculation, as shown in the appendix B, takes into account the self weight of the slab, the self weight multiplier should be set equal to zero. Otherwise the self weight will be added twice, leading to obviously irrational results.

Imposed load and Imposed load (shops): As shown in the table 4.2 the live loads for shops is greater than the live loads for common floors, thus two separate load patterns are defined.

Balcony Moment: The balconies are not included in the model. However the bending moment that causes torsion to the beams they are attached, is taken into account. The calculation of the bending moment due to the balconies is:

$$\left(Permanent\ Load\ of\ the\ Balcony\ \left(kN/m\right)\ +0.3\cdot Imposed\ Load\ of\ the\ Balcony\ \left(kN/m\right)\right)\cdot$$
$$\cdot Beam\ Length\ \left(m\right)\cdot\ Balcony\ width\ \left(m\right)$$

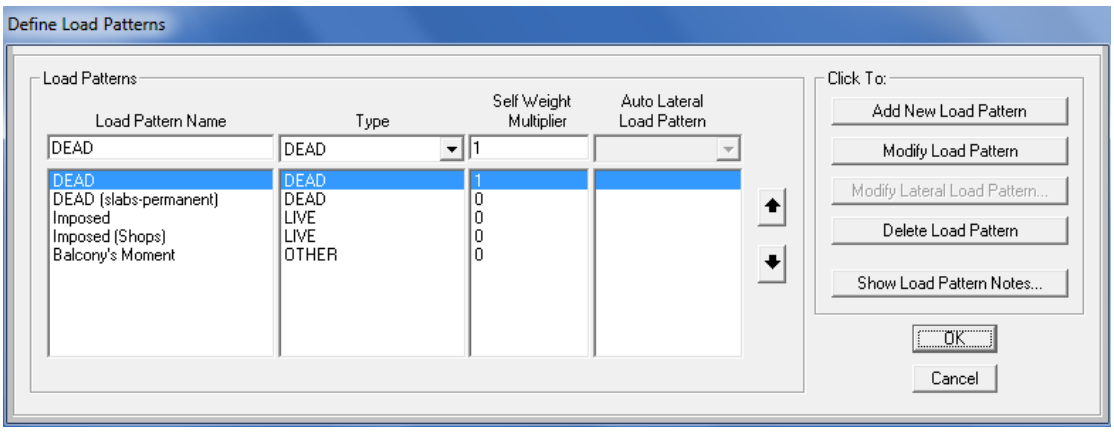

Figure 4.27 Load Patterns Definition

The loads are assigned to the beams, following the commands:

Assign⇒Frame Loads⇒Distributed

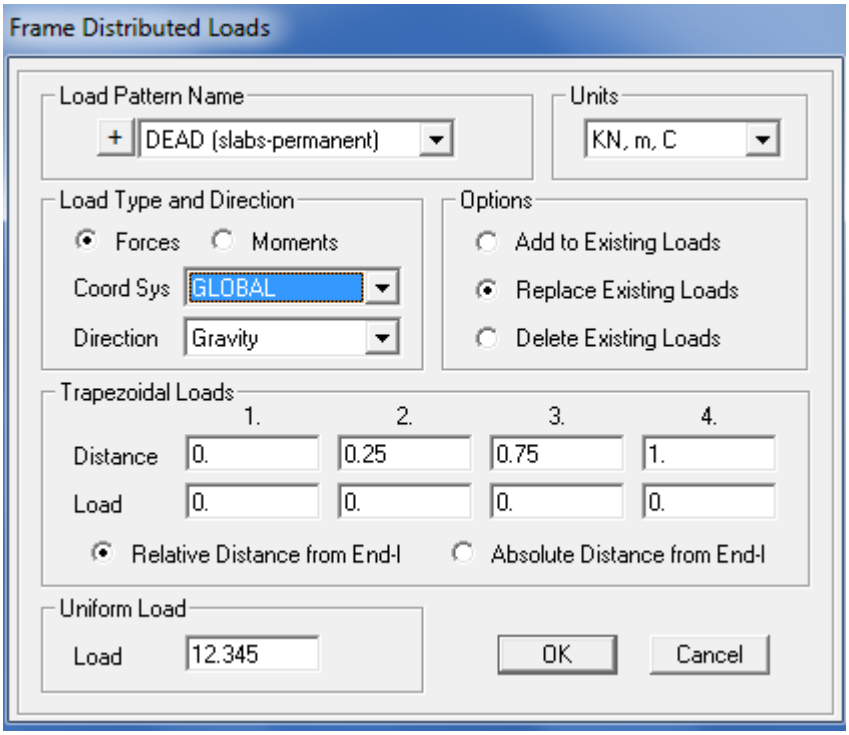

Figure 4.28 Loads Assignment to the Beams

The load patterns and the coordinate system are selected. The direction of all loads is set to gravity (except the balcony moment which is set about the appropriate local axis). The value of the uniform load is typed in the field "Load", as shown in figure 4.28.

4.3.5 Diaphragms

The diaphragmatic behaviour of the slab is considered. The slabs are flexible towards the perpendicular to their plane direction (z-direction), however in-plane they are considered to act as non-deformed plates (their deformation is low enough to be neglected). As a result the deformations of the in-plane (plane xy) joints of the slabs are not independent. They are constrained by the three degrees of freedom of the diaphragm, which is able to move as a solid body in the xy plane (Katsikadelis, 2012).

In SAP2000 a diaphragm constraint may be used to represent the behaviour of the slab, since it causes all of its constrained joints to move together as a planar

diaphragm that is rigid against membrane deformation, but do not affect out-of-plane (plate) deformation.

It is very useful in the lateral (horizontal) dynamic analysis of buildings, as it results in a significant reduction in the size of the eigenvalue problem to be solved CSi, 1995).

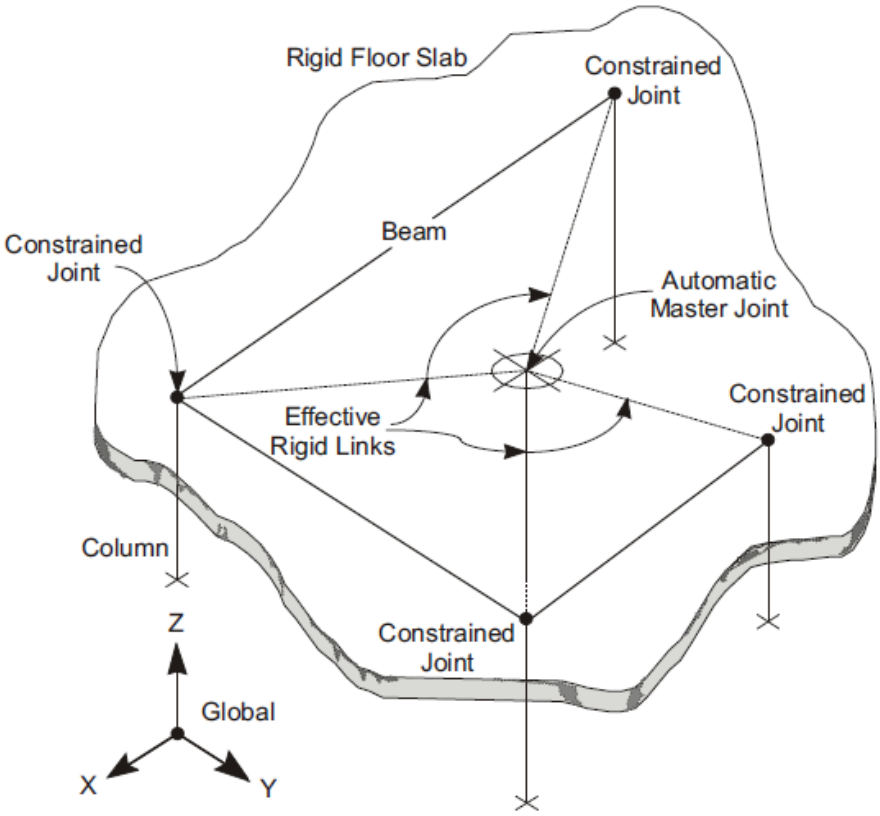

Figure 4.29 Use of Diaphragm Constraint to Model a Rigid Floor Slab (CSi, 1995)

The diaphragm constraint is applied in SAP 2000 through the following steps, since all the joints of the desirable level are selected.

Assign⇒Joint⇒Constraints⇒Diaphragm

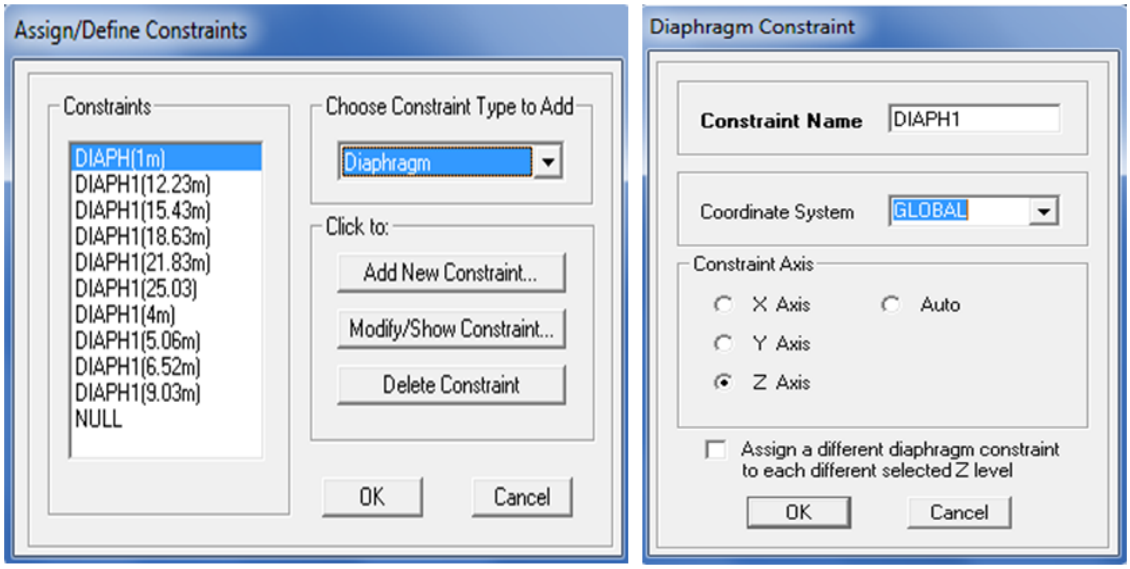

Figure 4.30 Diaphragm Constraints Definition

The Z-axis constrained should be selected, since it defines a perpendicular to the Z-axis diaphragm (CSi, 1997).

Chapter 5

Modal Response Spectrum Analysis of the Existing Structure

5.1 Modal Analysis

A modal analysis is defined by creating a load case and setting its type to modal. Modal analysis is always linear. The values of the stiffness of the structure elements are taken from table 4.1, which is appropriate for linear analyses.

The Eigen Vectors type of modes and stiffness from zero initial conditions-unstressed state are chosen. The number of modes is set high enough, so all modes with effective modal mass greater than 5% of the total mass are taken into account as suggested in EN 1998-1 (2004). Thus the number of modes is set to: 170

The mass source has to be defined; otherwise the program is not able to solve the generalized eigenvalue problem:

$[K - \Omega^2 M]\, \Phi = 0$ (31) (CSi, 1995)

The mass is defined from elements, additional masses and loads. By selecting this option, the mass from the elements of the structure and the mass from permanent and imposed loads (due to slabs and infill walls that are not modelled) are taken into account (there are no additional masses). As a result the total mass of the structure is considered for the modal analysis. The loads are combined through the combination $G+\psi_2 Q$, where ψ_2 is the coefficient for imposed (live) loads.

ψ_2=0.3 for usual residences (Category A)

ψ_2=0.6 for shops (Category D) (EN 1990, (2002) Greek National Annex)

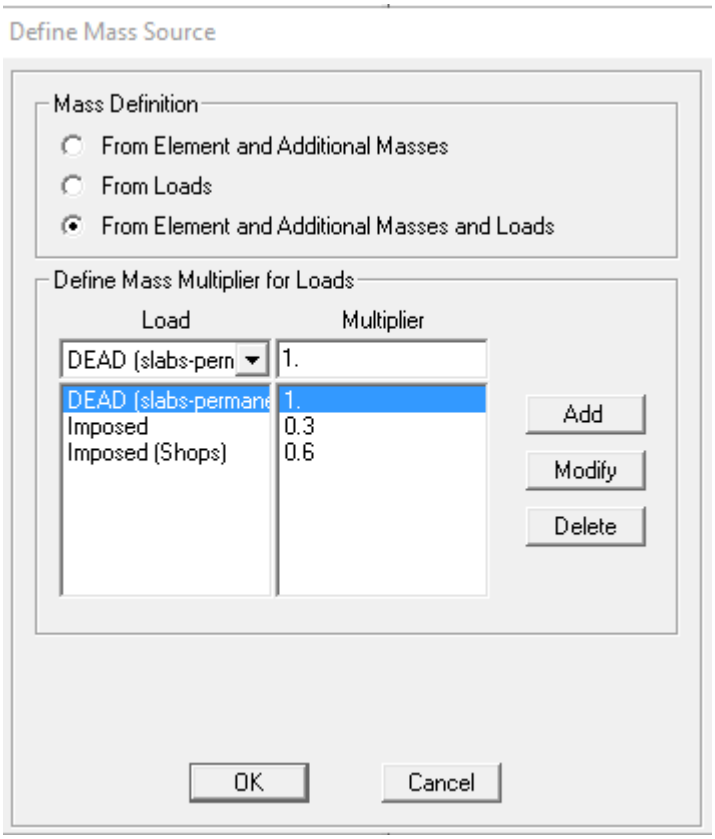

Figure 5.1 Mass Sources Definition

The modal participating mass ratios of the first 5 and the last 5 modes are presented in the following table:

Table 5.1 Modal Analysis Results: Modal Participating Mass Ratios of the first 5 and the last five modes of the structure

OutputCase	StepType	StepNum	Period	UX	UY	UZ	RX	RY	RZ
Text	Text	Unitless	Sec	Unitless	Unitless	Unitless	Unitless	Unitless	Unitless
MODAL	Mode	1	1.627333	0.29517	0.09153	4.53E-08	0.0656	0.16849	0.12517
MODAL	Mode	2	1.404784	0.04641	0.42273	5.77E-06	0.3073	0.02621	0.04552
MODAL	Mode	3	1.141874	0.18555	0.00345	4.68E-08	0.00213	0.1039	0.32066
MODAL	Mode	4	0.522281	0.03225	0.01336	1.3E-05	0.01236	0.02985	0.01212
MODAL	Mode	5	0.463984	0.00602	0.05606	1.27E-05	0.04887	0.00632	0.00763
MODAL	Mode	165	0.050208	4.78E-05	1.9E-05	0.00071	0.00011	0.00029	0.00031
MODAL	Mode	166	0.050106	2.44E-06	0.00011	0.00072	3.37E-05	8.82E-06	1.08E-05
MODAL	Mode	167	0.049928	4.32E-06	2.45E-07	0.00012	3.73E-05	0.00022	0.00012
MODAL	Mode	168	0.049539	0.00015	1.54E-05	0.00035	5.79E-05	2.71E-05	0.00012
MODAL	Mode	169	0.049524	0.00049	3.39E-06	0.00347	0.00023	0.00184	3.44E-05
MODAL	Mode	170	0.049487	0.00019	5.16E-05	2.4E-05	8.91E-05	7.11E-05	0.00683

The deformed shapes of the first 3 modes are presented in the figures 5.2 to 5.4:

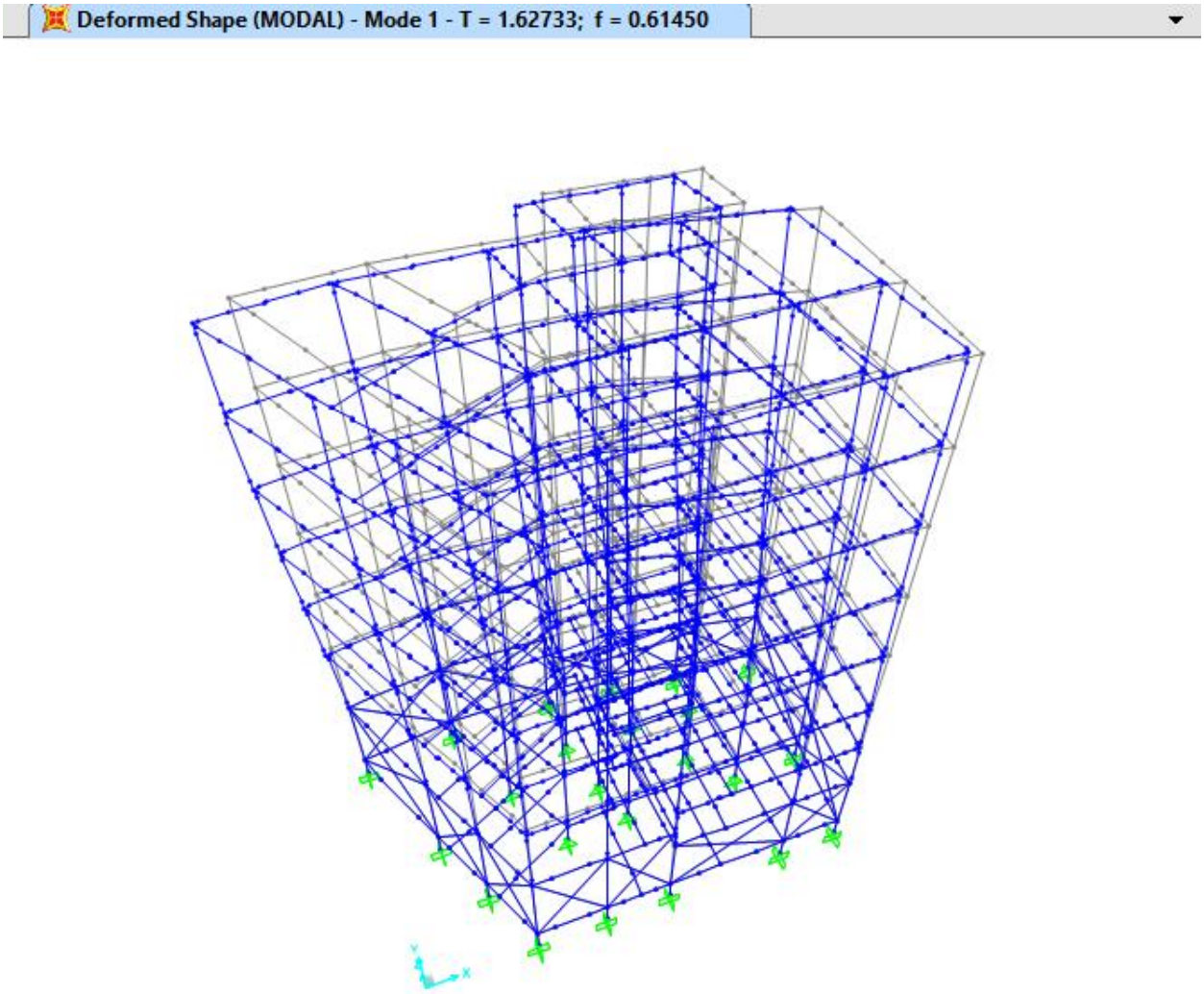

Figure 5.2 Deformed Shape of Mode 1: T1= 1.627sec. Translational along X axis

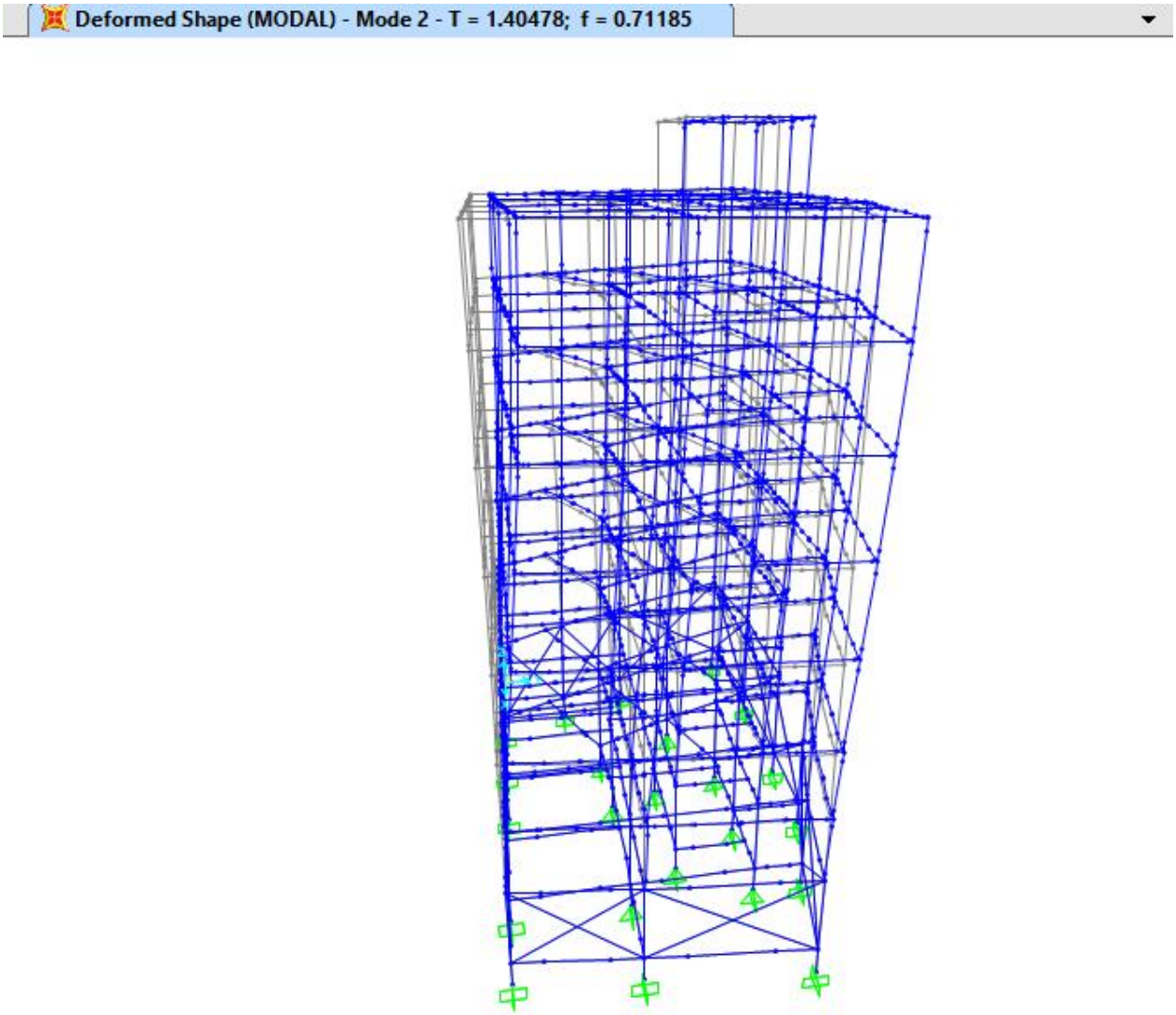

Figure 5.3 Deformed Shape of Mode 2: T2= 1.405sec. Translational along Y axis

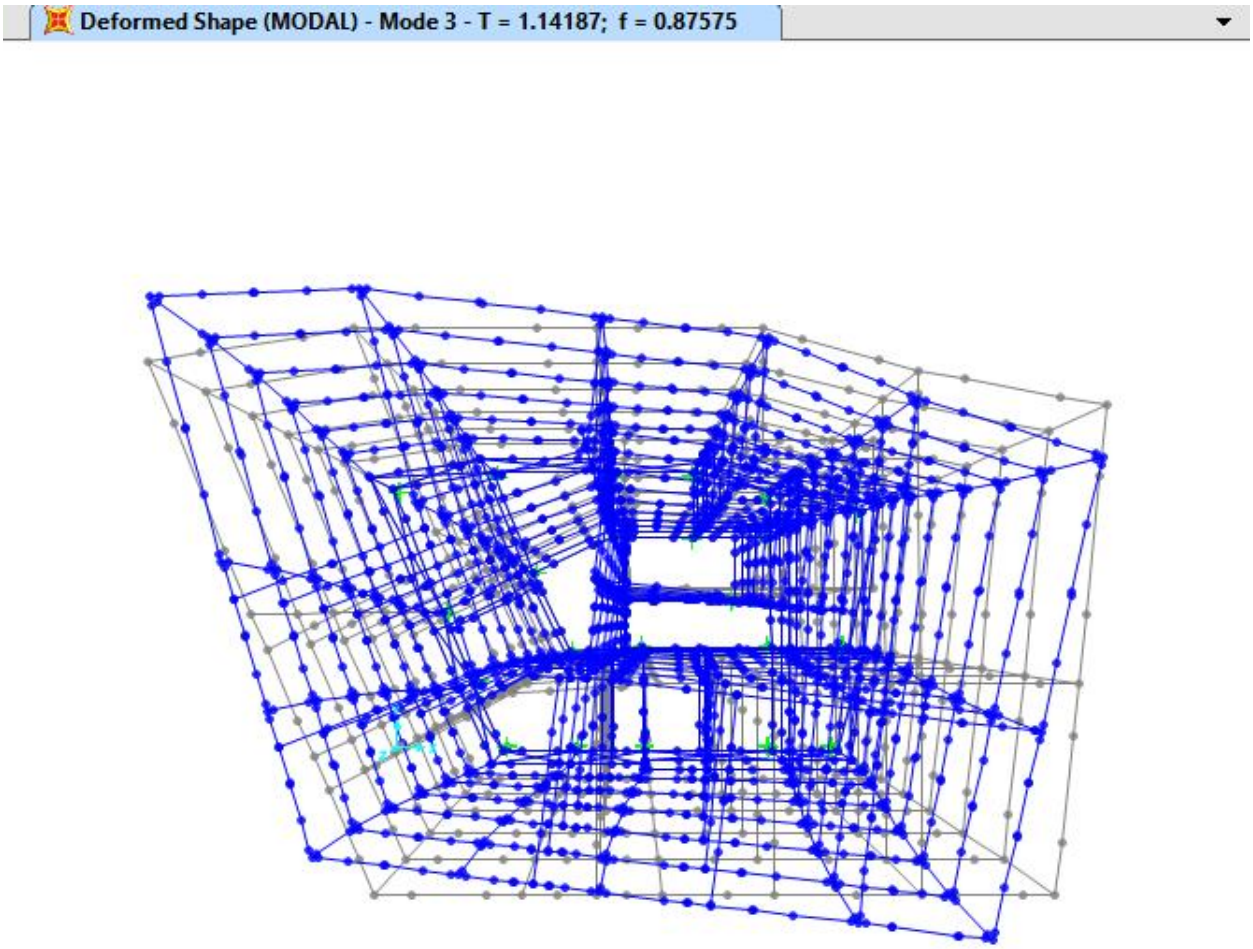

Figure 5.4 Deformed Shape of Mode 3: T3= 1.142sec. Rotational about Z axis

5.2 Response Spectrum Analysis

The response spectrum function is defined in SAP 2000 by the commands:

Define⇒Functions⇒Response Spectrum⇒ (Choose Function Type to Add) ⇒EuroCode 8 2004

Subsequently the required parameters are defined:

Horizontal Ground Acceleration: 0.24 a_g/g (where $a_g=a_{gr}\gamma_I$) ($\gamma_I=1$)

Spectrum Type: 1

Ground Type: B

Soil Factor, S: 1.2

Tb:0.15 sec

Tc: 0.5 sec

Td:2.5 sec

β:0.2

Behaviour factor q: 3.5

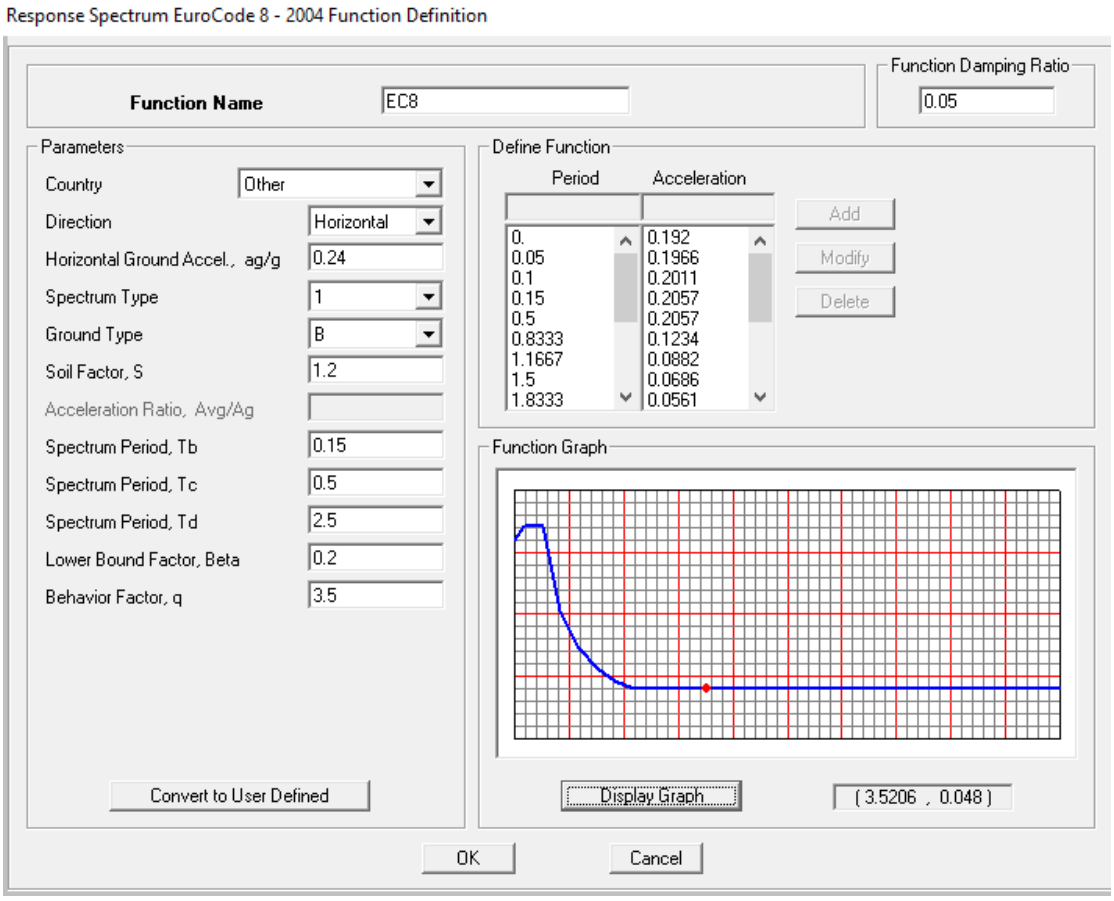

Figure 5.5 Response Spectrum Function Definition

The load case for the vertical static loads (G+0.3Q) is defined. The initial conditions are set to zero and the linear analysis type is chosen. The loads applied are shown in the figure 5.6.

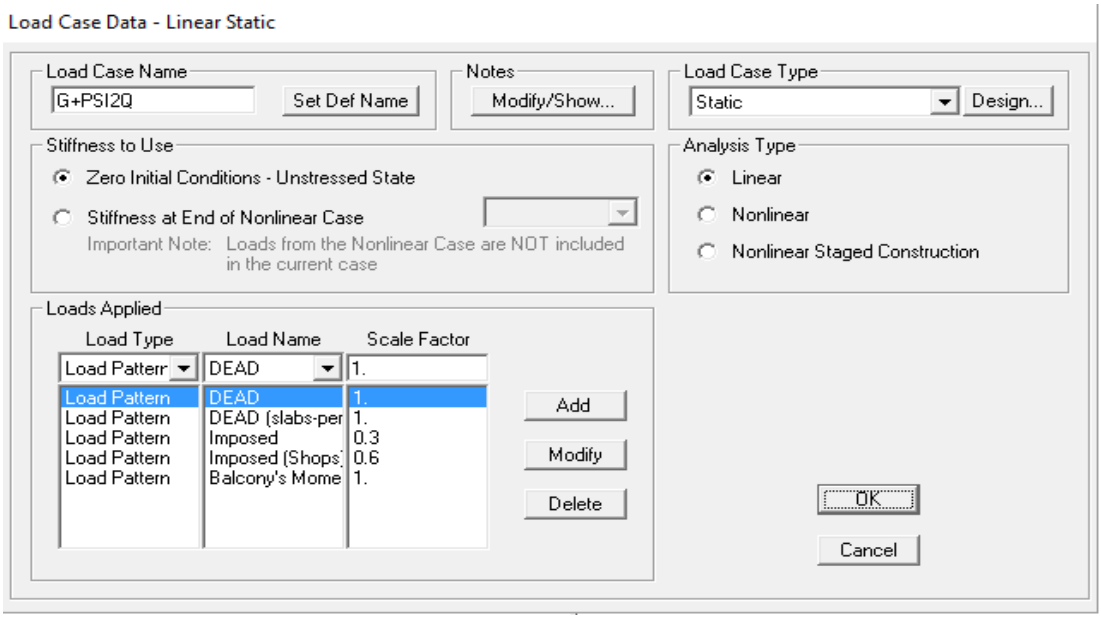

Figure 5.6 Vertical Loads-Case Definition

The earthquake load cases along the axis X and Y are defined.

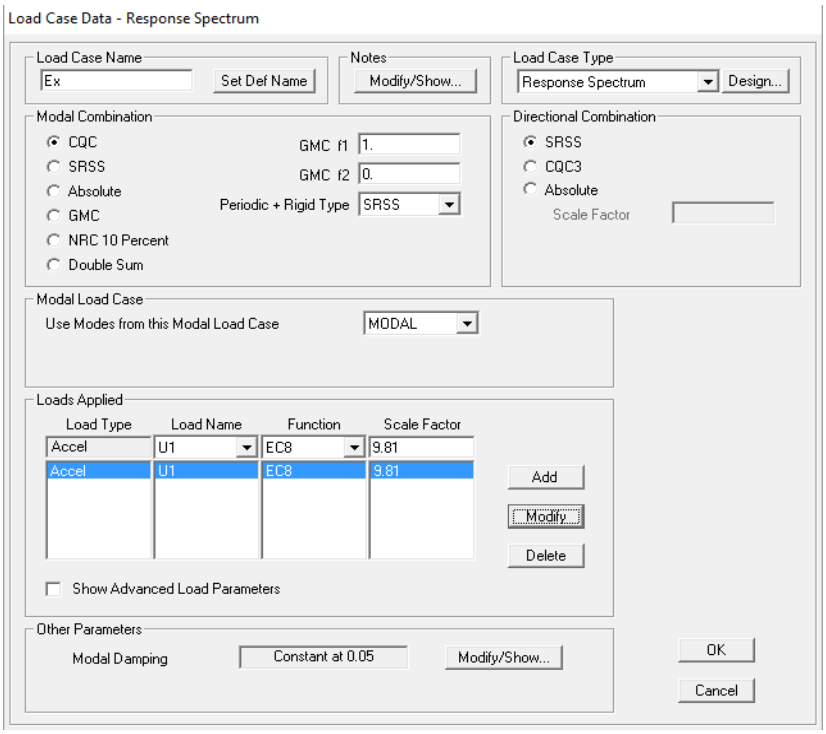

Figure 5.7 Definition of Load Case of Seismic Action Imposed to the Building along the X axis.

The vertical and seismic loads are combined through the commands: Define⇒Load Combinations⇒Add New Combo

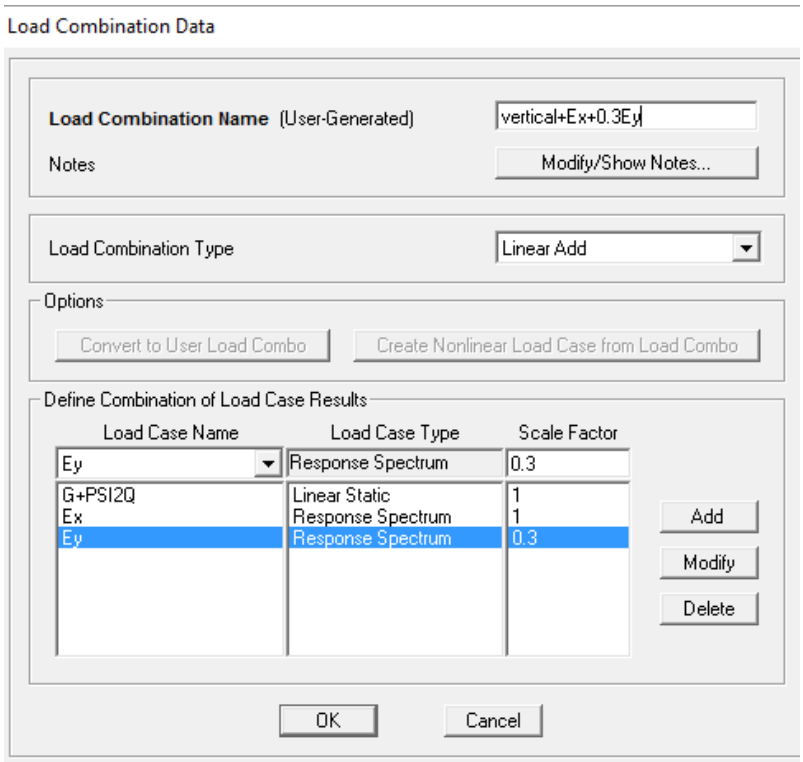

Figure 5.7 Definition of The combination of the Vertical Loads+Ex+0.3Ey

The response spectrum analyses are performed for the load combinations:

G+0.3Q+Ex+0.3Ey, G+0.3Q+Ex-0.3Ey, G+0.3Q-Ex+0.3Ey, G+0.3Q+Ex-0.3Ey, G+0.3Q+0.3Ex+Ey, G+0.3Q+0.3Ex-Ey, G+0.3Q-0.3Ex+Ey, G+0.3Q-0.3Ex-Ey, G+0.3Q+SRSS (Ex,Ey)

Where G+0.3Q is the combination of the vertical loads of the structure, taken into account for dynamic analyses according to EN 1998 (2004)

5.3 Modal Response Spectrum Analysis Results

The maximum displacements and the maximum forces along each axis, for each floor level, are presented in the following tables. The maximum due to the SRSS combination is common along both X and Y axes.

Table 5.2 Maximum Column Forces per Floor Level for Load Combinations: G+0.3Q+Ex+0.3Ey, G+0.3Q+Ex-0.3Ey, G+0.3Q-Ex+0.3Ey, G+0.3Q+Ex-0.3Ey, G+0.3Q+SRSS (Ex,Ey)

Column Forces (Earthquake along main axis X and SRSS combination)					
Floor Level	**P (KN)**	**V2 (KN)**	**V3 (KN)**	**M2 (KNm)**	**M3 (KNm)**
Ground Floor	-1267.9	-193.66	-176.558	-197.539	146.6952
Mezzanine Floor	-1137.12	92.966	-148.432	-152.307	102.8312
A	-1143.12	123.363	-128.519	167.8805	131.5493
B	-716.432	-93.819	-111.993	-143.18	-119.62
C	-495.46	-86.917	-102.469	133.6989	114.2687
D	-309.017	52.164	-75.609	99.7109	-71.9614
E	-143.359	76.19	-54.095	77.4287	112.7865

Table 5.3 Maximum Column Forces per Floor Level for Load Combinations: G+0.3Q+0.3Ex+Ey, G+0.3Q+0.3Ex-Ey, G+0.3Q-0.3Ex+Ey, G+0.3Q-0.3Ex-Ey, G+0.3Q+SRSS (Ex,Ey)

Column Forces (Earthquake along main axis Y and SRSS combination)					
Floor Level	**P (KN)**	**V2 (KN)**	**V3 (KN)**	**M2 (KNm)**	**M3 (KNm)**
Ground Floor	-1350.484	-187.63	-181.631	-197.5393	145.1213
Mezzanine Floor	-1128.76	90.843	-149.974	-154.1498	100.2469
A	-1143.121	123.363	-148.432	167.8805	128.1647
B	-711.273	-91.415	-111.993	-143.1798	-116.5706
C	-496.56	-84.867	-102.469	133.6989	111.5601
D	-309.017	51.895	-78.276	103.2685	-71.3941
E	-144.086	76.19	-55.757	79.8612	-110.8466

The magnitudes that share common values for a specific floor level, no matter which one is the main analysis axis, show that their maximum value is obtained by the SRSS combination.

For both the main directions of the earthquake, the maximum forces act in the ground floor level. In addition, it is observed that the same frames face the maximum forces no matter which one is the main direction of the earthquake.

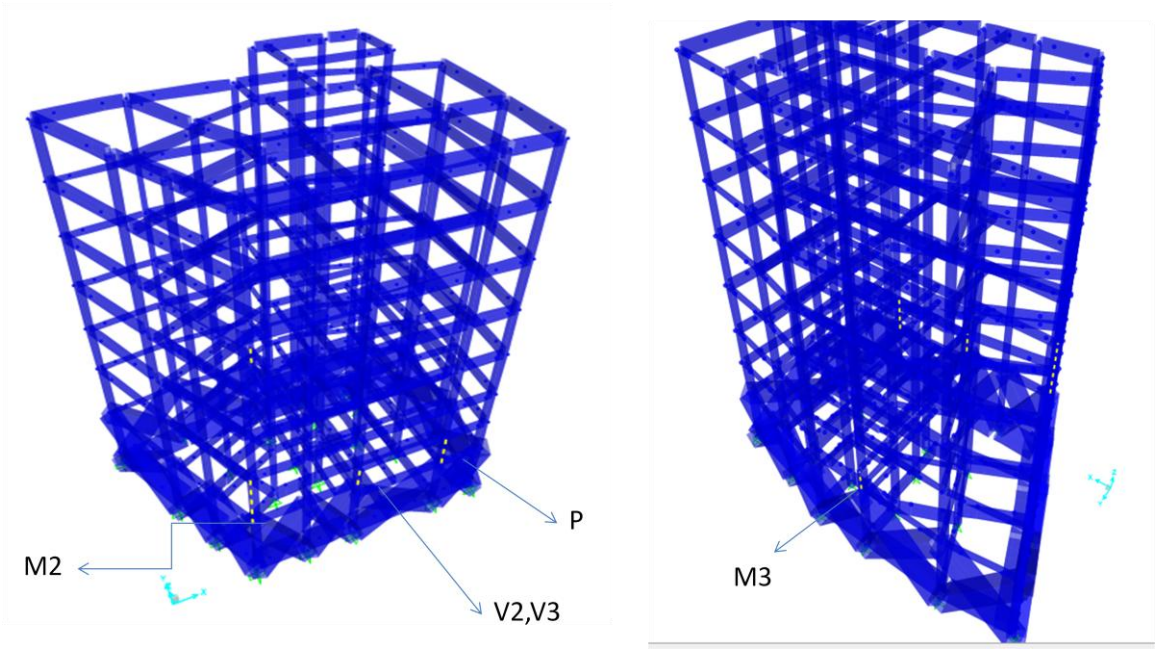

Figure 5.8 Column Frames Facing the Maximum Values of Magnitudes

The columns which face the maximum P,V2,V3,M2,M3 are shown in the figure 5.8. They are the columns C4, C3, C1 and C20 respectively. The maximum V2,V3, M3 are observed in short columns.

Table 5.4 Maximum displacements U1,U2,U3 per floor level due to earthquake along the X axis G+0.3Q+Ex+0.3Ey, G+0.3Q-Ex+0.3Ey, G+0.3Q Ex-0.3Ey, G+0.3Q -Ex-0.3Ey and G+0.3Q+SRSS (Ex, Ey)

Floor Level	Height (m)	U1 (m)	U2(m)	U3(m)
Non Approachable Roof	27.53	-0.0640	-0.0617	-0.0052
Approachable Roof	25.03	-0.0758	-0.0891	-0.0073
E Level	21.83	-0.0692	-0.0806	-0.0074
D Level	18.63	-0.0593	-0.0684	-0.0072
C Level	15.43	-0.0470	-0.0538	-0.0069
B Level	12.23	-0.0326	-0.0370	-0.0063
A Level	9.03	-0.0161	-0.0183	-0.0072
Mezzanine Floor	6.52	-0.0048	0.00509	-0.0063
Ground Floor (Shops)	5.06	0.00045	0.00084	-0.0046
Ground Floor (Hotel)	4	-0.00014	0.00041	-0.00538

Table 5.5 Maximum displacements U1,U2,U3 per Floor Level due to Earthquake along the Y axis G+0.3Q+0.3Ex+Ey, G+0.3Q-0.3Ex+Ey, G+0.3Q+0.3Ex-Ey, G+0.3Q - 0.3Ex-Ey, and G+0.3Q+SRSS (Ex, Ey)

Floor Level	Height (m)	U1 (m)	U2(m)	U3(m)
Non Approachable Roof	27.53	-0.0630	-0.0631	-0.0053
Approachable Roof	25.03	-0.0749	-0.0891	-0.0073
E Level	21.83	-0.0683	-0.0806	-0.0074
D Level	18.63	-0.0586	-0.0684	-0.0072
C Level	15.43	-0.0464	-0.0538	-0.0069
B Level	12.23	-0.0321	-0.0370	-0.0063
A Level	9.03	-0.0159	-0.0183	-0.0072
Mezzanine Floor	6.52	-0.0047	0.00516	-0.0062
Ground Floor (Shops)	5.06	0.00045	0.00087	-0.0046
Ground Floor (Hotel)	4	-0.00014	0.00043	-0.00538

The displacements U1, U2, U3 corresponds to the global axes X,Y,Z, of the SAP2000 model, respectively.

The common displacements between the two tables are the result of the SRSS combination of the seismic forces.

The results show that the upper floor levels face larger displacements than the lower floor levels.

The U3 displacement is always negative as expected.

The ground floor levels may be considered unshakable.

The larger displacement of the structure is observed at the approachable roof level (25.03m) along the U2 direction. It is -0.0891m at the joint 179 as shown in the figure 5.9. It is the result of the SRSS combination of the seismic forces.

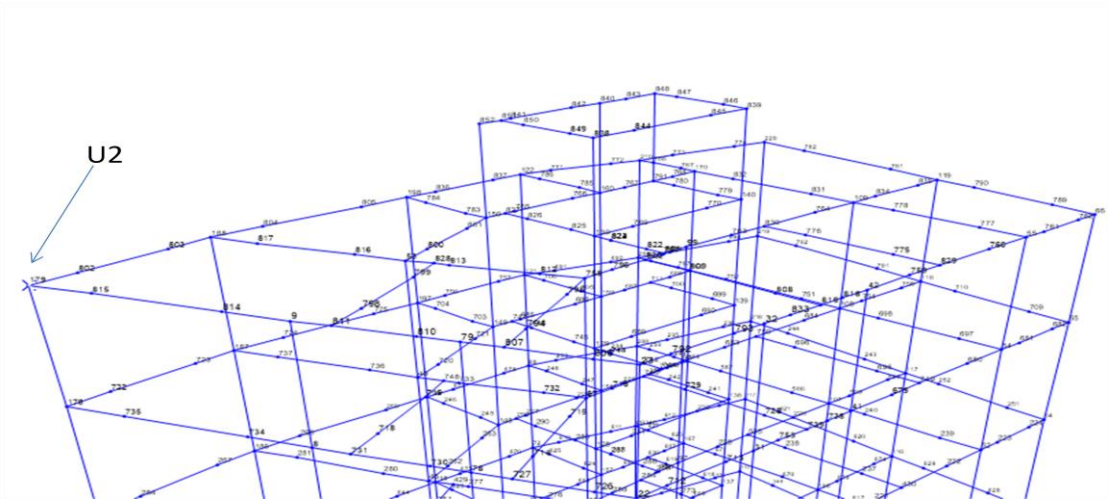

Figure 5.9 Joint that maximum displacement (-0.0891m) along the U2 axis is observed at the approachable roof level (25.03m)

The larger displacement of the structure along the U1 axis is -0.0758m at the approachable roof (25.03m). It is the result of the G+0.3Q+Ex+0.3Ey combination of forces. It is observed at the joints shown in the figure 5.10

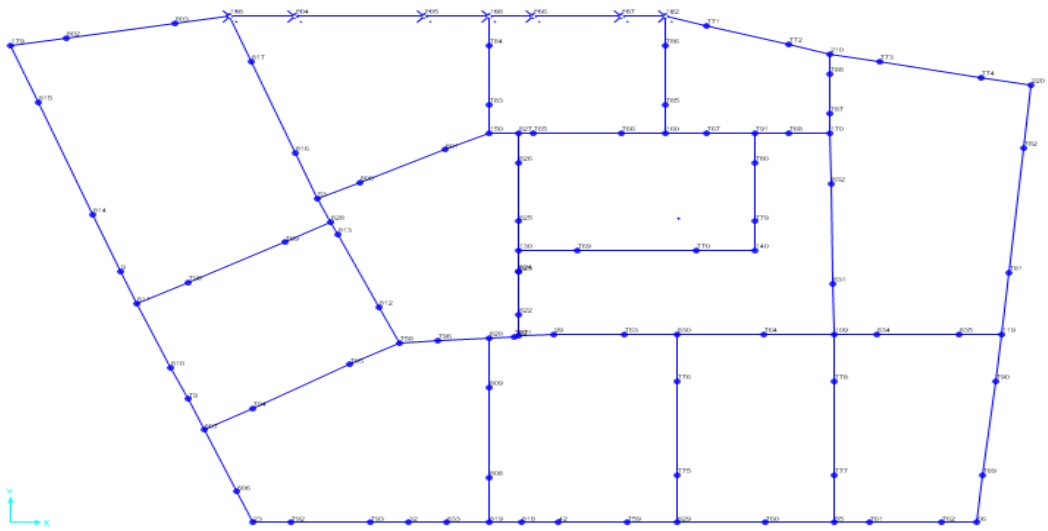

Figure 5.10 Joints that maximum displacement (-0.0758m) along the U1 axis is observed at the approachable roof level (25.03m)

Chapter 6

Nonlinear Static (Pushover) Analysis of the Existing Structure

According to KANEPE (2013), the nonlinear parameters of the materials should be taken into account when nonlinear analyses are performed. They are defined in section 4.3.1. The force-displacement behaviour of all components shall be explicitly included in the model using full backbone curves that include strength degradation and residual strength if any. They are assigned to the model through the plastic hinges.

The model is subjected to lateral loads. Use of more than one lateral load pattern is intended to bound the range of actions that may occur during actual dynamic response. Thus the uniform load distribution and the distribution of load patterns based on mode shapes are used. The loads are monotonically increased until the target displacement is reached, or the building is collapsed. The capacity curve is produced by the procedure described in 2.3.2.

The performance check for the whole building takes place, based on the deformations of each one of the elements, during the segmental increase of the lateral loads.

6.1 Limitations on Use of the Nonlinear Static Analysis-Higher Mode Participation Check

As mentioned in 2.3.2.1, static pushover analysis shall be permitted for structures that higher mode effects are not significant.

Two modal response spectrum analyses, suggested by KANEPE (2013) are performed. In the first the 90% of mass participation is captured and in the second only the fundamental mode in each direction is taken into account. The shear force in columns of all stories is compared, as indicated in the tables 6.1 and 6.2.

Table 6.1 Higher mode participation check for earthquake imposed along the X axis.

Earthquake imposed along X axis			
Floor Level	**Shear Force (KN)- Capturing the 90% of mass participation**	**Shear Force (KN)- Fundamental mode (X axis)**	**Variation (%)**
Ground Floor	986.40	767.92	128.45
A	527.23	436.57	120.77
B	466.98	379.99	122.89
C	389.92	301.71	129.24
D	297.92	228.65	130.29
E	186.34	142.30	130.95

Table 6.2 Higher mode participation check for earthquake imposed along the Y axis

Earthquake imposed along Y axis			
Floor Level	**Shear Force (KN)- Capturing the 90% of mass participation**	**Shear Force (KN)- Fundamental mode (Y axis)**	**Variation (%)**
Ground Floor	961.59	841.33	114.29
A	573.73	548.95	104.51
B	504.70	485.13	104.03
C	427.92	388.66	110.10
D	334.71	262.99	127.27
E	229.43	175.82	130.49

It is concluded that the higher mode effects are not significant, since the shear in any story resulting from the modal response spectrum analysis, considering modes required to obtain 90% of mass participation, does not exceed 130% of the corresponding story shear, considering only the fundamental mode response in either direction. Thus the non linear static analysis is permitted.

6.2 Secant Stiffness

For the nonlinear analyses, the secant stiffness of each element of the structure should be taken into account.

If the verification is carried out in terms of deformations, deformation demands should be obtained from an analysis of a structural model in which the stiffness of each element is taken to be equal to the mean value of $K = \frac{M_y \cdot L_v}{3 \cdot \Theta_y}$ at the two ends of the element. (For columns where the reinforcement at the bottom and at the top is usually the same, the calculation of the mean of the secant stiffness of the two ends is adequate. However in beams where the upper and the bottom reinforcement at the edge differ, the secant stiffness should be calculated for the upper and bottom of each edge. As a result the secant stiffness of the beam element is the mean of the four values calculated-two at each end). In this calculation the shear span at the end section, L_v, may be taken to be equal to the half of the element clear length (EN 1998-3, 2005). However for beams connected with a vertical element only at one end, the L_v may be taken to be equal to the total clear length of the beam. For shear walls L_v may be modified depending on the floor level- it may be taken equal to the half of the distance between the lower section of each floor and the top of the shear wall in the building (KANEPE, 2013). M_y is the yield moment and θ_y is the yield rotation of the end section of the element.

M_y is calculated automatically by the section designer of SAP2000. The program computes the moment-curvature diagram of each section, by analyzing the sections. The stress-strain relations of the materials, taking into account their nonlinear properties, defined in 4.3.1 are used for this purpose. The moment-curvature diagram is automatically transformed into a bi-linear diagram

according to Caltrans Seismic Design Criteria. The values of the bi-linear diagram are referred to the section designer as M_p and Phi-yield (idealized), thus those are used for the calculation of the secant stiffness. The behaviour of each section should be taken into account under the act of a representative axial force (for the columns). Thus a linear response spectrum analysis under the seismic combination of loads (G+0.3Q) is performed to provide the axial loads of the columns, used for the calculation of yield moment of the section. The behaviour of the beams which is different between the upper and bottom side of each end, due to asymmetry between the upper and bottom reinforcing steel, is taken into account through the angle option, available in section designer (Angle (Deg)=0 for tension in the bottom reinforcement, and Angle (Deg)=180 for tension in the upper reinforcement).

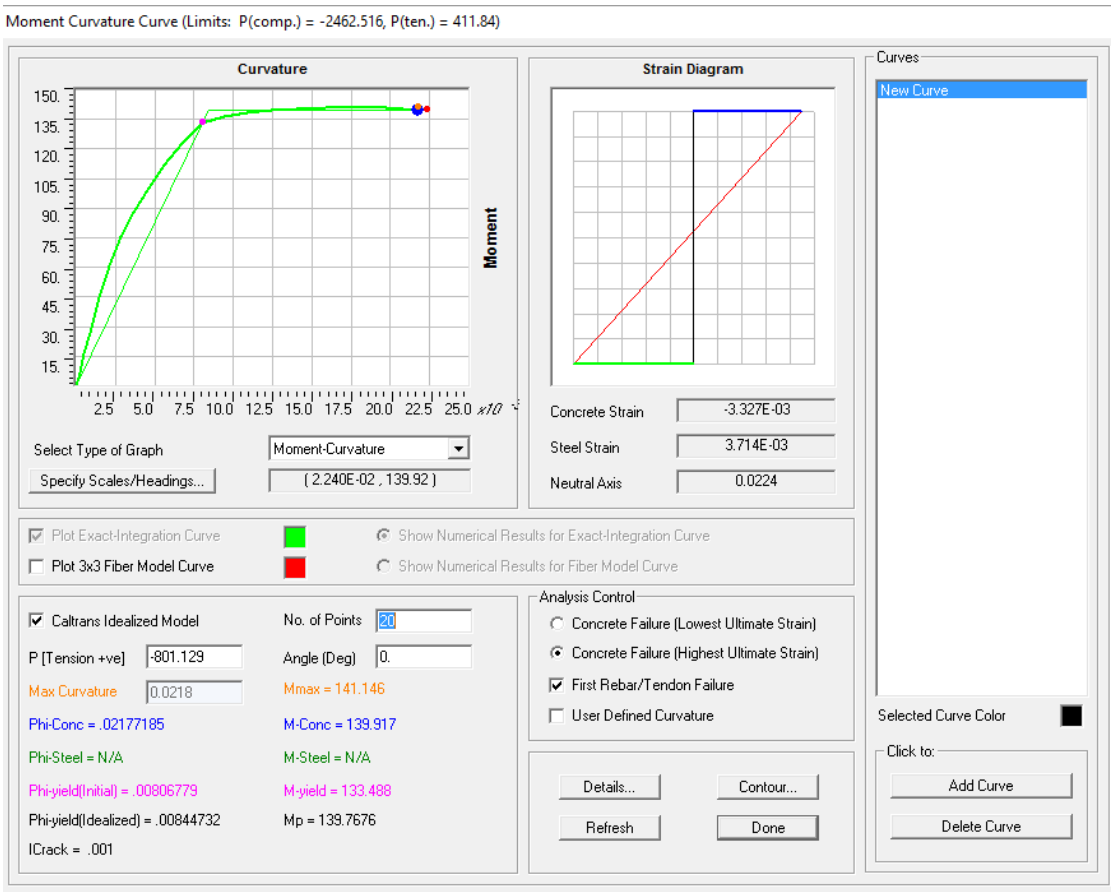

Figure 6.1 Moment-Curvature diagram of column C11 at the A floor level.

θ_y is computed using a Microsoft Excel Spreadsheet, by the equations provided in (EN 1998-3, 2005) and explained 2.4.6. As mentioned earlier the equations are:

For beams and columns:

$$\theta_y = \varphi_y \cdot \frac{Lv + a_v \cdot z}{3} + 0.0013 \cdot \left(1 + 1.5\frac{h}{Lv}\right) + 0.13 \cdot \varphi_y \frac{d_b \cdot f_y}{\sqrt{f_c}} \quad (32) \text{ (EN 1998-3, 2005)}$$

And for walls of rectangular, T- barbelled section:

$$\theta_y = \varphi_y \cdot \frac{L_v + a_v \cdot z}{3} + 0.002 \cdot \left(1 - 0.125 \cdot \frac{L_v}{h}\right) + 0.13 \cdot \varphi_y \cdot \frac{d_b \cdot f_y}{\sqrt{f_c}} \quad (33) \text{ (EN 1998-3, 2005)}$$

Φ_y is taken by section designer of SAP2000 as described above.

The stiffness modification should be applied to the SAP 2000 model by the commands described in 4.3.3. The percentage of the section that is effective and is able to sustain loads is represented by the ratio $\frac{K_{eff}}{K_{el}}$ where K_{eff} is the secant stiffness and K_{el} is the elastic stiffness of the section $K_{el} = E \cdot I$.

The properties that must be modified, as mentioned in the 4.3.3 are the moment of inertia about 3 for the beams and the moment of inertia about 3 and about 2 for the columns, since the columns receive biaxial bending moment about those two local axes.

The maximum and minimum values of $\frac{K_{eff}}{K_{el}}$ for columns are 0.329 and 0.119, respectively. The average value is 0.230.

The maximum and minimum values of $\frac{K_{eff}}{K_{el}}$ for beams are 0.217 and 0.045, respectively. The average value is 0.130.

An example of the calculations is shown in the tables 6.3 and 6.4:

Table 6.3 Secant Stiffness of Beams

Frames	keff(2) /Kel(2)	keff(3) /Kel(3)	Sections	BEAM	h(m)	b (m)	db (m)	angle 0 θy	angle 180 θy	angle 0 Keff	angle 180 Keff	Μέσος Όρος Keff
225	1	0.149	B20X30 4F12	B7(4m)	0.3	0.2	0.012	0.0058	0.0057	1361.78	2267.19	1814.48
298	1	0.136	B20X30 4F12	B6(4m)	0.3	0.2	0.012	0.0052	0.0051	1240.92	2062.61	1651.76
226	1	0.170	B20X30 4F14	B8(4m)	0.3	0.2	0.014	0.0054	0.0057	1733.96	2390.43	2062.20

Table 6.4 Secant Stiffness of Columns

Section	Frame	Lv (m)	h(m)	b (m)	db (m)	Start θy	End θy	Start Keff	End Keff	Mean Keff	Keff/Kel2	Keff/Kel3
K11A	4	1.5	0.35	0.35	0.018	0.0070	0.0069	10054	10062	10058	0.297883	0.297883
K11B	5	1.5	0.35	0.35	0.017	0.0066	0.0066	9695.5	9671.3	9683.4	0.286795	0.286795
K4Ground	42	1.26	0.35	0.35	0.019	0.0068	0.0068	9144.8	9159.1	9152	0.271057	0.271057
K4Mezzanine	43	1.26	0.35	0.35	0.019	0.0066	0.0066	9250.8	9255.5	9253.2	0.274053	0.274053

6.3 Plastic Hinges

It is considered that the plastic deformation is concentrated in the plastic hinges at the two edges of each column and beam. In addition here a plastic hinge in the middle of each beam is defined in order to research its behaviour.

The hinges are applied to each element by the commands:

Assign⇒Frame⇒Hinges

The hinge properties-backbone curve is taken from FEMA 356 tables which are included in SAP2000. The automatic calculation of the properties of each hinge is based on the section properties of the elements (dimensions, materials, reinforcing steel), which have been designed in section designer.

For the columns, the degree of freedom is set to P-M2-M3, because the axial force and the biaxial bending moment influence the element deformation. For the beams the degree of freedom is set to M3.

It is assumed that the transverse reinforcement does not provide confinement. It is assumed that the FEMA 356 criterion (a component is conforming if, within the flexural plastic hinge region, hoops are spaced at ≤ of d/3, and if, for components of moderate and high ductility demand, the strength provided by the hoops (Vs) is at least three-fourths of the design shear) is not satisfied.

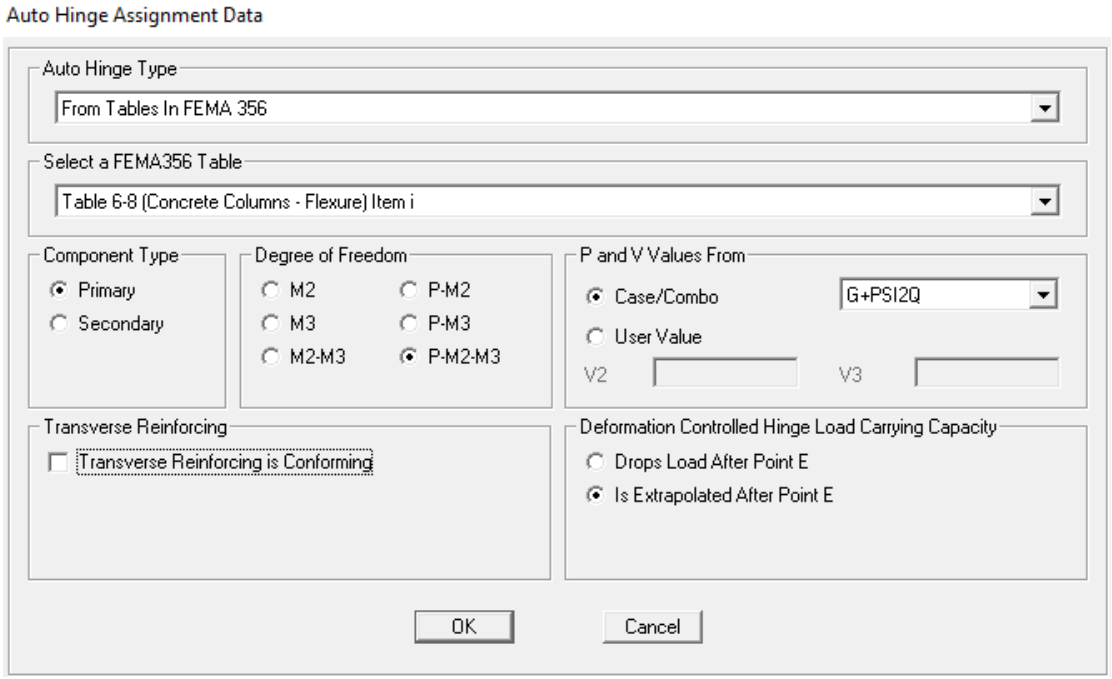

Figure 6.2 Auto Hinge Assignment Data for Concrete Columns

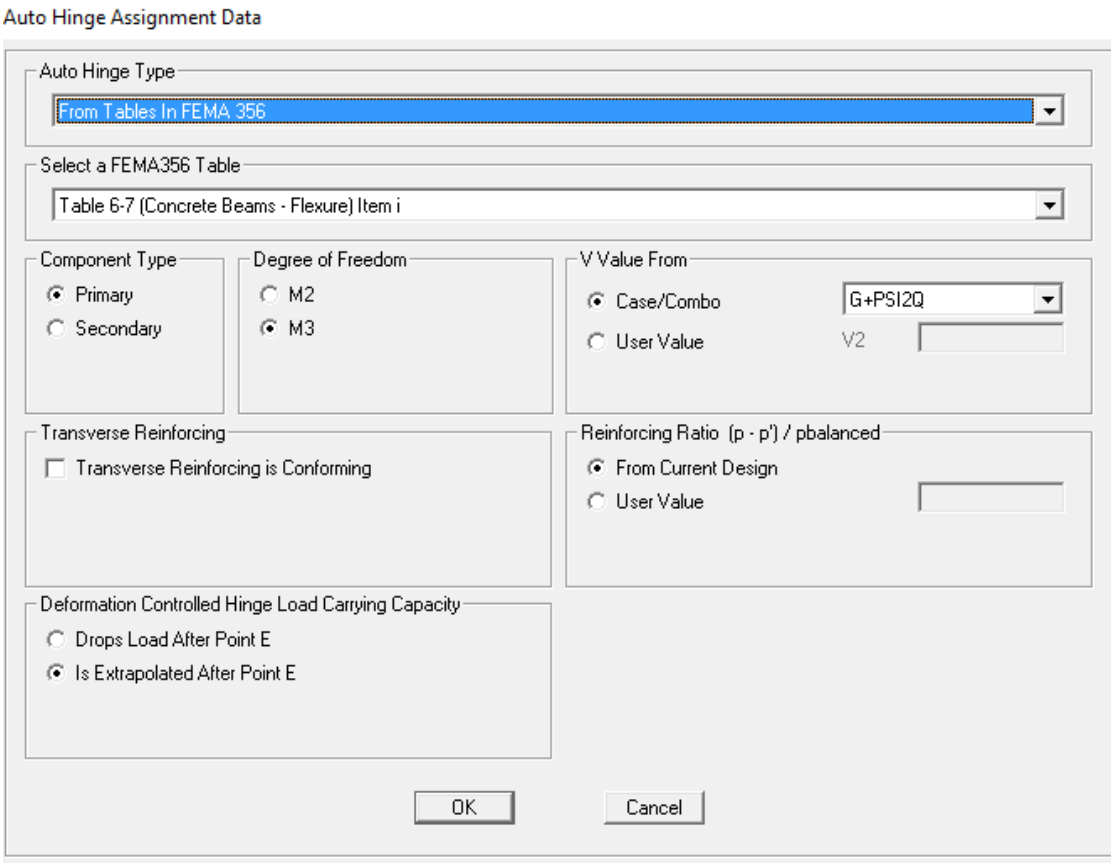

Figure 6.3 Auto Hinge Assignment Data for Concrete Beams

Subsequently the FEMA 356 tables, which define the backbone curve of the hinges, for concrete beams and concrete columns are shown.

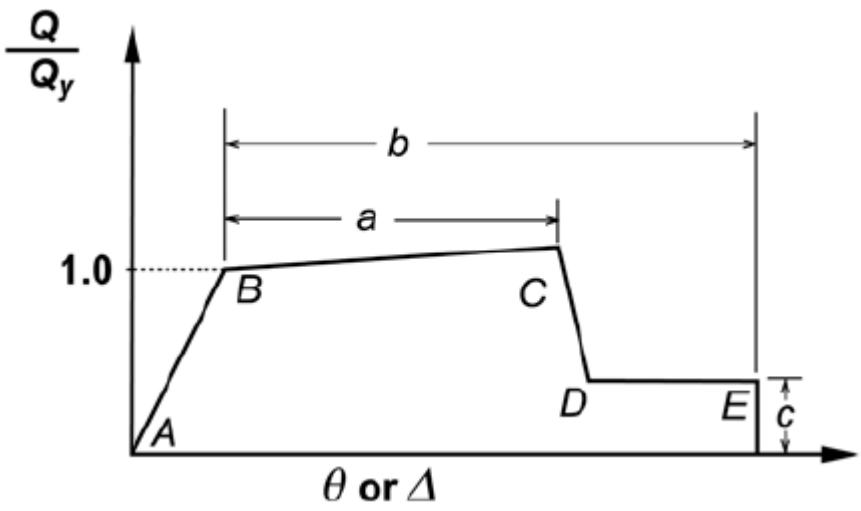

Figure 6.4 Hinge Backbone Curve according to FEMA 356 (2000)

Table 6-7 Modeling Parameters and Numerical Acceptance Criteria for Nonlinear Procedures—Reinforced Concrete Beams

Conditions			Modeling Parameters[3]			Acceptance Criteria[3]				
						Plastic Rotation Angle, radians				
						Performance Level				
			Plastic Rotation Angle, radians		Residual Strength Ratio		Component Type			
							Primary		Secondary	
			a	b	c	IO	LS	CP	LS	CP
i. Beams controlled by flexure[1]										
$\frac{\rho-\rho'}{\rho_{bal}}$	Trans. Reinf.[2]	$\frac{V}{b_w d\sqrt{f'_c}}$								
≤ 0.0	C	≤ 3	0.025	0.05	0.2	0.010	0.02	0.025	0.02	0.05
≤ 0.0	C	≥ 6	0.02	0.04	0.2	0.005	0.01	0.02	0.02	0.04
≥ 0.5	C	≤ 3	0.02	0.03	0.2	0.005	0.01	0.02	0.02	0.03
≥ 0.5	C	≥ 6	0.015	0.02	0.2	0.005	0.005	0.015	0.015	0.02
≤ 0.0	NC	≤ 3	0.02	0.03	0.2	0.005	0.01	0.02	0.02	0.03
≤ 0.0	NC	≥ 6	0.01	0.015	0.2	0.0015	0.005	0.01	0.01	0.015
≥ 0.5	NC	≤ 3	0.01	0.015	0.2	0.005	0.01	0.01	0.01	0.015
≥ 0.5	NC	≥ 6	0.005	0.01	0.2	0.0015	0.005	0.005	0.005	0.01
ii. Beams controlled by shear[1]										
Stirrup spacing ≤ d/2			0.0030	0.02	0.2	0.0015	0.0020	0.0030	0.01	0.02
Stirrup spacing > d/2			0.0030	0.01	0.2	0.0015	0.0020	0.0030	0.005	0.01
iii. Beams controlled by inadequate development or splicing along the span[1]										
Stirrup spacing ≤ d/2			0.0030	0.02	0.0	0.0015	0.0020	0.0030	0.01	0.02
Stirrup spacing > d/2			0.0030	0.01	0.0	0.0015	0.0020	0.0030	0.005	0.01
iv. Beams controlled by inadequate embedment into beam-column joint[1]										
			0.015	0.03	0.2	0.01	0.01	0.015	0.02	0.03

1. When more than one of the conditions i, ii, iii, and iv occurs for a given component, use the minimum appropriate numerical value from the table.
2. "C" and "NC" are abbreviations for conforming and nonconforming transverse reinforcement. A component is conforming if, within the flexural plastic hinge region, hoops are spaced at ≤ $d/3$, and if, for components of moderate and high ductility demand, the strength provided by the hoops (V_s) is at least three-fourths of the design shear. Otherwise, the component is considered nonconforming.
3. Linear interpolation between values listed in the table shall be permitted.

Figure 6.5 Modelling Parameters and Numerical Acceptance Criteria for Nonlinear Procedures-Reinforced Concrete Beams (FEMA 356, 2000)

Table 6-8 Modeling Parameters and Numerical Acceptance Criteria for Nonlinear Procedures—Reinforced Concrete Columns

			Modeling Parameters[4]			Acceptance Criteria[4]				
						Plastic Rotation Angle, radians				
						Performance Level				
							Component Type			
			Plastic Rotation Angle, radians		Residual Strength Ratio		Primary		Secondary	
Conditions			a	b	c	IO	LS	CP	LS	CP
i. Columns controlled by flexure[1]										
$\frac{P}{A_g f'_c}$	Trans. Reinf.[2]	$\frac{V}{b_w d \sqrt{f'_c}}$								
≤ 0.1	C	≤ 3	0.02	0.03	0.2	0.005	0.015	0.02	0.02	0.03
≤ 0.1	C	≥ 6	0.016	0.024	0.2	0.005	0.012	0.016	0.016	0.024
≥ 0.4	C	≤ 3	0.015	0.025	0.2	0.003	0.012	0.015	0.018	0.025
≥ 0.4	C	≥ 6	0.012	0.02	0.2	0.003	0.01	0.012	0.013	0.02
≤ 0.1	NC	≤ 3	0.006	0.015	0.2	0.005	0.005	0.006	0.01	0.015
≤ 0.1	NC	≥ 6	0.005	0.012	0.2	0.005	0.004	0.005	0.008	0.012
≥ 0.4	NC	≤ 3	0.003	0.01	0.2	0.002	0.002	0.003	0.006	0.01
≥ 0.4	NC	≥ 6	0.002	0.008	0.2	0.002	0.002	0.002	0.005	0.008
ii. Columns controlled by shear[1, 3]										
All cases[5]			—	—	—	—	—	—	.0030	.0040
iii. Columns controlled by inadequate development or splicing along the clear height[1,3]										
Hoop spacing ≤ d/2			0.01	0.02	0.4	0.005	0.005	0.01	0.01	0.02
Hoop spacing > d/2			0.0	0.01	0.2	0.0	0.0	0.0	0.005	0.01
iv. Columns with axial loads exceeding $0.70P_o$[1, 3]										
Conforming hoops over the entire length			0.015	0.025	0.02	0.0	0.005	0.01	0.01	0.02
All other cases			0.0	0.0	0.0	0.0	0.0	0.0	0.0	0.0

1. When more than one of the conditions i, ii, iii, and iv occurs for a given component, use the minimum appropriate numerical value from the table.
2. "C" and "NC" are abbreviations for conforming and nonconforming transverse reinforcement. A component is conforming if, within the flexural plastic hinge region, hoops are spaced at ≤ $d/3$, and if, for components of moderate and high ductility demand, the strength provided by the hoops (V_s) is at least three-fourths of the design shear. Otherwise, the component is considered nonconforming.
3. To qualify, columns must have transverse reinforcement consisting of hoops. Otherwise, actions shall be treated as force-controlled.
4. Linear interpolation between values listed in the table shall be permitted.
5. For columns controlled by shear, see Section 6.5.2.4.2 for acceptance criteria.

Figure 6.6 Modelling Parameters and Numerical Acceptance Criteria for Nonlinear Procedures-Reinforced Concrete Columns (FEMA 356, 2000)

6.4 Nonlinear Static (Pushover) Analysis

The pushover analysis is performed in two phases. Firstly, the load case of the vertical loads (G+0.3Q) is set to nonlinear and it is run from zero initial conditions- "start from unstressed state". Secondly the load case of the lateral loads is set to analysis type: Nonlinear and it is set to run from the end of the nonlinear case of the vertical loads, by the command: "Continue from state at end of nonlinear case": G+0.3Q.

The lateral loads distributions used are the uniform load distribution and the distribution based on the mode shapes. (When the latter is chosen, a modal analysis is run before the vertical and lateral loads application to the structure). The load type ⇒ Accel is set for uniform distribution of loads and the load type ⇒ Mode is set for modal pattern. If modal pattern is selected the distribution of lateral loads is based on the mode shape of the fundamental mode of the corresponding direction (Mode 1 is set for X axis and Mode 2 for Y axis).

It is interesting to note the modal analysis results, since the secant stiffness of the elements is used.

In the following table the modal mass participation ratios and the fundamental periods of the first 5 modes are shown.

Table 6.5 Modal Participating Mass Ratios of the first 5 Modes

TABLE: Modal Participating Mass Ratios									
OutputCase	**StepType**	**StepNum**	**Period**	**UX**	**UY**	**UZ**	**RX**	**RY**	**RZ**
Text	Text	Unitless	Sec	Unitless	Unitless	Unitless	Unitless	Unitless	Unitless
MODAL	Mode	1	2.639646	0.32636	0.08261	4.702E-08	0.06237	0.19121	0.09604
MODAL	Mode	2	2.368858	0.05254	0.42026	0.000006131	0.31761	0.03047	0.03167
MODAL	Mode	3	1.942065	0.13775	0.0017	0.000001648	0.00139	0.0805	0.35319
MODAL	Mode	4	0.870279	0.03751	0.01383	0.00000785	0.00992	0.02946	0.00918
MODAL	Mode	5	0.797585	0.00962	0.0556	0.000005013	0.0399	0.0068	0.00381

By comparing the results of the modal analysis using the secant stiffness of the elements and the modal analysis using the stiffness that is proposed by the table 4.1 (KANEPE, 2013), it is shown that even if the participating mass ratios are not significantly different, the periods of the first three modes are

approximately 1sec higher when secant stiffness is used, resulting to a much more flexible structure.

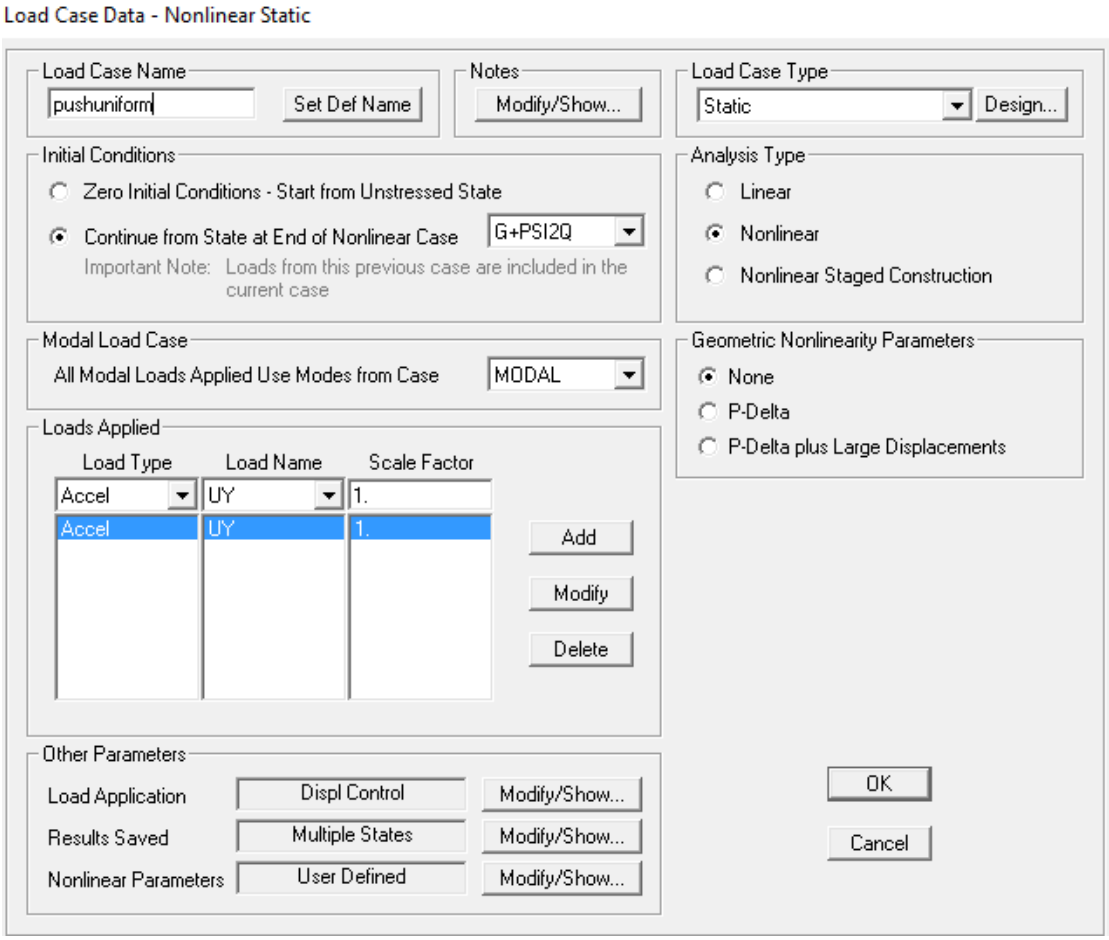

Figure 6.7 Definition of the Load Case of a Nonlinear Static Analysis. Uniform Distribution of Lateral Loads along the +Y axis.

The control node is the joint 130 of the structure, since it is the closer to the center of mass of the approachable roof (25.03m).

Eight nonlinear static analyses are performed (4 for each load distribution along the axes +X, -X, +Y, -Y).

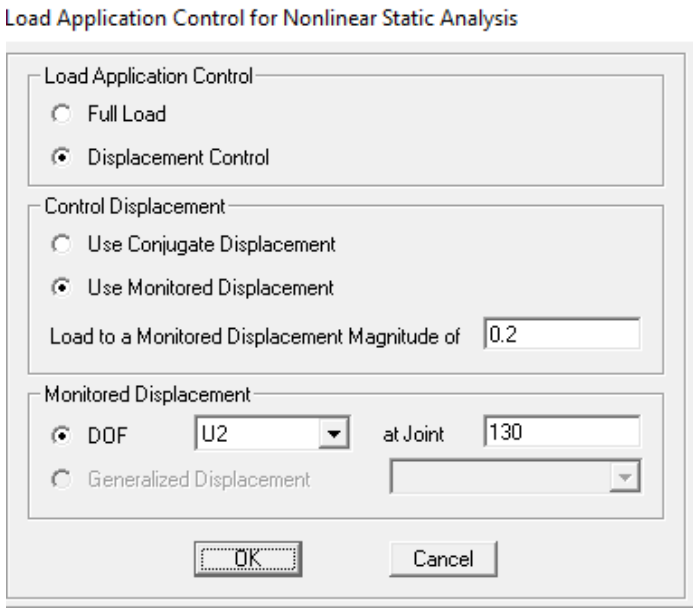

Figure 6.8 Load Application Control for Nonlinear Static Analysis

The displacement control option is set if the desirable displacement of the control node is known, but how much load is required is unknown. Using displacement control is not the same thing as applying displacement loading on the structure. Displacement control is simply used to measure the displacement at one point that results from the applied loads, and to adjust the magnitude of the loading in an attempt to reach a certain measured displacement value. The overall displaced shape of the structure will be different for different load patterns, even if the same displacement is controlled (CSi, 1995).

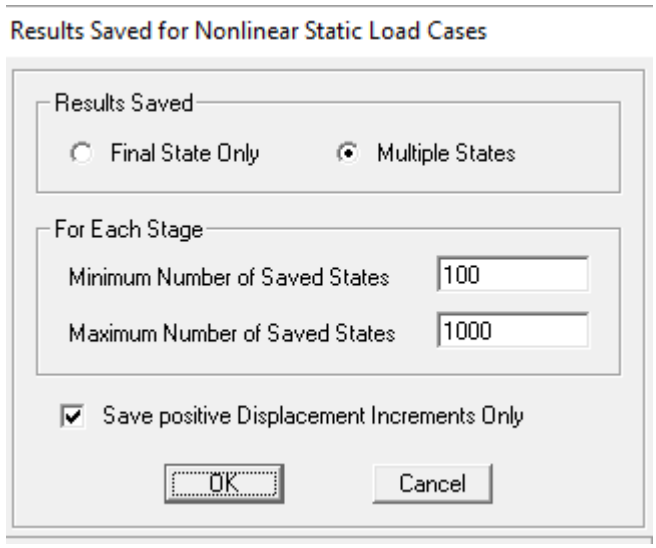

Figure 6.9 The results are saved in multiple states.

6.5 Results of Nonlinear Static (Pushover) Analysis

The results of the pushover analyses include the pushover curves and the capacity spectrums in ADRS format. In addition the deformed shape of the structure and tables showing the hinge results at the performance point are presented.

In the ADRS format, the red line represents the elastic response spectrum of Eurocode 8 (reduced according to the ATC-40 methodology), the green line represents the capacity curve of the equivalent single degree of freedom system and the cross-section of the green with the orange line indicates the performance point.

<u>Nonlinear Static Analysis along –X Axis (Uniform Distribution of Lateral Loads)</u>

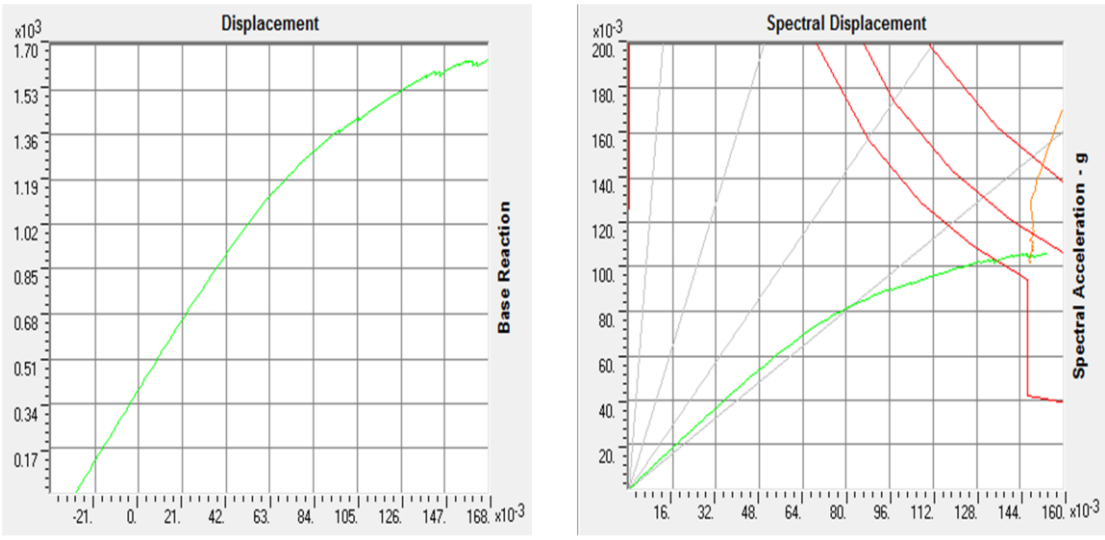

a b

Figure 6.10 a) Pushover Curve (Uniform Distribution of Lateral Loads along –X Axis) b) ATC-40 Capacity Spectrum-ADRS (Uniform Distribution of Lateral Loads along –X Axis)

Performance Point: V=1625.041KN, D=0.161m, S_a=0.105g, S_d=0.148m

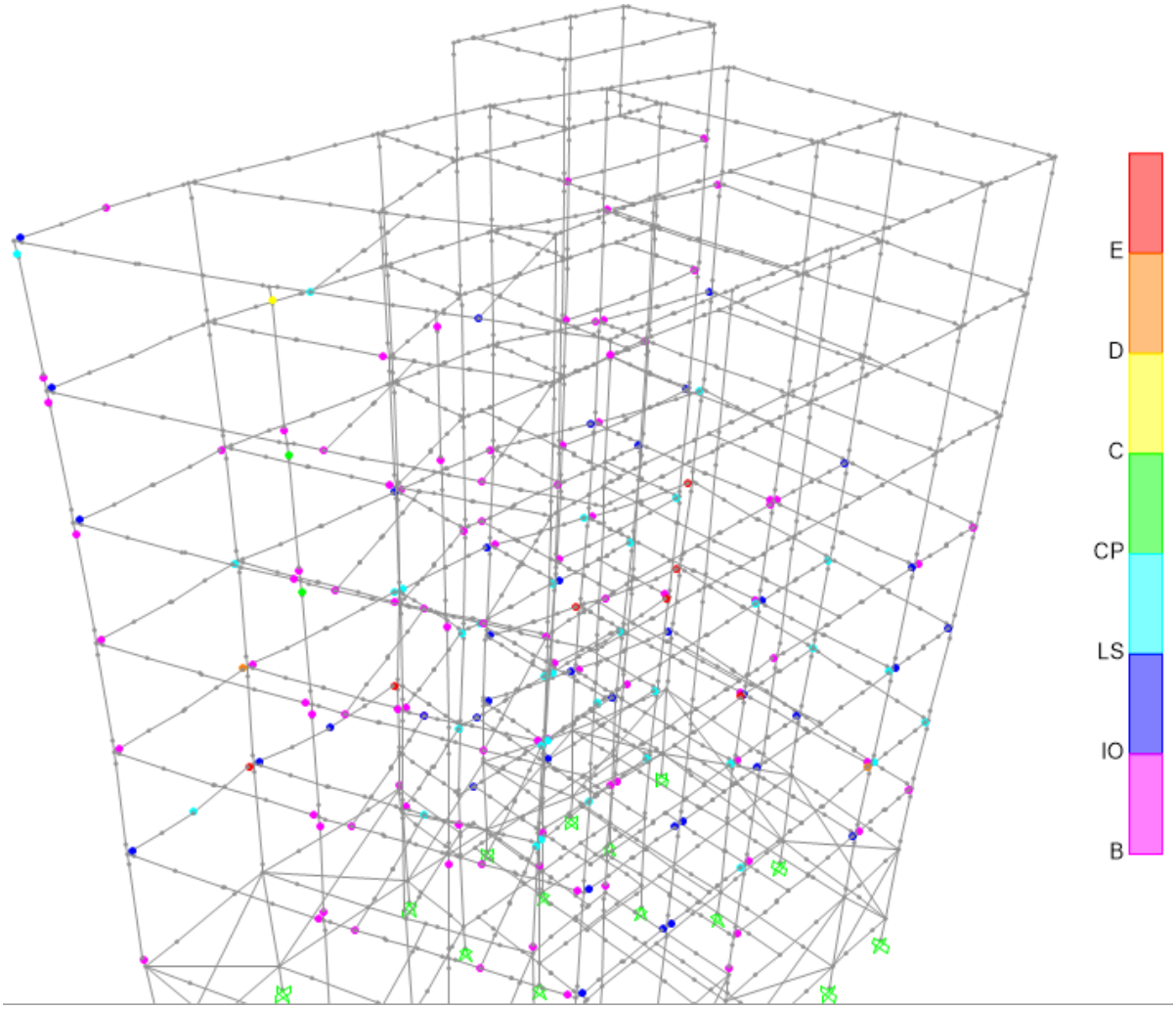

Figure 6.11 Deformed Shape of the Structure at Performance Point- Step 91-92 (Uniform Distribution of Lateral Loads along –X Axis)

Table 6.6 Hinges Limit State Results at Performance Point (Step 91-92)

Step	Displacement	BaseForce	AtoB	BtoIO	IOtoLS	LStoCP	CPtoC	CtoD	DtoE	BeyondE	Total
	m	KN									
90	0.160247	1643.613	924	97	39	34	2	1	1	7	1105
91	**0.160249**	**1622.208**	**924**	**97**	**39**	**34**	**2**	**1**	**1**	**7**	**1105**
92	**0.162503**	**1635.329**	**924**	**96**	**39**	**34**	**2**	**1**	**2**	**7**	**1105**
93	0.162505	1620.953	923	95	41	34	2	1	1	8	1105
94	0.164674	1632.083	921	94	43	35	2	1	1	8	1105

It is shown that 46 hinges exceed the life safety limit state in total. 34 hinges are between the limit states life safety and collapse prevention, 5 face significant strength degradation since they exceed the collapse prevention limit state and 7 hinges lose even their residual strength (Beyond E).

The hinges beyond E are found in beams in the West of the floor level A and in the North-West and centre of the floor level B.

The column C11 faces significant damage since two hinges exceed the collapse prevention limit state and one hinge exceeds the collapse limit state, in floor levels C,D and E.

The column C18 faces significant problems since there is one hinge exceeding the limit state life safety in floor level E.

<u>Nonlinear static analysis along +X Axis (Uniform Distribution of Lateral Loads)</u>

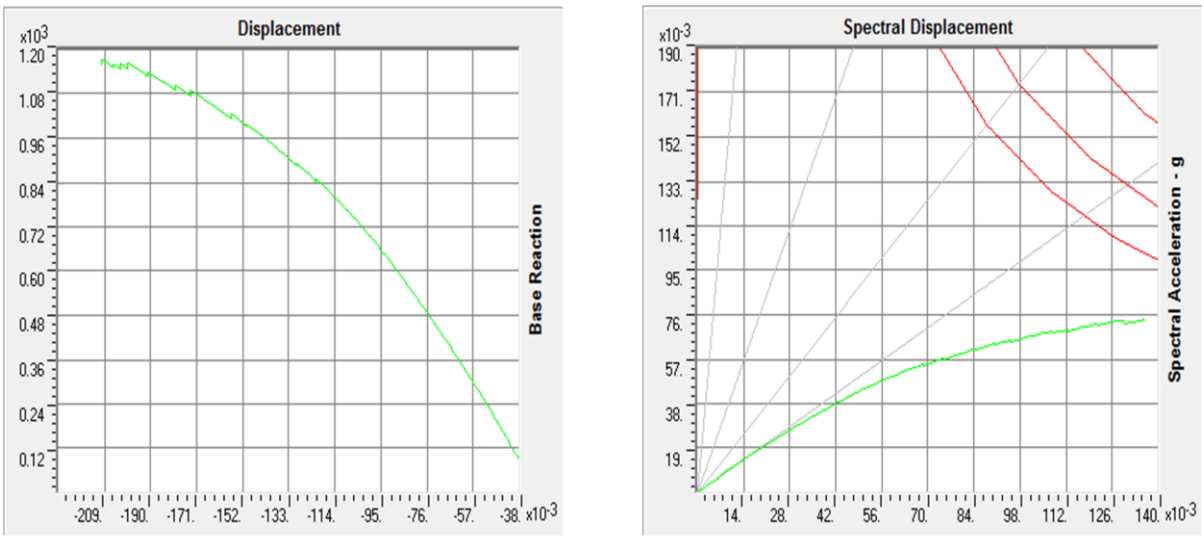

a b

Figure 6.12 a) Pushover Curve (Uniform Distribution of Lateral Loads along +X Axis) b) ATC-40 Capacity Spectrum-ADRS (Uniform Distribution of Lateral Loads along +X Axis)

Performance Point: Not found

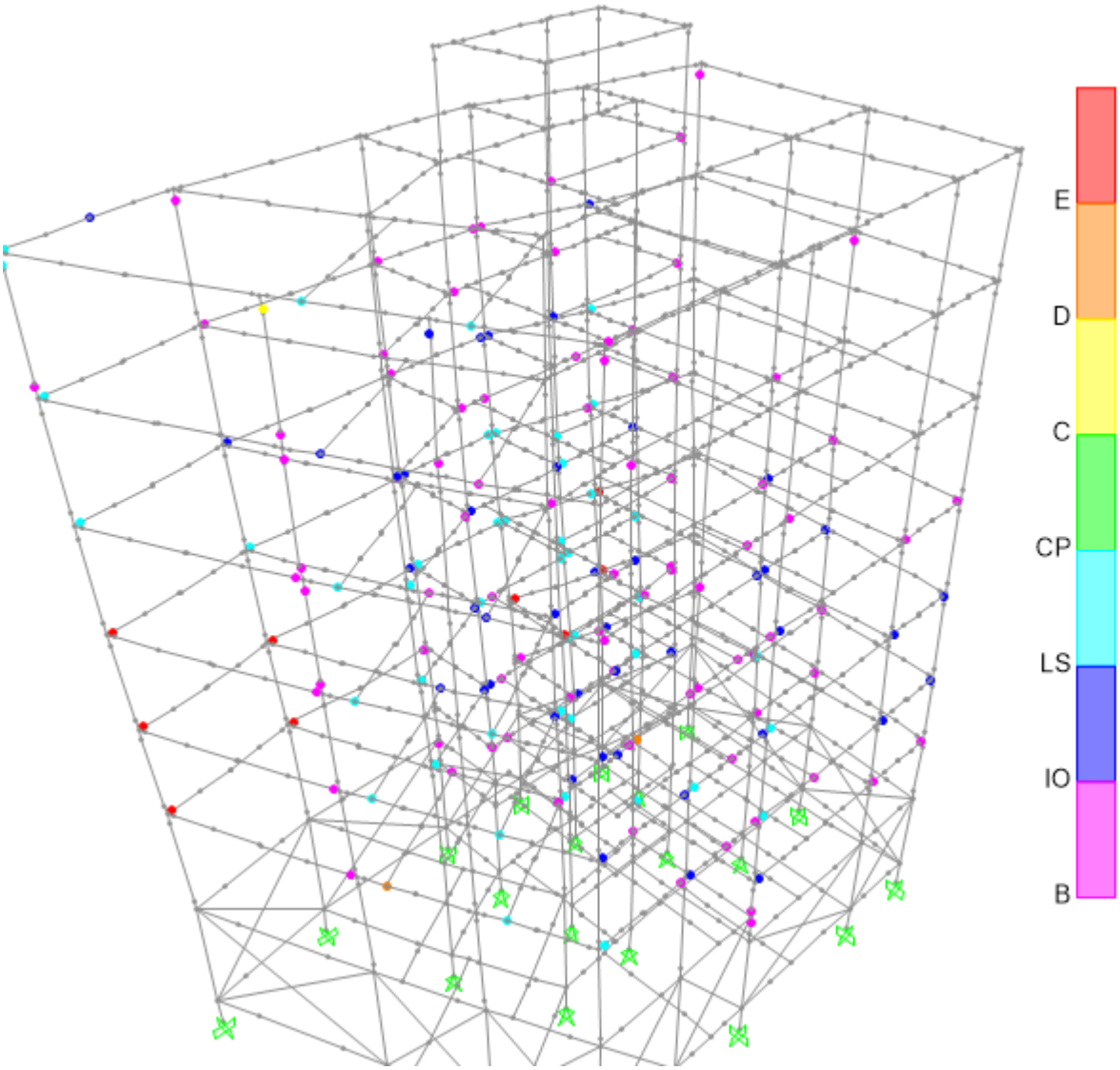

Figure 6.13 Deformed Shape of the Structure at Maximum Step of the Analysis (Uniform Distribution of Lateral Loads along +X Axis)

Table 6.7 Hinges Limit State Results

Step	Displacement	BaseForce	AtoB	BtoIO	IOtoLS	LStoCP	CPtoC	CtoD	DtoE	BeyondE	Total
	m	KN									
98	-0.205377	1151.687	923	83	44	44	0	1	1	9	1105
99	-0.20835	1165.542	922	83	45	44	0	1	1	9	1105
100	-0.21015	1172.643	921	84	45	43	0	1	2	9	1105
101	-0.210152	1159.634	921	84	44	44	0	1	2	9	1105
102	-0.210449	1161.494	921	84	44	44	0	1	2	9	1105

The performance point is not obtained by the analysis, showing that the capacity of the building is inadequate. The capacity is lower than the seismic

demand. The pushover analysis cannot displace the structure beyond 0.21m due to the total strength loss of many hinges.

At the maximum step the analysis reached, the displacement of the control node is 0.21m the base force 1161.494 KN and totally 56 hinges exceed the life safety limit state. 9 hinges have no residual strength (Beyond E), 2 exceed the collapse prevention limit state and 44 are between life safety and collapse prevention limit state.

Only two of the hinges that exceed life safety limit state are found in columns (C11 and C18). However the results indicate that the building faces severe damages to many elements. The most extreme damages (hinges beyond E), are in beams in the South-West, West, and in the centre of the building in the floor levels A and B.

<u>Nonlinear Static (Pushover) Analysis</u> (Uniform Distribution of Lateral Loads along +Y Axis)

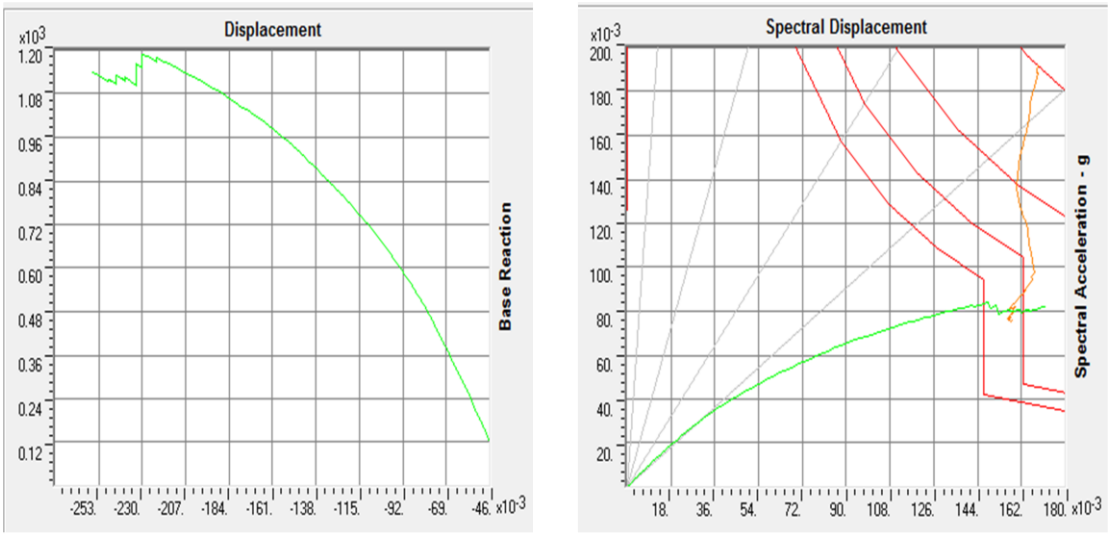

a b

Figure 6.14 a) Pushover Curve (Uniform Distribution of Lateral Loads along +Y Axis) b) ATC-40 Capacity Spectrum-ADRS (Uniform Distribution of Lateral Loads along +Y Axis)

Performance Point: V=1122.347 KN, D=-0.240m, S_a=0.080g, S_d=0.158m

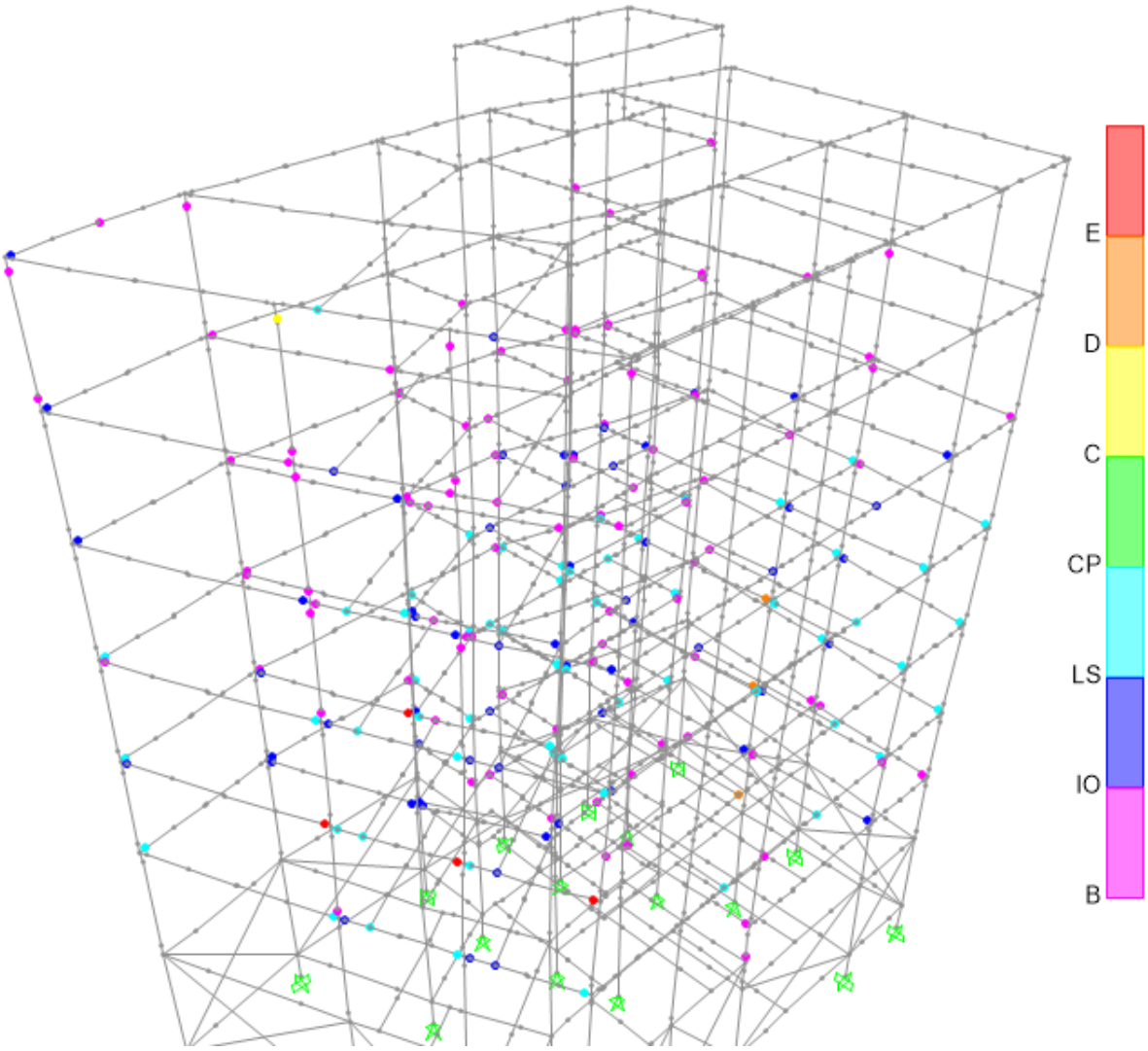

Figure 6.15 Deformed Shape of the Structure at Performance Point-Step 82 (Uniform Distribution of Lateral Loads along +Y Axis)

Table 6.8 Hinges Limit State Results at Performance Point (Step 82)

Step	Displacement	BaseForce	AtoB	BtoIO	IOtoLS	LStoCP	CPtoC	CtoD	DtoE	BeyondE	Total
	m	KN									
80	-0.23907	1128.462	881	95	59	63	0	0	4	3	1105
81	-0.239073	1116.047	881	95	59	63	0	0	4	3	1105
82	**-0.24048**	**1122.455**	**881**	**95**	**59**	**63**	**0**	**1**	**3**	**4**	**1105**
83	-0.240483	1118.072	881	95	59	63	0	0	3	4	1105
84	-0.243945	1130.918	881	94	59	63	0	0	4	4	1105

At the performance point (step 82), 71 hinges exceed the life safety limit state. The 4 hinges beyond E, indicating components having no residual strength, are found in beams in the South-East of the building at the floor levels B and C.

One hinge in column C11 exceeds the collapse limit state. It faces significant strength degradation.

Nonlinear Static Analysis along –Y Axis (Uniform Distribution of Lateral Loads)

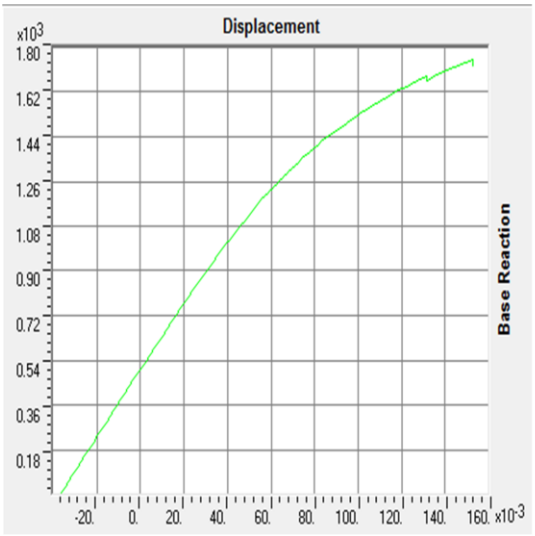

a

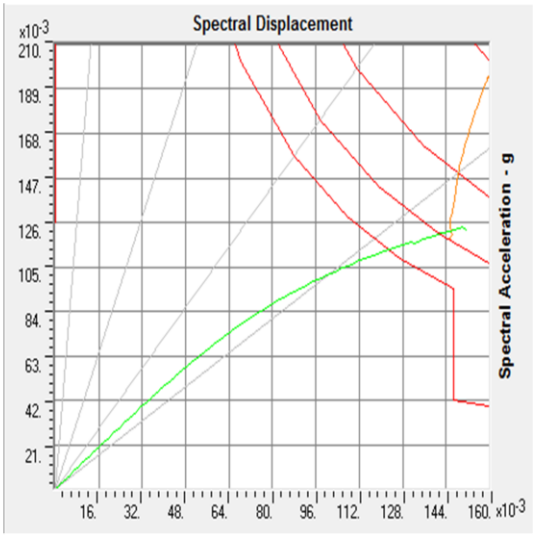

b

Figure 6.16 a) Pushover Curve (Uniform Distribution of Lateral Loads along –Y Axis) b) ATC-40 Capacity Spectrum-ADRS (Uniform Distribution of Lateral Loads along -Y Axis)

Performance Point: V= 1734.622KN, D=0.148m, S_a=0.122g, S_d=0.146m

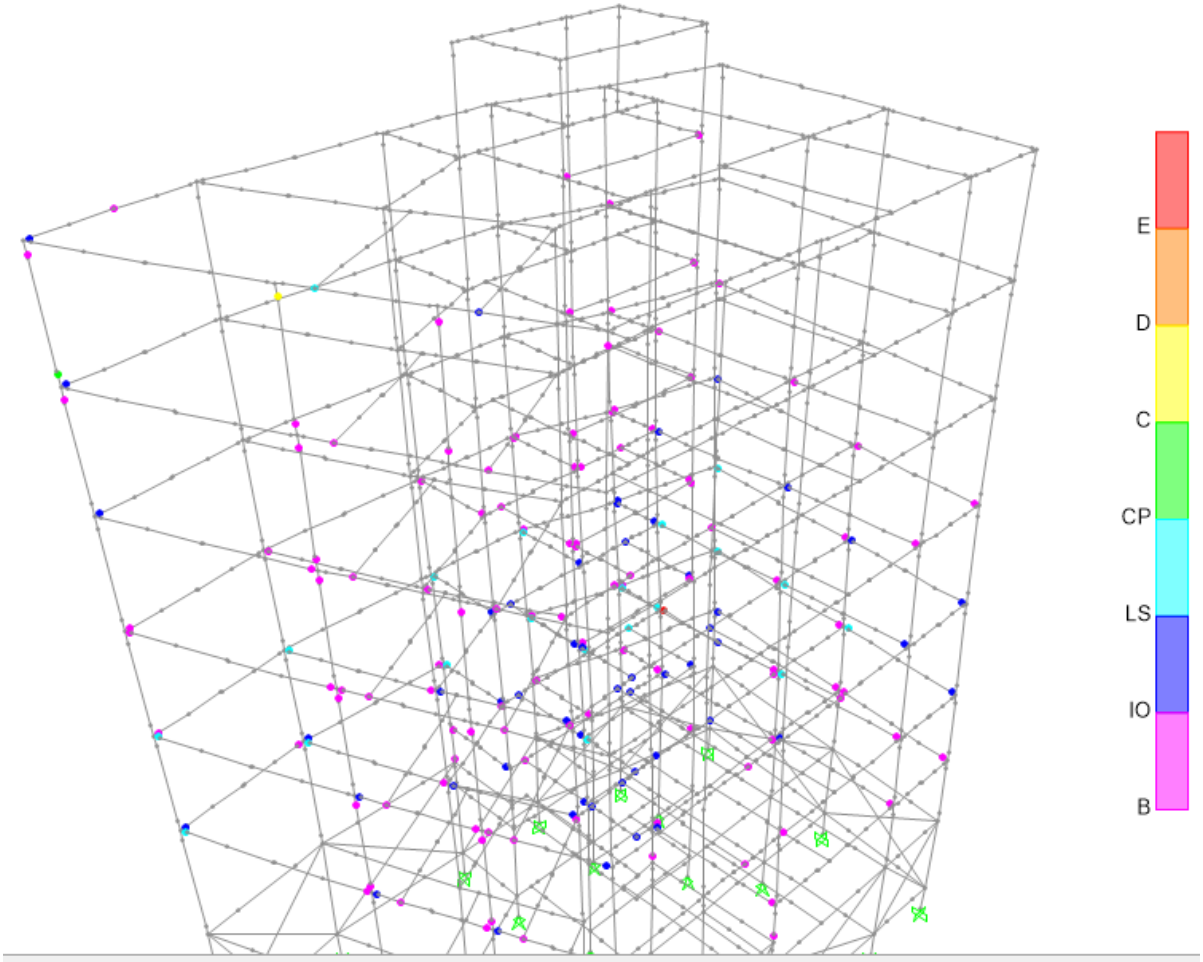

Figure 6.17 Deformed Shape of the Structure at Performance Point-Step 84 (Uniform Distribution of Lateral Loads along -Y Axis)

Table 6.9 Hinges Limit States at Performance Point (Step 84)

Step	Displacement	BaseForce	AtoB	BtoIO	IOtoLS	LStoCP	CPtoC	CtoD	DtoE	BeyondE	Total
	m	KN									
82	0.144424	1721.425	917	110	55	21	0	1	0	1	1105
83	0.147516	1732.874	915	112	53	23	0	1	0	1	1105
84	**0.149416**	**1739.577**	**915**	**111**	**53**	**24**	**1**	**1**	**0**	**1**	**1105**
85	0.152764	1751.2	914	107	55	26	0	1	1	1	1105
86	0.152766	1724.665	913	105	53	31	0	1	0	2	1105

At the performance point (step 84), 27 hinges exceed the life safety limit state, showing that the pushover analysis with uniform distribution of loads along the –Y axis caused lesser damages to the structure, than the other analyses of uniform distribution of lateral loads. One hinge exceeds limit state E. It is in the center of the building in the floor level A.

Hinges in columns C18 and C11 exceed limit states of collapse prevention and collapse, respectively. They face severe damages and strength degradation.

Nonlinear Static Analysis along +X Axis (Modal Distribution of Lateral Loads)

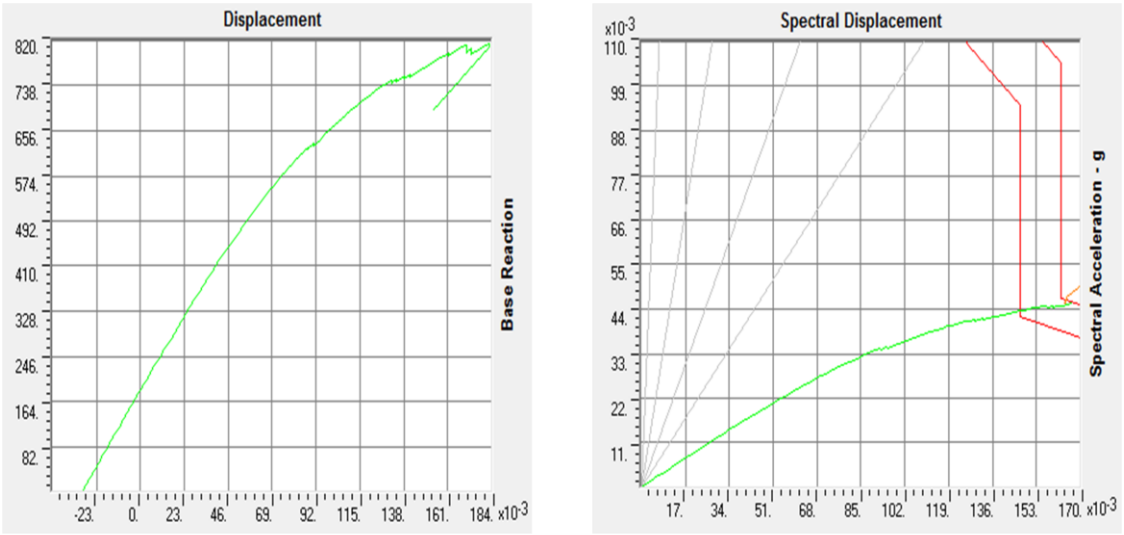

a b

Figure 6.18 a) Pushover Curve (Modal Distribution of Lateral Loads along +X Axis) b) ATC-40 Capacity Spectrum-ADRS (Modal Distribution of Lateral Loads along +X Axis)

Performance Point: V= 811.006, D=0.181m, S_a=0.045g, S_d=0.165m

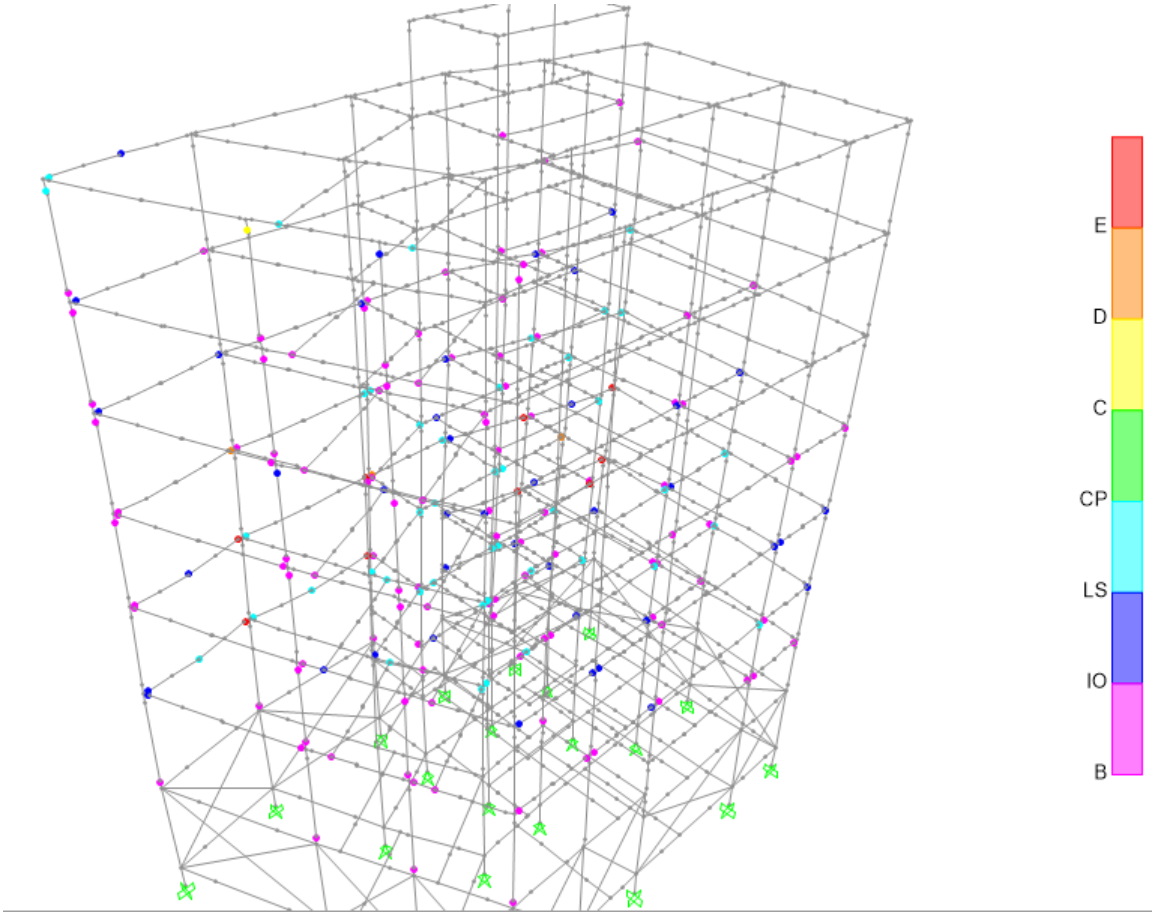

Figure 6.19 Deformed Shape of the Structure at Performance Point-Step 89 (Modal Distribution of Lateral Loads along +X Axis)

Table 6.10 Hinges Limit State Results at Performance Point (Step 89)

Step	Displacement	BaseForce	AtoB	BtoIO	IOtoLS	LStoCP	CPtoC	CtoD	DtoE	BeyondE	Total
	m	KN									
87	0.178721	806.886	901	110	40	42	0	1	2	9	1105
88	0.180871	810.972	898	111	40	44	0	1	2	9	1105
89	**0.182928**	**814.841**	**898**	**110**	**41**	**43**	**0**	**1**	**3**	**9**	**1105**
90	0.18293	808.104	898	110	41	43	0	1	1	11	1105
91	0.152823	692.86	898	110	41	43	0	1	1	11	1105

At the performance point there are 56 hinges that exceed the limit state of life safety. The most severe damages (hinges beyond E) are located in beams in the West of the building at A and B floor levels.

Nonlinear Static Analysis along -X Axis (Modal Distribution of Lateral Loads)

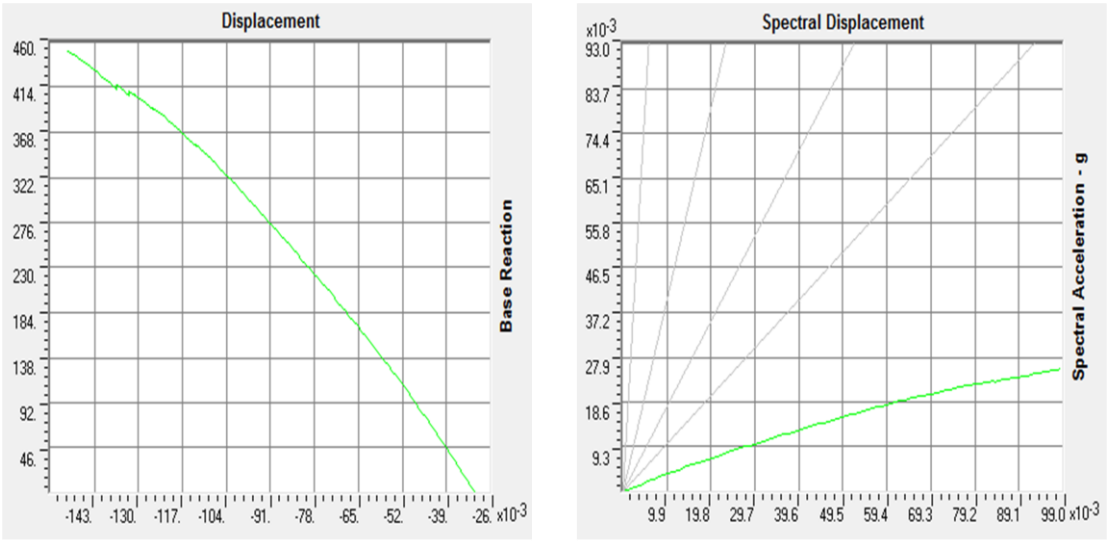

a b

Figure 6.20 a) Pushover Curve (Modal Distribution of Lateral Loads along -X Axis) b) ATC-40 Capacity Spectrum-ADRS (Modal Distribution of Lateral Loads along -X Axis)

Performance Point: Not found

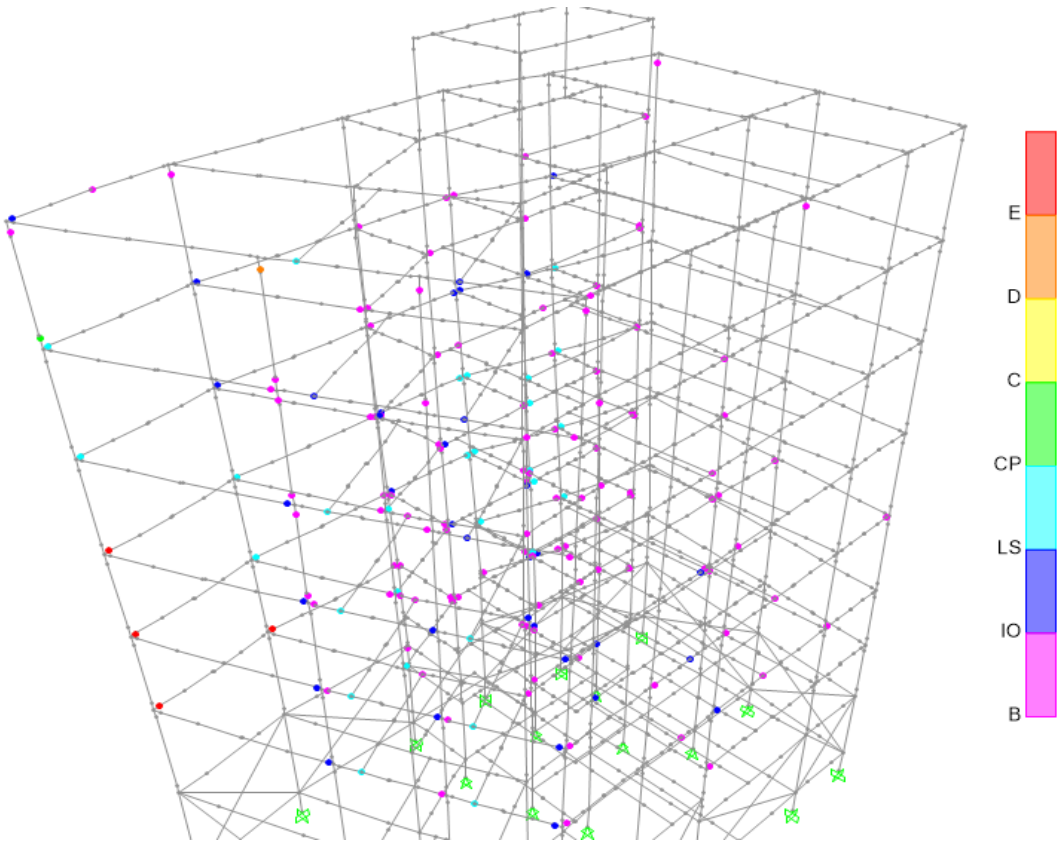

Figure 6.21 Deformed Shape of the Structure at Maximum Step of the Analysis (Modal Distribution of Lateral Loads along -X Axis)

Table 6.11 Hinges Limit State Results

Step	Displacement	BaseForce	AtoB	BtoIO	IOtoLS	LStoCP	CPtoC	CtoD	DtoE	BeyondE	Total
	m	KN									
92	-0.146768	440.759	926	108	34	32	0	0	1	4	1105
93	-0.147978	443.777	925	109	34	32	0	0	1	4	1105
94	-0.149188	446.774	923	111	34	32	1	0	1	4	1105
95	-0.150398	449.679	922	112	34	32	1	0	1	4	1105
96	-0.151449	452.173	922	112	33	33	1	0	1	4	1105

The maximum displacement of the control node is 0.151m. Beyond that displacement the analysis cannot run, because of the severe strength loss of the elements of the building. The most extended damages (beyond E) are found in beams in the South-West side of the building at the floor levels A,B and C. 39 hinges exceed life safety limit state.

The columns C11 and C18 face significant strength degradation

<u>Nonlinear Static Analysis along +Y Axis (Modal Distribution of Lateral Loads)</u>

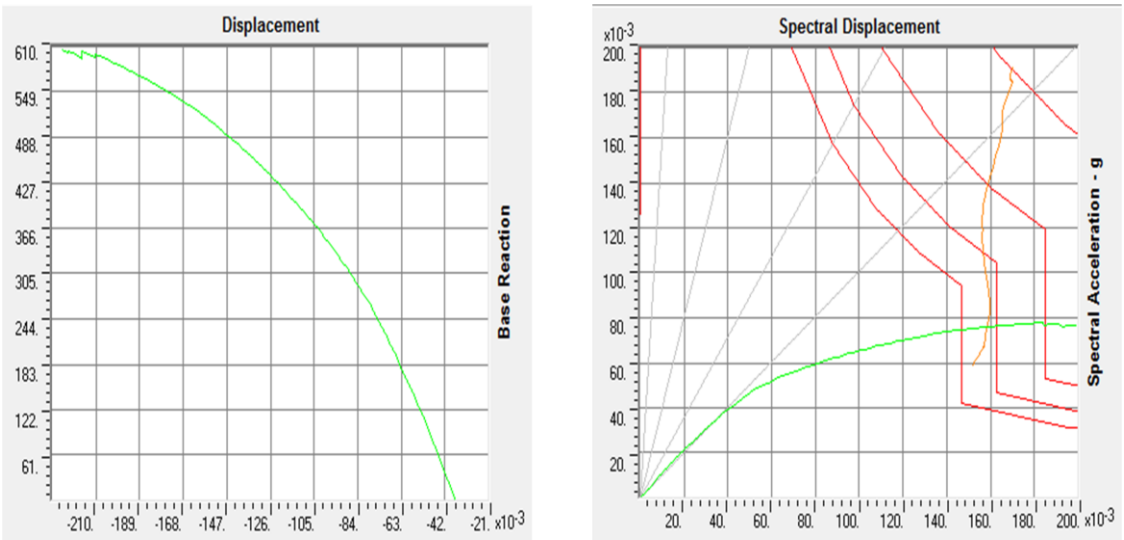

a b

Figure 6.22 a) Pushover Curve (Modal Distribution of Lateral Loads along +Y Axis) b) ATC-40 Capacity Spectrum-ADRS (Modal Distribution of Lateral Loads along +Y Axis)

Performance Point: V=561.429KN D=-0.183m, S_a=0.076g, S_d=0.158m

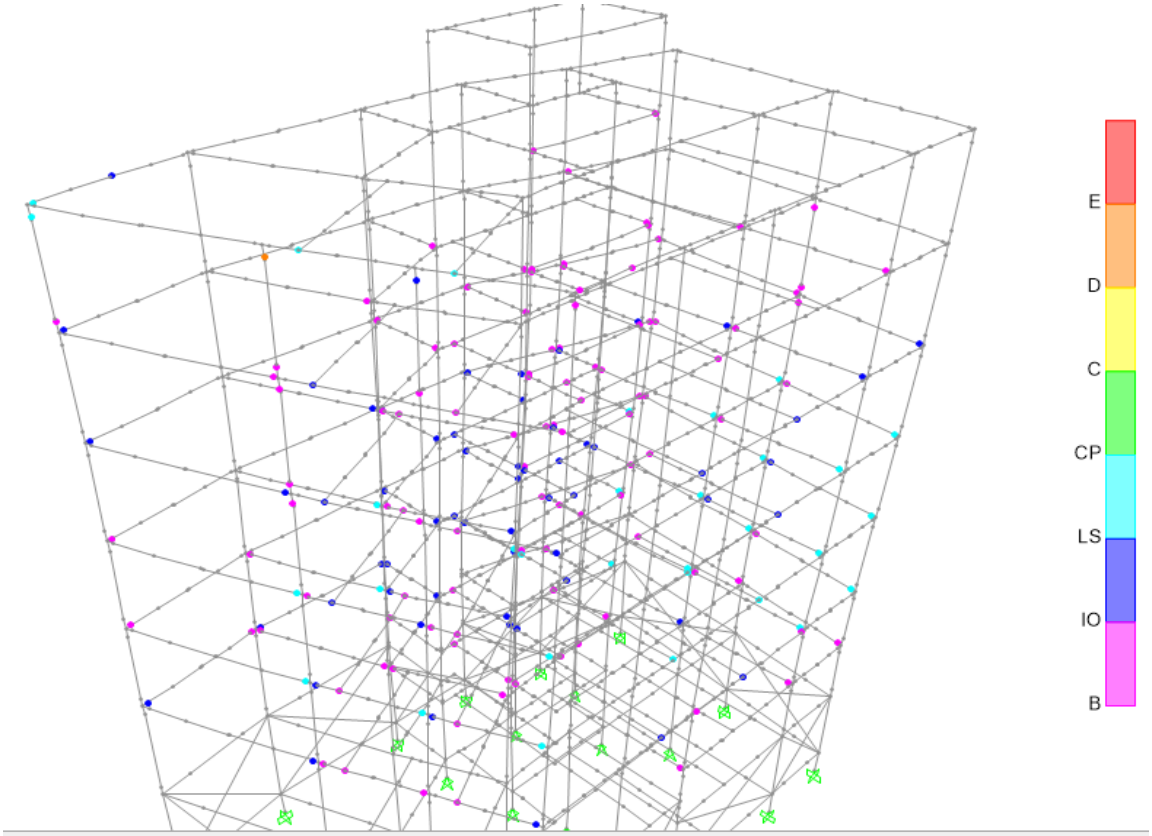

Figure 6.23 Deformed Shape of the Structure at Performance Point-Step 66 (Modal Distribution of Lateral Loads along +Y Axis)

Table 6.12 Hinges Limit State Results at Performance Point (Step 66)

Step	Displacement	BaseForce	AtoB	BtoIO	IOtoLS	LStoCP	CPtoC	CtoD	DtoE	BeyondE	Total
	m	KN									
65	-0.182084	560.028	905	108	60	31	0	0	1	0	1105
66	**-0.183984**	**562.945**	**905**	**108**	**60**	**31**	**0**	**0**	**1**	**0**	**1105**
67	-0.185884	565.861	903	107	61	33	0	0	1	0	1105
68	-0.187784	568.675	901	109	60	34	0	0	1	0	1105
69	-0.189684	571.472	900	109	61	34	0	0	1	0	1105

At the performance point (step 66), there are 32 hinges that exceed life safety limit state. The total of those are found in beams, except one which is found in Column C18 and one in column C11 that faces significant strength degradation (D to E).

Nonlinear Static Analysis along -Y Axis (Modal Distribution of Lateral Loads)

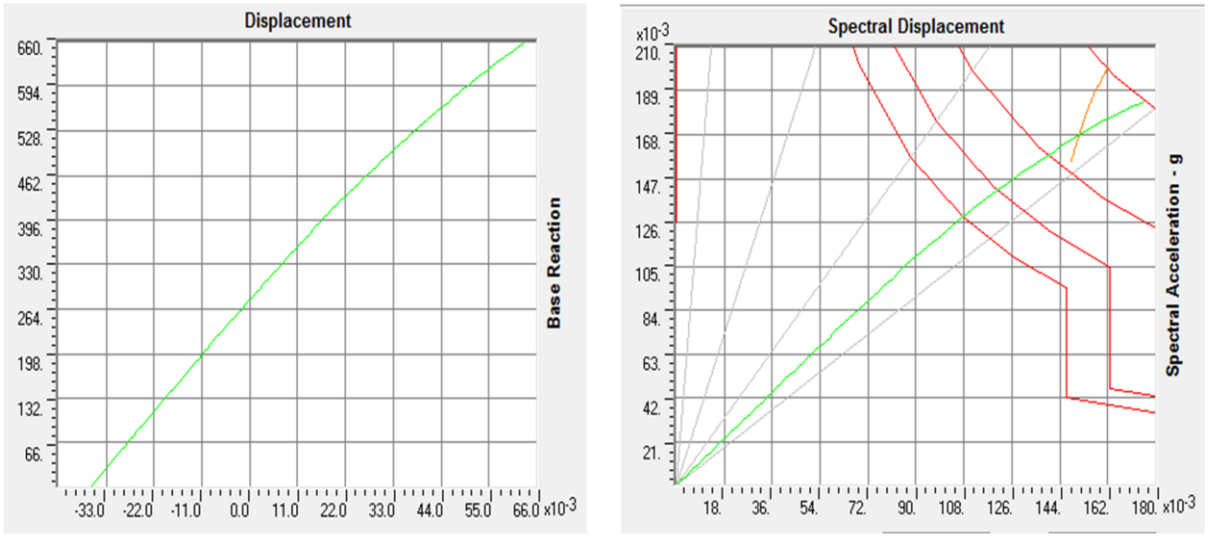

a b

Figure 6.24 a) Pushover Curve (Modal Distribution of Lateral Loads along -Y Axis) b) ATC-40 Capacity Spectrum-ADRS (Modal Distribution of Lateral Loads along -Y Axis)

Performance Point: V=591.894 KN, D= 0.049m, S_a=0.168g, S_d=0.151m

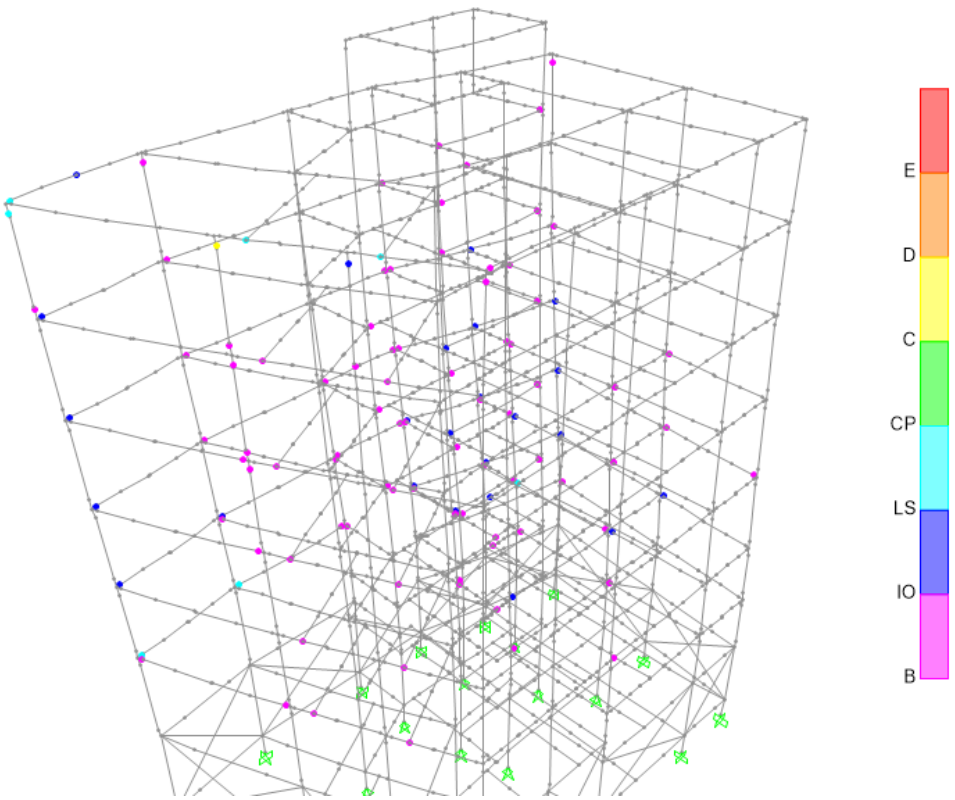

Figure 6.25 Deformed Shape of the Structure at Performance Point-Step 84 (Modal Distribution of Lateral Loads along -Y Axis)

Table 6.13 Hinges Limit State Results at Performance Point (Step 84)

Step	Displacement	BaseForce	AtoB	BtoIO	IOtoLS	LStoCP	CPtoC	CtoD	DtoE	BeyondE	Total
	m	KN									
82	0.047681	582.364	991	83	23	7	0	1	0	0	1105
83	0.048681	587.692	991	83	23	7	0	1	0	0	1105
84	**0.049681**	**593.02**	**991**	**82**	**24**	**7**	**0**	**1**	**0**	**0**	**1105**
85	0.050681	598.348	987	85	24	8	0	1	0	0	1105
86	0.051681	603.424	984	87	25	8	0	1	0	0	1105

At the performance point step 84, only 8 hinges exceed life safety limit state. This analysis causes the less damage in comparison to all the other pushover analyses. In addition the lowest base shear force and displacement to the structure is obtained at its performance point.

The results of a hinge are shown in order to indicate the hinge backbone curve. It is taken from beam B30 of floor A (9.03m) and the pushover analysis with modal lateral load distribution along –Y axis. It is shown that when the performance point is reached (step 84) the hinge status (for the degree of freedom M3 which is crucial for the beams) is between the life safety and collapse prevention limit states.

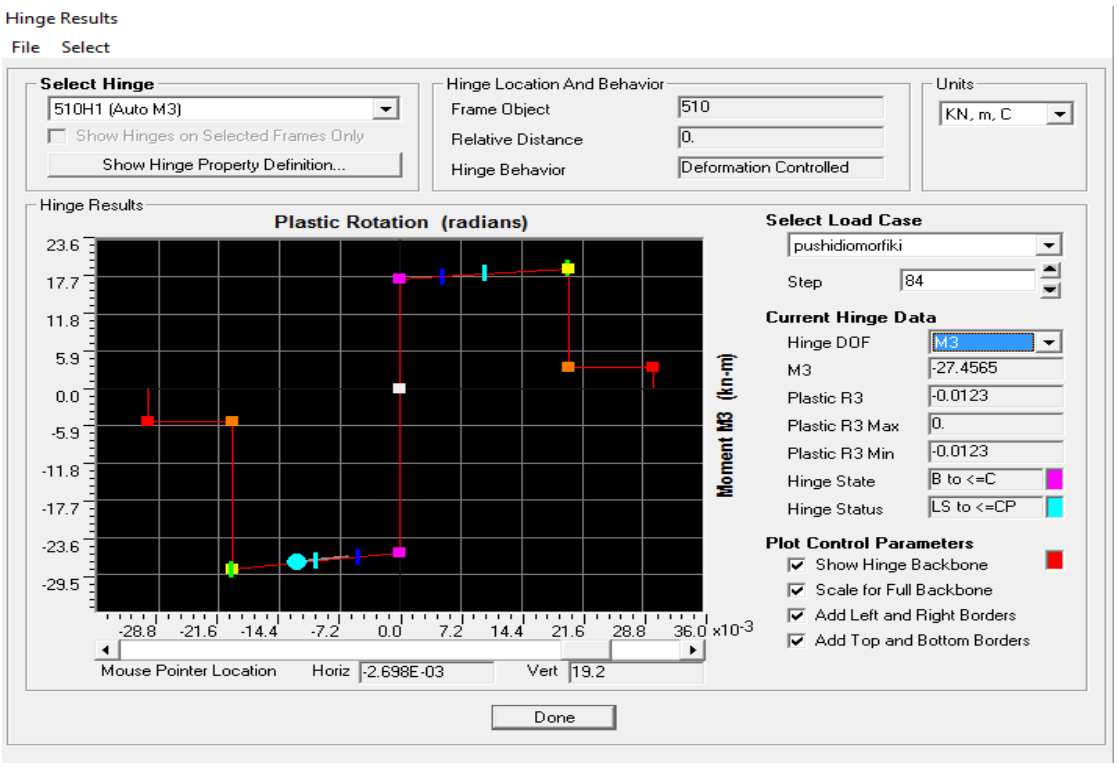

Figure 6.26 Hinge Results-Backbone Curve

In the figures 6.27 and 6.28, the maximum displacement per floor level and per distribution of the lateral loads, along X and Y axis are shown.

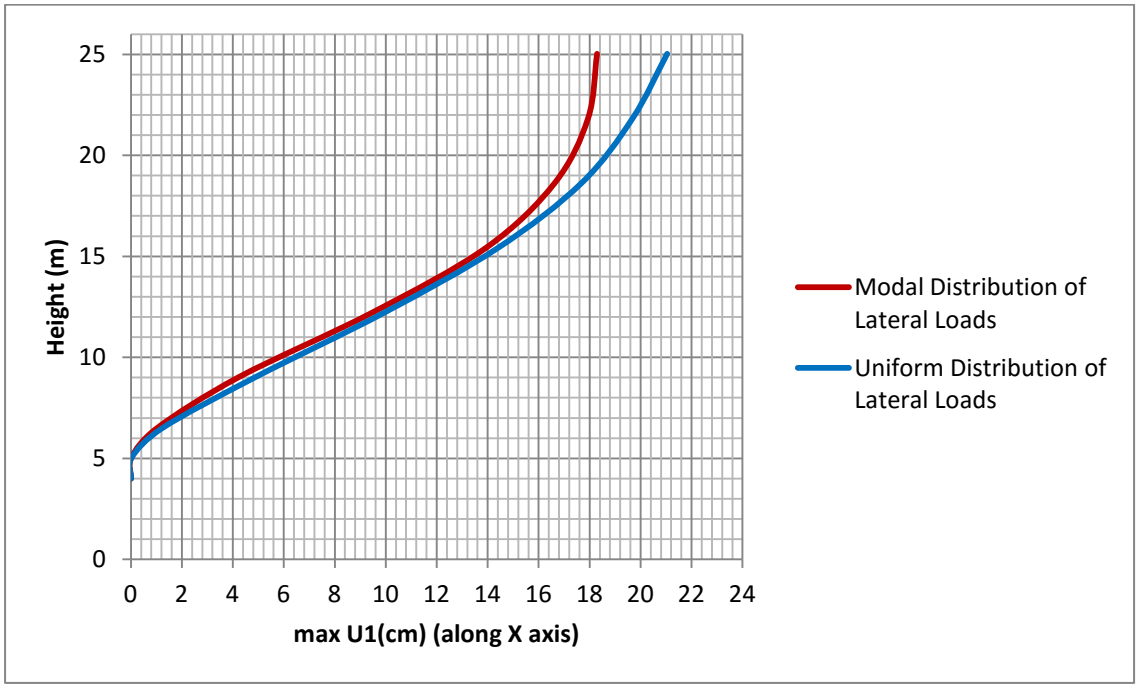

Figure 6.27 Maximum Displacement per Height along X axis for Uniform and Modal Distribution of Lateral Loads

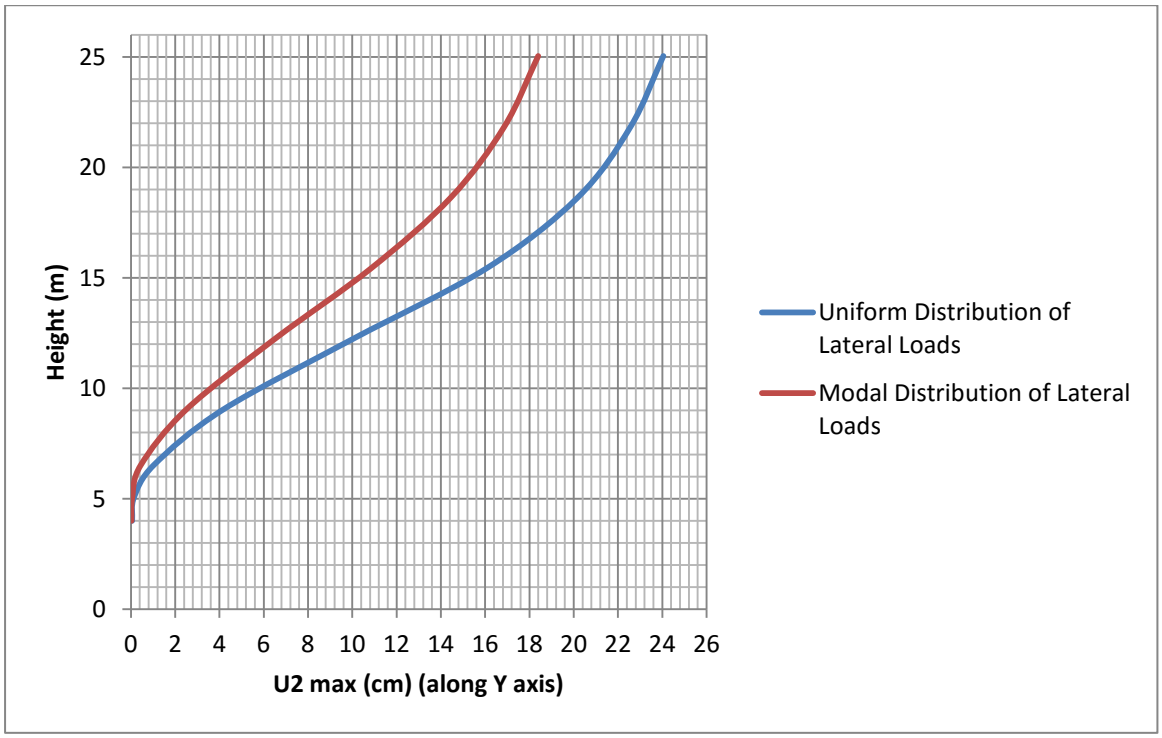

Figure 6.28 Maximum Displacement per Height along Y axis for Uniform and Modal Distribution of Lateral Loads

In the figures 6.29 and 6.30, the inter-story drift ratios, which is an important indicator of structural behavior in performance-based seismic analysis, are shown for uniform and modal distribution of lateral loads, along X and Y axis.

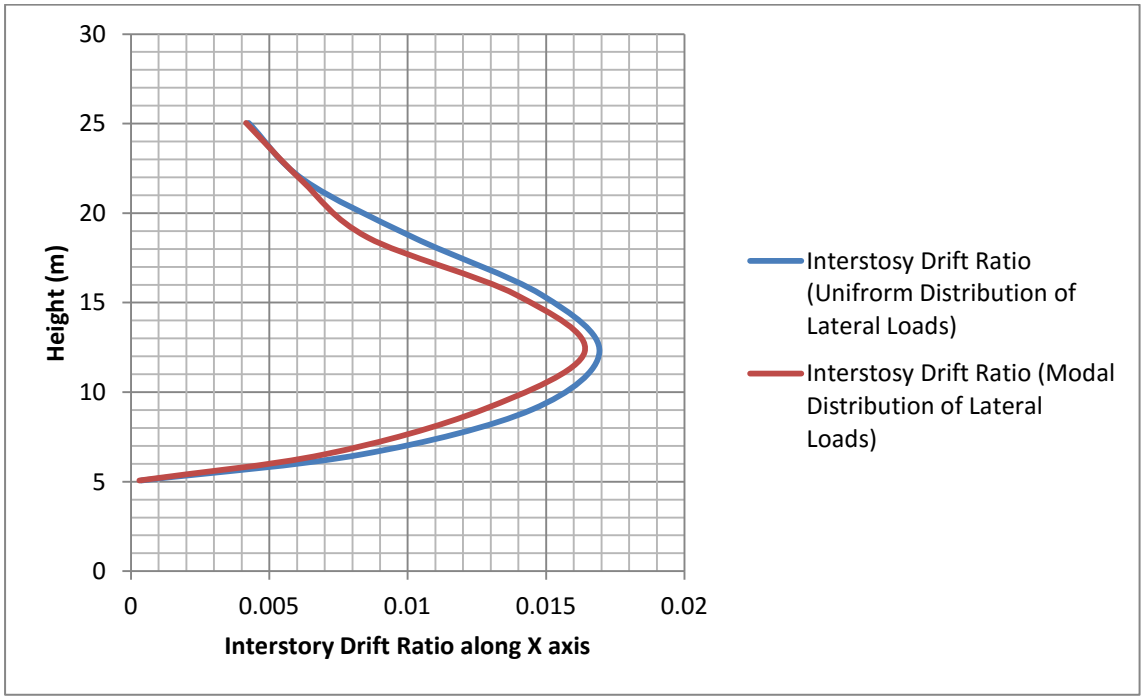

Figure 6.29 Inter-story Drift Ratios along X Axis for Uniform and Modal Distribution of Lateral Loads

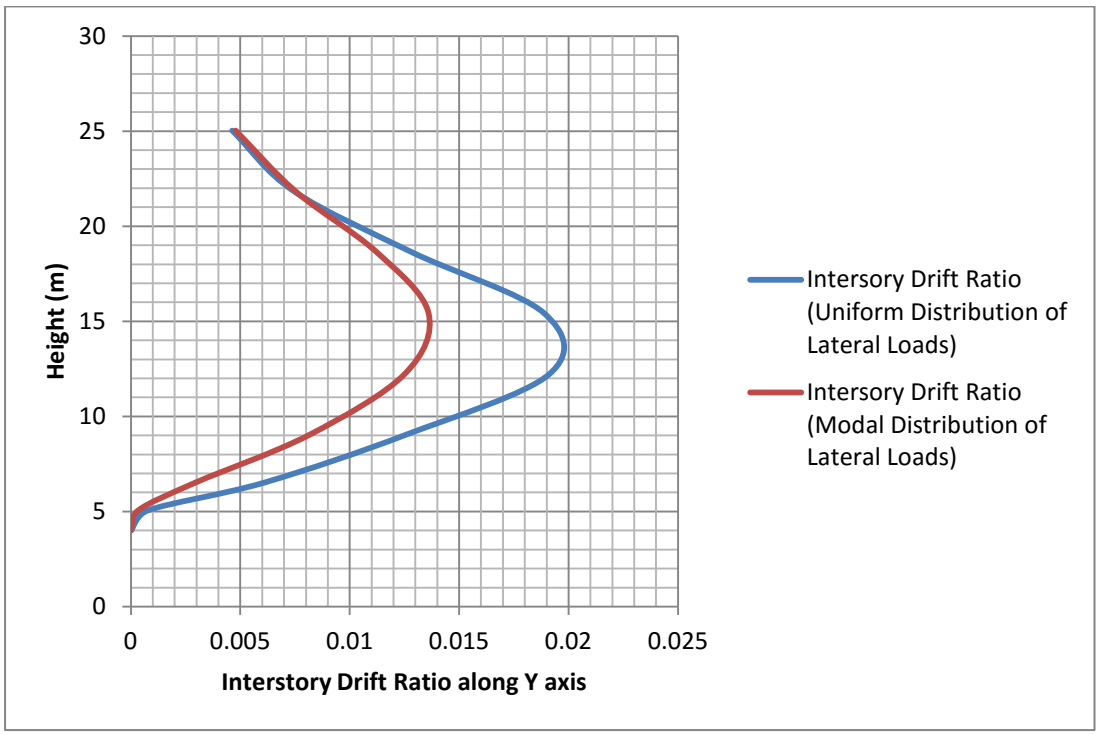

Figure 6.30 Inter-story Drift Ratios along Y Axis for Uniform and Modal Distribution of Lateral Loads

6.6 Discussions on the Pushover Analysis Results

- The maximum displacement of the control node is caused by the pushover analysis with uniform distribution of lateral loads along +Y axis (D=0.24m). The maximum base shear force is caused by the pushover analysis with uniform distribution of lateral loads along the –Y axis (V=1739.577KN).
- Performance point is not obtained for the pushover analyses with modal distribution of loads along –X axis and with uniform distribution of loads along +X axis, showing that the capacity of the structure is inadequate and the structure faces very significant damages and strength degradation when the seismic force is imposed along the X axis.
- The highest number of hinges (70 hinges) exceeding the life safety limit state is obtained for the pushover analysis with uniform distribution of lateral loads along +Y axis (which also causes the maximum displacements).
- The highest number of hinges (9 hinges) beyond E is obtained for the pushover analysis with modal and uniform distribution of lateral loads along +X axis.
- In general the uniform distribution causes 198 hinges to exceed life safety limit state and 21 to lose their residual strength (beyond E), while the modal distribution causes 134 and 13 hinges, respectively. As a result the uniform distribution of lateral loads causes more damages to the structure than the modal distribution.
- The minimum displacement is caused by the pushover analysis with modal distribution of lateral loads along –Y axis (0.049681m). In addition it causes the minimum number of hinges (8) that exceed the life safety limit state.
- The most severe damages are obtained in beams in floor levels A (9.03m) and B (12.23m). Many hinges in those floor levels lose their residual strength and others face significant strength degradation.
- Columns C11 and C18 face the most significant damages since their hinges range from life safety limit state to D (point on hinge backbone

curve defined by FEMA 356), in floor levels D and E, for all the analyses. The hinges of the rest of the columns do not exceed the life safety limit state for none of the pushover analyses performed.

- The maximum absolute displacements increase with floor height for both the lateral load distributions and axes. The maximum displacement is observed in Y axis, as mentioned above.
- The uniform distribution of lateral loads causes higher absolute displacements than the modal distribution, for both the axes X,Y. However it is shown that their difference is larger in Y axis than in X axis.
- The maximum displacements caused by the pushover analyses with modal distribution of lateral loads are approximately 0.18m for both the X and Y axis.
- The inter-story drift ratios are larger for uniform distribution of lateral loads, than they are for modal distribution, for both X and Y axis. However it is shown that their difference is larger in Y axis than in X axis.
- The largest inter-story drift ratio is observed along the Y axis and it is approximately 2%, which is far beyond the acceptable limits.
- The uniform distribution of lateral loads causes higher inter-story drift ratios along axis Y (2%) than along the X axis (1.7%). However the modal distribution of lateral loads causes higher inter-story drift ratios along axis X (1.65%) than along the axis Y (1.35%).
- It is mentioned that the maximum inter-story drift ratios are observed at medium heights of the building, in the floor levels A (9.03M), B (12.23m) and C (15.43m).

Chapter 7

Nonlinear Time-History Dynamic Analyses of the Existing Structure

Time-history analysis is a step-by-step analysis of the dynamic response of a structure to a specified loading that may vary with time. The nonlinear time-history analysis is highly dependent on the time history used. Thus many nonlinear analyses, using a variety of accelerograms are required, in order to obtain reliable results. The response of the building is directly calculated in discrete time steps.

The dynamic equilibrium equations to be solved are given by:

$$K\,u(t) + C\,\dot{u}(t) + M\,\ddot{u}\,(t) = r(t) \qquad (34) \qquad \text{(CSi, 1995)}$$

Where K is the stiffness matrix, C is the damping matrix and M is the diagonal mass matrix. u, $\dot{u}$, $\ddot{u}$ are the displacements, velocities and accelerations of the structure and r is the applied load. Here the applied load refers to the ground motion, so the displacements, velocities and accelerations are relative to this ground motion (CSi, 1995).

7.1 Nonlinear Characteristics of the structure elements

The nonlinear characteristics of the structure elements are exactly the same as for the pushover analysis.

7.2 Earthquake Ground Motion Time-Histories

Three pairs of acceleration time histories are used. They are obtained by the earthquakes of Corinth (1981, magnitude: 6.6), Kalamata (1986, magnitude 6.2) and L'Aquila-Italy (2009 magnitude: 6.3). The acceleration time histories are obtained by the PEER Ground Motion Data Base-Beta version. It is an interactive web based application that allows the user to select sets of ground motion acceleration time series that are representative of design ground

motions. The user may specify the design ground motions in terms of a target response spectrum and the desired characteristics of the earthquake ground motions in terms of earthquake magnitude, source-to-site distance and other characteristics (Pacific Earthquake Engineering Research Center (PEER), 2010).

Consistent pairs of earthquake ground motion records are simultaneously imposed to the structure, along each of the horizontal axes (longitudinal and transverse).

The values of the acceleration time histories are scaled, to the value of a_g.S, where for seismic zone II and ground type B is $0.24g \cdot 1.2 = 0.288g$. According to EN 1998-1 (2004) the zero period response spectrum acceleration values should not be lower than the value of a_g.S for the site in question.

In the figures 7.1 to 7.18, the scaled and non scaled acceleration time-histories and their corresponding response spectrums are shown.

Earthquake Event of Corinth

Scaling factors: Longitudinal Axis: 1.114, Transverse Axis: 0.972

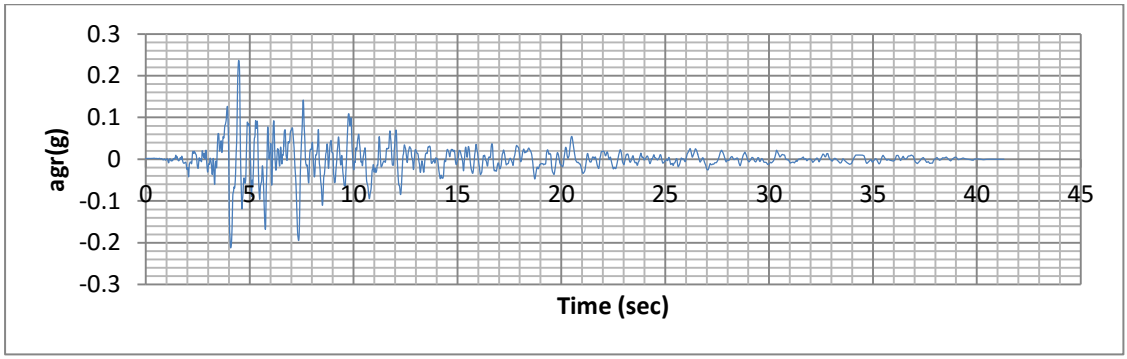

Figure 7.1 Non Scaled Acceleration Time History of Corinth Earthquake (longitudinal axis)

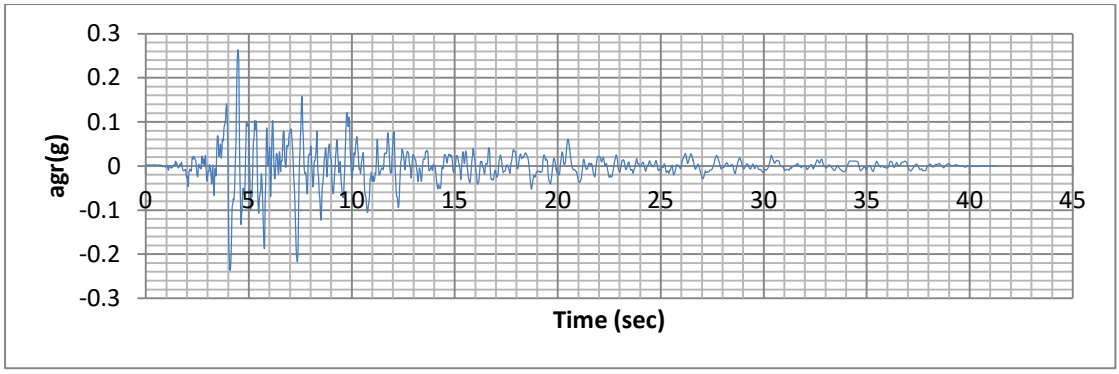

Figure 7.2 Scaled Acceleration Time History of Corinth Earthquake (longitudinal axis)

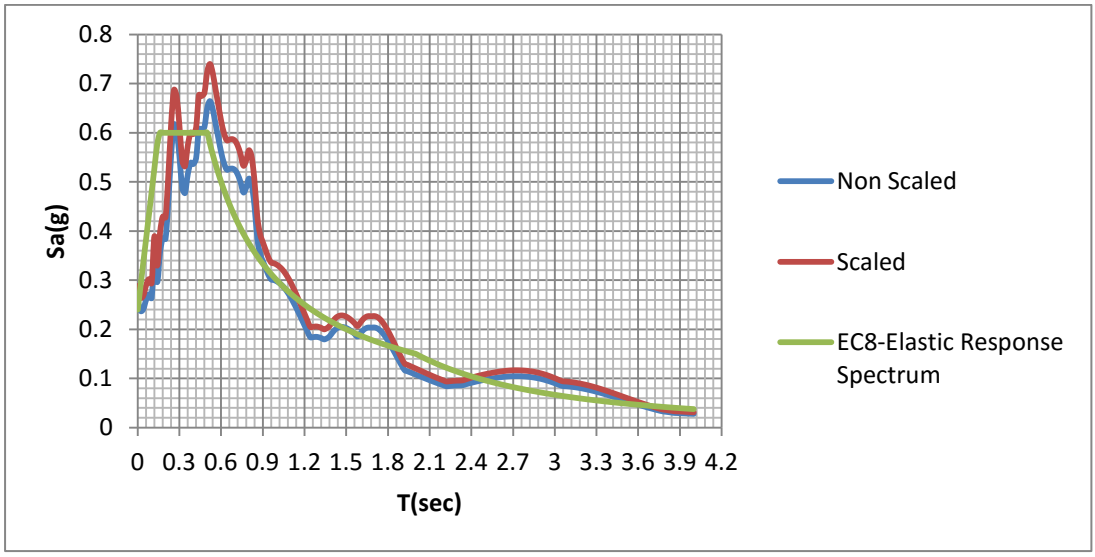

Figure 7.3 Scaled and Non-scaled Acceleration Response Spectrum of Corinth Earthquake (longitudinal axis)

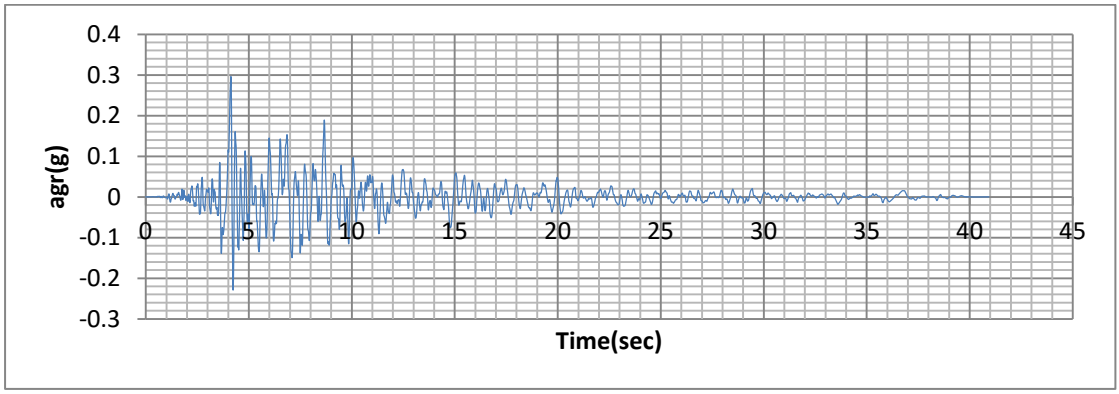

Figure 7.4 Non Scaled Acceleration Time History of Corinth Earthquake (transverse axis)

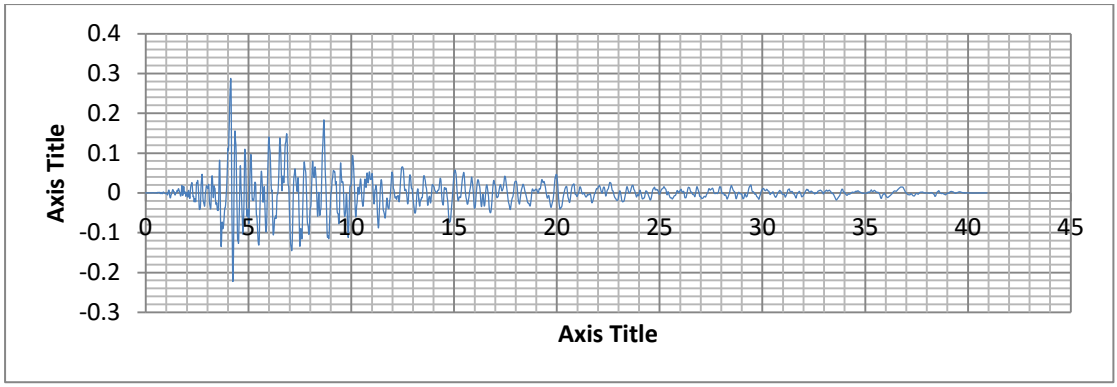

Figure 7.5 Scaled Acceleration Time History of Corinth Earthquake (transverse axis)

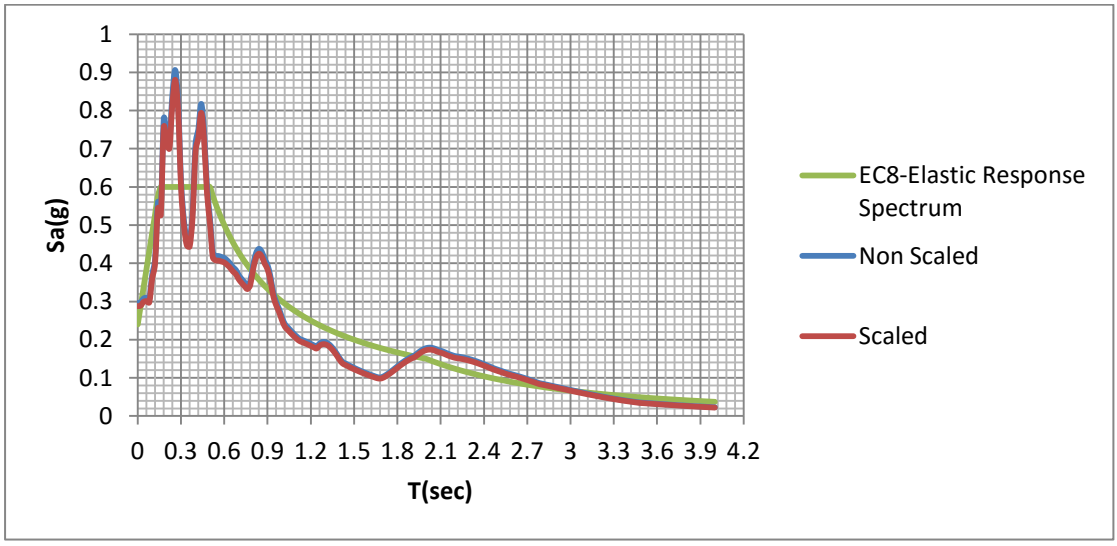

Figure 7.6 Scaled and Non-scaled Acceleration Response Spectrum of Corinth Earthquake (transverse axis)

Earthquake Event of Kalamata

Scaling factors: Longitudinal Axis: 1.159 Transverse Axis: 1.057

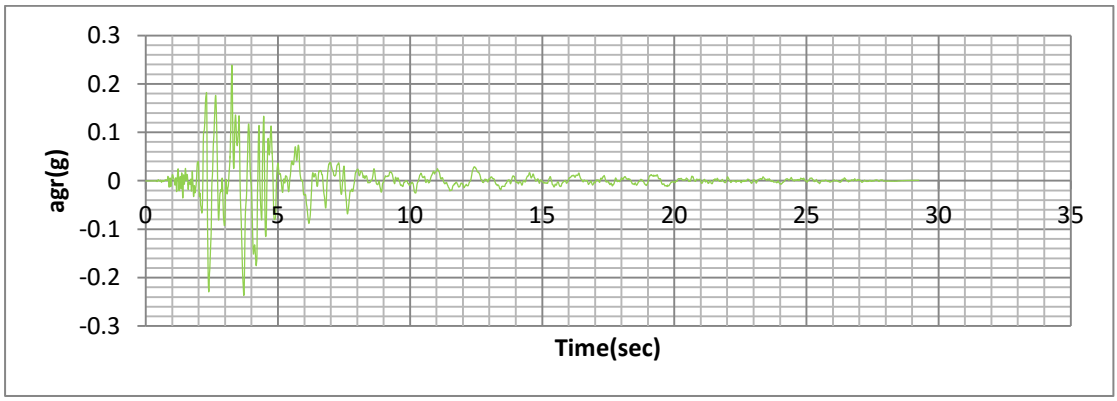

Figure 7.7 Non Scaled Acceleration Time History of Kalamata Earthquake (longitudinal axis)

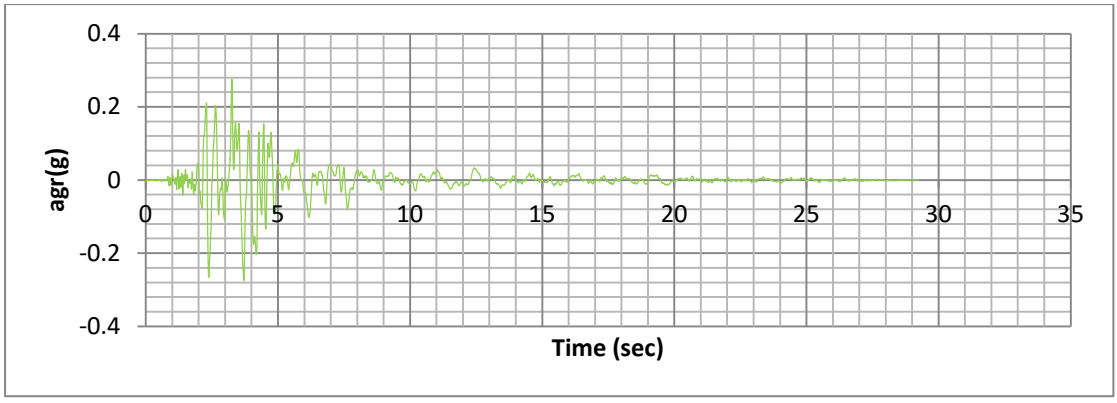

Figure 7.8 Scaled Acceleration Time History of Kalamata Earthquake (longitudinal axis)

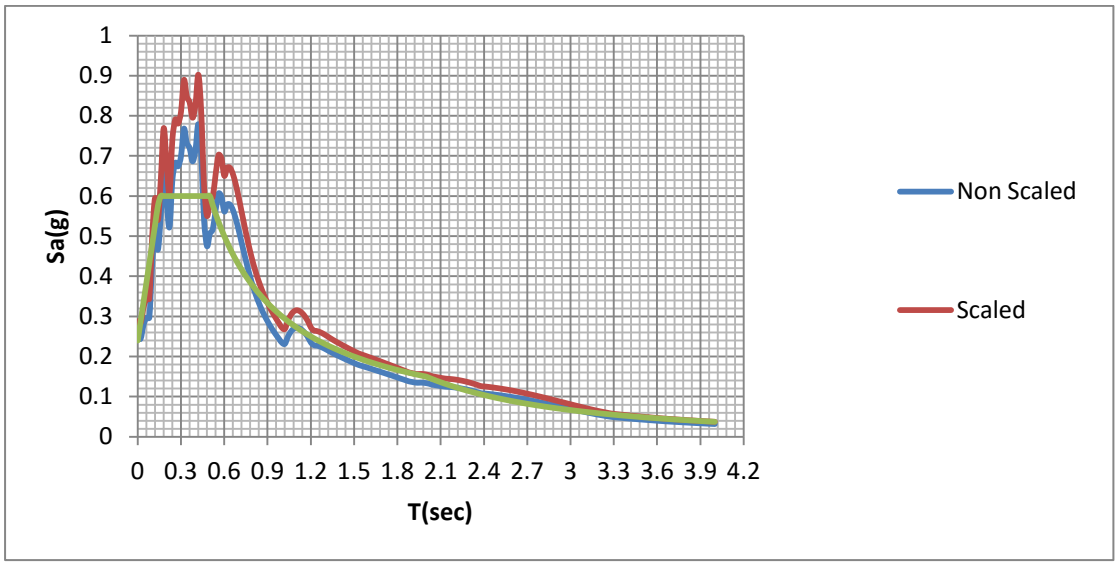

Figure 7.9 Scaled and Non-scaled Acceleration Response Spectrum of Kalamata Earthquake (longitudinal axis)

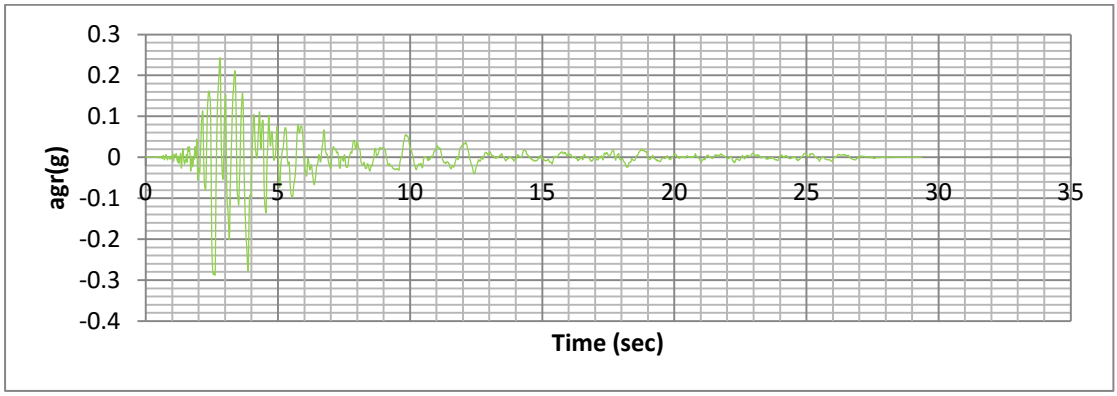

Figure 7.10 Non Scaled Acceleration Time History of Kalamata Earthquake (transverse axis)

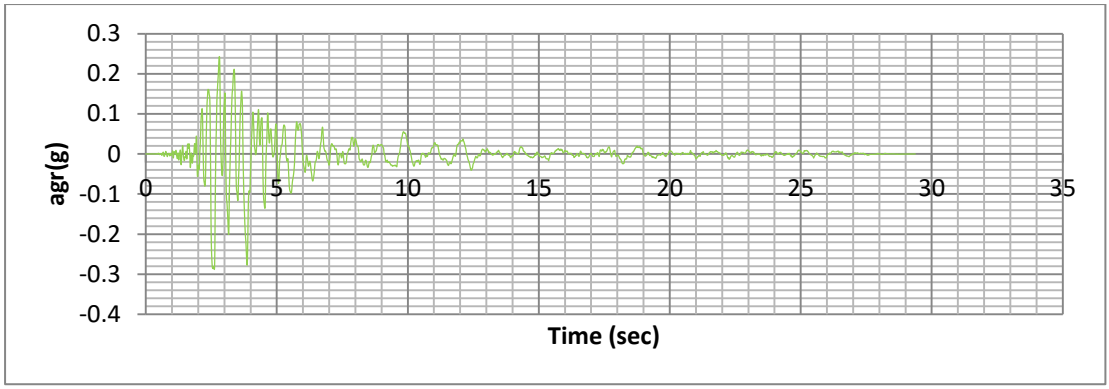

Figure 7.11 Scaled Acceleration Time History of Kalamata Earthquake (transverse axis)

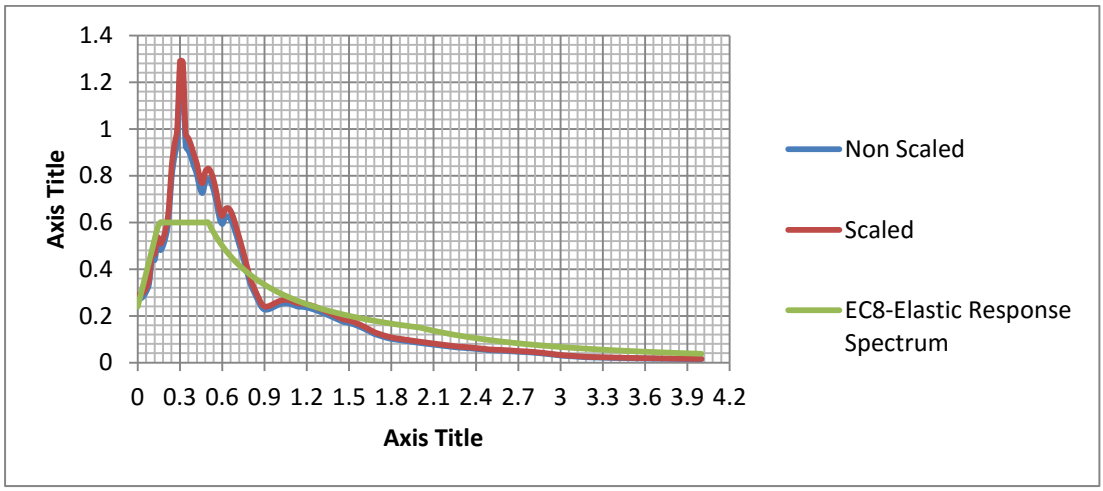

Figure 7.12 Scaled and Non-scaled Acceleration Response Spectrum of Kalamata Earthquake (transverse axis)

Earthquake Event of L'Aquila

Scaling factors: Longitudinal Axis: 0.857, Transverse Axis: 0.797

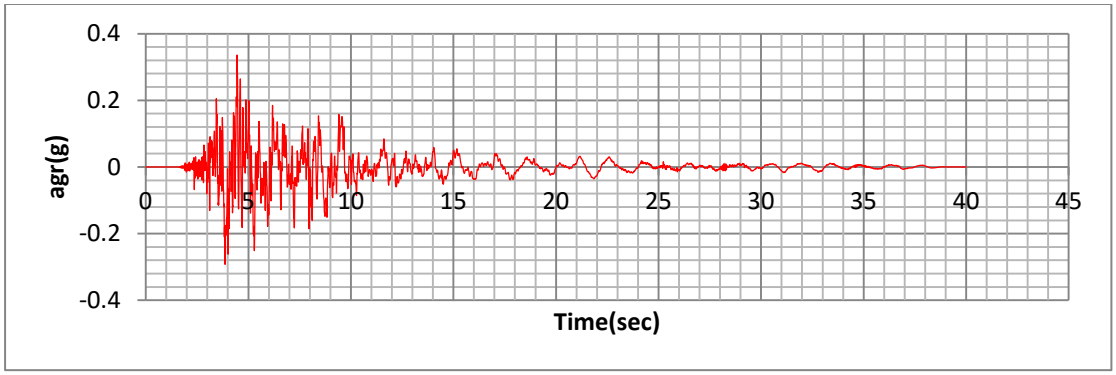

Figure 7.13 Non Scaled Acceleration Time History of L'Aquila Earthquake (longitudinal axis)

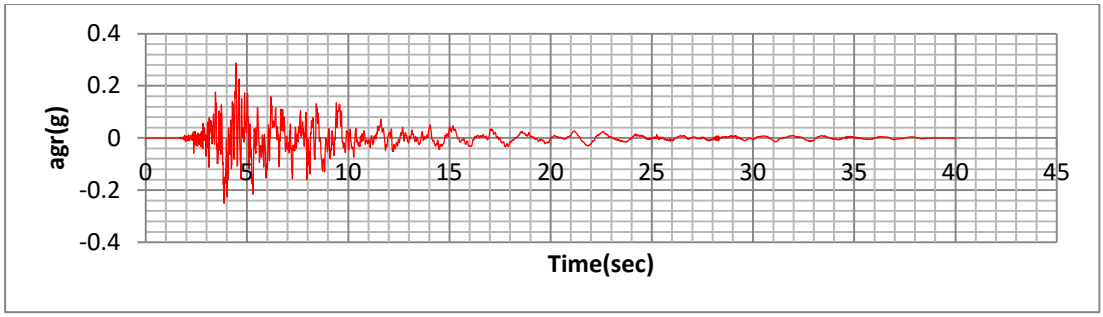

Figure 7.14 Scaled Acceleration Time History of L'Aquila Earthquake (longitudinal axis)

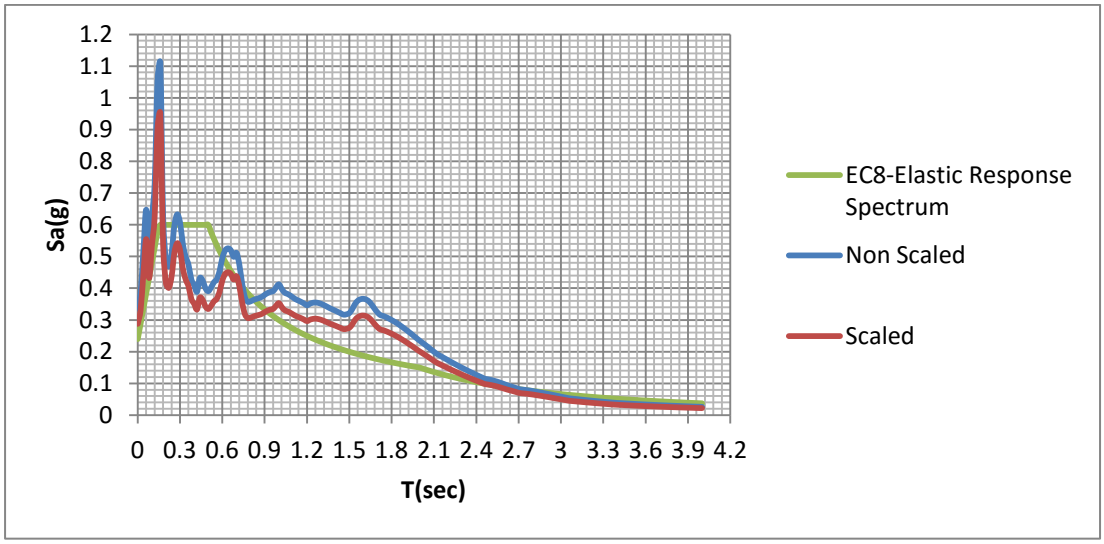

Figure 7.15 Scaled and Non-scaled Acceleration Response Spectrum of L'Aquila Earthquake (longitudinal axis)

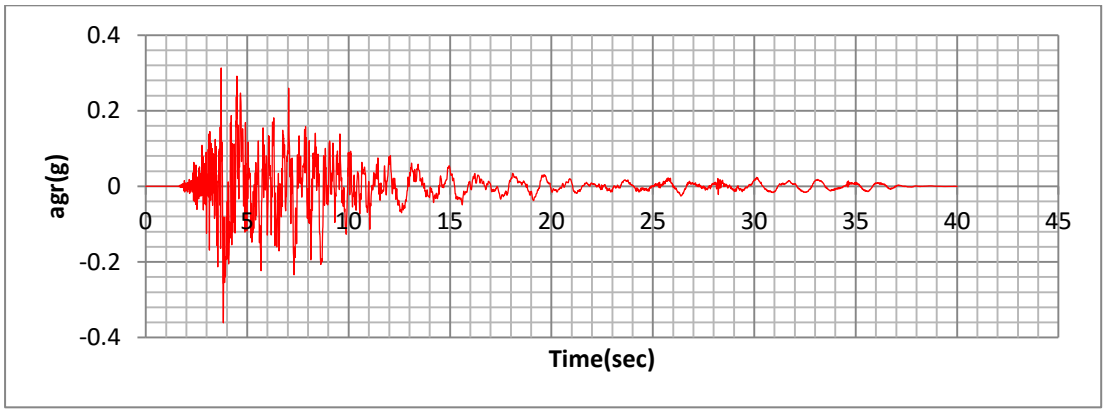

Figure 7.16 Non Scaled Acceleration Time History of L'Aquila Earthquake (transverse axis)

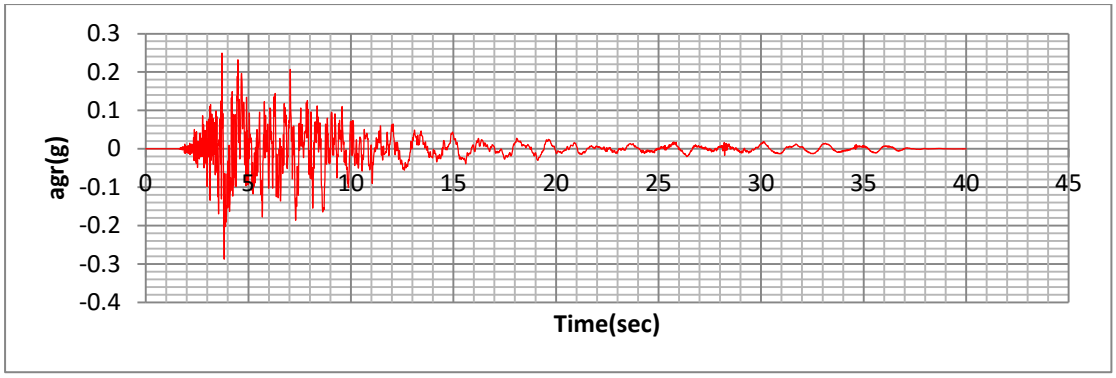

Figure 7.17 Scaled Acceleration Time History of L'Aquila Earthquake (transverse axis)

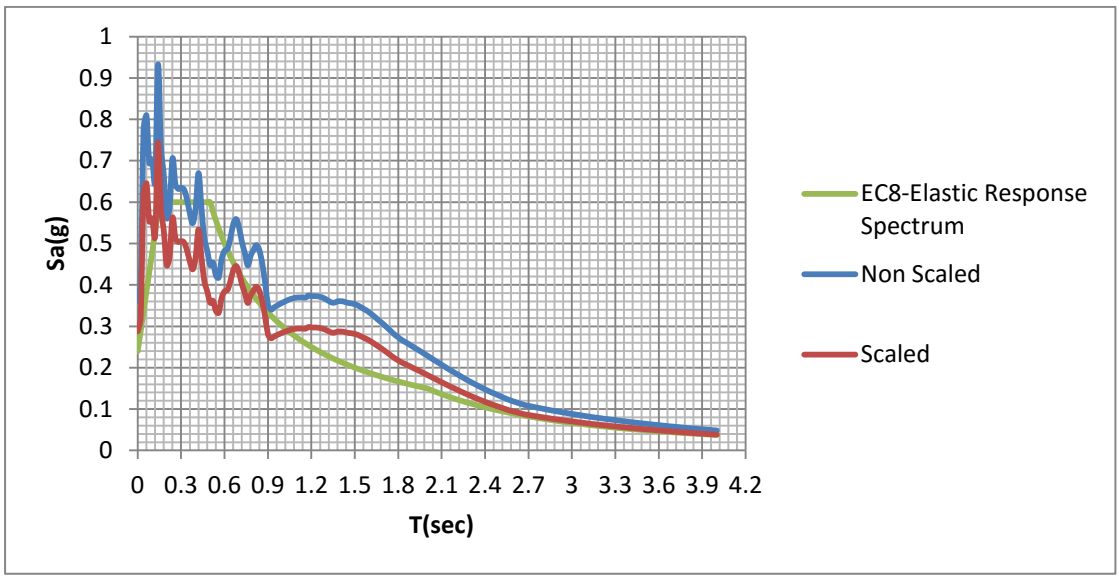

Figure 7.18 Scaled and Non-scaled Acceleration Response Spectrum of L'Aquila Earthquake (transverse axis)

7.3 Time-History Function Definition in SAP 2000

The time series shown above are defined in SAP 2000 by the commands:

Define⇒ Function⇒ Time History⇒ (Choose Function Type to Add) ⇒From File

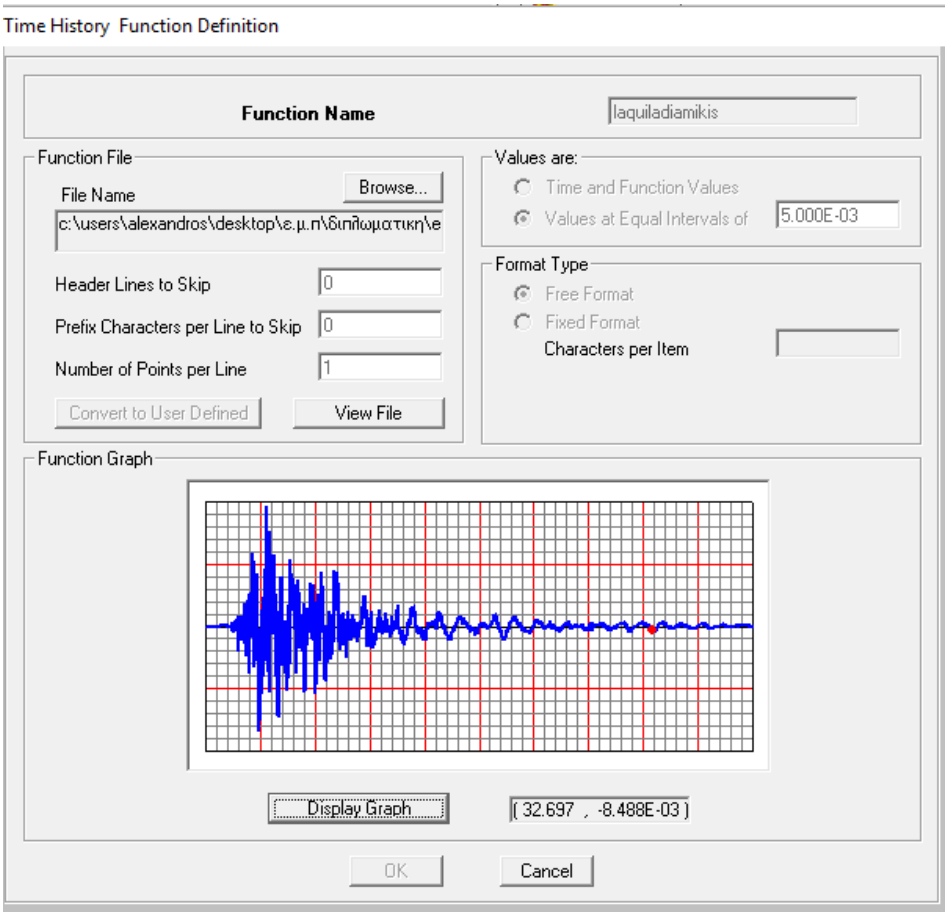

Figure 7.19 Time History Function Definition

Time-histories are defined for the longitudinal and transverse direction of the 3 earthquake events mentioned above.

The loads are combined according to the combinations:

G+0.3Q+Ex+0.3Ey, G+0.3Q+Ex-0.3Ey, G+0.3Q-Ex+0.3Ey, G+0.3Q-Ex-0.3Ey, G+0.3Q+0.3Ex+Ey, G+0.3Q+0.3Ex-Ey, G+0.3Q-0.3Ex+Ey, G+0.3Q-0.3Ex-Ey

Where it is assumed that the longitudinal time histories are along the X axis and the transverse time histories are along the Y axis of the structure.

7.4 Load Case Definition in SAP 2000

The time-histories are added on the vertical loads, already acting, at the end of the previous case. When performing a nonlinear time-history analysis, such as for earthquake loading, it is necessary to start from a nonlinear static state, such as due to gravity loading (CSi, 1995). The output time step size and the number of output time steps are set according to the time history time step size

and number of steps. The nonlinear analysis will internally solve the equations of motion at each output time step and at each load function time step. The values of the time-history functions are multiplied by 9.81m/s^2 since the values imported are in g. The value 2.943 shown in the figure 7.20 is the result of the multiplication $9.81 \cdot 0.3$, where the value 0.3 is due to the load combination.

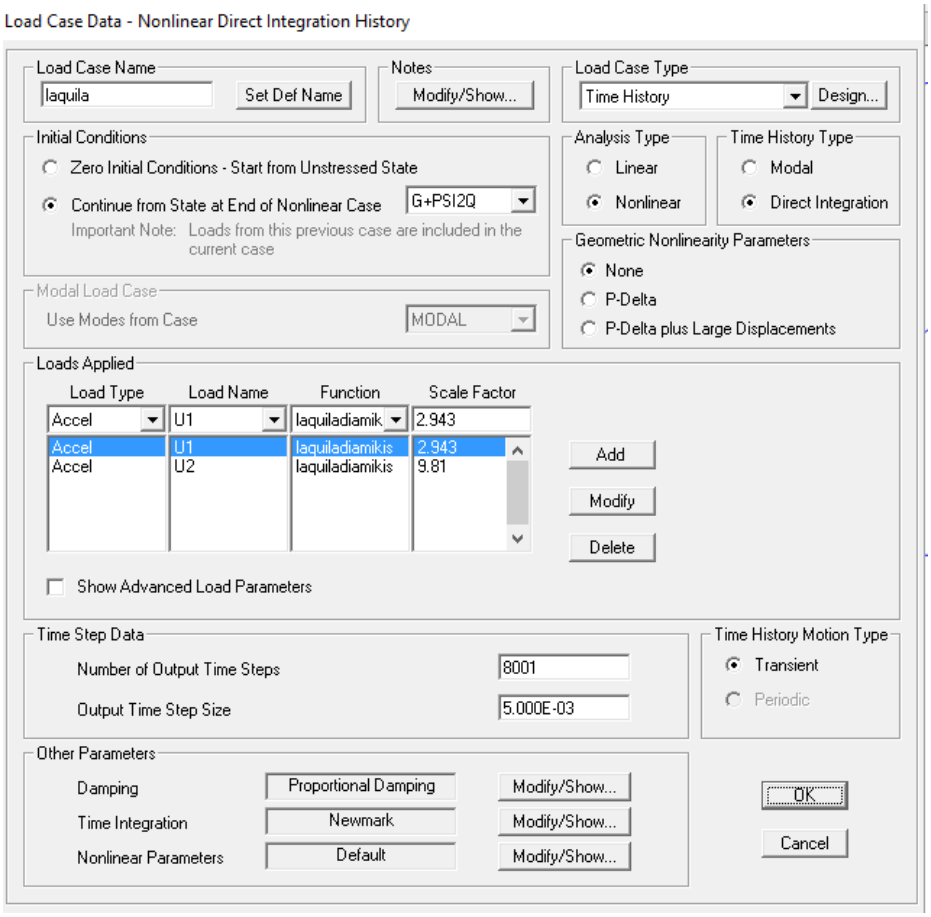

Figure 7.20 Load Case Definition: L'Aquila. Load Combination: G+0.3Q+0.3Ex+Ey

The time-history motion type is set to transient, indicating that the applied load is considered as a one-time event, with a beginning and end.

The time-history type is set to direct integration. Direct Integration is applied to the equations of motion, without the use of modal superposition. Direct integration results are extremely sensitive to time-step size in a way that is not true for modal superposition (CSi, 1995).

In direct integration time-history analysis, the damping in the structure is modeled using a full damping matrix, which allows coupling between modes to be considered (CSi, 1995).

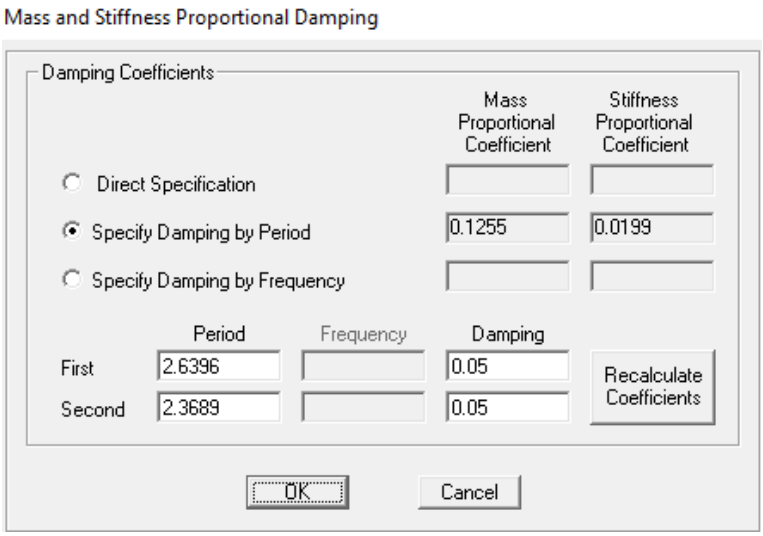

Figure 7.21 Mass and Stiffness Proportional Damping Coefficients

For each direct integration time-history load case, proportional damping coefficients that apply to the structure as a whole may be specified. The damping matrix is calculated as a linear combination of the stiffness matrix, scaled by a coefficient C_K and the mass matrix scaled by a coefficient, C_M.

Here, the coefficients are specified by the two fundamental periods of the structure.

$$C = C_M \cdot M + C_K \cdot K \qquad (35) \qquad \text{(Katsikadelis, 2012)}$$

The nonlinear equations are solved iteratively in each time step, which may require reforming and resolving the stiffness and damping matrices. The iterations are carried out until the solution converges.

The Newmark time integration method is used and the parameters gamma and beta are set to 0.5 and 0.25, respectively.

7.5 Results of Nonlinear Time-History Analyses

The nonlinear time-history analyses cause significant damages to the structure. In the following figures, the deformed shapes of the most unfavorable load combination for each of the three earthquake events are presented.

L'Aquila Earthquake Event

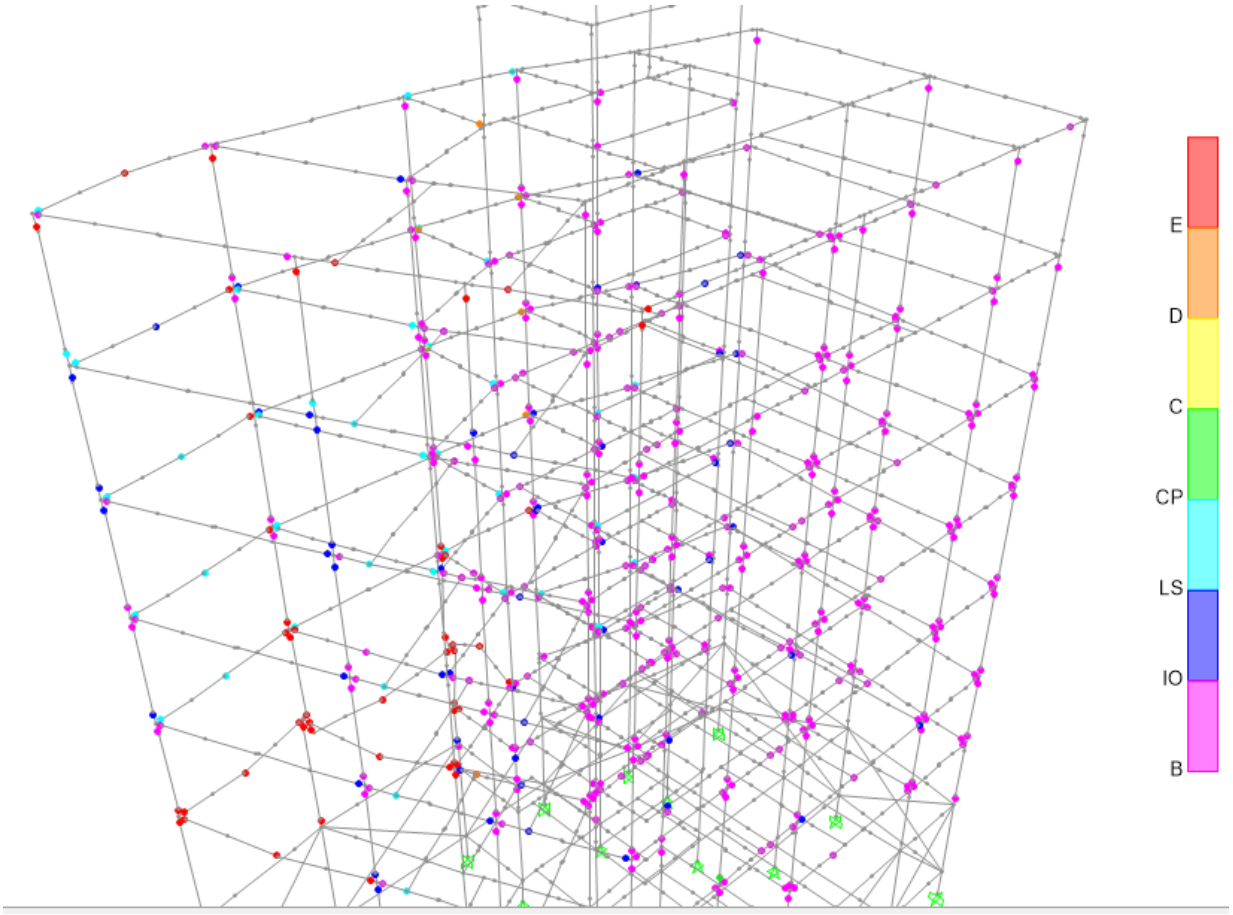

Figure 7.22 Earthquake Event: L'Aquila. Most Unfavourable Load Combination: G+0.3Q+Ex+0.3Ey

The most unfavorable load combination, that causes the most severe damages to the structure, due to the L'Aquila Earthquake event is the G+0.3Q+Ex+0.3Ey. (However all the load combinations of L'Aquila earthquake event cause hinges in columns to exceed limit state E).

In the columns C1,C6,C11,C12,C18,C19,C20 there are hinges that have no residual strength (beyond E). Two hinges of column C18 have no residual strength. The hinges of C12, C18, C19, C20 are formed in the floor levels A and B.

In addition, C2 faces significant strength degradation (one hinge in the limit state: collapse prevention to collapse), and C11 is above life safety limit state.

Summarizing, hinges in 7 columns exceed limit state E and in total (including the 7 above E) 9 columns exceed life safety limit state.

In addition there are 21 hinges beyond E in beams in several floor levels.

As a result of the extended damages, probably the building is collapsed.

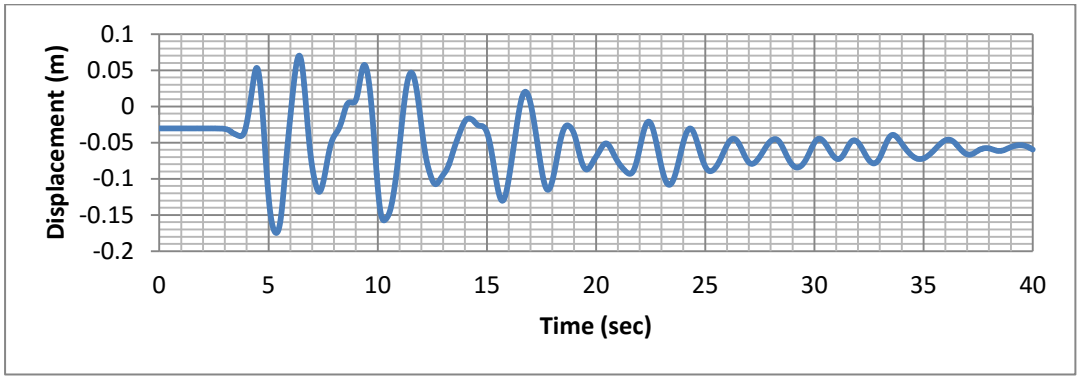

Figure 7.23 Displacement Time-History of the Center of Mass (joint 130) of the Approachable Roof due to L'Aquila Earthquake Event

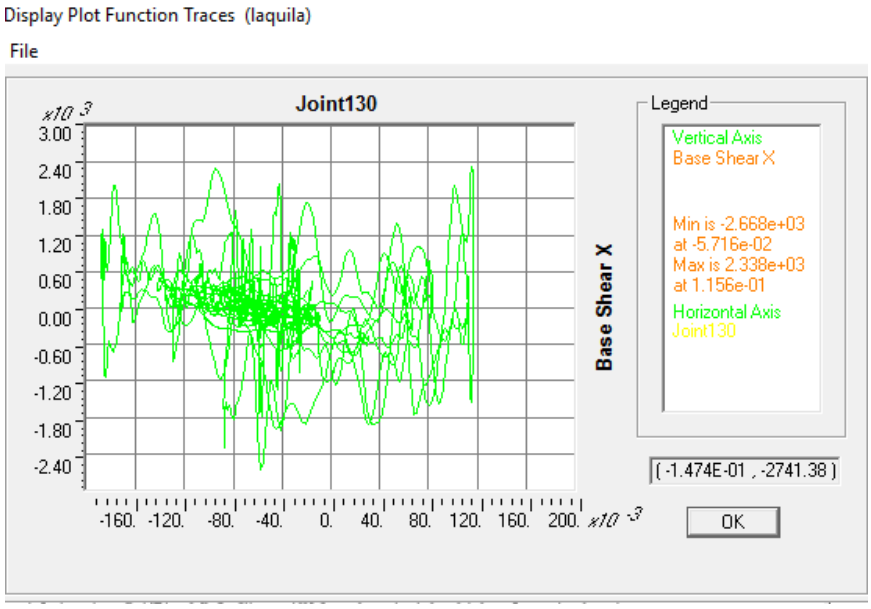

Figure 7.24 Hysteretic Loop of base shear force along X- Displacement along X of joint 130–(center of mass of the approachable roof) - L'Aquila

Corinth Earthquake Event

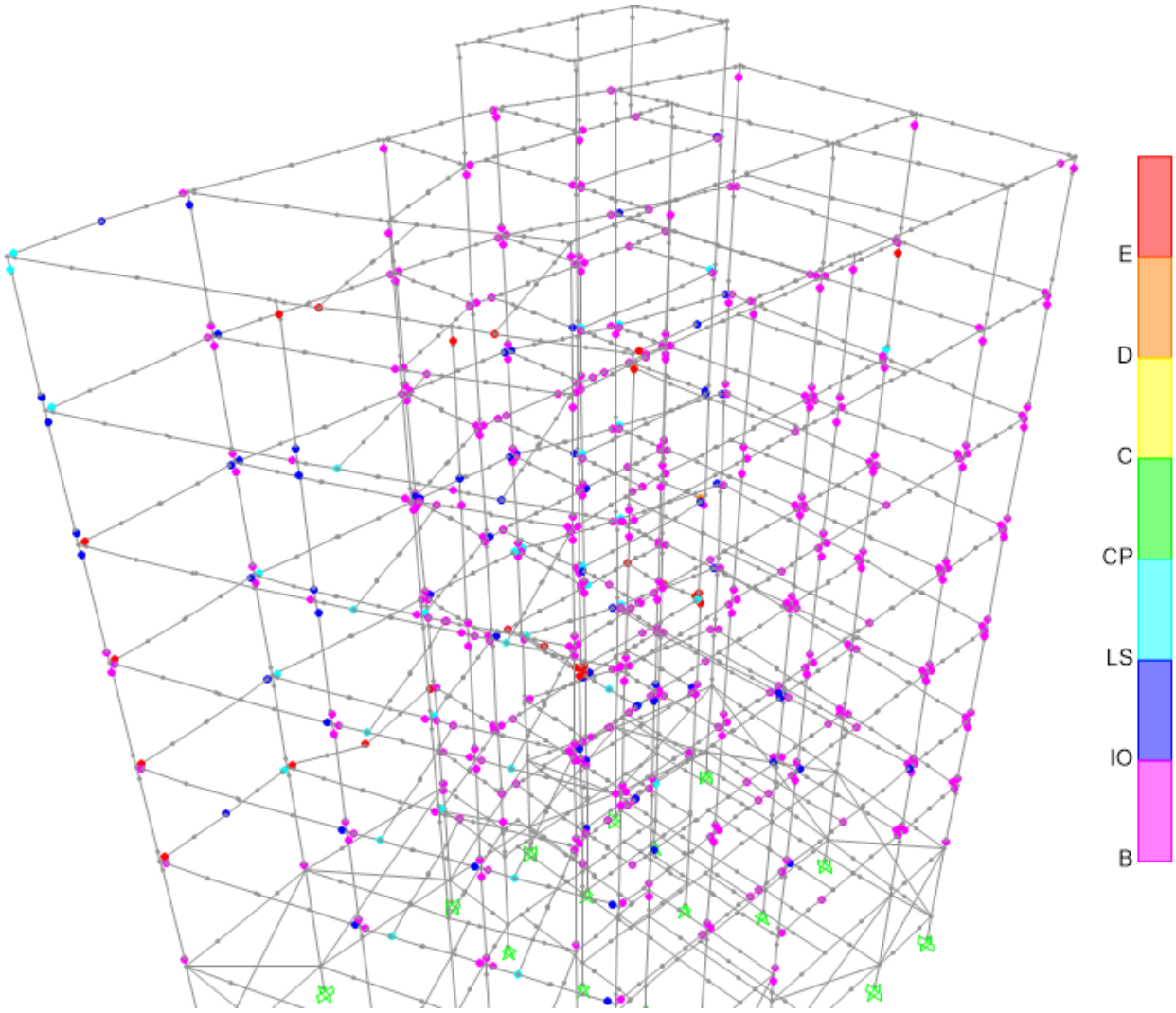

Figure 7.25 Earthquake Event: Corinth. Most Unfavourable Load Combination: G+0.3Q-Ex-0.3Ey

The most unfavorable load combination that causes the most severe damages to the structure, due to Corinth Earthquake event is the G+0.3Q-Ex-0.3Ey. (However all the load combinations of Corinth earthquake event cause hinges in columns to exceed life safety limit state. Many load combinations cause hinges in columns to exceed limit state E. There are hinges that exceed limit state E in beams for all the load combinations).

In columns C1,C6,C10,C11,C13,C14 there are hinges that have no residual strength (beyond E). The hinges in C10 are formed in floor level D and the hinges in columns C13 and C14 are formed in floor levels A and B. In addition

there are 16 hinges beyond E in beams. Summarizing, hinges in 6 columns exceed limit state E.

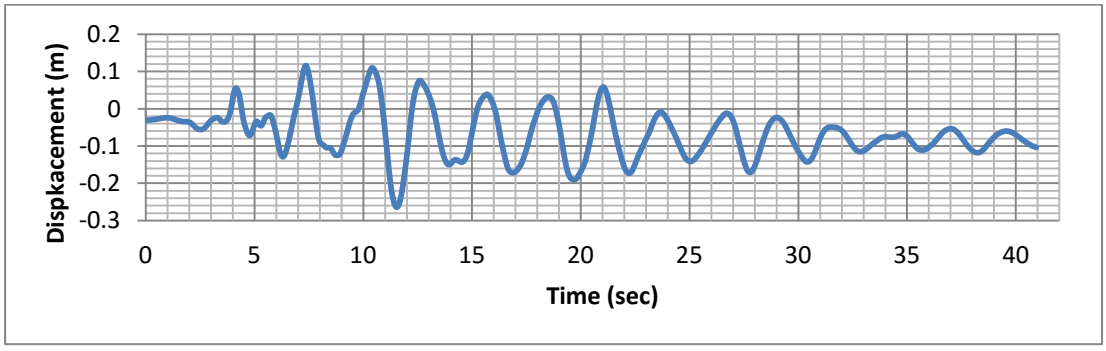

Figure 7.26 Displacement Time-History of the Center of Mass (joint 130) of the Approachable Roof due to Corinth Earthquake Event

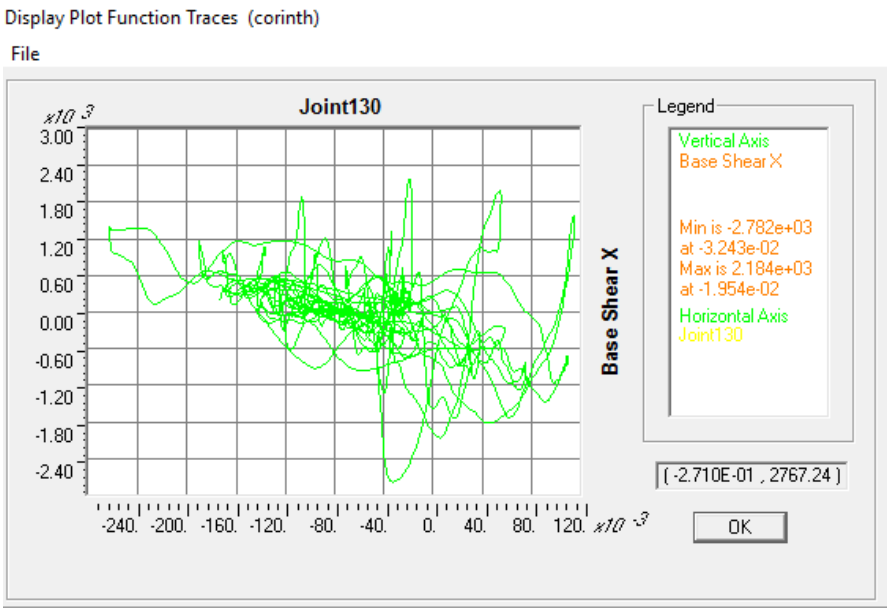

Figure 7.27 Hysteretic Loop of base shear force along X- Displacement along X of joint 130–(center of mass of the approachable roof)- Corinth

Kalamata Earthquake Event

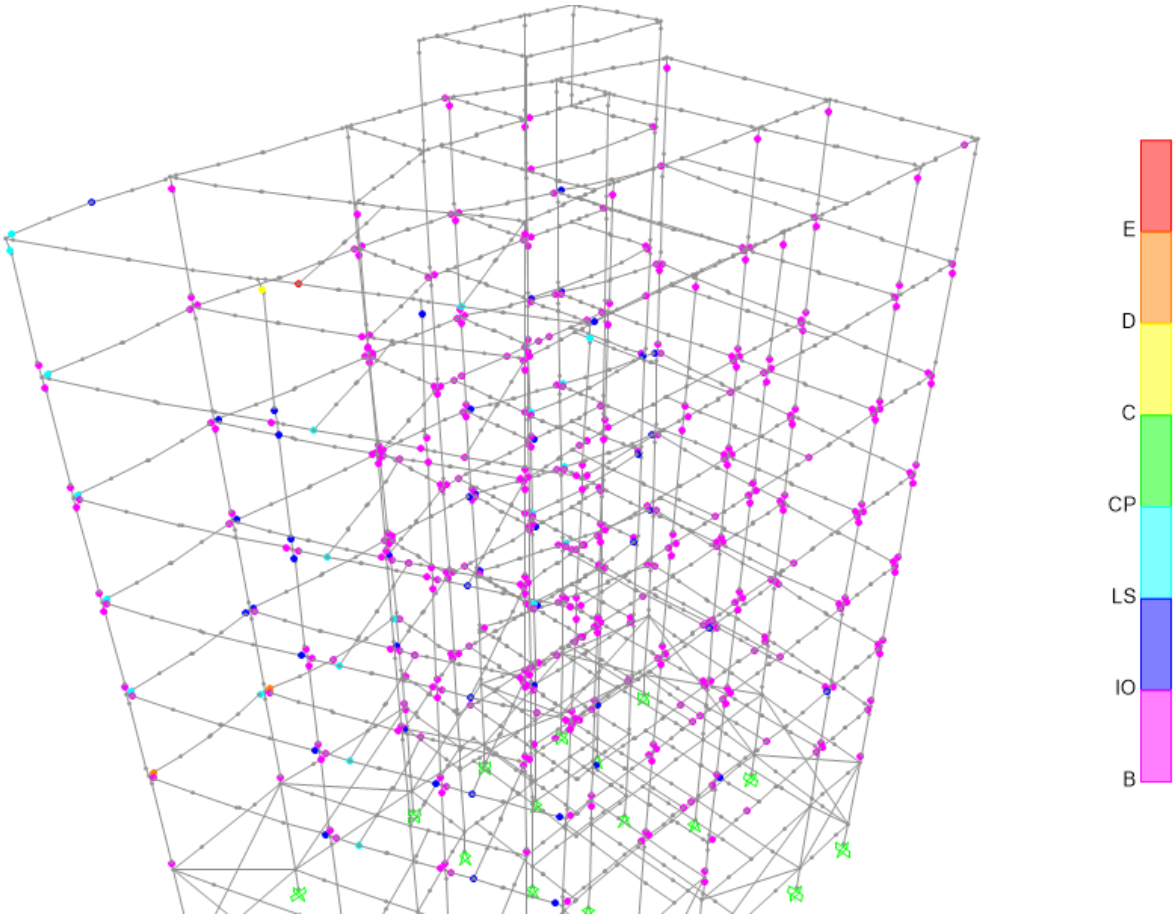

Figure 7.28 Earthquake Event: Kalamata. Most Unfavourable Load Combination: G+0.3Q-Ex-0.3Ey

The most unfavorable load combination that causes the most severe damages to the structure, due to Kalamata Earthquake event is the G+0.3Q-Ex-0.3Ey. In columns C1 and C18 are formed hinges between life safety and collapse prevention limit states. In column C11 there is hinge between C and D limit states. (However all the load combination of Corinth event cause hinges in columns and beams to exceed life safety limit state).

The building faces the lesser damages due to Kalamata Earthquake in comparison to the Corinth and the L'Aquila earthquake events.

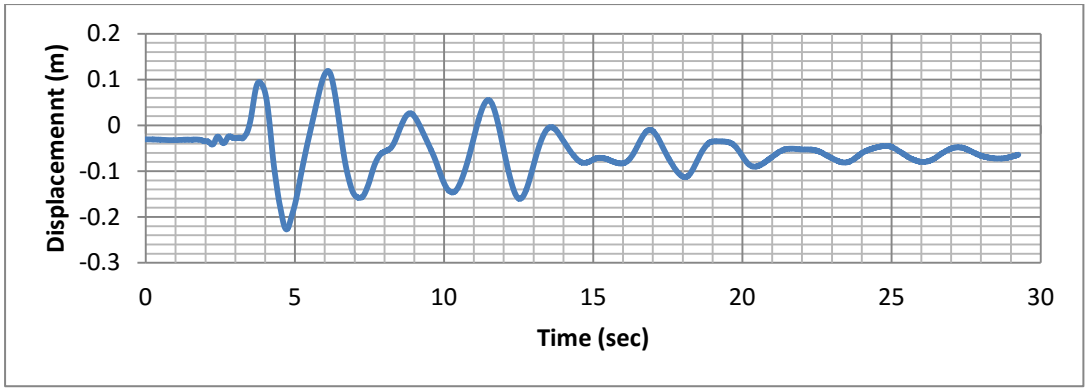

Figure 7.29 Displacement Time-History of the Center of Mass (joint 130) of the Approachable Roof due to Kalamata Earthquake Event

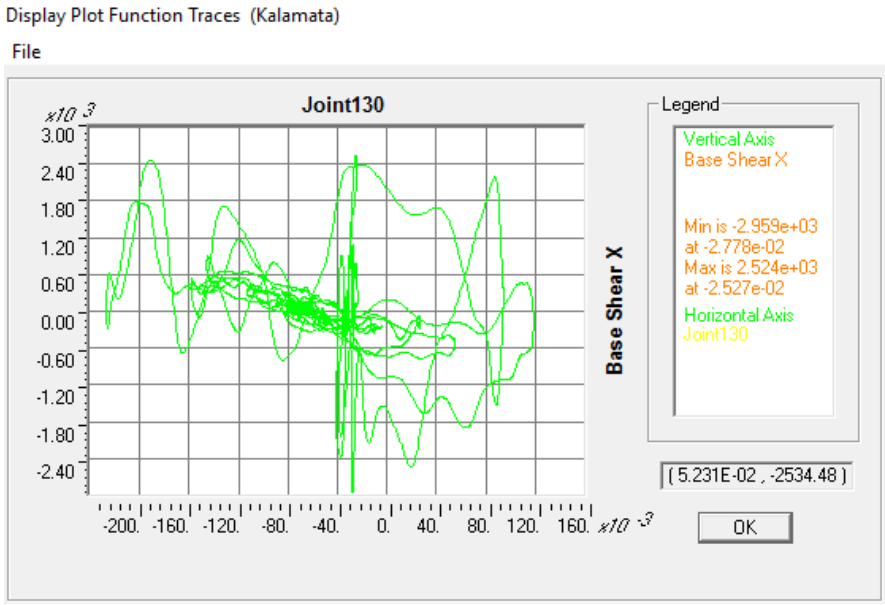

Figure 7.30 Hysteretic Loop of base shear force along X- Displacement along X of joint 130–(center of mass of the approachable roof)- Kalamata

In the figures 7.31 and 7.32 the maximum absolute displacements of each floor level for the three earthquake events are shown for axis X and Y.

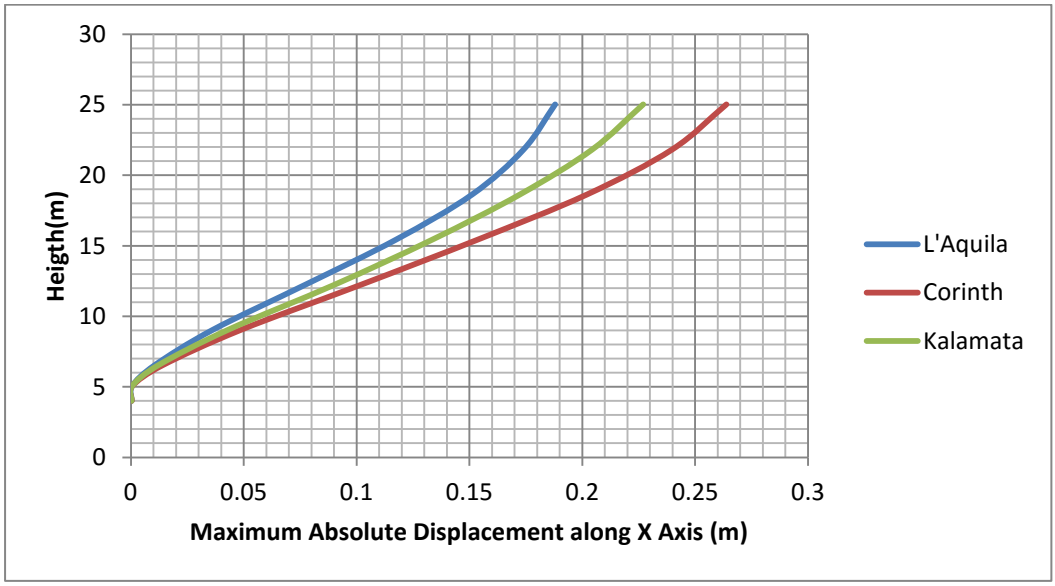

Figure 7.31 Maximum Absolute Displacement per Floor Level for Earthquakes imposed along the X axis

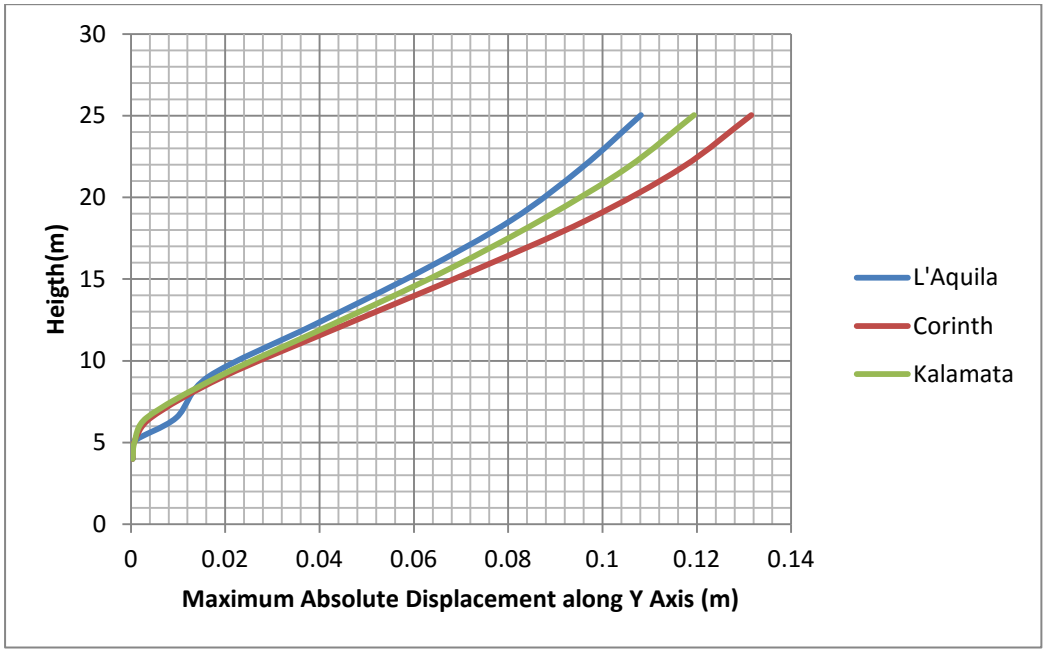

Figure 7.32 Maximum Absolute Displacement per Floor Level for Earthquakes imposed along the Y axis

In the figures 7.33 and 7.34 the inter-story drift ratios for the three earthquake events are shown for axes X and Y.

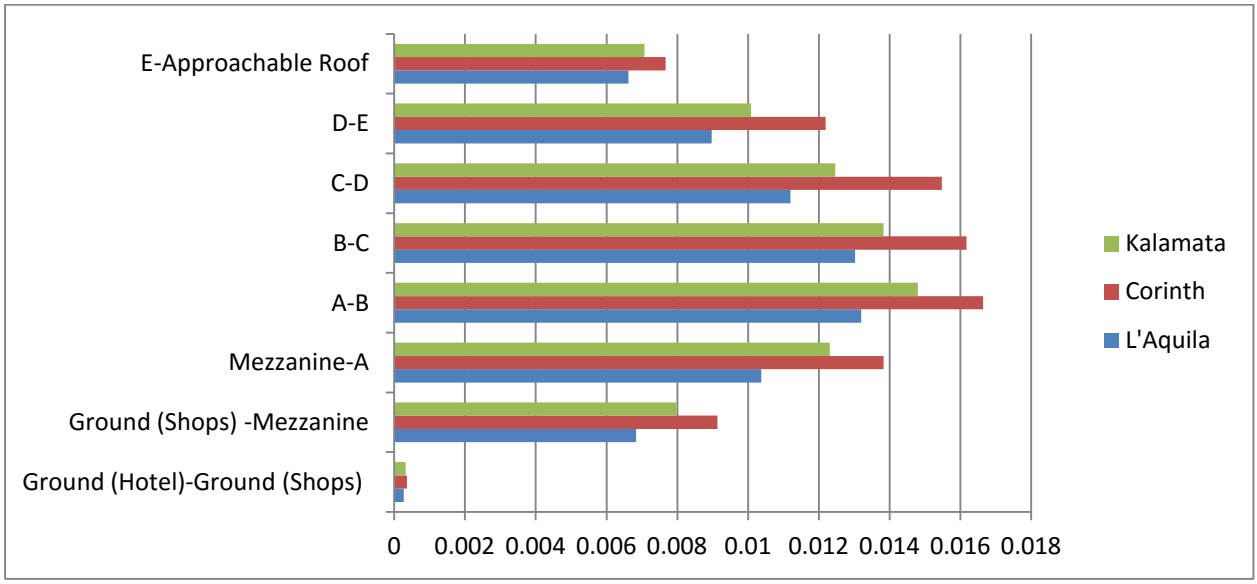

Figure 7.33 Inter-story Drift Ratios along X axis

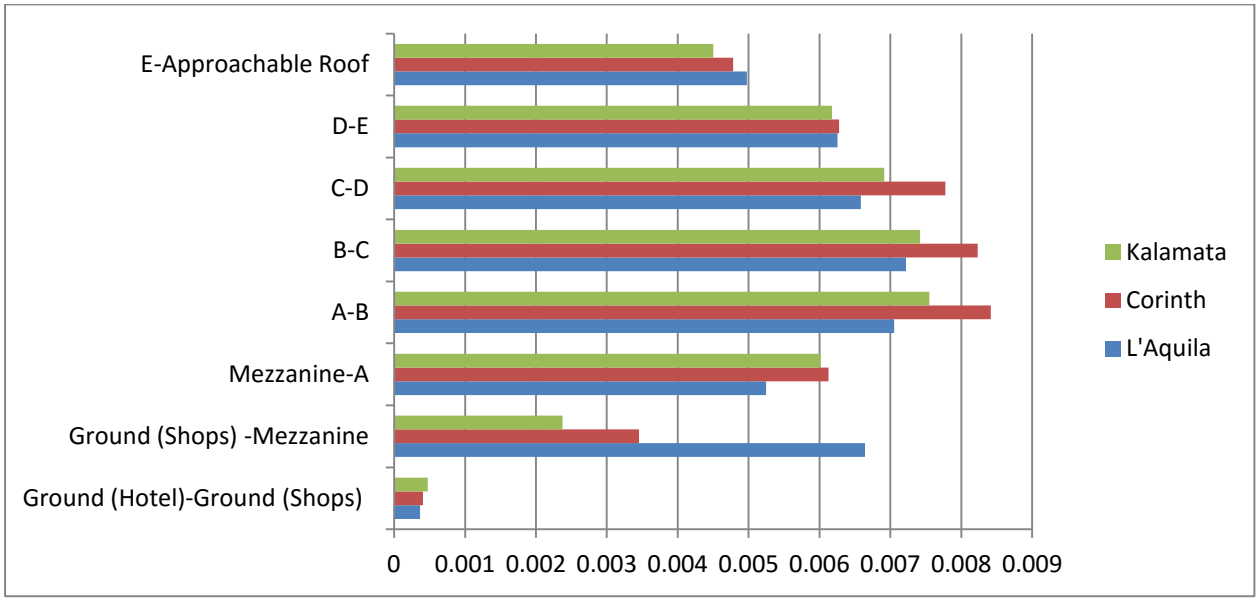

Figure 7.34 Inter-story Drift Ratios along Y axis

In the following figures the time-histories of the bending moments and shear forces along axis X (M3, V2) and along axis Y (M2,V3) of the column C20, for each floor level, for the L'Aquila earthquake event are shown.

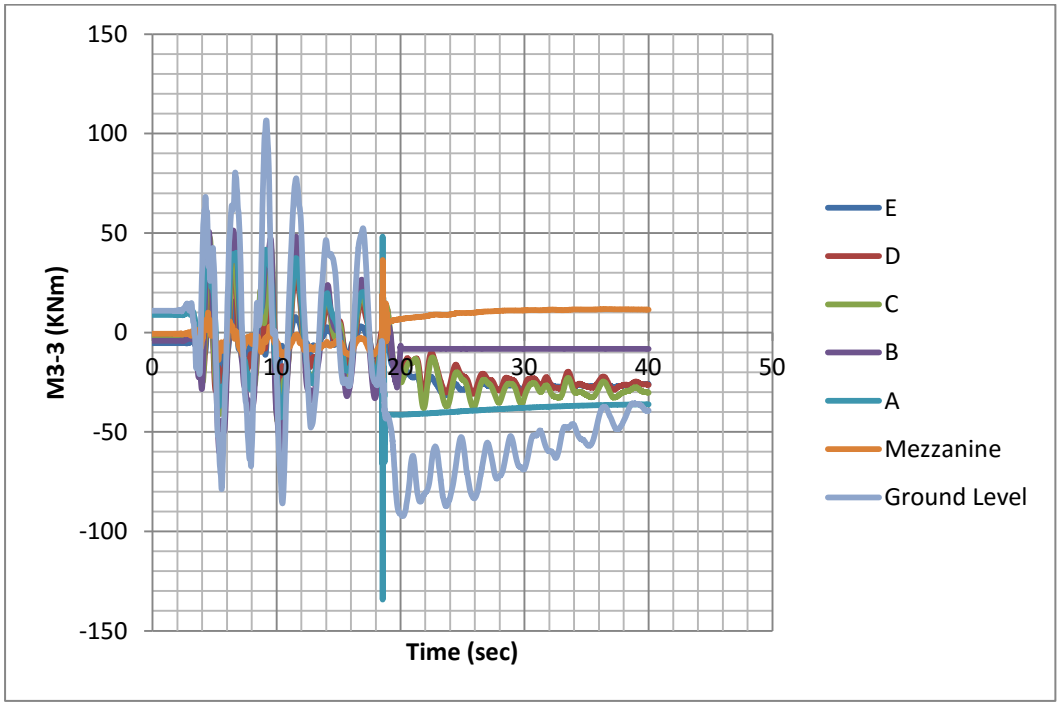

Figure 7.35 Time-History of Bending Moments of Column C20 along axis X (M3-3)

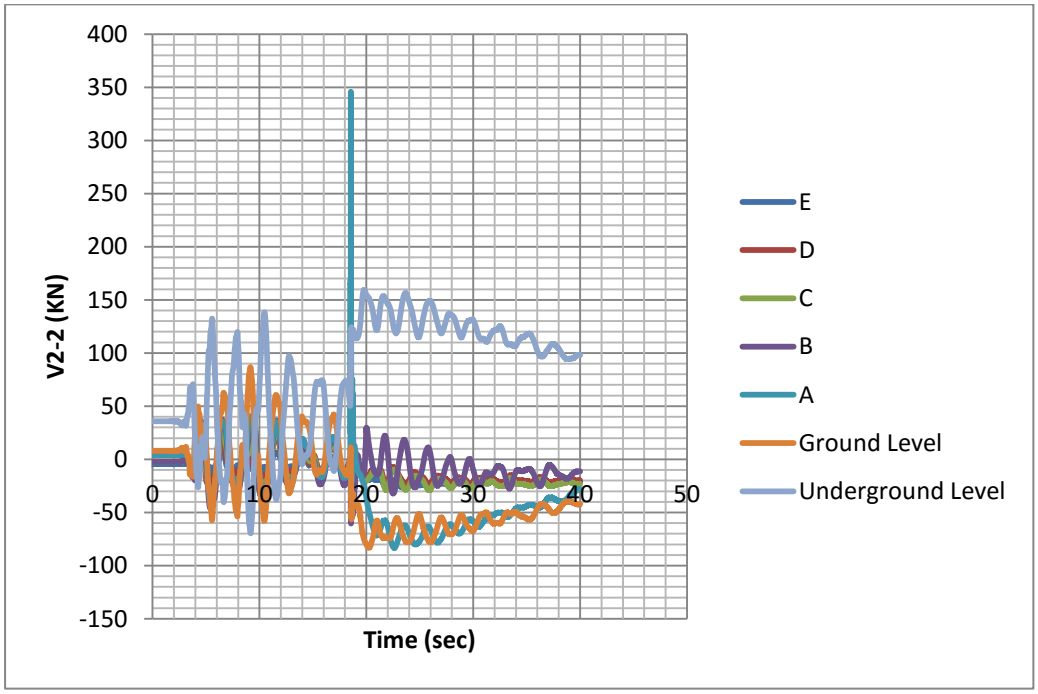

Figure 7.36 Time-History of Shear Forces of Column C20 along axis X (V2-2)

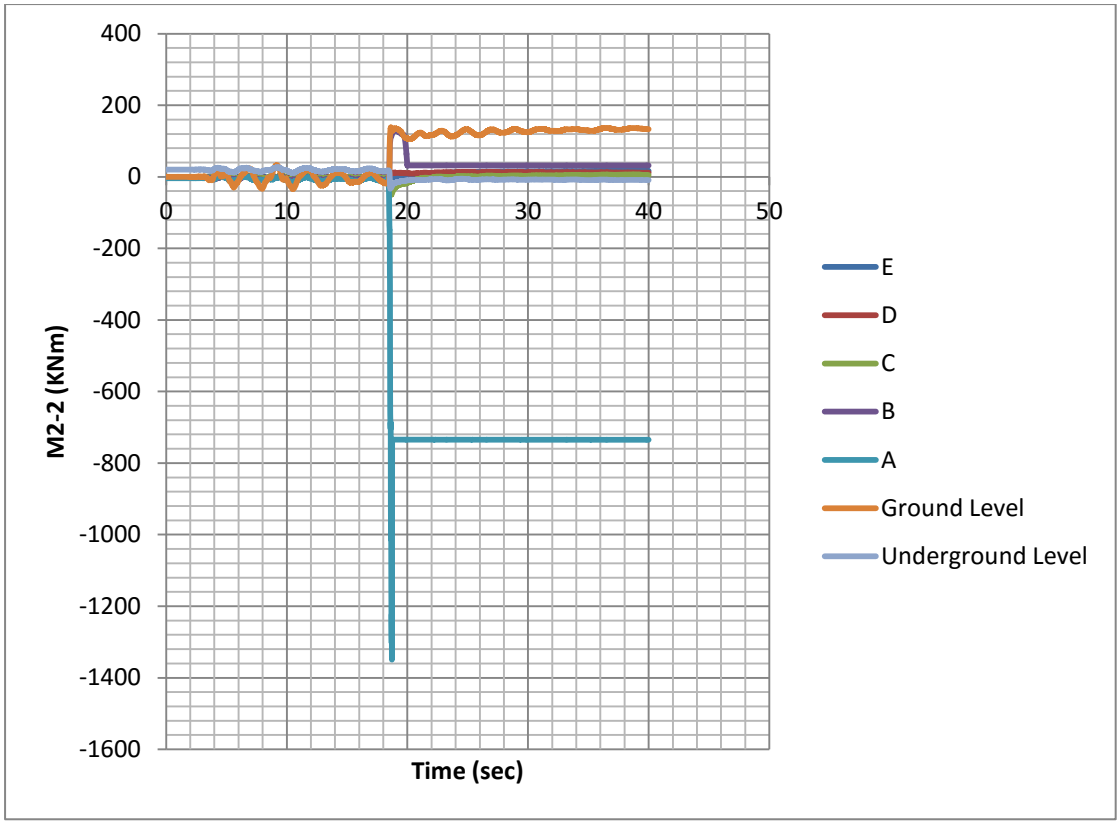

Figure 7.37 Time-History of Bending Moments of Column C20 along axis Y (M2-2)

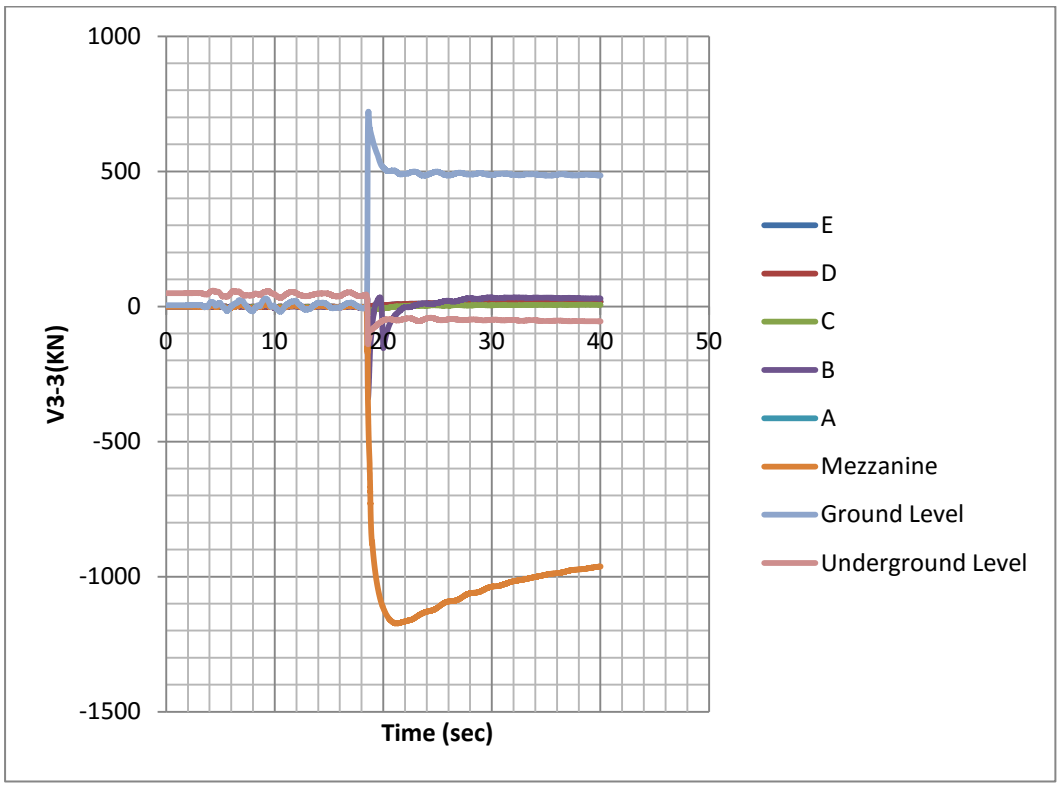

Figure 7.38 Time-History of Shear Forces of Column C20 along axis Y (V3-3)

7.6 Discussions on Nonlinear Time History Analyses Results

- All the earthquake events, form hinges in columns that exceed life safety limit state.
- The earthquake events of Corinth and L'Aquila for each one of the load combinations, form hinges in 6 and 7 columns respectively, that exceed limit state E. In addition many hinges beyond E are formed in beams. Thus the building is probably collapsed when Corinth or L'Aquila acceleration time-histories are imposed to the structure. The lesser damages are caused by the Kalamata earthquake event.
- The most extended damages, no matter which earthquake event is imposed, are observed when the main axis of the acceleration time-history is imposed along the X axis of the structure.
- It is shown from the displacement time history of the joint 130 (closer to the center of mass of the roof) that the maximum displacement for the L'Aquila earthquake event is -0.19m and occurs at 5 sec approximately, the maximum displacement for the Corinth earthquake event is -0.26m and occurs at 11 sec approximately and the maximum displacement for the Kalamata earthquake event is -0.23m and occurs at 5 sec approximately.
- From the maximum absolute displacements per floor level and axis of the building, it is shown that the maximum absolute displacements increase with height.
- The maximum absolute displacements on the structure are caused by the Corinth earthquake event for both the axis X and Y, while the L'Aquila earthquake event causes the minimum.
- The highest inter-story drift ratios for Corinth and Kalamata earthquake events are observed in the floor levels A-B for both axes (X,Y), while for L'Aquila they are observed at floor levels A-B and B-C.
- In general the ratios are higher along the X axis than they are along the Y axis. It does make sense, since the worst load combinations, for which the drift ratios are calculated, are taken along the main axis X (because those combinations caused the most significant damages).

- The inter-story drift ratios are proportional to the maximum displacements caused by the earthquake. The higher the displacements the higher the inter-story drift ratios. Thus the higher inter-story drift ratios in both X and Y axes are caused by the Corinth earthquake event in the most floor levels.
- The maximum inter-story drift ratios are observed for Corinth earthquake event along the X axis in the floor levels A-B (1.7%).
- It is shown from the time histories of the forces of the column C20 that the highest values for all the magnitudes, are approximately occurring at 18 sec. M3-3=-135KNm, V2-2=350KN, M2-2=-1380KNm, V3-3=-1150KN. The maximum of V3-3 is observed in the mezzanine floor level, while the maximum of the others is observed in the A floor level. It is shown from the hinge's backbone curve that prior the 18th sec the member is highly rotated, thus in the 18th sec the strength of the element is lost. The loss of the strength last from 18.4 to 18.8 sec. The M2-2 (along Y axis) is higher than M3-3 (along X axis), even if the main axis of the imposed seismic accelerogram is the X axis. This is because the C20 is in the edge of the building and there is no other member beyond (to the West) C20 in the Y axis, that could contribute to resist against the earthquake motion.

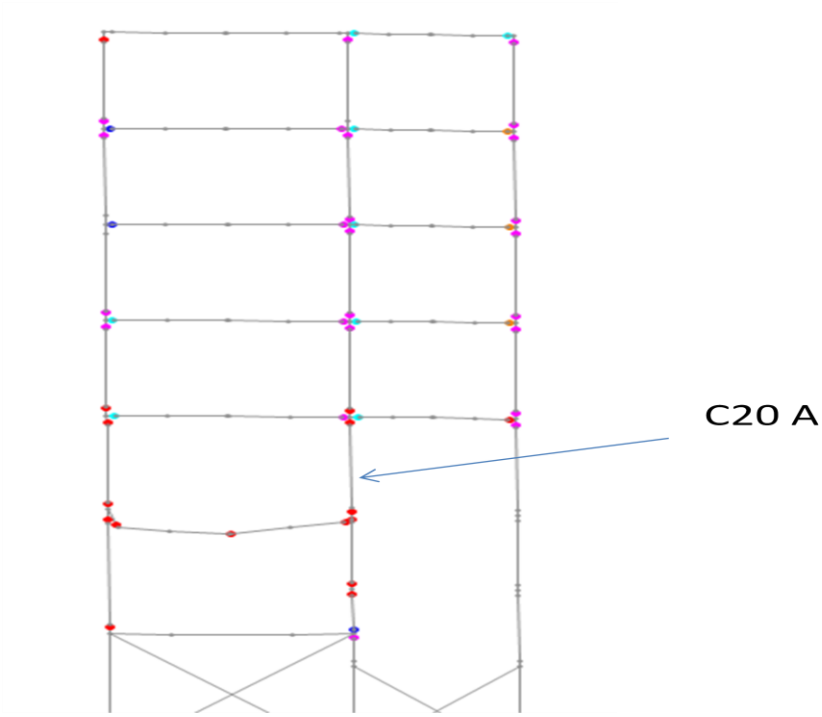

Figure 7.39 Deformed shape and hinges results of the Columns C19,C20,C21 due to the L'Aquila earthquake event (Load Combination: G+0.3Q+Ex+0.3Ey)

7.7 Conclusions on the Assessment of the Bearing Capacity of the Structure

From the nonlinear static (pushover) and the nonlinear dynamic analyses, it is concluded that the building faces significant and extended damages in many members. The structure cannot satisfy the current codes and the seismic action it is subjected to, thus seismic retrofitting is necessary. The assessment shows that the building is probably collapsed when subjected to the Corinth or the L'Aquila earthquake events.

The building has no lateral force resisting system.

Too many elements-columns and beams, exceed the life safety limit state.

Hinges formed in columns C1, C6, C10, C11, C12, C13, C14, C18, C19, C20 exceed limit state E (beyond E). In other words, the 10 out 23 columns of the structure have no residual strength.

The most severe damages are observed in floor levels A and B and in the top of the columns, in the West, South-West and South side of the building.

The maximum inter-story drift ratios from all of the analyses are approximately 2% along the Y axis, due to pushover analysis with uniform distribution of lateral loads. The ratio of 2% is too high. The inter-story drift ratios are generally higher than permitted.

The Corinth earthquake event causes the highest inter-story drift ratios (1.7% along the X axis in floor levels A-B), of the three earthquake events.

The pushover analyses with modal distribution of lateral loads along the –X axis and the uniform distribution along the +X axis do not find a performance point, indicating that the structure capacity is inadequate.

The maximum displacement of the center of mass of the approachable roof is 0.26m, due to the Corinth earthquake event, which is too high.

Chapter 8

Strengthening of the Structure

The target of the retrofitting is the life safety performance level. None of the columns is allowed to exceed life safety limit state.

The structure has no lateral force resisting system, leading to excessive lateral deformations and the elements have inadequate ductility to sustain resulting deformations. In addition the strength and stiffness of the structure is inadequate and the under-strength elements that require modifications are too many.

Thus, the global structural strengthening and stiffening in combination with local modification of inadequate column elements are the chosen strategies. By structural stiffening the deformation demand of the structure is reduced, and by local modification the ductility and strength of the members are increased.

The retrofitting systems that are used to satisfy the above strategies are the addition of shear walls within the existing frames and the local modification of the inadequate columns by concrete jacketing.

To that purpose 7 shear walls and jackets to 17 out of 23 columns are added.

The shear walls are added within the existing frames:

Shear wall 1: between the columns C16 and C17

Shear wall 2: between the columns C4 and C9

Shear wall 3: between the columns C1 and C6

Shear wall 4: between the columns C18 and C19

Shear wall 5: between the columns C20 and C15

Shear wall 6: between the columns C2 and C3

Shear wall 7: between the columns C13 and C14

The jackets are applied to the columns: C1, C2, C3, C4, C5, C6, C9, C11, C13, C14, C15, C16, C17, C18, C19, C20, C23.

In other words the jackets are applied to the columns at the sides of the added shear walls, to the columns at the corners of the building and to the column C11.

All the interventions take into account the architectural plan drawings, so the functionality of the hotel is not influenced. All the rooms existing before the intervention will be fully functional after the construction of the shear walls and column jackets at the positions shown in the figure 8.1.

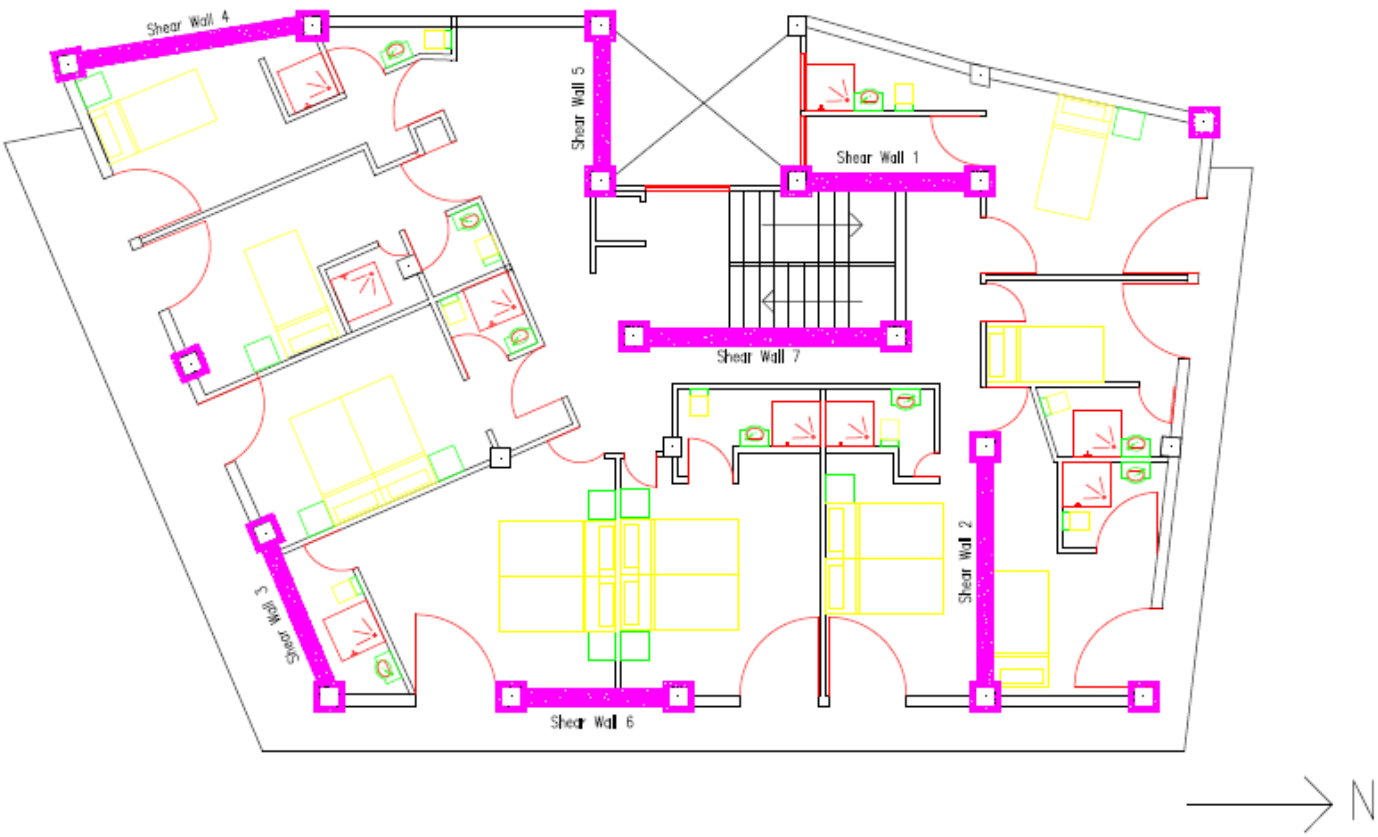

Figure 8.1 Structural Interventions- Addition of Shear walls and jackets

The dimensions of the shear walls are:

Shear wall 1: 2.65m x 0.30m

Shear wall 2: 3.20m x 0.30m

Shear wall 3: 2.60m x 0.40m

Shear wall 4: 3.20m x 0.40m

Shear wall 5: 2.00m x 0.30m

Shear wall 6: 2.30m x 0.30m

Shear wall 7: 3.60m x 0.30m

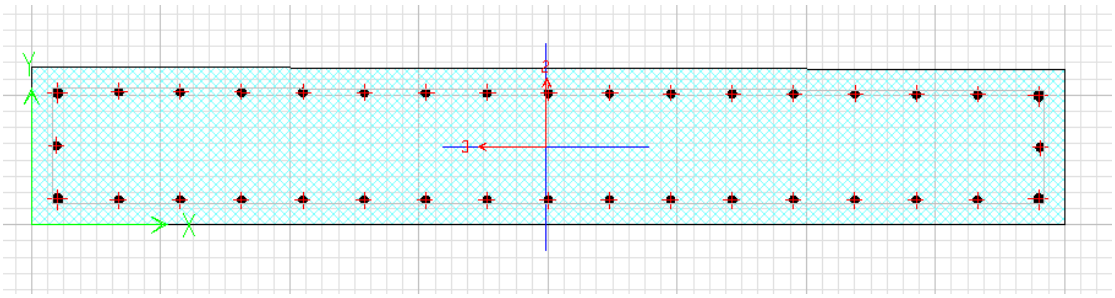

Figure 8.2 Section of Shear Wall 5 (section designer)

The reinforcing steel of the shear walls is Φ16/0.125m and in the corners Φ20.

The shear walls are considered to be monolithically connected to the frames they are added in, and their joints are included to the diaphragmatic behaviour of each floor level.

The width of the jacket is 10cm and the reinforcing steel is 16Φ16+4Φ20. Confining reinforcement is also added Φ10/10 (2 ties in height and width).

The bar cover is 4cm.

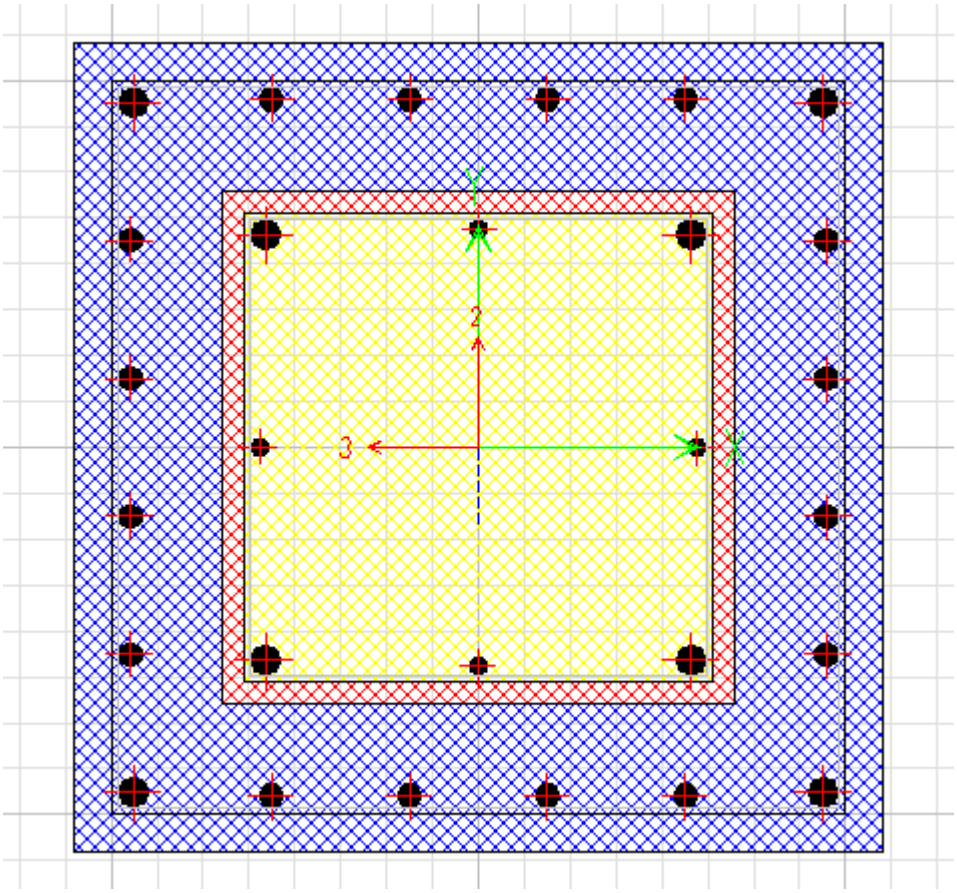

Figure 8.3 Jacket of Column C5 at the floor level E. Jacket Width:10cm, Reinforcing Steel: 16Φ16+ 4Φ20 Bar Cover: 4cm

The jackets may be modelled using section designer of SAP2000. The existing section is added on the new section (which parameters are the new-concrete-reinforcing steel etc.).

The concrete of the new members is C20/25 and the reinforcing steel is S500. Their parameters are given below:

Concrete:

Characteristic compressive cylinder strength of concrete at 28 days: f_{ck}=20 MPa

Characteristic compressive cube strength of concrete at 28 days: $f_{ck,cube}$=25 MPa

Mean value of concrete cylinder compressive strength: f_{cm}=28 MPa (f_{cm}= f_{ck}+8)

Mean value of axial tensile strength of concrete: f_{ctm}=2.2 MPa

Young's modulus: E_{cm}=30 GPa

Stain at maximum unconfined compressive strength, f'_c: ε_{c1}=2 ‰

Ultimate unconfined stain capacity: ε_{cu1}=3,5 ‰

Reinforcing Steel:

The S500 reinforcing steel minimum yield point (fy) is 500 MPa and the minimum tensile stress (fu) 550 MPa.

E=200 GPa, Strain at onset of strain hardening: 0.02, ultimate strain capacity: 0.12, weight per unit volume: 78.5 KN/m^3

8.1 Modal Analysis Results

A modal analysis of the retrofitted structure is performed. The secant stiffness of the elements is used.

Table 8.1 Modal Participating mass ratios of the retrofitted structure using the secant stiffness

TABLE: Modal Participating Mass Ratios									
OutputCas	StepType	StepNur	Period	UX	UY	UZ	RX	RY	RZ
Text	Text	Unitless	Sec	Unitless	Unitless	Unitless	Unitless	Unitless	Unitless
MODAL	Mode	1	1.265863	0.13965	0.39769	9.2E-07	0.26175	0.07473	0.00013
MODAL	Mode	2	1.117586	0.33231	0.11996	2.1E-06	0.07892	0.18677	0.06803
MODAL	Mode	3	0.936403	0.05646	0.01853	1.6E-06	0.01362	0.03049	0.45089
MODAL	Mode	4	0.34637	0.0187	0.0905	5.5E-06	0.05201	0.00765	0.00152

In addition a modal analysis of the retrofitted structure when the stiffness proposed by the table 4.1 of KANEPE is performed. It would be interesting to compare the periods and the participating mass ratios when the stiffness proposed by the table 4.1 and the secant stiffness are used.

Table 8.2 Modal Participating mass ratios of the retrofitted structure using the stiffness proposed by the table 4.1 of KANEPE

TABLE: Modal Participating Mass Ratios									
utputCas	StepType	StepNum	Period	UX	UY	UZ	RX	RY	RZ
Text	Text	Unitless	Sec	Unitless	Unitless	Unitless	Unitless	Unitless	Unitless
MODAL	Mode	1	0.78999	0.07806	0.4583	1.4E-06	0.30989	0.04359	0.00086
MODAL	Mode	2	0.69811	0.33722	0.05088	3.2E-06	0.03324	0.20011	0.12206
MODAL	Mode	3	0.55175	0.11497	0.02705	7.2E-06	0.02199	0.06177	0.38467
MODAL	Mode	4	0.20998	0.00771	0.10858	1.5E-07	0.06414	0.00406	0.00214

It can be seen that the periods do have significant differences.

For the nonlinear analyses presented in the following, the secant stiffness is used.

8.2 Wall System Check

The structural system of the retrofitted building is a wall system, since lateral loads are mainly resisted by vertical shear walls, whose shear resistance at the building base exceeds 65% of the total shear resistance of the whole structural system (in this definition, the fraction of shear resistance may be submitted by the fraction of shear forces in the seismic design situation).

Modal Response Spectrum analyses are performed. The seismic action is imposed on the X and on the Y axis separately.

Table 8.3 Wall System Check

	Seismic Action Along X axis	**Seismic Action Along Y axis**
Percentage of shear force taken by shear walls	0.702 (V2-2)	0.654 (V3-3)

Chapter 9

Nonlinear Static (Pushover) Analysis Results of the Retrofitted Structure

The significance of the effect of higher modes should be examined as described in chapter 5.

Table 9.1 Higher Mode Participation Check for Earthquake Imposed along the X Axis

Earthquake imposed along X axis			
Floor Level	**Shear Force (KN) Capturing the 90% of mass participation**	**Shear Force (KN) Fundamental mode (X axis)**	**Variation (%)**
Ground Floor	2386.32	1944.68	1.22
A	1449.09	1263.19	1.14
B	1213.12	1111.23	1.09
C	1033.83	825.89	1.25
D	843.92	658.43	1.28
E	700.14	536.08	1.30

Table 9.2 Higher Mode Participation Check for Earthquake Imposed along the y Axis

Earthquake imposed along Y axis			
Floor Level	**Shear Force (KN) Capturing the 90% of mass participation**	**Shear Force (KN) Fundamental mode (Y axis)**	**Variation (%)**
Ground Floor	2478.70	2348.52	1.06
A	1130.12	1059.50	1.07
B	954.08	921.42	1.035
C	850.15	779.26	1.09
D	692.17	546.62	1.27
E	481.85	367.22	1.31

It is concluded that the higher mode effects are not significant; since the shear in any story resulting from the modal response spectrum analysis, considering modes required to obtain 90% mass participation, does not exceed 130% of the corresponding story shear, considering only the fundamental mode response in either direction.

A Pushover analysis is performed exactly as described in the chapter 6.

Nonlinear Static Analysis along +Y Axis (Modal Distribution of Lateral Loads)

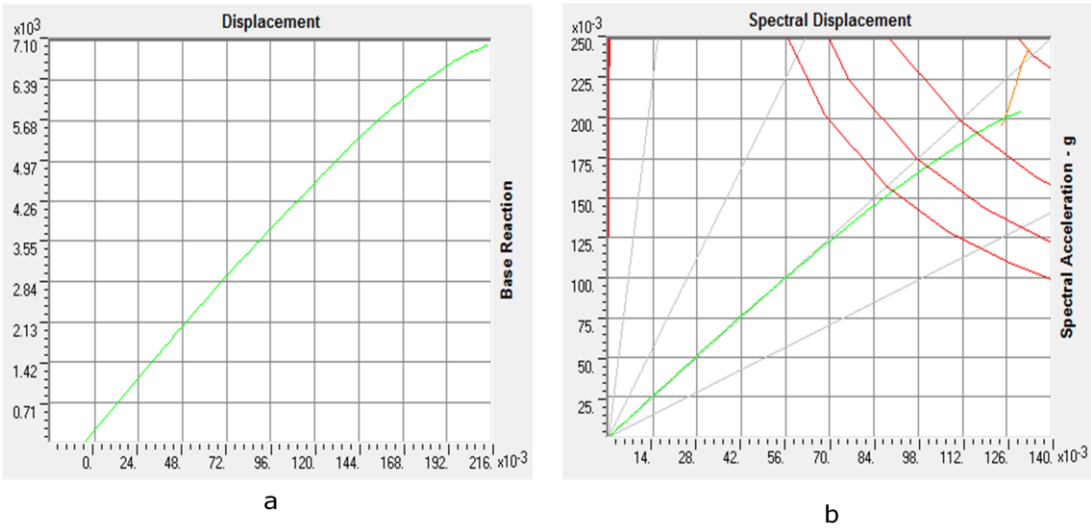

Figure 9.13 a) Pushover Curve (Modal Distribution of Lateral Loads along +Y Axis) b) ATC-40 Capacity Spectrum-ADRS (Modal Distribution of Lateral Loads along +Y Axis)

Performance Point: V=6895.38KN D=0.205m, S_a=0.200g, S_d=0.125m

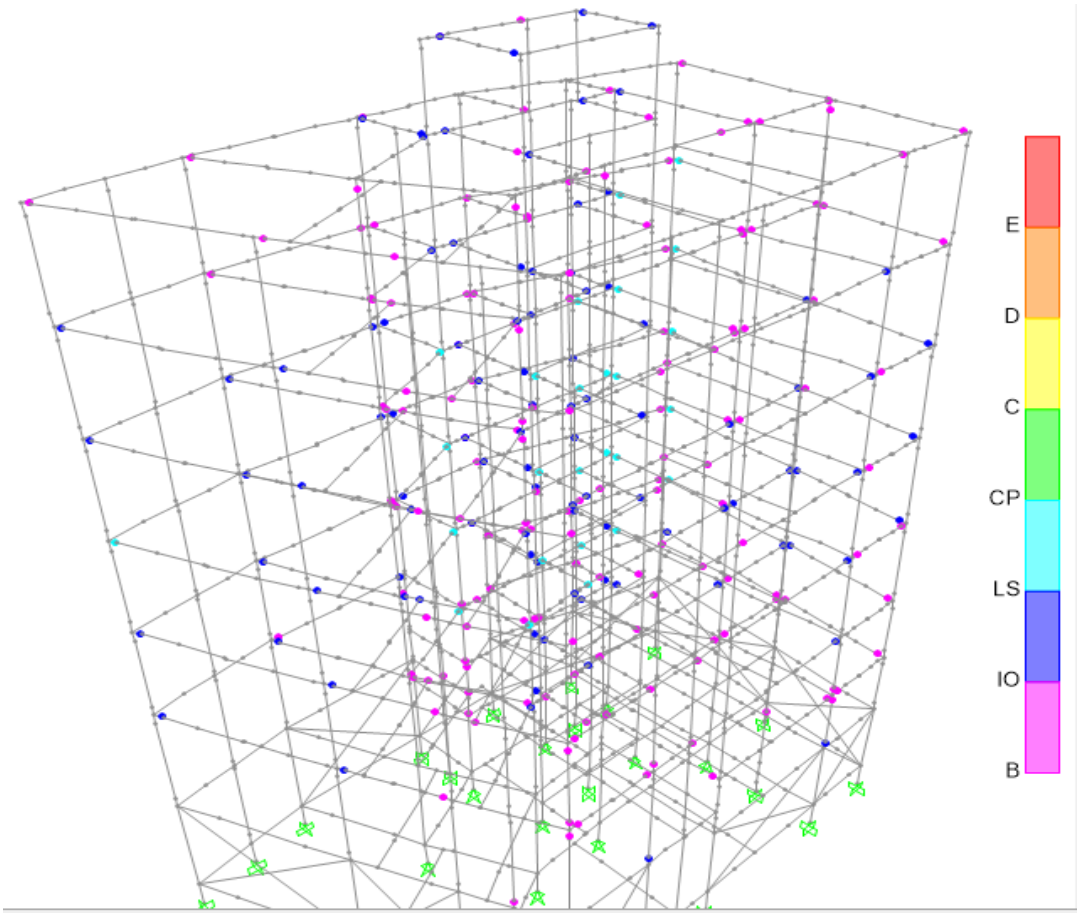

Figure 9.14 Deformed Shape of the Structure at Performance Point-Step 79 (Modal Distribution of Lateral Loads along +Y Axis)

Table 9.9 Hinges Limit State Results at Performance Point (Step 79)

Step	Displacement	BaseForce	AtoB	BtoIO	IOtoLS	LStoCP	CPtoC	CtoD	DtoE	BeyondE	Total
	m	KN									
77	0.201696	6840.175	774	161	97	24	0	0	0	0	1056
78	0.203896	6872.531	773	161	97	25	0	0	0	0	1056
79	**0.206096**	**6904.41**	**771**	**161**	**98**	**26**	**0**	**0**	**0**	**0**	**1056**
80	0.208296	6935.646	771	158	100	27	0	0	0	0	1056
81	0.210496	6966.5	769	158	101	28	0	0	0	0	1056

There are 26 hinges that exceed the life safety limit state. However no hinge exceeds life safety limit state in columns. Hinges between the limit states immediate occupancy and life safety are formed in two columns (JC2, JC4).

Nonlinear Static Analysis along -Y Axis (Modal Distribution of Lateral Loads)

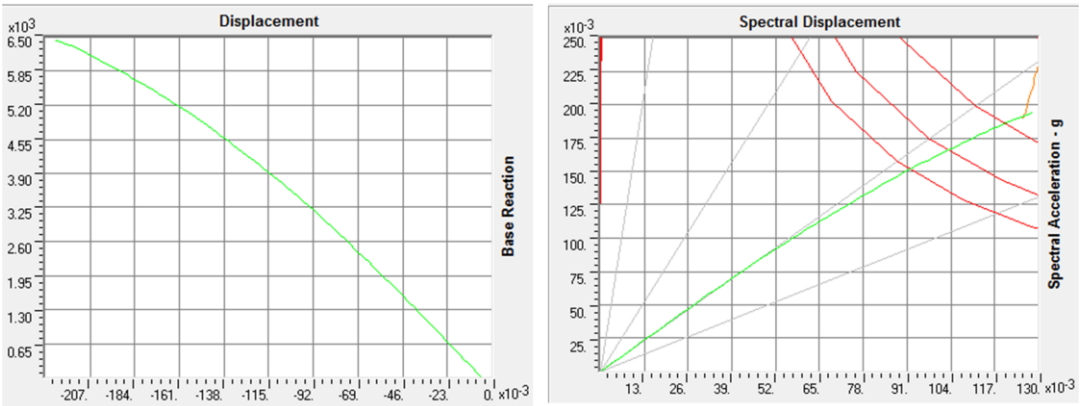

a b

Figure 9.15 a) Pushover Curve (Modal Distribution of Lateral Loads along -Y Axis) b) ATC-40 Capacity Spectrum-ADRS (Modal Distribution of Lateral Loads along -Y Axis)

Performance Point: V=6381.76 D=-0.220m, S_a=0.191g, S_d=0.126m

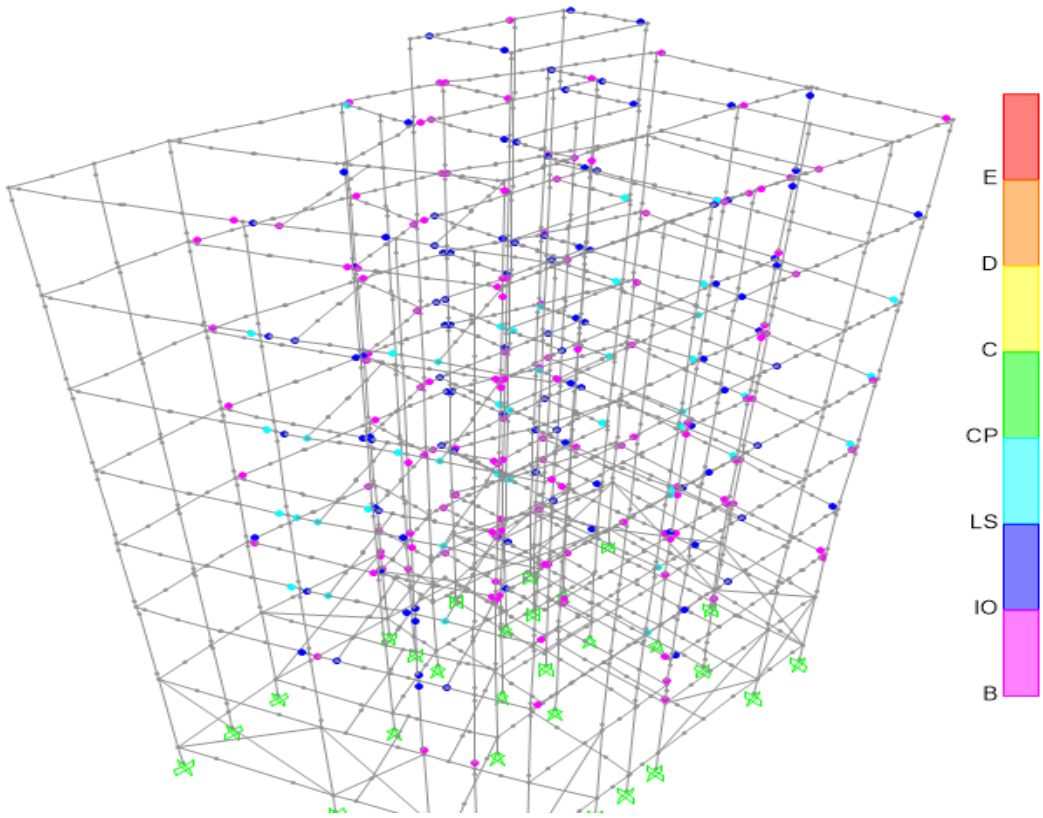

Figure 9.16 Deformed Shape of the Structure at Performance Point-Step 84 (Modal Distribution of Lateral Loads along -Y Axis)

Table 9.10 Hinges Limit State Results at Performance Point (Step 84)

Step	Displacement	BaseForce	AtoB	BtoIO	IOtoLS	LStoCP	CPtoC	CtoD	DtoE	BeyondE	Total
	m	KN									
82	-0.217619	6346.62	773	142	103	38	0	0	0	0	1056
83	-0.219819	6374.353	771	140	104	41	0	0	0	0	1056
84	**-0.222019**	**6401.453**	**769**	**137**	**107**	**43**	**0**	**0**	**0**	**0**	**1056**
85	-0.224219	6427.897	769	136	108	43	0	0	0	0	1056
86	-0.225354	6441.526	767	138	105	46	0	0	0	0	1056

At the performance point (step 84), 43 hinges exceed limit safety limit state. However all of them are in beams and there is no hinge exceeding life safety limit state in column or shear wall. There are hinges between the limit states immediate occupancy and life safety in three columns (JC6, C10, C12).

Nonlinear Static Analysis along +X Axis (Modal Distribution of Lateral Loads)

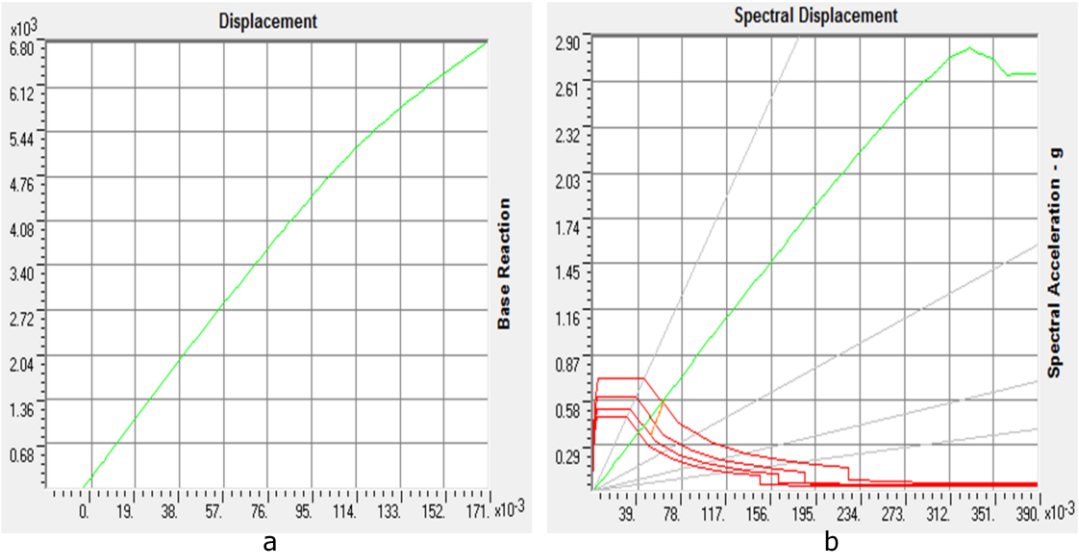

Figure 9.9 a) Pushover Curve (Modal Distribution of Lateral Loads along +X Axis) b) ATC-40 Capacity Spectrum-ADRS (Modal Distribution of Lateral Loads along +X Axis)

Performance Point: V=1081.86 KN, D=0.019m, S_a=0.587g, S_d=0.062m

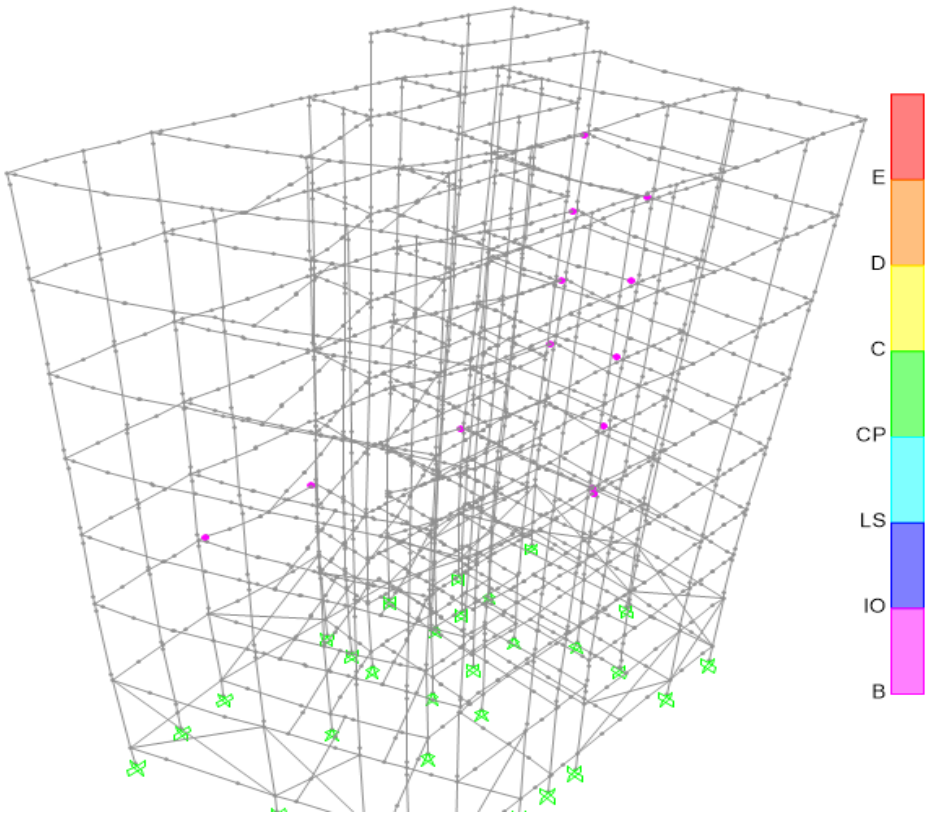

Figure 9.10 Deformed Shape of the Structure at Performance Point-Step 12 (Modal Distribution of Lateral Loads along +X Axis)

Table 9.7 Hinges Limit State Results at Performance Point (Step 12)

Step	isplacemer	BaseForce	AtoB	BtoIO	IOtoLS	LStoCP	CPtoC	CtoD	DtoE	BeyondE	Total
	m	KN									
10	0.013988	832.23	1049	7	0	0	0	0	0	0	1056
11	0.017497	997.52	1048	8	0	0	0	0	0	0	1056
12	**0.019468**	**1090.28**	**1043**	**13**	**0**	**0**	**0**	**0**	**0**	**0**	**1056**
13	0.021268	1174.822	1043	13	0	0	0	0	0	0	1056
14	0.023068	1259.368	1042	14	0	0	0	0	0	0	1056

Nonlinear Static Analysis along -X Axis (Modal Distribution of Lateral Loads)

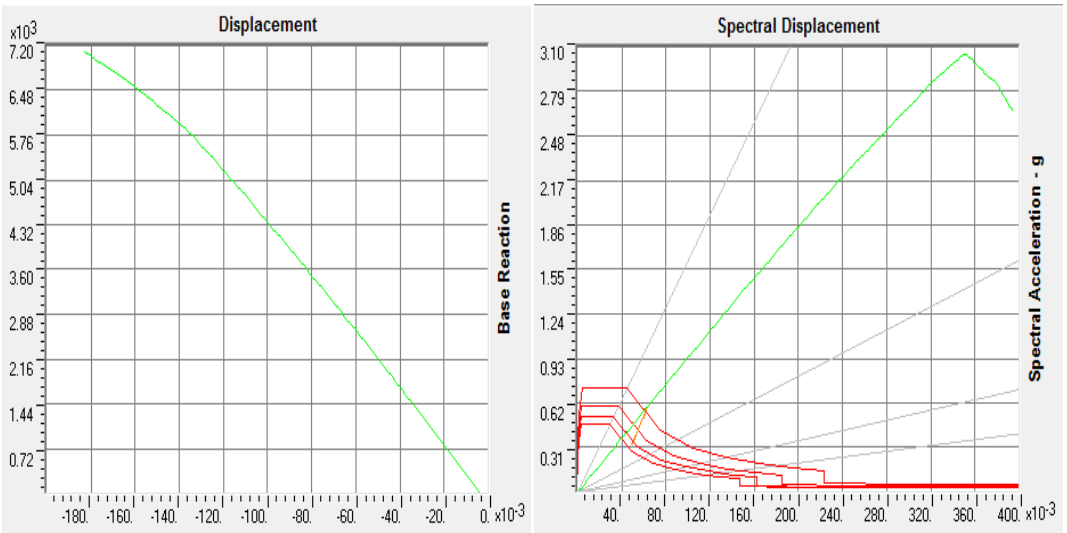

Figure 9.11 a) Pushover Curve (Modal Distribution of Lateral Loads along -X Axis) b) ATC-40 Capacity Spectrum-ADRS (Modal Distribution of Lateral Loads along -X Axis)

Performance Point: V=1085.73KN, D=-0.027m, S_a=0.585g, S_d=0.062m

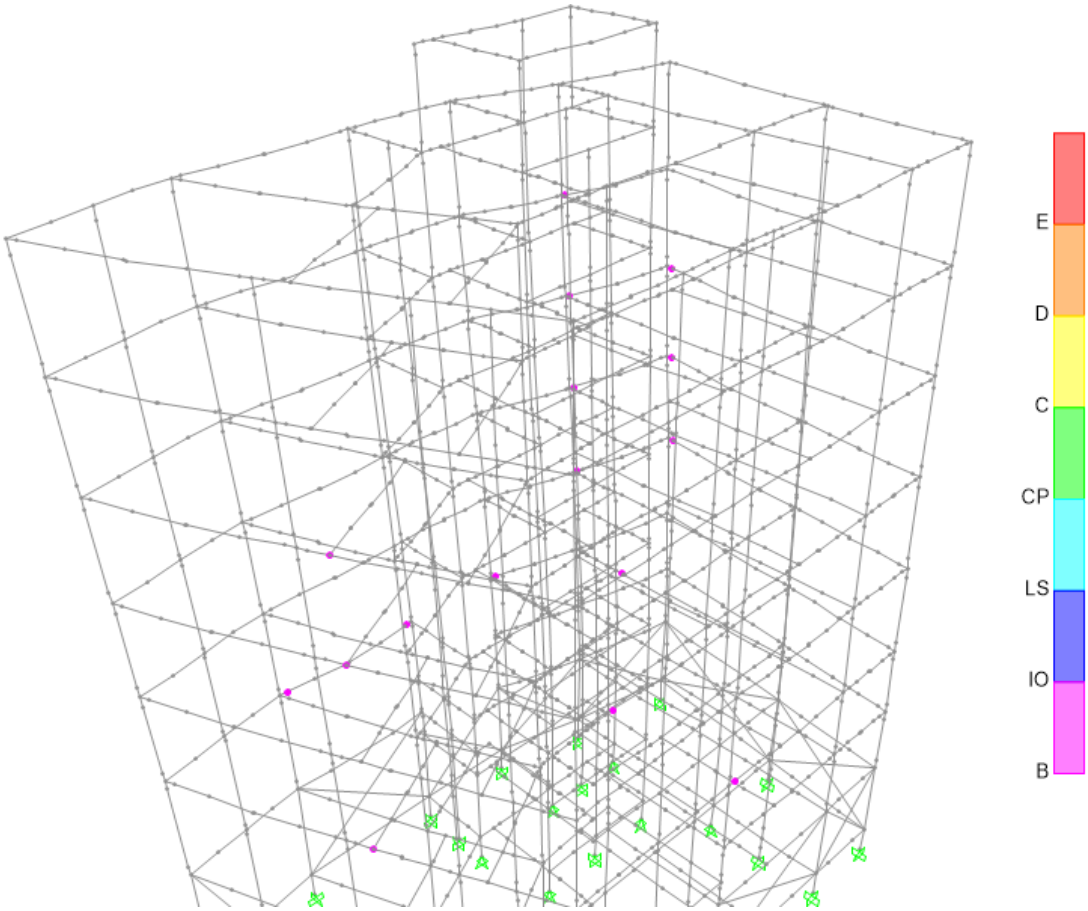

Figure 9.12 Deformed Shape of the Structure at Performance Point-Step 13 (Modal Distribution of Lateral Loads along -X Axis)

Table 9.8 Hinges Limit State Results at Performance Point (Step 13)

Step	Displacement	BaseForce	AtoB	BtoIO	IOtoLS	LStoCP	CPtoC	CtoD	DtoE	BeyondE	Total
	m	KN									
11	-0.022927	912.165	1050	6	0	0	0	0	0	0	1056
12	-0.025906	1052.374	1043	13	0	0	0	0	0	0	1056
13	**-0.027706**	**1136.88**	**1040**	**16**	**0**	**0**	**0**	**0**	**0**	**0**	**1056**
14	-0.029506	1221.295	1040	16	0	0	0	0	0	0	1056
15	-0.032555	1364.184	1037	19	0	0	0	0	0	0	1056

Nonlinear Static Analysis along +Y Axis (Uniform Distribution of Lateral Loads)

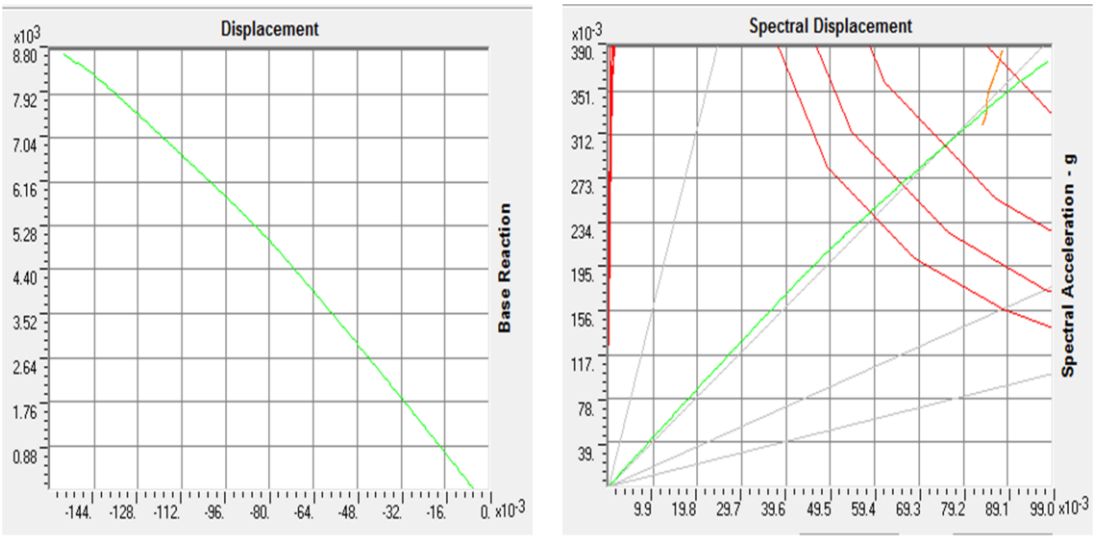

a b

Figure 9.5 a) Pushover Curve (Uniform Distribution of Lateral Loads along +Y Axis) b) ATC-40 Capacity Spectrum-ADRS (Uniform Distribution of Lateral Loads along +Y Axis)

Performance Point: V=7824.82 KN, D=-0.134m, S_a=0.334g, S_d=0.084m

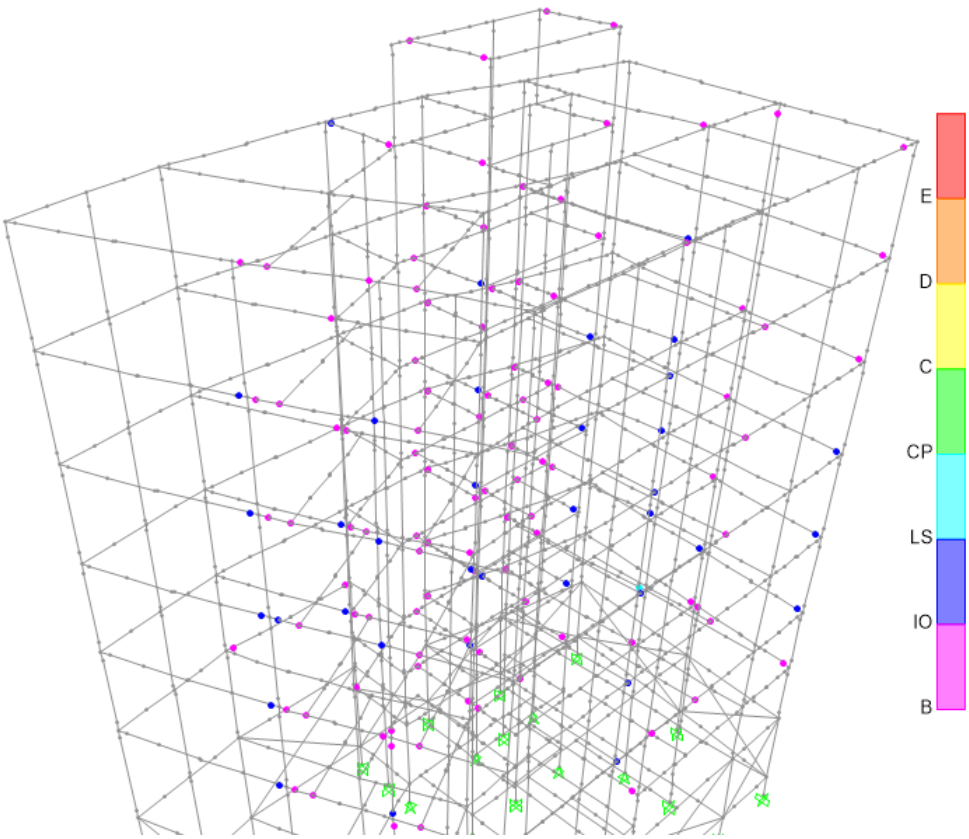

Figure 9.6 Deformed Shape of the Structure at Performance Point-Step 173 (Uniform Distribution of Lateral Loads along +Y Axis)

Table 9.5 Hinges Limit State Results at Performance Point (Step 173)

Step	isplaceme	BaseForce	AtoB	BtoIO	IOtoLS	LStoCP	CPtoC	CtoD	DtoE	BeyondE	Total
	m	KN									
171	-0.13353	7778.487	916	107	32	1	0	0	0	0	1056
172	-0.13428	7816.167	915	105	35	1	0	0	0	0	1056
173	**-0.135**	**7853.84**	**913**	**106**	**36**	**1**	**0**	**0**	**0**	**0**	**1056**
174	-0.13578	7890.736	912	106	37	1	0	0	0	0	1056
175	-0.13653	7927.598	911	106	38	1	0	0	0	0	1056

It is shown that at the performance point, only one hinge exceeds life safety limit state. It is a hinge beam.

<u>Nonlinear Static Analysis along –Y Axis (Uniform Distribution of Lateral Loads)</u>

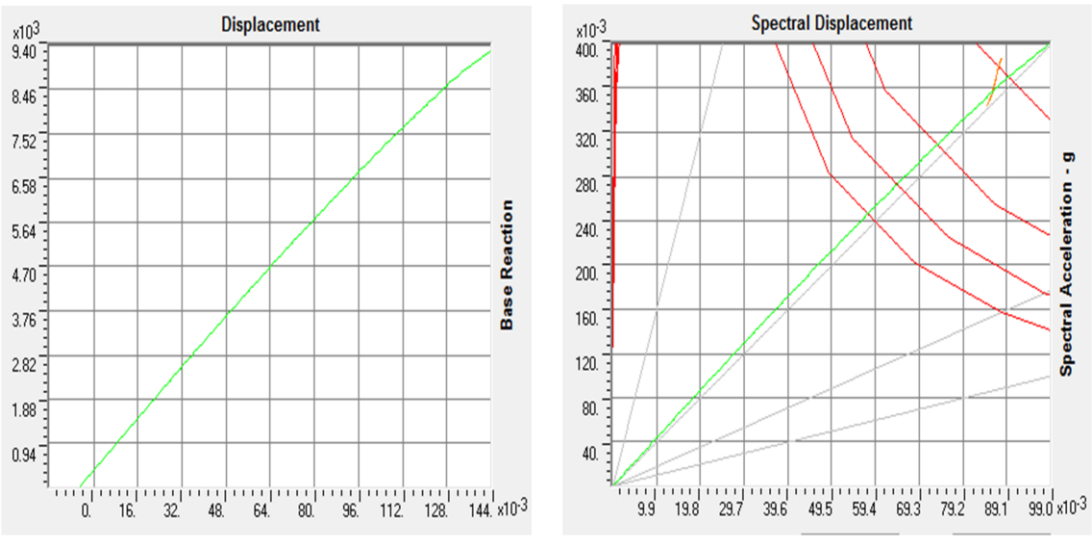

a b

Figure 9.7 a) Pushover Curve (Uniform Distribution of Lateral Loads along -Y Axis) b) ATC-40 Capacity Spectrum-ADRS (Uniform Distribution of Lateral Loads along -Y Axis)

Performance Point: V=8417.83 KN, D=0.126m, S_a=0.357g, S_d=0.086m

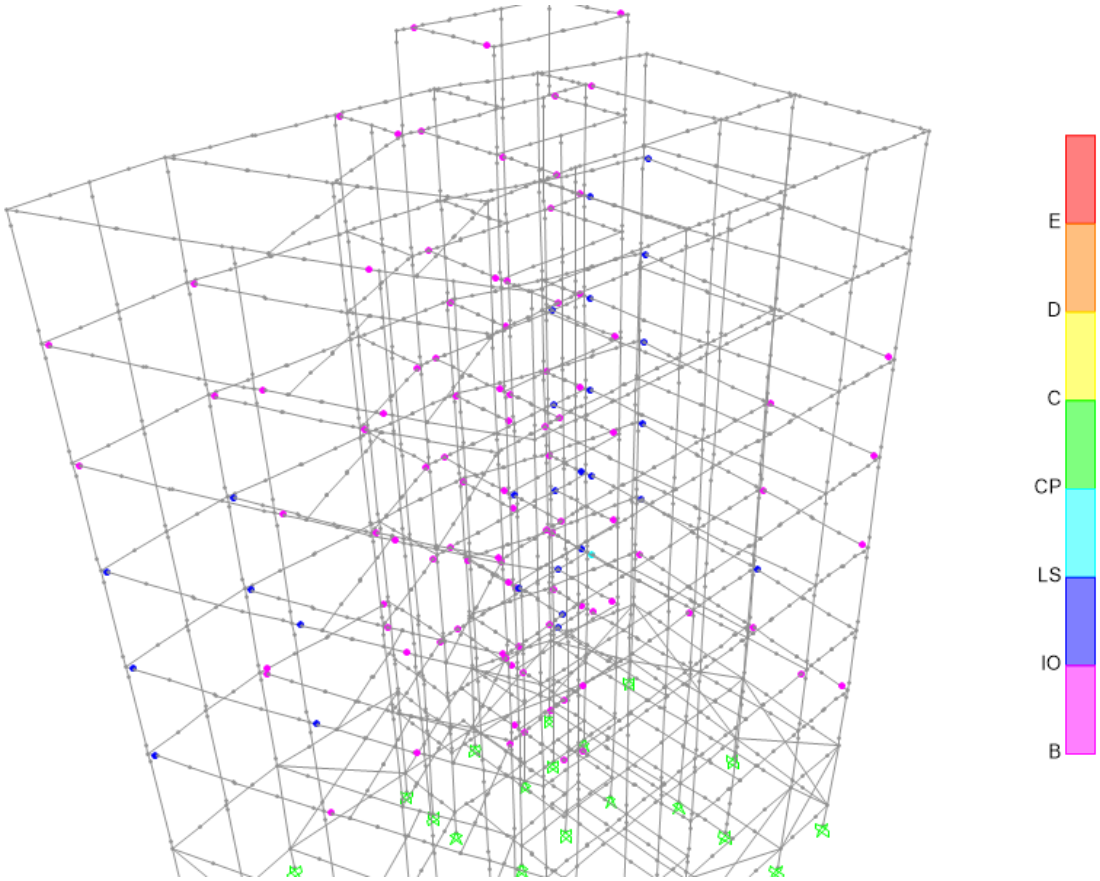

Figure 9.8 Deformed Shape of the Structure at Performance Point-Step 176 (Uniform Distribution of Lateral Loads along -Y Axis)

Table 9.6 Hinges Limit State Results at Performance Point (Step 176)

Step	isplaceme	BaseForce	AtoB	BtoIO	IOtoLS	LStoCP	CPtoC	CtoD	DtoE	BeyondE
	m	KN								
174	0.125146	8383.598	931	97	27	1	0	0	0	0
175	0.125896	8425.605	929	99	27	1	0	0	0	0
176	**0.12665**	**8467.56**	**929**	**99**	**27**	**1**	**0**	**0**	**0**	**0**
177	0.127396	8509.508	929	98	28	1	0	0	0	0
178	0.128146	8551.46	928	99	28	1	0	0	0	0

It is shown that at the performance point, only one hinge exceeds life safety limit state. It is a hinge beam.

Nonlinear static analysis along +X Axis (Uniform Distribution of Lateral Loads)

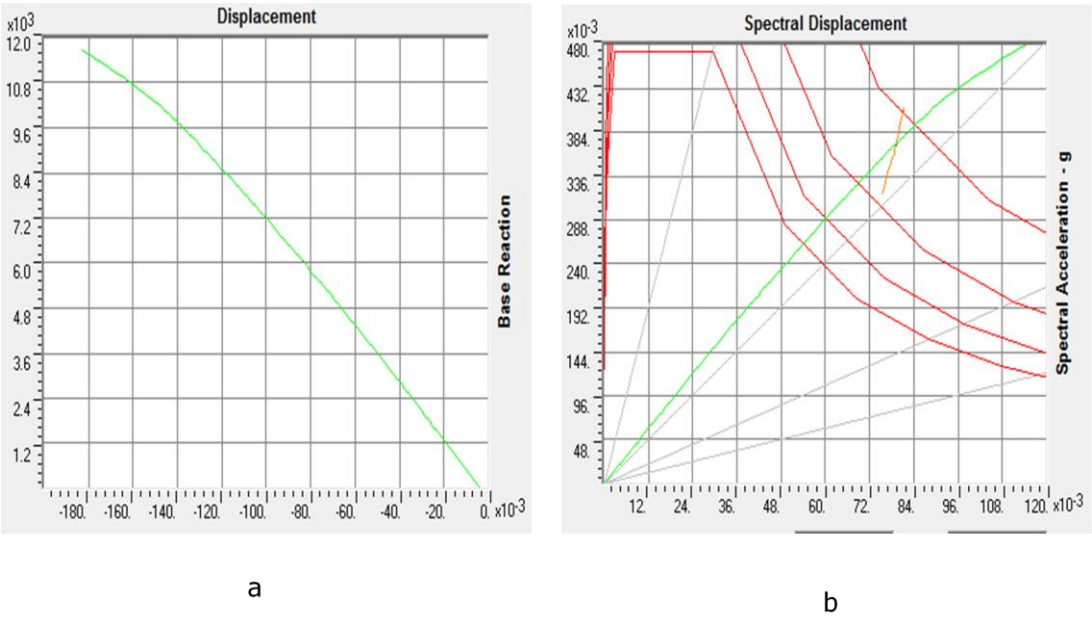

Figure 9.1 a) Pushover Curve (Uniform Distribution of Lateral Loads along +X Axis) b) ATC-40 Capacity Spectrum-ADRS (Uniform Distribution of Lateral Loads along +X Axis)

Performance Point: V=9032.91KN, D=-0.128m, S_a=0.371g, S_d=0.079m

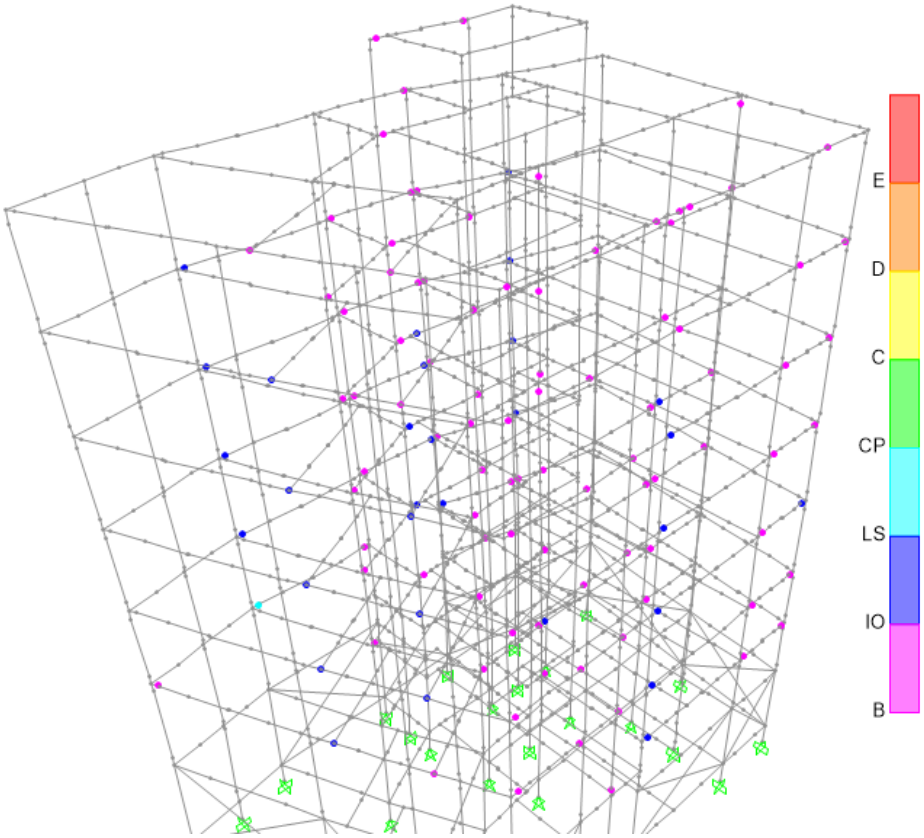

Figure 9.2 Deformed Shape of the Structure at Performance Point-Step 59 (Uniform Distribution of Lateral Loads along +X Axis)

Table 9.3 Hinges Limit State Results at Performance Point (Step 59)

Step	Displacement	BaseForce	AtoB	BtoIO	IOtoLS	LStoCP	CPtoC	CtoD	DtoE	BeyondE	Total
	m	KN									
57	-0.12612	8892.762	940	89	26	1	0	0	0	0	1056
58	-0.12792	9006.866	937	91	27	1	0	0	0	0	1056
59	**-0.12972**	**9120.32**	**934**	**91**	**30**	**1**	**0**	**0**	**0**	**0**	**1056**
60	-0.13152	9233.714	934	88	33	1	0	0	0	0	1056
61	-0.13332	9346.982	933	86	36	1	0	0	0	0	1056

It is shown that at the performance point, only one hinge exceeds life safety limit state. It is a hinge beam.

Nonlinear Static Analysis along –X Axis (Uniform Distribution of Lateral Loads)

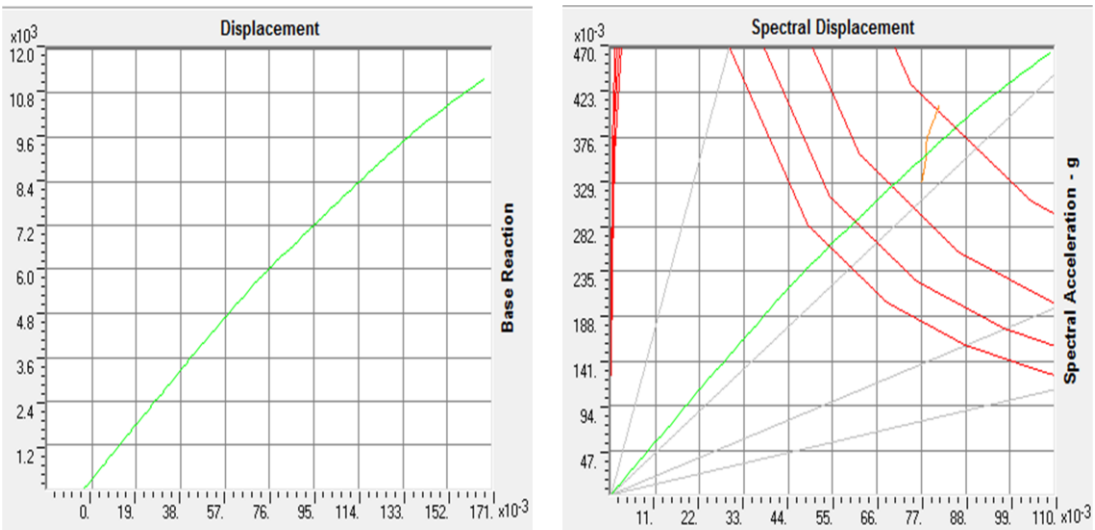

a b

Figure 9.3 a) Pushover Curve (Uniform Distribution of Lateral Loads along -X Axis) b) ATC-40 Capacity Spectrum-ADRS (Uniform Distribution of Lateral Loads along -X Axis)

Performance Point: V=8663.27, D=0.119m, S_a=0.358g, S_d=0.078m

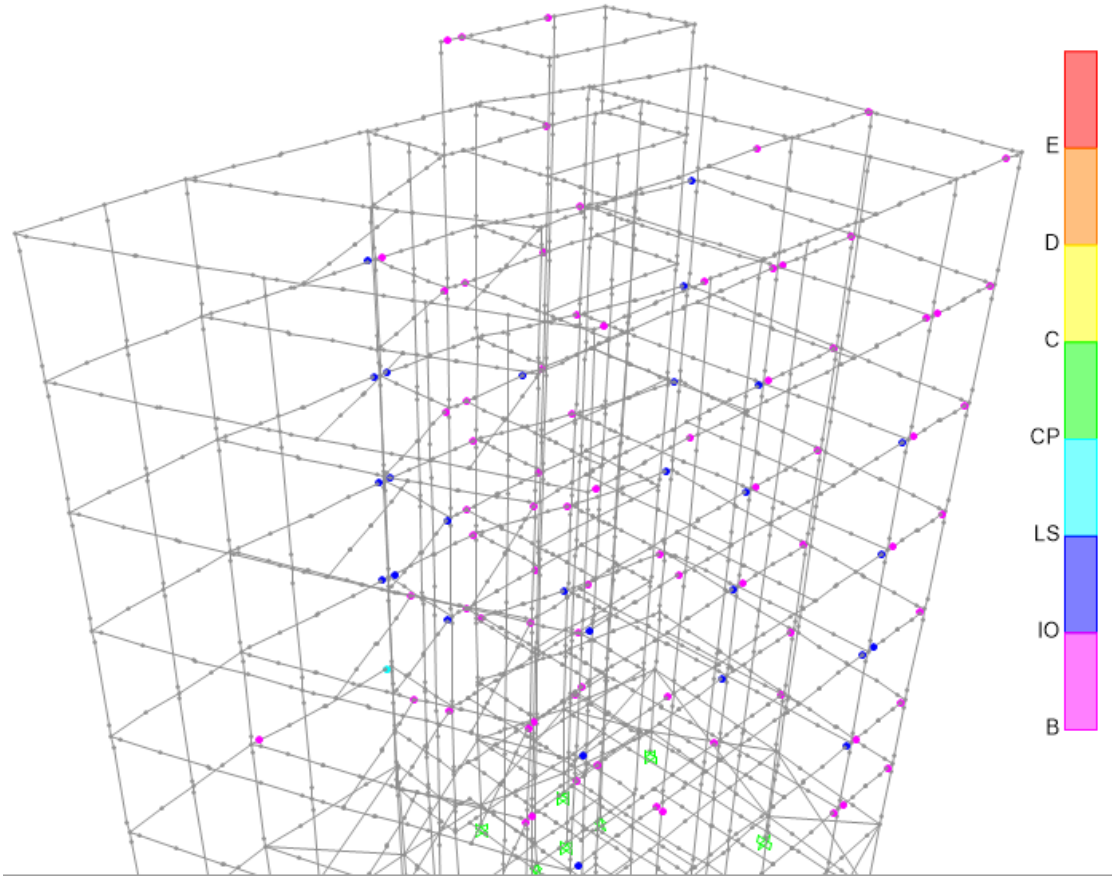

Figure 9.4 Deformed Shape of the Structure at Performance Point-Step 57 (Uniform Distribution of Lateral Loads along -X Axis)

Table 9.4 Hinges Limit State Results at Performance Point (Step 57)

Step	isplaceme	BaseForce	AtoB	BtoIO	IOtoLS	LStoCP	CPtoC	CtoD	DtoE	BeyondE	Total
	m	KN									
55	0.116271	8501.67	947	88	20	1	0	0	0	0	1056
56	0.118071	8610.094	947	83	25	1	0	0	0	0	1056
57	**0.11987**	**8718.52**	**947**	**80**	**28**	**1**	**0**	**0**	**0**	**0**	**1056**
58	0.122925	8898.693	942	80	33	1	0	0	0	0	1056
59	0.124725	9003.157	942	79	34	1	0	0	0	0	1056

Life safety limit state is exceeded by one hinge which is formed in a beam.

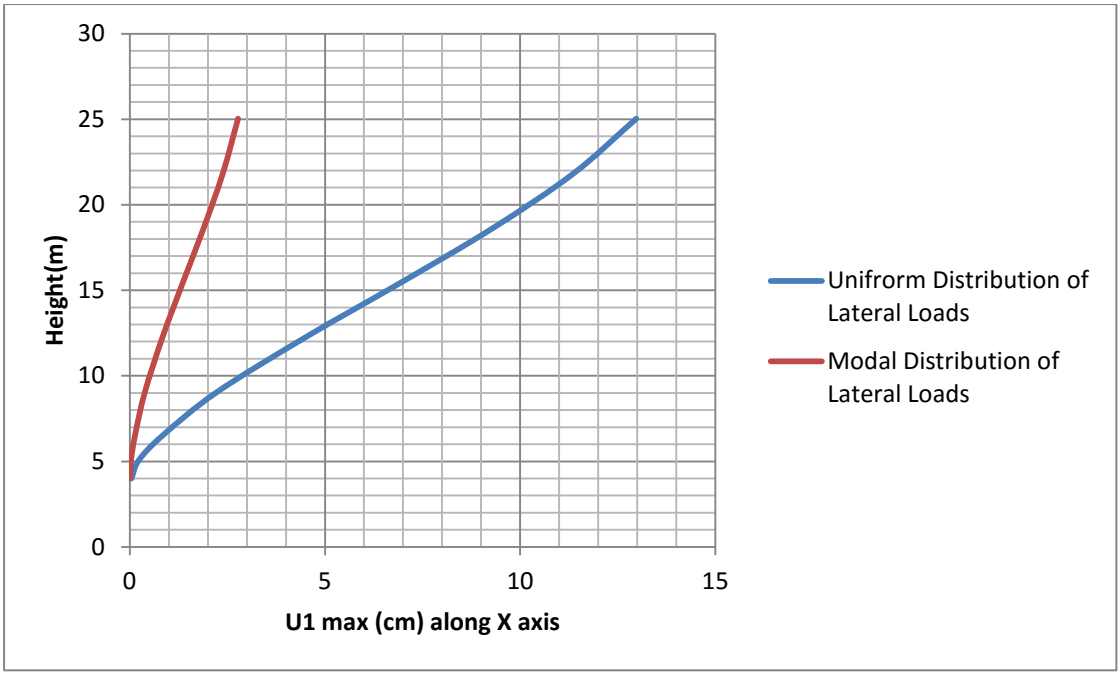

Figure 9.17 Maximum Displacement per Height along X axis for Uniform and Modal Distribution of Lateral Loads

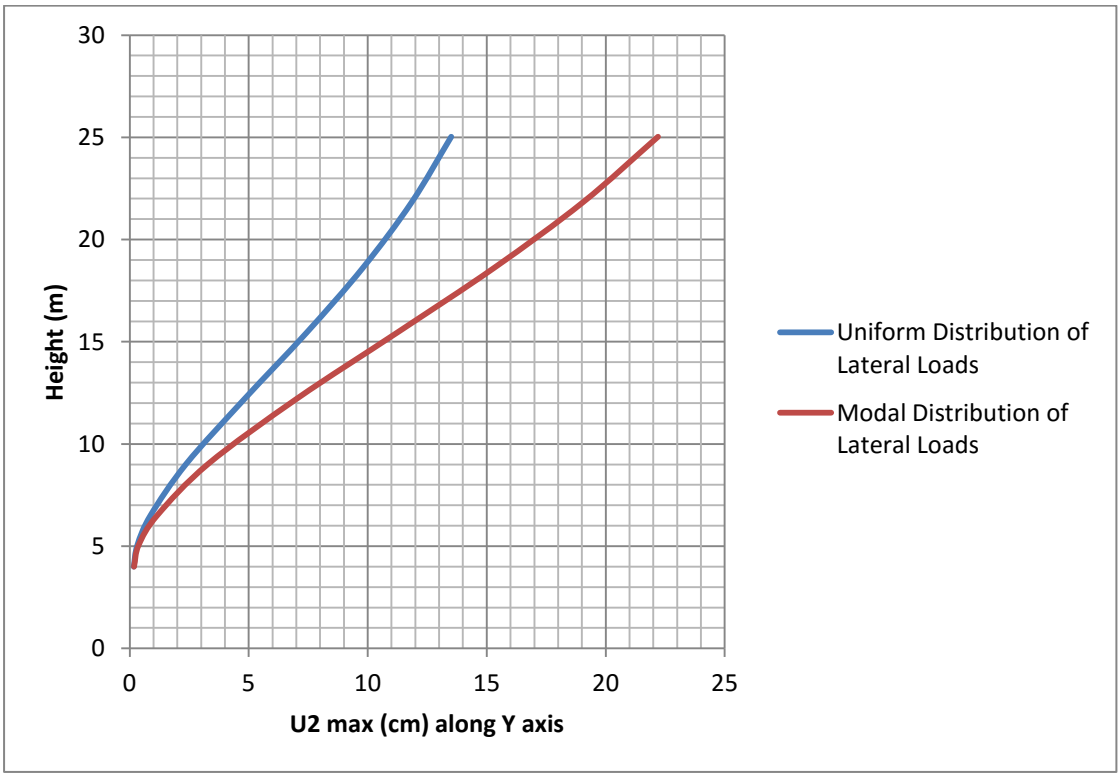

Figure 9.18 Maximum Displacement per Height along Y axis for Uniform and Modal Distribution of Lateral Loads

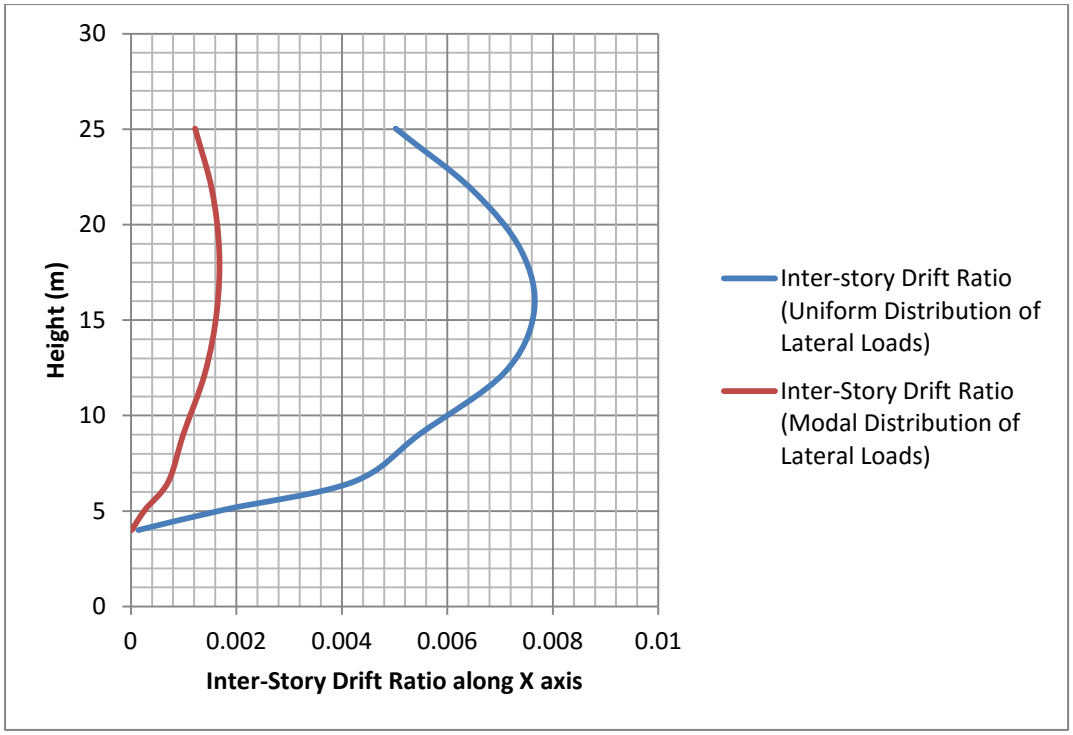

Figure 9.19 Inter-story Drift Ratios along X Axis for Uniform and Modal Distribution of Lateral Loads

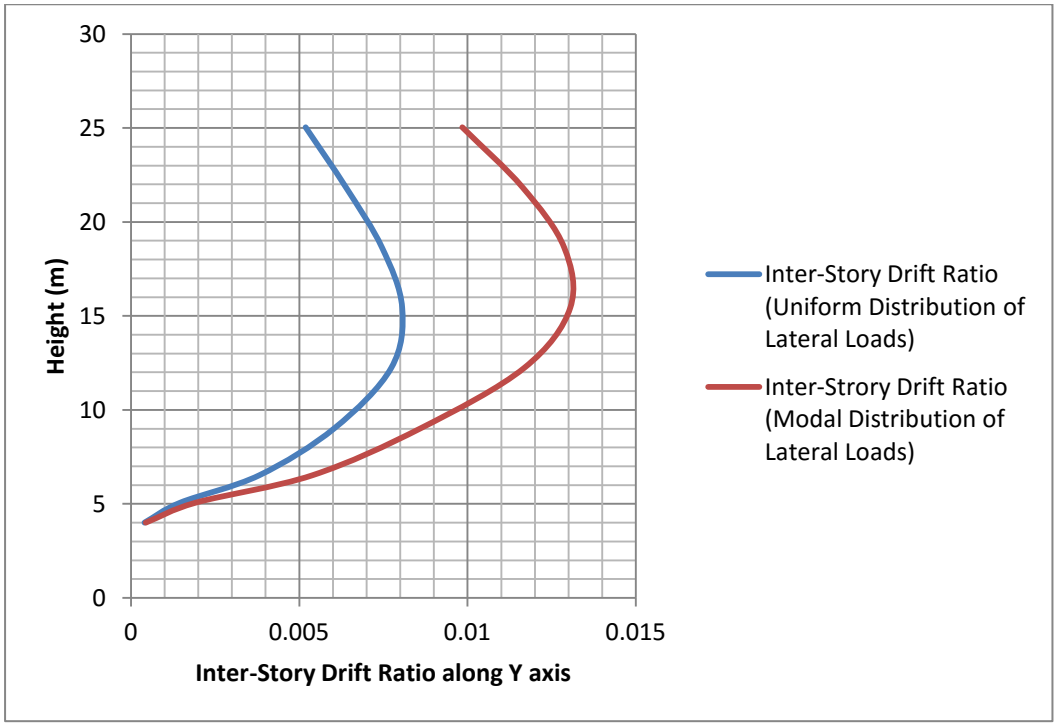

Figure 9.20 Inter-story Drift Ratios along Y Axis for Uniform and Modal Distribution of Lateral Loads

9.1 Discussions on Pushover Analyses Results

Only beam-hinges exceed the life safety limit state, for the analyses of modal distribution of lateral loads along the –Y and +Y axes. Nearly no hinge exceeds life safety limit state by other analyses.

The maximum displacement of the control node of the building is caused for modal distribution of lateral loads along the –Y axis (-0.22m). In addition, the maximum number of hinges exceeding life safety limit state is observed by this analysis (however as mentioned earlier no hinge exceeds life safety limit state in column or shear wall).

The maximum absolute displacements of the building per height due to the uniform distribution of lateral loads are higher than due to the modal distribution of lateral loads, along the X axis.

The maximum absolute displacements of the building per height due to the modal distribution of lateral loads are higher than due to the uniform distribution of lateral loads, along the Y axis.

The inter-story drift ratios due to the uniform distribution of lateral loads are higher than due to the modal distribution of lateral loads, along the X axis.

The inter-story drift ratios due to the modal distribution of lateral loads are higher than due to the uniform distribution of lateral loads, along the Y axis.

Chapter 10

Nonlinear Time-History Dynamic Analyses Results of the Retrofitted Structure

Nonlinear time-history analyses performed as described in chapter 7. There is no hinge in columns, shear wall or beam that exceeds life safety limit state. The results of load combinations that are presented in chapter 7, are also presented in this chapter, in order to be comparable.

L'Aquila Earthquake Event

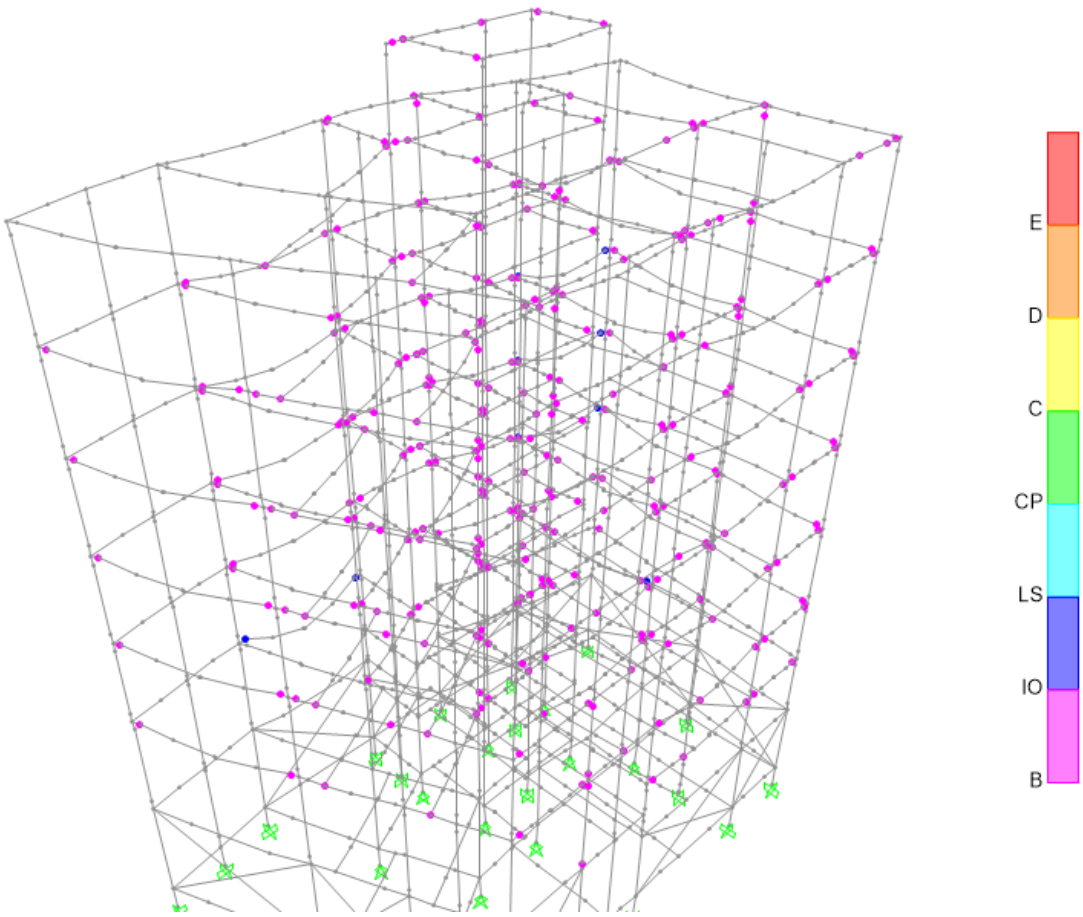

Figure 10.1 Earthquake Event: L'Aquila, Load Combination: G+0.3Q+Ex+0.3Ey

No column-hinge is exceeding immediate occupancy limit state.

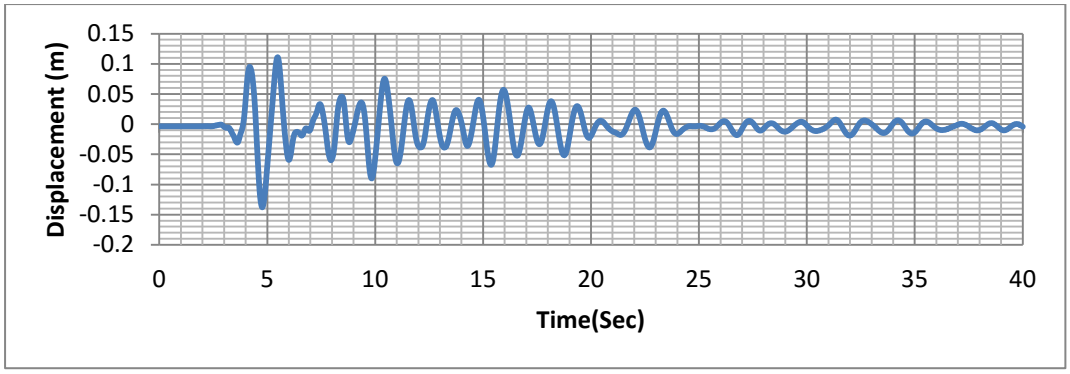

Figure 10.2 Displacement Time-History of the Center of Mass (joint 130) of the Approachable Roof due to L'Aquila Earthquake Event

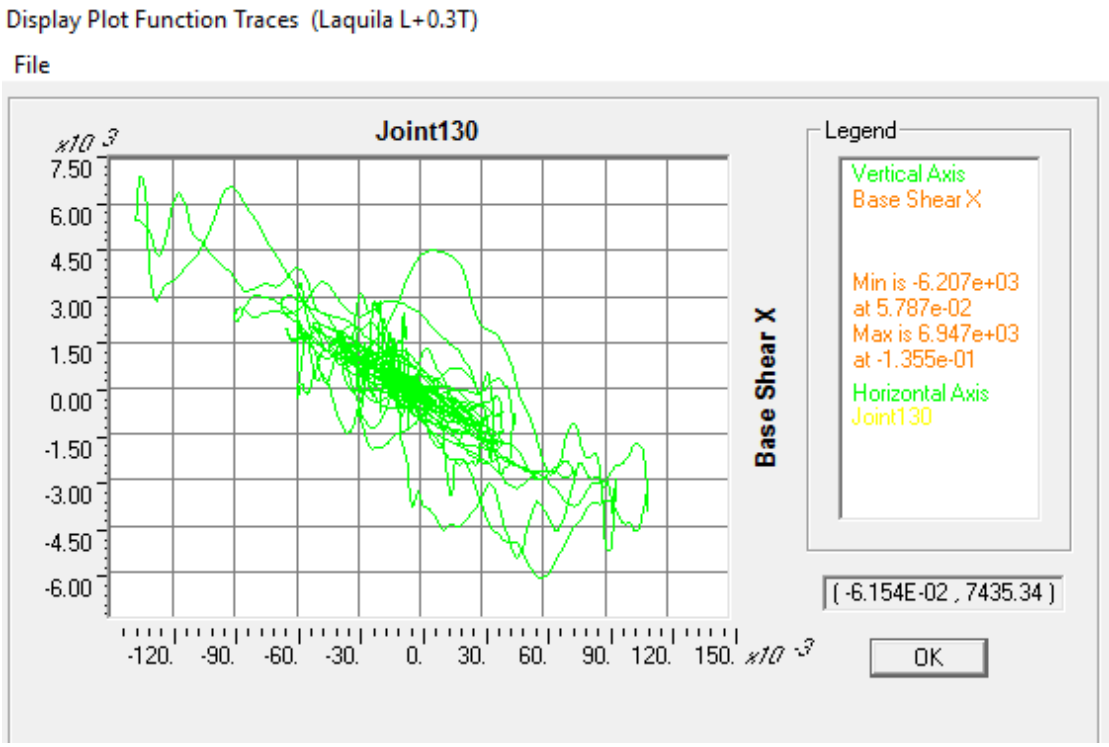

Figure 10.3 Hysteretic Loop of base shear force along X- Displacement along X of joint 130–(center of mass of the approachable roof)- L'Aquila

Corinth Earthquake Event

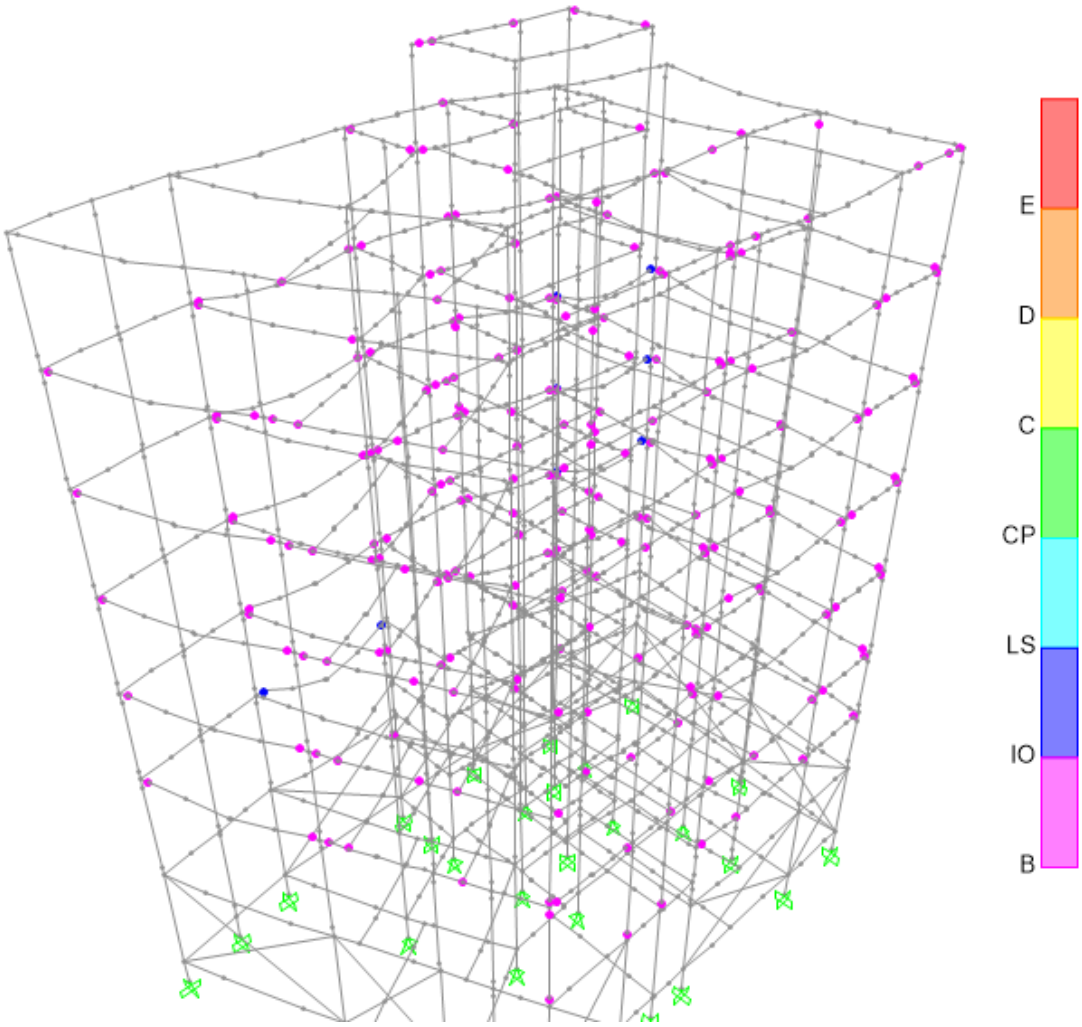

Figure 10.4 Earthquake Event: Corinth, Load Combination: G+0.3Q-Ex-0.3Ey

No column-hinge is exceeding immediate occupancy limit state.

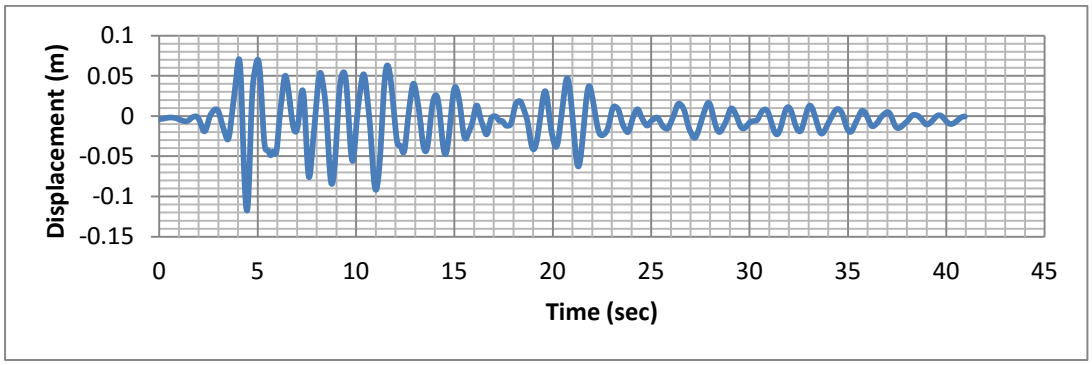

Figure 10.5 Displacement Time-History of the Center of Mass (joint 130) of the Approachable Roof due to Corinth Earthquake Event

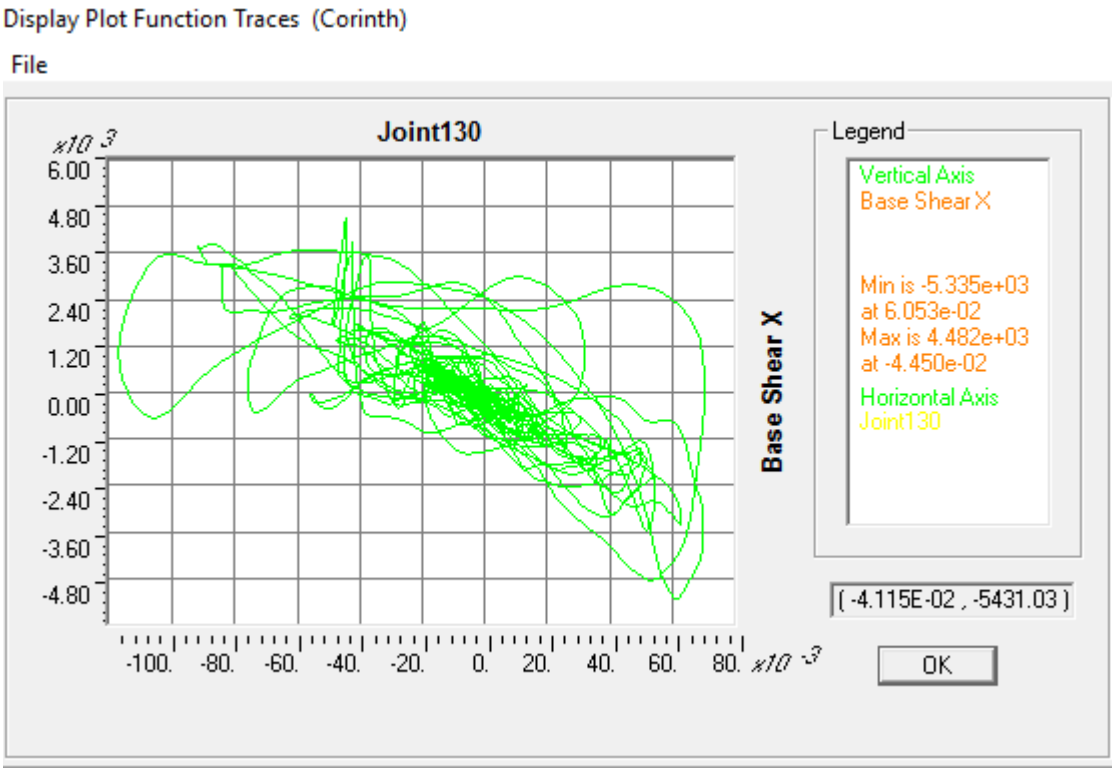

Figure 10.6 Hysteretic Loop of base shear force along X- Displacement along X of joint 130–(center of mass of the approachable roof)- Corinth

Kalamata Earthquake Event

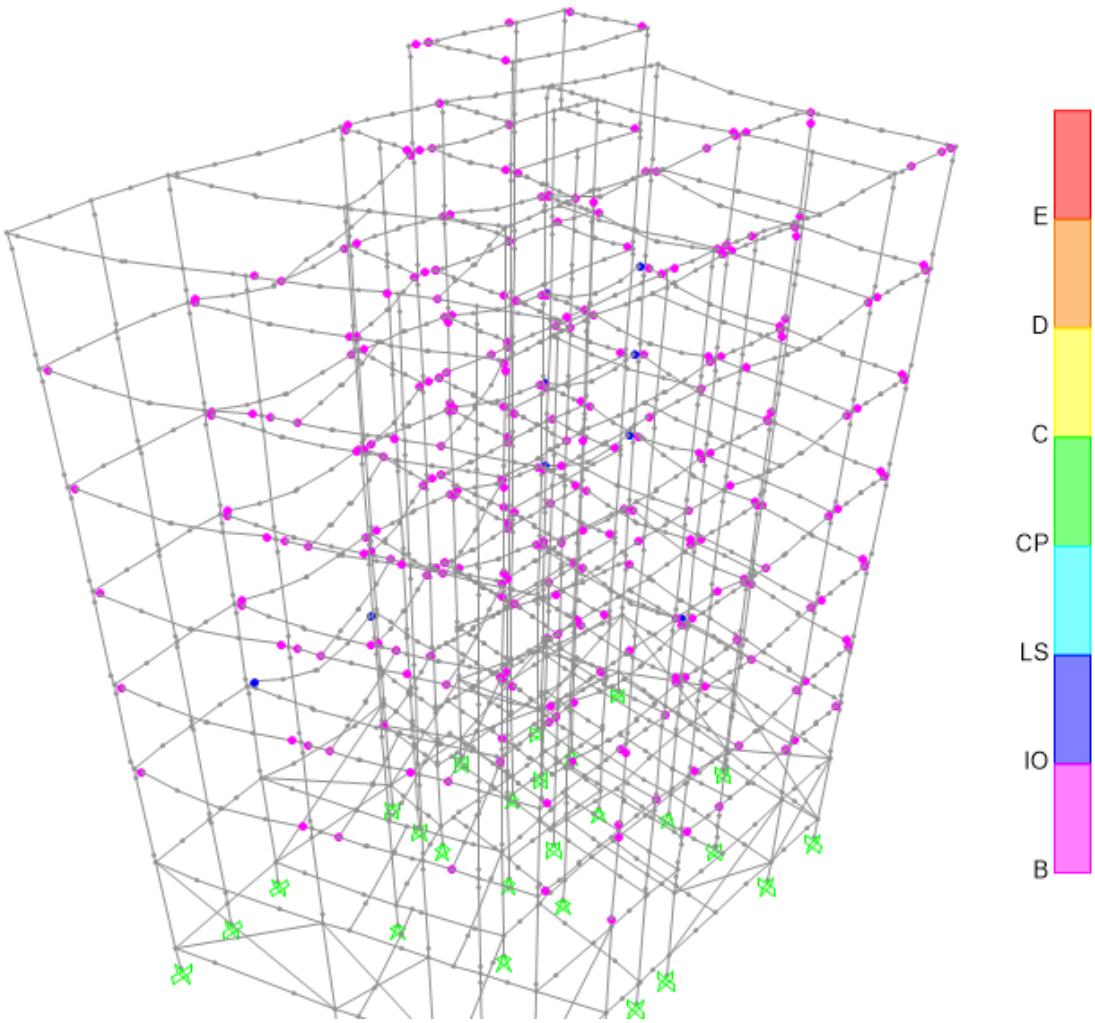

Figure 10.7 Earthquake Event: Kalamata, Load Combination: G+0.3Q-Ex-0.3Ey

No column-hinge is exceeding immediate occupancy limit state.

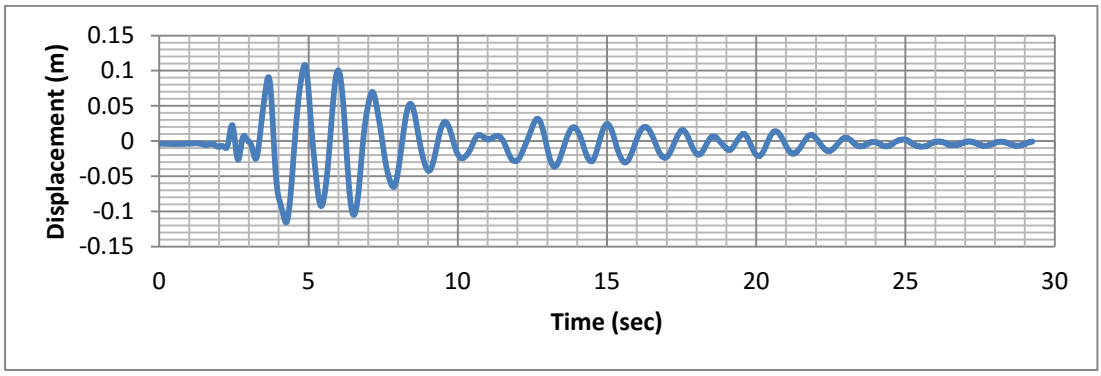

Figure 10.8 Displacement Time-History of the Center of Mass (joint 130) of the Approachable Roof due to Kalamata Earthquake Event

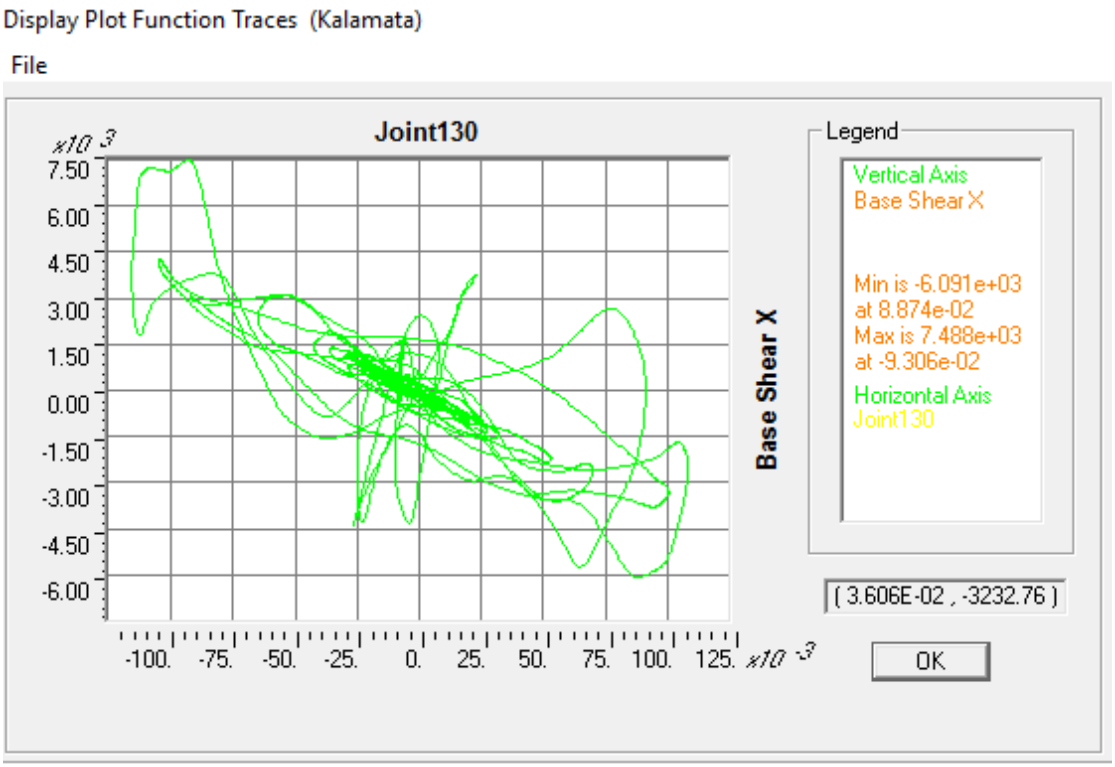

Figure 10.9 Hysteretic Loop of base shear force along X- Displacement along X of joint 130–(center of mass of the approachable roof)- Kalamata

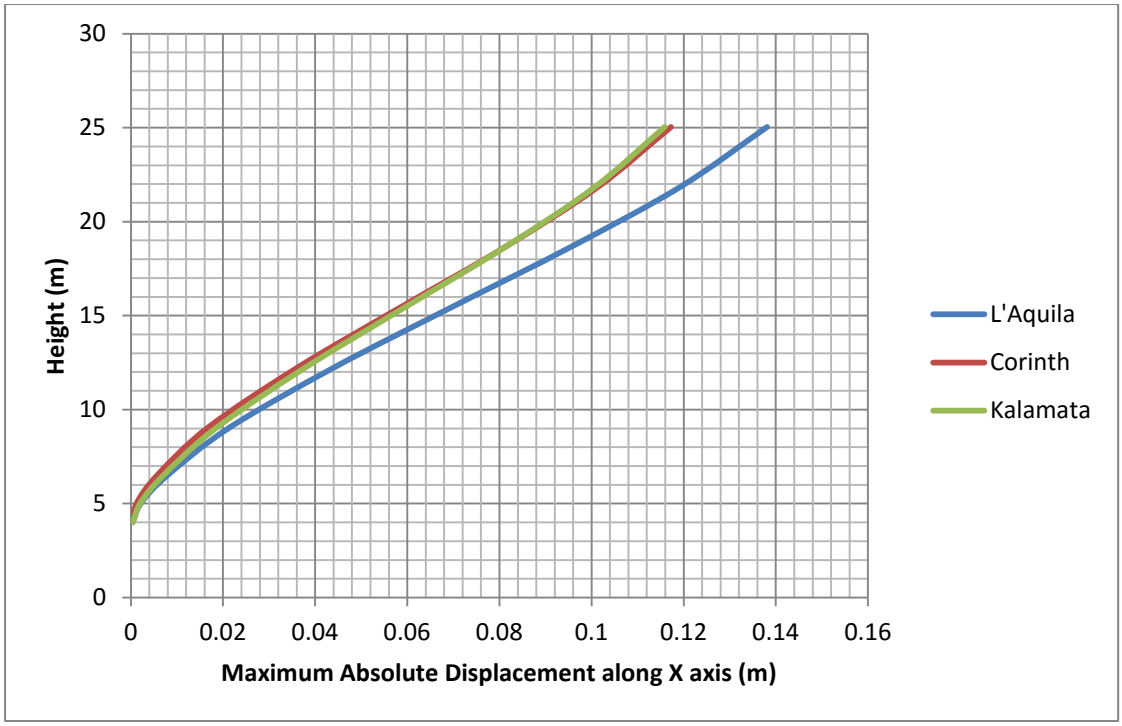

Figure 10.10 Maximum Absolute Displacement per Floor Level for Earthquakes imposed along the X axis

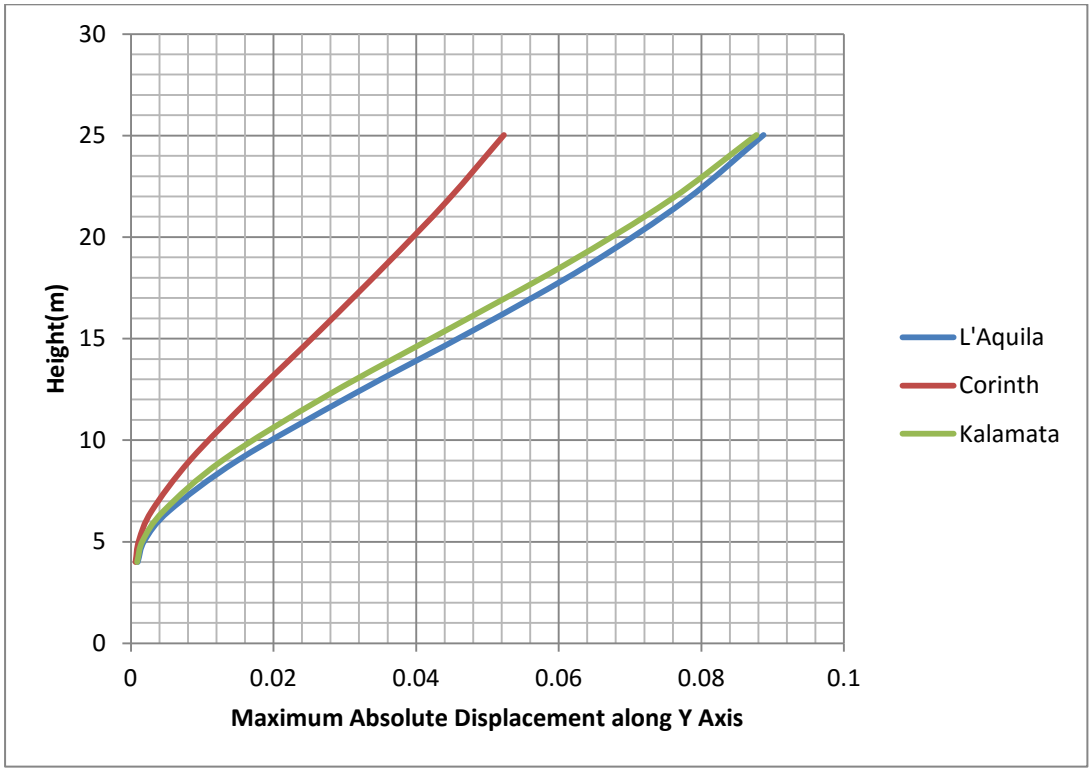

Figure 10.11 Maximum Absolute Displacement per Floor Level for Earthquakes imposed along the Y axis

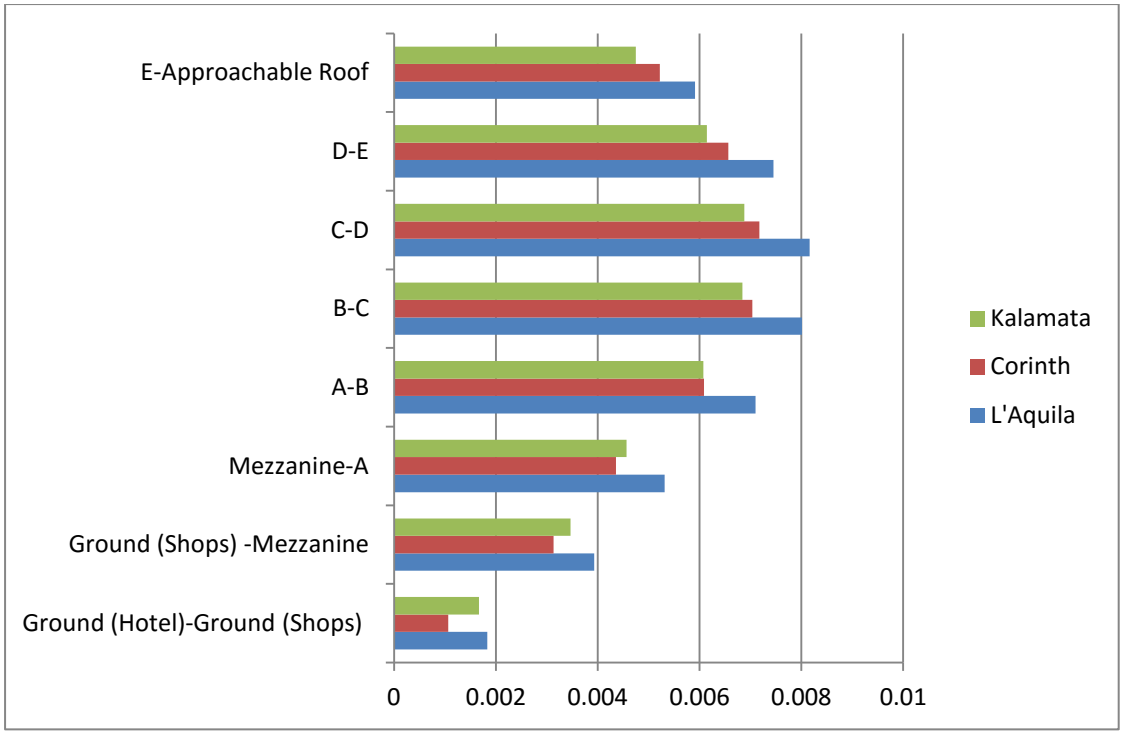

Figure 10.12 Inter-story Drift Ratios along X axis

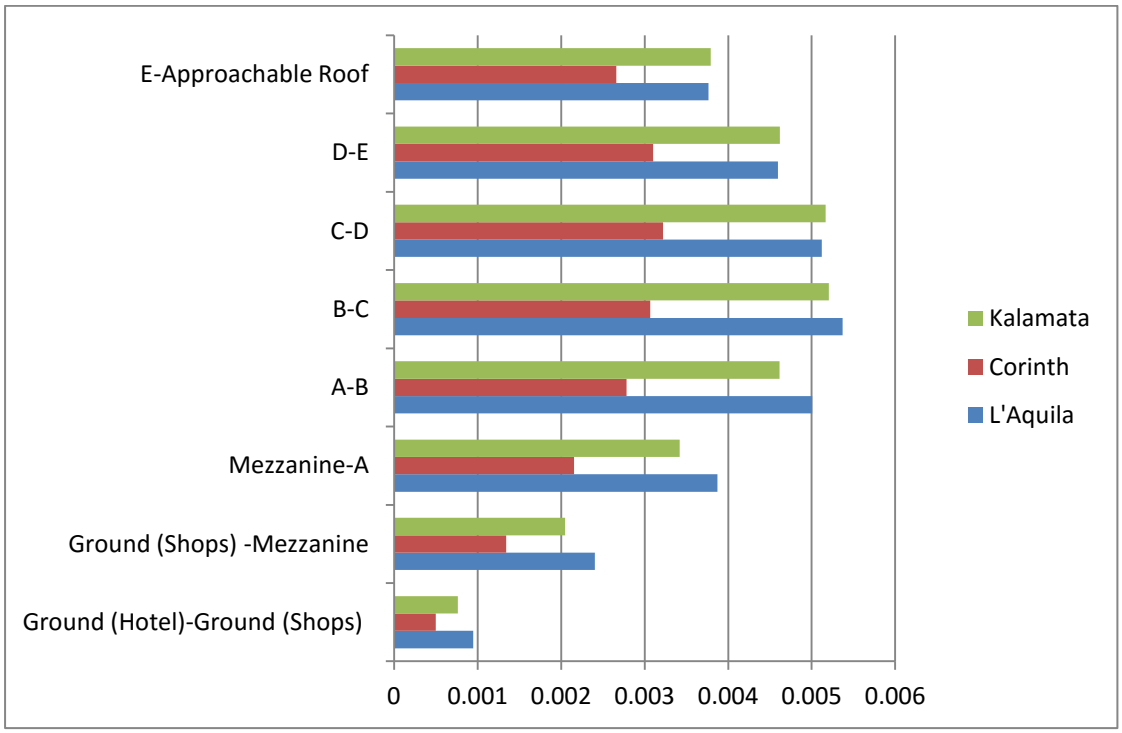

Figure 10.13 Inter-story Drift Ratios along Y axis

In the following figures the time-histories of the bending moments and shear forces along axis X (M3, V2) and along axis Y (M2,V3) of the column C20, for each floor level, for the L'Aquila earthquake event are shown.

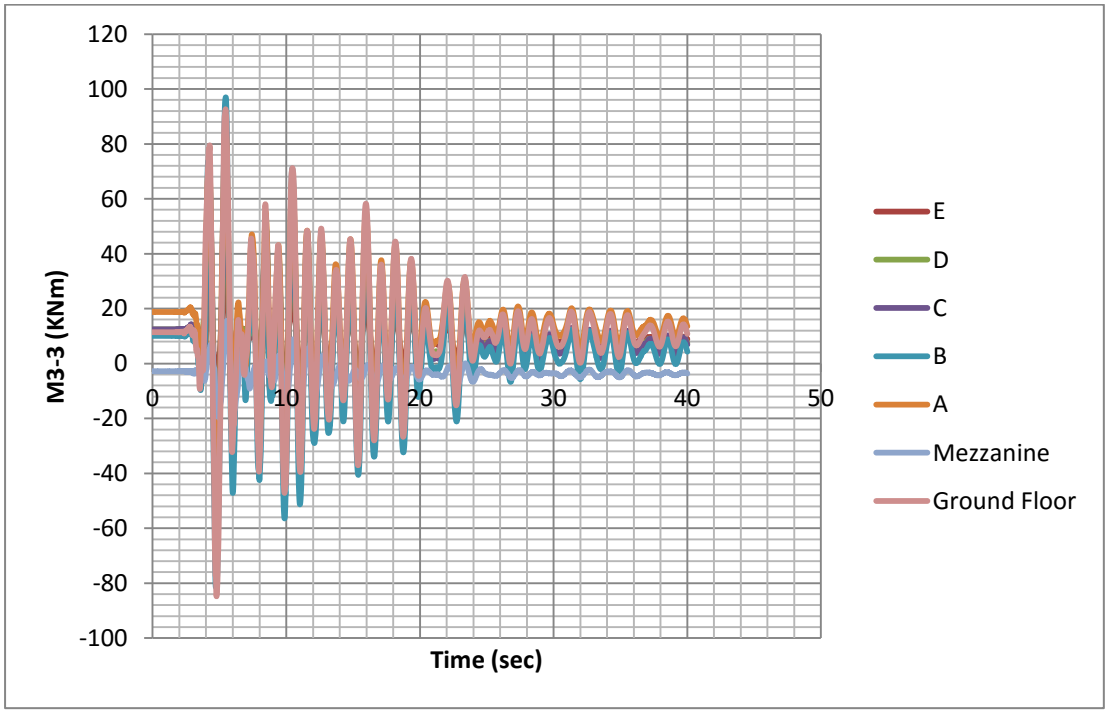

Figure 10.14 Time-History of Bending Moments of Column C20 along axis X (M3-3)

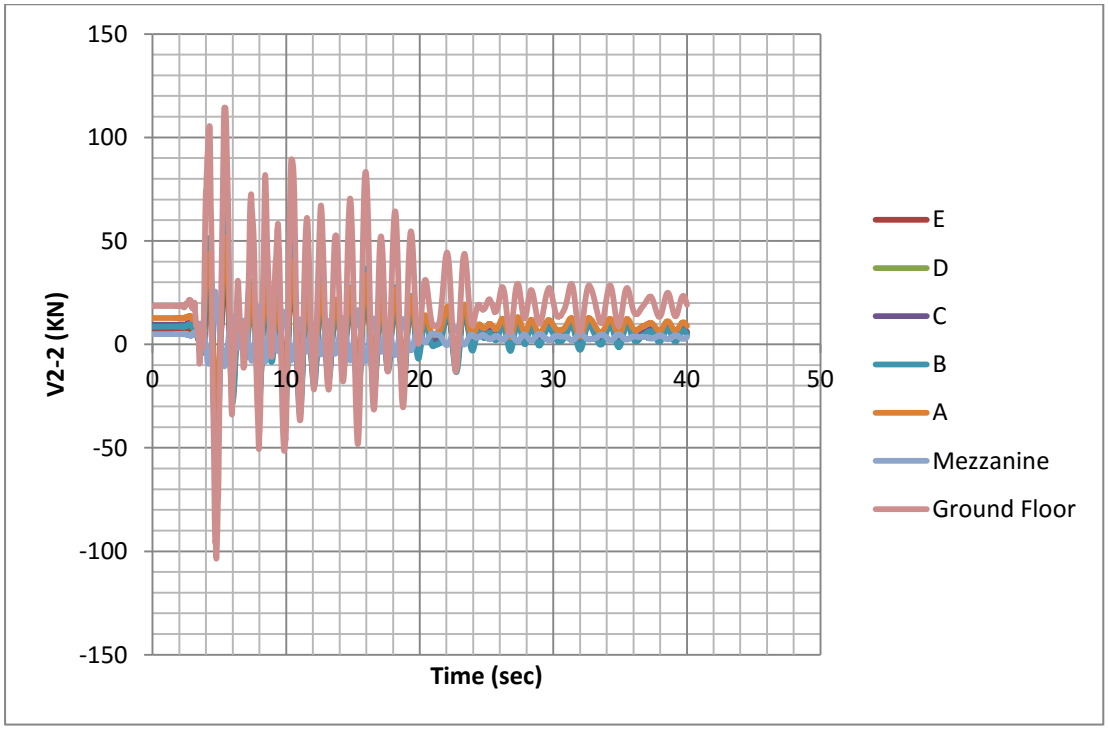

Figure 10.15 Time-History of Shear Forces of Column C20 along axis X (V2-2)

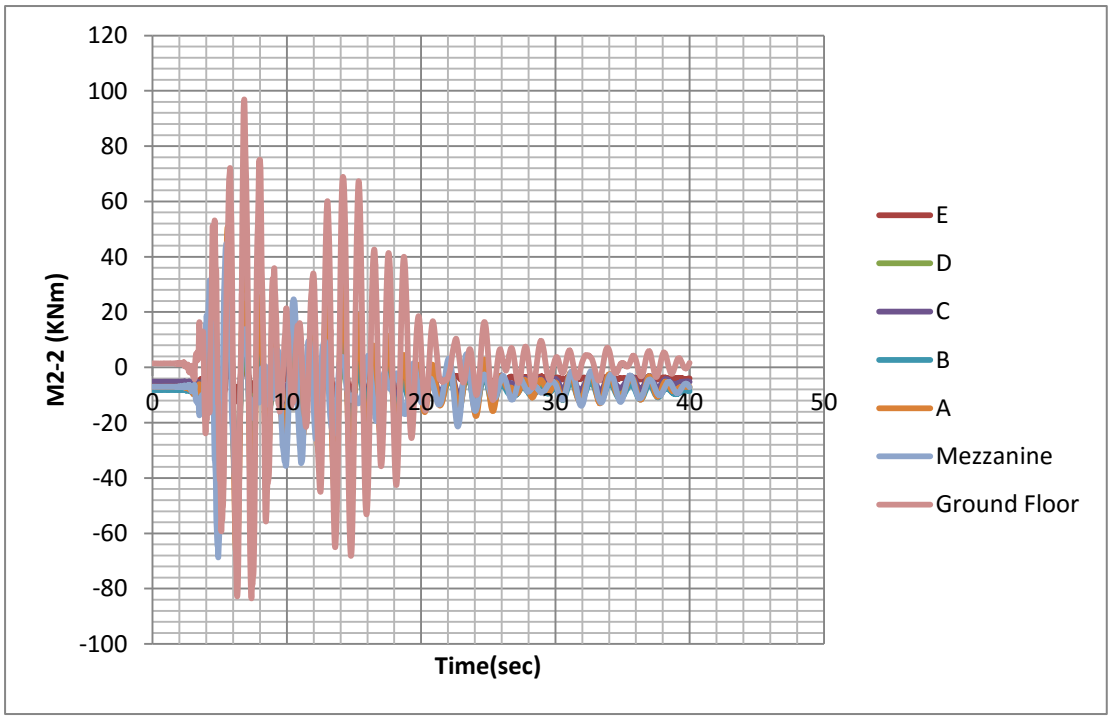

Figure 10.16 Time-History of Bending Moments of Column C20 along axis Y (M2-2)

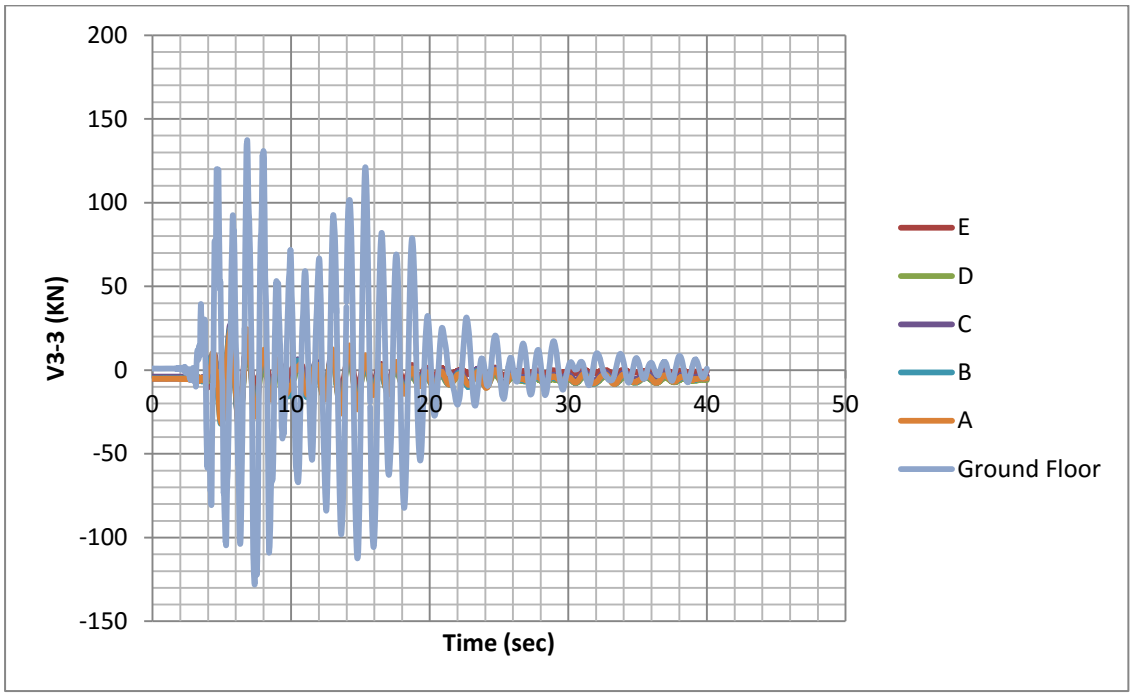

Figure 10.17 Time-History of Shear Forces of Column C20 along axis Y (V3-3)

10.1 Discussions on Nonlinear Time-History Analyses Results of the Retrofitted Structure

- No hinge in column or shear wall exceeds life safety limit sate for none of the earthquake events the structure is subjected to.
- It is shown by the time-histories of the displacement of the center of mass of the approachable roof (joint 130) that the maximum displacement (-0.14m) is caused by the L'Aquila earthquake event at approximately 5 seconds, while for both Corinth and Kalamata the maximum displacement (-0.12m) is caused at approximately 4 seconds.
- The charts of the maximum absolute displacements show that the maximum absolute displacements increase with the building's height.
- The maximum absolute displacement is caused by the L'Aquila earthquake event (0.14m) along the X axis.
- Along the X axis, the maximum absolute displacements observed are caused by the L'Aquila earthquake event, while the displacements caused by Corinth and Kalamata are lower and approximately equal.
- Along the Y axis, the maximum absolute displacements of the structure are caused by the earthquake events of Kalamata and L'Aquila, while those caused by Corinth are significantly lower.
- The inter-story drift ratios are generally higher along the X axis than they are along the Y axis.
- The maximum inter-story drift ratio is caused by the L'Aquila earthquake event (0.8% approximately) at the floor levels B-C, along the X axis.
- The inter-story drift ratios are proportional to the maximum absolute displacements. Thus the higher drift ratios are caused by the L'Aquila earthquake event in X and Y (Kalamata is close enough along Y) axes, and the lower by Corinth earthquake event.
- The time-histories of the forces of C20 per height due to the L'aquila earthquake event show that the maximum V2 (along X), M3 (along Y), V3 (along Y) occur at the ground level, while the peak of the M2 (along X) occurs at the floor level B. In addition it is observed that the time the peaks occur is approximately 5 seconds, when the maximum

displacement due to the L'aquila earthquake event is caused to the structure.

10.2 Conclusions on the Assessment of the Bearing Capacity of the Retrofitted Structure

- From the nonlinear static (pushover) and the nonlinear dynamic analyses, it is concluded that the building is satisfactory retrofitted to the performance level of life safety, since there is no hinge in columns or shear walls exceeding life safety limit state.
- The maximum displacement of the building is caused for the pushover analysis with modal distribution of lateral loads along the –Y axis (0.22m). In addition, the maximum number of hinges exceeding life safety limit state (43) is observed by this analysis. However as mentioned earlier there is no hinge exceeding life safety limit state in column or shear wall.
- The maximum inter-story drift ratio (1.3%) is caused by the pushover analyses along the Y axis with a modal distribution of lateral loads at floor levels B-C and C-D.

Chapter 11

Shear Resistance Checks

11.1 Check of Shear Resistance of Shear Walls

According to EN 1992-1 (2004), in regions of the member that $V_{Ed} \leq V_{Rd,c}$ no calculated shear reinforcement is necessary. V_{Ed} is the design shear force in the section considered resulting from external loading. In regions where $V_{Ed} > V_{Rd,c}$ sufficient shear reinforcement should be provided in order that $V_{Ed} \leq V_{Rd,c}$.

The design value for the shear resistance $V_{Rd,c}$ is given by:

$$V_{Rd,c} = \left[C_{Rd,c} k \left(100 \rho_1 f_{ck}\right)^{1/3} + k_1 \sigma_{cp} \right] b_w d \qquad (36)$$

With a minimum of

$$V_{Rd,c} = \left(v_{\min} + k_1 \sigma_{cp}\right) b_w d \qquad (37)$$

Where:

f_{ck} is in MPa

$k = 1 + \sqrt{\frac{200}{d}} \leq 2,0$ with d in mm (38) (EN 1992-1 ,2004)

$$\rho_1 = \frac{A_{sl}}{b_w d} \leq 0.02$$

A_{sl} is the area of the tensile reinforcement, which extends $\geq (l_{bd}+d)$ beyond the section considered

b_w is the smallest width of the cross-section in the tensile area (mm)

$\sigma_{cp} = N_{Ed}/A_C < 0.2\ f_{cd}$ [MPa]

N_{Ed} is the axial force in the cross-section due to loading ($N_{Ed} > 0$ for compression)

A_c is the area of concrete cross section (mm^2)

$V_{Rd,c}$ is [N]

The values of $C_{Rd,c}$, v_{min} and K_1 according to the Greek National Annex of EN 1992-1 are $0.18/\gamma_c$, given from $v_{min}=0.035\ k^{3/2}\ fck^{1/2}$, 0.15 respectively.

And γ_c is 1.5 for concrete, for persistent and transient design situations according to table 2.1N of EN 1992-1.

In the following table the check of shear resistance of the shear wall 7 is shown.

The maximum values of V_{Ed} obtained by the analyses are used.

Table 11.1 Check of Shear Resistance of Sheart Wall 7

$C_{Rd,c}$	0.12
f_{ck}(MPa)	20
d(mm)	3570
k	1.23
b_w(mm)	300
A_{sl} (mm^2)	2814.86
ρ_1	0.0026
N_{Ed} (N)	1661331
Ac (mm^2)	1080000
σ_{cp} (MPa)	1.538
K1	0.15
v_{min}	0.215
$V_{Rd,c}$ (KN)	521.952
V_{Ed} (KN)	302.615

It is shown that $V_{Ed} \leq V_{Rd,c}$ for shear wall 7, so the shear wall resistance to shear forces is adequate and shear reinforcement is not required. According to the

same procedures the checks are performed for all the shear walls and the results are shown in table 9.2.

Table 11.2 Results of Checks of Shear Resistance of Shear Walls

Shear Walls	V_{Ed} (KN)	$V_{Rd,c}$ (KN)	V_{Rd} (KN) (When Shear Reinforcement is Required)
Shear Wall 1	668.05	508.73	842.65
Shear Wall 2	1001.40	558.17	1019.54
Shear Wall 3	514.44	582.74	
Shear Wall 4	817.13	689.99	1019.54
Shear Wall 5	163.27	304.80	
Shear Wall 6	225.18	391.92	
Shear Wall 7	302.62	521.95	

11.2 Check of Shear Resistance of Existing Members

According to EN 1998-3 (2005), the cyclic shear resistance, V_R, decreases with the plastic part of ductility demand, expressed in terms of ductility factor of the transverse deflection of the shear span of the chord rotation at member end: $\mu_\Delta^{pl}=\mu_\Delta-1$. For this purpose μ_Δ^{pl} may be calculated as the ratio the plastic part of the chord rotation, θ, normalized to the chord rotation at yielding, θ_y, calculated as described in section 6.2

The following expression may be used for the shear strength, as controlled by the stirrups, accounting for the above reduction (units: MN and meters):

$$V_R = \frac{1}{\gamma_{el}}\left[\frac{h-x}{2L_v}\min\left(N;0.55A_c f_c\right)+\left(1-0.05\min\left(5;\mu_\Delta{}^{pl}\right)\right)\left[0.16\max\left(0.5;100\rho_{tot}\right)\left(1-0.16\min\left(5;\frac{L_v}{h}\right)\right)\sqrt{f_c}A_c+V_W\right]\right]$$

(39) (EN 1998-3, 2005)

where:

γ_{el}=1.15 for primary seismic elements and 1 for secondary,

h is the depth of the cross-section,

x is the compression zone depth,

N is the compressive axial force (positive, taken being zero for tension)

L_v =M/V is the ratio moment/shear at the end section

A_c is the cross-section area, taken as being equal to $b_w d$ for a cross-section with a rectangular web of width (thickness) b_w and structural depth d,

f_c is the concrete compressive strength (should further be divided by the partial factor for concrete in accordance with EN1998-1:2004, 5.2.4,

Ptot is the total longitudinal reinforcement ratio,

V_w is the contribution of transverse reinforcement to shear resistance, taken as being equal to: (for cross-sections with rectangular web of width (thickness) b_w)

$$V_W = \rho_W b_W z f_{yW} \qquad (40) \quad \text{(EN 1998-3, 2005)}$$

Where:

ρ_w is the transverse reinforcement ratio,

z is the length of the internal level arm

f_{yw} is the yield stress of the transverse reinforcement (for primary seismic elements should further be divided by the partial factor for steel in accordance with EN 1998-1:2004, 5.2.4.

The shear resistance of the column C10 is checked according to the procedure described above. The column C10 is chosen because it is one of the columns that concrete jacket is not applied. The shear resistance is checked in two parts of the column, in the ground floor level, where the maximum shear forces are

observed-but no plastic deformation occurs, and in the floor level C-where plastic hinge in the life safety limit state is formed.

C10 at the ground floor: 0.45X0.45 4Φ20+4Φ16

C10 at floor level C: 0.3X0.3 4Φ16

Table 11.3 Shear check of the column C10 (no jacket is applied)

	Column C10 at the Ground Floor Level	Column C10 at the Floor C Level
γ_{el}	1.15	1.15
h (m)	0.45	0.3
N (MN)	0.71445	0.33096
L_v (M/V)	1.708	1.6
A_c (m^2)	0.1935	0.084
f_c (MPa)	16.667	16.667
Ptot	0.0106506	0.0095744
r_w	0.0005195	0.0011968
b_w (m)	0.45	0.3
z (m)	0.41	0.28
f_{yW} (MPa)	220	220
V_w (MN)	0.02108	0.00221
V_w (KN)	21.088	22.117
V_R (MN)	0.1052161	0.034765
V_R (KN)	105.216	34.764
V_{Ed} (KN)	87.93	31.24

The shear resistance is adequate in both cases, since $V_{Ed} < V_R$

Chapter 12

Retrofitted and Non-retrofitted Building Comparison

The results of the modal analyses of the retrofitted and the non-retrofitted building are compared, when both the secant stiffness and the values of stiffness of the table 4.1 are used.

The results of the nonlinear static analyses, including the pushover curves, the hinges' limit state results, the maximum absolute displacements and the inter-storey drift ratios, between the retrofitted building and the non retrofitted building are compared.

In addition, the corresponding results of the nonlinear dynamic analyses and the forces on the column C20 between the retrofitted and the non-retrofitted building are compared.

12.1 Modal Analyses Comparison

Stiffness proposed in table 4.1:

Non-Retrofitted:

Table 12.1 Modal Participating Mass Ratios of the Non-Retrofitted Structure using the Stiffness proposed in Table 4.1 of KANEPE

StepType	StepNum	Period	UX	UY	UZ	RX	RY	RZ
Text	Unitless	Sec	Unitless	Unitless	Unitless	Unitless	Unitless	Unitless
Mode	1	1.627333	0.29517	0.09153	4.532E-08	0.0656	0.16849	0.12517
Mode	2	1.404784	0.04641	0.42273	0.00000577	0.3073	0.02621	0.04552
Mode	3	1.141874	0.18555	0.00345	4.679E-08	0.00213	0.1039	0.32066

Retrofitted:

Table 12.2 Modal Participating Mass Ratios of the Retrofitted Structure using the Stiffness proposed in Table 4.1 of KANEPE

StepType	StepNum	Period	UX	UY	UZ	RX	RY	RZ
Text	Unitless	Sec	Unitless	Unitless	Unitless	Unitless	Unitless	Unitless
Mode	1	0.789987	0.07806	0.4583	1.444E-06	0.30989	0.04359	0.00086
Mode	2	0.698112	0.33722	0.05088	3.246E-06	0.03324	0.20011	0.12206
Mode	3	0.551747	0.11497	0.02705	7.199E-06	0.02199	0.06177	0.38467

Secant Stiffness:

Non-Retrofitted:

Table 12.3 Modal Participating Mass Ratios of the Non-Retrofitted Structure using the Secant Stiffness

StepType	StepNum	Period	UX	UY	UZ	RX	RY	RZ
Text	Unitless	Sec	Unitless	Unitless	Unitless	Unitless	Unitless	Unitless
Mode	1	2.639646	0.32636	0.08261	4.702E-08	0.06237	0.19121	0.09604
Mode	2	2.368858	0.05254	0.42026	0.000006131	0.31761	0.03047	0.03167
Mode	3	1.942065	0.13775	0.0017	0.000001648	0.00139	0.0805	0.35319

Retrofitted:

Table 12.4 Modal Participating Mass Ratios of the Retrofitted Structure using the Secant Stiffness

StepType	StepNum	Period	UX	UY	UZ	RX	RY	RZ
Text	Unitless	Sec	Unitless	Unitless	Unitless	Unitless	Unitless	Unitless
Mode	1	1.265863	0.13965	0.39769	9.152E-07	0.26175	0.07473	0.00013
Mode	2	1.117586	0.33231	0.11996	2.116E-06	0.07892	0.18677	0.06803
Mode	3	0.936403	0.05646	0.01853	1.595E-06	0.01362	0.03049	0.45089

- It is observed that either the secant stiffness is used, or the stiffness proposed by the table 4.1, the periods are significantly reduced when the building is retrofitted.
- The fundamental periods of the structure when secant stiffness is used, are much higher (approximately 1 sec for the non-retrofitted and 0.5 sec for the retrofitted) than when the stiffness proposed by the table 4.1 of KANEPE is used, for both the retrofitted and the non-retrofitted building, indicating that the secant stiffness, leads to much more flexible structures.
- The highest mass participating ratio of the fundamental period T_1, of the non-retrofitted building, when both secant and the stiffness of the table 4.1 are used, is along axis X. The corresponding mass participating ratio of the retrofitted building is along axis Y.

12.2 Pushover Analyses

12.2.1 Comparison of the Capacity Curves of the Non-Retrofitted and the Retrofitted Building

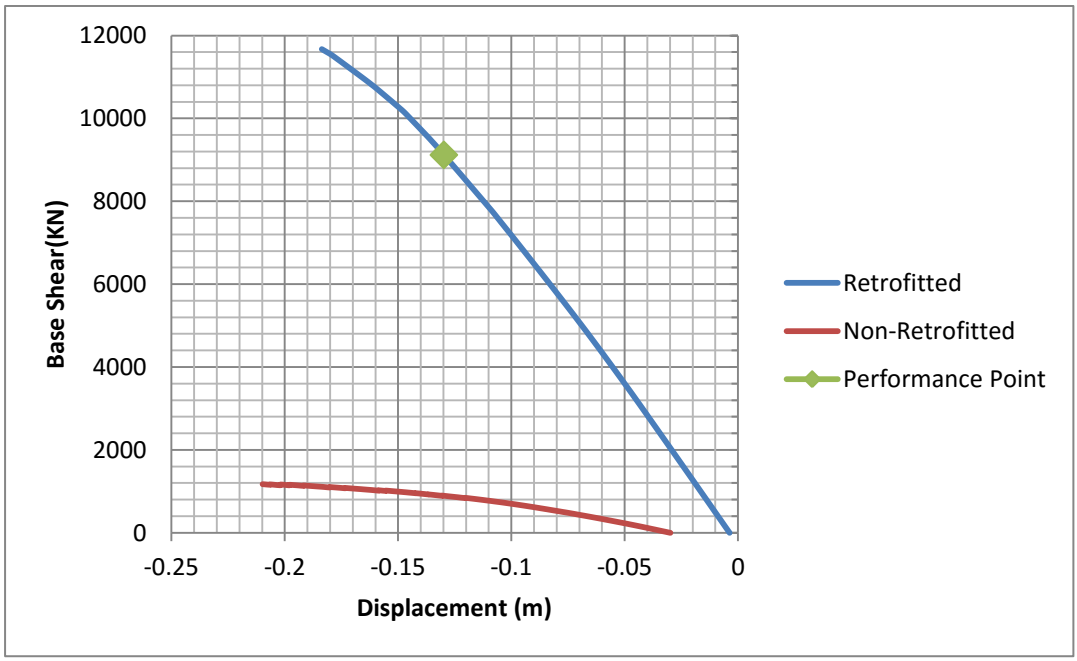

Figure 12.1 Pushover Analysis-Uniform Distribution of Lateral Loads along +X Axis

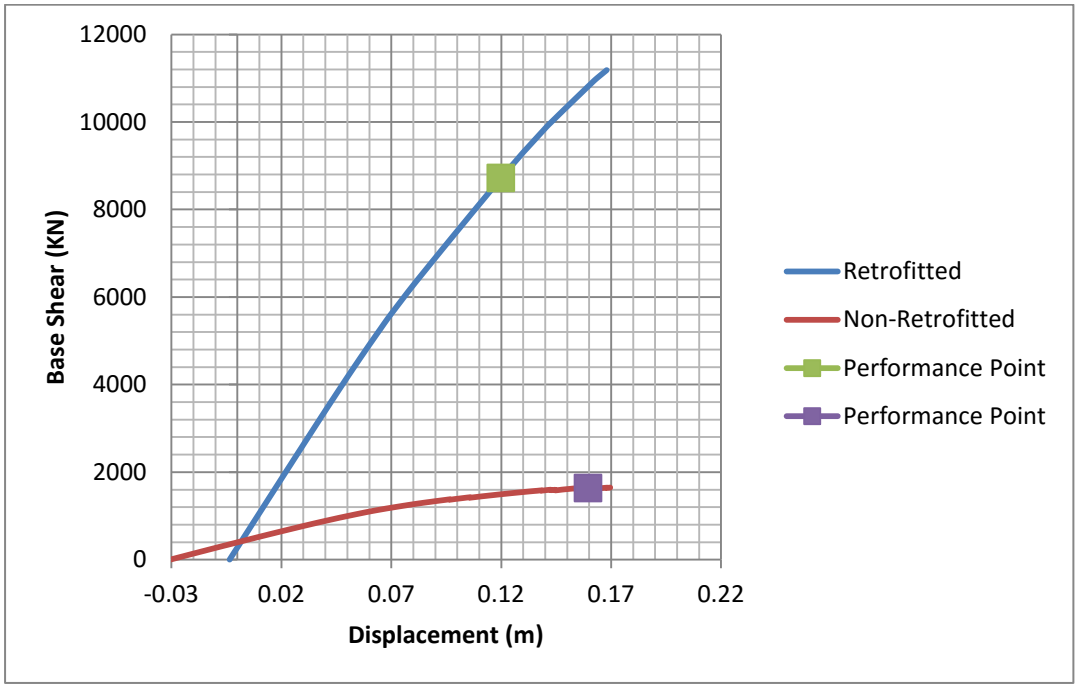

Figure 12.2 Pushover Analysis-Uniform Distribution of Lateral Loads along -X Axis

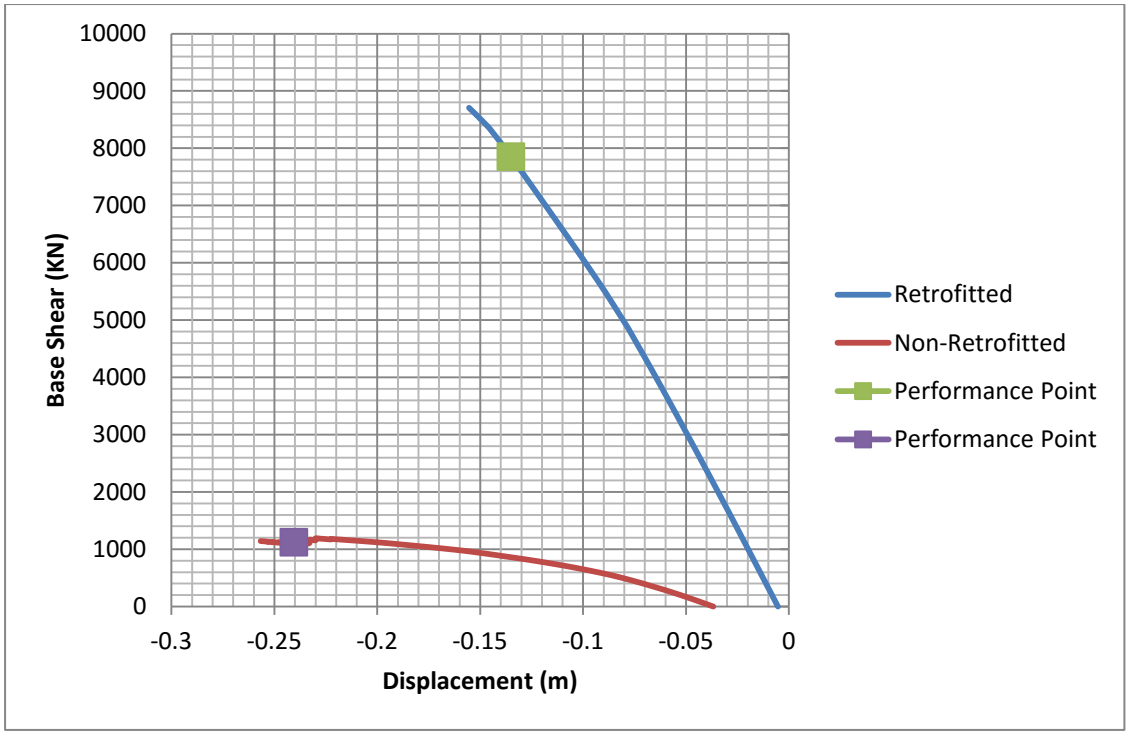

Figure 12.3 Pushover Analysis-Uniform Distribution of Lateral Loads along +Y Axis

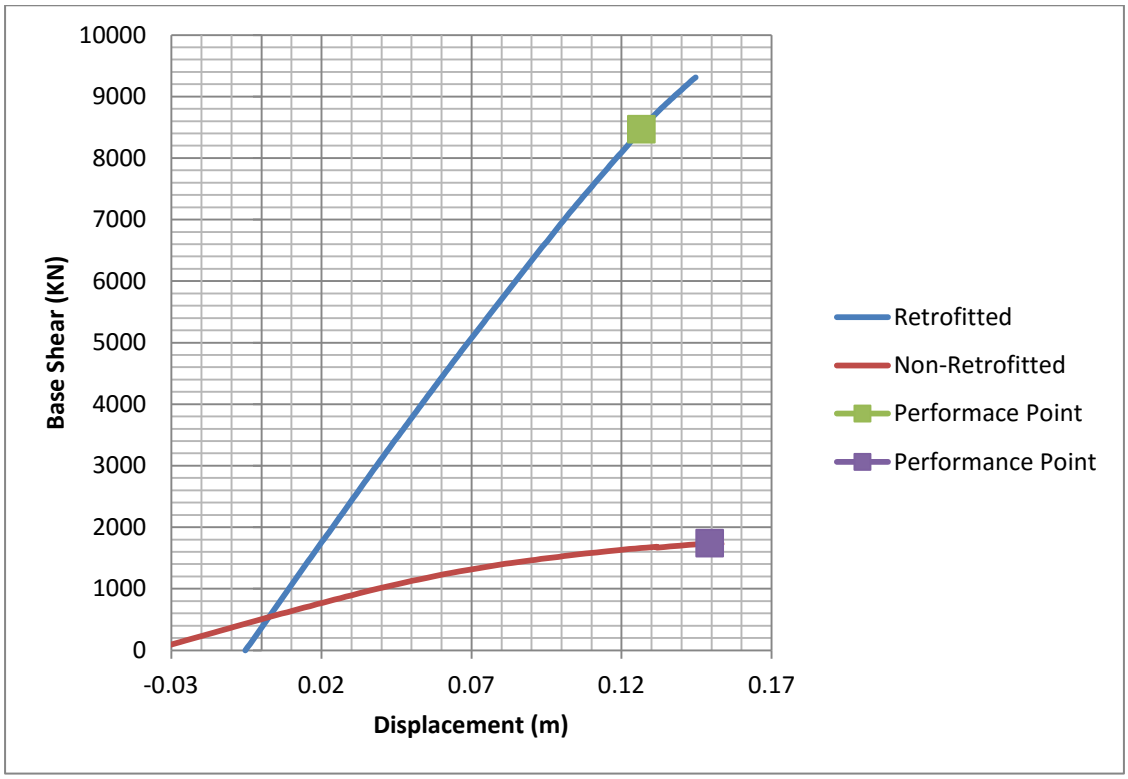

Figure 12.4 Pushover Analysis-Uniform Distribution of Lateral Loads along -Y Axis

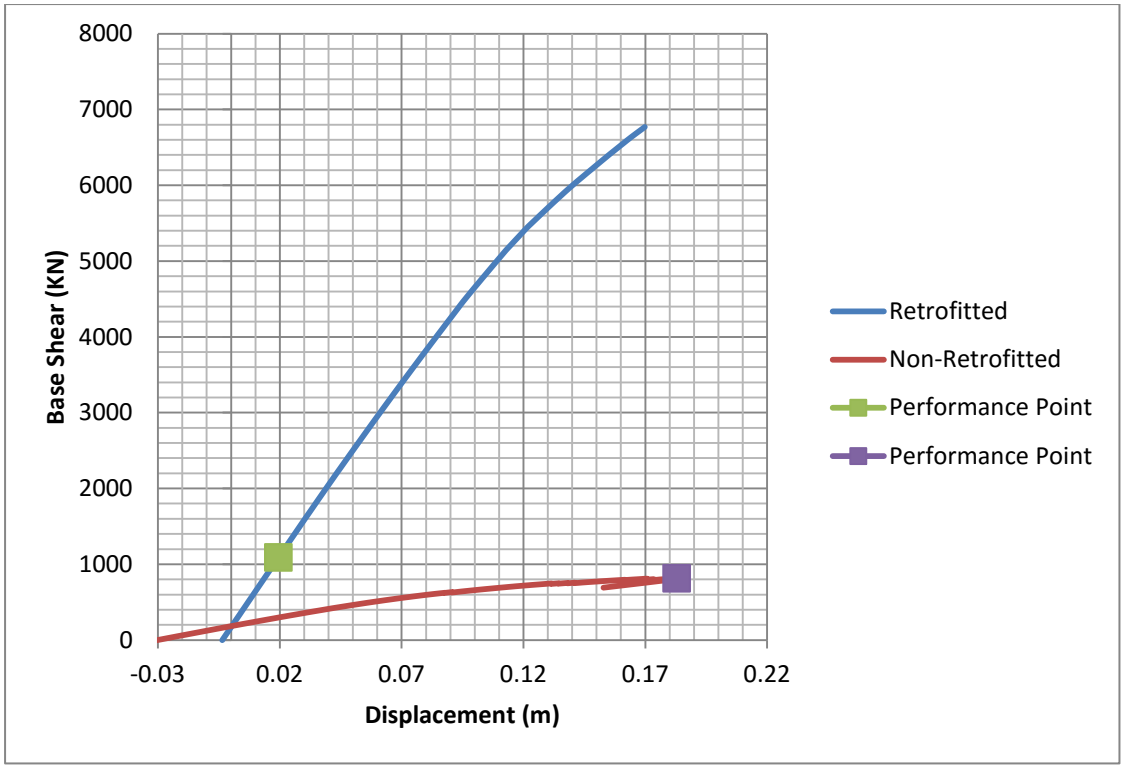

Figure 12.5 Pushover Analysis-Modal Distribution of Lateral Loads along +X Axis

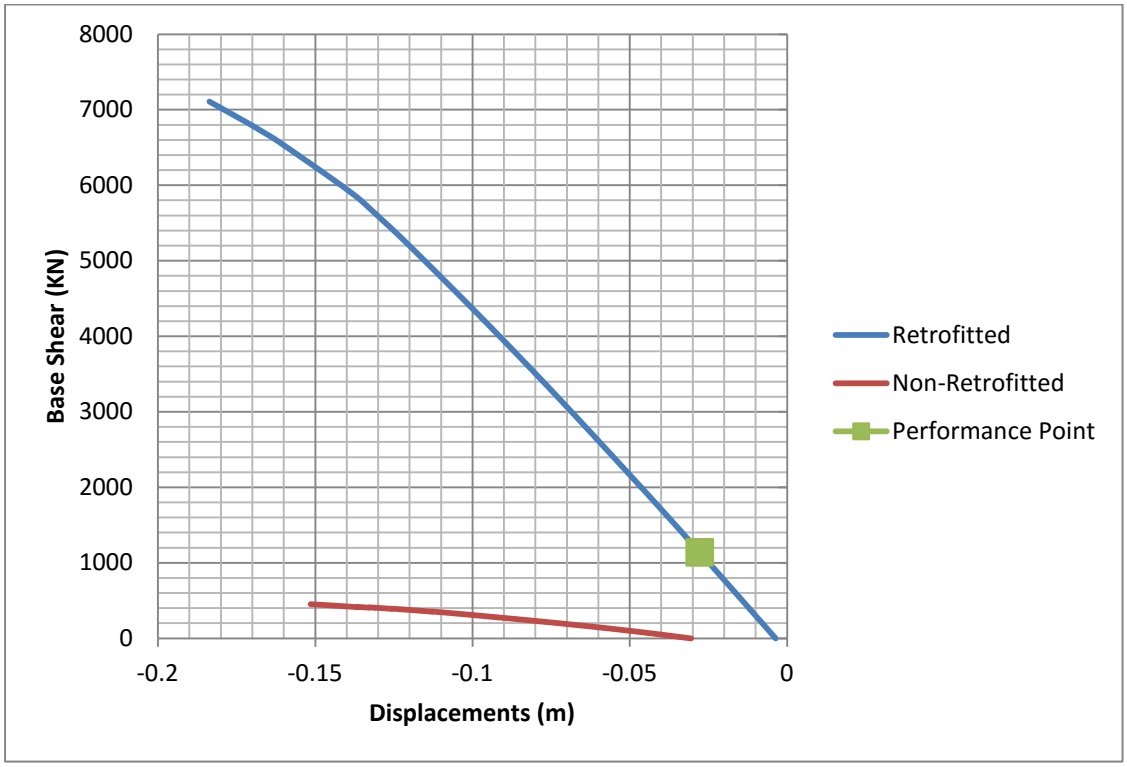

Figure 12.6 Pushover Analysis-Modal Distribution of Lateral Loads along -X Axis

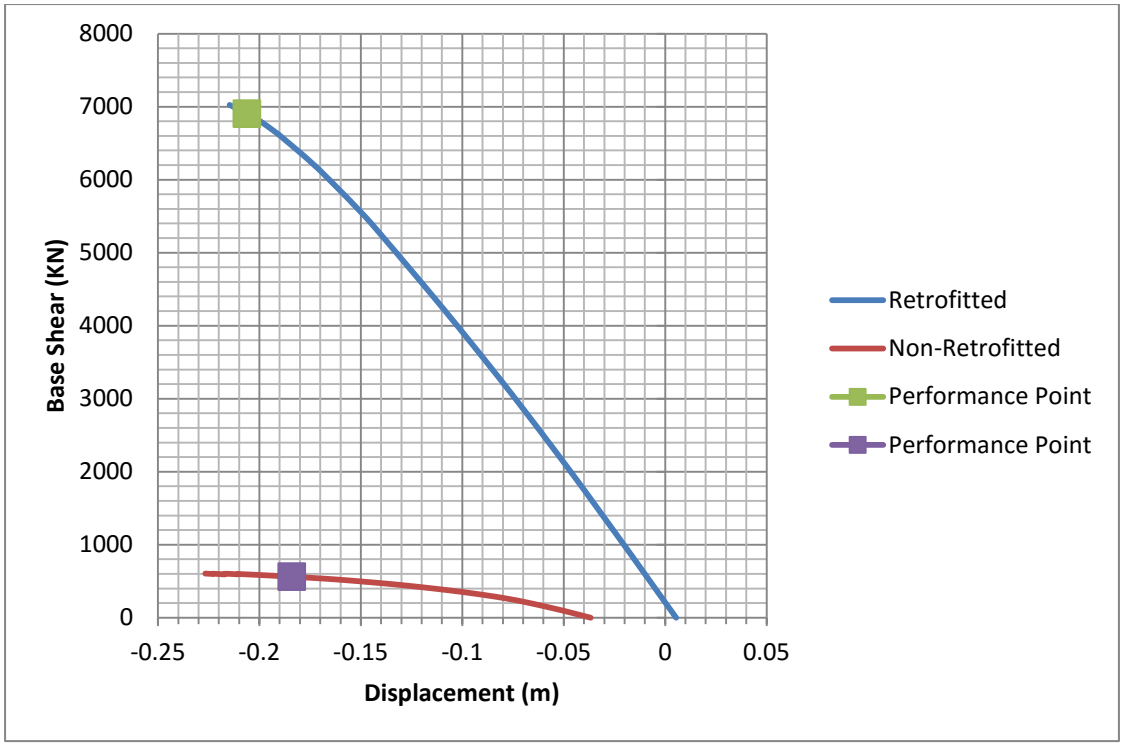

Figure 12.7 Pushover Analysis-Modal Distribution of Lateral Loads along +Y Axis

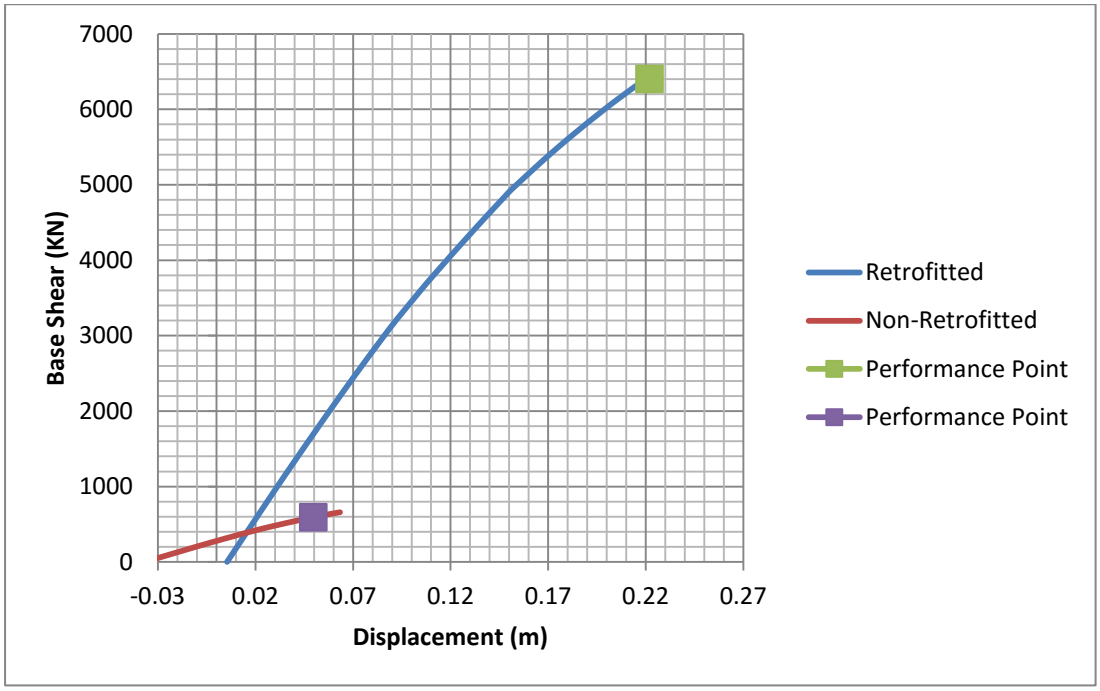

Figure 12.8 Pushover Analysis-Modal Distribution of Lateral Loads along -Y Axis

From the comparison of the pushover curves of the non-retrofitted and the retrofitted building, it is obvious that the capacity and the ductility of the retrofitted building are much higher.

12.2.2 Hinges Limit States Results

Hinges Results	
Retrofitted Building	**Non Retrofitted Building**
• None of the hinges that exceed the limit state of life safety is formed in column or shear wall. • Hinges that exceed life safety limit state do not exceed collapse prevention limit state. None of the hinges exceeds collapse prevention limit state. • The pushover analysis with a modal distribution of lateral loads along –Y formed 43 hinges between the limit states life safety and collapse prevention (all beam-hinges).	• According to every one of the pushover analyses results, hinges that exceed life safety limit state are formed in columns. • The columns C11 and C18 face significant strength degradation. • Many hinges that exceed limit state E are formed in beams. • The most severe damages are concentrated in the West, South-West and South side of the building, in floor levels A and B. • The pushover analyses with a modal distribution of lateral loads along –X and a uniform distribution along +X cannot reach a performance point, due to significant strength loss and damage. • The pushover analyses with a modal distribution of lateral loads along +X and a uniform distribution along +X form 9 hinges beyond E.

12.2.3 Maximum Absolute Displacements Comparison

- The higher the floor level under consideration, the higher the maximum absolute displacements.
- It is observed that the maximum absolute displacements of the retrofitted building are always lower than of the non-retrofitted (except in the case of modal distribution of lateral loads along U2(Y axis)).
- The maximum absolute displacements of the top, both for the retrofitted and the non retrofitted building are observed along U2. For the retrofitted building it is caused by a modal lateral load distribution, while for the non-retrofitted it is caused by a uniform lateral load distribution.
- Along the U1(X axis), the maximum absolute displacements of the retrofitted building are much lower than the non-retrofitted for both the uniform and modal lateral loads distribution, for all the floor levels.

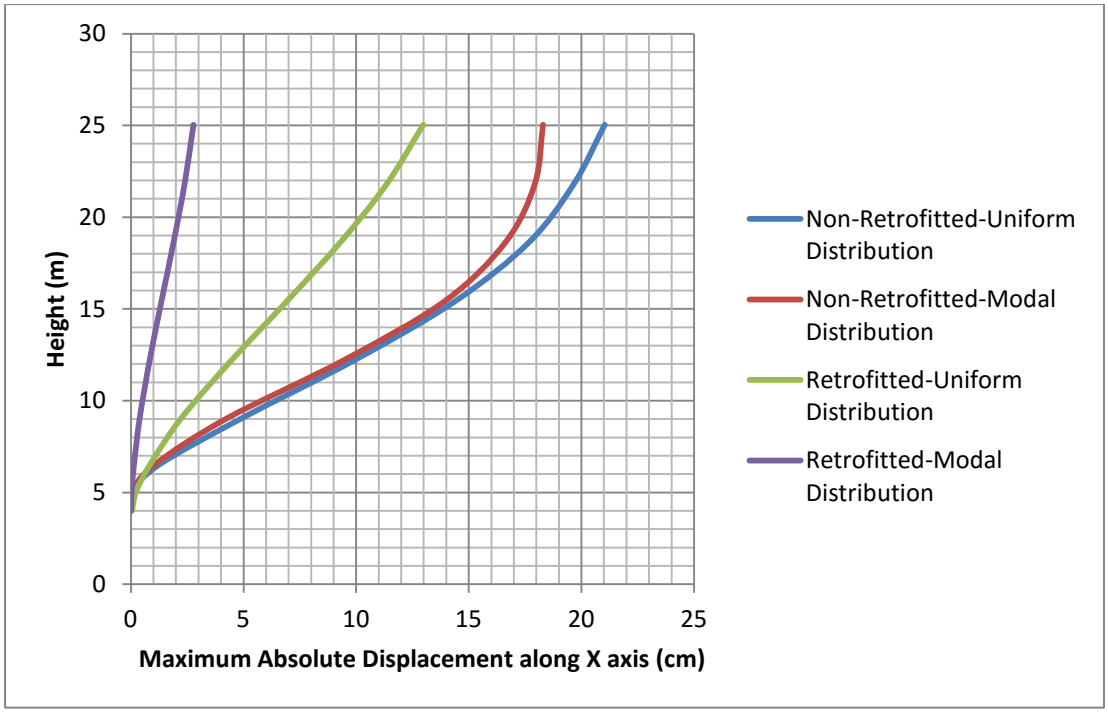

Figure 12.9 Maximum Absolute Displacements along X axis for Uniform and Modal Distribution of Lateral Loads for the Non-Retrofitted and the Retrofitted Building

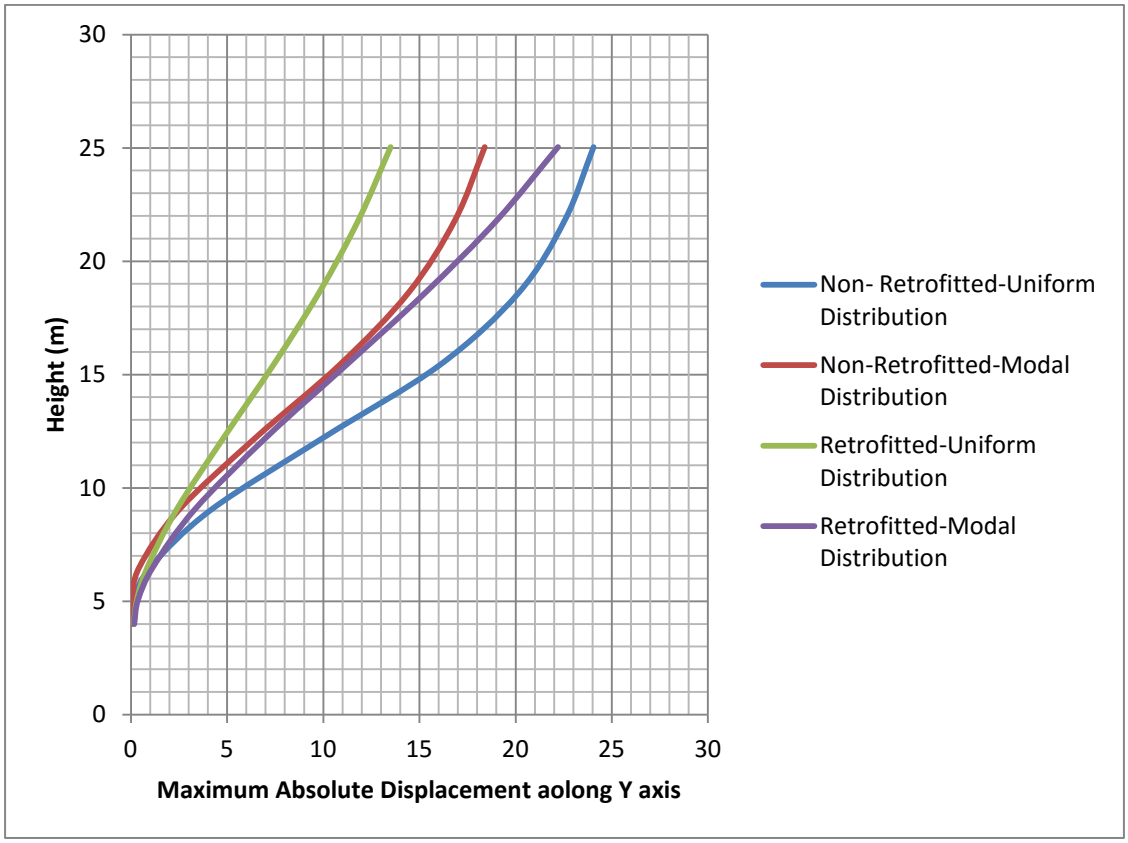

Figure 12.10 Maximum Absolute Displacements along Y axis for Uniform and Modal Distribution of Lateral Loads for the Non-Retrofitted and the Retrofitted Building

12.2.4 Inter-Storey Drift Ratios Comparison

- The maximum inter-storey drift ratios of the non retrofitted building are too high, much higher than the permitted values.
- The inter-storey drift ratios of the retrofitted building are significant lower (except for the pushover analysis with a modal distribution of lateral loads along U2), than those of the non-retrofitted.
- The maximum inter-story drift ratios are observed at the floor levels A-B-C of the non-retrofitted building and at the floor levels B-C-D of the retrofitted. In general the ratios are higher around at mid heights of the building, than they are at the top and at the bottom.
- The highest ratios are observed along the Y axis for both the non-retrofitted and the retrofitted building.

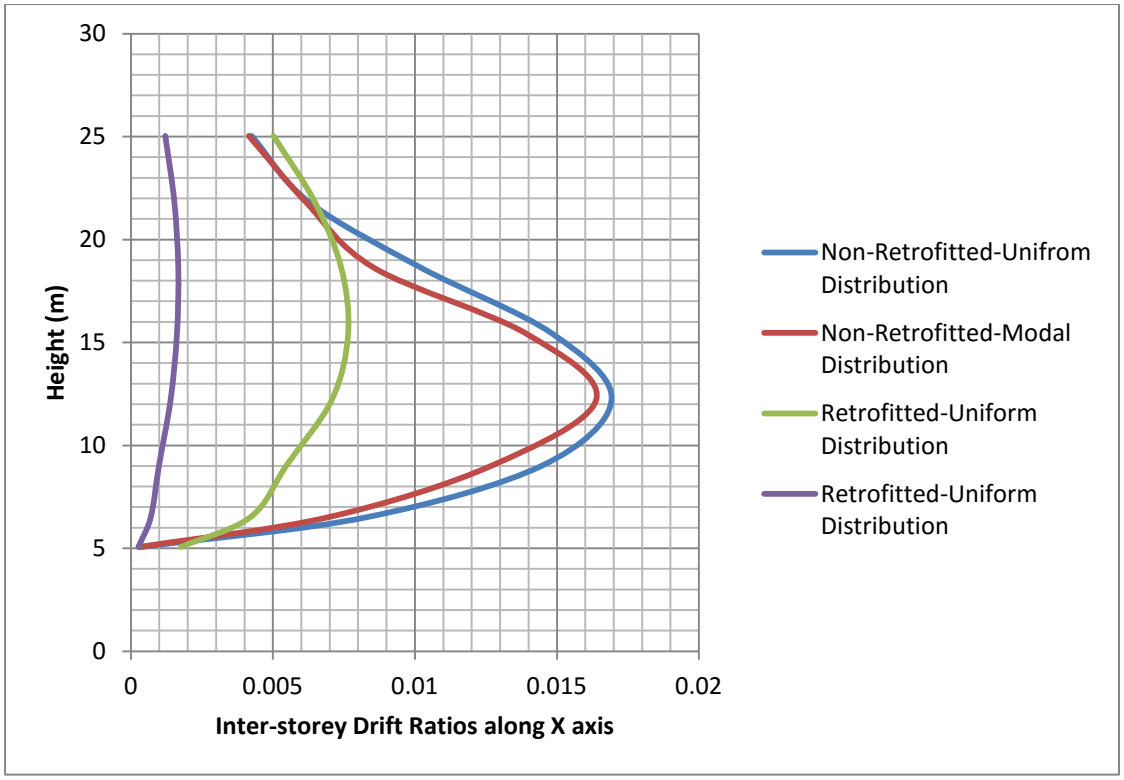

Figure 12.11 Inter-Storey Drift Ratios along X axis for Uniform and Modal Distribution of Lateral Loads for the Non-Retrofitted and the Retrofitted Building

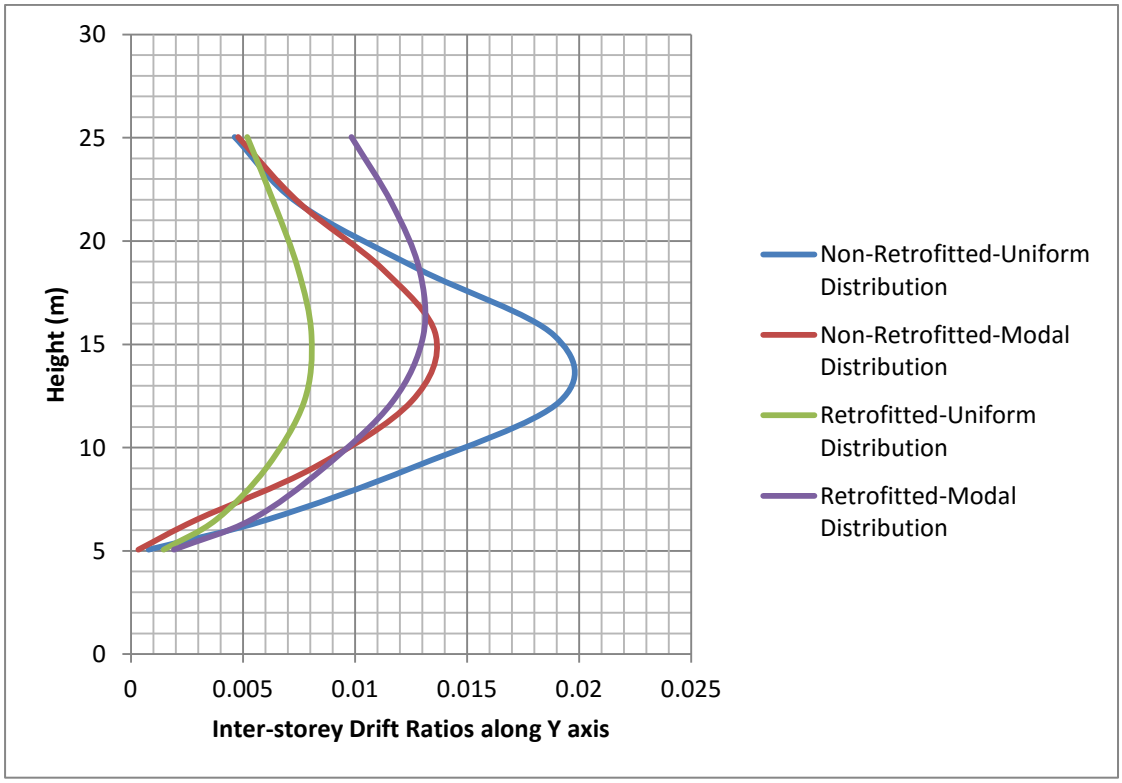

Figure 12.12 Inter-Storey Drift Ratios along Y axis for Uniform and Modal Distribution of Lateral Loads for the Non-Retrofitted and the Retrofitted Building

12.3 Nonlinear Time-History Dynamic Analyses

12.3.1 Hinges Limit States

Hinges Results	
Retrofitted Building	**Non Retrofitted Building**
• No hinge in column or shear wall exceeds life safety limit state.	• Hinges exceeding life safety limit state are caused by all the earthquake events imposed to the structure and for each one of the combinations of the seismic forces. • There are 6 columns whose hinges exceed limit state E due to Corinth earthquake event and 7 columns due to L'Aquila. In addition many beam-hinges beyond E are caused by both earthquakes. Probably the building is collapsed.

12.3.2 Comparison of the Maximum Absolute Displacements of the Non-Retrofitted and the Retrofitted Building due to the Earthquake events: L'Aquila, Corinth, Kalamata

- The displacements of the retrofitted building are significantly lower than those of the non-retrofitted (especially along the X axis).
- Both the retrofitted and the non-retrofitted face larger displacements along the X axis than along the Y axis.
- The maximum absolute displacements of the retrofitted building are caused by the L'Aquila earthquake event and those of the non-retrofitted by the Corinth earthquake event.
- The lower maximum absolute displacements of the non-retrofitted are caused by the L'aquila earthquake event for both the X and Y axis. The lower maximum absolute displacements of the retrofitted are caused by the Kalamata and Corinth along the X axis, and by Corinth along the Y axis.

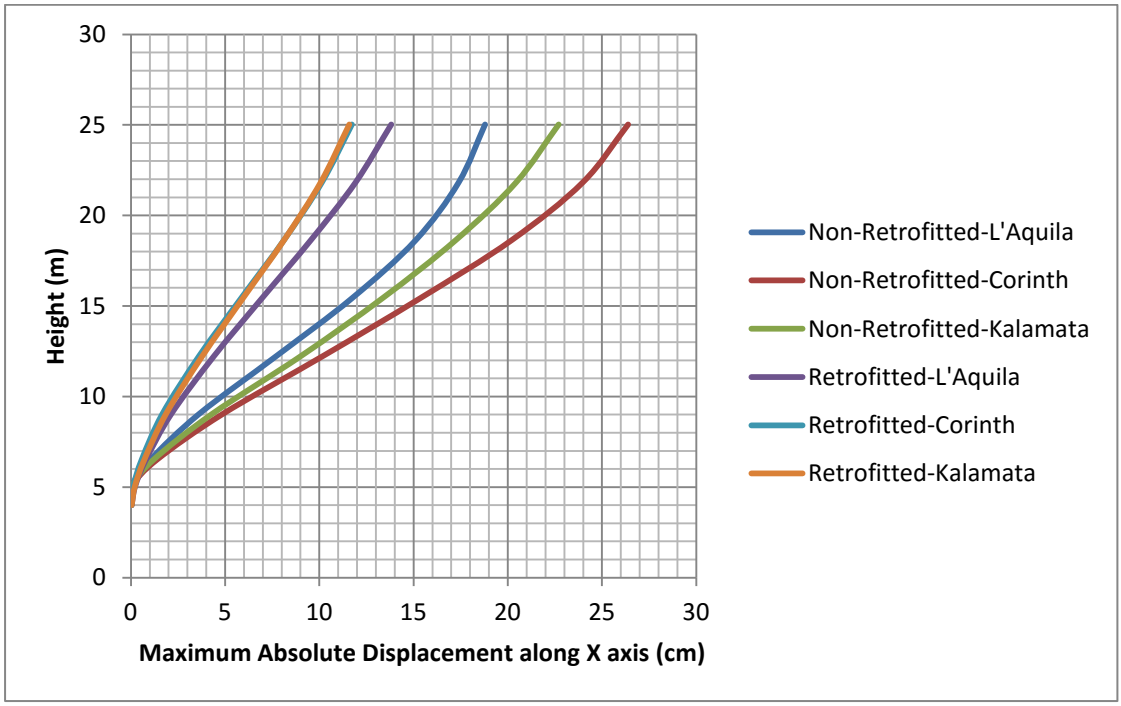

Figure 12.13 Maximum Absolute Displacements along X axis of the Non-Retrofitted and the Retrofitted Building due to the Earthquake events: L'Aquila, Corinth, Kalamata

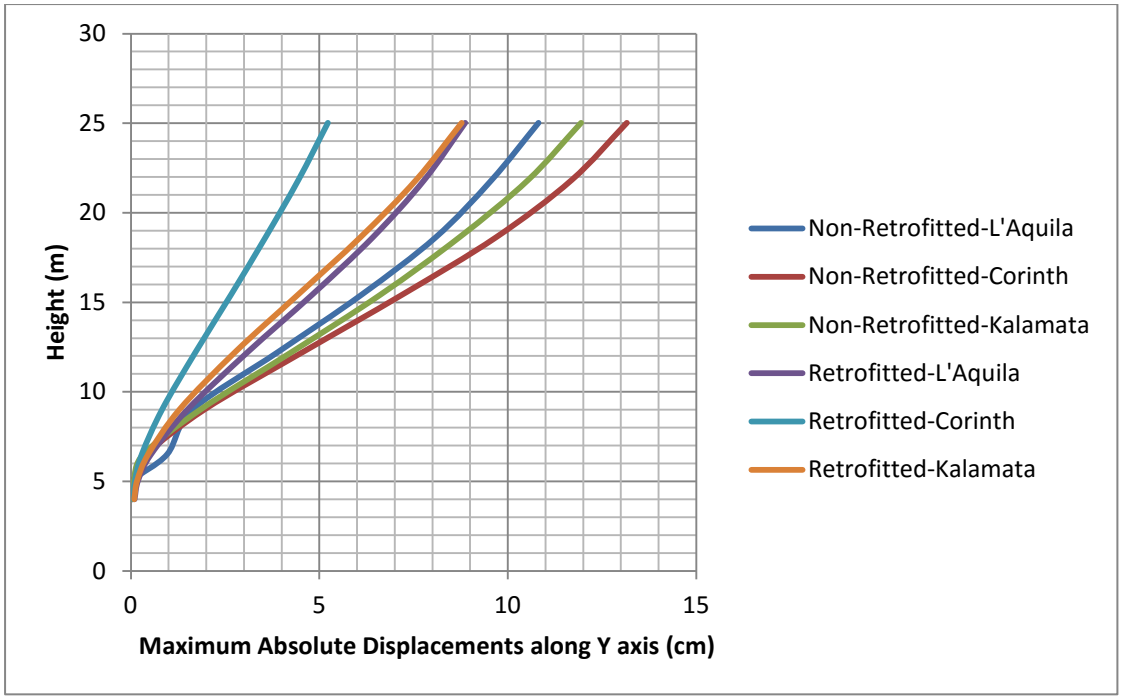

Figure 12.14 Maximum Absolute Displacements along Y axis of the Non-Retrofitted and the Retrofitted Building due to the Earthquake events: L'Aquila, Corinth, Kalamata

12.3.3 Comparison of the Inter-storey Drift Ratios of the of the Non-Retrofitted and the Retrofitted Building due to the Earthquake events: L'Aquila, Corinth, Kalamata

- The inter-story drift ratios of the retrofitted building are lower than those of the non-retrofitted, for both X and Y axes. The ratios are corresponding to the maximum displacements.
- The maximum inter-story drift ratios of the non-retrofitted are observed at the floor levels A-B-C-D, while those of the retrofitted are observed at the floor levels B-C-D.
- Both the retrofitted and the non-retrofitted face higher inter-story drift ratios at the mid heights of the building than at the top and bottom.
- The highest inter-storey drift ratio of the non-retrofitted building is given by the Corinth earthquake event, while the highest of the retrofitted is given by L'Aquila earthquake events for both X and Y axes.

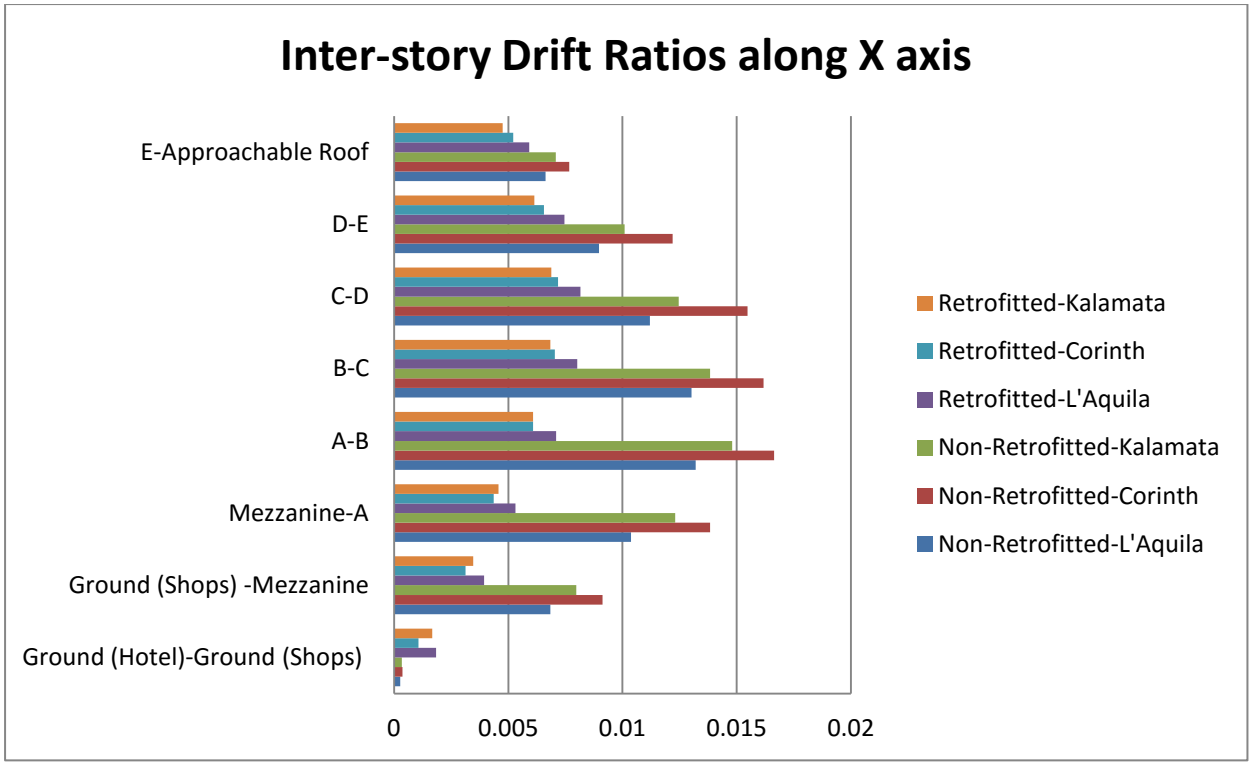

Figure 12.15 Inter-Storey Drift Ratios along X axis for the Non-Retrofitted and the Retrofitted Building due to the Earthquake events: L'Aquila, Corinth, Kalamata

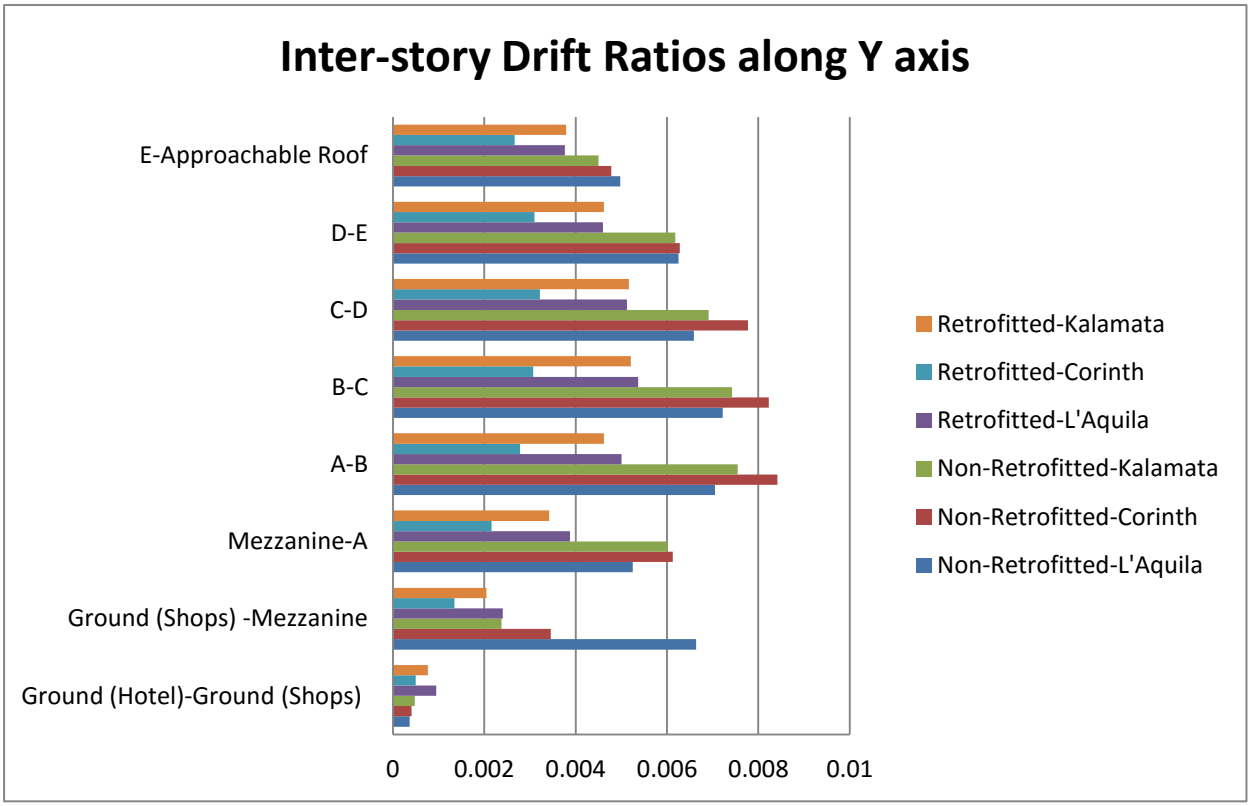

Figure 12.16 Inter-Storey Drift Ratios along Y axis for the Non-Retrofitted and the Retrofitted Building due to the Earthquake events: L'Aquila, Corinth, Kalamata

12.3.4 Comparison of the Maximum Forces along the Column C20 of the Retrofitted and the Non-Retrofitted Building (L'Aquila Earthquake Event)

It can be seen from the following figures that in some cases (excepting the extremely high values observed) the envelope of the forces of the retrofitted column is higher than the corresponding forces of the non-retrofitted (especially along X axis above mezzanine floor level).

On the one hand the seismic action imposed in the building remains the same, on the other hand the stiffness of the retrofitted element is increased, thus it takes higher forces. However, not only the stiffness, but also the strength of the element is increased, thus it is able to sustain the higher forces.

The extremely high values of the forces of the non-retrofitted element are obtained when a plastic hinge is being formed. Probably the hinges of neighboring elements are unloading, so the redistribution of forces inside the structure cause extremely high values of bending moments and shear forces within column C20.

The higher strength and ductility of the retrofitted structure ensures that hinges remain in the elastic area or they get into plastic in lower-acceptable levels. As a result the extremely high values of the non-retrofitted building are not observed for the retrofitted.

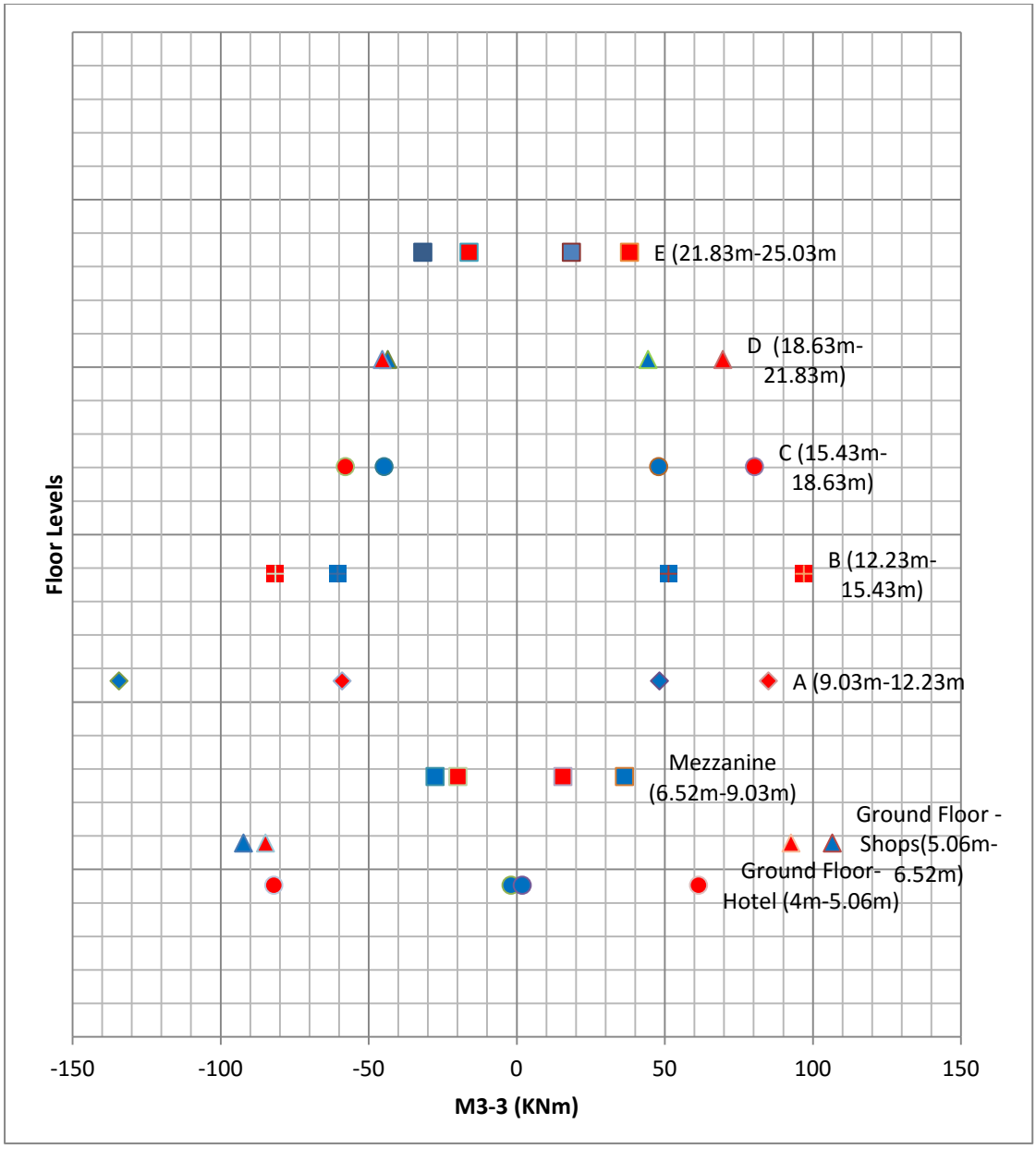

Figure 12.17 Envelope of the Bending Moments of Column C20 along Axis X (M3-3) per Floor Level of the Non-Retrofitted (blue) and the Retrofitted (red) Building

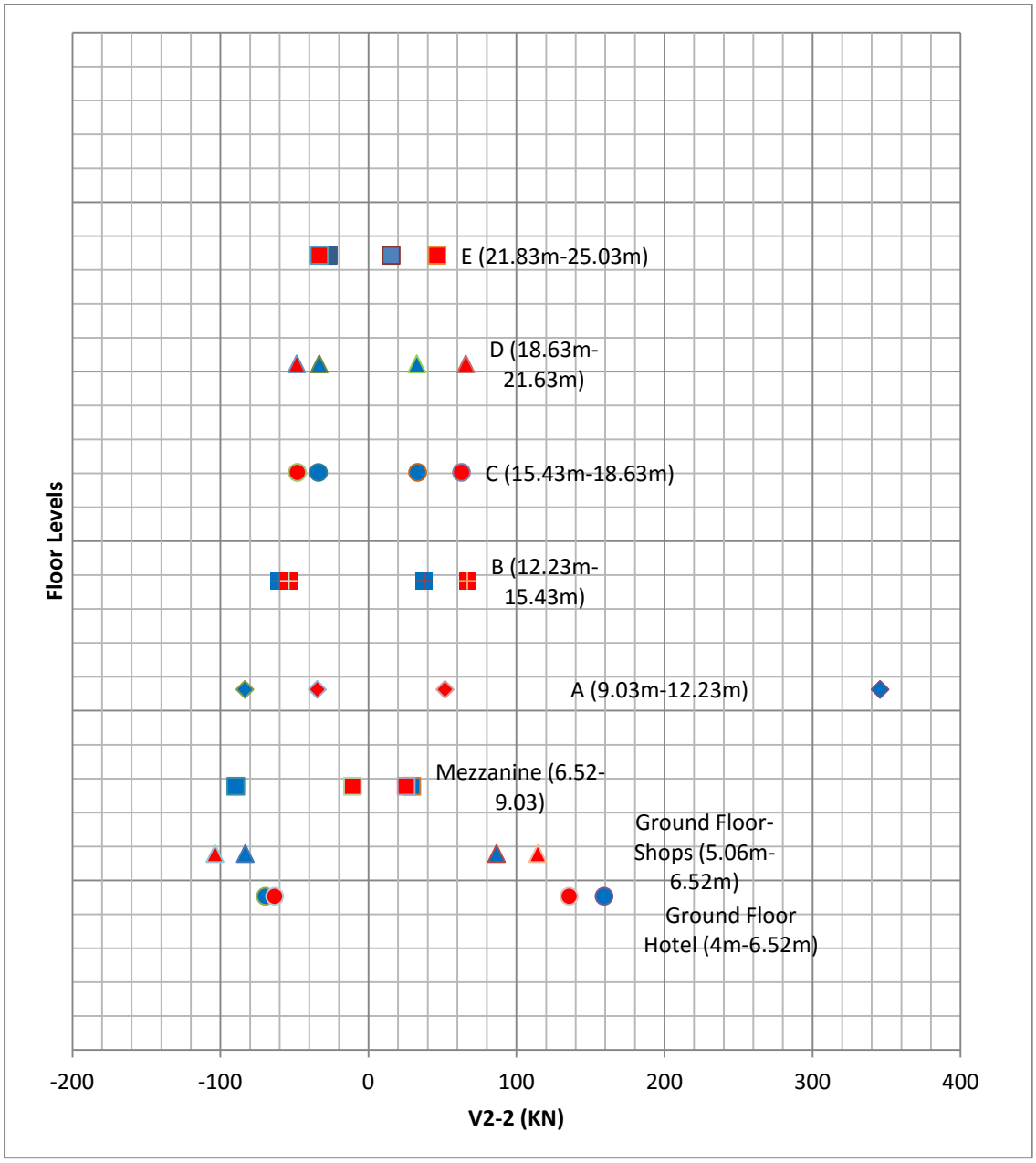

Figure 12.18 Envelope of the Shear Forces of Column C20 along Axis X (V2-2) per Floor Level of the Non-Retrofitted (blue) and the Retrofitted (red) Building

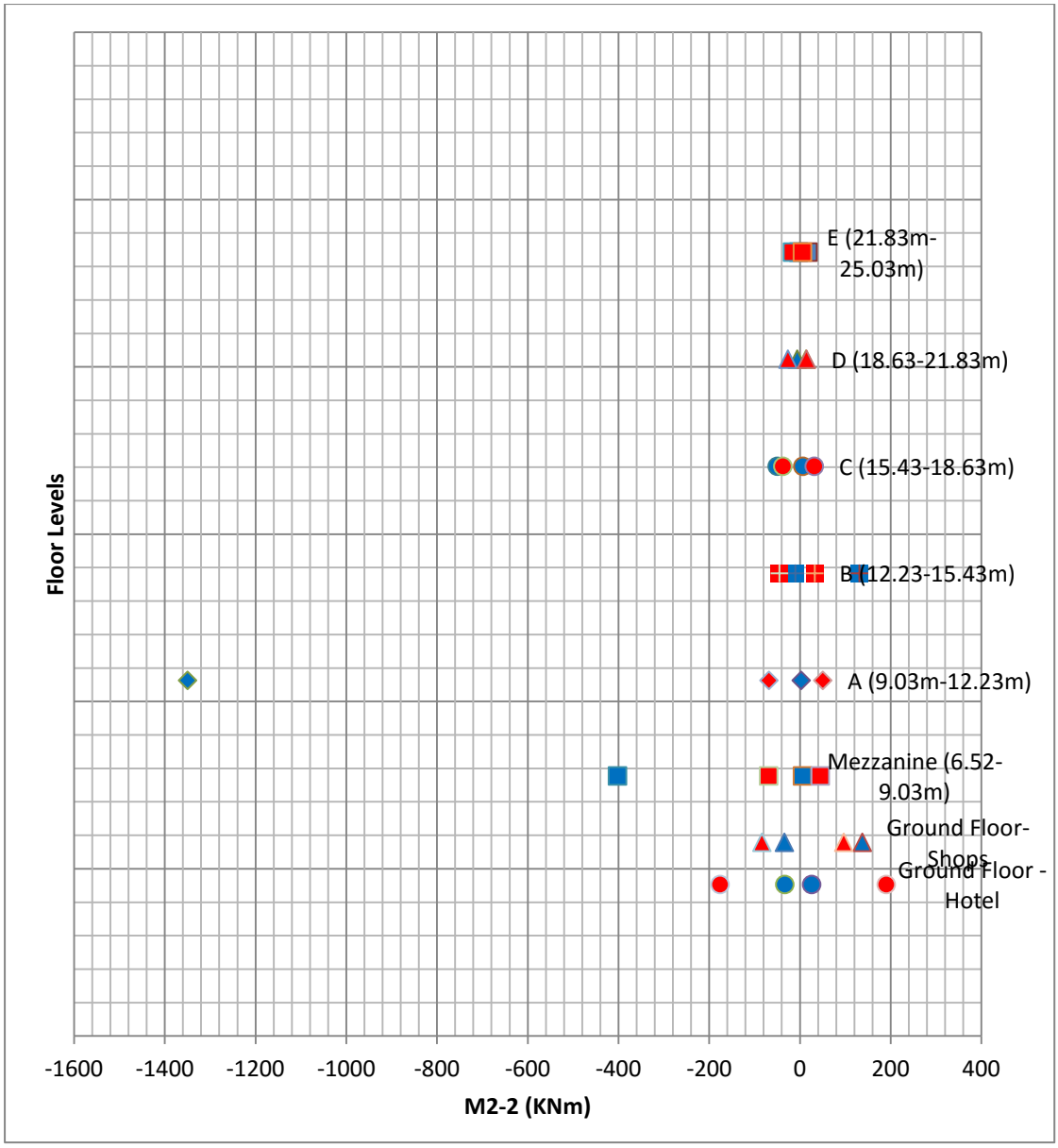

Figure 12.19 Envelope of the Bending Moments of Column C20 along Axis Y (M2-2) per Floor Level of the Non-Retrofitted (blue) and the Retrofitted (red) Building

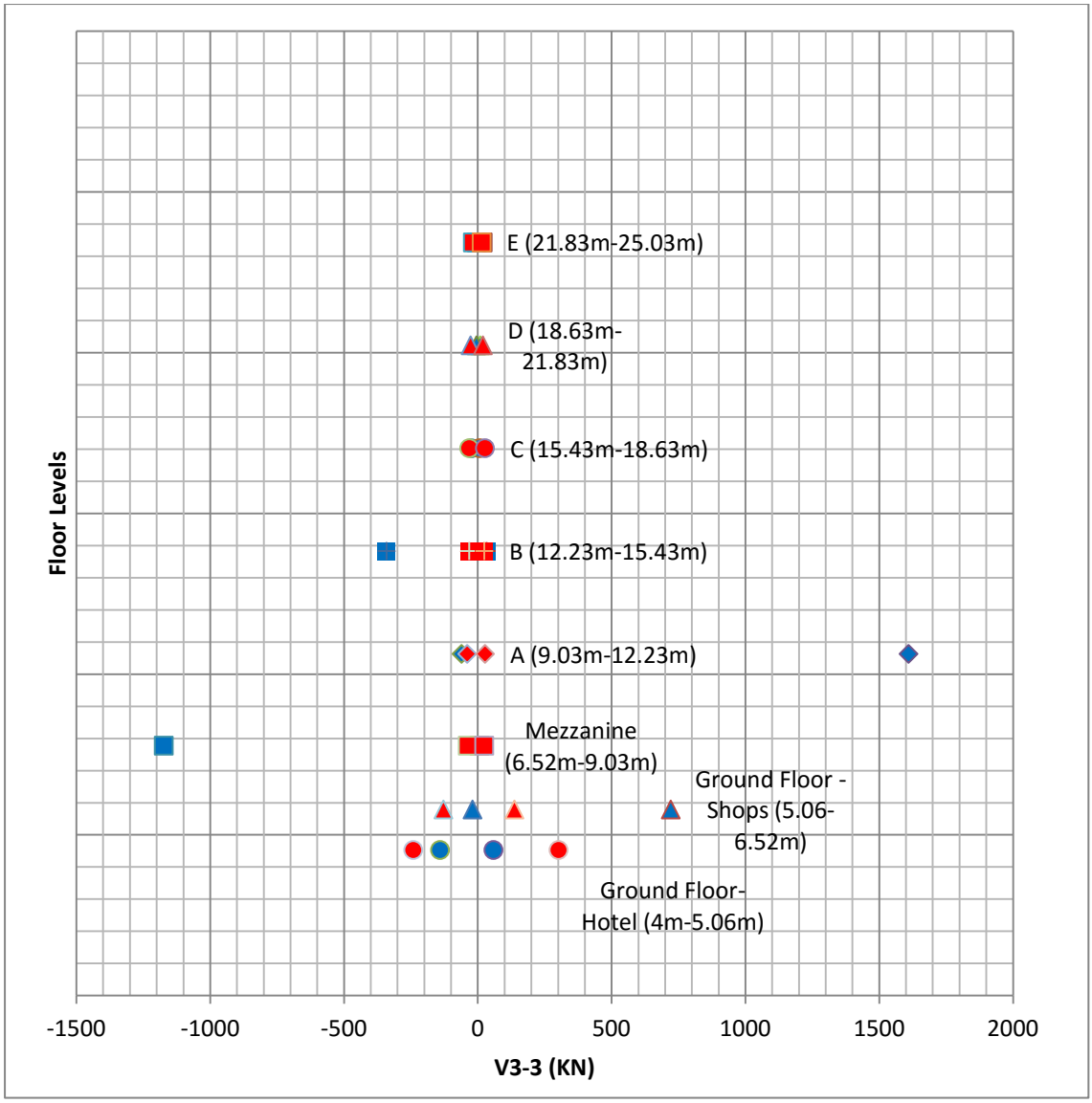

Figure 12.20 Envelope of the Shear Forces of Column C20 along Axis Y (V3-3) per Floor Level of the Non-Retrofitted (blue) and the Retrofitted (red) Building

Chapter 13

Summary and Conclusions

13.1 Summary

The aim of this project is to assess the bearing capacity of the reinforced concrete hotel and to strengthen it. The hotel was constructed in 1967 in Greece. The building was designed and constructed under the provision of the national codes of Members of Reinforced Concrete (1954) and the Design Code for Earthquake Resistant structures (1959). The code of 1959 did not provide safety against earthquakes in comparison with the modern codes. The hotel is in seismic zone 2 (Z2, $a_{GR}/g=0.24$). It is a 5-storey reinforced concrete building with underground floor, ground floor (two levels), mezzanine floor, approachable and non approachable roof. The total number of levels is 11. Its overall high is 27.53m, including the non approachable roof, while the typical high of floors is 3.2m (except the underground, ground and mezzanine floor).

The building is modelled using the SAP2000 software. It is general purpose civil engineering software. It is ideal for the analysis and design of any type of structural system.

Firstly, modal response spectrum analysis is performed. The purpose of this type of analysis is to detect possible deficiencies the building would have if it was designed according to the modern codes, and not to assess its bearing capacity. The bearing capacity is assessed by performing nonlinear static and dynamic analyses.

Nonlinear static analyses are performed. The target displacement is calculated according to the ATC-40 method, which is applied automatically by SAP 2000. In addition nonlinear dynamic time-history analyses are performed. Three pairs of acceleration time histories are used. They are the obtained by the earthquakes of Corinth (1981, magnitude: 6.6), Kalamata (1986, magnitude 6.2) and

L'Aquila-Italy (2009 magnitude: 6.3). The acceleration time histories are obtained by the PEER Ground Motion Data Base-Beta version. The acceleration time-histories are scaled.

The assessment of the bearing capacity shows that the structure requires rehabilitation, since the building faces significant damages due to its inadequate bearing capacity. Thus 7 shear walls and concrete jackets to 17 out of 23 columns are added to the structure.

The analyses described above are repeated. The retrofitted structure satisfies the target performance level-life safety, when seismic action corresponding to seismic return period of 475 years, or the scaled L'Aquila, Corinth, Kalamata acceleration time-histories are imposed.

13.2 Conclusions

- It is a very flexible structure. The fundamental period of the non-retrofitted structure is 1.63 sec (30% along X) when the stiffness of the elements according to the table 4.1 is used, while it is 2.64 sec (33% along X) when the secant stiffness is used. The stiffness of the retrofitted structure is higher, thus the fundamental period is lower, 0.79 sec (46% along Y) when the stiffness of the elements according to the table 4.1 is used, while it is 1.27 sec (40% along Y) when the secant stiffness is used, indicating that the structure remains flexible although the rehabilitation.
- The use of the secant stiffness leads to higher flexibility and periods because the part of the sections that is considered effective is lower than when the values of the table 4.1 are used. When the values of the table 4.1 are used, the modification factor of SAP 2000 is set to 0.8 or 0.6 for columns (internal and outer respectively), 0.5 for cracked shear walls and 0.4 for beams. When the secant stiffness is used, the average values of the modification factor Keff/Kel is 0.23 for columns and 0.13 for beams. As a result, it is indicated that only a small part of the section is considered effective, uncracked and contributes to earthquake

resistance. The effective section of the beams is considered even smaller than the effective section of the columns.

Non-Retrofitted Structure:

- The geometric dimensions of the sections of the elements of the non-retrofitted building (both columns and beams) are not adequate in comparison with the modern codes and there is no lateral force resisting system.
- The building exceeds the life safety performance level, since the hinges of its columns exceed it. More plastic hinges are formed in beams than in columns.
- The most severe damages are observed in the West, South-West and South side of the building at the floor levels A and B.
- The low stiffness of the building leads to high maximum absolute displacements per height and high inter-storey drifts along both X and Y axis.
- The earthquake events of L'Aquila and Corinth probably cause the collapse of the building, since hinges in 7 and 6 columns, respectively, exceed limit state E-they have no residual strength and cannot sustain loads.
- The non-retrofitted building has inadequate strength, low stiffness and ductility.
- Global and local retrofitting is required. The elements' strength and ductility should be increased. The stiffness should be increased to reduce the lateral displacements and the inter-storey drift ratios. The ductility of the elements should be increased, so they will be able to absorb the seismic energy more effectively.

Retrofitted Structure:

- The rehabilitation of the building is global, since the acceleration time-histories imposed are from very intense and catastrophic earthquakes. In

addition the time histories are scaled and the L'Aquila earthquake influences especially the flexible buildings.

- The 7 shear walls add strength and stiffness to the structure. The concrete jackets increase the bearing capacity, the flexural/shear strength and the deformation capacity of the elements.
- The higher modes are insignificant, thus the pushover analysis is permitted.
- The retrofitted building is a wall system building, since more than 65% of the shear force is taken by the shear walls.
- The retrofitted building satisfies the design criteria of the life safety performance level, since no hinge in columns exceeds the life safety limit state.
- The bearing capacity of the retrofitted building is much higher than the bearing capacity of the non-retrofitted.
- The maximum absolute displacements and the inter-story drift ratios per floor level of the retrofitted structure are lower than those of the non-retrofitted, since the shear walls increase the stiffness of the structure.
- The shear walls are able to sustain the shear forces as shown by the shear check.

References

Applied Technology Council (ATC-40) (1996) *Seismic Evaluation and Retrofit of Concrete Buildings.* Volume 1, 555 Twin Dolphin Drive, Suite 550 Redwood City, California [Online] Available at: https://www.civil.iitb.ac.in/~p0saurabhrs/ATC-40.pdf

Belarbi A. and Acun B. (2013) *FRP Systems in Shear Strengthening of Reinforced Concrete Structures.* Procedia Engineering Volume 57 (2013) Pages 2-8 Modern Building Materials, Structures and Techniques [Online] Available at: http://www.sciencedirect.com/science/article/pii/S1877705813007340

(Assessed: 11 March 2016)

Chopra, A. (1995) *DYNAMICS OF STRUCTURES Theory and Applications to Earthquake Engineering.* 3rd edition. Upper Saddle River: Pearson Education Inc

Computers and Structures Inc. (1995) *CSI Analysis Reference Manual for SAP2000, ETABS, SAFE and CSIBridge.*USA: University Avenue Berkeley, California

Computers and Structures Inc. (1997) *SAP2000 Integrated Finite Elements Analysis and Design of Structures Tutorial Manual Version 6.1.* USA: University Avenue Berkeley, California

Computers and Structures Inc. (2008) *Technical Note Material Stress-Strain Curves.* USA: University Avenue Berkeley, California

Computers and Structures Inc. (2013) *Knowledge Base.* USA: Berkeley, California [Online] Available at: https://wiki.csiamerica.com/display/SAP2000/Home

(Assessed: 22/04/2016)

EN 1990 Basis of Structural Design, Greek National Annex

EN 1991-1, (2002) *Eurocode 1: Actions on structures-Part 1-1: General actions-Densities, self-weight, imposed loads for buildings.*

EN 1992-1(2004) *Eurocode 2: Design of concrete structures- Part 1-1: General rules and rules for buildings.*

EN 1998-1, (2004) *Eurocode 8: Design of structures for earthquake resistance-Part 1:General rules, seismic actions and rules for buildings.*

EN 1998-3, (2005) *Eurocode 8-Design of structures for earthquake resistance-Part 3: Assessment and retrofitting of buildings.*

Fardis, M. and Dritsos, S. (2003) *Assessment of Seismic Damage, Repair and Retrofit of Reinforced Concrete Buildings.* Patras: ESPI Editors L.L.C. (Limited Liability Company*)*

Federal Emergency Management Agency (FEMA 356) (2000) *Prestandard and Commentary for the Seismic Rehabilitation of Buildings. Washington, D.C.*

Government Gazette of Greek Kingdom, (1954) *Reinforced Concrete Regulation (KOS) issue 1.* Athens.

Government Gazette of Greek Kingdom, (1959) *Aseismic Regulation issue 1.* Athens.

Katsikadelis, I. (2012) *Dynamic Analysis of Structures Theory and Applications*. Athens: Symmetria Editions

Ministry for the Environment, Physical Planning and Public Works, (2008) *Reinforcing Steel New Regulation (FEK 1416/B/17-07-2008 and FEK 2113/B/13-10-2008).* Athens

O.A.S.P., (2000) *EKOS 2000 (Reinforced Concrete Greek Regulation).* Athens

O.A.S.P. (2013) *KANEPE (Intervention regulations) FEK 2187/B/05-09-2013 1st review.* Athens

Psycharis, I. (2015) *Notes of the module: Aseismic Design and Analysis of Structures.* Athens: National Technical University of Athens

Spyrakos, C. (2004) *Retrofitting of Structures for Seismic Actions.* Athens: Technical Chamber of Greece

Tarabia, A.M. and Albarky H.F.(2014) *Strenghtening of RC columns by steel angles and strips.* Alexandria Engineering Journal Volume 5, Issue 3, September 2014, pages 615-626 [Online] Available at: http://www.sciencedirect.com/science/article/pii/S1110016814000404

(Assessed: 11 March 2016)

Tasios, T. (2015) *Design Theory of Repairs and Retrofits.* Athens: National Technical University of Athens

Pacific Earthquake Engineering Research Center (PEER), (2010) Users Manual for the PEER Ground Motion Database Web Application, Beta Version-October 1 2010 [Online] Available at: http://peer.berkeley.edu/products/strong_ground_motion_db.html

(Assessed: 10 January 2016)

Viswanath K.G., Prakash K.B., Desai A. (2010) *Seismic Analysis of Steel Braced Reinforced Concrete Frames.* International Journal of Civil and Structural Engineering Volume, No 1,2010 [Online] Available at: http://ipublishing.co.in/jcandsevol1no12010/EIJCSE1010.pdf

(Assessed: 11 March 2016)

Appendix A

Sections Dimensions and Reinforcement:

Columns:

Columns coordinates on the grid:

Columns	X (m)	Y (m)
C1	4.85	0
C2	8	0
C3	11	0
C4	16.55	0
C5	19.4	0
C6	3.55	2.95
C7	7.8	4.3
C8	10.9	4.5
C9	16.55	4.5
C10	19.9	4.5
C11	2.2	6
C12	6.15	7.75
C13	10.2	6.5
C14	14.95	6.5
C15	9.6	9.3
C16	13.15	9.3
C17	16.45	9.3
C18	0	11.4
C19	4.4	12.1
C20	9.6	12.1
C21	13.15	12.1
C22	16.45	11.2
C23	20.5	10.45

Foundation Level (0-1m)		
Columns	Dimensions (cm)	Reinforcement
C1	40X35	4Φ20+4Φ12
C2	35X35	4Φ20+4Φ12
C3	40X35	4Φ20+4Φ14
C4	35X35	4Φ20+4Φ16
C5	40X40	4Φ20
C6	35X35	4Φ20+4Φ12
C7	35X35	4Φ20+4Φ14
C8	35X35	8Φ20
C9	40X40	8Φ20
C10	45X45	4Φ20+4Φ16
C11	35X35	4Φ20+4Φ14
C12	35X35	4Φ20+4Φ14
C13	35X35	4Φ20
C14	40X35	4Φ20
C15	35X35	4Φ20+4Φ16
C16	40X40	4Φ20+4Φ16
C17	45X45	4Φ20+4Φ16
C18	40X40	4Φ20+4Φ12
C19	40X40	4Φ20+4Φ12
C20	40X40	4Φ20
C21	40X40	4Φ20
C22	40X40	4Φ20
C23	40X40	4Φ20+4Φ16

Underground Level (1-4m)		
Columns	Dimensions (cm)	Reinforcement
C1	40X35	4Φ20+4Φ12
C2	35X35	4Φ20+4Φ12
C3	40X35	4Φ20+4Φ14
C4	35x35	4Φ20+4Φ16
C5	40X40	4Φ20
C6	35X35	4Φ20+4Φ12
C7	35X35	4Φ20+4Φ14
C8	35x35	8Φ20
C9	40x40	8Φ20
C10	45x45	4Φ20+4Φ16
C11	35x35	4Φ20+4Φ14
C12	35X35	4Φ20+4Φ14
C13	35x35	4Φ20
C14	35x40	4Φ20
C15	35x35	4Φ20+4Φ16
C16	40x40	4Φ20+4Φ16
C17	45x45	4Φ20+4Φ16
C18	40X40	4Φ20+4Φ12
C19	40X40	4Φ20+4Φ12
C20	35x40	4Φ20
C21	35x40	4Φ20
C22	35x40	4Φ20
C23	40x40	4Φ20+4Φ16

Ground Level (4-6.52m)		
Columns	Dimensions (cm)	Reinforcement
C1	40X35	4Φ20+4Φ12
C2	35X35	4Φ20+4Φ12
C3	40X35	4Φ20+4Φ14
C4	35x35	4Φ20+4Φ16
C5	40X40	4Φ20
C6	35X35	4Φ20+4Φ12
C7	35X35	4Φ20+4Φ14
C8	35X35	8Φ20
C9	40X40	8Φ20
C10	45x45	4Φ20+4Φ16
C11	35x35	4Φ20+4Φ14
C12	35X35	4Φ20+4Φ14
C13	35X35	4Φ20
C14	35x40	4Φ20
C15	35X35	4Φ20+4Φ16
C16	40X40	4Φ20+4Φ16
C17	45x45	4Φ20+4Φ16
C18	40X40	4Φ20+4Φ12
C19	40X40	4Φ20+4Φ12
C20	35x40	4Φ20
C21	35x40	4Φ20
C22	35x40	4Φ20
C23	40X40	4Φ20+4Φ16

Mezzanine Level (6.52-9.03m)		
Columns	Dimensions (cm)	Reinforcement
C1	40X35	4Φ20+4Φ12
C2	35X35	4Φ20+4Φ12
C3	40X35	4Φ20+4Φ14
C4	35x35	4Φ20+4Φ16
C5	35x35	4Φ20
C6		
C7		
C8	55x55	4Φ20+4Φ16
C9	55x55	4Φ20+4Φ16
C10	40x40	4Φ12+4Φ12
C11		
C12		
C13	35x35	4Φ20
C14	35x35	4Φ20
C15	35x35	8Φ14
C16	35x35	4Φ20
C17	35x35	4Φ20
C18		
C19		
C20	35x35	4Φ20
C21	35x35	4Φ20
C22	35x35	4Φ20
C23	35x35	4Φ20

Gaps indicate that those columns do not cross the mezzanine floor.

A Level (9.03-12.23m)		
Columns	Dimensions (cm)	Reinforcement
C1	35x35	4Φ20+4Φ12
C2	35x35	4Φ20+4Φ12
C3	35x35	4Φ20+4Φ14
C4	35x35	4Φ20+4Φ14
C5	35x35	4Φ20+4Φ12
C6	35x35	4Φ20+4Φ12
C7	35x35	4Φ20+4Φ12
C8	35x35	4Φ20+4Φ14
C9	35x35	4Φ20+4Φ14
C10	35x35	4Φ20+4Φ12
C11	35x35	4Φ20+4Φ14
C12	35x35	4Φ20+4Φ14
C13	35x35	4Φ20+4Φ12
C14	35x35	4Φ20+4Φ12
C15	35x35	4Φ20+4Φ12
C16	35x35	4Φ20+4Φ12
C17	35x35	4Φ20+4Φ12
C18	35x35	4Φ20+4Φ12
C19	35x35	4Φ20+4Φ12
C20	35x35	4Φ20+4Φ12
C21	35x35	4Φ20+4Φ12
C22	35x35	4Φ20+4Φ12
C23	35x35	4Φ20+4Φ12

B Level (12.23-15.43m)		
Columns	Dimensions (cm)	Reinforcement
C1	30x30	4Φ20
C2	30x30	4Φ20
C3	35x35	4Φ20+4Φ12
C4	35x35	4Φ20+4Φ12
C5	30x30	4Φ20
C6	30x30	4Φ20
C7	30x30	4Φ20
C8	35x35	4Φ20+4Φ12
C9	35x35	4Φ20+4Φ12
C10	30x30	4Φ20
C11	35x35	4Φ20+4Φ12
C12	35x35	4Φ20+4Φ12
C13	30x30	4Φ20
C14	30x30	4Φ20
C15	30x30	4Φ20
C16	30x30	4Φ20
C17	30x30	4Φ20
C18	30x30	4Φ20
C19	30x30	4Φ20
C20	30x30	4Φ20
C21	30x30	4Φ20
C22	30x30	4Φ20
C23	30x30	4Φ20

C Level (15.43-18.63m)		
Columns	Dimensions (cm)	Reinforcement
C1	30x30	4Φ16
C2	30x30	4Φ16
C3	35x35	4Φ16
C4	35x35	4Φ16
C5	30x30	4Φ16
C6	30x30	4Φ16
C7	30x30	4Φ16
C8	35x35	4Φ16
C9	35x35	4Φ16
C10	30x30	4Φ16
C11	35x35	4Φ16
C12	35x35	4Φ16
C13	30x30	4Φ16
C14	30x30	4Φ16
C15	30x30	4Φ16
C16	30x30	4Φ16
C17	30x30	4Φ16
C18	30x30	4Φ16
C19	30x30	4Φ16
C20	30x30	4Φ16
C21	30x30	4Φ16
C22	30x30	4Φ16
C23	30x30	4Φ16

D Level (18.63-21.83m)		
Columns	Dimensions (cm)	Reinforcement
C1	30x30	4Φ18
C2	30x30	4Φ18
C3	30x30	4Φ18
C4	30x30	4Φ18
C5	30x30	4Φ18
C6	30x30	4Φ18
C7	30x30	4Φ18
C8	30x30	4Φ18
C9	30x30	4Φ18
C10	30x30	4Φ18
C11	30x30	4Φ18
C12	30x30	4Φ18
C13	30x30	4Φ18
C14	30x30	4Φ18
C15	30x30	4Φ18
C16	30x30	4Φ18
C17	30x30	4Φ18
C18	30x30	4Φ18
C19	30x30	4Φ18
C20	30x30	4Φ18
C21	30x30	4Φ18
C22	30x30	4Φ18
C23	30x30	4Φ18

E Level (21.83-25.03m)		
Columns	Dimensions (cm)	Reinforcement
C1	30x30	4Φ18
C2	30x30	4Φ18
C3	30x30	4Φ18
C4	30x30	4Φ18
C5	30x30	4Φ18
C6	30x30	4Φ18
C7	30x30	4Φ18
C8	30x30	4Φ18
C9	30x30	4Φ18
C10	30x30	4Φ18
C11	30x30	4Φ18
C12	30x30	4Φ18
C13	30x30	4Φ18
C14	30x30	4Φ18
C15	30x30	4Φ18
C16	30x30	4Φ18
C17	30x30	4Φ18
C18	30x30	4Φ18
C19	30x30	4Φ18
C20	30x30	4Φ18
C21	30x30	4Φ18
C22	30x30	4Φ18
C23	30x30	4Φ18

Beams:

The dimensions and reinforcement of all the connecting beams are 20X100cm 8Φ14.

Ground Floor Level (Hotel) 4m		
Beams	Dimensions (cm)	Reinforcement
B1	20X42	4Φ14
B2	20X42	4Φ14
B3	20X35	4Φ14
B4	20X35	4Φ14
B5	20X35	4Φ14
B6	20x30	4Φ12
B7	20X30	4Φ12
B8	20X30	4Φ14
B9	20X50	4Φ14
B10	20X50	4Φ14
B11	20X30	4Φ12
B12	20X30	4Φ12
B13	20x50	4Φ18
B14	20X42	4Φ14
B15	20X42	4Φ14
B16	20X60	4Φ18
B17	20X60	4Φ18
B18	20x50	4Φ18
B19	20X60	4Φ18
B20	20X60	4Φ18
B21	20x50	4Φ18

Ground Floor Level (Shops) 5.06m		
Beams	Dimensions (cm)	Reinforcement
B1	20x60	4Φ18
B2	20x60	4Φ18
B3	20x60	4Φ18
B4	20x50	4Φ18
B5	20x50	4Φ18
B6	20x60	4Φ16
B7	20x60	4Φ16
B8	20x60	4Φ16
B9	20x30	4Φ14
B10	20x50	4Φ18
B11	20x30	4Φ14
B12	20x30	4Φ14
B13	20x60	4Φ18
B14	20x60	4Φ16
B15	20x30	4Φ12
B16	20x30	4Φ14
B17	20x30	4Φ14
B18	20x50	4Φ18

Mezzanine Floor Level 6.52m		
Beams	Dimensions (cm)	Reinforcement
B1	20X42	4Φ14
B2	20X42	4Φ14
B3	20X35	4Φ14
B4	20X35	4Φ14
B5	20X35	4Φ14
B6	20x30	4Φ12
B7	20X30	4Φ12
B8	20X30	4Φ14
B9	20X50	4Φ14
B10	20X50	4Φ14
B11	20X30	4Φ12
B12	20X30	4Φ12
B13	20x50	4Φ18
B14	20X42	4Φ14
B15	20X42	4Φ14
B16	20X60	4Φ18
B17	20X60	4Φ18
B18	20x50	4Φ18
B19	20X60	4Φ18
B20	20X60	4Φ18
B21	20x50	4Φ18

A Floor Level 9.03m		
Beams	Dimensions (cm)	Reinforcement
B1	25X50	4Φ16
B2	20X45	4Φ14
B3	20X35	4Φ14
B4	20X35	4Φ14
B5	20X30	4Φ12
B6	20X30	4Φ14
B7	20X30	4Φ12
B8	20X30	4Φ12
B9	20X30	4Φ12
B10	20X50	4Φ14
B11	20X50	4Φ14
B12	20X50	4Φ12
B13	20X60	4Φ18
B14	20X60	4Φ18
B15	20X50	4Φ18
B16	20X50	4Φ18
B17	20X60	4Φ18
B18	20X60	4Φ18
B19	20X60	4Φ18
B20	20X50	4Φ18
B21	20X60	4Φ16
B22	20X30	4Φ14
B23	20X30	4Φ14
B24	20X30	4Φ14
B25	20X30	4Φ16
B26	20x60	4Φ16
B27	20x50	4Φ18
B28	20x60	4Φ20
B29	20x60	4Φ16

B30	20X50	4Φ14
B31	20x50	4Φ16
B32	20x60	4Φ18
B33	20X60	4Φ18

B and C Floor Level (12.23m and 15.43m respectively)		
Beams	Dimensions (cm)	Reinforcement
B1	25X65	2Φ14+2Φ16
B2	25X65	2Φ14+2Φ16
B3	25X65	2Φ18+2Φ20
B4	25X65	2Φ14+2Φ16
B5	20X50	4Φ18
B6	25X65	4Φ16
B7	25X65	4Φ20
B8	25X65	4Φ16
B9	20X50	4Φ18
B10	20X30	2Φ14+2Φ16
B11	20X45	4Φ14
B12	20X45	4Φ14
B13	20X30	2Φ14+2Φ16
B13’	20X50	2Φ14+2Φ16
B14	20X50	2Φ14+2Φ16
B15	20X50	4φ12
B16	20χ30	4φ12
B17	20χ30	4φ12
B18	25X65	2Φ14+2Φ16
B19	20X50	4Φ18
B20	20X50	4Φ18
B21	20X60	2Φ14+2Φ16
B22	25X65	2Φ14+2Φ16

B23	25X65	2Φ14+2Φ16
B24	20X65	2Φ14+2Φ16
B25	20X30	4Φ14
B26	20X30	4Φ14
B27	20X30	4Φ14
B28	20X60	2Φ14+2Φ16
B29	25X65	4Φ18
B30	25X65	2Φ18+2Φ20
B31	20X65	4Φ16
B32	20X30	4Φ12
B33	20X30	4Φ12
B34	20X60	4Φ12

D, E Floor Levels and Approachable Roof (18.63m, 21.83m and 25.03m respectively)		
Beams	Dimensions (cm)	Reinforcement
B1	20X65	2Φ14+2Φ16
B2	20X65	2Φ14+2Φ16
B3	20X65	2Φ18+2Φ20
B4	20X65	2Φ14+2Φ16
B5	20X50	4Φ18
B6	25X65	4Φ16
B7	25X65	4Φ20
B8	25X65	4Φ16
B9	20X50	4Φ18
B10	20X30	2Φ14+2Φ16
B11	20X45	4Φ14
B12	20X45	4Φ14
B13	20X30	2Φ14+2Φ16
B13’	20X50	2Φ14+2Φ16

B14	20X50	2Ф14+2Ф16
B15	20X50	4φ12
B16	20χ30	4φ12
B17	20χ30	4φ12
B18	25X65	2Ф14+2Ф16
B19	20X50	4Ф18
B20	20X50	4Ф18
B21	20X60	2Ф14+2Ф16
B22	20X65	2Ф14+2Ф16
B23	25X65	2Ф14+2Ф16
B24	20X65	2Ф14+2Ф16
B25	20X30	4Ф14
B26	20X30	4Ф14
B27	20X30	4Ф14
B28	20X60	2Ф14+2Ф16
B29	20X65	4Ф18
B30	25X65	2Ф18+2Ф20
B31	20X65	4Ф16
B32	20X30	4Ф12
B33	20X30	4Ф12
B34	20X60	4Ф12

Appendix B

Calculations of the distribution of slab loads to the beams:

Slab and wall loads to the connecting beams-underground floor, z=1m

					Permanent Loads (KN/m^2)			Imposed Loads (KN/m^2)			Walls' Loads (Permanent) (KN/m^2)				
Beams	**Area Influence**	**Total Slab Area (m^2)**	**Stairs Area (m^2)**	**Beam Length (m)**	**Concrete self weight**	**Floors**	**Total Permanent (due to slab) (KN/m)**	**Floors**	**Stairs**	**Total Imposed) (KN/m)**	**Stretcher Bond**	**Wall Height (m)**	**Walls' Load (KN/m)**	**Total Permanent Load (KN/m)**	**Total Imposed Load (KN/m)**
B1	A2,B4	3.55		2.8	2.88	1.5	5.553	2		2.536			0	5.553	2.536
B2	A5,A65	1.18		2.65	2.88	1.5	1.950	2		0.891			0	1.950	0.891
B3	A48,A54	2.62		5.2	2.88	1.5	2.207	2		1.008			0	2.207	1.008
B4	A47,B7	1.38		2.5	2.88	1.5	2.418	2		1.104			0	2.418	1.104
B5	A3,A7	11.31		4.169	2.88	1.5	11.882	2		5.426			0	11.882	5.426
B6	A6,A11,A56	4.07		2.752	2.88	1.5	6.478	2		2.958	2.1	2.35	4.935	11.413	2.958
B7	A51,A35,A52	8.97		5.30	2.88	1.5	7.413	2		3.385	2.1	2.35	4.935	12.348	3.385
B8	A43,A44	6.43		3	2.88	1.5	9.388	2		4.287			0	9.388	4.287
B9	A9,A17	9.9		4.23	2.88	1.5	10.251	2		4.681			0	10.251	4.681
B10	A15,A22	6.83		3.422	2.88	1.5	8.742	2		3.992			0	8.742	3.992
B11	A31,ST1	1.17	1.59	3.2	2.88	1.5	3.778	0	3.5	1.591	2.1	2.75	5.775	9.553	1.591
B12	A26,A38, ST2	3.3	1.46	2.95	2.88	1.5	7.067	2	3.5	3.919	2.1	2.9	6.09	13.157	3.919
B13	A29,A34,ST4	5.26	3.04	4.4	2.88	1.5	8.262	2	3.5	3.877	2.1	2.9	6.09	14.352	3.877
B13'	A20	4.27		4.14	2.88	1.5	4.518	2		2.063			0	4.518	2.063
B14	A23	4.4		4.85	2.88	1.5	3.974	2		1.814			0	3.974	1.814
B15	NO LOAD			3.2	2.88	1.5	0.000	2		0.000			0	0.000	0.000

B16	A27	1.86		3.08	2.88	1.5	2.645	2		1.208			0	2.645	1.208
B17	A40	2.67		3.789	2.88	1.5	3.086	2		1.409			0	3.086	1.409
B18	A1	1.47		2.867	2.88	1.5	2.246	2		1.025			0	2.246	1.025
B19	A4,A55	10.59		4.221	2.88	1.5	10.989	2		5.018			0	10.989	5.018
B20	A50,A53	9.41		4.25	2.88	1.5	9.698	2		4.428			0	9.698	4.428
B21	A49,A46	9.17		4.15	2.88	1.5	9.678	2		4.419			0	9.678	4.419
B22	A45	3		4.164	2.88	1.5	3.156	2		1.441			0	3.156	1.441
B23	A8	1.18		2.99	2.88	1.5	1.729	2		0.789			0	1.729	0.789
B24	A10,A12	5.51		3.5	2.88	1.5	6.895	2		3.149			0	6.895	3.149
B25	A13,A32	2.57		1.764	2.88	1.5	6.381	2		2.914	2.1	2.7	5.67	12.051	2.914
B26	A14,A30	4.83		2.45	2.88	1.5	8.635	2		3.943	2.1	2.7	5.67	14.305	3.943
B27	A36,ST3,ST5	1.9	1.67	2.45	2.88	1.5	6.382	2	3.5	3.661	2.1	2.9	6.09	12.472	3.661
B28	A37,A41	10.55		4.45	2.88	1.5	10.384	2		4.742			0	10.384	4.742
B29	A42	5.4		5.549	2.88	1.5	4.262	2		1.946			0	4.262	1.946
B30	A18	6.17		5.52	2.88	1.5	4.896	2		2.236			0	4.896	2.236
B31	A19,A21	12.9		4.368	2.88	1.5	12.935	2		5.907			0	12.935	5.907
B32	A24	2.13		2.45	2.88	1.5	3.808	2		1.739	2.1	2.9	6.09	9.898	1.739
B33	A25	1.25		2.45	2.88	1.5	2.235	2		1.020	2.1	2.9	6.09	8.325	1.020
B34	A28,A39	3.24		1.512	2.88	1.5	9.386	2		4.286			0	9.386	4.286

Slab and wall loads to the beams-ground floor (hotel), z=4m

					Permanent loads (KN/m^2)			Imposed Loads (KN/m^2)			Walls' Loads (Permanent) (KN/m^2)					
Beams	**Area Influence**	**Total Slab Area (m^2)**	**Stairs Area (m^2)**	**Beam Length**	**Concrete self weight**	**Floors**	**Total Permanent (due to slab) (KN/m)**	**Floors**	**Stairs**	**Total Imposed (KN/m)**	**Stretcher Bond**	**Header Bond**	**Wall Height (m)**	**Walls' Load (KN/m)**	**Total Permanent Load (KN/m)**	**Total Imposed Load (KN/m)**
B1	A35, A68, A31	7.800		5.30	2.88	1.5	6.446	2		2.943				0	6.446	2.943
B2	A34,A31,A44	6.39		3	2.88	1.5	9.329	2		4.260	2.1		2.1	4.41	13.739	4.260
B3	A34,A29,ST4	5.26	3.04	4.4	2.88	1.5	8.262	2	3.5	4.809		3.6	2.17	7.812	16.074	4.809
B4	A31,ST1	1.17	1.59	3.2	2.88	1.5	3.778	2	3.5	2.470		3.6	2.17	7.812	11.590	2.470
B5	A26, A38,ST2	3.3	1.46	2.95	2.88	1.5	7.067	2	3.5	3.969		3.6	2.17	7.812	14.879	3.969
B6	A25.	1.25		2.45	2.88	1.5	2.235	2		1.020		3.6	2.22	7.992	10.227	1.020
B7	A27	1.86		3.08	2.88	1.5	2.645	2		1.208		3.6	2.22	7.992	10.637	1.208
B8	A40	2.67		3.789	2.88	1.5	3.086	2		1.409		3.6	2.22	7.992	11.078	1.409
B9	A32	0.78		1.764	2.88	1.5	1.937	2		0.884	2.1		2.02	4.242	6.179	0.884
B10	A30	1.69		2.45	2.88	1.5	3.021	2		1.380	2.1		2.02	4.242	7.263	1.380
B11					0	0	0.000			0.000	2.1		2.22	4.662	4.662	0.000
B12	A36,ST3,ST5	1.9	1.67	2.45	2.88	1.5	6.382	2	3.5	3.937		3.6	2.22	7.992	14.374	3.937
B13	A67	3.93		4.15	2.88	1.5	4.148	2		1.894	2.1		2.02	4.242	8.390	1.894
B14	A37.A41	10.55		4.45	2.88	1.5	10.384	2		4.742				0	10.384	4.742
B15	A28.A39	3.24		1.512	2.88	1.5	9.386	2		4.286				0	9.386	4.286
B16	A42	5.4		5.549	2.88	1.5	4.262	2		1.946		3.6	1.92	6.912	11.174	1.946
B17	A66,A48	2.05		5.2	2.88	1.5	1.727	2		0.788		3.6	1.92	6.912	8.639	0.788
B18	A49,A46	9.17		4.15	2.88	1.5	9.678	2		4.419	2.1		2.02	4.242	13.920	4.419
B19	A47	1.39		2.5	2.88	1.5	2.435	2		1.112		3.6	1.92	6.912	9.347	1.112
B20	A45	3		4.164	2.88	1.5	3.156	2		1.441		3.6	1.92	6.912	10.068	1.441
B21	A68,A50	8.45		4.25	2.88	1.5	8.708	2		3.976				0	8.708	3.976

Slab and wall loads to the beams-ground floor (shops), z=5.06m

					Permanent loads (KN/m^2)		Imposed Loads (KN/m^2)		Walls Loads (Permanent) (KN/m^2)					
Beams	**Area Influence**	**Total Slab Area (m^2)**	**Beam Length**	**Concrete self weight**	**Floors**	**Total Permanent (due to slab) (KN/m)**	**Shops**	**Total Imposed (KN/m)**	**Stretcher Bond**	**Header Bond**	**Wall Height (m)**	**Walls Load (KN/m)**	**Total Permanent Load (KN/m)**	**Total Imposed Load (KN/m)**
B1	A2	3.55	2.8	2.88	1.5	5.553	5	6.339		3.6	3.37	12.132	17.685	6.339
B2	A5,A25	1.18	2.65	2.88	1.5	1.950	5	2.226		3.6	3.37	12.132	14.082	2.226
B3	A1	1.47	2.867	2.88	1.5	2.246	5	2.564		3.6	3.37	12.132	14.378	2.564
B4	A3	6.71	4.169	2.88	1.5	7.050	5	8.047	2.1		3.47	7.287	14.337	8.047
B5	A4,A26	7.01	4.221	2.88	1.5	7.274	5	8.304				0	7.274	8.304
B6	A6,A28	2.13	2.752	2.88	1.5	3.390	5	3.870	2.1		3.37	7.077	10.467	3.870
B7	A8	1.16	2.99	2.88	1.5	1.699	5	1.940		3.6	3.37	12.132	13.831	1.940
B8	A10,A12	5.51	3.5	2.88	1.5	6.895	5	7.871				0	6.895	7.871
B9	A13	1.8	1.764	2.88	1.5	4.469	5	5.102	2.1		3.67	7.707	12.176	5.102
B10	A9,A17	9.9	4.23	2.88	1.5	10.251	5	11.702	2.1		3.37	7.077	17.328	11.702
B11	A15,A22	6.83	3.422	2.88	1.5	8.742	5	9.980	2.1		3.67	7.707	16.449	9.980
B12	A14	3.14	2.45	2.88	1.5	5.614	5	6.408	2.1		3.67	7.707	13.321	6.408
B13	A18	6.17	5.52	2.88	1.5	4.896	5	5.589		3.6	3.37	12.132	17.028	5.589
B14	A19,A21	12.9	4.368	2.88	1.5	12.935	5	14.766				0	12.935	14.766
B15	A24	2.13	2.45	2.88	1.5	3.808	5	4.347	2.1		3.67	7.707	11.515	4.347
B16	A20	4.27	4.14	2.88	1.5	4.518	5	5.157		3.6	3.67	13.212	17.730	5.157
B17	A23	4.4	4.85	2.88	1.5	3.974	5	4.536		3.6	3.67	13.212	17.186	4.536
B18	A27	1.79	4.15	2.88	1.5	1.889	5	2.157	2.1		3.47	7.287	9.176	2.157

Slab and wall loads to the beams-mezzanine floor, z=6.52m

					Permanent loads (KN/m^2)			Imposed Loads (KN/m^2)			Walls' Loads (Permanent) (KN/m^2)					
Beams	**Area Influence**	**Total Slab Area (m^2)**	**Stairs Area (m^2)**	**Beam Length (m)**	**Concrete's self weight**	**Floors**	**Total Permanent (due to slab) (KN/m)**	**Floors**	**Stairs**	**Total Imposed (KN/m)**	**Stretcher Bond**	**Header Bond**	**Wall Height (m)**	**Walls' Load (KN/m)**	**Total Permanent Load (KN/m)**	**Total Imposed Load (KN/m)**
B1	A35, A68, A31	7.800		5.30	2.88	1.5	6.446	2		2.943				2.01	8.456	2.943
B2	A431,A44	6.39		3	2.88	1.5	9.329	2		4.260				2.06	11.389	4.260
B3	A34,A29,ST4	5.26	3.04	4.4	2.88	1.5	8.262	2	3.5	4.809		3.6		2.16	10.422	4.809
B4	A31,ST1	1.17	1.59	3.2	2.88	1.5	3.778	2	3.5	2.470		3.6		2.16	5.938	2.470
B5	A26, A38,ST2	3.3	1.46	2.95	2.88	1.5	7.067	2	3.5	3.969		3.6		2.21	9.277	3.969
B6	A25.	1.25		2.45	2.88	1.5	2.235	2		1.020		3.6		2.21	4.445	1.020
B7	A27	1.86		3.08	2.88	1.5	2.645	2		1.208		3.6		2.21	4.855	1.208
B8	A40	2.67		3.789	2.88	1.5	3.086	2		1.409		3.6		2.21	5.296	1.409
B9	A32	0.78		1.764	2.88	1.5	1.937	2		0.884	2.1			2.21	4.147	0.884
B10	A30	1.69		2.45	2.88	1.5	3.021	2		1.380	2.1			2.01	5.031	1.380
B11							0.000			0.000	2.1			2.01	2.010	0.000
B12	A36,ST3,ST5	1.9	1.67	2.45	2.88	1.5	6.382	2	3.5	3.937		3.6		2.01	8.392	3.937
B13	A67	3.93		4.15	2.88	1.5	4.148	2		1.894	2.1			1.91	6.058	1.894
B14	A37.A41	10.55		4.45	2.88	1.5	10.384	2		4.742				1.91	12.294	4.742
B15	A28.A39	3.24		1.512	2.88	1.5	9.386	2		4.286	2.1			1.91	11.296	4.286
B16	A42	5.4		5.549	2.88	1.5	4.262	2		1.946		3.6		2.01	6.272	1.946
B17	A66,A48	2.05		5.2	2.88	1.5	1.727	2		0.788		3.6		2.01	3.737	0.788
B18	A49,A46	9.17		4.15	2.88	1.5	9.678	2		4.419	2.1			1.91	11.588	4.419
B19	A47	1.39		2.5	2.88	1.5	2.435	2		1.112		3.6		1.91	4.345	1.112
B20	A45	3		4.164	2.88	1.5	3.156	2		1.441		3.6		2.01	5.166	1.441
B21	A68,A50	8.45		4.25	2.88	1.5	8.708	2		3.976				1.91	10.618	3.976

Slab and wall loads to the beams-Floor A, z=9.03m

						Permanent Load (KN/m^2)			Imposed Load (KN/m^2)				Wall Loads (Permanent) (KN/m^2)						
Beams	**Area Influence**	**Total Slab Area (m^2)**	**Stairs Area (m^2)**	**Balconies Area (m^2)**	**Beam Length**	**Concrete self weight**	**Floors**	**Total Permanent (due to slab) (KN/m)**	**Floors**	**Stairs**	**Balconies**	**Total Imposed (KN/m)**	**Stretcher Bond**	**Header Bond**	**Wall Height (m)**	**Stretcher bond (not on the beams) (KN/m)**	**Wall Load (KN/m)**	**Total Permanent Load (KN/m)**	**Total Imposed Load (KN/m)**
B1	A51,A35,A52	8.97			5.30	2.88	1.5	7.413	2			3.385			2.55	1.747	1.747	9.160	3.385
B2	A29,A34,ST4	5.26	3.04		4.4	2.88	1.5	8.262	2	3.5		4.809			2.9		0.000	8.262	4.809
B3	A31,ST1	1.17	1.59		3.2	2.88	1.5	3.778	2	3.5		2.470			2.75		0.000	3.778	2.470
B4	A26,A38, ST2	3.3	1.46		2.95	2.88	1.5	7.067	2	3.5		3.969			3.05		0.000	7.067	3.969
B5	A27	1.86			3.08	2.88	1.5	2.645	2			1.208		3.6	2.9		10.440	13.085	1.208
B6	A40	2.67			3.789	2.88	1.5	3.086	2			1.409		3.6	2.9		10.440	13.526	1.409
B7	A24	2.13			2.45	2.88	1.5	3.808	2			1.739	2.1		2.9		6.090	9.898	1.739
B8	A25	1.25			2.45	2.88	1.5	2.235	2			1.020	2.1		2.9		6.090	8.325	1.020
B9	A36,ST3,ST5	1.9	1.67		2.45	2.88	1.5	6.382	2	3.5		3.937			2.9		0.000	6.382	3.937
B10	A49,A46	9.17			4.15	2.88	1.5	9.678	2			4.419	2.1		2.6		5.460	15.138	4.419
B11	A37,A41	10.55			4.45	2.88	1.5	10.384	2			4.742	2.1		2.6	3.822	9.282	19.667	4.742
B12	A28,A39	3.24			1.512	2.88	1.5	9.386	2			4.286	2.1		2.6		5.460	14.846	4.286
B13	A45, B8	3		3.47	4.164	2.88	1.5	6.806	2		5	5.608		3.6	2.55		9.180	15.986	5.608

B14	A42,B9	5.4		3.76	5.549	2.88	1.5	7.230	2		5	5.334		3.6	2.55	2.044	11.224	18.454	5.334
B15	A4,A55	10.59			4.221	2.88	1.5	10.989	2			5.018	2.1		2.7		5.670	16.659	5.018
B16	A50,A53	9.41			4.25	2.88	1.5	9.698	2			4.428	2.1		2.7		5.670	15.368	4.428
B17	A5,A65,B5	1.18		2.4	2.65	2.88	1.5	5.917	2		5	5.419		3.6	2.55		9.180	15.097	5.419
B18	A2,B4	3.55		3.13	2.8	2.88	1.5	10.449	2		5	8.125		3.6	2.55		9.180	19.629	8.125
B19	A1,B3	1.47		4.85	2.867	2.88	1.5	9.655	2		5	9.484		3.6	2.55		9.180	18.835	9.484
B20	A3,A7	11.31			4.169	2.88	1.5	11.882	2			5.426	2.1		2.7		5.670	17.552	5.426
B21	A6,A11,A56	4.07			2.752	2.88	1.5	6.478	2			2.958			2.55		0.000	6.478	2.958
B22	A13,A32	2.57			1.764	2.88	1.5	6.381	2			2.914			2.9		0.000	6.381	2.914
B23	A14,A30	4.83			2.45	2.88	1.5	8.635	2			3.943			2.9	2.691	2.691	11.326	3.943
B24	A15,A22	6.83			3.422	2.88	1.5	8.742	2			3.992			2.9	1.853	1.853	10.595	3.992
B25	A10,A12	5.51			3.5	2.88	1.5	6.895	2			3.149			2.55		0.000	6.895	3.149
B26	A8,B2	1.18		4.62	2.99	2.88	1.5	8.496	2		5	8.515		3.6	2.55		9.180	17.676	8.515
B27	A9,A17	9.9			4.23	2.88	1.5	10.251	2			4.681	2.1		2.7		5.670	15.921	4.681
B28	A18,B1	6.17		6.87	5.52	2.88	1.5	10.347	2		5	8.458		3.6	2.55	2.321	11.501	21.848	8.458
B29	A19,A21	12.9			4.368	2.88	1.5	12.935	2			5.907			2.55	4.038	4.038	16.974	5.907
B30	A20	4.27			4.14	2.88	1.5	4.518	2			2.063		3.6	2.9	2.166	12.606	17.123	2.063
B31	A23	4.4			4.85	2.88	1.5	3.974	2			1.814		3.6	2.7		9.720	13.694	1.814
B32	A48,A54,B6	2.62		4.44	5.2	2.88	1.5	5.947	2		5	5.277		3.6	2.55		9.180	15.127	5.277
B33	A47,B7	1.38		2.65	2.5	2.88	1.5	7.061	2		5	6.404		3.6	2.55		9.180	16.241	6.404
B34	A43,A44	6.43			3	2.88	1.5	9.388	2			4.287	2.1		2.55		5.355	14.743	4.287

Slab and wall loads to the beams-Floors B, C, D, E z=12.23, 15.43, 18.63, 21.83m respectively

						Permanent Loads (KN/m^2)			Imposed Loads (KN/m^2)				Walls' Loads (Permanent) (KN/m^2)						
Beams	**Area Influence**	**Total Slab Area (m^2)**	**Stairs Area (m^2)**	**Balconies Area (m^2)**	**Beam Length**	**Concrete self weight**	**Floors**	**Total Permanent (due to slab) (KN/m)**	**Floors**	**Stairs**	**Balconies**	**Total Imposed (KN/m)**	**Stretcher Bond**	**Header Bond**	**Wall Height (m)**	**Stretcher bond (not on the beams) (KN/m)**	**Walls Load (KN/m)**	**Total Permanent Load (KN/m)**	**Total Imposed Load (KN/m)**
B1	A2,B4	3.55		3.13	2.8	2.88	1.5	10.449	2		5	8.125		3.6	2.55		9.18	19.629	8.125
B2	A5,A65,B5	1.18		2.4	2.65	2.88	1.5	5.917	2		5	5.419		3.6	2.55		9.18	15.097	5.419
B3	A48,A54,B6	2.62		4.44	5.2	2.88	1.5	5.947	2		5	5.277		3.6	2.55		9.18	15.127	5.277
B4	A47,B7	1.38		2.65	2.5	2.88	1.5	7.061	2		5	6.404		3.6	2.55		9.18	16.241	6.404
B5	A3,A7	11.31			4.169	2.88	1.5	11.882	2			5.426	2.1		2.6		5.46	17.342	5.426
B6	A6,A11,A56	4.07			2.752	2.88	1.5	6.478	2			2.958					0	6.478	2.958
B7	A51,A35,A52	8.97			5.30	2.88	1.5	7.413	2			3.385				1.747	1.75	9.160	3.385
B8	A43,A44	6.43			3	2.88	1.5	9.388	2			4.287	2.1		2.55		5.36	14.743	4.287
B9	A9,A17	9.9			4.23	2.88	1.5	10.251	2			4.681	2.1		2.7		5.67	15.921	4.681
B10	A15,A22	6.83			3.422	2.88	1.5	8.742	2			3.992				1.853	1.85	10.595	3.992
B11	A31,ST1	1.17	1.59		3.2	2.88	1.5	3.778	0	3.5		1.739		3.6	2.75		9.9	13.678	1.739
B12	A26,A38, ST2	3.3	1.46		2.95	2.88	1.5	7.067	2	3.5		3.969		3.6	2.9		10.44	17.507	3.969
B13	A29,A34,ST4	5.26	3.04		4.4	2.88	1.5	8.262	2	3.5		4.809		3.6	2.9		10.44	18.702	4.809
B13'	A20	4.27			4.14	2.88	1.5	4.518	2			2.063		3.6	2.9	2.166	12.61	17.123	2.063
B14	A23	4.4			4.85	2.88	1.5	3.974	2			1.814		3.6	2.7		9.72	13.694	1.814
B15	NO LOAD				3.2	2.88	1.5	0.000	2			0.000					0	0.000	0.000
B16	A27	1.86			3.08	2.88	1.5	2.645	2			1.208		3.6	2.6		9.36	12.005	1.208
B17	A40	2.67			3.789	2.88	1.5	3.086	2			1.409		3.6	2.9		10.44	13.526	1.409

B18	A1,B3	1.47		4.85	2.867	2.88	1.5	9.655	2		5	9.484		3.6	2.55		9.18	18.835	9.484
B19	A4,A55	10.59			4.221	2.88	1.5	10.989	2			5.018	2.1		2.7		5.67	16.659	5.018
B20	A50,A53	9.41			4.25	2.88	1.5	9.698	2			4.428					0	9.698	4.428
B21	A49,A46	9.17			4.15	2.88	1.5	9.678	2			4.419	2.1		2.6		5.46	15.138	4.419
B22	A45, B8	3		3.47	4.164	2.88	1.5	6.806	2		5	5.608		3.6	2.55		9.18	15.986	5.608
B23	A8,B2	1.18		4.62	2.99	2.88	1.5	8.496	2		5	8.515		3.6	2.55		9.18	17.676	8.515
B24	A10,A12	5.51			3.5	2.88	1.5	6.895	2			3.149			2.55		0	6.895	3.149
B25	A13,A32	2.57			1.764	2.88	1.5	6.381	2			2.914					0	6.381	2.914
B26	A14,A30	4.83			2.45	2.88	1.5	8.635	2			3.943				2.691	2.69	11.326	3.943
B27	A36,ST3,ST5	1.9	1.67		2.45	2.88	1.5	6.382	2	3.5		3.937		3.6	2.9		10.44	16.822	3.937
B28	A37,A41	10.55			4.45	2.88	1.5	10.384	2			4.742	2.1		2.7	3.822	9.49	19.877	4.742
B29	A42,B9	5.4		3.76	5.549	2.88	1.5	7.230	2		5	5.334		3.6	2.55	2.044	11.22	18.454	5.334
B30	A18,B1	6.17		6.87	5.52	2.88	1.5	10.347	2		5	8.458		3.6	2.55	2.321	11.50	21.848	8.458
B31	A19,A21	12.9			4.368	2.88	1.5	12.935	2			5.907			2.55	4.038	4.04	16.974	5.907
B32	A24	2.13			2.45	2.88	1.5	3.808	2			1.739	2.1		2.9		6.09	9.898	1.739
B33	A25	1.25			2.45	2.88	1.5	2.235	2			1.020	2.1		2.9		6.09	8.325	1.020
B34	A28,A39	3.24			1.512	2.88	1.5	9.386	2			4.286	2.1		2.6		5.46	14.846	4.286

Slab and wall loads to the beams-approachable roof, z=25.03m

						Permanent Loads (KN/m2)			Imposed Loads (KN/m2)				Walls' Loads (Permanent) (KN/m2)					
Beams	**Area Influence**	**Total Slab Area (m2)**	**Stairs Area (m2)**	**Balconies Area (m2)**	**Beam Length**	**Concrete self weight**	**Roof**	**Total Permanent (due to slab) (KN/m)**	**Approachable Roof**	**Stairs**	**Balconies**	**Total Imposed (KN/m)**	**Stretcher Bond**	**Header Bond**	**Wall Height (m)**	**Walls Load (KN/m)**	**Total Permanent Load (KN/m)**	**Total Imposed Load (KN/m)**
B1	A2,B4	3.55		3.13	2.8	2.88	1.3	9.972	2		5	8.125				0	9.972	8.125
B2	A5,A65,B5	1.18		2.4	2.65	2.88	1.3	5.647	2		5	5.419				0	5.647	5.419
B3	A48,A54,B6	2.62		4.44	5.2	2.88	1.3	5.675	2		5	5.277				0	5.675	5.277
B4	A47,B7	1.38		2.65	2.5	2.88	1.3	6.738	2		5	6.404				0	6.738	6.404
B5	A3,A7	11.31			4.169	2.88	1.3	11.340	2			5.426				0	11.340	5.426
B6	A6,A11,A56	4.07			2.752	2.88	1.3	6.182	2			2.958				0	6.182	2.958
B7	A51,A35,A52	8.97			5.30	2.88	1.3	7.074	2			3.385				0	7.074	3.385
B8	A43,A44	6.43			3	2.88	1.3	8.959	2			4.287				0	8.959	4.287
B9	A9,A17	9.9			4.23	2.88	1.3	9.783	2			4.681				0	9.783	4.681
B10	A15,A22	6.83			3.422	2.88	1.3	8.343	2			3.992				0	8.343	3.992
B11	A31,ST1	1.17	1.59		3.2	2.88	1.3	3.605	0	3.5		1.739		3.6	2.75	9.9	13.505	1.739
B12	A26,A38, ST2	3.3	1.46		2.95	2.88	1.3	6.745	2	3.5		3.969		3.6	2.9	10.44	17.185	3.969
B13	A29,A34,ST4	5.26	3.04		4.4	2.88	1.3	7.885	2	3.5		4.809		3.6	2.9	10.44	18.325	4.809
B13'	A20	4.27			4.14	2.88	1.3	4.311	2			2.063				0	4.311	2.063
B14	A23	4.4			4.85	2.88	1.3	3.792	2			1.814				0	3.792	1.814
B15	NO LOAD				3.2	2.88	1.3	0.000	2			0.000				0	0.000	0.000
B16	A27	1.86			3.08	2.88	1.3	2.524	2			1.208				0	2.524	1.208
B17	A40	2.67			3.789	2.88	1.3	2.946	2			1.409				0	2.946	1.409
B18	A1,B3	1.47		4.85	2.867	2.88	1.3	9.214	2		5	9.484				0	9.214	9.484
B19	A4,A55	10.59			4.221	2.88	1.3	10.487	2			5.018				0	10.487	5.018
B20	A50,A53	9.41			4.25	2.88	1.3	9.255	2			4.428				0	9.255	4.428
B21	A49,A46	9.17			4.15	2.88	1.3	9.236	2			4.419				0	9.236	4.419
B22	A45, B8	3		3.47	4.164	2.88	1.3	6.495	2		5	5.608				0	6.495	5.608
B23	A8,B2	1.18		4.62	2.99	2.88	1.3	8.108	2		5	8.515				0	8.108	8.515

B24	A10,A12	5.51			3.5	2.88	1.3	6.581	2			3.149				0	6.581	3.149
B25	A13,A32	2.57			1.764	2.88	1.3	6.090	2			2.914				0	6.090	2.914
B26	A14,A30	4.83			2.45	2.88	1.3	8.241	2			3.943		3.6	2.9	10.44	18.681	3.943
B27	A36,ST3,ST5	1.9	1.67		2.45	2.88	1.3	6.091	2	3.5		3.937		3.6	2.9	10.44	16.531	3.937
B28	A37,A41	10.55			4.45	2.88	1.3	9.910	2			4.742				0	9.910	4.742
B29	A42,B9	5.4		3.76	5.549	2.88	1.3	6.900	2		5	5.334				0	6.900	5.334
B30	A18,B1	6.17		6.87	5.52	2.88	1.3	9.874	2		5	8.458				0	9.874	8.458
B31	A19,A21	12.9			4.368	2.88	1.3	12.345	2			5.907				0	12.345	5.907
B32	A24	2.13			2.45	2.88	1.3	3.634	2			1.739				0	3.634	1.739
B33	A25	1.25			2.45	2.88	1.3	2.133	2			1.020				0	2.133	1.020
B34	A28,A39	3.24			1.512	2.88	1.3	8.957	2			4.286				0	8.957	4.286

Slab load to the beams-non approachable roof, z=27.53m

				Permanent Loads (KN/m^2)			**Imposed Loads (KN/m^2)**			
Beams	**Area Influence**	**Total Slab Area (m^2)**	**Beam Length**	**Concrete self weight**	**Roof**	**Total Permanent (due to slab) (KN/m)**	**Non Approachable Roof**	**Total Imposed (KN/m)**	**Total Permanent Load (KN/m)**	**Total Imposed Load (KN/m)**
B11	A3	2.76	3.2	2.88	1.3	3.60525	1	0.8625	3.605	0.863
B12	A4	1.46	2.95	2.88	2.3	2.563661017	1	0.494915254	2.564	0.495
B13	A1	4.21	4.4	2.88	3.3	5.913136364	1	0.956818182	5.913	0.957
B26	A2	1.69	2.45	2.88	4.3	4.952734694	1	0.689795918	4.953	0.690
B27	A5	1.68	2.45	2.88	5.3	5.609142857	1	0.685714286	5.609	0.686

Appendix C

Secant Stiffness (Keff/Kel) values of the elements:

Beams:

Frames	keff(2)/ Kel(2)	keff(3) /Kel(3)	Sections	BEAM	h(m)	b (m)	db (m)	θy(angle0)	θy (angle 180)
425	1	0.1359	B20X30 4F12LR	B15(5.06m)	0.3	0.2	0.012	0.00522	0.00510
426	1	0.1359	B20X30 4F12	B15(5.06m)	0.3	0.2	0.012	0.00522	0.00510
427	1	0.1359	B20X30 4F12LR	B15(5.06m)	0.3	0.2	0.012	0.00522	0.00510
223	1	0.1493	B20X30 4F12LR	B7(4m)	0.3	0.2	0.012	0.00581	0.00567
224	1	0.1493	B20X30 4F12	B7(4m)	0.3	0.2	0.012	0.00581	0.00567
225	1	0.1493	B20X30 4F12LR	B7(4m)	0.3	0.2	0.012	0.00581	0.00567
298	1	0.1359	B20X30 4F12LR	B6(4m)	0.3	0.2	0.012	0.00522	0.00510
299	1	0.1359	B20X30 4F12	B6(4m)	0.3	0.2	0.012	0.00522	0.00510
300	1	0.1359	B20X30 4F12LR	B6(4m)	0.3	0.2	0.012	0.00522	0.00510
236	1	0.1359	B20X30 4F12LR	B11(4m)	0.3	0.2	0.012	0.00522	0.00510
277	1	0.1359	B20X30 4F12	B11(4m)	0.3	0.2	0.012	0.00522	0.00510
238	1	0.1359	B20X30 4F12LR	B11(4m)	0.3	0.2	0.012	0.00522	0.00510
269	1	0.1775	B20X30 4F12	B12(6.52m)	0.3	0.2	0.012	0.00802	0.00780
270	1	0.1775	B20X30 4F12	B12(6.52m)	0.3	0.2	0.012	0.00802	0.00780
271	1	0.1775	B20X30 4F12LR	B12(6.52m)	0.3	0.2	0.012	0.00802	0.00780
295	1	0.1359	B20X30 4F12LR	B6(6.52m)	0.3	0.2	0.012	0.00522	0.00510
296	1	0.1359	B20X30 4F12	B6(6.52m)	0.3	0.2	0.012	0.00522	0.00510
297	1	0.1359	B20X30 4F12LR	B6(6.52m)	0.3	0.2	0.012	0.00522	0.00510
311	1	0.1359	B20X30 4F12LR	B11(6.52m)	0.3	0.2	0.012	0.00522	0.00510
333	1	0.1359	B20X30 4F12LR	B11(6.52m)	0.3	0.2	0.012	0.00522	0.00510
334	1	0.1359	B20X30 4F12	B11(6.52m)	0.3	0.2	0.012	0.00522	0.00510
254	1	0.1493	B20X30 4F12LR	B7(6.52m)	0.3	0.2	0.012	0.00581	0.00567
255	1	0.1493	B20X30 4F12	B7(6.52m)	0.3	0.2	0.012	0.00581	0.00567
256	1	0.1493	B20X30 4F12LR	B7(6.52m)	0.3	0.2	0.012	0.00581	0.00567
315	1	0.1359	B20X30 4F12LR	B7(9.03m)	0.3	0.2	0.012	0.00522	0.00510
316	1	0.1359	B20X30 4F12	B7(9.03m)	0.3	0.2	0.012	0.00522	0.00510
317	1	0.1359	B20X30 4F12LR	B7(9.03m)	0.3	0.2	0.012	0.00522	0.00510
289	1	0.1359	B20X30 4F12LR	B8(9.03m)	0.3	0.2	0.012	0.00522	0.00510
290	1	0.1359	B20X30 4F12	B8(9.03m)	0.3	0.2	0.012	0.00522	0.00510
291	1	0.1359	B20X30 4F12LR	B8(9.03m)	0.3	0.2	0.012	0.00522	0.00510
318	1	0.1775	B20X30 4F12	B9(9.03m)	0.3	0.2	0.012	0.00802	0.00780
319	1	0.1775	B20X30 4F12	B9(9.03m)	0.3	0.2	0.012	0.00802	0.00780
320	1	0.1775	B20X30 4F12LR	B9(9.03m)	0.3	0.2	0.012	0.00802	0.00780
480	1	0.1359	B20X30 4F12LR	B32(12.23m)	0.3	0.2	0.012	0.00522	0.00510
481	1	0.1359	B20X30 4F12	B32(12.23m)	0.3	0.2	0.012	0.00522	0.00510

482	1	0.1359	B20X30 4F12LR	B32(12.23m)	0.3	0.2	0.012	0.00522	0.00510
469	1	0.1359	B20X30 4F12LR	B33(12.23m)	0.3	0.2	0.012	0.00522	0.00510
470	1	0.1359	B20X30 4F12	B33(12.23m)	0.3	0.2	0.012	0.00522	0.00510
471	1	0.1359	B20X30 4F12LR	B33(12.23m)	0.3	0.2	0.012	0.00522	0.00510
466	1	0.1493	B20X30 4F12LR	B16(12.23m)	0.3	0.2	0.012	0.00581	0.00567
467	1	0.1493	B20X30 4F12	B16(12.23m)	0.3	0.2	0.012	0.00581	0.00567
468	1	0.1493	B20X30 4F12LR	B16(12.23m)	0.3	0.2	0.012	0.00581	0.00567
463	1	0.1418	B20X30 4F12LR	B17(12.23m)	0.3	0.2	0.012	0.00546	0.00533
464	1	0.1418	B20X30 4F12	B17(12.23m)	0.3	0.2	0.012	0.00546	0.00533
465	1	0.1418	B20X30 4F12LR	B17(12.23m)	0.3	0.2	0.012	0.00546	0.00533
CB32A	1	0.1359	B20X30 4F12LR	B32(15.43m)	0.3	0.2	0.012	0.00522	0.00510
CB32B	1	0.1359	B20X30 4F12	B32(15.43m)	0.3	0.2	0.012	0.00522	0.00510
CB32C	1	0.1359	B20X30 4F12LR	B32(15.43m)	0.3	0.2	0.012	0.00522	0.00510
CB33A	1	0.1359	B20X30 4F12LR	B33(15.43m)	0.3	0.2	0.012	0.00522	0.00510
CB33B	1	0.1359	B20X30 4F12	B33(15.43m)	0.3	0.2	0.012	0.00522	0.00510
CB33C	1	0.1359	B20X30 4F12LR	B33(15.43m)	0.3	0.2	0.012	0.00522	0.00510
CB16A	1	0.1493	B20X30 4F12LR	B16(15.43m)	0.3	0.2	0.012	0.00581	0.00567
CB16B	1	0.1493	B20X30 4F12	B16(15.43m)	0.3	0.2	0.012	0.00581	0.00567
CB16C	1	0.1493	B20X30 4F12LR	B16(15.43m)	0.3	0.2	0.012	0.00581	0.00567
CB17A	1	0.1418	B20X30 4F12LR	B17(15.43m)	0.3	0.2	0.012	0.00546	0.00533
CB17B	1	0.1418	B20X30 4F12	B17(15.43m)	0.3	0.2	0.012	0.00546	0.00533
CB17C	1	0.1418	B20X30 4F12LR	B17(15.43m)	0.3	0.2	0.012	0.00546	0.00533
431	1	0.1359	B20X30 4F12LR	B32(18.63m)	0.3	0.2	0.012	0.00522	0.00510
367	1	0.1359	B20X30 4F12LR	B32(18.63m)	0.3	0.2	0.012	0.00522	0.00510
368	1	0.1359	B20X30 4F12	B32(18.63m)	0.3	0.2	0.012	0.00522	0.00510

357	1	0.1359	B20X30 4F12LR	B33(18.63m)	0.3	0.2	0.012	0.00522	0.00510
358	1	0.1359	B20X30 4F12	B33(18.63m)	0.3	0.2	0.012	0.00522	0.00510
359	1	0.1359	B20X30 4F12LR	B33(18.63m)	0.3	0.2	0.012	0.00522	0.00510
351	1	0.1493	B20X30 4F12LR	B16(18.63m)	0.3	0.2	0.012	0.00581	0.00567
352	1	0.1493	B20X30 4F12	B16(18.63m)	0.3	0.2	0.012	0.00581	0.00567
353	1	0.1493	B20X30 4F12LR	B16(18.63m)	0.3	0.2	0.012	0.00581	0.00567
301	1	0.1418	B20X30 4F12LR	B17(18.63m)	0.3	0.2	0.012	0.00546	0.00533
305	1	0.1418	B20X30 4F12	B17(18.63m)	0.3	0.2	0.012	0.00546	0.00533
346	1	0.1418	B20X30 4F12LR	B17(18.63m)	0.3	0.2	0.012	0.00546	0.00533
850	1	0.1359	B20X30 4F12LR	B32(21.83m)	0.3	0.2	0.012	0.00522	0.00510
851	1	0.1359	B20X30 4F12	B32(21.83m)	0.3	0.2	0.012	0.00522	0.00510
852	1	0.1359	B20X30 4F12LR	B32(21.83m)	0.3	0.2	0.012	0.00522	0.00510
844	1	0.1359	B20X30 4F12LR	B33(21.83m)	0.3	0.2	0.012	0.00522	0.00510
845	1	0.1359	B20X30 4F12	B33(21.83m)	0.3	0.2	0.012	0.00522	0.00510
846	1	0.1359	B20X30 4F12LR	B33(21.83m)	0.3	0.2	0.012	0.00522	0.00510
841	1	0.1493	B20X30 4F12LR	B16(21.83m)	0.3	0.2	0.012	0.00581	0.00567
842	1	0.1493	B20X30 4F12	B16(21.83m)	0.3	0.2	0.012	0.00581	0.00567
843	1	0.1493	B20X30 4F12LR	B16(21.83m)	0.3	0.2	0.012	0.00581	0.00567
838	1	0.1418	B20X30 4F12LR	B17(21.83m)	0.3	0.2	0.012	0.00546	0.00533
839	1	0.1418	B20X30 4F12	B17(21.83m)	0.3	0.2	0.012	0.00546	0.00533
840	1	0.1418	B20X30 4F12LR	B17(21.83m)	0.3	0.2	0.012	0.00546	0.00533
963	1	0.1359	B20X30 4F12LR	B32(25.03m)	0.3	0.2	0.012	0.00522	0.00510
964	1	0.1359	B20X30 4F12	B32(25.03m)	0.3	0.2	0.012	0.00522	0.00510
965	1	0.1359	B20X30 4F12LR	B32(25.03m)	0.3	0.2	0.012	0.00522	0.00510
957	1	0.1359	B20X30 4F12LR	B33(25.03m)	0.3	0.2	0.012	0.00522	0.00510

958	1	0.1359	B20X30 4F12	B33(25.03m)	0.3	0.2	0.012	0.00522	0.00510
959	1	0.1359	B20X30 4F12LR	B33(25.03m)	0.3	0.2	0.012	0.00522	0.00510
954	1	0.1493	B20X30 4F12LR	B16(25.03m)	0.3	0.2	0.012	0.00581	0.00567
955	1	0.1493	B20X30 4F12	B16(25.03m)	0.3	0.2	0.012	0.00581	0.00567
956	1	0.1493	B20X30 4F12LR	B16(25.03m)	0.3	0.2	0.012	0.00581	0.00567
951	1	0.1418	B20X30 4F12LR	B17(25.03m)	0.3	0.2	0.012	0.00546	0.00533
952	1	0.1418	B20X30 4F12	B17(25.03m)	0.3	0.2	0.012	0.00546	0.00533
953	1	0.1418	B20X30 4F12LR	B17(25.03m)	0.3	0.2	0.012	0.00546	0.00533
220	1	0.1697	B20X30 4F14LR	B8(4m)	0.3	0.2	0.014	0.00538	0.00571
226	1	0.1697	B20X30 4F14	B8(4m)	0.3	0.2	0.014	0.00538	0.00571
227	1	0.1697	B20X30 4F14LR	B8(4m)	0.3	0.2	0.014	0.00538	0.00571
414	1	0.1981	B20X30 4F14LR	B16 (5.06m)	0.3	0.2	0.014	0.00670	0.00717
415	1	0.1981	B20X30 4F14	B16 (5.06m)	0.3	0.2	0.014	0.00670	0.00717
416	1	0.1981	B20X30 4F14LR	B16 (5.06m)	0.3	0.2	0.014	0.00670	0.00717
428	1	0.2082	B20X30 4F14LR	B17 (5.06m)	0.3	0.2	0.014	0.00743	0.00797
429	1	0.2082	B20X30 4F14	B17 (5.06m)	0.3	0.2	0.014	0.00743	0.00797
430	1	0.2082	B20X30 4F14LR	B17 (5.06m)	0.3	0.2	0.014	0.00743	0.00797
398	1	0.1864	B20X30 4F14LR	B11(5.06m)	0.3	0.2	0.014	0.00606	0.00646
399	1	0.1864	B20X30 4F14	B11(5.06m)	0.3	0.2	0.014	0.00606	0.00646
403	1	0.1864	B20X30 4F14LR	B11(5.06m)	0.3	0.2	0.014	0.00606	0.00646
354	1	0.1905	B20X30 4F14LR	B9(5.06m)	0.3	0.2	0.014	0.00626	0.00669
355	1	0.1905	B20X30 4F14	B9(5.06m)	0.3	0.2	0.014	0.00626	0.00669
356	1	0.1905	B20X30 4F14LR	B9(5.06m)	0.3	0.2	0.014	0.00626	0.00669
360	1	0.2128	B20X30 4F14LR	B12(5.06m)	0.3	0.2	0.014	0.00783	0.00840
361	1	0.2128	B20X30 4F14	B12(5.06m)	0.3	0.2	0.014	0.00783	0.00840
362	1	0.2128	B20X30 4F14LR	B12(5.06m)	0.3	0.2	0.014	0.00783	0.00840
389	1	0.2128	B20X30 4F14LR	B12(5.06m)	0.3	0.2	0.014	0.00783	0.00840
266	1	0.1697	B20X30 4F14LR	B8(6.52m)	0.3	0.2	0.014	0.00538	0.00571
267	1	0.1697	B20X30 4F14	B8(6.52m)	0.3	0.2	0.014	0.00538	0.00571
268	1	0.1697	B20X30 4F14LR	B8(6.52m)	0.3	0.2	0.014	0.00538	0.00571
510	1	0.1981	B20X30 4F14LR	B30(9.03m)	0.3	0.2	0.014	0.00670	0.00717
511	1	0.1981	B20X30 4F14	B30(9.03m)	0.3	0.2	0.014	0.00670	0.00717
512	1	0.1981	B20X30 4F14LR	B30(9.03m)	0.3	0.2	0.014	0.00670	0.00717
538	1	0.2082	B20X30 4F14LR	B31(9.03m)	0.3	0.2	0.014	0.00743	0.00797
539	1	0.2082	B20X30 4F14	B31(9.03m)	0.3	0.2	0.014	0.00743	0.00797
540	1	0.2082	B20X30 4F14LR	B31(9.03m)	0.3	0.2	0.014	0.00743	0.00797
524	1	0.1864	B20X30 4F14LR	B24(9.03m)	0.3	0.2	0.014	0.00606	0.00646
525	1	0.1864	B20X30 4F14	B24(9.03m)	0.3	0.2	0.014	0.00606	0.00646

526	1	0.1864	B20X30 4F14LR	B24(9.03m)	0.3	0.2	0.014	0.00606	0.00646
517	1	0.1905	B20X30 4F14LR	B22 (9.03m)	0.3	0.2	0.014	0.00626	0.00669
518	1	0.1905	B20X30 4F14	B22 (9.03m)	0.3	0.2	0.014	0.00626	0.00669
519	1	0.1905	B20X30 4F14LR	B22 (9.03m)	0.3	0.2	0.014	0.00626	0.00669
520	1	0.2128	B20X30 4F14LR	B23(9.03m)	0.3	0.2	0.014	0.00783	0.00840
521	1	0.2128	B20X30 4F14	B23(9.03m)	0.3	0.2	0.014	0.00783	0.00840
522	1	0.2128	B20X30 4F14LR	B23(9.03m)	0.3	0.2	0.014	0.00783	0.00840
283	1	0.1697	B20X30 4F14LR	B6(9.03m)	0.3	0.2	0.014	0.00538	0.00571
284	1	0.1697	B20X30 4F14	B6(9.03m)	0.3	0.2	0.014	0.00538	0.00571
285	1	0.1697	B20X30 4F14LR	B6(9.03m)	0.3	0.2	0.014	0.00538	0.00571
483	1	0.2128	B20X30 4F14	B27(12.23m)	0.3	0.2	0.014	0.00783	0.00840
484	1	0.2128	B20X30 4F14LR	B27(12.23m)	0.3	0.2	0.014	0.00783	0.00840
485	1	0.2128	B20X30 4F14LR	B27(12.23m)	0.3	0.2	0.014	0.00783	0.00840
579	1	0.2128	B20X30 4F14LR	B26(12.23m)	0.3	0.2	0.014	0.00783	0.00840
580	1	0.2128	B20X30 4F14	B26(12.23m)	0.3	0.2	0.014	0.00783	0.00840
581	1	0.2128	B20X30 4F14LR	B26(12.23m)	0.3	0.2	0.014	0.00783	0.00840
576	1	0.1905	B20X30 4F14LR	B25(12.23m)	0.3	0.2	0.014	0.00626	0.00669
577	1	0.1905	B20X30 4F14	B25(12.23m)	0.3	0.2	0.014	0.00626	0.00669
578	1	0.1905	B20X30 4F14LR	B25(12.23m)	0.3	0.2	0.014	0.00626	0.00669
CB25A	1	0.1905	B20X30 4F14LR	B25(15.23m)	0.3	0.2	0.014	0.00626	0.00669
CB25B	1	0.1905	B20X30 4F14	B25(15.23m)	0.3	0.2	0.014	0.00626	0.00669
CB25C	1	0.1905	B20X30 4F14LR	B25(15.23m)	0.3	0.2	0.014	0.00626	0.00669
CB26A	1	0.2128	B20X30 4F14LR	B26(15.23m)	0.3	0.2	0.014	0.00783	0.00840
CB26B	1	0.2128	B20X30 4F14	B26(15.23m)	0.3	0.2	0.014	0.00783	0.00840
CB26C	1	0.2128	B20X30 4F14LR	B26(15.23m)	0.3	0.2	0.014	0.00783	0.00840
CB27A	1	0.2128	B20X30 4F14LR	B27(15.23m)	0.3	0.2	0.014	0.00783	0.00840
CB27B	1	0.2128	B20X30 4F14	B27(15.23m)	0.3	0.2	0.014	0.00783	0.00840
CB27C	1	0.2128	B20X30 4F14LR	B27(15.23m)	0.3	0.2	0.014	0.00783	0.00840
557	1	0.1905	B20X30 4F14LR	B25(18.63m)	0.3	0.2	0.014	0.00626	0.00669
558	1	0.1905	B20X30 4F14	B25(18.63m	0.3	0.2	0.014	0.00626	0.00669

				)					
562	1	0.1905	B20X30 4F14LR	B25(18.63m)	0.3	0.2	0.014	0.00626	0.00669
569	1	0.2128	B20X30 4F14LR	B26(18.63m)	0.3	0.2	0.014	0.00783	0.00840
570	1	0.2128	B20X30 4F14	B26(18.63m)	0.3	0.2	0.014	0.00783	0.00840
571	1	0.2128	B20X30 4F14LR	B26(18.63m)	0.3	0.2	0.014	0.00783	0.00840
432	1	0.2128	B20X30 4F14	B27(18.63m)	0.3	0.2	0.014	0.00783	0.00840
453	1	0.2128	B20X30 4F14LR	B27(18.63m)	0.3	0.2	0.014	0.00783	0.00840
454	1	0.2128	B20X30 4F14LR	B27(18.63m)	0.3	0.2	0.014	0.00783	0.00840
875	1	0.1905	B20X30 4F14LR	B25(21.83m)	0.3	0.2	0.014	0.00626	0.00669
876	1	0.1905	B20X30 4F14	B25(21.83m)	0.3	0.2	0.014	0.00626	0.00669
877	1	0.1905	B20X30 4F14LR	B25(21.83m)	0.3	0.2	0.014	0.00626	0.00669
878	1	0.2128	B20X30 4F14LR	B26(21.83m)	0.3	0.2	0.014	0.00783	0.00840
879	1	0.2128	B20X30 4F14	B26(21.83m)	0.3	0.2	0.014	0.00783	0.00840
880	1	0.2128	B20X30 4F14LR	B26(21.83m)	0.3	0.2	0.014	0.00783	0.00840
853	1	0.2128	B20X30 4F14	B27(21.83m)	0.3	0.2	0.014	0.00783	0.00840
854	1	0.2128	B20X30 4F14LR	B27(21.83m)	0.3	0.2	0.014	0.00783	0.00840
855	1	0.2128	B20X30 4F14LR	B27(21.83m)	0.3	0.2	0.014	0.00783	0.00840
988	1	0.1905	B20X30 4F14LR	B25(25.03m)	0.3	0.2	0.014	0.00626	0.00669
989	1	0.1905	B20X30 4F14	B25(25.03m)	0.3	0.2	0.014	0.00626	0.00669
990	1	0.1905	B20X30 4F14LR	B25(25.03m)	0.3	0.2	0.014	0.00626	0.00669
991	1	0.2128	B20X30 4F14LR	B26(25.03m)	0.3	0.2	0.014	0.00783	0.00840
992	1	0.2128	B20X30 4F14	B26(25.03m)	0.3	0.2	0.014	0.00783	0.00840
993	1	0.2128	B20X30 4F14LR	B26(25.03m)	0.3	0.2	0.014	0.00783	0.00840
966	1	0.2128	B20X30 4F14	B27(25.03m)	0.3	0.2	0.014	0.00783	0.00840
967	1	0.2128	B20X30 4F14LR	B27(25.03m)	0.3	0.2	0.014	0.00783	0.00840
968	1	0.2128	B20X30 4F14LR	B27(25.03m	0.3	0.2	0.014	0.00783	0.00840

				)					
279	1	0.1521	B20X50 4F18	B13(4m)	0.5	0.2	0.018	0.00508	0.00596
292	1	0.1521	B20X50 4F18LR	B13(4m)	0.5	0.2	0.018	0.00508	0.00596
293	1	0.2102	B20X50 4F18LR	B18(4m)	0.5	0.2	0.018	0.00777	0.00822
294	1	0.2102	B20X50 4F18	B18(4m)	0.5	0.2	0.018	0.00777	0.00822
307	1	0.2102	B20X50 4F18LR	B18(4m)	0.5	0.2	0.018	0.00777	0.00822
308	1	0.2102	B20X50 4F18LR	B21(4m)	0.5	0.2	0.018	0.00777	0.00822
309	1	0.2102	B20X50 4F18	B21(4m)	0.5	0.2	0.018	0.00777	0.00822
310	1	0.2102	B20X50 4F18LR	B21(4m)	0.5	0.2	0.018	0.00777	0.00822
404	1	0.2102	B20X50 4F18LR	B5(5.06m)	0.5	0.2	0.018	0.00777	0.00822
405	1	0.2102	B20X50 4F18	B5(5.06m)	0.5	0.2	0.018	0.00777	0.00822
406	1	0.2102	B20X50 4F18LR	B5(5.06m)	0.5	0.2	0.018	0.00777	0.00822
1083	1	0.1521	B20X50 4F18LR	B18 (5.06m)	0.5	0.2	0.018	0.00508	0.00596
1082	1	0.1521	B20X50 4F18	B18 (5.06m)	0.5	0.2	0.018	0.00508	0.00596
1081	1	0.1521	B20X50 4F18LR	B18 (5.06m)	0.5	0.2	0.018	0.00508	0.00596
394	1	0.2095	B20X50 4F18LR	B4(5.06m)	0.5	0.2	0.018	0.00770	0.00815
395	1	0.2095	B20X50 4F18	B4(5.06m)	0.5	0.2	0.018	0.00770	0.00815
396	1	0.2095	B20X50 4F18LR	B4(5.06m)	0.5	0.2	0.018	0.00770	0.00815
419	1	0.2095	B20X50 4F18LR	B10 (5.06m)	0.5	0.2	0.018	0.00770	0.00815
420	1	0.2095	B20X50 4F18	B10 (5.06m)	0.5	0.2	0.018	0.00770	0.00815
421	1	0.2095	B20X50 4F18LR	B10 (5.06m)	0.5	0.2	0.018	0.00770	0.00815
335	1	0.1521	B20X50 4F18LR	B13(6.52m)	0.5	0.2	0.018	0.00508	0.00596
336	1	0.1521	B20X50 4F18	B13(6.52m)	0.5	0.2	0.018	0.00508	0.00596
337	1	0.1521	B20X50 4F18LR	B13(6.52m)	0.5	0.2	0.018	0.00508	0.00596
374	1	0.2102	B20X50 4F18LR	B21(6.52m)	0.5	0.2	0.018	0.00777	0.00822
375	1	0.2102	B20X50 4F18	B21(6.52m)	0.5	0.2	0.018	0.00777	0.00822
376	1	0.2102	B20X50 4F18LR	B21(6.52m)	0.5	0.2	0.018	0.00777	0.00822
338	1	0.2102	B20X50 4F18LR	B18(6.52m)	0.5	0.2	0.018	0.00777	0.00822
372	1	0.2102	B20X50 4F18	B18(6.52m)	0.5	0.2	0.018	0.00777	0.00822
373	1	0.2102	B20X50 4F18LR	B18(6.52m)	0.5	0.2	0.018	0.00777	0.00822
529	1	0.2095	B20X50 4F18LR	B27(9.03m)	0.5	0.2	0.018	0.00770	0.00815
530	1	0.2095	B20X50 4F18	B27(9.03m)	0.5	0.2	0.018	0.00770	0.00815
531	1	0.2095	B20X50 4F18LR	B27(9.03m)	0.5	0.2	0.018	0.00770	0.00815
493	1	0.2095	B20X50 4F18LR	B20 (9.03m)	0.5	0.2	0.018	0.00770	0.00815
494	1	0.2095	B20X50 4F18	B20 (9.03m)	0.5	0.2	0.018	0.00770	0.00815
495	1	0.2095	B20X50 4F18LR	B20 (9.03m)	0.5	0.2	0.018	0.00770	0.00815
500	1	0.2102	B20X50 4F18LR	B15 (9.03m)	0.5	0.2	0.018	0.00777	0.00822
501	1	0.2102	B20X50 4F18	B15 (9.03m)	0.5	0.2	0.018	0.00777	0.00822
502	1	0.2102	B20X50 4F18LR	B15 (9.03m)	0.5	0.2	0.018	0.00777	0.00822
435	1	0.2102	B20X50 4F18LR	B16(9.03m)	0.5	0.2	0.018	0.00777	0.00822
436	1	0.2102	B20X50 4F18	B16(9.03m)	0.5	0.2	0.018	0.00777	0.00822
437	1	0.2102	B20X50 4F18LR	B16(9.03m)	0.5	0.2	0.018	0.00777	0.00822
587	1	0.2095	B20X50 4F18LR	B9(12.23m)	0.5	0.2	0.018	0.00770	0.00815
588	1	0.2095	B20X50 4F18	B9(12.23m)	0.5	0.2	0.018	0.00770	0.00815
589	1	0.2095	B20X50 4F18LR	B9(12.23m)	0.5	0.2	0.018	0.00770	0.00815

552	1	0.2095	B20X50 4F18LR	B5(12.23m)	0.5	0.2	0.018	0.00770	0.00815
553	1	0.2095	B20X50 4F18	B5(12.23m)	0.5	0.2	0.018	0.00770	0.00815
554	1	0.2095	B20X50 4F18LR	B5(12.23m)	0.5	0.2	0.018	0.00770	0.00815
559	1	0.2102	B20X50 4F18LR	B19(12.23m)	0.5	0.2	0.018	0.00777	0.00822
560	1	0.2102	B20X50 4F18	B19(12.23m)	0.5	0.2	0.018	0.00777	0.00822
561	1	0.2102	B20X50 4F18LR	B19(12.23m)	0.5	0.2	0.018	0.00777	0.00822
600	1	0.2102	B20X50 4F18LR	B20(12.23m)	0.5	0.2	0.018	0.00777	0.00822
601	1	0.2102	B20X50 4F18	B20(12.23m)	0.5	0.2	0.018	0.00777	0.00822
602	1	0.2102	B20X50 4F18LR	B20(12.23m)	0.5	0.2	0.018	0.00777	0.00822
CB9A	1	0.2095	B20X50 4F18LR	B9(15.23m)	0.5	0.2	0.018	0.00770	0.00815
CB9B	1	0.2095	B20X50 4F18	B9(15.23m)	0.5	0.2	0.018	0.00770	0.00815
CB9C	1	0.2095	B20X50 4F18LR	B9(15.23m)	0.5	0.2	0.018	0.00770	0.00815
CB5A	1	0.2095	B20X50 4F18LR	B5(15.23m)	0.5	0.2	0.018	0.00770	0.00815
CB5B	1	0.2095	B20X50 4F18	B5(15.23m)	0.5	0.2	0.018	0.00770	0.00815
CB5C	1	0.2095	B20X50 4F18LR	B5(15.23m)	0.5	0.2	0.018	0.00770	0.00815
CB19A	1	0.2102	B20X50 4F18LR	B19(15.23m)	0.5	0.2	0.018	0.00777	0.00822
CB19B	1	0.2102	B20X50 4F18	B19(15.23m)	0.5	0.2	0.018	0.00777	0.00822
CB19C	1	0.2102	B20X50 4F18LR	B19(15.23m)	0.5	0.2	0.018	0.00777	0.00822
CB20A	1	0.2102	B20X50 4F18LR	B20(15.23m)	0.5	0.2	0.018	0.00777	0.00822
CB20B	1	0.2102	B20X50 4F18	B20(15.23m)	0.5	0.2	0.018	0.00777	0.00822
CB20C	1	0.2102	B20X50 4F18LR	B20(15.23m)	0.5	0.2	0.018	0.00777	0.00822
582	1	0.2095	B20X50 4F18LR	B9(18.63m)	0.5	0.2	0.018	0.00770	0.00815
583	1	0.2095	B20X50 4F18	B9(18.63m)	0.5	0.2	0.018	0.00770	0.00815
584	1	0.2095	B20X50 4F18LR	B9(18.63m)	0.5	0.2	0.018	0.00770	0.00815
476	1	0.2095	B20X50 4F18LR	B5(18.63m)	0.5	0.2	0.018	0.00770	0.00815
499	1	0.2095	B20X50 4F18	B5(18.63m)	0.5	0.2	0.018	0.00770	0.00815
523	1	0.2095	B20X50 4F18LR	B5(18.63m)	0.5	0.2	0.018	0.00770	0.00815
535	1	0.2102	B20X50 4F18LR	B19(18.63m)	0.5	0.2	0.018	0.00777	0.00822
536	1	0.2102	B20X50 4F18	B19(18.63m)	0.5	0.2	0.018	0.00777	0.00822
537	1	0.2102	B20X50 4F18LR	B19(18.63m)	0.5	0.2	0.018	0.00777	0.00822
596	1	0.2102	B20X50 4F18LR	B20(18.63m)	0.5	0.2	0.018	0.00777	0.00822
597	1	0.2102	B20X50 4F18	B20(18.63m)	0.5	0.2	0.018	0.00777	0.00822

598	1	0.2102	B20X50 4F18LR	B20(18.63m)	0.5	0.2	0.018	0.00777	0.00822
883	1	0.2095	B20X50 4F18LR	B9(21.83m)	0.5	0.2	0.018	0.00770	0.00815
884	1	0.2095	B20X50 4F18	B9(21.83m)	0.5	0.2	0.018	0.00770	0.00815
885	1	0.2095	B20X50 4F18LR	B9(21.83m)	0.5	0.2	0.018	0.00770	0.00815
861	1	0.2095	B20X50 4F18LR	B5(21.83m)	0.5	0.2	0.018	0.00770	0.00815
862	1	0.2095	B20X50 4F18	B5(21.83m)	0.5	0.2	0.018	0.00770	0.00815
863	1	0.2095	B20X50 4F18LR	B5(21.83m)	0.5	0.2	0.018	0.00770	0.00815
864	1	0.2102	B20X50 4F18LR	B19(21.83m)	0.5	0.2	0.018	0.00777	0.00822
865	1	0.2102	B20X50 4F18	B19(21.83m)	0.5	0.2	0.018	0.00777	0.00822
866	1	0.2102	B20X50 4F18LR	B19(21.83m)	0.5	0.2	0.018	0.00777	0.00822
889	1	0.2102	B20X50 4F18LR	B20(21.83m)	0.5	0.2	0.018	0.00777	0.00822
890	1	0.2102	B20X50 4F18	B20(21.83m)	0.5	0.2	0.018	0.00777	0.00822
891	1	0.2102	B20X50 4F18LR	B20(21.83m)	0.5	0.2	0.018	0.00777	0.00822
996	1	0.2095	B20X50 4F18LR	B9(25.03m)	0.5	0.2	0.018	0.00770	0.00815
997	1	0.2095	B20X50 4F18	B9(25.03m)	0.5	0.2	0.018	0.00770	0.00815
998	1	0.2095	B20X50 4F18LR	B9(25.03m)	0.5	0.2	0.018	0.00770	0.00815
974	1	0.2095	B20X50 4F18LR	B5(25.03m)	0.5	0.2	0.018	0.00770	0.00815
975	1	0.2095	B20X50 4F18	B5(25.03m)	0.5	0.2	0.018	0.00770	0.00815
976	1	0.2095	B20X50 4F18LR	B5(25.03m)	0.5	0.2	0.018	0.00770	0.00815
977	1	0.2102	B20X50 4F18LR	B19(25.03m)	0.5	0.2	0.018	0.00777	0.00822
978	1	0.2102	B20X50 4F18	B19(25.03m)	0.5	0.2	0.018	0.00777	0.00822
979	1	0.2102	B20X50 4F18LR	B19(25.03m)	0.5	0.2	0.018	0.00777	0.00822
1002	1	0.2102	B20X50 4F18LR	B20(25.03m)	0.5	0.2	0.018	0.00777	0.00822
1003	1	0.2102	B20X50 4F18	B20(25.03m)	0.5	0.2	0.018	0.00777	0.00822
1004	1	0.2102	B20X50 4F18LR	B20(25.03m)	0.5	0.2	0.018	0.00777	0.00822
278	1	0.1521	B20X50 4F18LR	B13(4m)	0.5	0.2	0.018	0.00508	0.00596
219	1	0.1556	B20X60 4F18LR	B16(4m)	0.6	0.2	0.018	0.00513	0.00536
222	1	0.1556	B20X60 4F18	B16(4m)	0.6	0.2	0.018	0.00513	0.00536
221	1	0.1556	B20X60 4F18LR	B16(4m)	0.6	0.2	0.018	0.00513	0.00536
342	1	0.1190	B20X60 4F18LR	B20(4m)	0.6	0.2	0.018	0.00509	0.00531
343	1	0.1190	B20X60 4F18	B20(4m)	0.6	0.2	0.018	0.00509	0.00531
344	1	0.1190	B20X60 4F18LR	B20(4m)	0.6	0.2	0.018	0.00509	0.00531
348	1	0.0845	B20X60 4F18LR	B19(4m)	0.6	0.2	0.018	0.00452	0.00469
349	1	0.0845	B20X60 4F18	B19(4m)	0.6	0.2	0.018	0.00452	0.00469
350	1	0.0845	B20X60 4F18LR	B19(4m)	0.6	0.2	0.018	0.00452	0.00469

345	1	0.1413	B20X60 4F18LR	B17(4m)	0.6	0.2	0.018	0.00494	0.00577
347	1	0.1413	B20X60 4F18LR	B17(4m)	0.6	0.2	0.018	0.00494	0.00577
449	1	0.1413	B20X60 4F18	B17(4m)	0.6	0.2	0.018	0.00494	0.00577
450	1	0.1413	B20X60 4F18	B17(4m)	0.6	0.2	0.018	0.00494	0.00577
386	1	0.0918	B20X60 4F18LR	B1(5.06m)	0.6	0.2	0.018	0.00460	0.00477
387	1	0.0918	B20X60 4F18	B1(5.06m)	0.6	0.2	0.018	0.00460	0.00477
388	1	0.0918	B20X60 4F18LR	B1(5.06m)	0.6	0.2	0.018	0.00460	0.00477
402	1	0.0882	B20X60 4F18	B2(5.06m)	0.6	0.2	0.018	0.00456	0.00473
407	1	0.0882	B20X60 4F18	B2(5.06m)	0.6	0.2	0.018	0.00456	0.00473
390	1	0.0882	B20X60 4F18LR	B2(5.06m)	0.6	0.2	0.018	0.00456	0.00473
391	1	0.0935	B20X60 4F18LR	B3(5.06m)	0.6	0.2	0.018	0.00462	0.00480
392	1	0.0935	B20X60 4F18	B3(5.06m)	0.6	0.2	0.018	0.00462	0.00480
393	1	0.0935	B20X60 4F18LR	B3(5.06m)	0.6	0.2	0.018	0.00462	0.00480
411	1	0.1450	B20X60 4F18LR	B13(5.06m)	0.6	0.2	0.018	0.00506	0.00591
412	1	0.1450	B20X60 4F18	B13(5.06m)	0.6	0.2	0.018	0.00506	0.00591
413	1	0.1450	B20X60 4F18LR	B13(5.06m)	0.6	0.2	0.018	0.00506	0.00591
445	1	0.1413	B20X60 4F18	B17(6.52m)	0.6	0.2	0.018	0.00494	0.00577
446	1	0.1621	B20X60 4F18	B17(6.52m)	0.6	0.2	0.018	0.00539	0.00564
447	1	0.1717	B20X60 4F18LR	B17(6.52m)	0.6	0.2	0.018	0.00586	0.00615
448	1	0.1796	B20X60 4F18LR	B17(6.52m)	0.6	0.2	0.018	0.00634	0.00666
383	1	0.0845	B20X60 4F18LR	B19(6.52m)	0.6	0.2	0.018	0.00452	0.00469
384	1	0.0845	B20X60 4F18	B19(6.52m)	0.6	0.2	0.018	0.00452	0.00469
385	1	0.0845	B20X60 4F18LR	B19(6.52m)	0.6	0.2	0.018	0.00452	0.00469
339	1	0.1190	B20X60 4F18LR	B20 (6.52m)	0.6	0.2	0.018	0.00509	0.00531
340	1	0.1190	B20X60 4F18	B20 (6.52m)	0.6	0.2	0.018	0.00509	0.00531
341	1	0.1190	B20X60 4F18LR	B20 (6.52m)	0.6	0.2	0.018	0.00509	0.00531
251	1	0.1556	B20X60 4F18LR	B16(6.52m)	0.6	0.2	0.018	0.00513	0.00536
252	1	0.1665	B20X60 4F18LR	B16(6.52m)	0.6	0.2	0.018	0.00559	0.00586
253	1	0.1753	B20X60 4F18	B16(6.52m)	0.6	0.2	0.018	0.00606	0.00637
486	1	0.0918	B20X60 4F18LR	B18(9.03m)	0.6	0.2	0.018	0.00460	0.00477
487	1	0.0918	B20X60 4F18	B18(9.03m)	0.6	0.2	0.018	0.00460	0.00477
488	1	0.0918	B20X60 4F18LR	B18(9.03m)	0.6	0.2	0.018	0.00460	0.00477
624	1	0.0882	B20X60 4F18LR	B17 (9.03m)	0.6	0.2	0.018	0.00456	0.00473
623	1	0.0882	B20X60 4F18	B17 (9.03m)	0.6	0.2	0.018	0.00456	0.00473
503	1	0.0882	B20X60 4F18	B17 (9.03m)	0.6	0.2	0.018	0.00456	0.00473
489	1	0.0882	B20X60 4F18LR	B17 (9.03m)	0.6	0.2	0.018	0.00456	0.00473
438	1	0.1413	B20X60 4F18LR	B32(9.03m)	0.6	0.2	0.018	0.00494	0.00577
439	1	0.1413	B20X60 4F18	B32(9.03m)	0.6	0.2	0.018	0.00494	0.00577
440	1	0.1413	B20X60 4F18	B32(9.03m)	0.6	0.2	0.018	0.00494	0.00577
441	1	0.1413	B20X60 4F18LR	B32(9.03m)	0.6	0.2	0.018	0.00494	0.00577
442	1	0.0845	B20X60 4F18LR	B33(9.03m)	0.6	0.2	0.018	0.00452	0.00469
443	1	0.0845	B20X60 4F18	B33(9.03m)	0.6	0.2	0.018	0.00452	0.00469
444	1	0.0845	B20X60 4F18LR	B33(9.03m)	0.6	0.2	0.018	0.00452	0.00469
312	1	0.1190	B20X60 4F18LR	B13(9.03m)	0.6	0.2	0.018	0.00509	0.00531
313	1	0.1190	B20X60 4F18	B13(9.03m)	0.6	0.2	0.018	0.00509	0.00531

314	1	0.1190	B20X60 4F18LR	B13(9.03m)	0.6	0.2	0.018	0.00509	0.00531
280	1	0.1556	B20X60 4F18LR	B14(9.03m)	0.6	0.2	0.018	0.00513	0.00536
281	1	0.1556	B20X60 4F18LR	B14(9.03m)	0.6	0.2	0.018	0.00513	0.00536
282	1	0.1556	B20X60 4F18	B14(9.03m)	0.6	0.2	0.018	0.00513	0.00536
490	1	0.0935	B20X60 4F18LR	B19(9.03m)	0.6	0.2	0.018	0.00462	0.00480
491	1	0.0935	B20X60 4F18	B19(9.03m)	0.6	0.2	0.018	0.00462	0.00480
492	1	0.0935	B20X60 4F18LR	B19(9.03m)	0.6	0.2	0.018	0.00462	0.00480
507	1	0.1450	B20X60 4F18LR	B28(9.03m)	0.6	0.2	0.018	0.00506	0.00591
508	1	0.1450	B20X60 4F18	B28(9.03m)	0.6	0.2	0.018	0.00506	0.00591
509	1	0.1450	B20X60 4F18LR	B28(9.03m)	0.6	0.2	0.018	0.00506	0.00591
408	1	0.1048	B20x60 4F16LR	B7(5.06m)	0.6	0.2	0.016	0.00464	0.00496
409	1	0.1048	B20X60 4F16	B7(5.06m)	0.6	0.2	0.016	0.00464	0.00496
410	1	0.1048	B20x60 4F16LR	B7(5.06m)	0.6	0.2	0.016	0.00464	0.00496
397	1	0.0990	B20x60 4F16LR	B6(5.06Mm)	0.6	0.2	0.016	0.00457	0.00487
400	1	0.0990	B20X60 4F16	B6(5.06Mm)	0.6	0.2	0.016	0.00457	0.00487
401	1	0.0990	B20X60 4F16	B6(5.06Mm)	0.6	0.2	0.016	0.00457	0.00487
274	1	0.0990	B20x60 4F16LR	B6(5.06Mm)	0.6	0.2	0.016	0.00457	0.00487
276	1	0.0990	B20x60 4F16LR	B6(5.06Mm)	0.6	0.2	0.016	0.00457	0.00487
237	1	0.1157	B20x60 4F16LR	B8(5.06m)	0.6	0.2	0.016	0.00481	0.00515
272	1	0.1157	B20X60 4F16	B8(5.06m)	0.6	0.2	0.016	0.00481	0.00515
417	1	0.1157	B20x60 4F16LR	B8(5.06m)	0.6	0.2	0.016	0.00481	0.00515
418	1	0.1157	B20x60 4F16LR	B8(5.06m)	0.6	0.2	0.016	0.00481	0.00515
422	1	0.1322	B20x60 4F16LR	B14(5.06m)	0.6	0.2	0.016	0.00515	0.00555
423	1	0.1322	B20X60 4F16	B14(5.06m)	0.6	0.2	0.016	0.00515	0.00555
424	1	0.1322	B20x60 4F16LR	B14(5.06m)	0.6	0.2	0.016	0.00515	0.00555
504	1	0.1048	B20x60 4F16LR	B26 (9.03m)	0.6	0.2	0.016	0.00464	0.00496
505	1	0.1048	B20X60 4F16	B26 (9.03m)	0.6	0.2	0.016	0.00464	0.00496
506	1	0.1048	B20x60 4F16LR	B26 (9.03m)	0.6	0.2	0.016	0.00464	0.00496
513	1	0.1157	B20x60 4F16LR	B25 (9.03m)	0.6	0.2	0.016	0.00481	0.00515
514	1	0.1157	B20X60 4F16	B25 (9.03m)	0.6	0.2	0.016	0.00481	0.00515
527	1	0.1157	B20x60 4F16LR	B25 (9.03m)	0.6	0.2	0.016	0.00481	0.00515
528	1	0.1157	B20x60 4F16LR	B25 (9.03m)	0.6	0.2	0.016	0.00481	0.00515
532	1	0.1322	B20x60 4F16LR	B29(9.03m)	0.6	0.2	0.016	0.00515	0.00555
533	1	0.1322	B20X60 4F16	B29(9.03m)	0.6	0.2	0.016	0.00515	0.00555
534	1	0.1322	B20x60 4F16LR	B29(9.03m)	0.6	0.2	0.016	0.00515	0.00555
496	1	0.0990	B20x60 4F16LR	B21(9.03m)	0.6	0.2	0.016	0.00457	0.00487
497	1	0.0990	B20X60 4F16	B21(9.03m)	0.6	0.2	0.016	0.00457	0.00487
498	1	0.0990	B20X60 4F16	B21(9.03m)	0.6	0.2	0.016	0.00457	0.00487
515	1	0.0990	B20x60 4F16LR	B21(9.03m)	0.6	0.2	0.016	0.00457	0.00487
516	1	0.0990	B20x60 4F16LR	B21(9.03m)	0.6	0.2	0.016	0.00457	0.00487
206	1	0.1399	B20X42 4F14	B1(4m)	0.42	0.2	0.014	0.00609	0.00646

207	1	0.1399	B20X42 F414L	B1(4m)	0.42	0.2	0.014	0.00609	0.00646
209	1	0.1399	B20X42 4F14R	B1(4m)	0.42	0.2	0.014	0.00609	0.00646
1222	1	0.1019	B20X42 F414L	B2(4m)	0.42	0.2	0.014	0.00462	0.00547
1223	1	0.1019	B20X42 4F14	B2(4m)	0.42	0.2	0.014	0.00462	0.00547
1224	1	0.1019	B20X42 4F14R	B2(4m)	0.42	0.2	0.014	0.00462	0.00547
234	1	0.1481	B20X42 4F14R	B1(4m)	0.42	0.2	0.014	0.00678	0.00722
213	1	0.1327	B20X42 F414L	B14(4m)	0.42	0.2	0.014	0.00561	0.00594
214	1	0.1327	B20X42 4F14	B14(4m)	0.42	0.2	0.014	0.00561	0.00594
215	1	0.1327	B20X42 4F14R	B14(4m)	0.42	0.2	0.014	0.00561	0.00594
216	1	0.0655	B20X42 F414L	B15 (4m)	0.42	0.2	0.014	0.00454	0.00474
217	1	0.0655	B20X42 4F14	B15 (4m)	0.42	0.2	0.014	0.00454	0.00474
218	1	0.0655	B20X42 4F14R	B15 (4m)	0.42	0.2	0.014	0.00454	0.00474
275	1	0.1404	B20X42 4F14R	B1(6.52m)	0.42	0.2	0.014	0.00612	0.00650
240	1	0.1404	B20X42 F414L	B1(6.52m)	0.42	0.2	0.014	0.00612	0.00650
714	1	0.1404	B20X42 4F14	B1(6.52m)	0.42	0.2	0.014	0.00612	0.00650
715	1	0.1404	B20X42 4F14	B1(6.52m)	0.42	0.2	0.014	0.00612	0.00650
241	1	0.1404	B20X42 4F14R	B1(6.52m)	0.42	0.2	0.014	0.00612	0.00650
242	1	0.1038	B20X42 F414L	B2(6.52m)	0.42	0.2	0.014	0.00468	0.00553
243	1	0.1038	B20X42 4F14	B2(6.52m)	0.42	0.2	0.014	0.00468	0.00553
244	1	0.1038	B20X42 4F14R	B2(6.52m)	0.42	0.2	0.014	0.00468	0.00553
245	1	0.1327	B20X42 F414L	B14(6.52m)	0.42	0.2	0.014	0.00561	0.00594
246	1	0.1327	B20X42 4F14	B14(6.52m)	0.42	0.2	0.014	0.00561	0.00594
247	1	0.1327	B20X42 4F14R	B14(6.52m)	0.42	0.2	0.014	0.00561	0.00594
248	1	0.0655	B20X42 F414L	B15(6.52m)	0.42	0.2	0.014	0.00454	0.00474
249	1	0.0655	B20X42 4F14	B15(6.52m)	0.42	0.2	0.014	0.00454	0.00474
250	1	0.0655	B20X42 4F14R	B15(6.52m)	0.42	0.2	0.014	0.00454	0.00474
30	1	0.1027	B20X50 4F14LR	B9(4m)	0.5	0.2	0.014	0.00453	0.00538
31	1	0.1027	B20X50 4F14	B9(4m)	0.5	0.2	0.014	0.00453	0.00538
233	1	0.1027	B20X50 4F14LR	B9(4m)	0.5	0.2	0.014	0.00453	0.00538
231	1	0.1295	B20X50 4F14LR	B10(4m)	0.5	0.2	0.014	0.00536	0.00568
232	1	0.1295	B20X50 4F14	B10(4m)	0.5	0.2	0.014	0.00536	0.00568
235	1	0.1295	B20X50 4F14LR	B10(4m)	0.5	0.2	0.014	0.00536	0.00568
378	1	0.1027	B20X50 4F14LR	B9(6.52m)	0.5	0.2	0.014	0.00453	0.00538
379	1	0.1027	B20X50 4F14LR	B9(6.52m)	0.5	0.2	0.014	0.00453	0.00538
380	1	0.1027	B20X50 4F14	B9(6.52m)	0.5	0.2	0.014	0.00453	0.00538
377	1	0.1295	B20X50 4F14LR	B10(6.52m)	0.5	0.2	0.014	0.00536	0.00568
381	1	0.1295	B20X50 4F14	B10(6.52m)	0.5	0.2	0.014	0.00536	0.00568
382	1	0.1295	B20X50 4F14LR	B10(6.52m)	0.5	0.2	0.014	0.00536	0.00568
451	1	0.1170	B20X50 4F14LR	B10(9.03m)	0.5	0.2	0.014	0.00478	0.00505
452	1	0.1170	B20X50 4F14	B10(9.03m)	0.5	0.2	0.014	0.00478	0.00505
455	1	0.1170	B20X50 4F14LR/F12	B10(9.03m)	0.5	0.2	0.014	0.00478	0.00505
457	1	0.1208	B20X50 4F14LR/F12	B11(9.03m)	0.5	0.2	0.014	0.00493	0.00522
458	1	0.1208	B20X50 4F14	B11(9.03m)	0.5	0.2	0.014	0.00493	0.00522

459	1	0.1208	B20X50 4F14LR	B11(9.03m)	0.5	0.2	0.014	0.00493	0.00522
2	1	0.1268	B20X35 4F14LR	B3(4m)	0.35	0.2	0.014	0.00703	0.00753
3	1	0.1268	B20X35 4F14	B3(4m)	0.35	0.2	0.014	0.00703	0.00753
10	1	0.1268	B20X35 4F14LR	B3(4m)	0.35	0.2	0.014	0.00703	0.00753
210	1	0.1133	B20X35 4F14LR	B4(4m)	0.35	0.2	0.014	0.00589	0.00627
11	1	0.1133	B20X35 4F14LR	B4(4m)	0.35	0.2	0.014	0.00589	0.00627
156	1	0.1133	B20X35 4F14	B4(4m)	0.35	0.2	0.014	0.00589	0.00627
157	1	0.1133	B20X35 4F14LR	B4(4m)	0.35	0.2	0.014	0.00589	0.00627
164	1	0.1097	B20X35 4F14LR	B5(4m)	0.35	0.2	0.014	0.00567	0.00602
664	1	0.1097	B20X35 4F14	B5(4m)	0.35	0.2	0.014	0.00567	0.00602
665	1	0.1097	B20X35 4F14	B5(4m)	0.35	0.2	0.014	0.00567	0.00602
208	1	0.1097	B20X35 4F14LR	B5(4m)	0.35	0.2	0.014	0.00567	0.00602
257	1	0.1268	B20X35 4F14LR	B3(6.52m)	0.35	0.2	0.014	0.00703	0.00753
258	1	0.1268	B20X35 4F14	B3(6.52m)	0.35	0.2	0.014	0.00703	0.00753
259	1	0.1268	B20X35 4F14LR	B3(6.52m)	0.35	0.2	0.014	0.00703	0.00753
211	1	0.1133	B20X35 4F14LR	B4(6.52m)	0.35	0.2	0.014	0.00589	0.00627
212	1	0.1133	B20X35 4F14LR	B4(6.52m)	0.35	0.2	0.014	0.00589	0.00627
261	1	0.1133	B20X35 4F14	B4(6.52m)	0.35	0.2	0.014	0.00589	0.00627
262	1	0.1133	B20X35 4F14LR	B4(6.52m)	0.35	0.2	0.014	0.00589	0.00627
263	1	0.1097	B20X35 4F14LR	B5(6.52m)	0.35	0.2	0.014	0.00567	0.00602
265	1	0.1097	B20X35 4F14LR	B5(6.52m)	0.35	0.2	0.014	0.00567	0.00602
662	1	0.1097	B20X35 4F14	B5(6.52m)	0.35	0.2	0.014	0.00567	0.00602
663	1	0.1097	B20X35 4F14	B5(6.52m)	0.35	0.2	0.014	0.00567	0.00602
433	1	0.1133	B20X35 4F14LR	B3(9.03m)	0.35	0.2	0.014	0.00589	0.00627
434	1	0.1133	B20X35 4F14LR	B3(9.03m)	0.35	0.2	0.014	0.00589	0.00627
302	1	0.1133	B20X35 4F14	B3(9.03m)	0.35	0.2	0.014	0.00589	0.00627
303	1	0.1133	B20X35 4F14LR	B3(9.03m)	0.35	0.2	0.014	0.00589	0.00627
304	1	0.1097	B20X35 4F14LR	B4(9.03m)	0.35	0.2	0.014	0.00567	0.00602
260	1	0.1097	B20X35 4F14	B4(9.03m)	0.35	0.2	0.014	0.00567	0.00602
660	1	0.1097	B20X35 4F14	B4(9.03m)	0.35	0.2	0.014	0.00567	0.00602
306	1	0.1097	B20X35 4F14LR	B4(9.03m)	0.35	0.2	0.014	0.00567	0.00602
330	1	0.0446	B20X50 4F12LR	B12 (9.03m)	0.5	0.2	0.012	0.00447	0.00434
331	1	0.0446	B20X50 4F12	B12 (9.03m)	0.5	0.2	0.012	0.00447	0.00434
332	1	0.0446	B20X50 4F12LR	B12 (9.03m)	0.5	0.2	0.012	0.00447	0.00434
679	1	0.0837	B20X50 4F12LR/F14	B15(12.23m)	0.5	0.2	0.012	0.00447	0.00431
680	1	0.0837	B20X50 4F12	B15(12.23m)	0.5	0.2	0.012	0.00447	0.00431
681	1	0.0837	B20X50 4F12LR	B15(12.23m)	0.5	0.2	0.012	0.00447	0.00431
CB15A	1	0.0837	B20X50 4F12LR/F14	B15(15.43m)	0.5	0.2	0.012	0.00447	0.00431
CB15B	1	0.0837	B20X50 4F12	B15(15.43m)	0.5	0.2	0.012	0.00447	0.00431
CB15C	1	0.0837	B20X50 4F12LR	B15(15.43m)	0.5	0.2	0.012	0.00447	0.00431

831	1	0.0837	B20X50 4F12LR/F14	B15(18.63m)	0.5	0.2	0.012	0.00447	0.00431
832	1	0.0837	B20X50 4F12	B15(18.63m)	0.5	0.2	0.012	0.00447	0.00431
833	1	0.0837	B20X50 4F12LR	B15(18.63m)	0.5	0.2	0.012	0.00447	0.00431
944	1	0.0837	B20X50 4F12LR/F14	B15(21.83m)	0.5	0.2	0.012	0.00447	0.00431
945	1	0.0837	B20X50 4F12	B15(21.83m)	0.5	0.2	0.012	0.00447	0.00431
946	1	0.0837	B20X50 4F12LR	B15(21.83m)	0.5	0.2	0.012	0.00447	0.00431
1057	1	0.0837	B20X50 4F12LR/F14	B15(25.03m)	0.5	0.2	0.012	0.00447	0.00431
1058	1	0.0837	B20X50 4F12	B15(25.03m)	0.5	0.2	0.012	0.00447	0.00431
1059	1	0.0837	B20X50 4F12LR	B15(25.03m)	0.5	0.2	0.012	0.00447	0.00431
324	1	0.1346	B20X45 4F14LR	B2(9.03m)	0.45	0.2	0.014	0.00514	0.00566
325	1	0.1346	B20X45 4F14	B2(9.03m)	0.45	0.2	0.014	0.00514	0.00566
326	1	0.1346	B20X45 4F14LR	B2(9.03m)	0.45	0.2	0.014	0.00514	0.00566
656	1	0.1086	B20X45 4F14LR	B11(12.23m)	0.45	0.2	0.014	0.00448	0.00550
657	1	0.1086	B20X45 4F14LR	B11(12.23m)	0.45	0.2	0.014	0.00448	0.00550
658	1	0.1086	B20X45 4F14	B11(12.23m)	0.45	0.2	0.014	0.00448	0.00550
659	1	0.1086	B20X45 4F14LR	B11(12.23m)	0.45	0.2	0.014	0.00448	0.00550
666	1	0.1039	B20X45 4F14LR	B12(12.23m0	0.45	0.2	0.014	0.00435	0.00535
667	1	0.1039	B20X45 4F14	B12(12.23m1	0.45	0.2	0.014	0.00435	0.00535
668	1	0.1039	B20X45 4F14	B12(12.23m2	0.45	0.2	0.014	0.00435	0.00535
669	1	0.1039	B20X45 4F14LR	B12(12.23m3	0.45	0.2	0.014	0.00435	0.00535
CB11A	1	0.1086	B20X45 4F14LR	B11(15.43m)	0.45	0.2	0.014	0.00448	0.00550
CB11B	1	0.1086	B20X45 4F14LR	B11(15.43m)	0.45	0.2	0.014	0.00448	0.00550
CB11C	1	0.1086	B20X45 4F14	B11(15.43m)	0.45	0.2	0.014	0.00448	0.00550
CB11D	1	0.1086	B20X45 4F14LR	B11(15.43m)	0.45	0.2	0.014	0.00448	0.00550
CB12A	1	0.1039	B20X45 4F14LR	B12 (15.43m)	0.45	0.2	0.014	0.00435	0.00535
CB12B	1	0.1039	B20X45 4F14	B12 (15.43m)	0.45	0.2	0.014	0.00435	0.00535
CB12C	1	0.1039	B20X45 4F14	B12	0.45	0.2	0.014	0.00435	0.00535

				(15.43m)					
CB12D	1	0.1039	B20X45 4F14LR	B12 (15.43m)	0.45	0.2	0.014	0.00435	0.00535
814	1	0.1086	B20X45 4F14LR	B11(18.63m)	0.45	0.2	0.014	0.00448	0.00550
815	1	0.1086	B20X45 4F14LR	B11(18.63m)	0.45	0.2	0.014	0.00448	0.00550
816	1	0.1086	B20X45 4F14	B11(18.63m)	0.45	0.2	0.014	0.00448	0.00550
817	1	0.1086	B20X45 4F14LR	B11(18.63m)	0.45	0.2	0.014	0.00448	0.00550
818	1	0.1039	B20X45 4F14LR	B12(18.63m)	0.45	0.2	0.014	0.00435	0.00535
819	1	0.1039	B20X45 4F14	B12(18.63m)	0.45	0.2	0.014	0.00435	0.00535
820	1	0.1039	B20X45 4F14	B12(18.63m)	0.45	0.2	0.014	0.00435	0.00535
821	1	0.1039	B20X45 4F14LR	B12(18.63m)	0.45	0.2	0.014	0.00435	0.00535
927	1	0.1086	B20X45 4F14LR	B11(21.83m)	0.45	0.2	0.014	0.00448	0.00550
928	1	0.1086	B20X45 4F14LR	B11(21.83m)	0.45	0.2	0.014	0.00448	0.00550
929	1	0.1086	B20X45 4F14	B11(21.83m)	0.45	0.2	0.014	0.00448	0.00550
930	1	0.1086	B20X45 4F14LR	B11(21.83m)	0.45	0.2	0.014	0.00448	0.00550
931	1	0.1039	B20X45 4F14LR	B12(21.83m)	0.45	0.2	0.014	0.00435	0.00535
932	1	0.1039	B20X45 4F14	B12(21.83m)	0.45	0.2	0.014	0.00435	0.00535
933	1	0.1039	B20X45 4F14	B12(21.83m)	0.45	0.2	0.014	0.00435	0.00535
934	1	0.1039	B20X45 4F14LR	B12(21.83m)	0.45	0.2	0.014	0.00435	0.00535
1040	1	0.1086	B20X45 4F14LR	B11(25.03m)	0.45	0.2	0.014	0.00448	0.00550
1041	1	0.1086	B20X45 4F14LR	B11(25.03m)	0.45	0.2	0.014	0.00448	0.00550
1042	1	0.1086	B20X45 4F14	B11(25.03m)	0.45	0.2	0.014	0.00448	0.00550
1043	1	0.1086	B20X45 4F14LR	B11(25.03m)	0.45	0.2	0.014	0.00448	0.00550
1044	1	0.1039	B20X45 4F14LR	B12(25.03m)	0.45	0.2	0.014	0.00435	0.00535
1045	1	0.1039	B20X45 4F14	B12(25.03m)	0.45	0.2	0.014	0.00435	0.00535
1046	1	0.1039	B20X45 4F14	B12(25.03m)	0.45	0.2	0.014	0.00435	0.00535
1047	1	0.1039	B20X45 4F14LR	B12(25.03m	0.45	0.2	0.014	0.00435	0.00535

				)					
327	1	0.1286	B25X50 4F16LR	B1(9.03m)	0.5	0.25	0.016	0.00526	0.00567
328	1	0.1286	B25X50 4F16	B1(9.03m)	0.5	0.25	0.016	0.00526	0.00567
329	1	0.1286	B25X50 4F16LR	B1(9.03m)	0.5	0.25	0.016	0.00526	0.00567
364	1	0.1286	B25X50 4F16	B1(9.03m)	0.5	0.25	0.016	0.00526	0.00567
616	1	0.0520	B25X65 2F14+2F16LR	B1(12.23m)	0.65	0.25	0.016	0.00418	0.00460
617	1	0.0520	B25X65 2F14+2F16	B1(12.23m)	0.65	0.25	0.016	0.00418	0.00460
618	1	0.0520	B25X65 2F14+2F16LR	B1(12.23m)	0.65	0.25	0.016	0.00418	0.00460
628	1	0.0500	B25X65 2F14+2F16LR	B2(12.23m)	0.65	0.25	0.016	0.00414	0.00456
629	1	0.0500	B25X65 2F14+2F16	B2(12.23m)	0.65	0.25	0.016	0.00414	0.00456
630	1	0.0500	B25X65 2F14+2F16	B2(12.23m)	0.65	0.25	0.016	0.00414	0.00456
631	1	0.0500	B25X65 2F14+2F16LR/F18	B2(12.23m)	0.65	0.25	0.016	0.00414	0.00456
549	1	0.0530	B25X65 2F14+2F16LR	B18(12.23m)	0.65	0.25	0.016	0.00420	0.00462
550	1	0.0530	B25X65 2F14+2F16	B18(12.23m)	0.65	0.25	0.016	0.00420	0.00462
682	1	0.0530	B25X65 2F14+2F16LR/F16	B18(12.23m)	0.65	0.25	0.016	0.00420	0.00462
563	1	0.0544	B25X65 2F14+2F16LR/F16	B23(12.23m)	0.65	0.25	0.016	0.00424	0.00465
564	1	0.0544	B25X65 2F14+2F16	B23(12.23m)	0.65	0.25	0.016	0.00424	0.00465
565	1	0.0544	B25X65 2F14+2F16LR/F16	B23(12.23m)	0.65	0.25	0.016	0.00424	0.00465
636	1	0.0478	B25X65 2F14+2F16LR/F14	B4(12.23m)	0.65	0.25	0.016	0.00410	0.00453
637	1	0.0478	B25X65 2F14+2F16	B4(12.23m)	0.65	0.25	0.016	0.00410	0.00453
638	1	0.0478	B25X65 2F14+2F16LR	B4(12.23m)	0.65	0.25	0.016	0.00410	0.00453
477	1	0.0675	B25X65 2F14+2F16LR	B22(12.23m)	0.65	0.25	0.016	0.00470	0.00504
478	1	0.0675	B25X65 2F14+2F16	B22(12.23m)	0.65	0.25	0.016	0.00470	0.00504

479	1	0.0675	B25X65 2F14+2F16LR/F20	B22(12.23m)	0.65	0.25	0.016	0.00470	0.00504
CB4A	1	0.0478	B25X65 2F14+2F16LR/F14	B4(15.43m)	0.65	0.25	0.016	0.00410	0.00453
CB4B	1	0.0478	B25X65 2F14+2F16	B4(15.43m)	0.65	0.25	0.016	0.00410	0.00453
CB4D	1	0.0478	B25X65 2F14+2F16LR	B4(15.43m)	0.65	0.25	0.016	0.00410	0.00453
CB1A	1	0.0520	B25X65 2F14+2F16LR	B1(15.43m)	0.65	0.25	0.016	0.00418	0.00460
CB1B	1	0.0520	B25X65 2F14+2F16	B1(15.43m)	0.65	0.25	0.016	0.00418	0.00460
CB1C	1	0.0520	B25X65 2F14+2F16LR	B1(15.43m)	0.65	0.25	0.016	0.00418	0.00460
CB2A	1	0.0500	B25X65 2F14+2F16LR	B2(15.43m)	0.65	0.25	0.016	0.00414	0.00456
CB2B	1	0.0500	B25X65 2F14+2F16	B2(15.43m)	0.65	0.25	0.016	0.00414	0.00456
CB2C	1	0.0500	B25X65 2F14+2F16	B2(15.43m)	0.65	0.25	0.016	0.00414	0.00456
CB2D	1	0.0500	B25X65 2F14+2F16LR/F18	B2(15.43m)	0.65	0.25	0.016	0.00414	0.00456
CB18A	1	0.0530	B25X65 2F14+2F16LR	B18(15.43m)	0.65	0.25	0.016	0.00420	0.00462
CB18B	1	0.0530	B25X65 2F14+2F16	B18(15.43m)	0.65	0.25	0.016	0.00420	0.00462
CB18C	1	0.0530	B25X65 2F14+2F16LR/F16	B18(15.43m)	0.65	0.25	0.016	0.00420	0.00462
CB23A	1	0.0544	B25X65 2F14+2F16LR/F16	B23(15.43m)	0.65	0.25	0.016	0.00424	0.00465
CB23B	1	0.0544	B25X65 2F14+2F16	B23(15.43m)	0.65	0.25	0.016	0.00424	0.00465
CB23C	1	0.0544	B25X65 2F14+2F16LR/F16	B23(15.43m)	0.65	0.25	0.016	0.00424	0.00465
CB22A	1	0.0675	B25X65 2F14+2F16LR	B22(15.43m)	0.65	0.25	0.016	0.00470	0.00504
CB22B	1	0.0675	B25X65 2F14+2F16	B22(15.43m)	0.65	0.25	0.016	0.00470	0.00504
CB22C	1	0.0675	B25X65 2F14+2F16LR/F20	B22(15.43m)	0.65	0.25	0.016	0.00470	0.00504
474	1	0.0530	B25X65 2F14+2F16LR	B18(18.63m)	0.65	0.25	0.016	0.00420	0.00462
475	1	0.0530	B25X65 2F14+2F16	B18(18.63m)	0.65	0.25	0.016	0.00420	0.00462

834	1	0.0530	B25X65 2F14+2F16LR/F16	B18(18.63m)	0.65	0.25	0.016	0.00420	0.00462
541	1	0.0544	B25X65 2F14+2F16LR/F16	B23(18.63m)	0.65	0.25	0.016	0.00424	0.00465
545	1	0.0544	B25X65 2F14+2F16	B23(18.63m)	0.65	0.25	0.016	0.00424	0.00465
546	1	0.0544	B25X65 2F14+2F16LR/F16	B23(18.63m)	0.65	0.25	0.016	0.00424	0.00465
859	1	0.0530	B25X65 2F14+2F16LR	B18(21.83m)	0.65	0.25	0.016	0.00420	0.00462
860	1	0.0530	B25X65 2F14+2F16	B18(21.83m)	0.65	0.25	0.016	0.00420	0.00462
947	1	0.0530	B25X65 2F14+2F16LR/F16	B18(21.83m)	0.65	0.25	0.016	0.00420	0.00462
867	1	0.0530	B25X65 2F14+2F16LR/F16	B23(21.83m)	0.65	0.25	0.016	0.00420	0.00462
868	1	0.0530	B25X65 2F14+2F16	B23(21.83m)	0.65	0.25	0.016	0.00420	0.00462
869	1	0.0530	B25X65 2F14+2F16LR/F16	B23(21.83m)	0.65	0.25	0.016	0.00420	0.00462
972	1	0.0530	B25X65 2F14+2F16LR	B18(25.03m)	0.65	0.25	0.016	0.00420	0.00462
973	1	0.0530	B25X65 2F14+2F16	B18(25.03m)	0.65	0.25	0.016	0.00420	0.00462
1060	1	0.0530	B25X65 2F14+2F16LR/F16	B18(25.03m)	0.65	0.25	0.016	0.00420	0.00462
980	1	0.0544	B25X65 2F14+2F16LR/F16	B23(25.03m)	0.65	0.25	0.016	0.00424	0.00465
981	1	0.0544	B25X65 2F14+2F16	B23(25.03m)	0.65	0.25	0.016	0.00424	0.00465
982	1	0.0544	B25X65 2F14+2F16LR/F16	B23(25.03m)	0.65	0.25	0.016	0.00424	0.00465
460	1	0.1165	B25X65 4F18LR/F20	B29(12.23m)	0	0	0	0.00000	0.00000
461	1	0.1165	B25X65 4F18LR	B29(12.23m)	0	0	0	0.00000	0.00000
462	1	0.1165	B25X65 4F18	B29(12.23m)	0	0	0	0.00000	0.00000
CB29A	1	0.1176	B25X65 4F18LR/F20	B29(15.43m)	0	0	0	0.00000	0.00000
CB29B	1	0.1176	B25X65 4F18	B29(15.43m)	0	0	0	0.00000	0.00000

CB29C	1	0.1176	B25X65 4F18LR	B29(15.43m)	0	0	0	0.00000	0.00000
650	1	0.0568	B25X65 4F16LR	B8(12.23m)	0.65	0.25	0.016	0.00488	0.00465
651	1	0.0568	B25X65 4F16	B8(12.23m)	0.65	0.25	0.016	0.00488	0.00465
652	1	0.0568	B25X65 4F16LR	B8(12.23m)	0.65	0.25	0.016	0.00488	0.00465
639	1	0.0533	B25X65 4F16LR	B6(12.23m)	0.65	0.25	0.016	0.00480	0.00459
640	1	0.0533	B25X65 4F16	B6(12.23m)	0.65	0.25	0.016	0.00480	0.00459
641	1	0.0533	B25X65 4F16	B6(12.23m)	0.65	0.25	0.016	0.00480	0.00459
644	1	0.0533	B25X65 4F16LR/2F16	B6(12.23m)	0.65	0.25	0.016	0.00480	0.00459
645	1	0.0533	B25X65 4F16LR/2F16	B6(12.23m)	0.65	0.25	0.016	0.00480	0.00459
CB8A	1	0.0568	B25X65 4F16LR	B8(15.43m)	0.65	0.25	0.016	0.00488	0.00465
CB8B	1	0.0568	B25X65 4F16	B8(15.43m)	0.65	0.25	0.016	0.00488	0.00465
CB8C	1	0.0568	B25X65 4F16LR	B8(15.43m)	0.65	0.25	0.016	0.00488	0.00465
CB6A	1	0.0533	B25X65 4F16LR	B6(15.43m)	0.65	0.25	0.016	0.00480	0.00459
CB6B	1	0.0533	B25X65 4F16	B6(15.43m)	0.65	0.25	0.016	0.00480	0.00459
CB6C	1	0.0533	B25X65 4F16	B6(15.43m)	0.65	0.25	0.016	0.00480	0.00459
CB6D	1	0.0533	B25X65 4F16LR/2F16	B6(15.43m)	0.65	0.25	0.016	0.00480	0.00459
CB6E	1	0.0533	B25X65 4F16LR/2F16	B6(15.43m)	0.65	0.25	0.016	0.00480	0.00459
808	1	0.0568	B25X65 4F16LR	B8(18.63m)	0.65	0.25	0.016	0.00488	0.00465
809	1	0.0568	B25X65 4F16	B8(18.63m)	0.65	0.25	0.016	0.00488	0.00465
810	1	0.0568	B25X65 4F16LR	B8(18.63m)	0.65	0.25	0.016	0.00488	0.00465
799	1	0.0533	B25X65 4F16LR	B6(18.63m)	0.65	0.25	0.016	0.00480	0.00459
800	1	0.0533	B25X65 4F16	B6(18.63m)	0.65	0.25	0.016	0.00480	0.00459
801	1	0.0533	B25X65 4F16	B6(18.63m)	0.65	0.25	0.016	0.00480	0.00459
802	1	0.0533	B25X65 4F16LR/2F16	B6(18.63m)	0.65	0.25	0.016	0.00480	0.00459
803	1	0.0533	B25X65 4F16LR/2F16	B6(18.63m)	0.65	0.25	0.016	0.00480	0.00459

921	1	0.0568	B25X65 4F16LR	B8(21.83m)	0.65	0.25	0.016	0.00488	0.00465
922	1	0.0568	B25X65 4F16	B8(21.83m)	0.65	0.25	0.016	0.00488	0.00465
923	1	0.0568	B25X65 4F16LR	B8(21.83m)	0.65	0.25	0.016	0.00488	0.00465
912	1	0.0533	B25X65 4F16LR	B6(21.83m)	0.65	0.25	0.016	0.00480	0.00459
913	1	0.0533	B25X65 4F16	B6(21.83m)	0.65	0.25	0.016	0.00480	0.00459
914	1	0.0533	B25X65 4F16	B6(21.83m)	0.65	0.25	0.016	0.00480	0.00459
915	1	0.0533	B25X65 4F16LR/2F16	B6(21.83m)	0.65	0.25	0.016	0.00480	0.00459
916	1	0.0533	B25X65 4F16LR/2F16	B6(21.83m)	0.65	0.25	0.016	0.00480	0.00459
1034	1	0.0568	B25X65 4F16LR	B8(25.03m)	0.65	0.25	0.016	0.00488	0.00465
1035	1	0.0568	B25X65 4F16	B8(25.03m)	0.65	0.25	0.016	0.00488	0.00465
1036	1	0.0568	B25X65 4F16LR	B8(25.03m)	0.65	0.25	0.016	0.00488	0.00465
1025	1	0.0533	B25X65 4F16LR	B6(25.03m)	0.65	0.25	0.016	0.00480	0.00459
1026	1	0.0533	B25X65 4F16	B6(25.03m)	0.65	0.25	0.016	0.00480	0.00459
1027	1	0.0533	B25X65 4F16	B6(25.03m)	0.65	0.25	0.016	0.00480	0.00459
1028	1	0.0533	B25X65 4F16LR/2F16	B6(25.03m)	0.65	0.25	0.016	0.00480	0.00459
1029	1	0.0533	B25X65 4F16LR/2F16	B6(25.03m)	0.65	0.25	0.016	0.00480	0.00459
646	1	0.1345	B25X65 4F20LR/2F16	B7(12.23m)	0.65	0.25	0.02	0.00494	0.00577
647	1	0.1345	B25X65 4F20	B7(12.23m)	0.65	0.25	0.02	0.00494	0.00577
648	1	0.1345	B25X65 4F20	B7(12.23m)	0.65	0.25	0.02	0.00494	0.00577
649	1	0.1345	B25X65 4F20LR	B7(12.23m)	0.65	0.25	0.02	0.00494	0.00577
CB7A	1	0.1345	B25X65 4F20LR/2F16	B7(15.43m)	0.65	0.25	0.02	0.00494	0.00577
CB7B	1	0.1345	B25X65 4F20	B7(15.43m)	0.65	0.25	0.02	0.00494	0.00577
CB7C	1	0.1345	B25X65 4F20	B7(15.43m)	0.65	0.25	0.02	0.00494	0.00577
CB7D	1	0.1345	B25X65 4F20LR	B7(15.43m)	0.65	0.25	0.02	0.00494	0.00577
804	1	0.1345	B25X65 4F20LR/2F16	B7(18.63m)	0.65	0.25	0.02	0.00494	0.00577

805	1	0.1345	B25X65 4F20	B7(18.63m)	0.65	0.25	0.02	0.00494	0.00577
806	1	0.1345	B25X65 4F20	B7(18.63m)	0.65	0.25	0.02	0.00494	0.00577
807	1	0.1345	B25X65 4F20LR	B7(18.63m)	0.65	0.25	0.02	0.00494	0.00577
917	1	0.1345	B25X65 4F20LR/2F16	B7(21.83m)	0.65	0.25	0.02	0.00494	0.00577
918	1	0.1345	B25X65 4F20	B7(21.83m)	0.65	0.25	0.02	0.00494	0.00577
919	1	0.1345	B25X65 4F20	B7(21.83m)	0.65	0.25	0.02	0.00494	0.00577
920	1	0.1345	B25X65 4F20LR	B7(21.83m)	0.65	0.25	0.02	0.00494	0.00577
1030	1	0.1345	B25X65 4F20LR/2F16	B7(25.03m)	0.65	0.25	0.02	0.00494	0.00577
1031	1	0.1345	B25X65 4F20	B7(25.03m)	0.65	0.25	0.02	0.00494	0.00577
1032	1	0.1345	B25X65 4F20	B7(25.03m)	0.65	0.25	0.02	0.00494	0.00577
1033	1	0.1345	B25X65 4F20LR	B7(25.03m)	0.65	0.25	0.02	0.00494	0.00577
613	1	0.0967	B20X60 2F14+2F16LR/F12	B28(12.23m)	0.6	0.2	0.016	0.00489	0.00524
614	1	0.0967	B20X60 2F14+2F16	B28(12.23m)	0.6	0.2	0.016	0.00489	0.00524
615	1	0.0967	B20X60 2F14+2F16LR	B28(12.23m)	0.6	0.2	0.016	0.00489	0.00524
610	1	0.0931	B20X60 2F14+2F16LR	B21(12.23m)	0.6	0.2	0.016	0.00475	0.00512
611	1	0.0931	B20X60 2F14+2F16	B21(12.23m)	0.6	0.2	0.016	0.00475	0.00512
612	1	0.0931	B20X60 2F14+2F16LR/F12	B21(12.23m)	0.6	0.2	0.016	0.00475	0.00512
CB21A	1	0.0931	B20X60 2F14+2F16LR	B21(15.43m)	0.6	0.2	0.016	0.00475	0.00512
CB21B	1	0.0931	B20X60 2F14+2F16	B21(15.43m)	0.6	0.2	0.016	0.00475	0.00512
CB21C	1	0.0931	B20X60 2F14+2F16LR/F12	B21(15.43m)	0.6	0.2	0.016	0.00475	0.00512
CB28A	1	0.0967	B20X60 2F14+2F16LR/F12	B28(15.43m)	0.6	0.2	0.016	0.00489	0.00524
CB28B	1	0.0967	B20X60 2F14+2F16	B28(15.43m)	0.6	0.2	0.016	0.00489	0.00524
CB28C	1	0.0967	B20X60 2F14+2F16LR	B28(15.43m)	0.6	0.2	0.016	0.00489	0.00524

599	1	0.0931	B20X60 2F14+2F16LR	B21(18.63m)	0.6	0.2	0.016	0.00475	0.00512
603	1	0.0931	B20X60 2F14+2F16	B21(18.63m)	0.6	0.2	0.016	0.00475	0.00512
604	1	0.0931	B20X60 2F14+2F16LR/F12	B21(18.63m)	0.6	0.2	0.016	0.00475	0.00512
605	1	0.0967	B20X60 2F14+2F16LR/F12	B28(18.63m)	0.6	0.2	0.016	0.00489	0.00524
606	1	0.0967	B20X60 2F14+2F16	B28(18.63m)	0.6	0.2	0.016	0.00489	0.00524
607	1	0.0967	B20X60 2F14+2F16LR	B28(18.63m)	0.6	0.2	0.016	0.00489	0.00524
892	1	0.0931	B20X60 2F14+2F16LR	B21(21.83m)	0.6	0.2	0.016	0.00475	0.00512
893	1	0.0931	B20X60 2F14+2F16	B21(21.83m)	0.6	0.2	0.016	0.00475	0.00512
894	1	0.0931	B20X60 2F14+2F16LR/F12	B21(21.83m)	0.6	0.2	0.016	0.00475	0.00512
895	1	0.0967	B20X60 2F14+2F16LR/F12	B28(21.83m)	0.6	0.2	0.016	0.00489	0.00524
896	1	0.0967	B20X60 2F14+2F16	B28(21.83m)	0.6	0.2	0.016	0.00489	0.00524
897	1	0.0967	B20X60 2F14+2F16LR	B28(21.83m)	0.6	0.2	0.016	0.00489	0.00524
1005	1	0.0931	B20X60 2F14+2F16LR	B21(25.03m)	0.6	0.2	0.016	0.00475	0.00512
1006	1	0.0931	B20X60 2F14+2F16	B21(25.03m)	0.6	0.2	0.016	0.00475	0.00512
1007	1	0.0931	B20X60 2F14+2F16LR/F12	B21(25.03m)	0.6	0.2	0.016	0.00475	0.00512
1008	1	0.0967	B20X60 2F14+2F16LR/F12	B28(25.03m)	0.6	0.2	0.016	0.00489	0.00524
1009	1	0.0967	B20X60 2F14+2F16	B28(25.03m)	0.6	0.2	0.016	0.00489	0.00524
1010	1	0.0967	B20X60 2F14+2F16LR	B28(25.03m)	0.6	0.2	0.016	0.00489	0.00524
542	1	0.0318	B20X60 4F12LR	B34(12.23m)	0.6	0.2	0.012	0.00461	0.00443
543	1	0.0318	B20X60 4F12	B34(12.23m)	0.6	0.2	0.012	0.00461	0.00443
544	1	0.0318	B20X60 4F12LR	B34(12.23m)	0.6	0.2	0.012	0.00461	0.00443
CB34A	1	0.0318	B20X60 4F12LR	B34(15.43m)	0.6	0.2	0.012	0.00461	0.00443
CB34B	1	0.0318	B20X60 4F12	B34(15.43m	0.6	0.2	0.012	0.00461	0.00443

				)					
CB34C	1	0.0318	B20X60 4F12LR	B34(15.43m)	0.6	0.2	0.012	0.00461	0.00443
456	1	0.0318	B20X60 4F12LR	B34(18.63m)	0.6	0.2	0.012	0.00461	0.00443
472	1	0.0318	B20X60 4F12	B34(18.63m)	0.6	0.2	0.012	0.00461	0.00443
473	1	0.0318	B20X60 4F12LR	B34(18.63m)	0.6	0.2	0.012	0.00461	0.00443
856	1	0.0318	B20X60 4F12LR	B34(21.83m)	0.6	0.2	0.012	0.00461	0.00443
857	1	0.0318	B20X60 4F12	B34(21.83m)	0.6	0.2	0.012	0.00461	0.00443
858	1	0.0318	B20X60 4F12LR	B34(21.83m)	0.6	0.2	0.012	0.00461	0.00443
969	1	0.0318	B20X60 4F12LR	B34(25.03m)	0.6	0.2	0.012	0.00461	0.00443
970	1	0.0318	B20X60 4F12	B34(25.03m)	0.6	0.2	0.012	0.00461	0.00443
971	1	0.0318	B20X60 4F12LR	B34(25.03m)	0.6	0.2	0.012	0.00461	0.00443
572	1	0.0760	B20X65 2F14+2F16LR	B24 (12.23m)	0.65	0.2	0.016	0.00438	0.00457
573	1	0.0760	B20X65 2F14+2F16	B24 (12.23m)	0.65	0.2	0.016	0.00438	0.00457
585	1	0.0760	B20X65 2F14+2F16LR/F14	B24 (12.23m)	0.65	0.2	0.016	0.00438	0.00457
586	1	0.0760	B20X65 2F14+2F16LR/F14	B24 (12.23m)	0.65	0.2	0.016	0.00438	0.00457
CB24A	1	0.0760	B20X65 2F14+2F16LR	B24(15.43m)	0.65	0.2	0.016	0.00438	0.00457
CB24B	1	0.0760	B20X65 2F14+2F16	B24(15.43m)	0.65	0.2	0.016	0.00438	0.00457
CB24C	1	0.0760	B20X65 2F14+2F16LR/F14	B24(15.43m)	0.65	0.2	0.016	0.00438	0.00457
CB24D	1	0.0760	B20X65 2F14+2F16LR/F14	B24(15.43m)	0.65	0.2	0.016	0.00438	0.00457
555	1	0.0760	B20X65 2F14+2F16LR	B24(18.63m)	0.65	0.2	0.016	0.00438	0.00457
556	1	0.0760	B20X65 2F14+2F16	B24(18.63m)	0.65	0.2	0.016	0.00438	0.00457
574	1	0.0760	B20X65 2F14+2F16LR/F14	B24(18.63m)	0.65	0.2	0.016	0.00438	0.00457
575	1	0.0760	B20X65 2F14+2F16LR/F14	B24(18.63m)	0.65	0.2	0.016	0.00438	0.00457

796	1	0.0568	B20X65 2F14+2F16LR/F14	B4(18..63m)	0.65	0.2	0.016	0.00474	0.00435
797	1	0.0568	B20X65 2F14+2F16	B4(18..63m)	0.65	0.2	0.016	0.00474	0.00435
798	1	0.0568	B20X65 2F14+2F16LR	B4(18..63m)	0.65	0.2	0.016	0.00474	0.00435
363	1	0.0854	B20X65 2F14+2F16LR	B22(18.63m)	0.65	0.2	0.016	0.00466	0.00479
365	1	0.0854	B20X65 2F14+2F16	B22(18.63m)	0.65	0.2	0.016	0.00466	0.00479
366	1	0.0854	B20X65 2F14+2F16LR/F20	B22(18.63m)	0.65	0.2	0.016	0.00466	0.00479
608	1	0.0619	B20X65 2F14+2F16LR	B1(18.63m)	0.65	0.2	0.016	0.00482	0.00440
609	1	0.0619	B20X65 2F14+2F16	B1(18.63m)	0.65	0.2	0.016	0.00482	0.00440
619	1	0.0619	B20X65 2F14+2F16LR	B1(18.63m)	0.65	0.2	0.016	0.00482	0.00440
620	1	0.0594	B20X65 2F14+2F16LR	B2(18.63m)	0.65	0.2	0.016	0.00478	0.00437
621	1	0.0594	B20X65 2F14+2F16	B2(18.63m)	0.65	0.2	0.016	0.00478	0.00437
622	1	0.0594	B20X65 2F14+2F16	B2(18.63m)	0.65	0.2	0.016	0.00478	0.00437
625	1	0.0594	B20X65 2F14+2F16LR/F18	B2(18.63m)	0.65	0.2	0.016	0.00478	0.00437
898	1	0.0619	B20X65 2F14+2F16LR	B1(21.83m)	0.65	0.2	0.016	0.00482	0.00440
899	1	0.0619	B20X65 2F14+2F16	B1(21.83m)	0.65	0.2	0.016	0.00482	0.00440
900	1	0.0619	B20X65 2F14+2F16LR	B1(21.83m)	0.65	0.2	0.016	0.00482	0.00440
901	1	0.0594	B20X65 2F14+2F16LR	B2(21.03)	0.65	0.2	0.016	0.00478	0.00437
902	1	0.0594	B20X65 2F14+2F16	B2(21.03)	0.65	0.2	0.016	0.00478	0.00437
903	1	0.0594	B20X65 2F14+2F16	B2(21.03)	0.65	0.2	0.016	0.00478	0.00437
904	1	0.0594	B20X65 2F14+2F16LR/F18	B2(21.03)	0.65	0.2	0.016	0.00478	0.00437
847	1	0.0854	B20X65 2F14+2F16LR	B22(21.83m)	0.65	0.2	0.016	0.00466	0.00479
848	1	0.0854	B20X65 2F14+2F16	B22(21.83m)	0.65	0.2	0.016	0.00466	0.00479
849	1	0.0854	B20X65 2F14+2F16LR/F20	B22(21.83m)	0.65	0.2	0.016	0.00466	0.00479

873	1	0.0760	B20X65 2F14+2F16LR	B24(21.83m)	0.65	0.2	0.016	0.00438	0.00457
874	1	0.0760	B20X65 2F14+2F16	B24(21.83m)	0.65	0.2	0.016	0.00438	0.00457
881	1	0.0760	B20X65 2F14+2F16LR/F14	B24(21.83m)	0.65	0.2	0.016	0.00438	0.00457
882	1	0.0760	B20X65 2F14+2F16LR/F14	B24(21.83m)	0.65	0.2	0.016	0.00438	0.00457
909	1	0.0568	B20X65 2F14+2F16LR/F14	B4(21.83m)	0.65	0.2	0.016	0.00474	0.00435
910	1	0.0568	B20X65 2F14+2F16	B4(21.83m)	0.65	0.2	0.016	0.00474	0.00435
911	1	0.0568	B20X65 2F14+2F16LR	B4(21.83m)	0.65	0.2	0.016	0.00474	0.00435
1022	1	0.0568	B20X65 2F14+2F16LR/F14	B4(25.03m)	0.65	0.2	0.016	0.00474	0.00435
1023	1	0.0568	B20X65 2F14+2F16	B4(25.03m)	0.65	0.2	0.016	0.00474	0.00435
1024	1	0.0568	B20X65 2F14+2F16LR	B4(25.03m)	0.65	0.2	0.016	0.00474	0.00435
986	1	0.0760	B20X65 2F14+2F16LR	B25(25.03m)	0.65	0.2	0.016	0.00438	0.00457
987	1	0.0760	B20X65 2F14+2F16	B25(25.03m)	0.65	0.2	0.016	0.00438	0.00457
994	1	0.0760	B20X65 2F14+2F16LR/F14	B25(25.03m)	0.65	0.2	0.016	0.00438	0.00457
995	1	0.0760	B20X65 2F14+2F16LR/F14	B25(25.03m)	0.65	0.2	0.016	0.00438	0.00457
960	1	0.0854	B20X65 2F14+2F16LR	B22(25.03m)	0.65	0.2	0.016	0.00466	0.00479
961	1	0.0854	B20X65 2F14+2F16	B22(25.03m)	0.65	0.2	0.016	0.00466	0.00479
962	1	0.0854	B20X65 2F14+2F16LR/F20	B22(25.03m)	0.65	0.2	0.016	0.00466	0.00479
1011	1	0.0619	B20X65 2F14+2F16LR	B1(25.03m)	0.65	0.2	0.016	0.00482	0.00440
1012	1	0.0619	B20X65 2F14+2F16	B1(25.03m)	0.65	0.2	0.016	0.00482	0.00440
1013	1	0.0619	B20X65 2F14+2F16LR	B1(25.03m)	0.65	0.2	0.016	0.00482	0.00440
1014	1	0.0594	B20X65 2F14+2F16LR	B2(25.03m)	0.65	0.2	0.016	0.00478	0.00437
1015	1	0.0594	B20X65 2F14+2F16	B2(25.03m)	0.65	0.2	0.016	0.00478	0.00437

1016	1	0.0594	B20X65 2F14+2F16	B2(25.03m)	0.65	0.2	0.016	0.00478	0.00437
1017	1	0.0594	B20X65 2F14+2F16LR/F18	B2(25.03m)	0.65	0.2	0.016	0.00478	0.00437
653	1	0.2001	B20X30 2F14+2F16LR	B10(12.23m)	0.3	0.2	0.016	0.00603	0.00676
654	1	0.2001	B20X30 2F14+2F16	B10(12.23m)	0.3	0.2	0.016	0.00603	0.00676
655	1	0.2001	B20X30 2F14+2F16LR	B10(12.23m)	0.3	0.2	0.016	0.00603	0.00676
673	1	0.2128	B20X30 2F14+2F16LR	B13'(12.23m)	0.3	0.2	0.016	0.00666	0.00750
674	1	0.2128	B20X30 2F14+2F16	B13'(12.23m)	0.3	0.2	0.016	0.00666	0.00750
675	1	0.2128	B20X30 2F14+2F16LR	B13'(12.23m)	0.3	0.2	0.016	0.00666	0.00750
670	1	0.2175	B20X30 2F14+2F16LR	B13(12.23m)	0.3	0.2	0.016	0.00694	0.00783
671	1	0.2175	B20X30 2F14+2F16	B13(12.23m)	0.3	0.2	0.016	0.00694	0.00783
672	1	0.2175	B20X30 2F14+2F16LR	B13(12.23m)	0.3	0.2	0.016	0.00694	0.00783
CB13'A	1	0.2128	B20X30 2F14+2F16LR	B13'(15.43m)	0.3	0.2	0.016	0.00666	0.00750
CB13'B	1	0.2128	B20X30 2F14+2F16	B13'(15.43m)	0.3	0.2	0.016	0.00666	0.00750
CB13'C	1	0.2128	B20X30 2F14+2F16LR	B13'(15.43m)	0.3	0.2	0.016	0.00666	0.00750
CB10A	1	0.2001	B20X30 2F14+2F16LR	B10(15.43m)	0.3	0.2	0.016	0.00603	0.00676
CB10B	1	0.2001	B20X30 2F14+2F16	B10(15.43m)	0.3	0.2	0.016	0.00603	0.00676
CB10C	1	0.2001	B20X30 2F14+2F16LR	B10(15.43m)	0.3	0.2	0.016	0.00603	0.00676
CB13A	1	0.2175	B20X30 2F14+2F16LR	B13(15.43m)	0.3	0.2	0.016	0.00694	0.00783
CB13B	1	0.2175	B20X30 2F14+2F16	B13(15.43m)	0.3	0.2	0.016	0.00694	0.00783
CB13C	1	0.2175	B20X30 2F14+2F16LR	B13(15.43m)	0.3	0.2	0.016	0.00694	0.00783
825	1	0.2128	B20X30 2F14+2F16LR	B13'(18.63m)	0.3	0.2	0.016	0.00666	0.00750
826	1	0.2128	B20X30 2F14+2F16	B13'(18.63m)	0.3	0.2	0.016	0.00666	0.00750
827	1	0.2128	B20X30 2F14+2F16LR	B13'(18.63m)	0.3	0.2	0.016	0.00666	0.00750
811	1	0.2001	B20X30 2F14+2F16LR	B10(18.63m)	0.3	0.2	0.016	0.00603	0.00676
812	1	0.2001	B20X30 2F14+2F16	B10(18.63m)	0.3	0.2	0.016	0.00603	0.00676

813	1	0.2001	B20X30 2F14+2F16LR	B10(18.63m)	0.3	0.2	0.016	0.00603	0.00676
822	1	0.2175	B20X30 2F14+2F16LR	B13(18.63m)	0.3	0.2	0.016	0.00694	0.00783
823	1	0.2175	B20X30 2F14+2F16	B13(18.63m)	0.3	0.2	0.016	0.00694	0.00783
824	1	0.2175	B20X30 2F14+2F16LR	B13(18.63m)	0.3	0.2	0.016	0.00694	0.00783
935	1	0.2175	B20X30 2F14+2F16LR	B13(21.83m)	0.3	0.2	0.016	0.00694	0.00783
936	1	0.2175	B20X30 2F14+2F16	B13(21.83m)	0.3	0.2	0.016	0.00694	0.00783
937	1	0.2175	B20X30 2F14+2F16LR	B13(21.83m)	0.3	0.2	0.016	0.00694	0.00783
924	1	0.2001	B20X30 2F14+2F16LR	B10(21.83m)	0.3	0.2	0.016	0.00603	0.00676
925	1	0.2001	B20X30 2F14+2F16	B10(21.83m)	0.3	0.2	0.016	0.00603	0.00676
926	1	0.2001	B20X30 2F14+2F16LR	B10(21.83m)	0.3	0.2	0.016	0.00603	0.00676
938	1	0.2128	B20X30 2F14+2F16LR	B13'(21.83 m)	0.3	0.2	0.016	0.00666	0.00750
939	1	0.2128	B20X30 2F14+2F16	B13'(21.83 m)	0.3	0.2	0.016	0.00666	0.00750
940	1	0.2128	B20X30 2F14+2F16LR	B13'(21.83 m)	0.3	0.2	0.016	0.00666	0.00750
1048	1	0.2175	B20X30 2F14+2F16LR	B13(25.03m)	0.3	0.2	0.016	0.00694	0.00783
1049	1	0.2175	B20X30 2F14+2F16	B13(25.03m)	0.3	0.2	0.016	0.00694	0.00783
1050	1	0.2175	B20X30 2F14+2F16LR	B13(25.03m)	0.3	0.2	0.016	0.00694	0.00783
1037	1	0.2001	B20X30 2F14+2F16LR	B10(25.03m)	0.3	0.2	0.016	0.00603	0.00676
1038	1	0.2001	B20X30 2F14+2F16	B10(25.03m)	0.3	0.2	0.016	0.00603	0.00676
1039	1	0.2001	B20X30 2F14+2F16LR	B10(25.03m)	0.3	0.2	0.016	0.00603	0.00676
1051	1	0.2128	B20x60 4F16LR	B13'(25.03 m)	0.3	0.2	0.016	0.00666	0.00750
1052	1	0.2128	B20X60 4F16	B13'(25.03 m)	0.3	0.2	0.016	0.00666	0.00750
1053	1	0.2128	B20x60 4F16LR	B13'(25.03 m)	0.3	0.2	0.016	0.00666	0.00750
590	1	0.0856	B20X65 4F16LR/F14	B31(12.23m)	0.65	0.2	0.016	0.00462	0.00462
591	1	0.0856	B20X65 4F16	B31(12.23m)	0.65	0.2	0.016	0.00462	0.00462
592	1	0.0856	B20X65 4F16LR	B31(12.23m)	0.65	0.2	0.016	0.00462	0.00462

CB31A	1	0.0856	B20X65 4F16LR/F14	B13(15.43m)	0.65	0.2	0.016	0.00462	0.00462
CB31B	1	0.0856	B20X65 4F16	B13(15.43m)	0.65	0.2	0.016	0.00462	0.00462
CB31C	1	0.0856	B20X65 4F16LR	B13(15.43m)	0.65	0.2	0.016	0.00462	0.00462
593	1	0.0856	B20X65 4F16LR/F14	B31(18.63m)	0.65	0.2	0.016	0.00462	0.00462
594	1	0.0856	B20X65 4F16	B31(18.63m)	0.65	0.2	0.016	0.00462	0.00462
595	1	0.0856	B20X65 4F16LR	B31(18.63m)	0.65	0.2	0.016	0.00462	0.00462
886	1	0.0856	B20X65 4F16LR/F14	B31(21.83m)	0.65	0.2	0.016	0.00462	0.00462
887	1	0.0856	B20X65 4F16	B31(21.83m)	0.65	0.2	0.016	0.00462	0.00462
888	1	0.0856	B20X65 4F16LR	B31(21.83m)	0.65	0.2	0.016	0.00462	0.00462
999	1	0.0856	B20X65 4F16LR/F14	B31(25.03m)	0.65	0.2	0.016	0.00462	0.00462
1000	1	0.0856	B20X65 4F16	B31(25.03m)	0.65	0.2	0.016	0.00462	0.00462
1001	1	0.0856	B20X65 4F16LR	B31(25.03m)	0.65	0.2	0.016	0.00462	0.00462
676	1	0.1349	B20X50 2F14+2F16LR	B14(12.23m)	0.5	0.2	0.016	0.00511	0.00567
677	1	0.1349	B20X50 2F14+2F16	B14(12.23m)	0.5	0.2	0.016	0.00511	0.00567
678	1	0.1349	B20X50 2F14+2F16LR/F14	B14(12.23m)	0.5	0.2	0.016	0.00511	0.00567
CB14A	1	0.1349	B20X50 2F14+2F16LR	B14(15.43m)	0.5	0.2	0.016	0.00511	0.00567
CB14B	1	0.1349	B20X50 2F14+2F16	B14(15.43m)	0.5	0.2	0.016	0.00511	0.00567
CB14C	1	0.1349	B20X50 2F14+2F16LR/F14	B14(15.43m)	0.5	0.2	0.016	0.00511	0.00567
828	1	0.1349	B20X50 2F14+2F16LR	B14(18.63m)	0.5	0.2	0.016	0.00511	0.00567
829	1	0.1349	B20X50 2F14+2F16	B14(18.63m)	0.5	0.2	0.016	0.00511	0.00567
830	1	0.1349	B20X50 2F14+2F16LR/F14	B14(18.63m)	0.5	0.2	0.016	0.00511	0.00567
941	1	0.1349	B20X50 2F14+2F16LR	B14(21.83m)	0.5	0.2	0.016	0.00511	0.00567
942	1	0.1349	B20X50 2F14+2F16	B14(21.83m)	0.5	0.2	0.016	0.00511	0.00567
943	1	0.1349	B20X50 2F14+2F16LR/F1	B14(21.83m)	0.5	0.2	0.016	0.00511	0.00567

			4						
1054	1	0.1349	B20X50 2F14+2F16LR	B14(25.03m)	0.5	0.2	0.016	0.00511	0.00567
1055	1	0.1349	B20X50 2F14+2F16	B14(25.03m)	0.5	0.2	0.016	0.00511	0.00567
1056	1	0.1349	B20X50 2F14+2F16LR/F14	B14(25.03m)	0.5	0.2	0.016	0.00511	0.00567
165	1	0.1422	B20X65 4F18LR/F20	B29(18.63m)	0.65	0.2	0.018	0.00507	0.00594
264	1	0.1422	B20X65 4F18/LR	B29(18.63m)	0.65	0.2	0.018	0.00507	0.00594
273	1	0.1422	B20X65 4F18	B29(18.63m)	0.65	0.2	0.018	0.00507	0.00594
835	1	0.1422	B20X65 4F18LR/F20	B29(21.83m)	0.65	0.2	0.018	0.00507	0.00594
836	1	0.1422	B20X65 4F18/LR	B29(21.83m)	0.65	0.2	0.018	0.00507	0.00594
837	1	0.1422	B20X65 4F18	B29(21.83m)	0.65	0.2	0.018	0.00507	0.00594
948	1	0.1422	B20X65 4F18LR/F20	B29(25.03m)	0.65	0.2	0.018	0.00507	0.00594
949	1	0.1422	B20X65 4F18/LR	B29(25.03m)	0.65	0.2	0.018	0.00507	0.00594
950	1	0.1422	B20X65 4F18	B29(25.03m)	0.65	0.2	0.018	0.00507	0.00594

Columns:

Section	Frame	Lv (m)	h(m)	b (m)	db (m)	θy (Start)	θy (End)	Keff (Start)	Keff (End)	Keff (Mean)	Keff/Kel2	Keff/Kel3
K11foundation	1	1	0.35	0.35	0.018	0.0063	0.0063	7734.8	7739.0	7736.88	0.2291	0.2291
K11A	4	1.5	0.35	0.35	0.018	0.0070	0.0069	10053.7	10061.7	10057.72	0.2979	0.2979
K11B	5	1.5	0.35	0.35	0.0173	0.0066	0.0066	9695.5	9671.3	9683.37	0.2868	0.2868
K11C	6	1.5	0.35	0.35	0.016	0.0060	0.0060	7405.6	7346.4	7376.03	0.2185	0.2185
K11D	7	1.5	0.3	0.3	0.018	0.0069	0.0069	4528.2	4504.1	4516.14	0.2478	0.2478
K11E	8	1.5	0.3	0.3	0.018	0.0059	0.0060	3689.0	3625.6	3657.29	0.2007	0.2007
K12Foundation	9	1	0.35	0.35	0.018	0.0064	0.0063	7717.7	7721.1	7719.39	0.2286	0.2286
K1Foundation	12	1	0.45	0.45	0.0173	0.0059	0.0059	14400.7	14397.2	14398.95	0.1561	0.1561
K1Underground	13	1.9	0.45	0.45	0.0173	0.0055	0.0055	17180.6	17180.6	17180.63	0.1862	0.1862
K1Ground	14	1.8	0.45	0.45	0.0173	0.0058	0.0058	21554.4	21429.2	21491.80	0.2329	0.2329
K1A	15	1.5	0.35	0.35	0.0173	0.0066	0.0066	9770.9	9737.8	9754.34	0.2889	0.2889
K1B	16	1.5	0.3	0.3	0.02	0.0076	0.0076	5547.0	5520.7	5533.88	0.3036	0.3036
K12A	17	1.5	0.35	0.35	0.018	0.0066	0.0066	9755.5	9740.6	9748.03	0.2887	0.2887
K1C	18	1.5	0.3	0.3	0.016	0.0070	0.0070	4567.1	4550.4	4558.76	0.2501	0.2501
K1D	19	1.5	0.3	0.3	0.016	0.0065	0.0064	3954.0	3932.4	3943.19	0.2164	0.2164
K1E	20	1.5	0.3	0.3	0.016	0.0059	0.0059	3048.3	2998.3	3023.27	0.1659	0.1659
K2Foundation	21	1	0.35	0.35	0.018	0.0065	0.0065	7413.6	7418.8	7416.20	0.2196	0.2196
K2Underground	22	1.9	0.35	0.35	0.0173	0.0064	0.0064	6773.6	6773.5	6773.53	0.2006	0.2006
K2Ground	23	1.8	0.35	0.35	0.0173	0.0071	0.0071	10134.4	10138.6	10136.54	0.3002	0.3002
K2A	24	1.5	0.35	0.35	0.0173	0.0063	0.0063	8987.1	8965.3	8976.19	0.2659	0.2659
K2B	25	1.5	0.3	0.3	0.02	0.0072	0.0072	5090.2	5081.0	5085.59	0.2790	0.2790
K2C	26	1.5	0.3	0.3	0.016	0.0066	0.0065	4021.4	3995.5	4008.44	0.2199	0.2199
K2D	27	1.5	0.3	0.3	0.018	0.0063	0.0062	3770.2	3749.1	3759.64	0.2063	0.2063

K2E	28	1.5	0.3	0.3	0.018	0.0059	0.0059	2984.3	2945.6	2964.92	0.1627	0.1627
K3Foundation	29	1	0.4	0.35	0.018	0.0067	0.0067	9213.7	9219.6	9216.66	0.2389	0.1829
K12B	32	1.5	0.35	0.35	0.0173	0.0064	0.0064	9105.8	9069.7	9087.73	0.2692	0.2692
K3A	33	1.5	0.35	0.35	0.0173	0.0066	0.0066	10087.2	10094.9	10091.04	0.2989	0.2989
K3B	34	1.5	0.35	0.35	0.0173	0.0065	0.0064	9356.9	9350.2	9353.56	0.2770	0.2770
K12C	35	1.5	0.35	0.35	0.016	0.0058	0.0058	6577.3	6526.3	6551.78	0.1940	0.1940
K3C	36	1.5	0.35	0.35	0.016	0.0059	0.0058	6883.2	6863.3	6873.24	0.2036	0.2036
K3D	37	1.5	0.3	0.3	0.018	0.0067	0.0067	4282.7	4256.3	4269.52	0.2343	0.2343
K4Foundation	39	1	0.35	0.35	0.0186	0.0061	0.0061	8075.6	8078.6	8077.12	0.2392	0.2392
K12D	40	1.5	0.3	0.3	0.018	0.0065	0.0065	4215.8	4202.8	4209.31	0.2310	0.2310
K4Underground	41	1.5	0.35	0.35	0.0186	0.0072	0.0071	4724.3	4712.6	4718.48	0.1397	0.1397
K4Ground	42	1.26	0.35	0.35	0.0186	0.0068	0.0068	9144.8	9159.1	9151.98	0.2711	0.2711
K4Mezzanine	43	1.26	0.35	0.35	0.0186	0.0066	0.0066	9250.8	9255.5	9253.15	0.2741	0.2741
K12E	44	1.5	0.3	0.3	0.018	0.0060	0.0060	3393.6	3335.9	3364.76	0.1846	0.1846
K4A	45	1.5	0.35	0.35	0.018	0.0067	0.0067	10014.0	10017.4	10015.70	0.2966	0.2966
K4B	46	1.5	0.35	0.35	0.0173	0.0065	0.0065	9444.9	9397.6	9421.26	0.2790	0.2790
K4C	47	1.5	0.35	0.35	0.016	0.0060	0.0059	6941.6	6906.8	6924.24	0.2051	0.2051
K13Foundation	48	1	0.35	0.35	0.02	0.0061	0.0061	7248.1	7248.2	7248.16	0.2147	0.2147
K4D	49	1.5	0.3	0.3	0.018	0.0067	0.0067	4330.0	4284.9	4307.45	0.2363	0.2363
K4E	50	1.5	0.3	0.3	0.018	0.0060	0.0060	3401.9	3345.4	3373.67	0.1851	0.1851
K5Foundation	51	1	0.4	0.4	0.02	0.0057	0.0057	11014.0	11007.0	11010.47	0.1912	0.1912
K5Underground	52	1.5	0.4	0.4	0.02	0.0051	0.0051	8273.5	8176.7	8225.09	0.1428	0.1428
K5Ground	53	1.26	0.4	0.4	0.02	0.0053	0.0053	11089.7	11012.1	11050.92	0.1919	0.1919
K5Mezzanine	54	1.26	0.35	0.35	0.02	0.0060	0.0060	7802.5	7744.6	7773.56	0.2302	0.2302
K5A	55	1.5	0.35	0.35	0.0173	0.0063	0.0063	9579.1	9554.5	9566.78	0.2833	0.2833

K5B	56	1.5	0.3	0.3	0.02	0.0072	0.0072	5086.4	5078.3	5082.36	0.2789	0.2789
K21A	57	1.5	0.35	0.35	0.018	0.0059	0.0059	7463.9	7463.9	7463.87	0.2211	0.2211
K5C	58	1.5	0.3	0.3	0.016	0.0066	0.0065	4047.6	4005.0	4026.29	0.2209	0.2209
K5D	59	1.5	0.3	0.3	0.018	0.0063	0.0063	3794.6	3773.6	3784.10	0.2076	0.2076
K5E	60	1.5	0.3	0.3	0.018	0.0060	0.0060	3099.3	3051.2	3075.27	0.1687	0.1687
K6Foundation	61	1	0.35	0.35	0.0173	0.0064	0.0063	7603.9	7607.7	7605.78	0.2253	0.2253
K6Underground	62	1.9	0.35	0.35	0.0173	0.0066	0.0064	7984.7	8055.7	8020.17	0.2375	0.2375
K21B	63	1.5	0.35	0.35	0.0173	0.0055	0.0055	7068.6	6994.6	7031.62	0.2083	0.2083
K13Underground	64	1.5	0.35	0.35	0.02	0.0070	0.0070	9056.3	9053.9	9055.07	0.2682	0.2682
K13Ground	65	1.26	0.35	0.35	0.02	0.0062	0.0062	8188.0	8179.4	8183.70	0.2424	0.2424
K13Mezzanine	66	1.26	0.35	0.35	0.02	0.0060	0.0060	7846.6	7855.8	7851.20	0.2325	0.2325
K6Ground	67	1.8	0.35	0.35	0.0173	0.0077	0.0077	10711.9	10745.3	10728.61	0.3178	0.3178
K6A	68	1.5	0.35	0.35	0.0173	0.0066	0.0066	9859.3	9817.1	9838.21	0.2914	0.2914
K6B	69	1.5	0.3	0.3	0.02	0.0078	0.0078	5511.7	5518.6	5515.17	0.3026	0.3026
K6C	70	1.5	0.3	0.3	0.016	0.0069	0.0070	4662.0	4583.6	4622.82	0.2537	0.2537
K6D	71	1.5	0.3	0.3	0.018	0.0067	0.0066	4249.5	4238.1	4243.79	0.2329	0.2329
K6E	72	1.5	0.3	0.3	0.018	0.0060	0.0060	3412.8	3355.9	3384.37	0.1857	0.1857
K7Foundation	73	1	0.35	0.35	0.0173	0.0061	0.0061	7824.3	7826.8	7825.55	0.2318	0.2318
K7Underground	74	1.9	0.35	0.35	0.0173	0.0081	0.0081	10858.0	10879.0	10868.50	0.3219	0.3219
K7Ground	75	1.8	0.35	0.35	0.0173	0.0073	0.0073	10729.3	10734.6	10731.99	0.3179	0.3179
K7A	76	1.5	0.35	0.35	0.0173	0.0064	0.0065	9595.0	9476.7	9535.83	0.2824	0.2824
K7B	77	1.5	0.3	0.3	0.02	0.0075	0.0074	5405.5	5403.3	5404.36	0.2965	0.2965
K7C	78	1.5	0.3	0.3	0.016	0.0068	0.0068	4345.5	4328.6	4337.06	0.2380	0.2380
K7D	79	1.5	0.3	0.3	0.018	0.0064	0.0064	4084.4	4021.1	4052.77	0.2224	0.2224
K21C	80	1.5	0.3	0.3	0.016	0.0059	0.0059	3093.6	3038.9	3066.25	0.1682	0.1682

K8Foundation	81	1	0.35	0.35	0.02	0.0064	0.0064	8128.4	8135.6	8131.99	0.2408	0.2408
K8Underground	82	1.5	0.35	0.35	0.02	0.0074	0.0074	10357.2	10360.8	10359.05	0.3068	0.3068
K21D	83	1.5	0.3	0.3	0.018	0.0060	0.0060	3105.8	3054.8	3080.28	0.1690	0.1690
K8Ground	84	1.26	0.35	0.35	0.02	0.0065	0.0065	9632.7	9635.3	9634.00	0.2853	0.2853
K8Mezzanine	85	1.26	0.35	0.35	0.02	0.0062	0.0062	9162.6	9140.0	9151.32	0.2710	0.2710
K8A	86	1.5	0.35	0.35	0.018	0.0065	0.0065	9574.9	9523.0	9548.93	0.2828	0.2828
K8B	87	1.5	0.35	0.35	0.0173	0.0063	0.0062	8955.8	8944.2	8949.99	0.2651	0.2651
K8C	88	1.5	0.35	0.35	0.016	0.0058	0.0057	6440.0	6393.2	6416.63	0.1900	0.1900
K8D	89	1.5	0.3	0.3	0.018	0.0065	0.0064	4203.1	4199.3	4201.21	0.2305	0.2305
K8E	90	1.5	0.3	0.3	0.018	0.0060	0.0060	3496.2	3436.3	3466.24	0.1902	0.1902
K9Foundation	91	1	0.4	0.4	0.02	0.0061	0.0061	11737.1	11744.3	11740.70	0.2038	0.2038
K9Underground	92	1.5	0.4	0.4	0.02	0.0069	0.0068	15473.7	15500.3	15487.01	0.2689	0.2689
K9Ground	93	1.26	0.4	0.4	0.02	0.0061	0.0061	14340.1	14346.5	14343.29	0.2490	0.2490
K9Mezzanine	94	1.26	0.4	0.4	0.0186	0.0058	0.0058	13951.4	13963.1	13957.25	0.2423	0.2423
K9A	95	1.5	0.35	0.35	0.018	0.0069	0.0069	10056.6	10062.7	10059.61	0.2979	0.2979
K9B	96	1.5	0.35	0.35	0.0173	0.0066	0.0066	9674.2	9655.2	9664.72	0.2862	0.2862
K9C	97	1.5	0.35	0.35	0.016	0.0060	0.0060	7340.5	7272.5	7306.50	0.2164	0.2164
K9D	98	1.5	0.35	0.35	0.018	0.0057	0.0057	6641.5	6529.8	6585.65	0.1950	0.1950
K9E	99	1.5	0.35	0.35	0.018	0.0053	0.0053	4853.2	4787.3	4820.25	0.1428	0.1428
K10Foundation	100	1	0.45	0.45	0.0186	0.0058	0.0058	14423.4	14416.4	14419.90	0.1563	0.1563
K10Underground	101	1.5	0.45	0.45	0.0186	0.0053	0.0053	18297.7	18226.3	18262.00	0.1979	0.1979
K10Ground	102	1.26	0.45	0.45	0.0186	0.0052	0.0052	19280.7	19183.8	19232.21	0.2084	0.2084
K10Mezzanine	103	1.26	0.4	0.4	0.012	0.0054	0.0054	11879.8	11848.5	11864.14	0.2060	0.2060
K10A	104	1.5	0.35	0.35	0.0173	0.0068	0.0068	9898.1	9894.3	9896.17	0.2931	0.2931
K10B	105	1.5	0.3	0.3	0.02	0.0080	0.0080	5544.2	5537.1	5540.65	0.3040	0.3040

K10C	106	1.5	0.3	0.3	0.016	0.0071	0.0070	4720.0	4722.1	4721.06	0.2590	0.2590
K10D	107	1.5	0.3	0.3	0.018	0.0067	0.0067	4358.8	4303.9	4331.38	0.2377	0.2377
K10E	108	1.5	0.3	0.3	0.018	0.0060	0.0060	3399.4	3344.0	3371.71	0.1850	0.1850
K21E	109	1.5	0.3	0.3	0.018	0.0057	0.0057	2797.9	2768.2	2783.06	0.1527	0.1527
K22Foundation	110	1	0.4	0.4	0.02	0.0061	0.0061	9218.2	9213.6	9215.92	0.1600	0.1600
K22Underground	111	1.5	0.4	0.35	0.02	0.0051	0.0051	7626.7	7526.8	7576.76	0.1964	0.1503
K22Ground	112	1.26	0.4	0.35	0.02	0.0059	0.0059	8924.8	8859.1	8891.97	0.2304	0.1764
K22Mezzanine	113	1.26	0.35	0.35	0.02	0.0058	0.0058	7388.2	7338.1	7363.13	0.2181	0.2181
K13A	114	1.5	0.35	0.35	0.0173	0.0063	0.0063	9853.6	9829.8	9841.73	0.2915	0.2915
K13B	115	1.5	0.3	0.3	0.02	0.0074	0.0073	5258.7	5274.2	5266.47	0.2890	0.2890
K13C	116	1.5	0.3	0.3	0.016	0.0068	0.0067	4328.6	4290.6	4309.63	0.2365	0.2365
K13D	117	1.5	0.3	0.3	0.018	0.0065	0.0065	4213.1	4201.1	4207.14	0.2308	0.2308
K13E	118	1.5	0.3	0.3	0.018	0.0061	0.0060	3699.4	3706.2	3702.80	0.2032	0.2032
K14Foundation	119	1	0.4	0.35	0.02	0.0060	0.0060	8690.8	8689.9	8690.39	0.2252	0.1724
K14Underground	120	1.5	0.4	0.35	0.02	0.0060	0.0060	12148.6	12098.2	12123.39	0.3142	0.2405
K14Ground	121	1.26	0.4	0.35	0.02	0.0055	0.0055	10562.1	10518.6	10540.34	0.2732	0.2091
K14Mezzanine	122	1.26	0.35	0.35	0.02	0.0059	0.0060	7850.4	7776.1	7813.27	0.2314	0.2314
K14A	123	1.5	0.35	0.35	0.0173	0.0063	0.0063	9278.3	9264.0	9271.14	0.2746	0.2746
K14B	124	1.5	0.3	0.3	0.02	0.0074	0.0073	5255.7	5263.6	5259.60	0.2886	0.2886
K14C	125	1.5	0.3	0.3	0.016	0.0068	0.0067	4338.6	4299.4	4318.96	0.2370	0.2370
K14D	126	1.5	0.3	0.3	0.018	0.0065	0.0064	4209.3	4198.9	4204.09	0.2307	0.2307
K14E	127	1.5	0.3	0.3	0.018	0.0060	0.0060	3705.2	3671.6	3688.37	0.2024	0.2024
K15Foundation	128	1	0.35	0.35	0.0186	0.0060	0.0060	8108.1	8108.2	8108.18	0.2401	0.2401
K15Underground	129	1.5	0.35	0.35	0.0186	0.0069	0.0069	10158.6	10151.3	10154.94	0.3008	0.3008

K15Ground	130	1.26	0.35	0.35	0.0186	0.0062	0.0062	9306.4	9304.9	9305.64	0.2756	0.2756
K15Mezzanine	131	1.26	0.35	0.35	0.014	0.0057	0.0059	7829.5	7838.9	7834.18	0.2320	0.2320
K15A	132	1.5	0.35	0.35	0.0173	0.0063	0.0064	9274.7	9140.3	9207.53	0.2727	0.2727
K15B	133	1.5	0.3	0.3	0.018	0.0072	0.0071	5351.1	5370.9	5360.96	0.2942	0.2942
K15C	134	1.5	0.3	0.3	0.016	0.0067	0.0067	4260.3	4237.9	4249.11	0.2331	0.2331
K15D	135	1.5	0.3	0.3	0.018	0.0063	0.0064	4184.2	4117.0	4150.60	0.2277	0.2277
K15E	136	1.5	0.3	0.3	0.018	0.0060	0.0060	3511.2	3447.6	3479.40	0.1909	0.1909
K16Foundation	137	1	0.4	0.4	0.0186	0.0058	0.0058	9701.6	9702.1	9701.87	0.1684	0.1684
K16Underground	138	1.5	0.4	0.4	0.0186	0.0060	0.0060	14538.9	14494.0	14516.44	0.2520	0.2520
K16Ground	139	1.26	0.4	0.4	0.0186	0.0062	0.0063	11254.8	11116.3	11185.56	0.1942	0.1942
K16Mezzanine	140	1.26	0.35	0.35	0.02	0.0060	0.0060	7851.4	7844.8	7848.06	0.2324	0.2324
K16A	141	1.5	0.35	0.35	0.0173	0.0060	0.0063	9201.6	9290.1	9245.82	0.2738	0.2738
K16B	142	1.5	0.3	0.3	0.02	0.0075	0.0074	5277.5	5261.1	5269.31	0.2891	0.2891
K16C	143	1.5	0.3	0.3	0.016	0.0068	0.0068	4376.9	4324.7	4350.78	0.2387	0.2387
K16D	144	1.5	0.3	0.3	0.018	0.0065	0.0065	4213.6	4201.2	4207.39	0.2309	0.2309
K16E	145	1.5	0.3	0.3	0.018	0.0060	0.0060	3703.4	3666.7	3685.01	0.2022	0.2022
K17Foundation	146	1	0.45	0.45	0.0186	0.0055	0.0055	12881.0	12874.0	12877.53	0.1396	0.1396
K17Underground	147	1.5	0.45	0.45	0.0186	0.0054	0.0054	19934.7	19861.2	19897.92	0.2157	0.2157
K17Ground	148	1.26	0.45	0.45	0.0186	0.0057	0.0057	15173.2	15115.4	15144.32	0.1641	0.1641
K17Mezzanine	149	1.26	0.35	0.35	0.02	0.0061	0.0061	8100.1	8048.0	8074.05	0.2391	0.2391
K17A	150	1.5	0.35	0.35	0.0173	0.0064	0.0064	9349.9	9351.2	9350.52	0.2769	0.2769
K17B	151	1.5	0.3	0.3	0.02	0.0074	0.0074	5266.1	5257.1	5261.57	0.2887	0.2887
K17C	152	1.5	0.3	0.3	0.016	0.0067	0.0067	4268.3	4241.1	4254.69	0.2335	0.2335
K17D	153	1.5	0.3	0.3	0.018	0.0064	0.0064	4048.2	3986.9	4017.54	0.2204	0.2204

K17E	154	1.5	0.3	0.3	0.018	0.0060	0.0060	3307.6	3254.1	3280.85	0.1800	0.1800
K18Foundation	155	1	0.4	0.4	0.0173	0.0058	0.0058	11598.4	11605.4	11601.90	0.2014	0.2014
K18A	158	1.5	0.35	0.35	0.0173	0.0065	0.0065	9645.5	9643.5	9644.50	0.2856	0.2856
K18B	159	1.5	0.35	0.35	0.02	0.0063	0.0063	8215.3	8202.5	8208.92	0.2431	0.2431
K18C	160	1.5	0.35	0.35	0.016	0.0058	0.0058	6564.8	6502.3	6533.56	0.1935	0.1935
K18D	161	1.5	0.35	0.35	0.016	0.0054	0.0054	6152.7	6107.1	6129.88	0.1816	0.1816
K18E	162	1.5	0.35	0.35	0.018	0.0052	0.0051	4708.4	4680.7	4694.55	0.1390	0.1390
K19Foundation	163	1	0.4	0.4	0.0173	0.0054	0.0054	11900.1	11900.5	11900.32	0.2066	0.2066
K19A	166	1.5	0.35	0.35	0.0173	0.0065	0.0065	9648.0	9589.9	9618.93	0.2849	0.2849
K19B	167	1.5	0.3	0.3	0.02	0.0075	0.0075	5415.2	5391.8	5403.53	0.2965	0.2965
K19C	168	1.5	0.3	0.3	0.016	0.0068	0.0068	4384.1	4332.1	4358.09	0.2391	0.2391
K19D	169	1.5	0.3	0.3	0.018	0.0064	0.0064	3957.5	3901.3	3929.43	0.2156	0.2156
K19E	170	1.5	0.3	0.3	0.018	0.0059	0.0059	2947.8	2906.8	2927.31	0.1606	0.1606
K20Foundation	171	1	0.4	0.4	0.02	0.0058	0.0058	8730.4	8729.6	8729.97	0.1516	0.1516
K20Underground	172	1.26	0.4	0.35	0.02	0.0050	0.0050	5700.8	5654.0	5677.40	0.1471	0.1126
K20Ground	173	1.26	0.4	0.35	0.02	0.0056	0.0054	7510.7	7719.3	7614.99	0.1973	0.1511
K20Mezzanine	174	1.26	0.35	0.35	0.02	0.0058	0.0058	7138.6	7095.6	7117.09	0.2108	0.2108
K20A	175	1.5	0.35	0.35	0.0173	0.0061	0.0061	8410.8	8384.6	8397.69	0.2487	0.2487
K20B	176	1.5	0.3	0.3	0.02	0.0070	0.0069	4781.8	4776.5	4779.14	0.2622	0.2622
K20C	177	1.5	0.3	0.3	0.016	0.0063	0.0063	3754.5	3693.7	3724.15	0.2043	0.2043
K20D	178	1.5	0.3	0.3	0.018	0.0060	0.0060	3666.3	3599.4	3632.86	0.1993	0.1993
K20E	179	1.5	0.3	0.3	0.018	0.0059	0.0059	2944.7	2902.7	2923.70	0.1604	0.1604
K21Foundation	180	1	0.4	0.4	0.02	0.0060	0.0060	8911.5	8904.3	8907.89	0.1547	0.1547
K21Underground	181	1.5	0.4	0.35	0.02	0.0048	0.0048	7113.0	7053.1	7083.05	0.1836	0.1405

K21Ground	182	1.26	0.4	0.35	0.02	0.0055	0.0055	7199.1	7139.7	7169.37	0.1858	0.1422
K21Mezzanine	183	1.26	0.35	0.35	0.02	0.0052	0.0054	6171.4	5953.7	6062.53	0.1796	0.1796
K22A	184	1.5	0.35	0.35	0.0173	0.0062	0.0062	8486.0	8437.4	8461.68	0.2506	0.2506
K22B	185	1.5	0.3	0.3	0.02	0.0070	0.0070	4820.2	4798.1	4809.16	0.2639	0.2639
K22C	186	1.5	0.3	0.3	0.016	0.0062	0.0063	3851.5	3790.1	3820.79	0.2096	0.2096
K22D	187	1.5	0.3	0.3	0.018	0.0059	0.0060	3695.7	3633.5	3664.59	0.2011	0.2011
K22E	188	1.5	0.3	0.3	0.018	0.0059	0.0058	2889.1	2852.2	2870.64	0.1575	0.1575
K23Foundation	189	1	0.4	0.4	0.0186	0.0062	0.0062	10360.8	10361.1	10360.99	0.1799	0.1799
K23Underground	190	1.5	0.4	0.4	0.0186	0.0397	0.0056	1709.8	12051.0	6880.40	0.1195	0.1195
K23Ground	191	1.26	0.4	0.4	0.0186	0.0062	0.0062	11296.4	11255.0	11275.70	0.1958	0.1958
K23Mezzanine	192	1.26	0.35	0.35	0.02	0.0061	0.0061	7872.5	7858.6	7865.57	0.2330	0.2330
K23A	193	1.5	0.35	0.35	0.0173	0.0064	0.0063	9066.0	9034.3	9050.16	0.2680	0.2680
K23B	194	1.5	0.3	0.3	0.02	0.0073	0.0073	5118.3	5104.4	5111.35	0.2805	0.2805
K23C	195	1.5	0.3	0.3	0.016	0.0065	0.0066	4097.6	4045.0	4071.30	0.2234	0.2234
K23D	196	1.5	0.3	0.3	0.018	0.0063	0.0062	3776.6	3755.6	3766.09	0.2066	0.2066
K23E	197	1.5	0.3	0.3	0.018	0.0059	0.0059	2983.2	2944.7	2963.95	0.1626	0.1626
K11Underground	198	1.9	0.35	0.35	0.018	0.0072	0.0071	9641.9	9593.8	9617.85	0.2849	0.2849
K11isogeio	199	1.8	0.35	0.35	0.018	0.0083	0.0083	10486.0	10504.1	10495.07	0.3108	0.3108
K12Underground	200	1.9	0.35	0.35	0.018	0.0084	0.0689	10834.2	137.7	5485.92	0.1625	0.1625
K12isogeio	201	1.8	0.35	0.35	0.018	0.0076	0.0075	10823.9	10822.3	10823.13	0.3206	0.3206
K18Underground	202	1.9	0.4	0.4	0.0173	100.3110	0.0061	0.9	13885.6	6943.23	0.1205	0.1205
K18Ground	203	1.8	0.4	0.4	0.0173	0.0065	0.0064	15541.5	15499.7	15520.57	0.2695	0.2695
K19Underground	204	1.9	0.4	0.4	0.0173	0.0060	0.0060	12167.7	11989.6	12078.66	0.2097	0.2097

K19isogeio	205	1.8	0.4	0.4	0.0173	0.0065	0.0064	15570.4	15509.9	15540.11	0.2698	0.2698
K3isogeio	239	1.26	0.4	0.35	0.018	94.1281	0.0058	0.8	12701.1	6350.97	0.1646	0.1260
K8Underground	321	1.5	0.35	0.35	0.02	0.0070	0.0070	10488.8	10488.5	10488.64	0.3106	0.3106
K13Ground	322	1.5	0.35	0.35	0.02	0.0066	0.0067	8833.7	8795.9	8814.78	0.2611	0.2611
K3Underground	369	1.5	0.4	0.35	0.018	0.0060	0.0060	9759.5	9742.4	9750.92	0.2527	0.1935
K3isogeio	239	1.26	0.4	0.35	0.0173	0.0058	0.0058	12777.0	12772.7	12774.87	0.3311	0.2535
K3Mezzanine	371	1.26	0.4	0.35	0.018	0.0057	0.0057	12603.2	12601.5	12602.34	0.3266	0.2500
K20isogeio	661	1.26	0.4	0.35	0.02	0.0057	0.0058	8518.2	8458.4	8488.30	0.2200	0.1684
K13E	1075	1.5	0.3	0.3	0.018	0.0058	0.0058	2867.7	2837.9	2852.81	0.1565	0.1565
K14E	1076	1.5	0.3	0.3	0.018	0.0059	0.0058	2892.0	2860.4	2876.21	0.1578	0.1578
K15E	1078	1.5	0.3	0.3	0.018	0.0057	0.0057	2783.9	2757.4	2770.66	0.1520	0.1520
K16E	1079	1.5	0.3	0.3	0.018	0.0058	0.0058	2870.0	2844.9	2857.43	0.1568	0.1568
K7E	1203	1.5	0.3	0.3	0.018	0.0060	0.0060	3158.3	3110.5	3134.39	0.1720	0.1720

Shear Walls:

Sections	Frames	Keff/Kel2	Keff/Kel3	Lv (m)	h (m)	b (m)
shear wall 1	511	0.353233	0.2277334	12.515	2.65	0.3
shear wall 1	512	0.331498	0.2131719	12.015	2.65	0.3
shear wall 1	599	0.320509	0.2001008	10.515	2.65	0.3
shear wall 1	603	0.313783	0.1878143	9.255	2.65	0.3
shear wall 1	604	0.307273	0.1733411	8	2.65	0.3
shear wall 1	610	0.297082	0.153275	6.4	2.65	0.3
shear wall 1	611	0.282146	0.1289025	4.8	2.65	0.3
shear wall 1	612	0.257281	0.097935	3.2	2.65	0.3
shear wall 1	660	0.18867	0.0572601	1.6	2.65	0.3
Shear Wall 4	239	0.301894	0.1700323	12.515	3.2	0.4
Shear Wall 4	321	0.293768	0.1628984	12.015	3.2	0.4
Shear Wall 4	322	0.285205	0.1489476	9.985	3.2	0.4
Shear Wall 4	323	0.274692	0.1309077	8	3.2	0.4
Shear Wall 4	414	0.262874	0.1142434	6.4	3.2	0.4
Shear Wall 4	415	0.246271	0.0945263	4.8	3.2	0.4
Shear Wall 4	416	0.201831	0.0705887	3.2	3.2	0.4
Shear Wall 4	510	0.147644	0.0402917	1.6	3.2	0.4
shearwall6	621	0.372412	0.2463139	12.515	2.3	0.3
shearwall6	623	0.347104	0.2345459	12.015	2.3	0.3
shearwall6	629	0.330637	0.2162436	9.985	2.3	0.3
shearwall6	902	0.311203	0.1948996	8	2.3	0.3
shearwall6	1015	0.296018	0.1729467	6.4	2.3	0.3
shearwall6	1085	0.279996	0.1431151	4.8	2.3	0.3
shearwall6	1086	0.254574	0.1092345	3.2	2.3	0.3
shearwall6	1097	0.18247	0.0651075	1.6	2.3	0.3
shearwall7	3	0.320585	0.1778441	12.515	3.6	0.3
shearwall7	258	0.319021	0.1716862	12.015	3.6	0.3
shearwall7	325	0.315258	0.1601783	10.515	3.6	0.3
shearwall7	671	0.314414	0.1493947	9.255	3.6	0.3
shearwall7	936	0.31117	0.1371008	8	3.6	0.3
shearwall7	1049	0.29995	0.1203848	6.4	3.6	0.3
shearwall7	1182	0.283556	0.0998669	4.8	3.6	0.3
shearwall7	1205	0.25672	0.074774	3.2	3.6	0.3
shearwall7	1206	0.182449	0.0428829	1.6	3.6	0.3
shearwall2	293	0.194883	0.3305372	12.515	3.2	0.3
shearwall2	294	0.189384	0.327997	12.015	3.2	0.3
shearwall2	307	0.176875	0.3227066	10.515	3.2	0.3
shearwall2	338	0.165107	0.3173778	9.255	3.2	0.3
shearwall2	372	0.151798	0.3109086	8	3.2	0.3
shearwall2	373	0.132772	0.3035183	6.4	3.2	0.3
shearwall2	451	0.110136	0.2894521	4.8	3.2	0.3
shearwall2	452	0.08257	0.2601932	3.2	3.2	0.3

shearwall2	455	0.047413	0.1854855	1.6	3.2	0.3
shearwall3	164	0.192139	0.3110659	12.515	2.6	0.4
shearwall3	208	0.188346	0.2943335	12.015	2.6	0.4
shearwall3	260	0.174224	0.2844142	9.985	2.6	0.4
shearwall3	263	0.155647	0.2737321	8	2.6	0.4
shearwall3	265	0.136954	0.2660414	6.4	2.6	0.4
shearwall3	304	0.114146	0.2558589	4.8	2.6	0.4
shearwall3	306	0.08616	0.209072	3.2	2.6	0.4
shearwall3	391	0.049935	0.1521824	1.6	2.6	0.4
shear wall 5	277	0.249176	0.3450385	12.515	2	0.3
shear wall 5	316	0.240391	0.3337608	12.015	2	0.3
shear wall 5	334	0.228156	0.327526	10.515	2	0.3
shear wall 5	368	0.224255	0.3235327	9.985	2	0.3
shear wall 5	426	0.21604	0.3190885	9.255	2	0.3
shear wall 5	481	0.201583	0.3111859	8	2	0.3
shear wall 5	757	0.181416	0.299466	6.4	2	0.3
shear wall 5	758	0.155829	0.2831827	4.8	2	0.3
shear wall 5	759	0.121951	0.2571825	3.2	2	0.3
shear wall 5	760	0.075218	0.1844199	1.6	2	0.3